National Library of Canada
Bibliothèque nationale du Canada

Acquisitions and Bibliographic Services Branch
Direction des acquisitions et des services bibliographiques

395 Wellington Street
Ottawa, Ontario
K1A 0N4

395, rue Wellington
Ottawa (Ontario)
K1A 0N4

Your file Votre référence

Our file Notre référence

NOTICE

The quality of this microform is heavily dependent upon the quality of the original thesis submitted for microfilming. Every effort has been made to ensure the highest quality of reproduction possible.

If pages are missing, contact the university which granted the degree.

Some pages may have indistinct print especially if the original pages were typed with a poor typewriter ribbon or if the university sent us an inferior photocopy.

Reproduction in full or in part of this microform is governed by the Canadian Copyright Act, R.S.C. 1970, c. C-30, and subsequent amendments.

AVIS

La qualité de cette microforme dépend grandement de la qualité de la thèse soumise au microfilmage. Nous avons tout fait pour assurer une qualité supérieure de reproduction.

S'il manque des pages, veuillez communiquer avec l'université qui a conféré le grade.

La qualité d'impression de certaines pages peut laisser à désirer, surtout si les pages originales ont été dactylographiées à l'aide d'un ruban usé ou si l'université nous a fait parvenir une photocopie de qualité inférieure.

La reproduction, même partielle, de cette microforme est soumise à la Loi canadienne sur le droit d'auteur, SRC 1970, c. C-30, et ses amendements subséquents.

Canada

Strength-Deformation Behaviour of a Weathered Clay Crust

Md. Mahbubul A. Khan, B. Sc. Eng., M. Eng.

A Thesis
Submitted to School of Graduate Studies
Under the supervision of

Dr. Vinod K. Garga

in partial fulfillment of the requirements for the degree of

Doctor of Philosophy in Civil Engineering

Department of Civil Engineering
University of Ottawa
Ottawa, Ontario
Canada K1N 6N5

June 1993

The Doctor of Philosophy in Civil Engineering is a joint program between Carleton University and the University of Ottawa, which is administered by the Ottawa-Carleton Institute for Civil Engineering

©1993 Md. Mahbubul A. Khan, Ottawa, Canada.

National Library of Canada
Bibliothèque nationale du Canada

Acquisitions and Bibliographic Services Branch
Direction des acquisitions et des services bibliographiques

395 Wellington Street
Ottawa, Ontario
K1A 0N4

395, rue Wellington
Ottawa (Ontario)
K1A 0N4

Your file Votre référence

Our file Notre référence

The author has granted an irrevocable non-exclusive licence allowing the National Library of Canada to reproduce, loan, distribute or sell copies of his/her thesis by any means and in any form or format, making this thesis available to interested persons.

L'auteur a accordé une licence irrévocable et non exclusive permettant à la Bibliothèque nationale du Canada de reproduire, prêter, distribuer ou vendre des copies de sa thèse de quelque manière et sous quelque forme que ce soit pour mettre des exemplaires de cette thèse à la disposition des personnes intéressées.

The author retains ownership of the copyright in his/her thesis. Neither the thesis nor substantial extracts from it may be printed or otherwise reproduced without his/her permission.

L'auteur conserve la propriété du droit d'auteur qui protège sa thèse. Ni la thèse ni des extraits substantiels de celle-ci ne doivent être imprimés ou autrement reproduits sans son autorisation.

ISBN 0-315-89673-6

Canada

UNIVERSITÉ D'OTTAWA
UNIVERSITY OF OTTAWA

ACKNOWLEDGEMENTS

The Author wishes to express his sincere thanks to his research supervisor, Dr. Vinod K. Garga, for his continuous support, generous advice and untiring supervision. He is specially thanked for his generous attitude toward the research freedom, given to the author, during this research programme. The author also wishes to thank Dr. G. Bauer, Dr. M. Bozozuk and Dr. B.H. Fellenius for serving as members on various examination committees during this study.

The financial support received from the University of Ottawa and the Natural Sciences and Engineering Research Council of Canada (NSERC) are gratefully acknowledged.

The author is indebted to the National Research Council of Canada (NRCC) and to Drs. M. Bozozuk and K.T. Law (previously working with NRC) in particular for the use of their field testing equipment.

The author would like to thank his parents and parents-in-law for their constant encouragement and moral support during the period of this study.

Finally, it is the authors wife, Silvana, whose hard work and encouragement made this programme a success. This acknowledgement would be incomplete if the patience of the author's son, Swat and 2-year old daughter, Anika, who have been waiting to see their dad's post-student life, would not be acknowledged.

ABSTRACT

The purpose of this research was to study the strength-deformation behaviour of a weathered clay crust in the Ottawa region. This study includes an extensive experimental programme, covering both field and laboratory tests. The field testing methods used were the field vane, the dilatometer, the piezocone, and the self-boring pressuremeter. Triaxial shear and consolidation tests were conducted in the laboratory testing programme. Conventional triaxial tests, in both compression and extension, and non-conventional stress-path tests covering various stress-paths in the triaxial space, were performed in this study. Constant rate of strain, constant rate of load, controlled gradient, as well as the conventional oedometer tests were conducted in the consolidation testing programme.

In order to perform the laboratory experiments, a computer-operated triaxial stress-path control system and an automated consolidation apparatus were developed. The software for the automation of the above apparatus was also developed in this research.

A laboratory method for the evaluation of *in situ* K_0 for highly overconsolidated soil has been proposed. Such a method is necessary for the stress-path triaxial tests, where reconsolidation of the triaxial sample to *in situ* state of stress is required. A new method of interpretation of field vane (FV) test, for anisotropic soil, has also been developed. In this method, the original equation for the interpretation of FV has been reformulated which includes the strength anisotropy of the soil, non-uniform stress distribution around the FV, effect of rate of shearing and the disturbance due to vane insertion.

From the analysis of the laboratory triaxial and consolidation tests, for various depths within the crust, a well defined yield envelope was obtained. This yield envelope can be used to estimate the elastic and plastic strains for any stress-path in the field.

The test results obtained from various laboratory and field tests have been compared with two case studies from the same site, and demonstrate the importance of the consideration of the *in situ* stress state.

TABLE OF CONTENTS

LIST OF TABLES

LIST OF FIGURES

CHAPTER 1

INTRODUCTION

1.1 Statement of Problem

The evaluation of strength-deformation characteristics of soil is a vital part of foundation analysis and design for civil engineering structures. These characteristics vary from soil to soil. Clay crusts are usually desiccated, fissured, anisotropic, highly overconsolidated, oxidized, and may be partially saturated. The overconsolidation developed in a crust is due to one or more of natural processes, such as erosion, delayed consolidation, ground water fluctuation, desiccation, or cementation. Generally, the weathered crusts have higher undrained shear strengths (S_u) and preconsolidation pressures (σ_p') with a corresponding lower water content and compressibility when compared with the underlying intact clay. The significantly less water content in this layer, often results in a liquidity index much less than unity, as compared with values generally higher than unity in underlying sensitive non-weathered clays.

In Eastern Canadian clay deposits, the thickness of the weathered crust generally varies between 1.0 and 5.0 m and is typically about 3.0 m (Lefebvre et al. 1987). Higher thickness of approximately 6.0 m has also been reported by Eden and Crawford (1957) for a weathered crust of the Ottawa region. The crust material to be studied in this research has a thickness of approximately 3.0 m.

The Ottawa region is underlain by a soil deposit originated in the marine environment of the Champlain Sea. The clay deposit is of particular interest since major failures have occurred, some of them with catastrophic consequences, such as collapses of silos and other structures and failures of natural slopes and embankments. As the thickness of the fissured crust may extend to a significant depth (approximately 6.0 m), it can be of considerable importance to account for its presence in the analysis and design of engineering structures resting on it.

The major factors on which strength-deformation behaviour of any soil depends are: (i) stress history, (ii) stress-path, (iii) loading rate, and (iv) *in situ* state of stress. The effect of these factors on the performance of crust materials when subjected to stresses from foundation loading is not well understood. The methods of interpretation of various test results, specially field tests, also have influence on the strength-deformation behaviour of a soil.

Many researchers (Dascal et al. 1972; La Rochelle et al. 1974; Lefebvre et al. 1987; for example) have observed that the undrained shear strengths (S_u) obtained from field vane tests, a commonly used *in-situ* test method to estimate S_u, are significantly higher than those obtained from laboratory tests or back analyses of field failures. These researchers suggested that further studies should be undertaken to investigate this inconsistency within the clay crust.

Previous studies by Haile (1977), Tanaka (1986), and Lefebvre et al. (1987) have indicated that shallow foundations founded in the clay crust can be feasible and economical alternative to deep foundations. Bozozuk (1983) studied the performance of 100 concrete silos constructed in the provinces of Ontario and Quebec. Problems found in these studies are bearing capacity failure, inadequate foundations, excessive settlement, and tilting. Further investigation has been suggested by Bozozuk (1983) to improve the silo foundation analysis founded on clays and clay crusts.

In order to evaluate representative strength-deformation properties of a clay crust from laboratory triaxial tests, it is essential to reconsolidate the sample to *in-situ* stress state before triaxial shearing. For a highly overconsolidated soil such as the clay crust, a value of K_0 greater than unity is expected. However, no suitable method of K_0 evaluation is available for such type of highly overconsolidated clays. Bauer et al. (1973), Shields and Bauer (1975), and Lefebvre et al. (1987) obtained values of K_0 smaller than unity in the absence of a suitable method of K_0 evaluation for weathered crust, and suggested further studies for better understanding of this aspect.

In addition to the above-mentioned problems, there is a general lack of information of stress-path dependent behaviour of such materials, investigation of which is also essential for the proper evaluation of the behaviour of weathered clay crusts.

The study of strength-deformation properties of these crustal clays is, therefore, of considerable importance to the geotechnical profession. However, because of the difficulties in sampling and testing of these soils and the difficulties in the analysis of this deposit, where the properties change rapidly with depth, no conclusive method has been developed to adequately estimate the crust's performance.

1.2 Research Objectives

The main objectives of this experimental research were:

1. To study the general and stress-path dependent strength-deformation behaviour of a weathered clay crust.

2. To develop an automated triaxial testing system capable of performing any type of stress-path test in the triaxial space to study the stress-path behaviour.

3. To develop a method for determining *in situ* horizontal stress which is required to study stress-path behaviour.

4. To study the inconsistency in the values of undrained shear strengths obtained from field vane tests and from laboratory triaxial tests or from back-analyzed field failures.

5. To compare test results obtained from laboratory and field tests with those obtained from case studies.

1.3 Scope of Research

In order to accomplish the research objectives, experimental work was undertaken on the following aspects:

1. Execute field and laboratory tests to evaluate strength-deformation behaviour. Field vane, dilatometer, self-boring pressuremeter, and piezocone tests were conducted in the field testing programme. Triaxial shear (conventional and stress-path), oedometer consolidation and direct shear tests were performed in the laboratory testing programme. Both vertically and horizontally oriented samples were used in laboratory tests.

2. Obtain a soil profile of the crust in terms of unit weight, density of soil particles, Atterberg limits, *in-situ* vertical and horizontal stresses, preconsolidation pressure, OCR, K_0, and undrained shear strength. Each of these soil parameters was obtained at least from five depths.

3. Compare and discuss the strength and deformation behaviour obtained by various field and laboratory test methods.

4. Develop a method for interpretation of field vane test results for anisotropic soils. In this method, basic equations for interpretation have been reformulated using an advanced fundamental approach.

5. Develop a new method of evaluation of K_0 for highly overconsolidated clays. Special laboratory tests were performed to check the validity of this method.

6. Examine the effect of stress history (OCR) and *in situ* state of stress (K_0) on the undrained shear strength and deformation behaviour. Values of K_0 were obtained by the new method developed during the course of this research.

7. Carry out stress-path tests to study the stress-path behaviour of the weathered crust. Tests were conducted for a variety of stress paths in both compression and extension sides. Isotropic triaxial compression tests were also conducted for this purpose.

8. Analyze field and laboratory tests to obtain the strength-deformation parameters from these tests, and compare them with those obtained from case studies.

1.4 Description of the Site and its Geological History

The location of the site for this research is the Fraser Farm in Fallowfield of Carleton County, approximately 30 Km southwest from the University of Ottawa, as shown in Fig. 1.1. This site was chosen for this research since it was studied and documented by a number of investigators as discussed below:

(i) At this site, there was a foundation failure of a tower silo which was documented and analyzed by Bozozuk (1977), Haile (1977), Tanaka (1986), and Tanaka et al. (1989).

(ii) After the failure, three new silos were constructed on raft foundations within the weathered crust at the same site. One of the new silos was instrumented (Haile 1977) to study the full-scale behaviour.

(iii) Tanaka (1986) carried out an intensive *in situ* testing programme at this site.

(iv) O'Shaunessy (1992) studied this site to determine the contaminant transport behaviour of the clay.

The weathered crust of this site is underlain by a soft sensitive clay deposit occupying large parts of the valley of St. Lawrence River and its tributaries. The soil within the crust is a clayey silt consisting occasional thin seams of silt and fine sand but does not show any detectable layering. The depth of the crust is 3 m which was easily determined from the change in field vane strength. Uncountable randomly oriented microfissures were observed in this crust. The groundwater table is located at a depth of 0.8 m with a seasonal variation of ±0.2 m. The soil shows overconsolidation behaviour with an overconsolidation ratio (OCR) of 16 at 1.0 m, decreasing with depth to a OCR value of 3.1 at a depth of 3.7 m.

The soil profile consists of a clayey silt of light brown colour from ground surface to 1.5 m, grey from 1.5 to 2.8 m and dark grey from 2.8 to 3.7 m. Since the purpose of this study was to investigate the properties of the weathered crust, classification tests for the intact clay below 3.7 m were not conducted, especially since the geotechnical properties of the underlying clay at the same Fallowfield site have been discussed in detail by

Bozozuk (1977) and Haile (1977). The Plasticity Index within the crust is approximately constant with a value of 22±2. Natural water content at a depth of 0.4 m is 24% which increases to 42% at 3.7 m. The Liquidity Index within the crust is less than unity. Grain size analysis showed 37% clay fraction and 63% silt at a depth of 2.0 m, changing almost linearly with depth to 58% clay and 42% silt at a depth of 16.0 m (Bozozuk 1977). The sensitivity of the soil evaluated from the field vane test increases with depth, ranging from 2.5 at 0.7 m to 40 at 8.5 m.

The Champlain clay is an extremely sensitive post-glacial marine clay occurring in the St Lawrence and Ottawa valleys. Generally the natural water content of the clay is higher than the liquid limit. Sensitivities range from extra-sensitive to quick.

In geological and agricultural literature, this clay has also been called "Leda" clay (the name "Leda" was applied to the deposit by Sir William Dawson to relate the clay to the most common fossil (*Leda glacialis*) found in it), "Laurentian" clay or "Rideau" clay but presently the name Champlain clay is most commonly used. The clay was deposited in the marine environment of the Champlain Sea which invaded the Ottawa and St Lawrence river valleys as glacial ice retreated from the region. Subsequent uplift resulted in present non-marine conditions. The environmental conditions during deposition of the clay are not completely understood. It is fairly certain that at least the inland deposits, such as in the Ottawa area, were laid down in the brackish water but the degree of influence of the inflow of fresh water is not known. It has been reported that two marine deposits, resulting from two distinct marine invasions, are present in the region (Eden and Crawford 1957).

A typical boring log in the Ottawa area would show glacial till over bedrock grading into gravel, sand, and silt and overlain by a substantial deposit of marine clay. The upper part of the marine clay, the brown weathered clay crust, is often fissured and desiccated. The marine clay is highly sensitive and exhibits notable thixotropic properties. Generally, Champlain clay has a liquidity index greater than one; this may partly account for its sensitivity.

Champlain clay is mainly composed of illite with a tendency toward mica, plagioclase feldspars, quartz, and chlorite with interstratification of the illite and chlorite minerals. Presence of small amounts of montmorillonite and kaolinite is also reported.

Eden and Crawford (1957) reported that the Champlain clay has experienced slight to medium precompression below the desiccated layer, and the magnitude appears to be related to present surface elevations. The precompression of the clay is attributed to erosion of overburden following emergence from the sea.

1.5 Outline of Thesis

Chapter 2 describes the literature review on previous studies made on weathered clay crusts and other overconsolidated similar soils.

Chapter 3 presents the field testing programme and their test results. Interpretation techniques for various field testing methods (field vane, dilatometer, self-boring pressuremeter and piezocone tests) are also described. Finally, the test results obtained by various testing methods are compared at the end of this chapter.

Chapter 4 gives the detailed description of the development of the vane interpretation method which was developed during the course of this research. This method re-formulates the conventional vane interpretation equation incorporating stress anisotropy, strength anisotropy, shearing rate effect, and disturbance due to vane insertion.

Chapter 5 explains the development of laboratory apparatuses which was essential for this research. Three apparatuses were developed during the course of this research: (i) a computerized triaxial control system for stress-path testing, (ii) an automated consolidation apparatus, and (iii) an improved volume gauge.

Chapter 6 gives the detailed description of the development of a laboratory method of K_0 evaluation for overconsolidated clays, which was also developed during the course of this research. Complete experimental technique and verification of the method have been described in this chapter.

Chapter 7 describes the results and analyzes of triaxial tests. Undrained tests for both vertical and horizontal samples were carried out. Drained tests for various stress-paths at different depths were also conducted in both compression and extension. A common yield envelope is obtained for all these stress-path tests on samples from different depths. The procedure to obtain the yield envelope is also described in this chapter.

Chapter 8 describes the consolidation tests and their test results. Various types of consolidation tests, constant rate of strain, constant rate of stress, controlled gradient, and conventional oedometer consolidation, were carried out during this testing programme. Test results obtained by these different methods are also compared and discussed.

Chapter 9 compares the strength-deformation parameters obtained from field and laboratory tests. This chapter also compares these parameters obtained from test results with those obtained from back-analyses of case studies.

Chapter 10 presents the conclusions of this research, and provides some recommendations for further research and development.

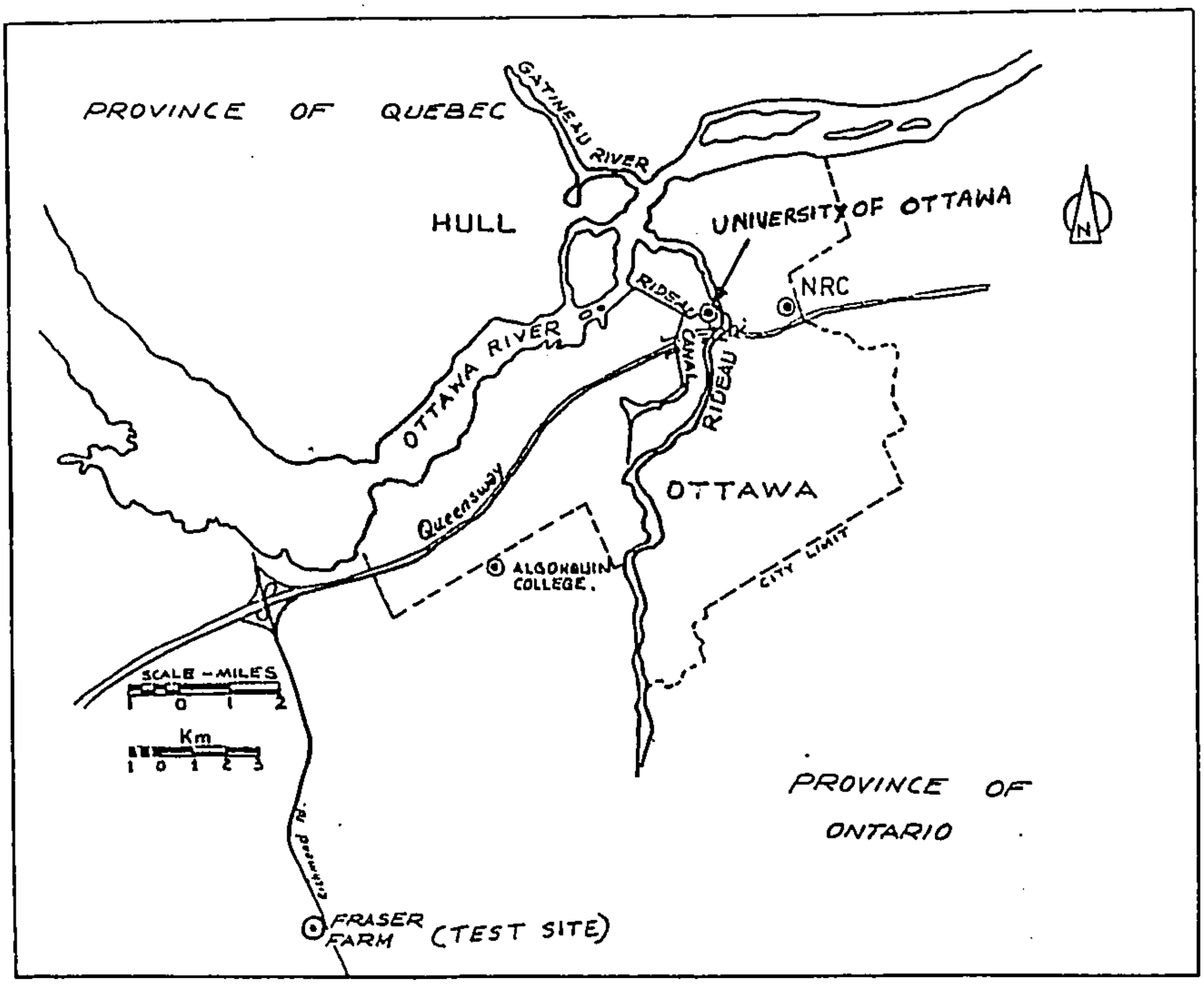

FIG. 1.1. Location of test site

CHAPTER 2

LITERATURE REVIEW

The literature review in this section is restricted to only the subject of the thesis, the weathered crust. While the underlying Champlain clay has been extensively investigated by a numerous researchers, considerably few studies (Webb 1971; Tanaka 1986; Lefebvre et al. 1987) have been undertaken on the overlying weathered crust.

In one of the initial attempts for investigation of strength-deformation properties of a weathered crust, Webb (1971) showed that the weathered crust of Ottawa Champlain clay has considerably higher strength than the underlying material. The maximum undrained shear strength of the crust was approximately four times that of the lower intact clay. It was also pointed out that the higher strength of the crust is due to overconsolidation most probably attributable to previous desiccation. The soil studied by Webb was from the Bronson-Heron road site where the depth of crust was approximately 3.8 m. The sensitivity within the crust obtained from field vane test was considerably low (6-14) when compared with the lower unweathered clay where sensitivity reported was up to 310. The clay fraction of this site was approximately constant (67-70%) for both crust and the lower clay. Natural water content increases with depth in the weathered crust and almost constant in the lower soft clay. Liquidity index within the crust is between 0.6 and 0.7, and below the crust is greater than unity and goes up to 8.3. This study has confirmed that a satisfactory design of shallow foundation instead of deep foundation is possible within the weathered crust. However, Webb recommended that further studies are required for a better understanding of this material. In the finite element analysis of elastic settlement calculation, the settlement value obtained was slightly higher than that obtained from a full-scale loading test. The soil parameters obtained in this finite element analysis were from constant mean pressure (p') triaxial compression tests and oedometer consolidation tests.

In a series of laboratory tests for both the crust and the underlying clay at a site in the Ottawa region, Mitchell et al. (1972) reported that a cementation yield curve or an elastic limit could be established in a non-dimensional stress space normalized by the preconsolidation pressure, p_c (Fig. 2.1). Two conclusions can be made from Fig. 2.1: (i) maximum elastic stress (normalized with p_c) is independent of pre-shear consolidation pressure for the values of η (=q/p) between 0.50 and 0.85; and (ii) the shear strength is also independent of the pre-shear consolidation pressure between η values of 0.6 and 1.3. Mitchell et al. termed this constant shear strength the cementation strength.

2.1 Deformation Properties of Clay Crusts and other Overconsolidated Clays.

The major part of the deformation in these crust deposits usually takes place rapidly and is composed of immediate deformation, closing of fissures, compression of air voids, and possibly some porewater drainage. Bauer et al. (1973) conducted a full-scale test on a specially constructed and instrumented footing (3.1 m x 3.1 m) for the characterization of deformation properties. Laboratory triaxial tests (UU and CK_0U) and field plate-bearing tests were also carried out for the same soil and depth. The results of these tests were compared to those obtained from the full-scale footing loading test. The plate bearing tests gave comparable results with the footing test when the proper depth of soil being deformed was considered. The laboratory values of deformation moduli were too low (in the range of less than 10 MPa to 25 MPa) and erratic. The deformation moduli show a decrease with increasing load intensity, as shown in Fig. 2.2, because of the non-linear stress-strain behaviour of the soil. The deformation modulus obtained from pressuremeter (Type GB-BX) test was also considerably lower when compared with plate loading or footing load test (Shields and Bauer 1975).

To obtain representative properties from the laboratory triaxial tests, it is essential to reconsolidate the sample to the *in-situ* stress state. The main reason why the results from the laboratory method did not compare well with the full-scale footing load test is believed to be the low values of K_0 used in the studies by Bauer et al. (1973) and Shields and Bauer (1975). K_0 used for these tests ranged from 0.20 to 0.40 which seem to be very low for a highly overconsolidated clay. K_0 values for these type of crust material are expected to be greater than unity. Therefore, research should be undertaken to determine the *in-situ* K_0 of clay crusts. Since a laboratory method to determine K_0 (where $K_0>1$) is unavailable, a method has been developed in this research for this purpose which is described in Chapter 6.

2.1.1 Elastic Deformation

In geotechnical engineering, the theory of elasticity is generally used for the solution of various stress-distribution and soil deformation problems. Many of these problems, such as stress distribution in layered systems and deformations under surface loadings, assume the soil to be an elastic material having certain elastic constants, such as Poisson's ratio and Young's modulus. These constants are often derived from stress-strain data from undrained triaxial shear tests. The calculation of immediate settlement assumes that the clay behaves as an isotropic linear-elastic material during shear. While the overconsolidated clay crust behaves as an essentially linear-elastic material, the normally consolidated clay does not. However, both clay deposits are generally subjected to *in situ* anisotropic stresses.

Ladd (1964) observed that the modulus of elasticity (sometimes the terms Young's modulus and deformation modulus are also used) is influenced by the following factors: (1) the level of applied shear stress; (2) the degree of overconsolidation; (3) the effects of time (thixotropy, aging, and strain rate); and (4) different types of stress systems (commonly known as stress path) applied to anisotropically consolidated samples. It was suggested that the correlations between laboratory results and well-documented case records are needed. The use of consolidated undrained (CU) tests, rather than unconsolidated undrained (UU) tests, is recommended by Ladd (1964) for establishing such correlations, because CU tests are generally less influenced by sample disturbance and can be better suited for evaluating the effects of different stress systems. Attention should also be paid to the value of K_0 since the in-situ state of stress of most clay deposits is anisotropic.

Ladd's (1964) study on the clay deposit of MIT campus showed that the samples from overconsolidated upper stratum yielded much higher values of modulus than the samples from the normally consolidated lower stratum. The value of K_0 for the overconsolidated clay was approximately 1. Therefore, isotropically consolidated undrained (CIU) triaxial compression tests were conducted to obtain the modulus for this overconsolidated upper stratum.

Heavily overconsolidated clays behave essentially in a linearly elastic manner for small changes of stress, and the incremental elastic moduli are dependent on the ambient effective pressure (Wroth 1971). This implies that the estimation of settlement for structures on such soils based on simple elastic theory should be satisfactory so long as the appropriate values of the moduli are known and used in the calculation. Because of the dependence on pressure, the elastic moduli vary with depth in a soil deposit, and this variation (increase) in stiffness with depth has an important influence on the magnitude of the calculated deformation. An example of such an approach of settlement calculation is given by Simons (1971). Wroth (1971) has investigated how the values of the moduli vary with pressure and whether any pattern of behaviour can be observed. It has been shown in this study that the moduli do vary in a systematic manner, being affected to a major degree by the ambient effective stress and to a minor degree by the overconsolidation ratio. The effects of anisotropy were also studied in this investigation by testing triaxial specimens in vertical, horizontal and inclined directions; the undrained Young's modulus for horizontal specimens E_h was consistently greater than that for vertical specimens E_v by a factor varying between 1.28 to 1.41. The Poisson's ratio evaluated in this study was 0.12 which was found to be independent of pressure and overconsolidation ratio.

Mitchell et al. (1972) used two layer isotropic elastic settlement theory to calculate the settlement of foundation placed in the crust overlying relatively deep deposits of sensitive clays in Eastern Ontario. Test data from a site in Ottawa, where, as mentioned previously, a stiff crust overlies a sensitive Champlain Sea deposit, were used to derive the elastic constants for the two layers. Case studies of some other similar soils, where a crust overlies sensitive clay, were also conducted for the verification of applicability of elastic theory for the determination of settlement. The use of elastic theory was justified by these data, and was found to be acceptable for foundation loads within the linear load-deformation range. The pore water pressure coefficient A, for undrained triaxial tests, was approximately 0.33 up to approximately 75% of the failure stress for tests carried out under confining pressures equal to the vertical stress. An A value of 0.33 is indicative of an elastic response to loading. The stress-strain curves are very linear and the strains are recoverable up to approximately 70% of failure. Consolidation tests carried out on block samples of this crust material indicated a linear e-logσ_v' curve to stress level of up to about 70% of preconsolidation pressure (σ_P'). K_0 determined by Mitchell et al. for this study was 0.30, which in the light of results from present research appears to be erroneous for the overconsolidated crust material.

The clay crust used in this study by Mitchell et al. (1972) was heavily overconsolidated. However, the method used for the determination of K_0 was for normally consolidated soil and resulted in a very small value of K_0. Clearly, there is a need for the development of a new method of K_0 determination which could be used for highly overconsolidated clays.

Atkinson (1975) reported that the laboratory tests on overconsolidated London clay taken from the Barbican Arts Centre have demonstrated a deformation behaviour which can be satisfactorily interpreted through the theory of elasticity, provided anisotropy is included in the elasticity model. The deformation behaviour was investigated in laboratory cylindrical and plane strain compression tests. It was observed that elastic deformations were approximately path-independent provided the loading increased monotonically. At any point on the loading path, the deformations were regarded as wholly elastic or wholly plastic, and the point at which the deformations changed from elastic to plastic was regarded as a yield point. It was also observed that the elastic parameters are dependent on the mean normal stress as well as on the stress history. In all the tests, the samples were loaded from an initial stage of isotropic stress. The overconsolidated London clay used in this investigation was significantly anisotropic in its elastic behaviour; the ratio of vertical stiffness to the horizontal stiffness was approximately 0.5.

The above research, in which tests were loaded monotonically from an initial state of isotropic stress, can be extended to study whether the samples behave in a similar way for other loading paths or for other initial stress states close to those in the ground. The applicability of the theory of elasticity can also be investigated for the overconsolidated weathered crust.

2.1.2 Effect of Stress Path on Deformation Behaviour

The effect of stress path on deformation behaviour of overconsolidated fissured London clay has been studied by Som (1968), Simons and Som (1969) and Simons (1971). Triaxial shear and oedometer consolidation tests were carried out to investigate the effect of stress path on the axial and volumetric compressibility of undisturbed samples of London clay. It was shown that the direct use of standard undrained compression tests to determine the elastic modulus, and oedometer tests to measure the axial compressibility, may lead to appreciable errors when calculating the settlements of structures on London clay. The volumetric compressibility was found to be reasonably independent of the magnitude of the lateral effective stress, but the axial compressibility was greatly influenced by the ratio of lateral to vertical effective stress, and a method was proposed for estimating the relative magnitude of axial and volumetric compressibilities as a function of this effective stress ratio. The value of K_0 for this overconsolidated fissured London clay was reported to be greater than unity, ranging between 1.4 and 3.4 for which OCR value ranged between 5.5 and 44.

Simons and Som (1969) found a relationship between the non-dimensional quantity $E/(\sigma_m')_0$ and the effective stress ratio (Fig. 2.3). This implies that for any effective stress ratio, the modulus is proportional to mean pre-shear effective stress $(\sigma_m')_0$, and that for any value of $(\sigma_m')_0$ the modulus decreases steadily with increasing stress level. Similar relationships have also been obtained for some other clays (Ladd 1964). It has been observed that the strain ratio $\varepsilon_1/\varepsilon_v$ decreases as the stress increment ratio $\Delta\sigma_3'/\Delta\sigma_1'$ increases (Fig. 2.4) indicating the influence of stress path. Both the weathered crust overlying the Champlain clay and the London clay are fissured and highly overconsolidated. A similar effect of stress path, as mentioned above for London clay, is also expected on the deformation behaviour of the weathered clay crusts in Eastern Ontario.

2.2 Undrained Shear Strength of Clay Crusts and other Overconsolidated Clays

One of the most significant characteristics of the crust is its much higher undrained shear strength measured by the field vane when compared with those values measured in the non-weathered clay underlying the crust. The field vane test is a commonly used method for evaluating the S_u of clayey materials for embankments and some other shallow foundations. The strength measured in the weathered crust may have significant effect on the calculated factor of safety, since it may be several times as high as that in the underlying non-weathered clay (Graham 1979). The various corrections used to reduce the vane shear strength in the crust varies from one engineer to the other and are purely arbitrary, based on the fact that the strength appears to be too high (Lefebvre et al. 1987).

La Rochelle et al. (1974) proposed a more fundamental approach by suggesting the use of so-called undrained residual strength determined in the laboratory by unconsolidated undrained tests. This approach leads to a difficulty since, the upper part of the crust does not show any peak shear strength in triaxial compression test. The stress continuously increases with the increment of strain most probably due to the negative pore-water pressure generated by the tendency of dilation in an undrained test (Lefebvre et al. 1987) as shown in Fig. 2.5.

Lefebvre et al. (1987) conducted field plate loading test, large shear box test, and undrained triaxial compression and extension tests to compare these results with field vane test. Since the values of S_u obtained from field vane test were considerably higher than those obtained from above-mentioned methods, Lefebvre et al. (1987) suggested that the field vane test should not be used to determine the undrained shear strength of a crust material, and should only be used to determine the depth of a crust. Therefore, to obtain a reasonable value of S_u, it has also been recommended that the S_u for crust should be considered same as that of the underlying non-weathered clay determined by field vane test.

Undrained shear strength determined in the laboratory is generally obtained from a fully saturated (artificially saturated in the laboratory) sample which contains higher water content than in the field. This might be one of the reasons why the field vane test gives higher shear strength than that determined in the laboratory. To overcome this problem, some triaxial shear tests may be conducted after consolidating the sample to *in-situ* stresses and applying back pressure equal to *in-situ* porewater pressure.

Law (1979) observed in laboratory triaxial-vane test that the S_u from vane shear test is highly influenced by the horizontal stress existing during shear. Becker et al. (1988) emphasized the importance of *in-situ* state of stress, and suggested that the *in-situ* field vane test data should be interpreted in terms of the *in-situ* horizontal and yield stresses. Conventional interpretation of vane shear test neither considers the anisotropic *in-situ* state of stress nor the strength anisotropy. Obviously, there is a need for research for development of a better interpretation method of vane shear test. With this idea in mind, a new interpretation method has been developed during the course of this research as discussed in chapter 4.

Bishop et al. (1965) obtained a correlation between strength and effective stress on undisturbed samples of London clay from the Ashford Common shaft. Since the London clay and the clay crust of this research have similar *in-situ* stress history (i.e. highly overconsolidated with $K_0>1$), a comparable correlation may also exist for the weathered crust. A similar study has been conducted in this research in addition to the study of stress-path behaviour.

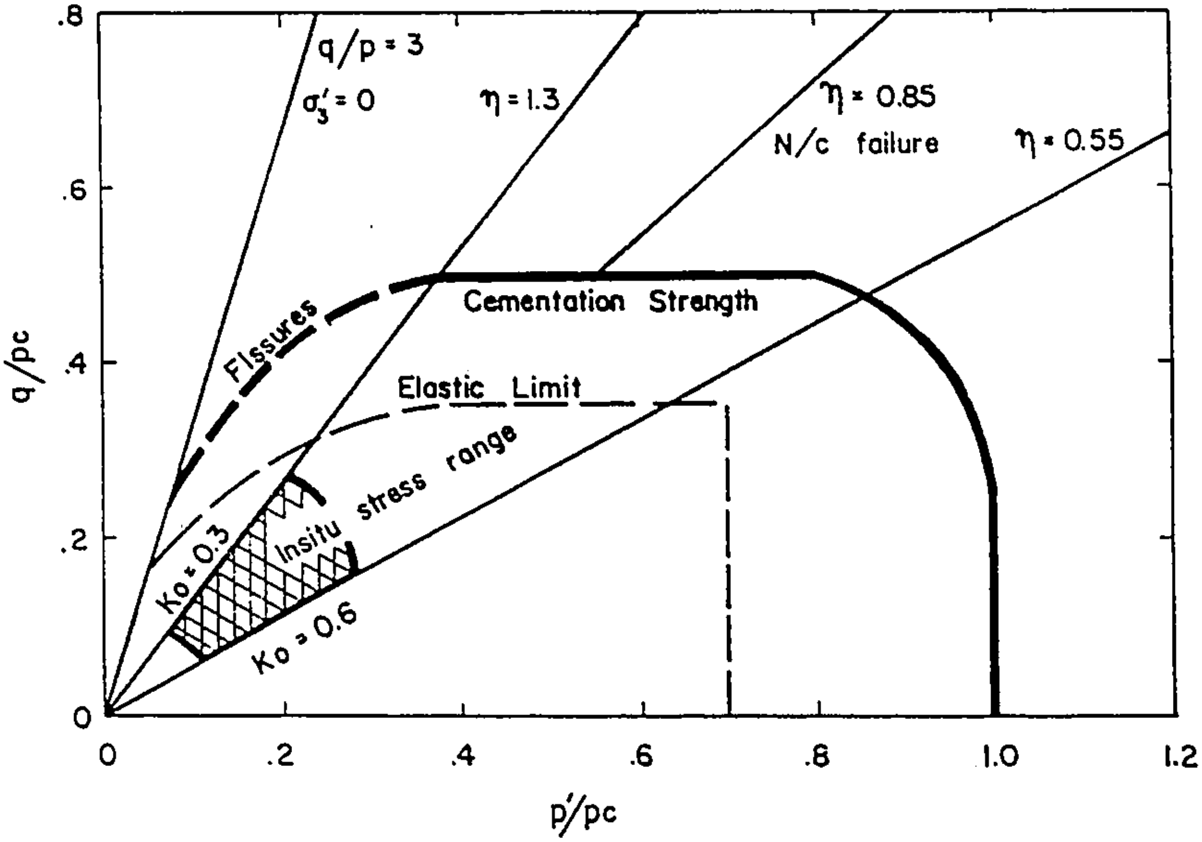

FIG. 2.1. Pattern of behaviour of cemented sensitive soils
(after Mitchell et al. 1972)

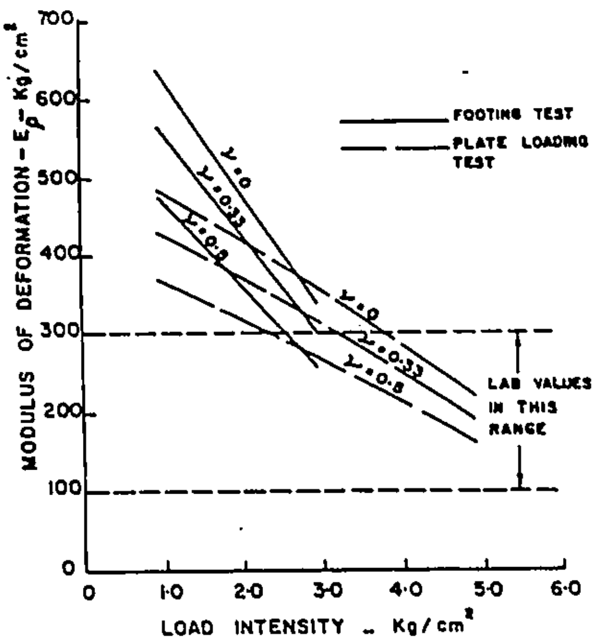

Fig. 2.2. Moduli of deformation from footing test and plate loading test (Bauer et al. 1973).

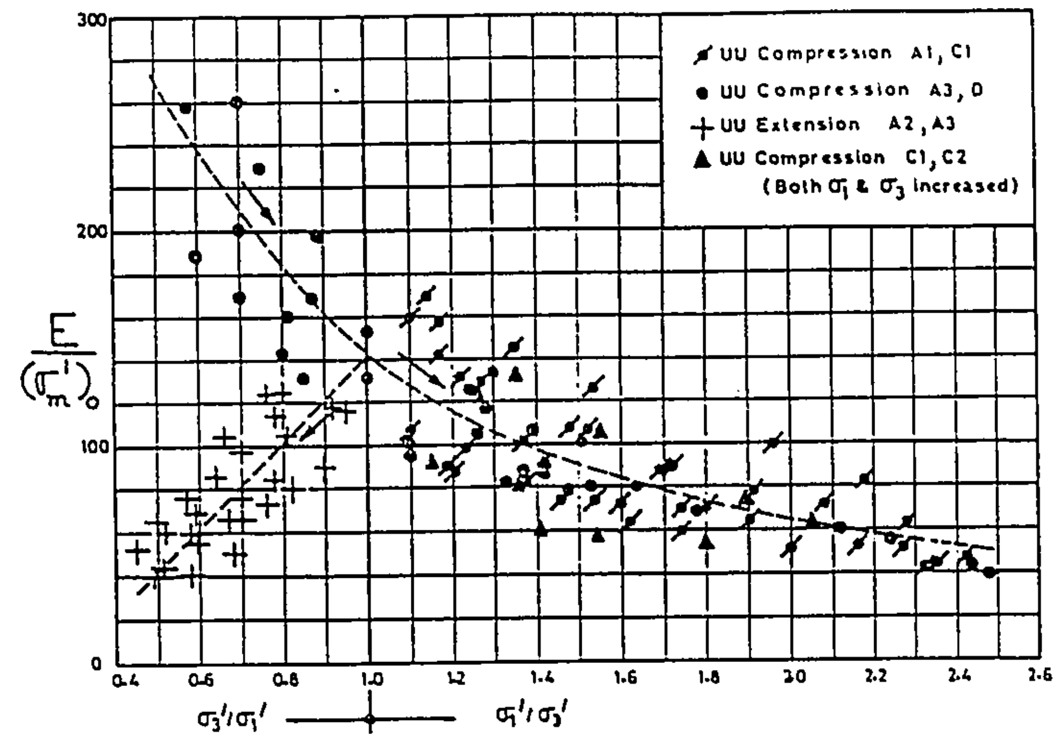

Fig. 2.3. Elastic modulus plotted against stress ratio (Simons 1971).

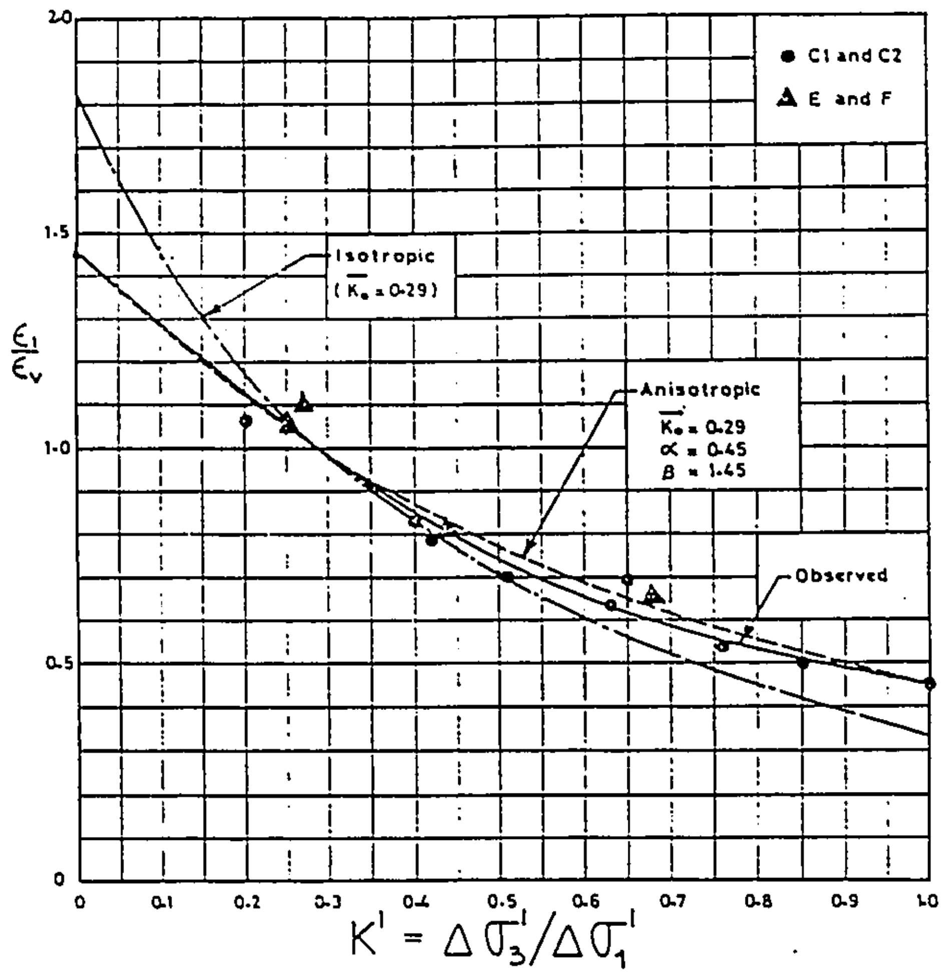

Fig. 2.4. Strain ratio plotted against stress increment ratio (Simons 1971).

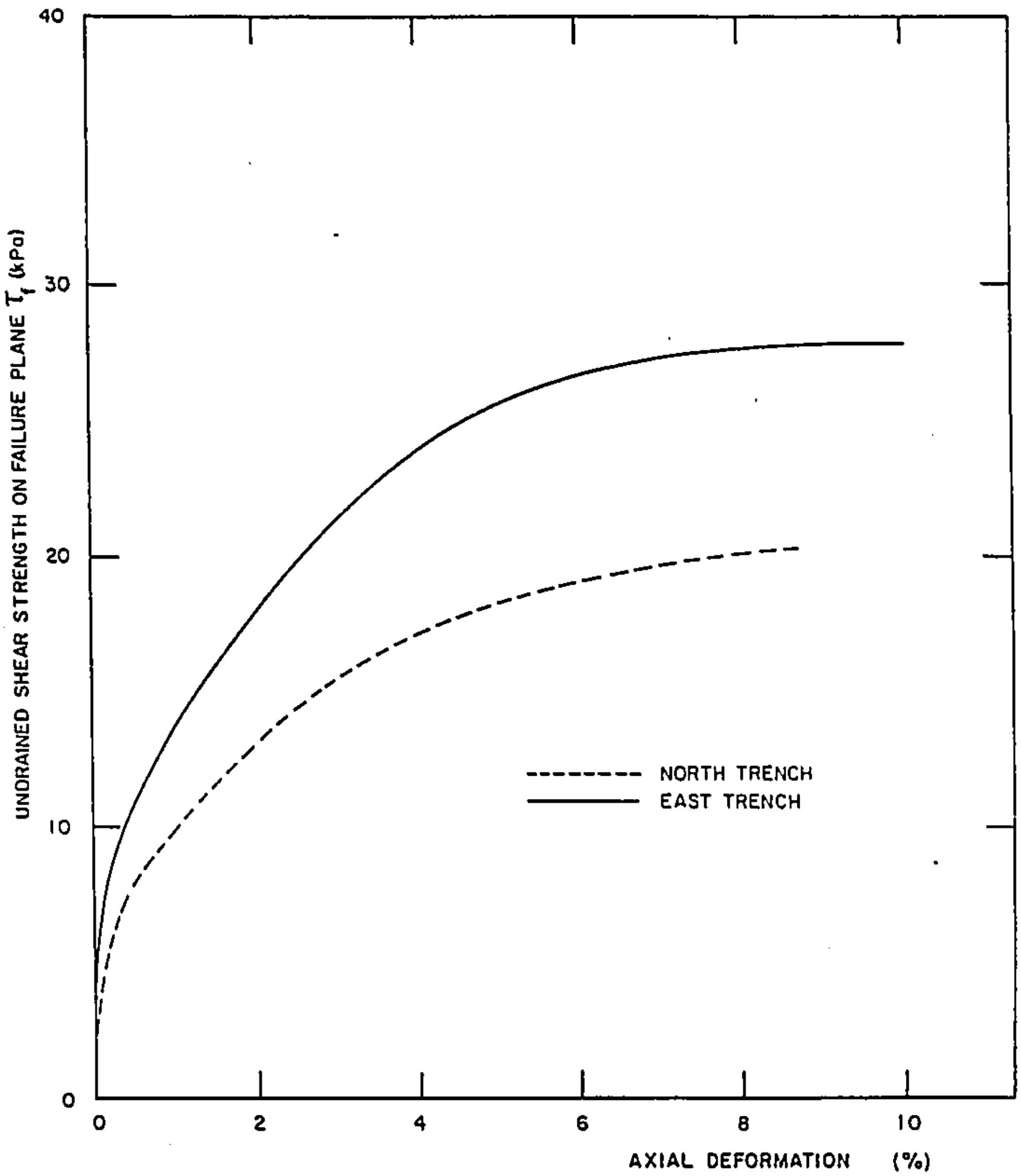

FIG. 2.5. Undrained shear strength on the failure plane averaged for compression and extension triaxial tests (Lefebvre et al. 1987).

CHAPTER 3

FIELD TESTS

3.1 General

A geotechnical investigation can be performed by using any one or a combination of the following three approaches: (i) field testing, (ii) laboratory testing, and (iii) back-analysis of a monitored structure. Major advances have been made in last three decades, in the first two investigation techniques with the development of new equipment and apparatuses, specially, by the use of electronic systems (e.g., data acquisition and processing as well as equipment controlling systems) which have significantly improved the quality and quantity of data. In geotechnical engineering, it is a good practice to resort to both field and laboratory test methods in order to assess soil properties, since it has been shown that these techniques can complement each other.

The field testing programme was undertaken, in this research, with the following objectives in mind: (i) to provide quantitative evaluation of strength-deformation characteristics of the weathered crust of Champlain clay, (ii) to compare the results obtained by various field testing methods (field vane, dilatometer, self-boring pressuremeter and piezocone), and to show and discuss the discrepancies among these test results, if any, and (iii) to examine the reliability of these *in situ* devices by comparing these test results with laboratory tests and case studies.

Ladd et al. (1977), Wroth (1984), and Jamiolkowski et al. (1985), among others, have discussed the advantages and disadvantages of each individual methods and can be summarized as follows:

(i) Field Tests:

Advantages:

- The ability to test a larger volume of soil thereby allowing the evaluation of the bulk properties of a soil mass.
- The testing of soil deposits where undisturbed sampling is difficult (e.g., sandy soils, highly fissured clays, etc.)
- The testing of soils in their natural environment (temperature, chemical, and biological conditions), and to allow the test to be initiated from the *in situ* stress state.
- Increased cost-effectiveness is realized in general.

Disadvantages:

- Boundary conditions in terms of stresses and/or strains are not well-defined for which the test results cannot be adequately analyzed.
- Drainage conditions during the test are usually unknown, and cannot be easily controlled.
- Effects of disturbance due to installation of field instruments cannot be evaluated easily and is of unknown magnitude.

(ii) Laboratory Tests:

Advantages:

- Well-defined boundary conditions can be maintained.
- Drainage conditions can be strictly controlled, and/or monitored .

- Any pre-selected and well-defined stress-paths can be followed during a test.

Disadvantages:

- Difficult to avoid the effect of sample disturbance.
- The soil specimens used in the laboratory may be too small in size to model the field behaviour.

(iii) Back-Analysis:

Advantages:

- Ability to verify a specific constitutive soil model.
- Ability to assess relevant soil parameters within the adopted soil model.
- In field cases involving failure, the factor of safety is known to be 1.0.

Disadvantages:

- Drainage and boundary conditions are not always well-defined in a geomechanical model.
- Analysis is dependent on some soil input variables, such as initial stress state, stress history of the deposit, etc.
- Analysis is highly dependent on the assumptions of the constitutive model.
- Field observations may be unreliable, few, and commonly incomplete.

Interpretation of most *in situ* tests are faced with some serious difficulties. Wroth (1984) attributes this to two factors: one is intrinsic to the nature of the soil and the other is related to the test itself. There is also the fact that some tests lack a proper basis for theoretical formulation in order to evaluate the soil properties.

The soil response depends on the geological history of the deposit, mineral composition, fabric and structure of the particle arrangement, stress history experienced after formation, and many other factors. The boundary conditions of any field test are in most cases unknown and uncontrolled, and therefore, solutions are based on simplified assumptions.

As a consequence, an unambiguous interpretation is invariably unattainable. The technique for interpretation of the test results is related to some empirical relationships or assumptions.

To illustrate, consider the common case of an anisotropic and non-homogeneous *in situ* soil. These *in situ* conditions may cause a non-homogeneous stress field to be generated around an *in situ* probe resulting in high localized hydraulic gradients. Some degree of drainage may, therefore, occur during the *in situ* testing procedure (Wroth 1984). The undrained condition supposed to exist during this test might not be true, and therefore, some erroneous interpretation is to be expected. In addition, the rate effect of the test and the rotation of the principal stress due to stress changes during the test can complicate the interpretation of any *in situ* test. Wroth (1984) has suggested to establishing empirical correlations from the results of various tests, both in field and in laboratory, and then to draw conclusions based on all these available experiences.

The variety of techniques and the range of applicability of field tests have been discussed by various researchers (e.g., Bjerrum 1973; Schmertmann 1975; Mitchell and Gardner 1975; Ladd et al. 1977; Wroth 1975,1984; Jamiolkowski et al. 1985 and others). This chapter, however, concentrates on only four *in situ* test devices as discussed in the following sections. A discussion of the interpretation techniques for these tests and the use of all these testing methods including the uncertainties associated with each of these methods have also been presented.

Four types of field tests: namely, field vane (FV), dilatometer (DMT), self-boring pressuremeter (SBP) and piezocone (CPTU) were conducted, for this research, at the Fraser Farm site. All these testing apparatuses were generously provided by the NRC (National Research Council) of Canada and the tests were performed in the field with the help of NRC technicians. For each type of testing method, at least two test holes were made and a minimum radial distance of 1.5 m (2.0 m for SBP) was maintained between the test holes to avoid influence from adjacent holes (Fig. 3.1).

There are four major sections in this chapter assigned to the four individual testing methods. In the initial part of each of these sections, a literature review has been made on the current understanding of the use of the respective testing method to measure the *in situ* undrained shear strength of clays. In the later part of these sections, the test results obtained during the current research has been presented and discussed. Discussion has also been presented to show how these values of strengths relate to other measurements of undrained shear strength.

3.2 Field Vane Test

3.2.1 Introduction

The field vane test is one of the most widely used method for the *in situ* determination of the undrained shear strength (S_u), particularly in soft clays. Schmertmann (1975) suggested phasing out of the FV testing method since it requires a number of corrections; and this testing method has been described as an example of the "correction crisis". However, this method is still being used with reasonable confidence in many parts of the world, more particularly, in Canada, the Scandinavian countries and Thailand. A detailed history of the use of vane shear test is published by Flodin and Broms (1981).

The Field Vane Apparatus

Elements of field vane apparatus are illustrated in Fig. 3.2. Although the apparatus has not yet been internationally standardized, there appears to be a general consensus that the ratio of height (H) to diameter (D) be 2:1, and that the vane consists of four blades set at right angles. A number of sizes of the field vane are being used. The widely used dimensions appear to be H=130 mm and D=65 mm. Other dimensions on which there is wide agreement are the vane blade thickness (≈2 mm) and the area ratio (the ratio of the volume of soil displaced by the vane to the soil volume swept by the rotation of the vane), which is almost universally specified to be less than 12%.

A major area of potential difference in the various national standards arises where field vane tests are carried out below the base of a borehole, in contrast to the more usual use of a self-contained vane device. Where a borehole is used it is clearly necessary to insert the vane to a depth below the base of the boring that is sufficient to ensure that the vane is in truly undisturbed soil (probably at least four borehole diameters), and that the *in situ* stresses are not affected by the presence of the borehole. The use of drilling fluid in the borehole may be of considerable value in this case, particularly in a sensitive clay.

The usual "rest-period" following vane insertion seems to be 5 min., and the rate of rotation is almost invariably specified as either 6° or 12°/min. In practice, this typically results in failure occurring at about 1 min. These two factors significantly influence the measured undrained shear strength, and are reviewed in detail in Chapter 4.

3.2.2 Interpretation of Field Vane Test Data

Undrained shear strength obtained from the field vane test is conventionally interpreted from the following equation:

$$S_u = \frac{6M}{7\pi D^3} \quad \ldots\ldots\ldots\ldots (3.1)$$

where, M = maximum torque recorded during the vane rotation.

An elaborate discussion on the present understanding of the interpretation of the FV test is given by Chandler (1988). Equation 3.1 assumes that the stress distribution during shear around the field vane is uniform, there is no disturbance due to the insertion of vane blades, there is no effect of the rate of vane rotation, and the soil is isotropic. The analysis does not take into account the anisotropic *in situ* stress state, especially observed in overconsolidated soils. The FV test data has been extensively used to obtain undrained shear strength in soft clays, where Bjerrum's (1972) correction factor is commonly applied to obtain a representative value. A detailed discussion about this subject will be made in Chapter 4, where a new method of FV interpretation has been discussed which was developed during the course of this research. This method uses more fundamental approach considering strength anisotropy, non-uniform stress distribution around the vane blades, disturbance due to vane insertion, and the effect of rate of vane rotation.

3.2.3 Results of Field Vane Test

Two series of field vane tests were performed at the standard rate of rotation of 6°/minute. The results of field vane tests, analyzed conventionally using Eq. 3.1, are presented in

Fig. 3.3. NGI (Norwegian Geotechnical Institute) vane of size 43 mm diameter and 86 mm high was used for these tests. Tests were performed at an interval of 400 mm within the crust and at an interval of 1 m below the crust to a depth of 10.5 m. In one of the boreholes, tests were undertaken to a depth of 21 m where the bedrock was encountered. From the undrained shear strength profile, the depth of crust may visually be taken as 3 m (Fig. 3.3a). Fig. 3.3b shows that the sensitivity increases with depth of soil, and it is obvious that the sensitivity in the intact Champlain clay is considerably higher than that of the weathered crust. Only a negligible scatter is noticeable between the two series of tests.

The calibration factor (2.73 kPa/unit) provided by the NRC was directly used to convert the dial readings into undrained shear strengths, S_u. Isotropic soil behavior was considered for this calibration.

3.2.4 Discussion of Field Vane Test Results

Bjerrum's correction factor which is a function of plasticity index and progressive failure (less predominant), reduces the FV undrained shear strength $S_{u(vane)}$, at this site, by only 3%, giving a μ value of 0.97 in Eq. 3.2. The interpreted data shown in Fig. 3.3 does not include this correction factor.

$$S_{u(field)} = S_{u(vane)} \cdot \mu \qquad (3.2)$$

Undrained shear strength obtained from the conventional interpretation of field vane test, where isotropic strength and uniform stress distribution are considered around the FV, is considerably higher than that obtained from other laboratory and field tests. Strength anisotropy, non-uniform stress distribution around the FV, and shearing rate are believed to be the reasons of this inconsistent result. Approximately 90% of the total resistance measured by the standard vane is provided by the vertical circumscribed failure surface. Consequently, vane test results are dominated by the strength mobilized on the vertical plane. Therefore, it is the horizontal *in situ* effective and/or yield stresses that dominantly control the vane shear strength. Yet, to date, vane strength interpretation has been considered in terms of vertical stresses only. A new interpretation method, which takes into account the strength anisotropy, non-uniform stress distribution around the vane, shearing rate effect and disturbance due to vane insertion, has been developed (Khan and Garga 1991; and Garga and Khan 1992) and is described in Chapter 4.

3.3 Dilatometer Test

3.3.1 Introduction

The flat dilatometer, a relatively new device for *in situ* investigation of soil properties (Marchetti 1980), was also used in this series of field testing program. Recent research (Schmertmann 1986) shows that this device tests sand in approximately fully drained conditions and clays in approximately fully undrained conditions. The best results are obtained at these extremes. Silts, clayey sands, fissured clays, and other soils may have only partial drainage during the test, to an unknown and possibly variable degree. This may lead to more variable and less accurate evaluations of their soil engineering properties.

The DMT test is a combination of two tests: firstly, a penetration test, and secondly, a controlled lateral expansion test. Only the second part of the test was used in this study, and no attempt was made to record the data in terms of penetration of the dilatometer test.

The Dilatometer Apparatus:

The apparatus (Fig. 3.4) consists of a thin stainless steel flat plate of 14 mm in thickness, 95 mm in width and 220 mm in length. An expandable circular steel membrane of 60 mm in diameter is located on one face of the blade. The flexible steel membrane is pneumatically pressurized laterally into the soil by 1.1 mm. The gas pressure used to inflate the diaphragm is either air or nitrogen supplied from the pressure cylinder. When at rest, the external surface of the membrane is flush with the surrounding flat surface of the blade.

During the test, the blade is pushed into the ground using a penetrometer rig, at a rate of 10-20 mm/sec. At 200 mm depth intervals penetration is stopped, and membrane is inflated by means of pressurized gas. Two pressure readings are taken while inflating the membrane: pressure A, required to just lift the membrane, and the pressure B, required to move the centre 1.1 mm laterally into the soil. The pressure on the diaphragm is increased in such a way that the expansion takes place in 15 to 30 seconds. The test is continued by successively pushing the blade into the ground and recording the A and B pressures at each depth. Testing and calibration procedures have been described in detail by Marchetti (1980), Marchetti and Crapps (1981), and Schmertmann (1986).

The interpretation technique, and the theoretical and practical limitations of the dilatometer test, as well as the usefulness of this *in situ* testing method, will be discussed in the following sections.

3.3.2 Interpretation of Dilatometer Test Data

The interpretation of dilatometer test is still being done on the basis of the original empirical equations proposed by Marchetti (1980) with some minor changes. These empirical correlations were based on the experience gained from performing DMT tests over 40 sites which were geotechnically well documented. Marchetti has proposed three index parameters, referred to as DMT material index I_D, horizontal stress index K_D, and dilatometer modulus E_D, as follows:

$$\text{DMT Material Index, } I_D = \frac{\Delta P}{p_0 - u_0} \qquad \text{(3.3)}$$

$$\text{Horizontal Stress Index, } K_D = \frac{p_0 - u_0}{\sigma_{v0}'} \qquad \text{(3.4)}$$

$$\text{DMT Modulus, } E_D = 34.7\Delta P \qquad \text{(3.5)}$$

where,

ΔP = $p_1 - p_0$

σ_{v0}' = *in situ* effective vertical stress

u_0 = *in situ* pore water pressure

p_0 = A + ΔA = pressure required to start the expansion of the membrane

p_l = B - ΔB = pressure required to expand the membrane up to 1.1 mm

A, B = respective pressures at the start and end of the expansion, directly taken from DMT dial reading

ΔA = the external pressure, in free air, to keep the membrane in contact with its seating

ΔB = internal pressure, in free air, to lift the membrane center 1.1 mm from its seating

From these three empirical soil index parameters, the following other correlations have been developed. These correlations were obtained empirically based on the experience gained from DMT tests at over 40 sites. The sites selected for these tests were reasonably homogeneous and geotechnically well documented.

(i) Soil Unit Weight and Soil Type:

The unit weight of a soil, at any depth, can be estimated from the soil classification chart (Fig. 3.5) developed by Marchetti and Crapps (1981). Based on this chart, soil classification can also be obtained using the index parameters I_D and E_D.

(ii) In Situ Stress History:

The *in situ* stress history, overconsolidation ratio (OCR) and coefficient of earth pressure at rest (K_0), can be obtained from the following correlations developed by Marchetti (1980) as shown in Figs. 3.6 and 3.7, respectively.

$$OCR = (0.5K_D)^{1.56} \quad \text{(3.6)}$$

$$K_0 = \left(\frac{K_D}{1.5}\right)^{0.47} - 0.6 \quad \text{(3.7)}$$

Equation 3.6 is valid only for the soils with $I_D < 1.2$.

(iv) Undrained Shear Strength:

Marchetti (1980) also suggested the following empirical correlation for the estimation of undrained shear strengths (S_u) of clays and clayey silts. This correlation is reproduced in Fig. 3.8, and is valid for soils with $I_D \leq 1.2$.

$$S_u = 0.22\sigma_{V0}' (0.5K_D)^{1.25} \quad \ldots\ldots \quad (3.8)$$

(v) Constrained Modulus:

A relationship between constrained modulus (M, defined as $1/m_v$), K_D and E_D was also obtained by Marchetti (1980). The values of M in such correlations are based on oedometer test results or were obtained from empirical correlations between M and other tests. In case of cohesive soil, the following relationship was obtained.

$$M = R_M.E_D \quad \ldots\ldots \quad (3.9)$$

where; $R_M = 0.14 + 2.36 \log K_D$, and E_D is the dilatometer modulus.

Similar relationships for cohesionless soil was also found by Marchetti (1980).

3.3.3 Results of Dilatometer Test

Two series of DMT tests were conducted to a depth of 4.4 m. A penetration rate of 20 mm/sec was used, and test data were recorded at an interval of 200 mm. The DMT test data were interpreted using the empirical correlations (Eqs. 3.3 through 3.9) developed by Marchetti (1980), and the interpreted test results are shown in Figs. 3.9a through 3.9h. The values of ΔA and ΔB, required for the determination of p_0 and p_1, from DMT test were calibrated as 11 kPa and 27 kPa, respectively. The DMT parameters I_D (Fig. 3.9b), K_D (Fig. 3.9c) and E_D (Fig. 3.9d) were calculated from Eqs. 3.3, 3.4 and 3.5, respectively, and the values of OCR (Fig. 3.9e), K_0 (Fig. 3.9f), S_u (Fig. 3.9g) and M (Fig. 3.9h) were estimated from the empirical Eqs. 3.6, 3.7, 3.8 and 3.9, respectively. Eq. 3.6 is valid only for the cohesive soils with $I_D<1.2$, and is applicable for the site of this research since these I_D values (Fig. 3.9b) satisfy the above criteria.

It should be mentioned here that different waiting periods between the end of probe pushing and the start the diaphragm inflation, were monitored to examine the influence of the waiting period. No noticeable effect was found, between the waiting periods of 15 seconds and 2 minutes, in the determination of dilatometer parameters. Schmertmann (1986) has also made similar observations.

3.3.4 Discussion of Dilatometer Test Results

The parameter I_D is a direct function of the physical and mechanical response controlled by the grain size distribution of a soil (Marchetti 1980). For the soil between the depths of 0.4 m and 2.5 m, the I_D value changes from 1.0 to 0.6. It can be observed from Fig. 3.5 that the soil type for these I_D values ranges between silt and clayey silt. From Fig. 3.5 it can also be observed that the soil between 2.5 m and 2.7 m is clayey silt to clay and the soil below 2.7 m is clay. Grain-size analysis of this research also gives close agreement to the dilatometer test results. Grain-size analysis indicates clayey silt within the crust, and shows a gradual increase in clay fraction with depth (39% at 1.0 m depth gradually increases to 45% at 3.7 m depth). Tanaka's (1986) study of DMT test shows that the clayey soil starts downward from the depth of 4.0 m, and the I_D values obtained from that study shows higher scatter than those obtained in this study.

The horizontal stress index, K_D, varies significantly (in the range between 30 and 10) in the upper 1.5 m. Similar trend was also observed in Tanaka's study, where K_D value varied between 50, close to the surface to about 10 at about 1.5 m depth. These values may be compared to those obtained by Marchetti for heavily overconsolidated (OCR between 17 and 35), fissured, marine silty clays tested at Numana, Italy where the K_D value ranges between 5 and over 20. There is very small scatter within the crust (0 - 3 m) between the K_D values of the two series of DMT tests carried out in this investigation, and negligible scatter is observed below the crust. Non-homogeneity of the crust could be the reason for the small scatter in the K_D values. The K_D value below the crust ranges between 8 (at 3.0 m depth) and 5 (at 4.4 m depth).

K_0 values obtained in this study, which are directly related to K_D, compares very well with those obtained from the DMT test results by Tanaka (1986), as shown in Fig. 3.10. The comparison for upper 0.8 m is poor. This may be because this upper layer is subjected to temporary surface loading due to movement of farm vehicles, etc.

The E_D values obtained in Tanaka's study are approximately double the E_D values obtained in this study. E_D values obtained by Tanaka range between 16 and 4 whereas the same values in this study range between 7 and 1.8.

Undrained shear strength obtained from DMT gradually increases with depth within the crust ranging between 28 and 38 kPa. This is a contrast to the results obtained from other laboratory and field methods where the S_u decreases with depth within the crust. These values of S_u are considerably lower than those of Tanaka's study, where these values range between 120 and 45 kPa.

The interpreted values of M (ranging between 70 and 10 MPa) obtained by Tanaka were also considerably higher than those obtained in this investigation (Fig. 3.9h), where M ranges between 15 MPa and 4 MPa) . No reason can be found for this discrepancy. Tanaka stated that the M values obtained were considerably higher when compared with those obtained from oedometer consolidation tests. However, the M values obtained from DMT tests in the present study are comparable to those obtained from oedometer consolidation tests, from present study (where M values range between 3 and 12) as well as from Haile's (1977) study (where M ranges between 4 and 7).

Very consistent result with negligible scatter, obtained in this study, indicates the suitability of the DMT test for the crust. Schmertmann (1986) also stated that the experience has shown the dilatometer test to be exceptionally reproducible and operator insensitive, and the estimated results by an experienced engineer are reproducible with a coefficient of variation of approximately 10%.

3.4 Self-Boring Pressuremeter Test

3.4.1 Introduction

The pressuremeter is an *in situ* device that can theoretically evaluate the lateral stress in the ground, the stress-strain behaviour, and the strength of the soil at depth. The concept of the pressuremeter test is relatively simple and involves expanding a cylindrical, flexible membrane against the sides of a hole drilled in the soil. In past practice, however, the test has been complicated by issues such as how much disturbance occurs to the soil prior to testing, before and during probe insertion, and how to determine standard geotechnical engineering parameters from the pressuremeter test data.

In the conventional Menard-type pressuremeter test (Menard 1956), the hole for the probe is drilled by a standard drill rig, the probe is lowered into the hole to the desired depth, and then the membrane is expanded to make contact with the soil. Unfortunately, the stress relaxation associated with the forming of the hole, as well as possible remoulding of the soil by the drilling process, raise questions concerning the reliability of the results. In order to address this problem, British (Wroth and Hughes 1973) and French (Baguelin et al. 1972) investigators simultaneously developed a new version of the pressuremeter with self-boring capability. This innovation allowed the pressuremeter to drill its own way into the ground, presumably with little or no disturbance. It represents an advance in the state-of-the-art of *in situ* testing, and the self-boring pressuremeter has found acceptance in the geotechnical practice. However, a firm skepticism remains since, in spite of the self-boring capability, most of the early published test results obtained using the new probes are inconsistent with established practice. For example, undrained shear strengths for clays obtained using the self-boring pressuremeter are reported to be as high as twice those obtained from other tests.

A research was undertaken by Denby and Clough (1980) to investigate the reasons of high undrained shear strengths obtained from pressuremeter tests. Denby and Clough (1980) found that there were more issues involved than just the reported disparity in shear strengths. The important issues they reported are:

1. Different parameters were obtained from pressuremeter tests using different interpretation procedures.
2. The interpretation procedures generally involved subjective judgments which could vary from one test to another or were difficult to carry out, or both.
3. Different soil responses were obtained depending upon the type of probe advancing techniques used.
4. It was not clear exactly how a small degree of disturbance would affect the parameters derived from the test.

The Self-Boring Pressuremeter Apparatus:

The self-boring pressuremeter used in this study was similar to that described by Wroth and Hughes (1973). The probe was 800 mm long and 80 mm in diameter, and the length of the whole pressuremeter assembly was 1.0 m. A typical self-boring pressuremeter is described in Fig. 3.11.

3.4.2 Interpretation of Self-boring Pressuremeter Test Data

The pressuremeter test relates displacement of a cylindrical cavity to the pressure causing that displacement. A method of interpretation is needed to obtain, from these data, the engineering parameters of the soil. Ideally, it would yield the entire stress-strain curve, the undrained shear strength, and the lateral earth pressure at rest.

There are a number of methods (Menard 1956; Gibson and Anderson 1961; Baguelin et al. 1974; Prevost and Hoeg 1975; Marsland and Randolph 1977; Denby and Clough 1980; Wroth 1980; Arnold 1981; Lacasse et al. 1981; Ghionna et al. 1985; Jefferies 1988; among others) available for interpreting the pressuremeter test results. The assumptions used in these methods, to obtain the soil characteristics (such as stress-strain curve, *in situ* horizontal stress, undrained shear strength, etc.), differ from each other. However, only the method by Denby and Clough (1980) was used in this study for interpreting the pressuremeter test data. This method has been selected for the following reasons:

(i) to minimize subjectivity in the analysis,

(ii) to provide one technique which yields lateral stress, stress-strain response and strength,

(iii) to reduce the effect of data points which might be influenced by seating or initial reading errors, and,

(iv) to allow for a range of possible shapes of stress-strain curves.

This method has been described in the following section.

Denby and Clough (1980) Method:

This method was derived using some features of some other existing methods. It has also incorporated the general idea of the widely accepted Duncan and Chang (1970) approach for fitting stress-strain data, in which the latter portions of the prefailure stress-strain curve can be used to generate the initial portions, where minor disturbances are likely to affect the experimental data.

The basic Duncan and Chang (1970) method assumes the stress-strain curve can be fitted by a hyperbola. However, in contrast to the Prevost and Hoeg (1975) technique, which only allows for a hyperbolic curve asymptotic to a peak stress at an infinite strain, the Duncan-Chang technique recognizes that the peak strength is reached at a finite strain. Thus, the actual soil strength $(\sigma_1-\sigma_3)_f$ is defined as $R_f\,(\sigma_1-\sigma_3)_{fh}$, in which $(\sigma_1-\sigma_3)_{fh}$ = the asymptotic value; and R_f = a factor normally less than one. In the extreme, the R_f value may be zero and a linear stress-strain curve is then defined by the Duncan-Chang technique.

Using the Duncan-Chang representation of the stress-strain curve for the undrained response of the soil, the expression relating principal stress difference, $\sigma_1-\sigma_3$, and axial strain, ε_a, is:

$$\sigma_1 - \sigma_3 = \frac{\varepsilon_a}{\dfrac{1}{E_i} + \dfrac{R_f \varepsilon_a}{(\sigma_1 - \sigma_3)}} \quad \ldots\ldots\ldots\ldots\ldots (3.10)$$

in which E_i = the initial tangent modulus. For the pressuremeter results, this equation must be transformed to radial stress and radial strain axes. Radial strain, ε_r, may be related to the axial strain through the shear strain γ, by the expression $\gamma = 2\varepsilon_r = 1.5\varepsilon_a$ (for small strains). Then, providing there is no volume change, $E_i = 3G_i$, where G_i is the initial tangent modulus of the shear stress versus shear strain curve. Noting that $(\sigma_1 - \sigma_3)$ in the pressuremeter test is $(\sigma_r - \sigma_0)$ and that $(\sigma_r - \sigma_0)/2$ = the undrained shear strength, S_u, and using the relationships for E_i and ε_a, Eq. 3.10 may be written as:

$$\frac{(\sigma_r - \sigma_\theta)}{2} = \frac{\varepsilon_r}{\frac{1}{2G_i} + \frac{R_f}{S_u}\varepsilon_r} \qquad (3.11)$$

Now, Baguelin et al. (1972), Palmer (1972), and Ladanyi (1973) established that for undrained behaviour and small strains:

$$\frac{(\sigma_r - \sigma_\theta)}{2} = \varepsilon_r \frac{d\sigma_r}{d\varepsilon_r} \qquad (3.12)$$

Thus, relating Eq. 3.11 to Eq. 3.12,

$$\frac{d\varepsilon_r}{d\sigma_r} = \frac{1}{2G_i} + \frac{R_f\varepsilon_r}{S_u} \qquad (3.13)$$

Equation 3.13 states that the inverse of the slope of the pressuremeter curve, $d\varepsilon_r/d\sigma_r$, is related to the radial strain by an equation for a straight line which has an intercept at $\varepsilon_r = 0$ of $1/2G_i$ and a slope of R_f/S_u. Therefore, by plotting $d\varepsilon_r/d\sigma_r$ versus ε_r, and obtaining the slope and intercept of the resulting straight line, the important parameters $2G_i$ and R_f/S_u can be obtained.

In order to isolate S_u and R_f, it is only necessary to assume that the shear stress will remain constant for at least a small period after yielding. Then,

$$\frac{(\sigma_r - \sigma_\theta)}{2} = \varepsilon_r \frac{d\sigma_r}{d\varepsilon_r} = S_u \qquad (3.14)$$

Rewriting Eq. 3.14 we obtain

$$\frac{d\varepsilon_r}{d\theta_r} = \frac{\varepsilon_r}{S_u} \qquad (3.15)$$

Equation 3.15 defines a second straight line relationship between the slope of the pressuremeter curve and the radial strain. The post-yield relationship is unique in that its slope is $1/S_u$, and it passes through the origin of the $d\varepsilon_r/d\sigma_r$ versus ε_r plot. Thus, the value of the undrained shear strength can be established and, since R_f/S_u is known, the parameter R_f can be defined.

Figure 3.12 shows hypothetical plots of $d\varepsilon_r/d\sigma_r$ versus ε_r for different values of R_f. Should R_f be 1.0, then the stress-strain curve corresponds to a true hyperbola and the data may be fitted by a single line of slope $1/S_u$, and intersection on the vertical axis of $1/2G_i$. If $R_f = 0$, then the data will plot parallel to the horizontal axis and the stress-strain curve will be linear with the same definition of G_i as for $R_f = 1.0$. However, since the stress-strain curve lies between a linear and true hyperbola, the data must be fitted by two straight lines; one for preyield conditions, as defined by Eq. 3.13; and one for approximating post-yield conditions, as defined by Eq. 3.15. The slope of the pre-yield line yields R_f/S_u, and that of the post-yield line approximately $1/S_u$. Thus, by measuring the slopes of the two straight lines and reading the intercept on the $d\varepsilon_r/d\sigma_r$ axis, G_i, S_u, and R_f may be determined.

To obtain the complete stress-strain curve using this method, the parameters G_i, S_u, and R_f are substituted into Eq. 3.11 to obtain $(\sigma_r\text{-}\sigma_\theta)/2$ values for any number of desired values of ε_r. Corresponding values of $(\sigma_1\text{-}\sigma_3)$ and ε_r may be determined using relationships described earlier.

The final step in the derivation involves the relationship for the lateral stress. This is relatively straightforward and is presented below.

Substituting $A = 1/G_i$, and $B = R_f/S_u$ and integrating Eq. 3.11,

$$\sigma_r = \frac{\ln(A + B\varepsilon_r)}{B} + K \quad \dots\dots\dots\dots \quad (3.16)$$

where, K = a constant. Now, at $x = 0$, $\sigma_r = \sigma_H$; thus from Eq. 3.16:

$$\sigma_h = \frac{\ln A}{B} + K \quad \dots\dots\dots\dots \quad (3.17)$$

Solving for K and substituting in Eq. 3.17 at the maximum mobilized shear stress:

$$\sigma_r = \frac{\ln\left(1 + \frac{B}{A}\varepsilon_r\right)}{B} + \sigma_H \quad \ldots\ldots \quad (3.18)$$

or, $$\sigma_h = \sigma_r - \frac{S_u}{R_f} \ln\left(1 + \frac{R_f}{S_u} 2G_i\varepsilon_r\right) \quad \ldots\ldots \quad (3.19)$$

It follows that σ_h may be calculated at other values of radial strain and mobilized shear stress to provide a check on the maximum value.

3.4.3 Results of Self-Boring Pressuremeter Tests

Self-boring pressuremeter tests were conducted at four depth levels (1.4 m, 2.4 m, 3.4 m and 4.4 m), one test at each level. All these tests were stress-controlled test; the diaphragm expansion rate used in these tests was 20 kPa/min (30 kPa/min for the test at the depth level 1.4 m). Each test was carried out with one unload-reload cycle. The rate of advance of the pressuremeter assembly was approximately 75 mm/min. A waiting period was observed, before the start of the test, to ensure that any small pore pressures developed by the advance of the probe were dissipated. This waiting period ranged between 1 hour to 3 hours.

During the progress of the tests, data were recorded by a personal computer on its harddisk. The correction factor for the diaphragm expansion was 40 kPa. The stress-strain curves (radial stress versus radial strain) of these tests are shown in Fig. 3.13. The diaphragm correction has not been applied in these curves. The interpreted soil parameters using two methods of interpretation are shown in Table 3.1. The diaphragm correction has been applied to results in Table 3.1.

3.4.4 Discussion of Self-Boring Pressuremeter Test Results

Estimation of initial shear modulus, G_i, using Denby and Clough (1980) method, was possible only for the test depth of 1.4 m where a straight line could be drawn with the initial few points on the $d\varepsilon_r/d\sigma_r$ versus ε_r curve. Initial points for other tests, on similar curves, were random and no reasonable straight line could be drawn; consequently, it was not possible to determine G_i values from this plot. Therefore, it can be inferred that the Denby-Clough method may not be always used to determine G_i for weathered crusts (Table 3.1).

Undrained shear strengths as shown in Table 3.1 were not obtained by applying the Denby-Clough method exactly. The method has been slightly modified by the author since $d\varepsilon_r/d\sigma_r$ versus ε_r curves were different to those expected by this method. The Denby-Clough method stated that the later part of the $d\varepsilon_r/d\sigma_r$ versus ε_r curve would be a straight line, and this straight line should pass through the origin as shown in Fig. 3.12. However, this is not the case; this later part of the plot is a curved line which concaves downward for which Denby-Clough method could not be used. However, with the concept and the theoretical basis of the Denby-Clough method, the tangent to the $d\varepsilon_r/d\sigma_r$ - ε_r curve will pass through the origin, with the slope $1/S_u$. The undrained shear strengths of Table 3.1 were obtained from this slope of $1/S_u$. The theoretical background of how this slope is $1/S_u$ is discussed in detail by Denby and Clough (1980). Tanaka (1986) used Gibson and Anderson (1961) method to estimate S_u from pressuremeter tests, and these S_u values are higher and more scatter than the same from the present study.

The values of *in situ* horizontal stress, σ_{h0}', were determined from the visual inspection of stress-strain curve, where the initial "lift-off" pressure (Ghionna et al. 1985) has been considered as the measurement of σ_{h0}'. The shear modulus, G_{ur} was determined from the average slope of unloading-reloading curve.

3.5 Piezocone Test

3.5.1 Introduction

The cone penetration test was developed from the idea of pushing a rod vertically into the ground. The force required to advance the rod was interpreted as the strength of the soil. The original and still commonly used static cone penetration test is known as the Dutch cone test. This basic cone penetration test has been used for many years as a standard tool in site investigation, especially, for establishing quickly and cheaply the soil profile at a particular site. It has grown in importance and acceptance with the recent special needs of offshore site investigation associated with oil exploration.

The first attempts to record porewater pressures during penetration of a probe into the ground were reported separately by Torstensson (1975), and Wissa et al. (1975). These pioneering works showed the clear promise of incorporating a pore pressure transducer in a cone penetrometer so that continuous profiles of pore pressures could be obtained at the same time as point resistance of the cone and measurement of sleeve friction. The resulting instrument has become known as the piezocone.

The Piezocone Apparatus:

The development of the piezocone since its invention has been rapid, with a variety of instruments on the market with most applications being offshore. Nearly all instruments have been built to the standard dimensions of the Dutch cone (60° apex angle and base area 1000 mm²), but the position of the pore pressure transducer has not been standardized. Porous filters are placed either on the cone tip (Fig.3.14a) or immediately above the cone tip (Fig.3.14b). The position has a marked influence on the magnitude of the observations (Wroth 1984). This requires both a standardization of equipment, test procedures and interpretation as well as a clear understanding of soil behaviour and the excess pore pressures generated during shear.

3.5.2 Interpretation of Piezocone Test Data

The interpretation of piezocone tests is done mainly by two methods: (i) the bearing capacity theory using classical plasticity approach (Terzaghi 1943; Meyerhof 1951; Caquot and Kerisel 1956; de Beer 1977; Robertson and Campanella 1983; among others), and, (ii) the cavity expansion theory combined with classical plasticity (Gibson 1950; Meyerhof 1951; Skempton 1951; Ladanyi 1967 and 1972; Vesic 1972 and 1975; Baligh 1975; and Konrad and Law 1987a and 1987b; among others). In the first approach, the basic bearing capacity theory has been used to determine the bearing capacity using shear strength parameters c and ϕ. The basic bearing capacity equation is

$$q_{ult} = cN_c + qN_q + \tfrac{1}{2}B\gamma N_\gamma \qquad (3.20)$$

where,

B = width of foundation

γ = unit weight of soil
q = surcharge (overburden pressure) at foundation level
N_c, N_q, N_γ = bearing capacity factors

For saturated clays, the strength parameters will be in terms of undrained condition and are denoted by S_u (or C_u) and ϕ_u. For fully saturated clays, $\phi_u = 0$ giving $N_\gamma = 0$ and $N_q = 1$. In this context q_{ult} may be written as q_c (cone resistance), and the Eq. 3.20 can be rewritten as:

$$q_c = S_u N_k + \gamma Z$$

where, N_k = cone factor, used instead of bearing capacity factor, N_c.

$$\text{or,} \quad S_u = \frac{q_c - \gamma Z}{N_k} \qquad \text{(3.21)}$$

The undrained shear strength can be estimated from piezocone test using Eq. 3.21. q_c is obtained from piezocone test and γZ can be obtained easily if the bulk unit weight of the soil at various depths are known. There are a number of direct and indirect methods by which N_k can be determined. The commonly used empirical method of the determination of N_k is to obtain this factor from the S_u back-calculated from a field failure or from the S_u obtained from other well accepted laboratory or field tests. Table 3.2 shows a number of other methods by which the cone factor N_k can be determined. The interpretation method of S_u by Konrad and Law (1987) does not require the determination of N_k. S_u is directly determined by this method if the soil parameters ϕ', θ, M and I_R (see Table 3.2 for definitions of these parameters) are known. In this study, three methods (Vesic 1975; de Beer 1977; and Konrad and Law 1987) have been used to determine and compare the values of S_u. Detailed discussions of these three methods can be obtained from the respective publications.

3.5.3 Results of Piezocone Test

The piezocone test was performed by hydraulically pushing a standard size conical tip, mounted on a cylindrical rod, into the soil. The conical tip had an apex angle of 60° with a projected base area of 1000 mm^2. A friction sleeve, placed above the cone tip, having the same outside diameter as the tip base with a cylindrical area of 15000 mm^2, measured the local shear resistance (local friction) of the soil acting on the sleeve. The porous stone, for the purpose of pore water pressure measurement, was located between the cone tip and the friction sleeve. The tip resistance (q_c), sleeve friction (f_s), pore water pressure (u), and depth of penetration were measured as the probe was pushed into the soil at a rate of 10 mm/sec. These values were recorded continuously and stored on a computer disk for subsequent interpretation.

The equivalent SPT, the soil material type and the sensitivity (S_t) determined from the piezocone tests are shown in Table 3.3. These properties are determined from the Technica CPT Soil Classification Chart (Fig. 3.15) which was originally developed by Robertson and Campanella (1983), and slightly modified by The Technica Ltd. The sensitivity was calculated from the following empirical equation as suggested by Robertson and Campanella (1983):

$$\text{Sensitivity } (S_t) = \frac{10}{FR(\%)} \qquad \text{(3.22)}$$

The corrected tip resistance (q_c) was determined from the following equation:

$$q_c = q_{c(measured)} + \alpha u \qquad \text{(3.23)}$$

Where,

$\alpha = 0.34$ (from instrument calibration),

u = generated or operational pore water pressure

Interpreted results of two series of piezocone test are shown in Fig. 3.16. Pore water pressure started generating at a depth of approximately 1.2 m (Fig. 3.16a). It should be mentioned that the groundwater table in the test holes was observed at approximately 0.80 m. The test results are shown to a depth of 3.50 m, although one of the tests went down to 21 m until the probe hit the hard layer. This deeper test (for which results are not presented in this thesis) showed higher generated pore water pressure than the tip resistance which may be for the reason that the natural water content is higher than the liquid limit. There were some other types of tests conducted at the same site by other investigators (Haile, 1977 and Tanaka, 1986), but this is the first attempt with the piezocone test. Therefore, more piezocone tests may be required to investigate this peculiarity. No attempt of studying this aspect has been made in this research since the purpose of this programme is to study the crust only.

3.5.4 Discussion of Piezocone Test Results

Although there are a number of methods (Table 3.2) available to estimate the S_u of a soil from piezocone tests, only three methods (Fig. 3.16d) have been used in this study. The complete analysis of CPTU test by using all the available methods is beyond the scope of this research. However, further research is encouraged in this direction. Among the three methods of analysis, the method proposed by Konrad and Law (1987) gave closest values of S_u when these values are compared with those of laboratory tests and case studies. The discrepancy among these three interpretation techniques is higher within the crust, whereas the S_u values from the three methods for below the crust are close to each other and comparable (Fig. 3.16d).

Determination of rigidity index I_R was essential, in this study, to obtain the values of cone factor N_K for methods in Table 3.2. These values of I_R were obtained from self-boring pressuremeter tests at various depths. Finally, I_R values were used (via N_K) in the evaluation of undrained shear strengths, using Eq. 3.21, for respective depth levels.

3.6 Comparison of Field Test Results

3.6.1 Comparison of Undrained Shear Strengths, S_u

A comparison of the values of undrained shear strengths, obtained from all the four *in situ* testing methods, is given in Fig. 3.17. The range of scatter of measurements in the overconsolidated crust, in contrast to that for the normally consolidated to slightly overconsolidated soil below the depth of 3.0 m, is remarkable. Within the crust (i.e., above the depth of approximately 3.0 m), the field vane test yields the highest values of S_u, whereas the dilatometer test yields the lowest. A detailed discussion of the reasons for high values of $S_u(FV)$ and the possibility of reinterpretation of FV test data is given in Chapter 4.

The value of $S_u(DMT)$ is a direct function of *in situ* effective vertical stress σ_{v0}', as shown in Eq. 3.8. This direct correlation between $S_u(DMT)$ and σ_{v0}' may be the reason for low $S_u(DMT)$ since the value of σ_{v0}' in the shallow crust is low. Although the values of $S_u(DMT)$ are low when compared to other *in situ* tests, they compare well with those obtained from laboratory tests and back-analyzed results as discussed in Chapter 9.

Although three methods were used in the interpretation of piezocone test results, only the values of $S_u(CPTU)$ obtained by Konrad and Law (1987) method are shown in Fig. 3.17 since this method provides reasonable values of S_u. The piezocone test also provides high S_u values within the crust which are comparable to FV test results. The high values of $S_u(CPTU)$ within the crust could be due to the high anisotropic *in situ* state of stress where σ_{h0}' is greater than σ_{v0}'. Further research may be undertaken to study this aspect to develop a new interpretation technique of piezocone data for a soil with anisotropic *in situ* state of stress, especially, where $K_0>1$.

It is interesting to note that, although the scatter of values of S_u obtained by different *in situ* methods within the crust is high, this scatter below the crust is low and comparable to each other.

3.6.2 Comparison of Deformation Modulus

The estimation of deformation modulus was possible by two methods, DMT and SBP, only. The modulus for SBP was calculated by multiplying the initial shear modulus, obtained from the initial tangent on the reloading part of the unloading-reloading stress-strain curve, by three. The constrained modulus M, obtained from DMT test is applicable for drained loading only (Schmertmann 1986), and, the modulus obtained from the SBP test is applicable for undrained loading only (Mair and Wood 1987). Therefore, these moduli are not precisely comparable. However, it is understood that the moduli values of undrained tests are generally higher than those from the drained tests. This was also observed in this study as shown in Fig. 3.18.

3.6.2 Comparison of Sensitivity, S_t

Two methods (FV and CPTU), for which interpretation techniques are available, were used to estimate the sensitivity of the crust. A comparison of S_t values obtained from piezocone tests using Eq. 3.22 and those obtained from field vane tests is shown in Fig. 3.19. The values of sensitivity obtained from the piezocone test are consistently lower than those from the field vane test. The sensitivity values from piezocone tests are approximately 50% of those from FV tests. From this study it can be concluded that the Eq. 3.22, developed by Robertson and Campanella (1983), cannot always be used for a crust.

3.6.3 Comparison of Coefficient of *in situ* Lateral Earth Pressure, K_0

Estimation of K_0 was possible only by two methods, dilatometer and self-boring pressuremeter, out of the four *in situ* methods used in this research. A comparison of values of K_0 obtained from dilatometer tests, using Eq. 3.7, and those obtained from self-boring pressuremeter tests is shown in Fig. 3.20. From Fig. 3.20, it is obvious that the values of K_0 obtained from the SBP test are significantly higher than those obtained from the DMT test. In this context, it should be mentioned that the K_0 values obtained from the DMT test compares well with the laboratory method (Garga and Khan 1991) as well as with the empirical methods (Brooker and Ireland 1965; and Mayne and Kulhawy 1982) available for the crust. A detailed discussion, on why K_0 is high for SBP and on these laboratory and empirical methods of K_0 evaluation, is provided in Chapter 7.

Table 3.1. Soil parameters interpreted from self-boring pressuremeter test data.

Depth (m)	Ghionna et al. (1985) σ'_{H0} (kPa)	K_0	Denby and Clough (1980) S_u (kPa)	G_i (MPa)	G_{ur} (MPa)
1.4	85	4.0	52.5	5.0	7.58
2.4	70	2.31	60.0	-	8.76
3.4	75	1.90	32.8	-	2.34
4.4	90	1.85	36.8	-	2.78

Table 3.2. Theoretical bearing capacity factor for deep circular foundations (after Konrad and Law 1987).

N_c ($\phi = 0$)	σ_i	Solution class	Remarks	Reference
7.41	σ_{vo}	1		Terzaghi (1943)
7.0	σ_{vo}	1		Caquot and Kerisel (1956)
9.34	σ_{vo}	1	Smooth base	Meyerhof (1951)
9.74	σ_{vo}	1	Rough base	
9.94	σ_{vo}	1		de Beer (1977)
$\frac{4}{3}\left[1 + \ln \frac{E_i}{3S_u}\right] + 1$	σ_{vo}	2	SCE E_i: Initial tangent modulus	Meyerhof (1951)
$\frac{4}{3}\left[1 + \ln \frac{E_s}{S_u}\right] + 1$	σ_{vo}	2	SCE E_s: secant modulus at 50% failure stress	Skempton (1951)
$\frac{4}{3}\left[1 + \ln \frac{E_s}{3S_u}\right] + \cot\theta$	σ_{vo}	2	SCE	Gibson (1950)
$\frac{4}{3}\left[1 + \ln \frac{E_s}{S_u}\right] + \cot\theta$	σ_{vo}	2	SCE, finite strain theory	Gibson (1950)
$\frac{4}{3}[1 + \ln I_R]$	σ_{vo}	2	SCE	Vesic (1972)
$\frac{4}{3}[1 + \ln I_R] + 2.57$	σ_o	3	SCE	Vesic (1975)
$[1 + \ln I_R] + 11$	σ_{ho}	3	CCE	Baligh (1975)
$\frac{S_a}{S_u} + \frac{4}{3}\frac{S_r}{S_u}\left[1 + \ln \frac{E_r}{3S_{ur}}\right] + \frac{4}{3}$	σ_{vo}	4	Trilinear stress–strain relationship	Ladanyi (1967)
$\left[\frac{E_u/S_u - E_r/S_{ur} \cdot S_{ur}/S_u}{E_u/S_u - E_r/S_{ur}}\right] \ln \frac{E_u S_{ur}}{S_u E_r}$				

NOTE: SCE: spherical cavity expansion; CCE: cylindrical cavity expansion; I_R: rigidity index $= G_u/S_u = E_u/3S_u$; σ_o: mean normal total stress $= (\sigma_{vo} + 2\sigma_{ho})/3$; θ: semiapex angle.

Table 3.3: Piezocone Tests Results from Technica Soil Classification Chart.

Depth (m)	Tip Resistance (kPa)	Sleeve Friction (kPa)	*FR(%)*	Material Type	Equivalent SPT	S_t
0.25	1800	110.0	6.0	Clay	18	1.7
0.50	2200	200.0	9.0	Clay	22	1.1
0.75	1200	110.0	9.0	Clay	12	1.1
1.00	1000	62.0	6.0	Clay	10	1.7
1.25	900	50.0	5.0	Clay	9	2.0
1.50	780	42.0	6.0	Clay	8	1.7
1.75	870	22.0	3.0	Silty clay to clay	6	3.3
2.00	845	26.0	3.0	Silty clay to clay	6	3.3
2.25	630	16.0	2.9	Silty clay to clay	4	3.5
2.50	556	15.0	3.5	Silty clay to clay	4	2.9
2.75	543	12.0	2.5	Silty clay to clay	4	4.0
3.00	446	4.6	2.0	Silty clay to clay	3	5.0
3.25	445	4.7	1.5	Silty clay to clay	3	6.7

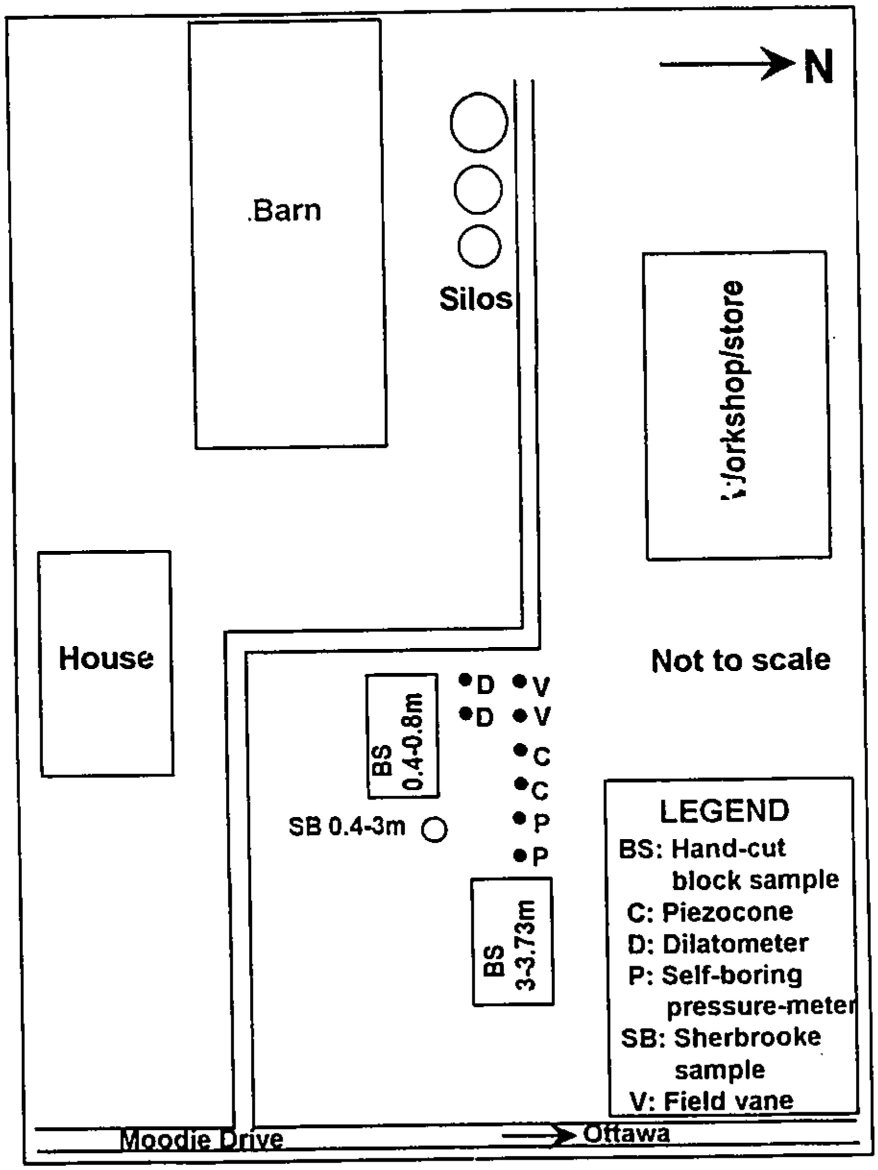

FIG. 3.1. Site plan of Fraser Farm showing location of test boreholes and collected samples.

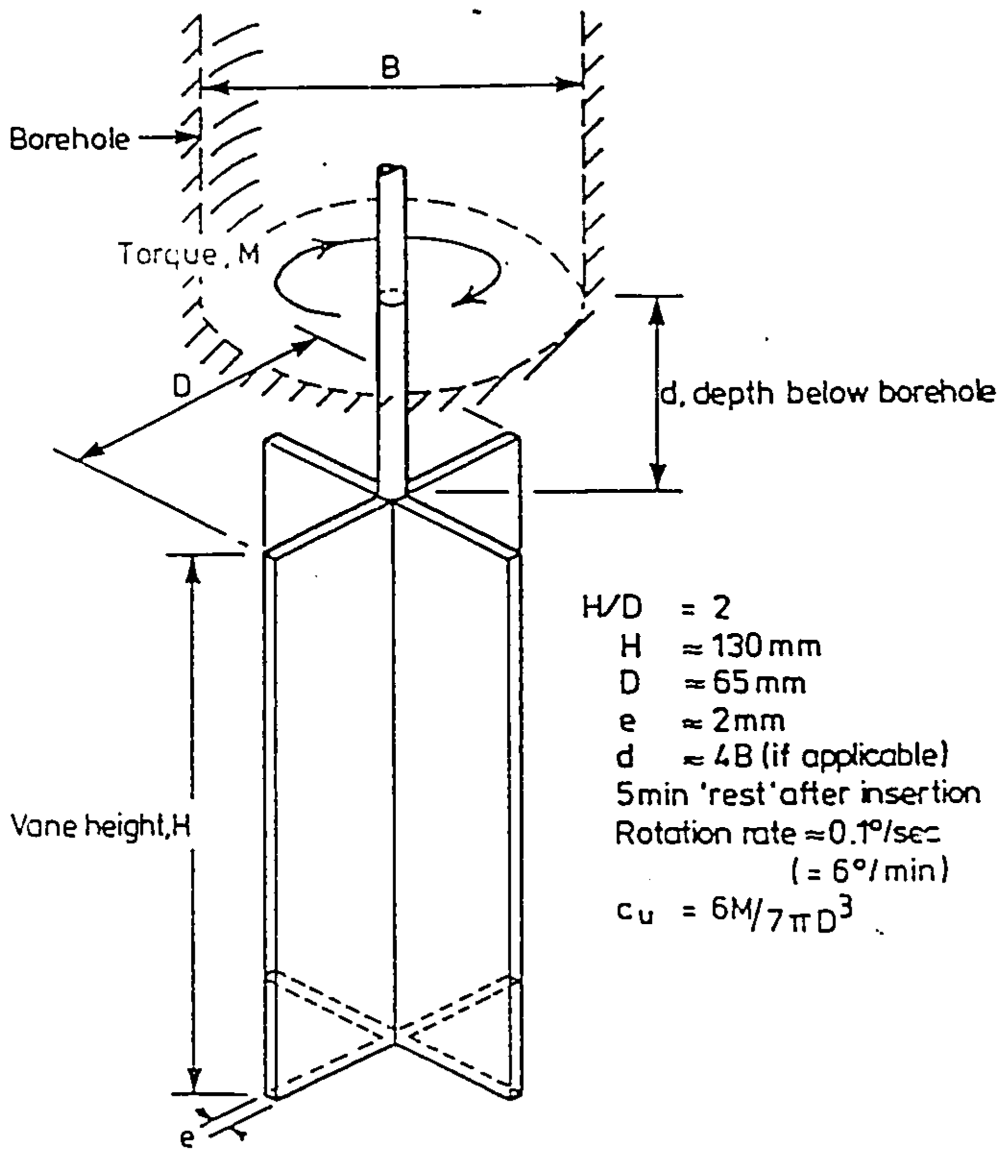

Fig. 3.2. The field vane apparatus (after Chandler 1988).

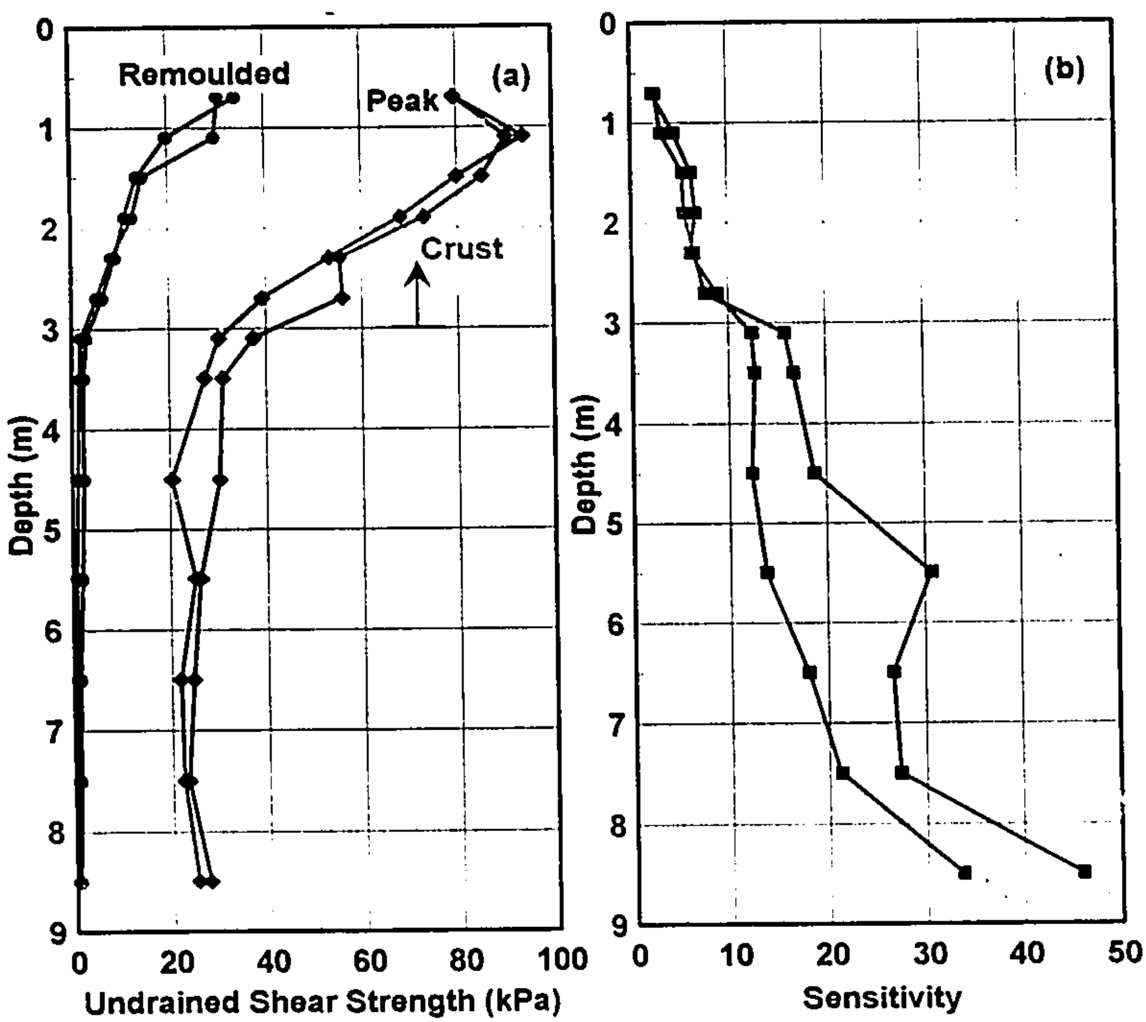

FIG. 3.3. Conventionally analyzed field vane test results.

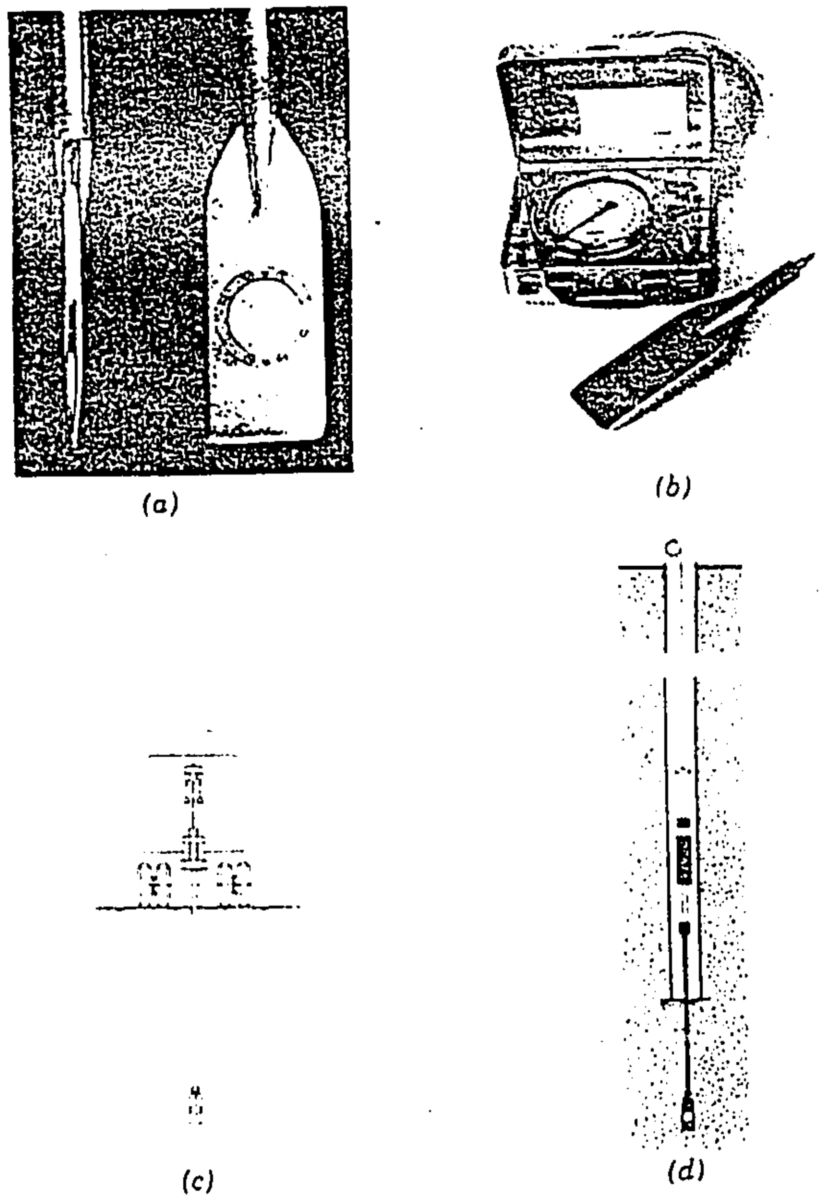

Fig. 3.4 The dilatometer apparatus (after Marchetti 1980): (a) side view and front view; (b) blade, control unit and cable; (c) dilatometer being jacked into ground; (d) dilatometer being driven by down-the-hole wireline hammer.

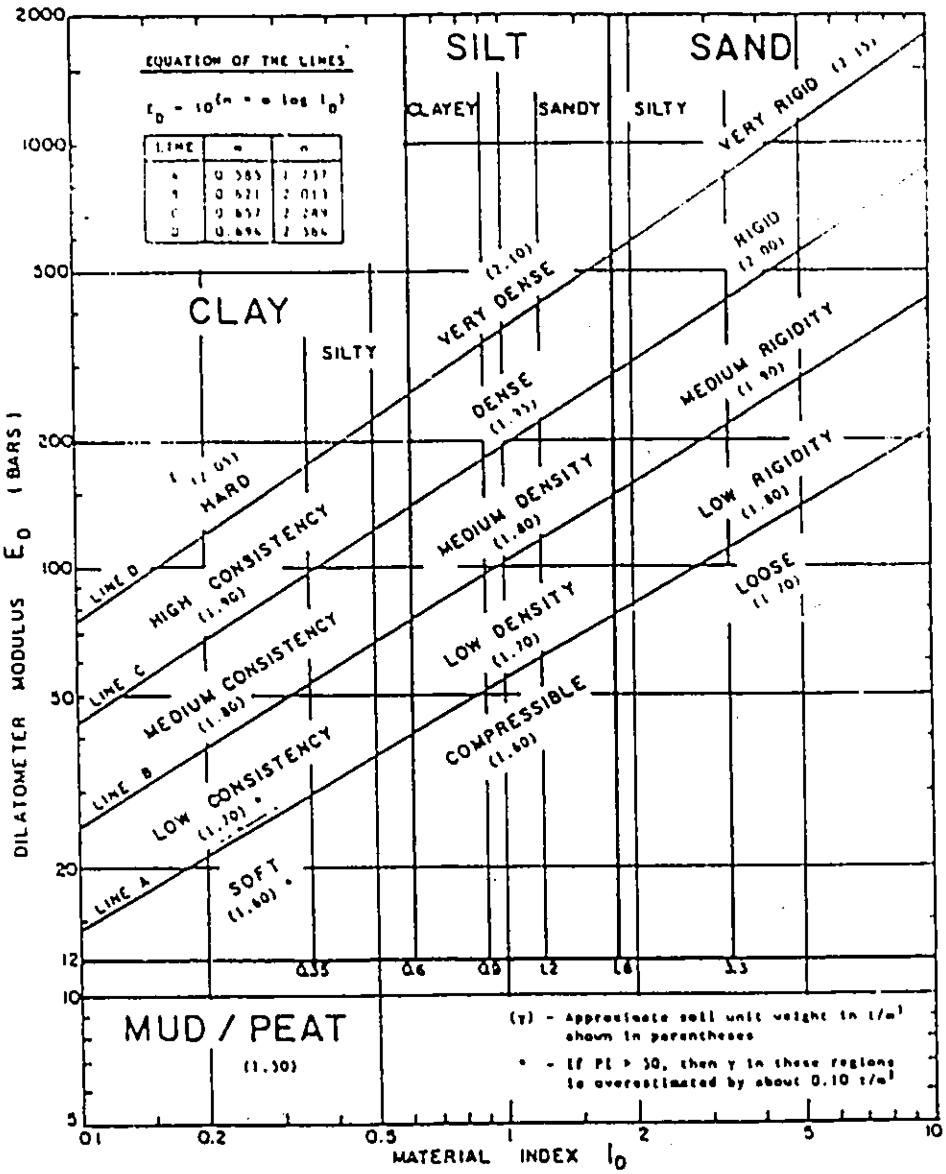

Fig. 3.5. Chart for the evaluation of the unit weight of a soil, and for the soil description (after Schmertmann 1986).

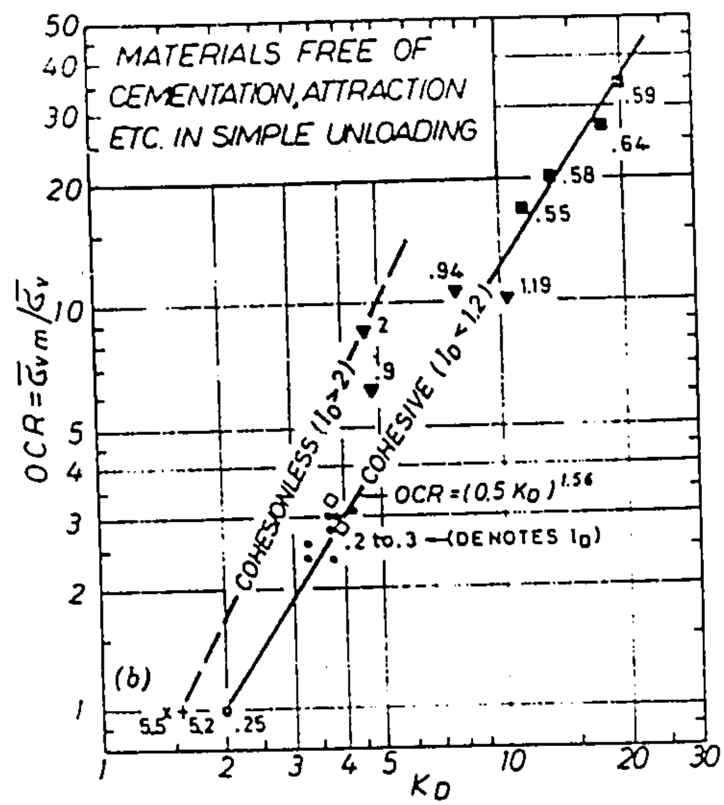

Fig. 3.6. Correlation between OCR and K_D (after Marchetti 1980).

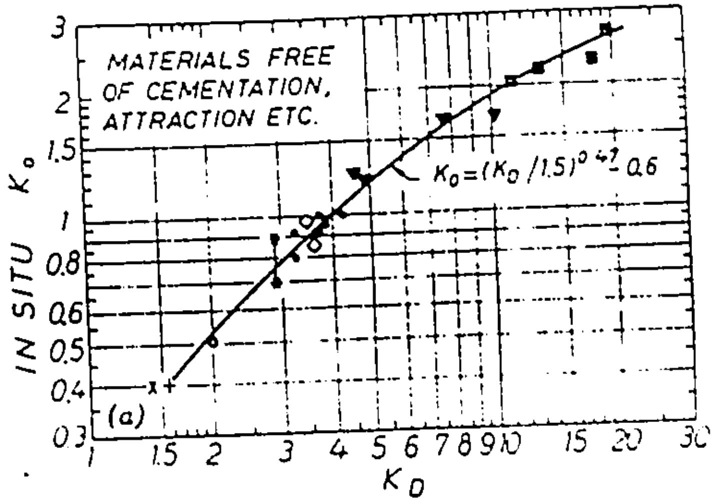

Fig. 3.7. Correlation between K_0 and K_D (after Marchetti 1980).

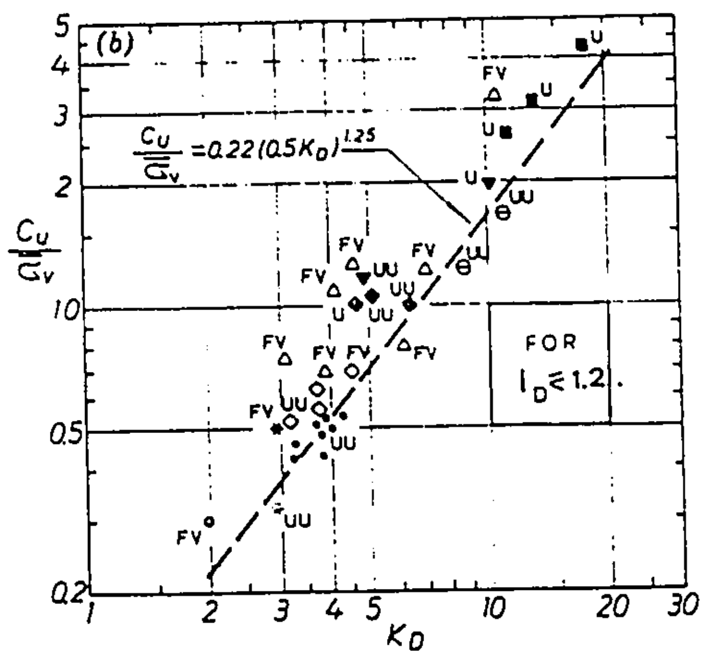

Fig. 3.8. Correlation between S_u/σ_{v0}' and K_0 (after Marchetti 1980).

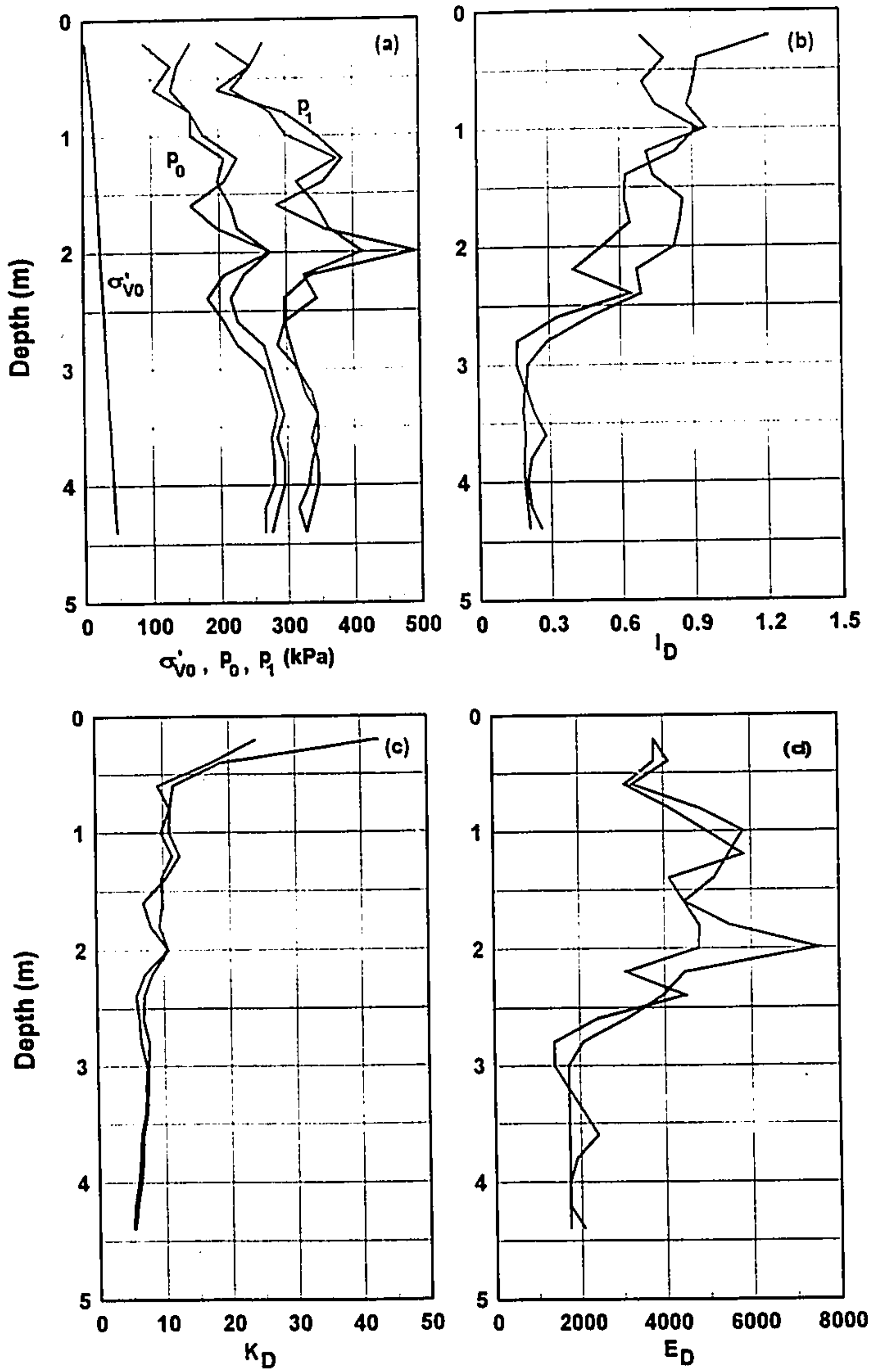

FIG. 3.9. Results from dilatometer test (continued to next page).

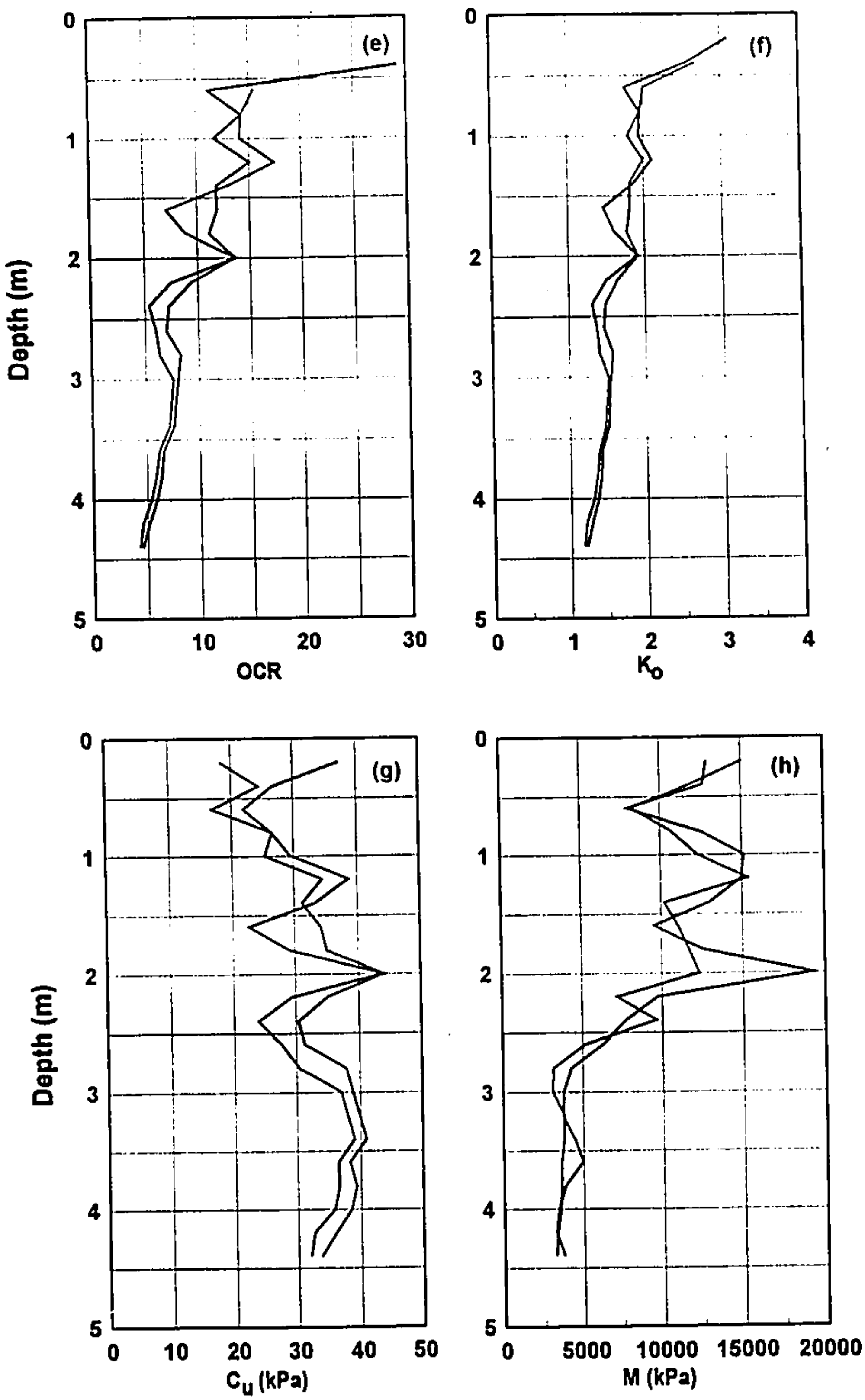

FIG. 3.9. Results from dilatometer test (continued from previous page).

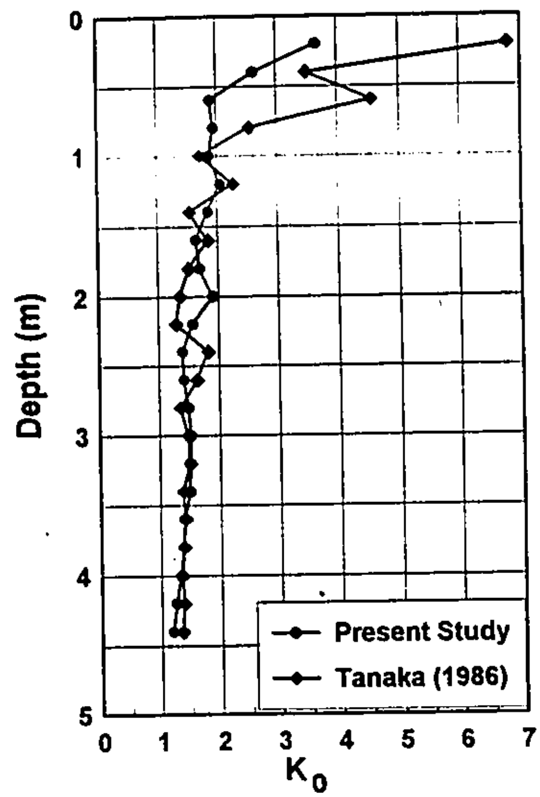

Fig. 3.10. Comparison of K_0 values between present study and Tanaka's (1986) study.

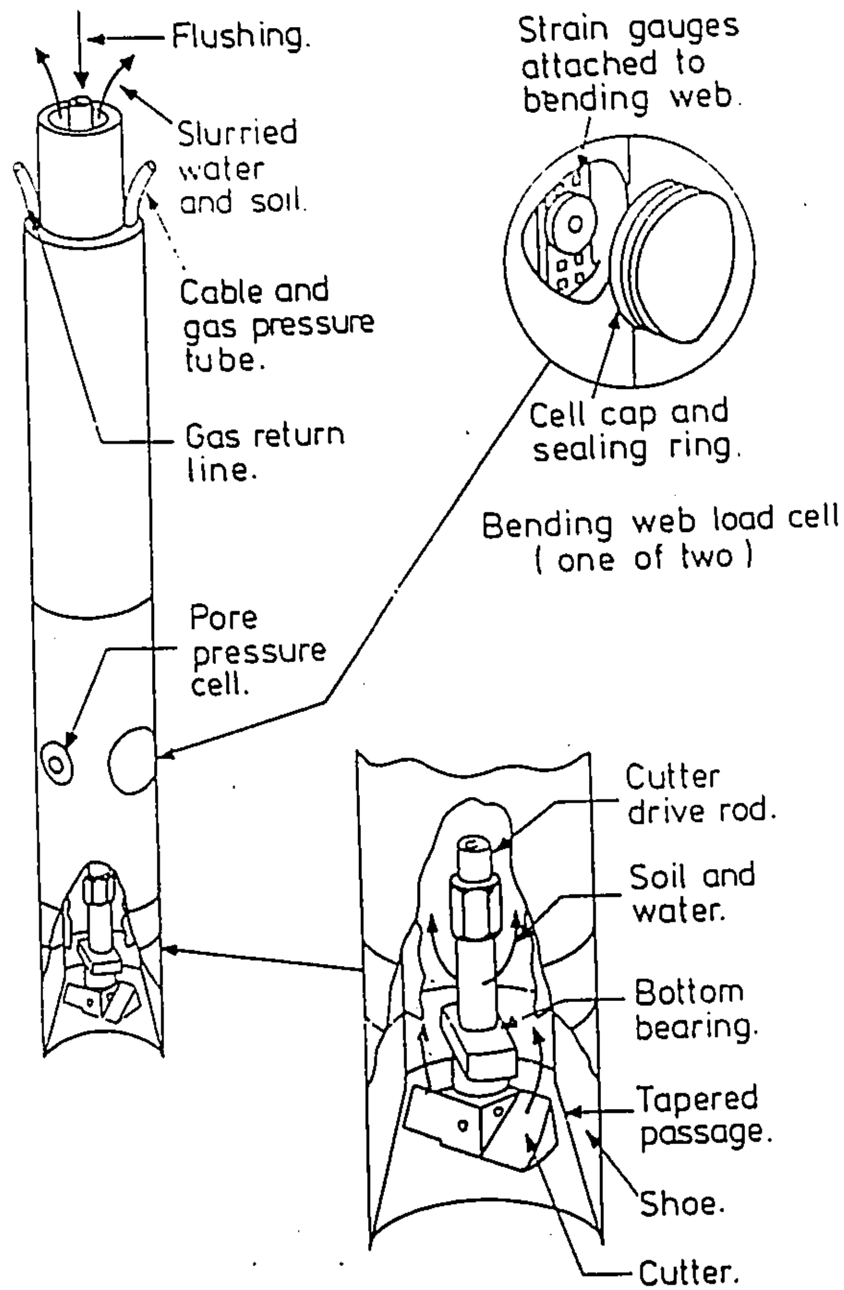

Fig. 3.11. Details of self-boring pressuremeter apparatus (after Windle and Wroth 1977).

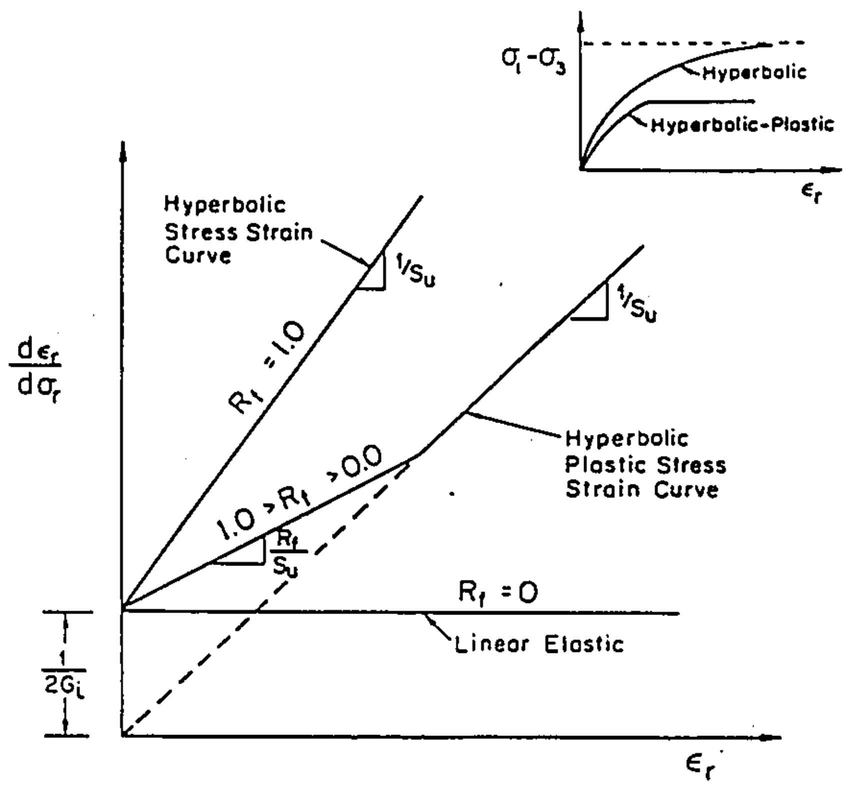

Fig. 3.12. Transformed plots of pressuremeter curves for hypothetical stress-strain curve (after Denby and Clough 1980).

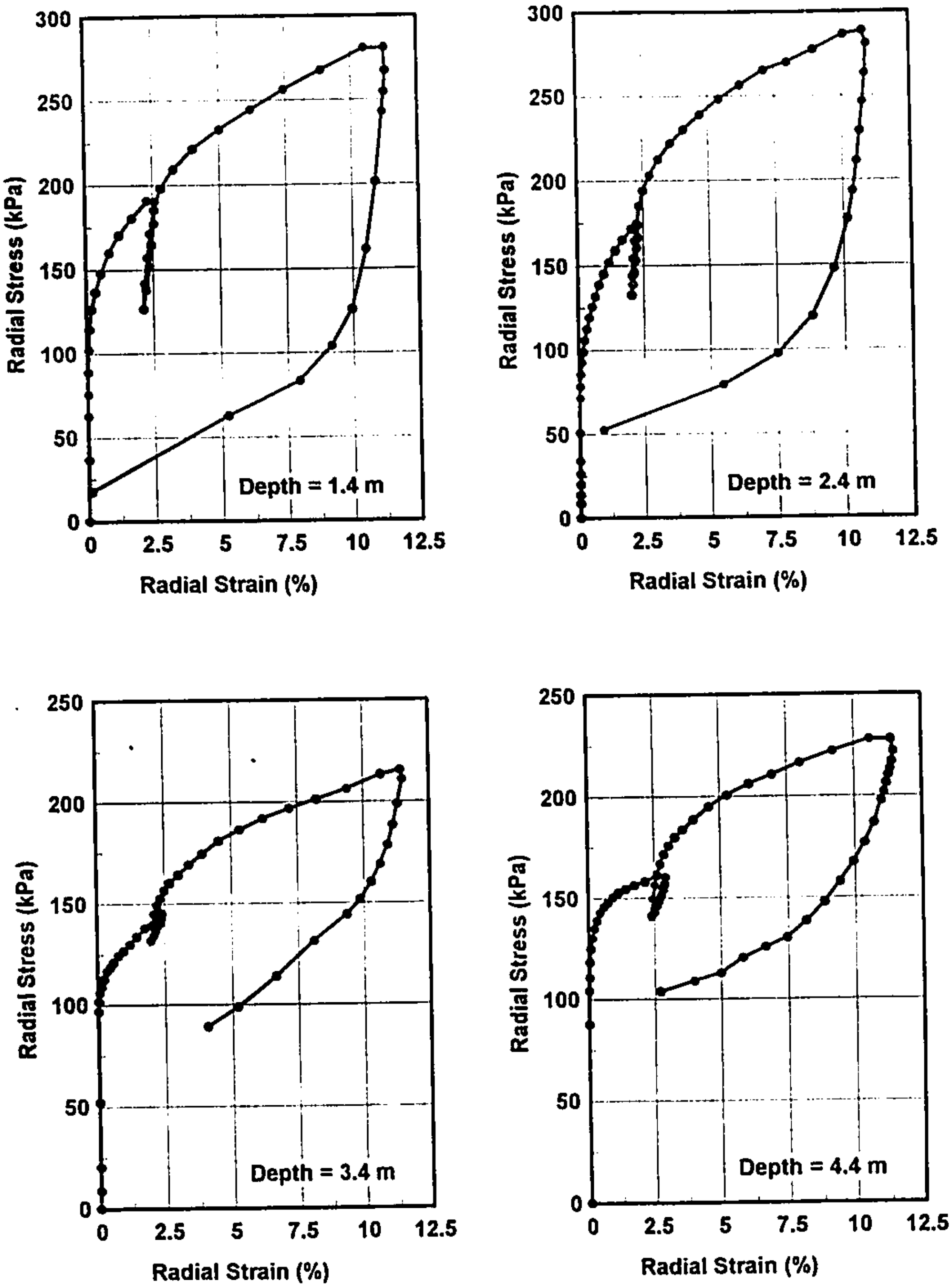

Fig. 3.13 Self-boring pressuremeter test results.

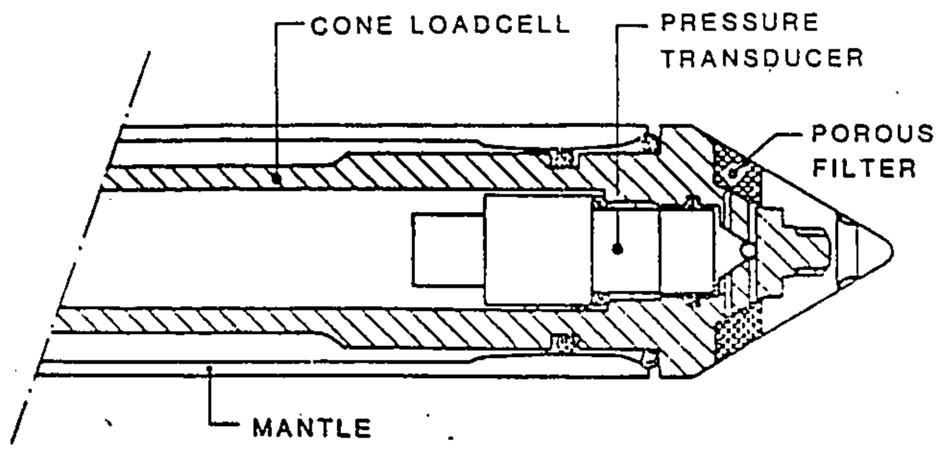

(a) FUGRO PORE PRESSURE TIP F5CW
(After Zuidberg et al, 1982)

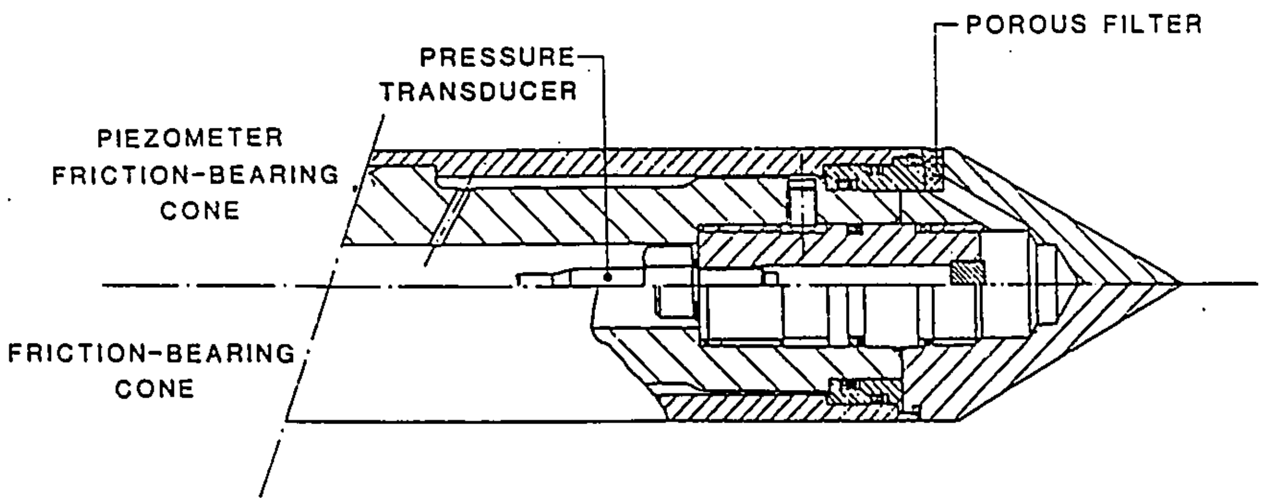

(b) HOGENTOGLER/GMF CONE

Fig. 3.14. The piezocone apparatus showing the positions of porous filters: (a) porous filter on the cone tip (Fugro type) and (b) porous filter immediately above the cone tip (Hogentogler/GMF type).

Technica CPT Soil Classification Chart

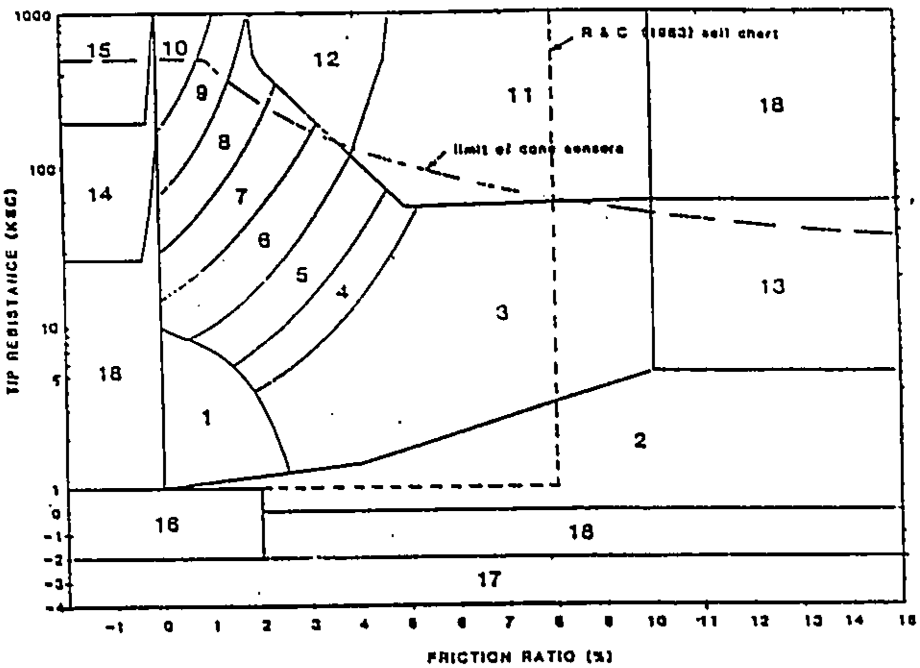

Zone Number	SPT q_c/N	Soil Behaviour Type: Printout Name	Soil Behaviour Type: Plot Name
1	2	Sensitive fine grained	Sens. fines
2	1	Organic material*	Organic
3	1	Clay	Clay
4	1.5	Silty clay to clay	Silty clay
5	2	Clayey silt to silty clay	Clayey silt
6	2.5	Sandy silt to clayey silt	Silt
7	3	Silty sand to sandy silt	Sandy silt
8	4	Sand to silty sand	Silty sand
9	5	Sand	Sand
10	6	Gravelly sand to sand	Grav. sand
11	1.6+	Very stiff fine grained*	Stiff fines*
12	2	Sand to clayey sand*	Clayey sand*
13+	1	Plastic clay	Plastic clay
14+	5	Cobble	Cobble
15+	6	Boulder	Boulder
16+	–	Void	Void
17+	–	– No data –	No data
18+	–	– No soil correlation –	No correl

* over consolidated or cemented
\+ Technica extension

Notes:

1) Original soil chart is from Robertson & Campanella (1983).
2) Technica extensions to the R & C chart are based on extensive local experience with Midwestern soils.
3) Zone 17 "– Bad data –" extends for all TIP values of -2 ksc and below.
4) All other areas not shown on the soil chart are Zone 18 "– No soil correlation –".
5) Cone sensor limit corresponds to a maximum tip load of 500 ksc and a maximum friction load of 5 ksc.

FIG. 3.15. Technica soil behaviour types from CPT data

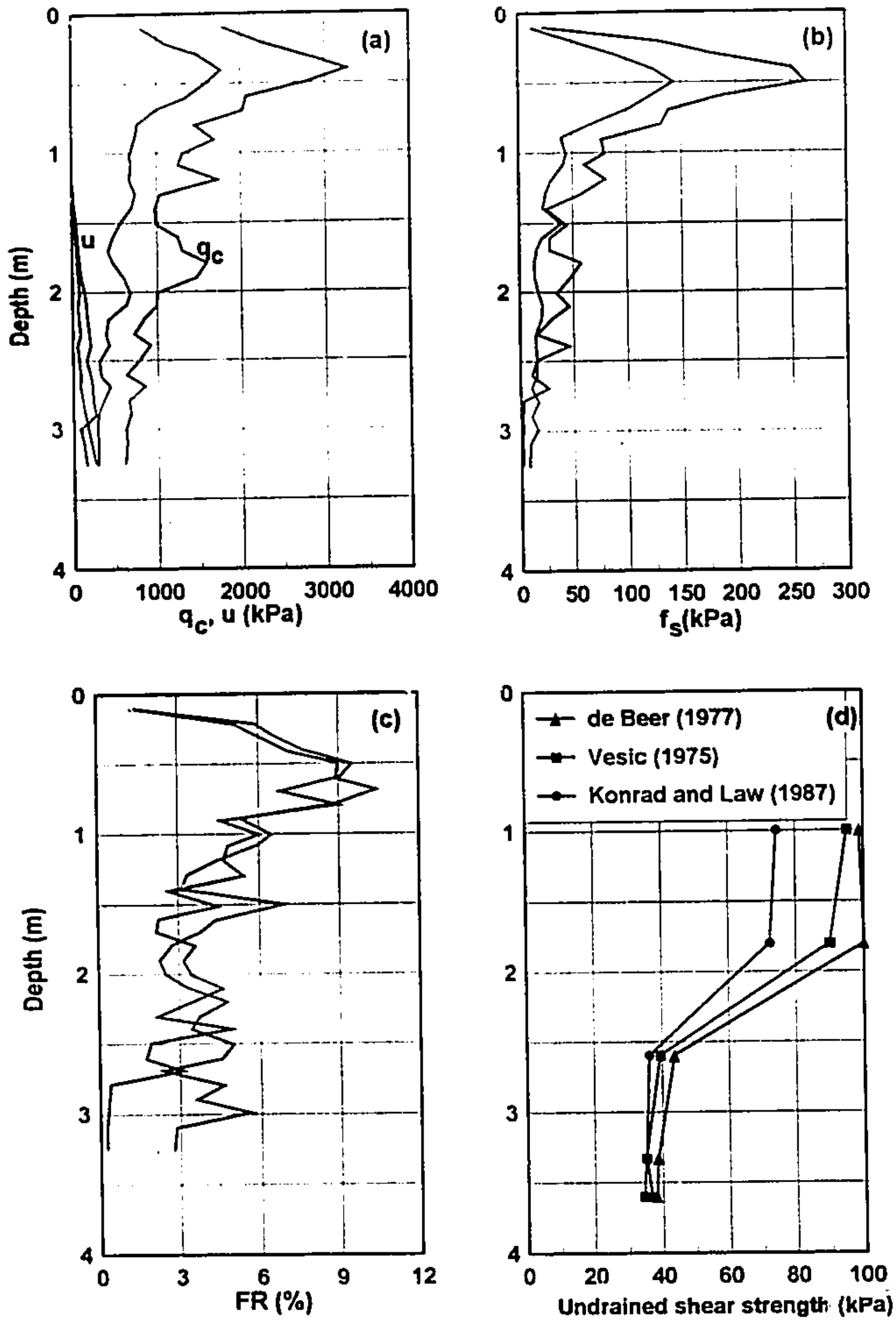

Fig. 3.16. Results from piezocone test.

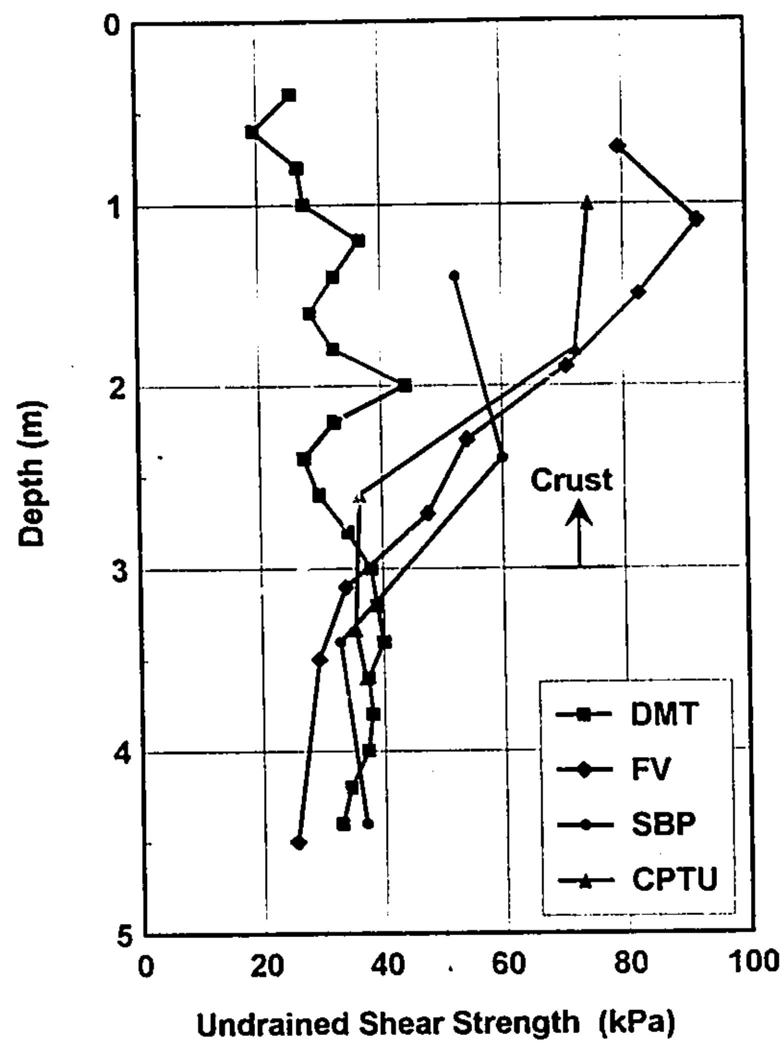

Fig. 3.17. Comparison of undrained shear strengths obtained from different *in situ* devices.

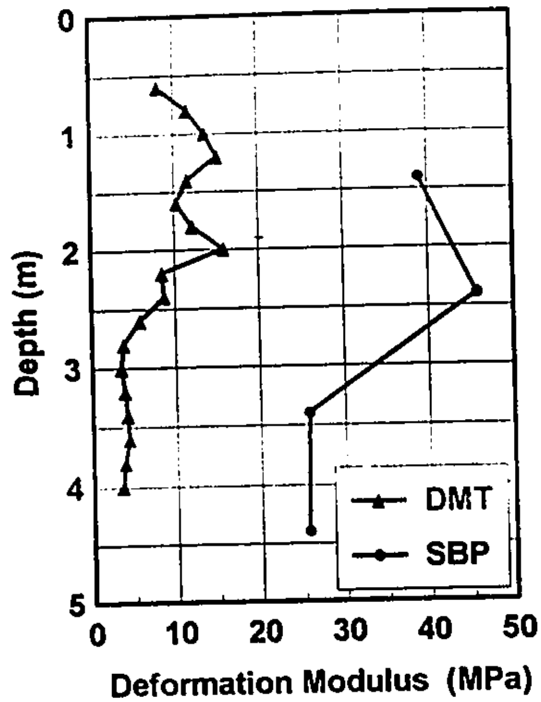

Fig. 3.18 Comparison of deformation moduli obtained from different *in situ* devices.

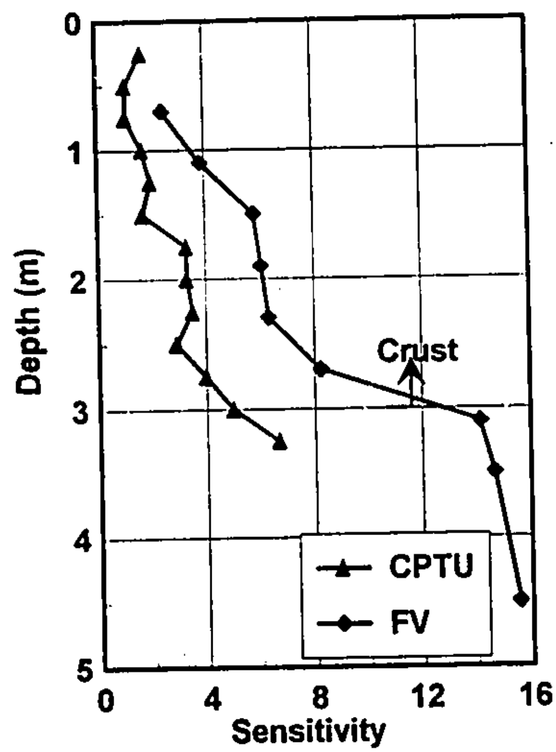

Fig. 3.19. Comparison of sensitivity obtained from different *in situ* devices.

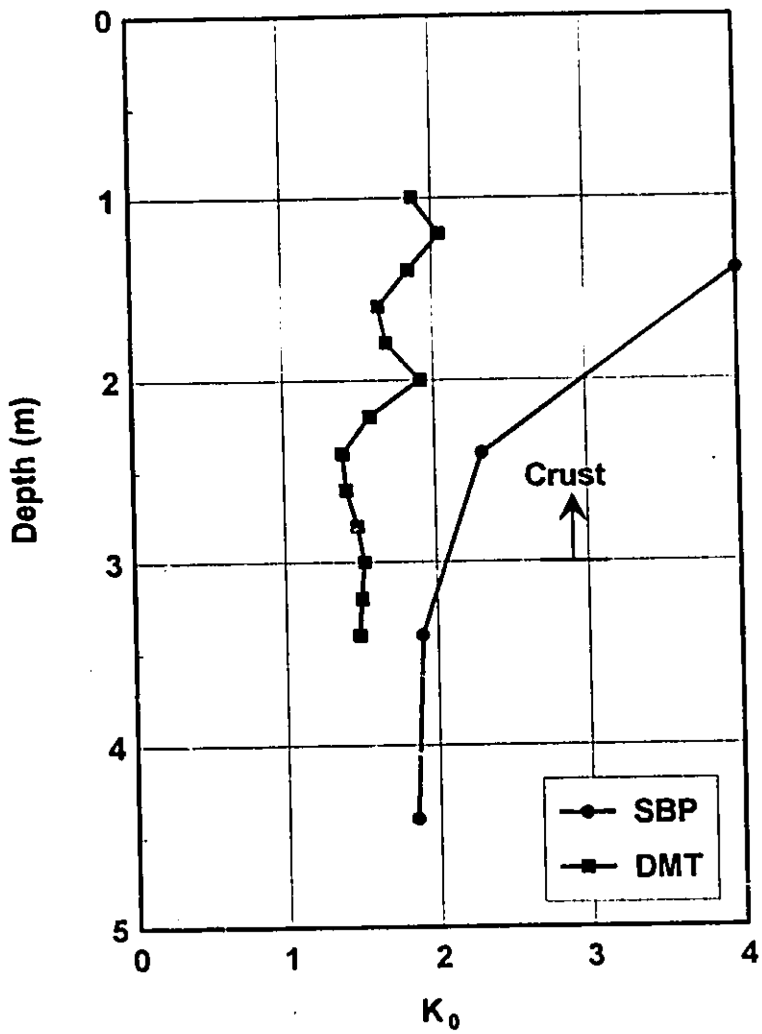

Fig. 3.20. Comparison of K_0 obtained from different *in situ* devices.

CHAPTER 4

DEVELOPMENT OF AN INTERPRETATION METHOD OF FIELD VANE STRENGTH

4.1 Introduction

The testing method and the interpretation method play an important role in the evaluation of the performance of any engineering structure. The estimation of the undrained shear strength (S_u) of overconsolidated soils such as the weathered clay crust overlying Champlain clay is important for the design of shallow foundations and embankments. *In-situ* vane shear tests and isotropically consolidated undrained triaxial tests have been conventionally used for this purpose. Contrasting test results from these two methods, low S_u obtained from triaxial tests and high S_u obtained from *in-situ* vane shear tests, motivated further research into this problem. Strength anisotropy, due to *in-situ* anisotropic state of stress and orientation of soil fabric during deposition, is believed to be the reason for these contrasting results. Improved testing and interpretation techniques for this type of anisotropic soils including the weathered clay crust have been proposed in this chapter.

Weathered crusts are generally heavily overconsolidated, with K_o values greater than unity. Undrained triaxial shear tests conducted to date by various researchers are either isotropically consolidated, or are anisotropically consolidated assuming K_o smaller than unity. Neither of these two methods represents the *in-situ* state of stress of a clay crust. Therefore, in this investigation, the undisturbed samples were reconsolidated anisotropically to the *in-situ* state of stress (K_o>1) before shearing undrained in the triaxial test. Direct shear tests on horizontal and vertical specimens consolidated to normal stresses equal to σ_{vo}' and σ_{ho}', respectively, were also conducted to investigate the strength anisotropy. Field vane tests have been re-interpreted in terms of this strength anisotropy. Although undrained shear strength on top and bottom horizontal planes (S_{uh}) obtained from these field vane tests within the crust provided comparable results with those from laboratory triaxial and direct shear tests which were reconsolidated to *in-situ* stresses, it underestimated S_u in the intact Champlain clay underlying the weathered crust.

A commonly used method of evaluation of undrained shear strength, for the analysis of embankments and shallow foundations, is the *in-situ* vane shear test. This method has been widely applied in *in-situ* testing because of its simple and economic nature despite a number of controversial corrections (Schmertmann 1975; Menzies 1976; Azzouz et al. 1983) related to the interpretation of test data. An important concern with the field vane (FV) shear test is whether S_u obtained from this test for overconsolidated soils can be used for foundation design. A number of researchers (Dascal et al. 1972; La Rochelle et al. 1974; Graham 1979; Lefebvre et al. 1987; for example) have observed significantly higher values of S_u from field vane tests than those obtained from conventional laboratory tests and back analyses of field failures. Dascal et al. (1972) conducted a full-scale embankment failure test, and the S_u obtained from the back analysis of this artificially failed embankment was compared with S_u(FV). S_u(FV) was found to be much higher than the back analyzed S_u even after reducing the S_u(FV) by using the correction factor proposed by Bjerrum (1972). The factor of safety determined from FV test was 1.6 instead of 1.0. At the same site, Lefebvre et al. (1987) conducted field plate loading and large shear box tests, and laboratory triaxial compression and extension tests to compare these results with those from the FV test. The FV test indicated much higher strength when compared with the above-mentioned field and laboratory tests. They have suggested that the FV test should not be used to determine the S_u of a clay crust, but only its thickness. These inconsistent observations challenge the validity of FV test for shallow foundations in the anisotropic, highly overconsolidated weathered crust.

Law (1979) observed that the S_u from triaxial-vane shear test is highly influenced by the applied horizontal stress. Becker et al. (1988) emphasized the importance of *in-situ* state of stress, and suggested that the *in-situ* field vane test data should be interpreted in terms of the *in-situ* horizontal and yield stresses. The purpose of this study is to further investigate this problem by considering the strength anisotropy in the crust induced by the anisotropic *in-situ* state of stress or the orientation of structured soil fabric. The FV test data have been re-interpreted in this study considering the coefficient of horizontal strength* ($K_s = S_{uh}/S_{uv}$), which varies from 0.49 at 1.0 m depth to 1.01 at a depth of 3.60 m. Triaxial tests on undisturbed samples isotropically consolidated to σ_{vo}' and anisotropically consolidated to *in-situ* stresses, and direct shear tests on horizontal and vertical undisturbed samples consolidated to σ_{vo}' and σ_{ho}', respectively, were also conducted to compare these results with the re-interpreted FV test results.

4.2 Interpretation of Field Vane Test Data

The undrained shear strength interpreted from field vane test data is influenced by the following factors which have been considered in the interpretation procedure described in this chapter.

(1) Shear stress distribution around the field vane,
(2) Strength anisotropy,
(3) Rate effect,
(4) Disturbance due to vane insertion.

(1) Shear stress distribution around the field vane

The conventional method of interpretation assumes that the shear stress distribution on both the cylindrical (vertical), and top and bottom (horizontal) surfaces is rectangular, i.e. uniform. The validity of this assumption has been critically re-examined by a number of researchers (Menzies and Mailey 1976; Donald et al. 1977; Menzies and Merrifield 1980; Wroth 1984; Griffiths and Lane 1990). Donald et al. (1977) have carried out a three-dimensional finite element analysis of the stress distribution around the vane in an elastic material, and have suggested the shear stress distribution along the shearing faces of a vane to be as shown in Fig. 4.1a. Menzies and Merrifield (1980) have confirmed this finding of non-linear stress distribution when they conducted some FV tests with instrumented vane blades. From these studies, the assumption of rectangular stress

* The undrained strength ratio K_s (= S_{uh}/S_{uv}) is termed as the coefficient of horizontal strength since the term "degree of strength anisotropy" or "strength anisotropy" is not meaningful when the value becomes less than 1.

distribution on the cylindrical vertical surface has been confirmed as reasonable, but the stress distributions on the horizontal (top and bottom) shear faces are far from the rectangular distribution as assumed in conventional interpretation. From these observations, Wroth (1984) obtained a relationship of shear stress distribution on the horizontal surfaces described by an expression of the form

$$\frac{S_{u(r)}}{S_{uh}} = \left(\frac{r}{D/2}\right)^n \qquad (4.1)$$

where

r = radial distance from the central axis on the horizontal surface

D= diameter of the cylinder circumscribed by the vane blades

$S_{u(r)}$ = undrained shear stress mobilized at a distance r

S_{uh} = maximum value of $S_{u(r)}$ on the horizontal surface

n = a coefficient that depends on the shape of the shear stress distribution, as shown in Table 4.1.

Thus the portion of the torque M_h carried by the horizontal surfaces is

$$M_h = 2\int_0^{D/2} S_{u(r)}\, 2\pi r^2\, dr$$

$$= 4\pi \int_0^{D/2} \frac{S_{uh}}{(D/2)^n} r^{n+2}\, dr$$

$$= \frac{\pi D^3 S_{uh}}{2(n+3)}$$

or

$$M_h = \frac{\pi D^3 S_{uh}}{p_n} \qquad (4.2)$$

where

p_n = $2(n+3)$ = shear stress distribution factor for horizontal shear planes as shown in Table 4.1.

The portion of the torque M_v provided by the vertical cylindrical surface is same as in the conventional analysis, i.e.

$$M_v = \pi DH \frac{D}{2} S_{uv}$$

where, H = height of the vane blades.

For a standard vane shape, $H/D = 2$, and,

$$M_v = \pi D^3 S_{uv} \tag{4.3}$$

The ratio of the torque carried by horizontal and vertical shear planes, from Eqs. 4.2 and 4.3, is

$$\frac{M_h}{M_v} = \frac{S_{uh}}{S_{uv}} \frac{1}{p_n}$$

or

$$\frac{M_h}{M_v} = \frac{K_s}{p_n} \tag{4.4}$$

where, $K_s = S_{uh}/S_{uv}$, the coefficient of horizontal undrained strength.

In conventional analysis, when the soil is considered isotropic (i.e. $K_s = 1$), and the shear stress distribution is considered uniform (i.e. $n = 0$ and $p_n = 6$)

$$\frac{M_h}{M_v} = \frac{1}{6} \tag{4.5}$$

From Menzies and Merrifield's data obtained from instrumented vane test, $n \approx 5$ and $p_n = 16$, giving

$$\frac{M_h}{M_v} = \frac{1}{16} \tag{4.6}$$

(2) Undrained strength anisotropy

Although the conventional analysis assumes that the shear strength of the soil being measured is isotropic (i.e. $S_{uv} = S_{uh}$), natural clays are generally anisotropic (Aas 1967; Richardson et al. 1975; Menzies and Mailey 1976; Garga 1988; Silvestri and Aubertin 1988).

Aas (1967) has conducted vane shear tests using rectangular vanes with different H/D ratio and diamond shaped vanes to determine the anisotropy of undrained shear strength along horizontal (top and bottom) and vertical (cylindrical side) shear planes. This series of tests was conducted for six sites of clays, varying from normally consolidated clay to overconsolidated clay. It was observed from this study that the value of K_s for normally consolidated clays was between 1.5 and 2.0; for overconsolidated clays K_s was less than 1, and that for slightly overconsolidated clays was close to 1. Aas concluded that in an overconsolidated clay where the *in-situ* effective horizontal stress is greater than the *in-situ* effective vertical stress, the coefficient of undrained horizontal strength should accordingly be less. Aas also concluded that the S_u(FV) is dependent on the *in-situ* effective normal stress on the failure plane. Similar studies were conducted by Richardson et al. (1975), and a value of K_s of less than 1 was obtained for the weathered crust as well as for the lower clay. The soil used was normally consolidated but showing quasi-preconsolidation characteristics; preconsolidation data were not provided in their paper. They found an average value of K_s of 0.67. The K_s value was less than 0.67 within the crust due to the overconsolidation effect. Laboratory vane borings in a vane-triaxial apparatus for isotropically and anisotropically consolidated samples showed that strength anisotropy could be expected for anisotropic state of stress (Kenney and Landva 1965; Law 1979).

Menzies and Mailey (1976) also measured strength anisotropy using diamond-shaped shear vanes with various apex angles (20°, 30°, 40°, 45°, 50°, 60° and 70°). The two clays used in this study, from North Sea and New Blind Yeo, showed high strength anisotropy giving K_s values of 0.55 and 0.53, respectively. Data on stress history of these clays have not been provided.

Silvestri and Aubertin (1988) suggested that there are mainly two reasons which explain strength anisotropy in a natural clay: (i) soil structure which results from particle orientation during sedimentation, and (ii) anisotropic *in-situ* state of stress which is related to stress history of the soil. In a natural soil, perfectly isotropic condition is not generally found. Therefore, for a realistic analysis, strength anisotropy should be incorporated in the interpretation of field vane test data where a major portion (greater than 86%) of torque is carried by the cylindrical vertical surface of a field vane.

The total torque carried by the vane, as obtained from Eqs. 4.2 and 4.3, is given by

$$M = M_v + M_h$$

$$M = \pi D^3 S_{uv} + \frac{\pi D^3 S_{uh}}{p_n}$$

$$= \pi D^3 S_{uv}\left(\frac{p_n + K_s}{p_n}\right)$$

or

$$S_{uv} = \frac{M}{\pi D^3}\left(\frac{p_n}{p_n + K_s}\right) \tag{4.7}$$

Similarly,

$$S_{uh} = \frac{M}{\pi D^3}\left(\frac{p_n K_s}{p_n + K_s}\right) \tag{4.8}$$

(3) Rate effect

It is well recognized that the rate of loading or rate of straining has a significant influence on the evaluation of undrained shear strength in the field as well as in the laboratory (Bjerrum 1972; Vaid et al. 1979; Sharifounnasab and Ullrich 1985; Chandler 1988; Roy and Leblanc 1988 among others). In a standard field vane test, rate of rotation during shearing is 6°/minute where the failure occurs in less than 1 minute. This time to failure (t_f) is small in comparison with that from various laboratory triaxial (UU, CIUC, CK_oUC, etc.) and undrained direct shear tests where t_f may vary from few minutes to several hours. The t_f for full-scale field failure may be much higher. Therefore, a correction for rate effect is essential in order to obtain strength from field vane tests which is comparable to laboratory tests or field failures. Bjerrum (1972) correlated this rate effect with plasticity index when he compared field vane test data with actual field failures.

(4) Disturbance due to vane insertion

According to Chandler (1988), there are mainly two consequences of soil displacement due to vane insertion:

(i) a local destruction of interparticle bonds within the soil, which in the case of more sensitive clays may significantly reduce the available undrained shear strength in the vicinity of the vane; and

(ii) a local displacement of soil particles together with a corresponding increase in the pore pressure around the vane, which on dissipation will result in an increase in effective stress.

Chandler has concluded from the data by La Rochelle et al. (1973) and Aas (1965) that the undrained shear strength could be underestimated for structured sensitive clays, by as much as 25% if the effect of disturbance (generation of pore water pressure and destruction of soil structure) due to vane insertion is not taken into account. Roy and Leblanc (1988) reported that the insertion of the vane creates disturbance which is linked to blade thickness and to the type of clay under study, and inferred that a better designed vane would reduce the disturbance with a 5 to 10% increase in measured strength. More research is necessary since only limited data related to this problem is available.

When the FV shear strengths are to be corrected for the rate effect and disturbance due to vane insertion, Eqs. 4.7 and 4.8 become

$$S_{uv} = \frac{M}{\pi D^3}\left(\frac{p_n}{p_n + K_s}\right)\mu_R \cdot \mu_D \tag{4.9}$$

and

$$S_{uh} = \frac{M}{\pi D^3}\left(\frac{p_n K_s}{p_n + K_s}\right)\mu_R \cdot \mu_D \tag{4.10}$$

where, μ_R and μ_D are correction factors for rate effect and disturbance due to vane insertion, respectively.

Undrained shear strengths on horizontal and vertical shear faces of a field vane can be obtained directly from the generalized Eqs. 4.9 and 4.10 for anisotropic soils with non-uniform shear stress distribution on horizontal surfaces.

4.3 Analysis of Test Results

Field vane tests were conducted at the standard rate of rotation of 6°/minute, at an interval of 400 mm within the crust and 1 m below the crust, using the NGI vane, 43 mm diameter by 86 mm high. Consistent results with negligible scatter were observed in two series of tests. Average results of these tests, analyzed conventionally (i.e. $S_u = 0.86M/\pi D^3$ considering uniform stress distributions and isotropic strength with no corrections), are shown in Fig. 4.2. There is a significant increase in sensitivity below the crust. The value of sensitivity at a depth of 2.7 m is 8 which suddenly increased to 14 at the next test depth at 3.1 m. From the sensitivity profile, it can be concluded that the sensitivity in the intact Champlain clay is considerably higher than that of the weathered crust.

As a part of this study, direct shear tests and triaxial compression tests were also conducted. Direct shear tests were carried out on horizontally and vertically trimmed undisturbed specimens to evaluate the undrained strengths on these two orthogonal planes, and to evaluate the coefficient of horizontal strength, which is assumed to be the same *in-situ*. Two types of triaxial compression tests were conducted: isotropically consolidated to σ_{vo}' (CIUC) (conventional type) and anisotropically consolidated to *in-situ* stress state (CK_oUC). Detailed discussions on these triaxial tests are given in Chapter 7. All these laboratory tests were performed for five depth levels: three (1.00, 1.80 and 2.60 m) within the crust and two (3.33 and 3.60 m) immediately below the crust. Utmost care was taken to trim laboratory samples to minimize disturbance. Below the crust, the soil was intact, sample preparation was much easier and the degree of disturbance was much less than in the crust material. Special sampling devices with sharp cutting edges were used, in order to obtain high quality samples minimizing disturbance to the lowest possible level. These laboratory specimens were obtained from cylindrical block samples (250 mm diameter x 400 mm high) which were collected from the field using Sherbrooke sampler (Lefebvre and Poulin 1979).

As discussed earlier, the undrained shear strength from FV test for any weathered crust is significantly higher than that obtained from laboratory and other *in-situ* tests. These test results will be reanalyzed in this chapter in terms of the four factors (non-uniform stress distribution, strength anisotropy, rate effect and vane insertion disturbance) mentioned in the previous section.

Stress distribution used in this analysis

Shear stress distribution along the cylindrical vertical face has been considered as uniform which is now well accepted in the geotechnical profession, as discussed earlier in this chapter. However, different shapes of stress distribution on horizontal edges have been proposed in various studies (Menzies and Mailey 1976; Donald et al. 1977; Menzies and Merrifield 1980; Wroth 1984; Silvestri and Aubertin 1988; Griffiths and Lane 1990). For strain-softening type of clays, the peak strength would be reached first at the vane corners, and by the time peak torque would be attained, the shear stress distribution would be as shown in Fig. 4.1b (Menzies and Mailey 1976; Silvestri and Aubertin 1988), and is a consequence of progressive failure (Flaate 1966; Donald et al. 1975). Therefore, the end shear stress distribution assumed in the present analysis is as shown in Fig. 4.1b since the soil showed strain-softening behaviour in triaxial (CK_oUC) and direct shear tests. The value of p_n in Eqs. 4.9 and 4.10, used in this analysis for strain-softening soil, was taken as 7.27 from Table 4.1. It should be noted that the stress-strain curves for depths 1.00 m and 1.80 m did not show a well-defined sharp peak although a strain-softening behaviour at large strain was indicated.

Estimation of strength anisotropy

The coefficients of horizontal strength (K_s), at various depths were estimated from direct shear tests. Lo and Morin (1972) determined strength anisotropy by testing samples trimmed at various angles. But, to simulate strength anisotropy on horizontal and vertical planes of a vane shear test, the direct shear test from horizontally and vertically trimmed samples is more appropriate. Therefore, in order to determine the values of K_s, direct shear (DS) tests were performed on two types of samples. First type of samples were conventional samples with the shear plane in the horizontal direction, where the applied normal stress was equal to the *in-situ* vertical stress σ_{vo}' (Fig. 4.3a). The second type of tests were conducted on samples with the shear plane in the vertical direction where the normal stress during shear was equal to σ_{ho}' (Fig. 4.3b). The strength anisotropy obtained from direct shear tests is assumed to be equal to that obtained from field vane tests, i.e. $S_{uh}(FV)/S_{uv}(FV) = S_{uh}(DS)/S_{uv}(DS) = K_s$.

The variation of K_s with depth (Z) is shown in Fig. 4.4 which indicates a good correlation. This correlation can be expressed by the following equation:

$$K_s = 0.49(Z)^{0.58} \quad \text{(where 1 m} < Z < \text{4 m)} \tag{4.11}$$

Strength anisotropy was accounted in the present analysis incorporating this value of K_s in Eqs. 4.9 and 4.10.

Adjustment for rate effect

Direct shear tests at various strain rates (0.004%-2.0%/minute) were conducted to determine the rate effect on the undrained shear strength of the crust, as shown in Fig. 4.5. The results indicate a decrease of strength by approximately 9% for each log cycle increase in time to failure (t_f). Similar observations were made by Donald et al. (1977) where strength changes per log cycle were 9% and 10% for Launceston and Yarra clay, respectively.

The time to failure in the laboratory undrained tests (triaxial and direct shear) varied between 30 minutes at 3.60 m depth and 160 minutes at 1.0 m depth although the same rate of strain of 0.04%/minute was used for all the laboratory triaxial and direct shear tests. The samples from more shallow depths failed at higher strain level than the samples from greater depths. Time to failure and consequently strain rate were determined using the method by Head (1986), where the following equation was suggested to determine t_f:

$$t_f = 0.51.t_{100} \text{ minutes} \tag{4.12}$$

where t_{100} is the required time for 100% primary consolidation obtained from triaxial consolidation test. Equation (4.12) is a simplified form of the equation originally proposed by Blight (1963).

The average t_f for laboratory undrained shear strength tests can be taken as 100 minutes. The t_f for FV tests was approximately 1 minute. Therefore, for the purpose of comparison between FV and laboratory tests, the S_u(FV) was corrected multiplying by 0.83 i.e. μ_R = 0.83 in Eqs. 4.9 and 4.10.

Correction for disturbance due to vane insertion

The weathered crust is permeable due to the presence of random micro-fissures. The sensitivity lies between 2 and 8. Hence, the pore-pressure build-up and destruction of structured bonds due to vane insertion can be assumed to be small and negligible. A μ_D value of 1.0 in Eqs. 4.9 and 4.10 has therefore been used in this analysis. According to Chandler (1988), this disturbance is unimportant for a soil with sensitivity of less than 15. However, for the soil below the crust, where the sensitivity is high and permeability is very low, a correction factor must be used; otherwise vane test would underestimate the undrained shear strengths.

The FV test data, re-interpreted considering the above four factors, are shown in Fig. 4.6. Undrained shear strengths from triaxial compression tests (CIUC and CK_oUC) and direct shear tests (horizontal and vertical samples) are also plotted in Fig. 4.6.

4.4 Comparison and Discussion of Test Results

It is evident from Fig. 4.6 that the undrained shear strengths on the vertical plane S_{uv}(FV), within the crust depth, obtained from field vane tests are significantly higher than the undrained shear strengths on horizontal planes S_{uh}(FV). This is to be expected for a soil with K_o>1 where the normal stress (σ_{ho}') on the vertical shearing face is greater than the normal stress (σ_{vo}') on the horizontal shearing face. It is also evident that the values of S_u(FV) obtained from conventional analysis (Fig. 4.2a) are close to the values of S_{uv}(FV) but are considerably higher than S_{uh}(FV) as well as the values of S_u obtained from laboratory triaxial compression and direct shear tests (Fig. 4.6). In this context, the author agrees with Lefebvre et al. (1987) that the S_u(FV) obtained from conventional analysis is considerably high and cannot be mobilized in the field; and should not be used for design in anisotropic overconsolidated soils. Moreover, the mode of failure in a vane shear test, where the strength is mobilized on the vertical and horizontal faces, is different from that in the field.

Although the values of S_u(FV) obtained from conventional analysis or S_{uv}(FV) obtained from the proposed interpretation technique give considerably higher values of undrained shear strengths within the crust, S_{uh}(FV) corresponds well with S_u(CK_OUC). The comparison between S_{uh}(FV) and S_u(CIUC) or S_{uh}(DS) is also reasonable. Therefore, from Fig. 4.6 it can be inferred that the S_{uh}(FV) can be used for geotechnical design since it matches reasonably well with K_o consolidated laboratory triaxial tests. The S_{uh}(FV) is expected to be smaller than the S_u(CK_OUC) since the normal stress on the shear plane for the earlier case is smaller. However, this has not been observed. The close match between S_{uh}(FV) and S_u(CK_OUC) may be caused by the vane blades shearing along a plane which is not necessarily the weakest shear plane whereas the shear plane of a CK_OUC test is the weakest plane.

The values of S_{uv} obtained from field vane tests and from direct shear tests on samples with vertical shear plane are expected to be similar since the mode of failure on the vertical plane for both of these tests is also similar. However, this is not the case. Two reasons may explain why S_{uv}(DS) is less than S_{uv}(FV). Firstly, although the normal stress equal to σ_{ho}' can be maintained on a sample with vertical shear plane (Fig. 4.3b), the lateral stresses, equal to σ_{ho}' and σ_{vo}', cannot be imposed in a direct shear test. Secondly, the specimens could be easily disturbed since the soil within the crust was loose, randomly micro-fissured, and composed of small rounded nuggets which were easily broken into individual pieces.

Undrained shear strengths, obtained from field vane tests, for any soil, by conventional analysis, will be close to the undrained shear strength on the cylindrical vertical face (S_{uv}) of the FV since the vertical surface carries major portion (86% or more) of the torque mobilized by the vane. Therefore, in any overconsolidated weathered crust with $\sigma_{ho}'>\sigma_{vo}'$ (i.e., $K_o>1$), it is anticipated that the undrained strength determined from conventional interpretation of the vane test will be higher than the shear strength back calculated from field failure, or from other laboratory tests. However, for normally consolidated clays where $\sigma_{ho}'<\sigma_{vo}'$, S_u(FV) would underestimate strength since, in this case, the normal stress on the vertical plane (σ_{ho}') is less than that on the horizontal plane (σ_{vo}'). Therefore, for realistic analysis, strength anisotropy should be incorporated in the field vane interpretation procedure and the use of a single correction factor for strength anisotropy is unsatisfactory. Assumption of isotropic behaviour of a soil may result in significant error in the estimation of the shear strength. The field vane would provide reasonable estimate of the undrained shear strength, from conventional analysis, only when the soil is isotropic. Bjerrum's correction factor, which is a function of plasticity index, reduces the conventional S_u, at this site, by only 3%. Bjerrum (1972), however, noted that the strength anisotropy generally varies along the depth, and this variation should be incorporated in the interpretation procedure. An attempt has been made in this study to integrate this variation of strength anisotropy in the interpretation of FV test data as shown in Eqs. 4.9 and 4.10.

The coefficient of horizontal strength K_s, for this weathered crust, varies between 0.49 (at OCR=16) and 1.01 (at OCR=3.1) as illustrated in Fig. 4.7a. It can be expected that the K_s will increase with increase in $\sigma_{vo}'/\sigma_{ho}'$ ratio, i.e., K_s will decrease with increase in K_o since the values of S_{uh} or S_{uv} depend on the normal stresses acting on the respective planes during shear. Data obtained from the present study confirms this tendency (Fig. 4.7b). Similar observation was made by Aas (1965) where the data for Drammen, Lierstranda and Manglerud clays were compared.

Undrained shear strengths obtained from CIUC tests are consistently lower than those from CK_oUC tests (Fig. 4.6), and this is reasonable for a soil with $K_o>1$. The ratio of the undrained strengths from K_0 consolidated and isotropically consolidated tests, $S_u(CK_0UC)/S_u(CIUC)$, decreases with depth and correlates well with the OCR and K_o (Fig. 4.8). This indicates that the values of undrained shear strengths are dependent on the stress history as well as on the *in-situ* state of stress.

Correlation between undrained strength ratio and in-situ stress history

It is well established that the undrained strength ratio S_u/σ_{vo}' has a correlation with the overconsolidation ratio indicating that the stress history influences the undrained shear strength of a soil. Similar correlation for field vane tests was observed in this study, as shown in Fig. 4.9a. In addition, a correlation between S_u/σ_{vo}' and K_o is also observed in this study (Fig. 4.9b) indicating that the *in-situ* stress state also has an influence on the undrained shear strength of a soil obtained from FV tests. The relationship between S_u/σ_{vo}' and OCR or K_o for this clay crust can be expressed by

$$S_u/\sigma_{vo}' = S_o(OCR)^m \tag{4.13}$$

$$S_u/\sigma_{vo}' = S_k(K_o)^q \tag{4.14}$$

The values of S_o, S_k, m and q are dependent on the soil type and the type of testing. The values of these parameters, as determined from regression analysis, are shown in Table 4.2. Minimum correlation coefficient obtained from this regression analysis was 0.97.

4.5 Concluding Remarks

The following observations have been made regarding the interpretation of the field vane test data for the weathered clay crust of anisotropic nature:

1. S_u obtained from FV tests, using conventional analysis, is considerably higher than those obtained from laboratory undrained shear strength tests, and cannot be used for design within the crust. This is attributed to the fact that the major portion of the torque mobilized by the field vane is developed on the cylindrical vertical face which is normal to the *in-situ* horizontal stress (σ_{ho}') where $\sigma_{ho}'>\sigma_{vo}'$. S_{uh}(FV) compares well with S_u obtained from K_o consolidated laboratory triaxial tests. Therefore, S_{uh}(FV) may be used for design analysis of a foundation within the overconsolidated crust instead of S_u(FV) from conventional analysis. An interpretation technique which takes the strength anisotropy into account, to obtain the values of S_{uh}(FV), has been discussed.

2. The undrained strength on horizontal plane in direct shear test, S_{uh}(DS), and is similar to that obtained from conventional triaxial shear test, S_u(CIUC). These strengths are, however, smaller than S_{uh}(FV) or S_u(CK$_0$UC).

3. Strength anisotropy varies with depth. This variation should be incorporated in the

interpretation of the field vane test data. The use of a single multiplying correction factor (Bjerrum 1972) is unsatisfactory.

4. The *in-situ* state of stress (K_o) correlates well with undrained strength ratio (S_u/σ_{vo}'), and clearly demonstrates the influence of the *in-situ* state of stress on undrained shear strength.

Table 4.1. End shear stress distribution for rectangular vanes (Silvestri and Aubertin 1988).

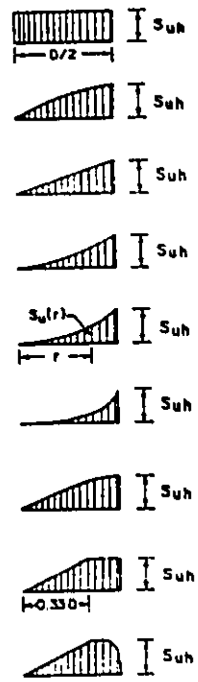

Type	Pattern	n	P_n
Uniform	S_{uh}; D/2	0	6
Parabolic	S_{uh}	1/2	7
Triangular	S_{uh}	1	8
Square power	S_{uh}	2	10
Cubic power	$S_u(r)$; S_{uh}; r	3	12
Fourth power	S_{uh}	4	14
Bessel function (Casson, 45)	S_{uh}	-	6.77
Trapezoidal	S_{uh}; 0.33D	-	6.48
Strain-softening	S_{uh}	-	7.27

Table 4.2. Values of parameters of S_o, S_k, m and q as expressed in (4.13) and (4.14).

Parameters	Conventional	Vertical plane	Horizontal plane
S_o	0.19	0.15	0.27
m	1.25	1.26	0.83
S_k	0.60	0.51	0.58
q	2.15	2.20	1.44

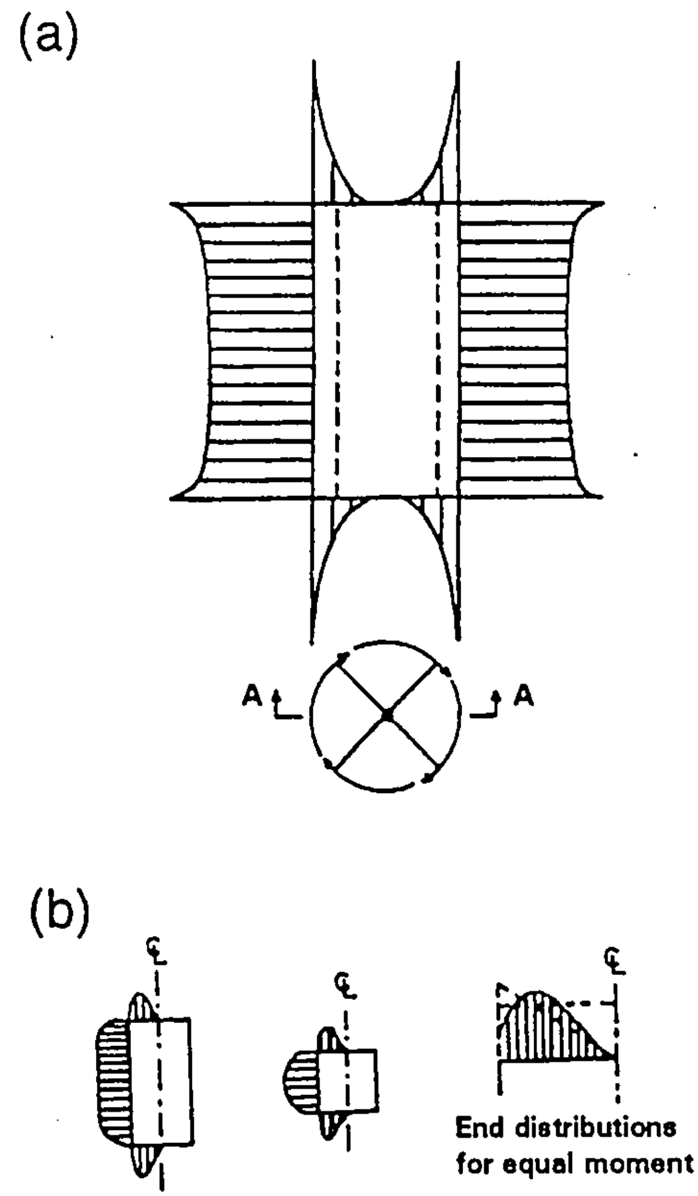

FIG. 4.1 Stress distribution (Donald et al. 1977). Elastic (a) and plastic (b) shear stress distributions.

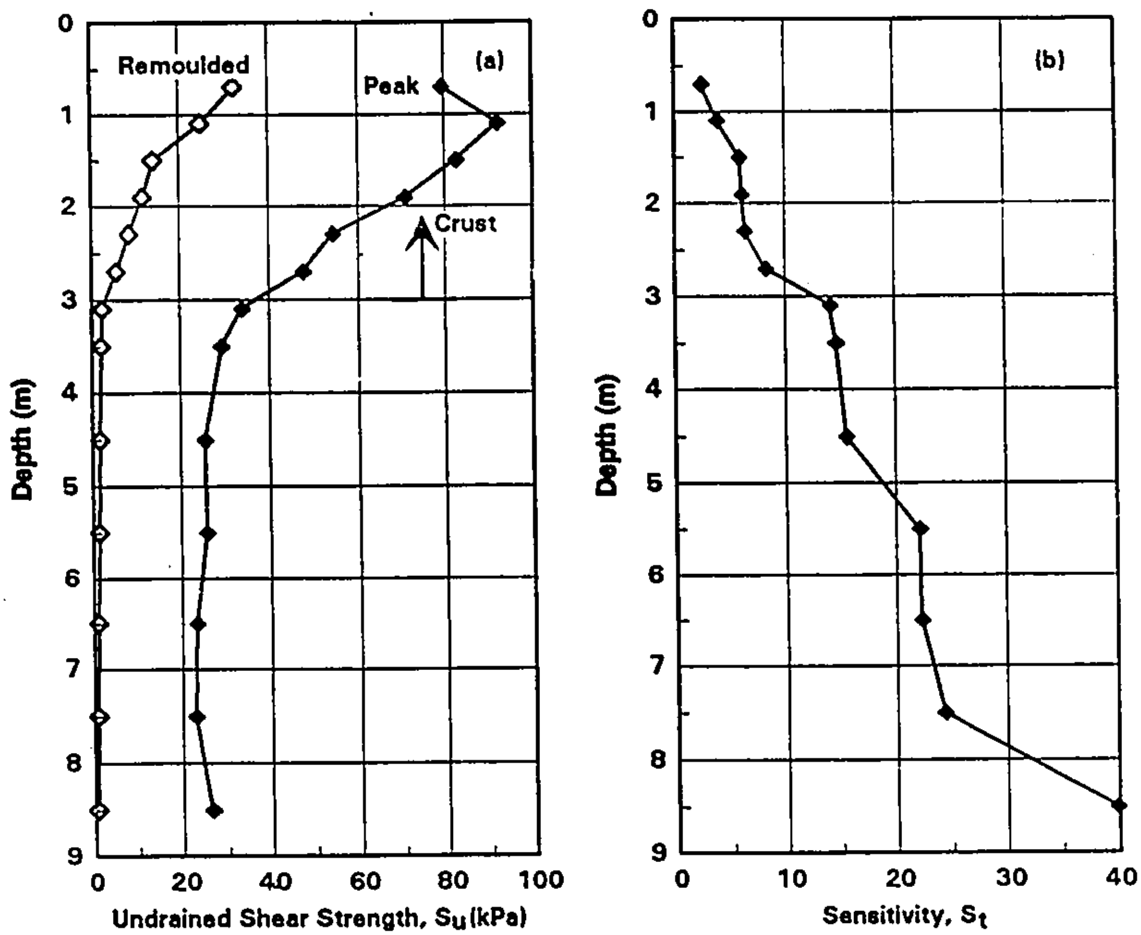

FIG. 4.2 Results of conventionally analyzed field vane test results.

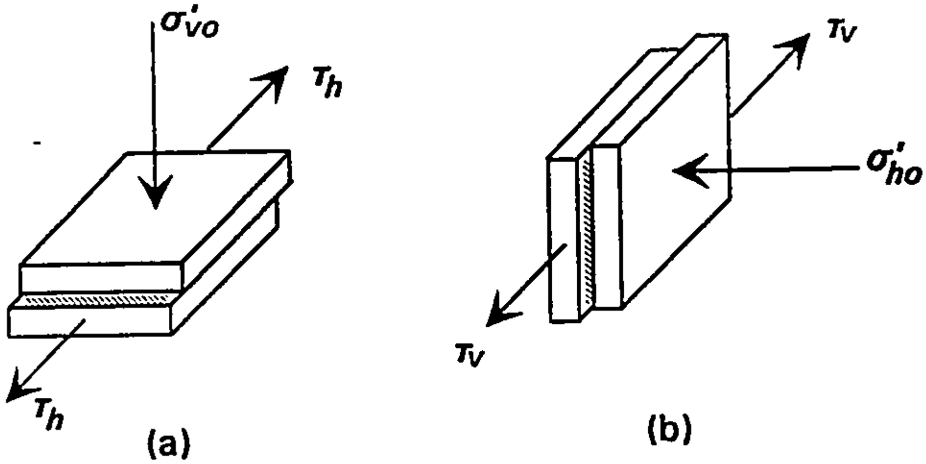

FIG. 4.3.Orientation of samples for direct shear tests: (a) shear plane in horizontal direction, and (b) shear plane in vertical direction.

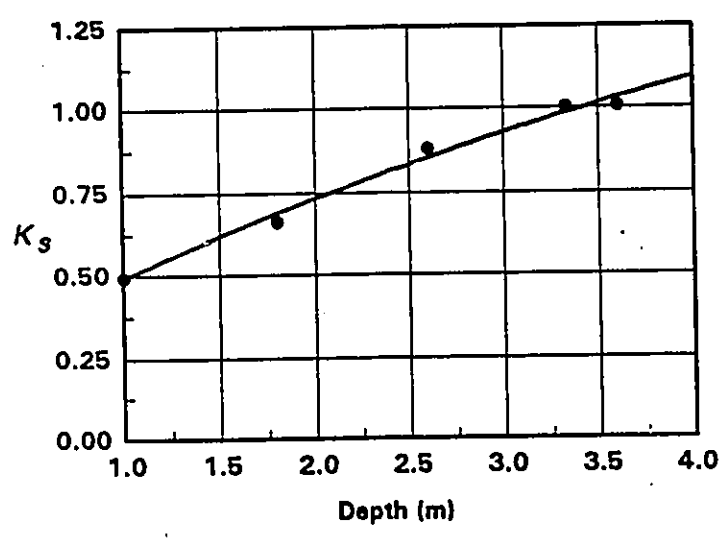

FIG. 4.4. Correlation between coefficient of horizontal strength (K_s) and depth (Z).

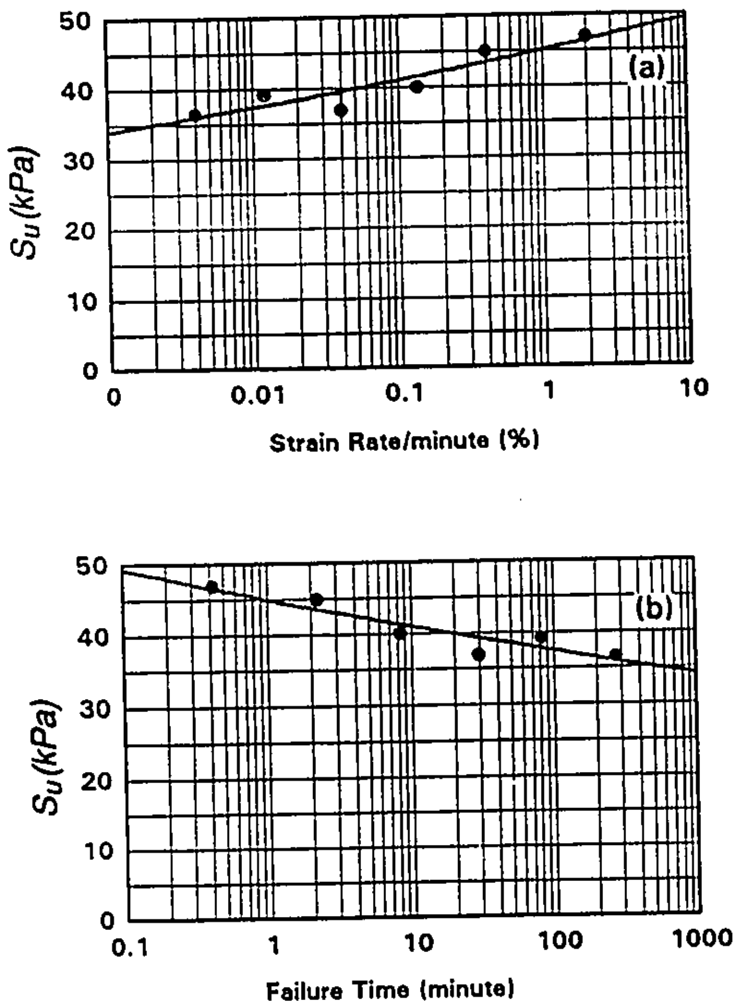

FIG. 4.5. Rate effect on undrained shear strength.

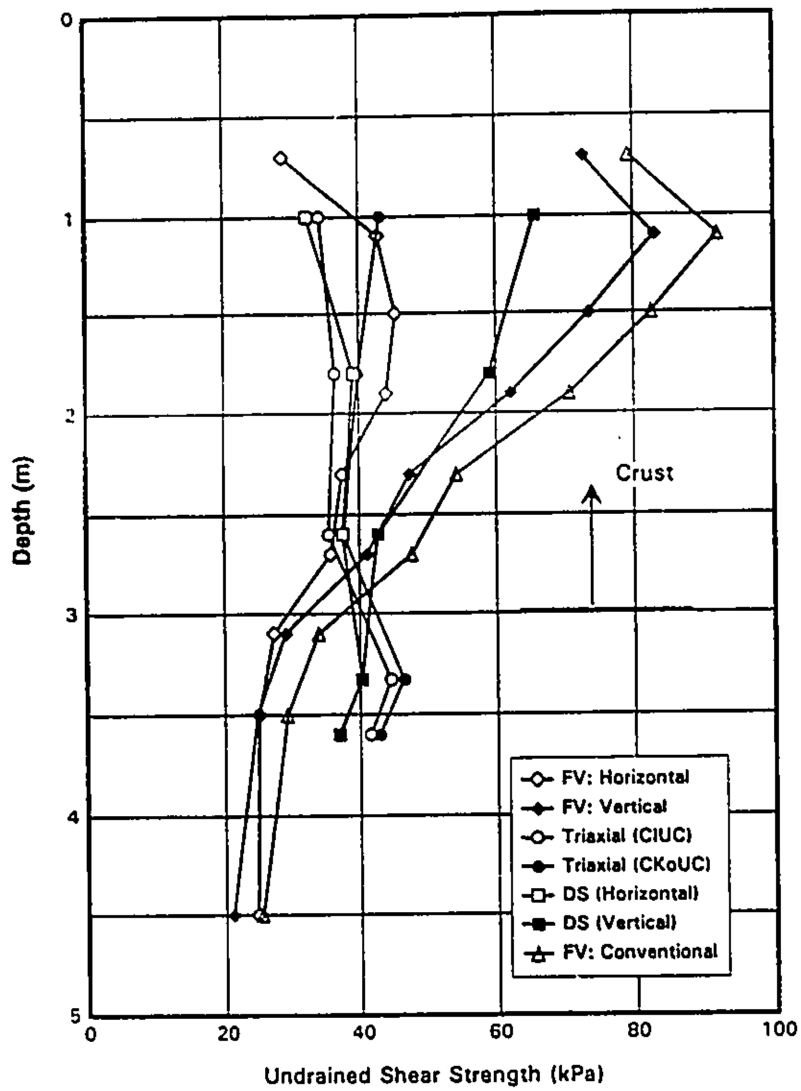

FIG. 4.6. Undrained shear strengths from field vane (re-interpreted), triaxial compression and direct shear tests.

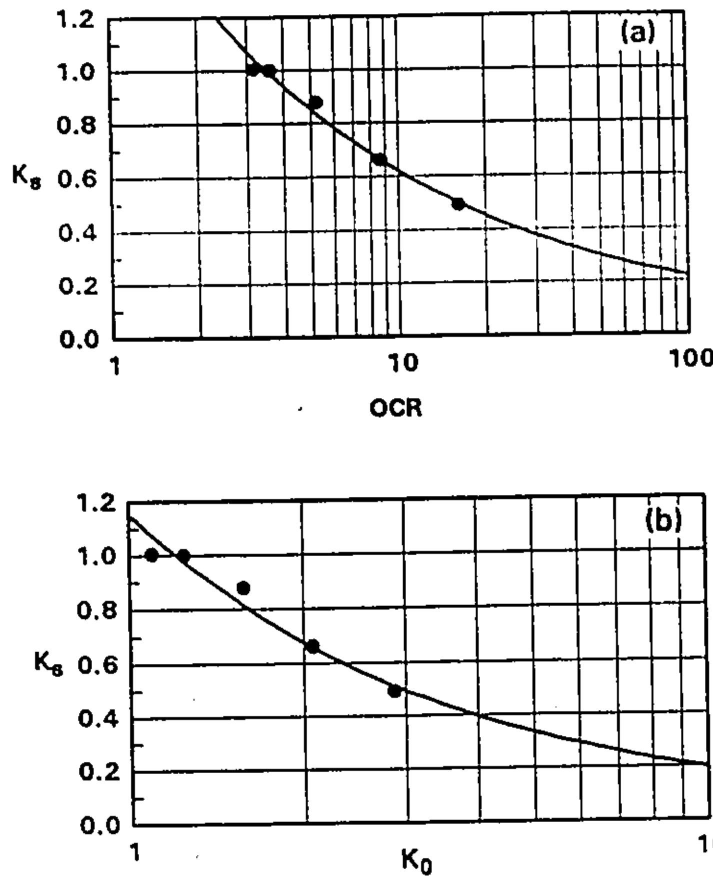

FIG. 4.7. Correlation between K_s and in-situ stress history: (a) K_s-OCR and (b) K_s-K_o.

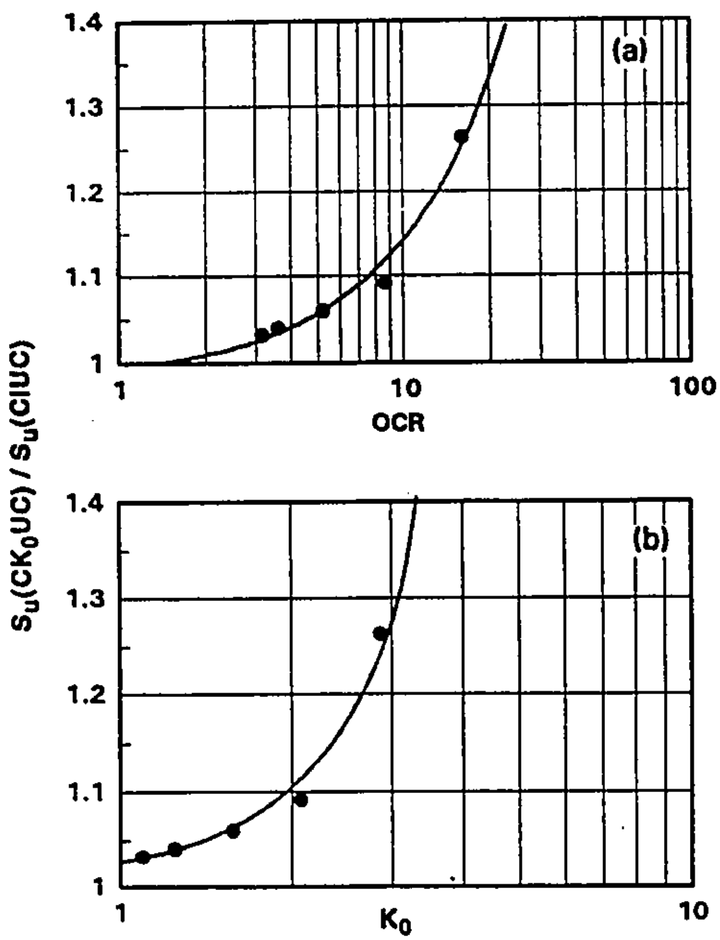

FIG. 4.8. Relationship between S_u(CK$_o$UC)/S_u(CIUC) and in-situ stress history: (a) OCR, and (b) K_o.

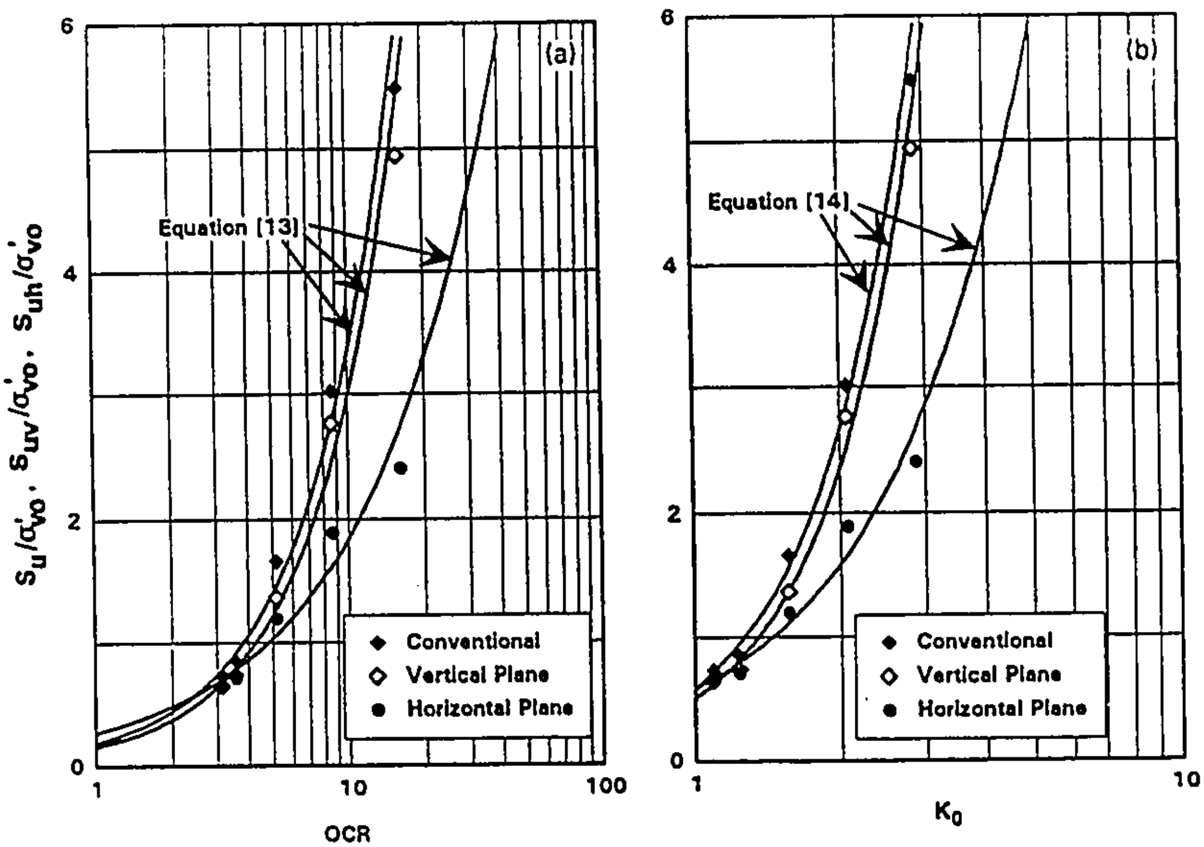

FIG. 4.9. Relationship between undrained shear strength ratio (S_u/σ_{vo}') and in-situ stress history: (a) OCR, and (b) K_o.

CHAPTER 5

DEVELOPMENT OF LABORATORY APPARATUS

Three laboratory apparatuses have been developed during the course of this research: (i) a computerized control system for triaxial testing, (ii) an improved consolidation apparatus, and (iii) an improved volume gauge. The detailed discussion of these apparatuses, including their advantages over the existing ones, are presented in the following sections.

5.1 A Computerized Control System for Triaxial Testing

5.1.1 Introduction

The conventional triaxial testing, i.e., triaxial compression or extension tests performed by increasing or decreasing axial stress, does not always simulate the stress path that is followed by a structure in the field. To obtain representative soil parameters from laboratory triaxial tests, the expected field stress path must be followed in the laboratory tests. Manual control of these stress paths in the laboratory is tedious, complicated, difficult to control, and requires continuous attendance of an operator. To overcome these disadvantages, a versatile computer-operated control system for triaxial stress/strain path testing has been developed. The system is capable of controlling any triaxial compression or extension stress path tests. It can be used for any stress-controlled, strain-controlled, or combination of both stress and strain controlled triaxial shear tests. The desired variety of stress and strain paths are followed by using a personal computer, and operating a set of stepper motors through a data acquisition and controller system. The apparatus, the control device, the testing method, and the versatility of the equipment are described in the following sections. The system can also be used for automatic sample saturation, K_0 consolidation, and stress, strain or gradient controlled isotropic consolidation tests.

Triaxial tests are either stress rate controlled or strain rate controlled, or less frequently, a combination of the two. Stress rate may be controlled by the simple method of application of dead loads at certain intervals or by using incremental pneumatic or hydraulic (Nagaraj et al. 1981) pressures. The strain rate tests are controlled by the conventional method of gear operation or by time dependant volume displacement (Campanella and Vaid 1972; Bishop and Wesley 1975) method. Both methods have some advantages and disadvantages in testing, and in the interpretation of stress-strain behaviour. Moreover, the conventional tests are performed with isotropic consolidation and monotonic loading which does not simulate the *in situ* stress conditions giving stress-strain characteristics which are different from those in the field.

Many researchers (Campanella and Vaid 1972; Bishop and Wesley 1975; Atkinson 1975; Ampadu and Tatsouka 1989; Pradhan et al. 1989) have developed various stress path testing apparatus to simulate the *in situ* stress conditions. The apparatus, developed at the University of Ottawa during this research, is simple and has some added advantages over the above mentioned ones.

Although the post-peak behaviour can be clearly defined by a strain controlled test, the initial stress-strain curve as well as initial modulus cannot be clearly defined. The main disadvantage of this method is that a desired stress path, to simulate the field condition, cannot be followed.

In a stress controlled test, a desired stress path can be followed to duplicate the field condition and also a well defined initial stress-strain curve can be obtained. The principal disadvantage of this method is that the post-failure stress-strain curve cannot be clearly defined.

The triaxial testing system, described in this chapter, has overcome the above-mentioned problems with the aid of computer-assisted control device. Interchange between stress controlled and strain controlled tests is possible, in the same shear test, by this equipment. To get a well defined stress-strain relationship, the experiment can be started with stress controlled test and then automatically switched to strain controlled test before failure and continues to the end of the test.

5.1.2 Description of the Triaxial Apparatus

The apparatus, mainly developed for the purpose of this research, has been in use at the Geotechnical Research Laboratory of the University of Ottawa for the last three and half years. The control device, described in this section, was developed for use with Bishop-Wesley stress path cell (Bishop and Wesley 1975). The Bishop-Wesley apparatus is not described in this paper since the complete description of this apparatus can be obtained from the original reference mentioned above.

A second conventional triaxial apparatus (UBC type) has also been operated from the same control system. This apparatus permits the application of either stress or strain control through a double chamber bellofram actuator connected to the ram. As mentioned earlier, the control device was originally developed for the Bishop-Wesley stress path cell. Thereafter, to make the conventional apparatus capable of stress path testing, a provision was made so that the same control device could be connected to the conventional triaxial apparatus with slight modifications. All the preliminary procedures including saturation and consolidation are performed using the existing mercury column system; and only at the time of stress path shear test, the apparatus is connected to the computerized control system. At all other times, the conventional apparatus works independently with conventional mercury column stress application assembly. A schematic diagram of the modified conventional triaxial apparatus is given in Fig. 5.1. During the sample saturation and/or consolidation time of the second triaxial apparatus, the control device is fully dedicated to the Bishop-Wesley triaxial stress path cell.

5.1.3 Description of the Control Device

The triaxial apparatus is controlled by a personal computer through a data acquisition and control system. The data acquisition and control system, known as LabMate, is manufactured locally by an Ottawa based company named Sciemetric Inc. The standard LabMate is capable of reading up to sixteen analog to digital (A/D) and two digital to analog (D/A) channels. The D/A channels are unused in this testing system. An optional custom made controller board has been added to the original LabMate to operate the stepper motors. There are three stepper motors dedicated individually to monitor axial, cell and back pressures separately. Although the LabMate system does not come with stepper controller board as a standard feature, this option can easily be added. This control system is simpler, easier in operation and more versatile when compared with the commercially available system. However, the cost of this data acquisition and control system appears to be less than other commercial systems.

The data acquisition system converts analog signals received from the va.ious sensors to digital signals to be used by the computer. These numerical values are fed to the computer for further control of the test and processing of the data. The computer analyzes the received data, compares with the desired stress or strain level, and operates a stepper motor, if required, through the stepper controller of LabMate to achieve the desired stress or strain level. The operation of the stress path control system is described in Fig. 5.2.

5.1.4 Stress Paths in Triaxial Shear Tests

The possible stress paths which can be followed by using this control device are illustrated in Fig.5.3, and are discussed below.

(1) *Passive Compression:* The conventional triaxial compression test where axial stress is monotonically increased maintaining constant radial stress.

(2) *Active Compression:* The compression test in which radial stress is decreased monotonically while axial stress is kept constant.

(3) *Passive Extension:* The extension test in which radial stress is increased while axial stress is maintained constant.

(4) *Active Extension:* The extension test in which axial stress is decreased maintaining constant radial stress.

(5) *Compression or Extension at K_0 condition:* When there is a change in axial stress in the field, there will always be a simultaneous change in the radial stress to maintain the K_0 condition. This stress path can also be simulated in the laboratory.

(6) *Compression or Extension at Constant Mean Pressure:* The axial and radial stresses are changed simultaneously in such a way that the mean pressure, $(\sigma_1+\sigma_2+\sigma_3)/3$, is always maintained constant.

(7) *Isotropic Compression:* Both axial and radial stresses increase simultaneously at the same rate.

A combination of two or more of above stress paths, in the same test, can also be followed to simulate a representative stress path in the field. An actual project, for example, may involve excavation in the first stage, and then the construction of the structure at the second stage. In this case, the soil below the foundation will experience extension during excavation and compression during construction. Such stress paths can also be followed.

Cyclic triaxial compression or extension, i.e., repeated loading and unloading by using any stress path as shown in Fig.5.3 can also be performed with this control device.

All the above-mentioned stress paths can be followed by using either stress controlled or strain controlled tests, or by using combination of both. It should be mentioned that any stress path in σ_v'-σ_h' space (Fig.5.3) can be followed by using this apparatus.

5.1.5 Operation and Control of Triaxial Shearing Stage

The desired stress or strain path is achieved by controlling the vertical stress (σ_v') and/or horizontal stress (σ_h') in the desired manner. The horizontal stress is measured directly from the cell pressure, and the axial stress is calculated from the following equation assuming negligible frictional loss.

$$\sigma_v' = \frac{W}{A_s} + \sigma_h' - \sigma_h A_p \qquad (5.1)$$

where, W = the load recorded by the load cell,

A_s = the cross-sectional area of the sample at any instant of time, and

A_p = the cross-sectional area of the piston rod.

The weight of top cap and the loading piston is not taken into consideration since the load cell was zeroed with these loads hanging.

A computer software, written in Microsoft QuickBasic, was custom-developed in this research to monitor the stress path test through the LabMate control device. The simplified flow diagram of the computer program, including the shear test control loop, is described in Fig. 5.4. The shearing stage of the triaxial stress path test is controlled by using feedback from the required transducers. For example, a strain controlled extension test is to be performed by increasing radial stress and keeping axial stress constant (stress path 3 in Fig. 5.3). In such a case, the main control is from the axial strain rate. The computer receives the digital reading, through the LabMate, from the axial displacement transducer and compares that reading with the desired reading as determined at that instant of time from the axial strain rate. If the current reading is not equal to the calculated desired reading, the computer sends signal to the stepper controller of LabMate to activate the stepper motor to achieve the desired strain. This control loop continues until the test is terminated or rerouted to a different stress path loop. The test terminates automatically when the maximum axial strain or maximum stress, specified by the operator, is reached. The test can also be terminated in case of emergency or for any other purposes by pressing Esc key on the keyboard.

Before starting the test the operator specifies, in response to the computer display, whether the test will be drained or undrained and stress controlled or strain controlled. When the test is an extension test, the stress or strain rates specified are in negative values.

The program operates the system, and stores the raw test data and the analyzed data on the hard disk at specified time intervals. The data saved on the hard disk are in ASCII code (American Standard Code for Information Interchange) so that they can be imported to any spreadsheet or graphic programs for further analyzes and plotting. It also prints the analyzed data on the printer. In addition to the above, it also displays, on the display monitor, the instant readings of all the channels in their respective units for visual inspection.

The program allows the operator to specify the desired stress rate for stress controlled test or strain rate for strain controlled tests or combination of both. To get a well defined stress strain curve, the test can be started with stress control and can then be rerouted to strain control before failure.

5.1.6 Versatility of the New Apparatus

This is an improved but simple triaxial stress path control device. The control system permits any desired stress/strain path for any triaxial shear test. Although the ease of use and versatility of the apparatus can be realized from the discussions in the previous sections, some of them are briefly mentioned below.

(a) Some of the disadvantages experienced with the previously developed stress path testing apparatus can be overcome by this system. Strain controlled tests can be performed directly from the feedback of the linear displacement transducer which measures the axial deformation of the sample directly. Constant rate of flow source is no longer required for axial strain controlled tests (Campanella and Vaid 1972; Bishop and Wesley 1975) making the triaxial apparatus simple and easy to operate. Also, for the Bishop-Wesley type cell, the load on the sample can directly be obtained from a submersible load cell placed directly on top of the sample. Hence, there is no need for complicated calculations of converting ram pressure to axial stress used in the conventional Bishop-Wesley type triaxial system. Internal load cell measurement also avoids correction for ram weight and ram friction in the ram chamber. However, the above complicacy does not arise for a conventional (UBC type) triaxial cell where the load is applied from the top of the sample, and the load cell is placed between the sample and the reversible pressure chamber.

(b) The main advantage of the system is that compression or extension tests in either stress controlled or strain controlled modes or a combination thereof, can be performed monitoring the cell pressure. For example, the extension tests with increasing radial stress and constant vertical stress can be performed as stress or strain controlled or both combined. Interchange between stress control and strain control can be obtained, during the progress of the test, ensuring a well defined pre-peak and post-peak stress-strain curve.

(c) K_0 consolidation test can easily be performed with this new system. The system can also be used for stress, strain or gradient controlled isotropic consolidation tests.

(d) Although the system was purposely designed for stress path triaxial testing, it can also be used for conventional drained and undrained compression or extension tests.

(e) The drained tests which may run for several weeks can easily be performed unattended, once it is started. The computer controls the apparatus, prints and stores the data at specified time intervals. It also stops the test when it reaches the termination value specified by the operator.

(f) This controlling system can be used with Bishop-Wesley type stress path triaxial cells or conventional triaxial cells with slight modification.

(g) Cyclic triaxial testing, i.e., a series of loading and unloading in the same test, can also be performed with this controlling device.

(h) Automatic sample saturation, as described by Brandon et al. (1990), can also be performed by using this apparatus.

5.2 An Automated Consolidation Apparatus

5.2.1 Introduction

A versatile computerized consolidation device has also been developed for this research. The development of the consolidation apparatus was accomplished in two stages:

(i) modification of the Rowe consolidation cell (Rowe and Barden 1966) to overcome the problems (Shields 1976) encountered while using this cell, and (ii) automation of this consolidation apparatus to speed-up the testing procedure and to make the device more versatile.

The consolidation test can be completed in 24 hours (or less) using this new device. This apparatus can be used for consolidation tests with stress-controlled, strain-controlled, gradient-controlled, or conventional 24-hour incremental loading. The description of the modified consolidation apparatus and its versatility have been provided in the following sections.

5.2.2 Modification of the Hydraulic Consolidation Cell

There are two significant problems which are encountered during the use of a hydraulic consolidation cell, commonly known as Rowe cell (Rowe and Barden 1966). Firstly, the trapped air and water in between the cell wall and the diaphragm stem or flange (Fig. 5.5): this air and water are expelled during the consolidation process giving incorrect readings of the volume change of the sample. With the existing hydraulic consolidation cell, it is difficult and tedious to get rid of this trapped air and water. Although under-water assembly of the consolidometer may get rid of the air, the trapped water may not be completely expelled before start of a consolidation test.

Secondly, the force exerted by diaphragm of a hydraulic consolidometer may differ considerably from that calculated on the basis of the hydraulic pressure and the cross-sectional area of the oedometer. Shields (1976) reported that in case of the 3 in. diameter cell, errors of 15 to 20% and greater were measured consistantly at pressures up to 400 or 500 kPa. In consolidation tests on identical specimens of a marine clay, the preconsolidation pressure, σ_p, measured in a 3 in. consolidometer was always about 30% greater than in the 6 in. consolidometer - 100 kPa against 76 kPa. Shields also reported that the tests using a conventional, mechanical loading system showed little discrepancy between the results in 3 in. and 6 in. cells.

From the above-mentioned two-fold problem, it is conceivable that the origin of the problems is the flexible diaphragm used in the Rowe type cell. It should be mentioned that the diaphragm in a hydraulic consolidometer is working as a sealant which prevents pressurizing water from moving in to the sample. Therefore, thought was given to replacing the diaphragm with an alternative sealant. Consequently, a loading ram, equipped with two U-cup seals (Fig. 5.6), was used instead of the flexible diaphragm.

U-cup seals are placed in opposite directions at upper and lower ends of the ram as shown in Fig. 5.6b. These U-cup seals are made of nitrile which is very pliable and has a low break-away resistance. The seals used in this study were obtained from D and D Packing and Seals Inc. (Part No: 8406-0250). The modified hydraulic consolidation cell including the U-cup seals on the loading piston is illustrated in Fig. 5.7.

Initially, during this research, both the loading ram and the cell body were made from aluminium. Later on, it was observed that the aluminium was reacting with soil where they were in contact with each other. Therefore, the aluminium cell body was replaced with brass which is believed to be inert with soil. No reaction has been observed with the loading ram presumably since it did not come in contact with the soil. However, it is preferable that both the cell body and the ram are made of brass.

5.2.3 Types of Consolidation Tests

Seven different varieties of consolidation tests, including the standard incremental loading (STD), can be performed using the modified consolidation apparatus. Other six types of tests, which are continuous loading tests, can also be performed with this consolidometer without any modification. Loading patterns of these tests are illustrated in Fig. 5.8, and their descriptions are briefly given below:

(a) ***Standard incremental loading (STD)***, this is the conventional consolidation test where the load is doubled (or is increased at a certain ratio) at a specified interval of time, commonly at 24-hour interval (Fig. 5.8a). This applied load is kept constant during each stage.

(b) ***Constant rate of strain (CRS)***, in which the consolidation pressure is applied in such a way that the rate of vertical deformation is constant (Fig. 5.8b). Consolidation tests with constant rate of volumetric strain can also be performed with this apparatus without any modification.

(c) ***Constant rate of loading (CRL)***, in which the applied stress is increased at a constant rate (Fig. 5.8c).

(d) ***Constant pore pressure gradient (CG)***, in which the difference in pore pressure between the upper and lower faces of the sample is kept constant (Fig. 5.8d).

(e) ***Constant pressure ratio (CPR)***, in which the loading is applied in such a way that the pore pressure developed at the non-drainage face is always a fixed proportion of the total applied stress (Fig. 5.8e).

(f) ***Restricted flow consolidation (RFC)***, in which the rate of drainage is restricted by a flow restrictor so that the pore pressure at the drainage face decreases slowly to the back pressure and the hydraulic gradient across the sample remains quite small (Fig. 5.8f).

(g) ***Back pressure controlled consolidation (BPC)***, in which the back pressure is initially equal to the pore pressure in the sample and is steadily reduced to a final value (Fig. 5.8g).

5.2.4 Automation of the Consolidation Apparatus

All the different varieties of consolidation tests described in the previous section require continuous attendance of an operator unless a computerized system is used. The modified consolidometer as discussed earlier, has been computerized during the course of this research so that the experiments can be performed without the continuous attendance of an operator. The operator can prepare the sample and start the test, specifying the loading pattern required (Fig. 5.8a-g), with the help of the computer. Thereafter, the computer controls the test following the loading pattern as specified at the start of the test.

The same computerized control system that was used with the stress path triaxial apparatus as discussed in section 5.1, was also used with this consolidometer. Although the basic controlling technique is same as that of the triaxial, a separate subroutine of computer programming has been added to the original program for the automatic operation of the modified hydraulic consolidometer.

At the begining of the experiment, the computer asks the operator for the loadiing pattern and the loading rate to be used during the test. When these values are given to the computer, the remainder of the work is continued automatically. At the begining of the test, the operator also specifies the time interval of recording the data and the limit of stress or strain after which the experiment will be terminated by the computer automatically. To avoid duplication of discussion, the controlling technique that has been programmed in the new subroutine will not be discussed in this section.

5.2.5 Versatility of the New Consolidometer

The versatility of the newly developed hydraulic consolidation apparatus can be realized from the following discussions:

(a) There are two obvious problems with the conventional Rowe hydraulic consolidation cells: (i) the load applied on the flexible diaphragm is not totally transfered to the soil sample (Shields 1976), and (ii) the entrapped air and water in between the cell wall and diaphragm stem contribute to the volume change of the sample giving incorrect consolidation readings. These two problems have been eliminated by replacing the diaphragm with a loading ram fitted with U-cup seals at upper and lower ends of the ram.

(b) The consolidation tests, more particularly the continuous loading type of consolidation tests, require continuous attendance of an operator. This continuous attendance is no longer required with the new consolidometer since it has been computerized to run tests automatically once the test is started.

(c) This is a single most versatile apparatus which can be used for any type of consolidation test, either for various types of continuous loading consolidation tests or for the standard incremental loading consolidation tests.

(d) Direct permeability tests, constant head type or variable head type, can also be easily performed with this apparatus without any further modification.

5.3 An Improved Simple Volume Gauge

5.3.1 Introduction

The existing volume gauges in the geotechnical research laboratory of the University of Ottawa, purchased from United Kingdom, have a capability for total volume change of 100 cc. These volume gauges use a piston fitted with a bellofram diaphragm. The vertical movement of the piston is calibrated to provide measurements of volume change. However, the calibration curve for these gauges is linear over only the middle 55 cc. The combination of the initial and final curved portions, including the middle straight line portion of the calibration curve, has an "S" shape. Larger volume change measurements are required in the isotropic triaxial consolidation tests, in the laboratory permeability tests, and in the larger diameter (76 mm and 152 mm) consolidation tests. To satisfy this requirement of higher volume capacity with linear calibration characteristics, a volume gauge of approximately 110 cc capacity has been developed. The complete calibration curve for this volume gauge is a straight line, and this volume gauge including its components can be fabricated easily in a machine shop.

5.3.2 Description of the Volume Gauge

The concept of the volume gauge has been borrowed from the modified consolidometer described in Section 5.2. The cylinder including the piston, is essentially identical to that of the consolidometer. The piston for the volume gauge is also sealed with U-cup seals (Fig. 5.6) at upper and lower ends of the piston perimeter. The schematic diagram of the volume gauge is shown in Fig. 5.9. The internal diameter of the volume gauge cylinder, fabricated for this research, is 76 mm, although the diameter of the cylinder can be made larger or smaller depending on the total volume change required and the availability of the size of the U-cup seals. While designing a volume gauge, it should be kept in mind that the precision of the volume measurement is coarser for a larger diameter volume gauge. The volume gauge developed in this research, including the piston and the cell body, is made of aluminium since there is no appreciable reaction between aluminium and water.

Volume measurement is obtained from the movement of the piston through an LVDT which is connected to the piston through the cell cap. This LVDT, which has been calibrated for the volume change, registers the movement of the piston.

The bellofram seals, which have been used with commercially available conventional volume gauges, have been replaced with U-cup seals in this new volume gauge. In addition to the non-linear calibration curve, the volume gauge equipped with bellofram seals has another potential disadvantage. When the pressure in the volume gauge on both sides (above and below) of the bellofram stabilizes (i.e., at the end of each stage of consolidation, at the end of each stage of saturation, etc.), occasionally, the direction of the curvature of the bellofram seal changes in the opposite direction giving an instantaneous false volume change of approximately 7 cc for the volume gauge presently being used in the laboratory. These commercial volume gauges, therefore, should be used for only those cases where the total volume change will be less than approximately 50 cc during a test, and will not require the reversal in the direction of the movement of the piston. The replacement of bellofram seals with U-cup seals has overcome both of these problems, and also the use of U-cup seals has made the use of volume gauge simple.

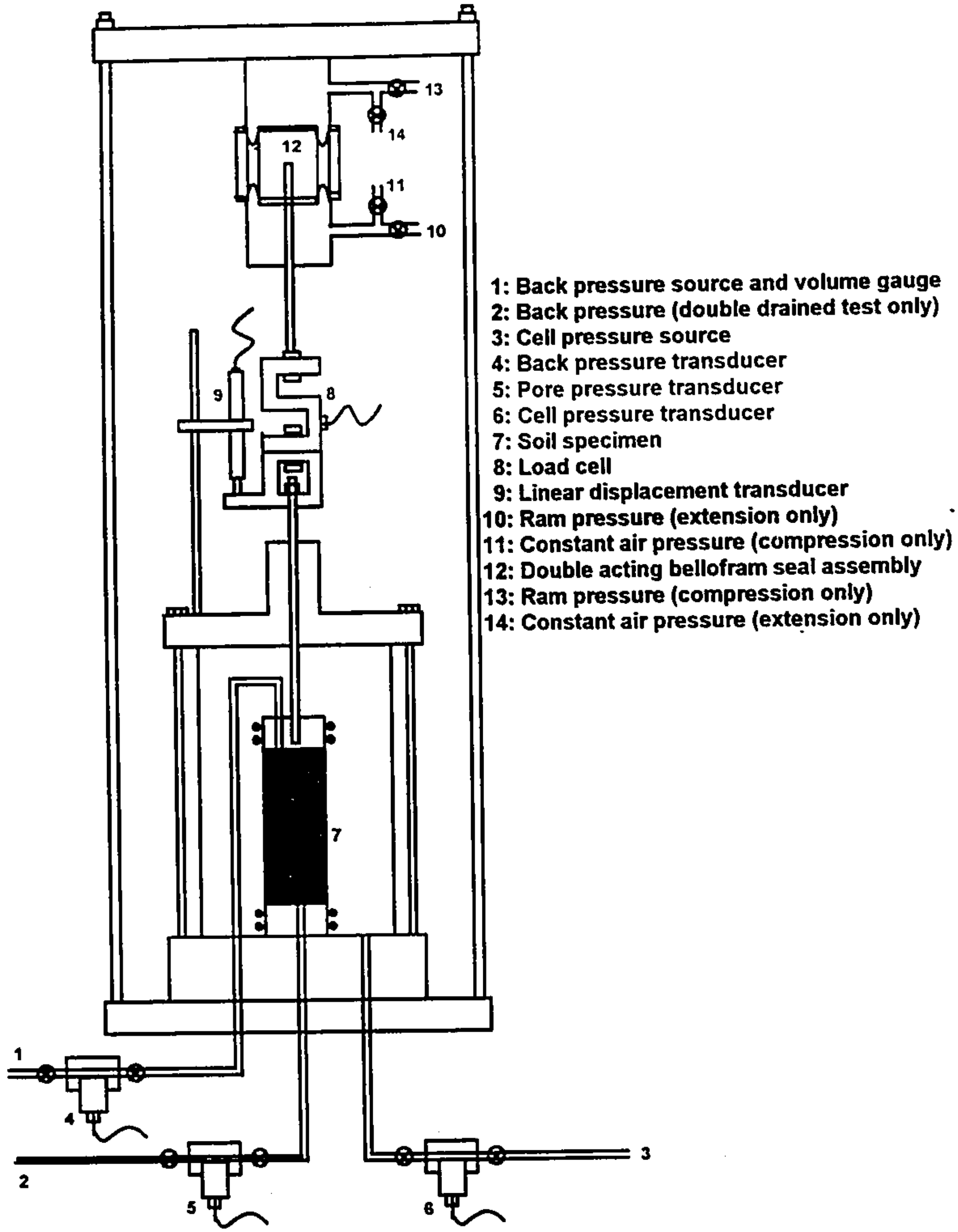

Fig. 5.1. Schematic diagram of the UBC type triaxial apparatus.

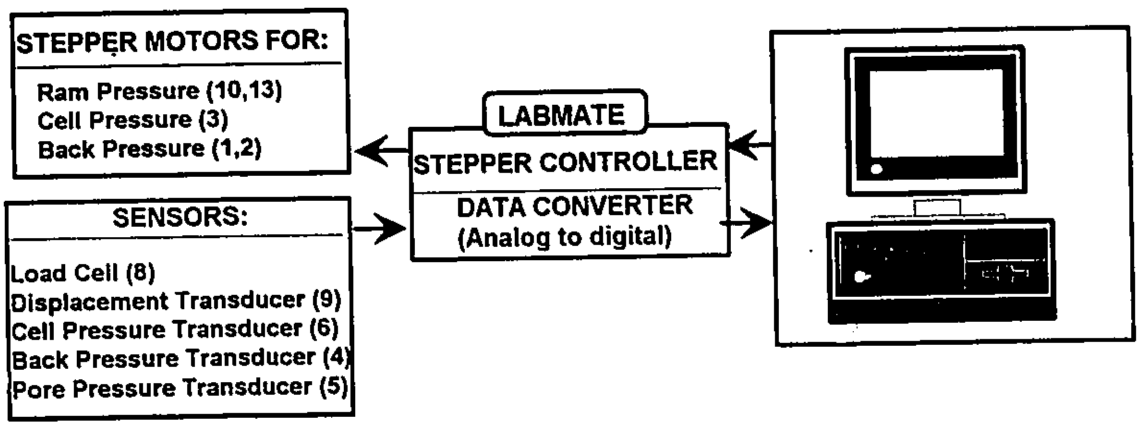

Fig. 5.2. Operation of computer-assisted stress path control system.
(See Fig. 5.1 for explanation of numbers in parentheses)

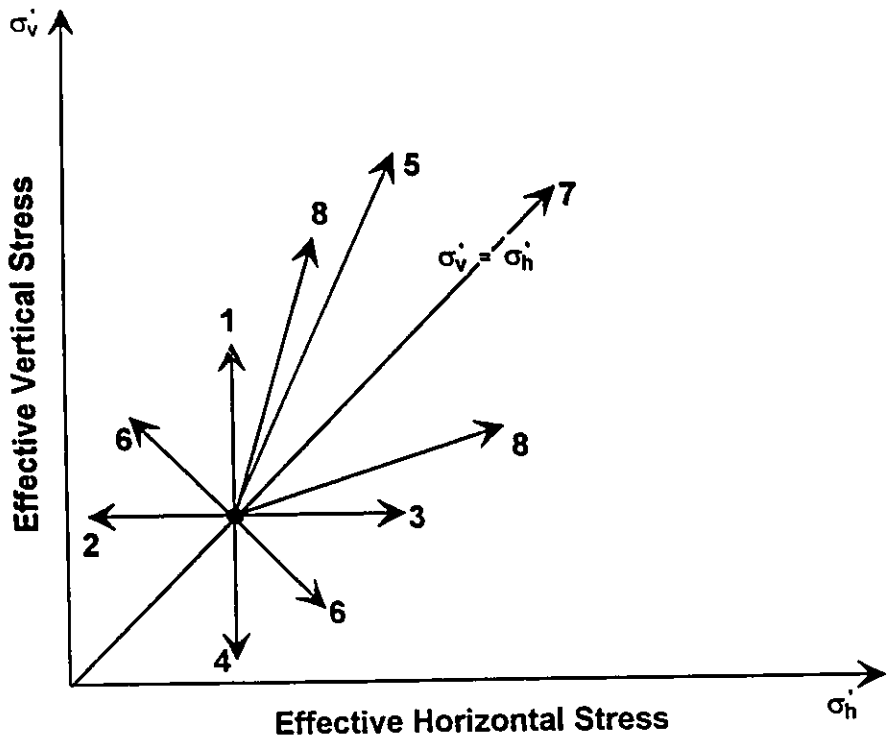

1: **Passive compression**	2: **Active compression**
3: **Passive extension**	4: **Active extension**
5: **Compression or extension at K_0 condition**	6: **Compression or extension at mean pressure**
7: **Isotropic compression**	8: **Any arbitrary stress path**

Fig. 5.3. Possible stress paths in a triaxial space.

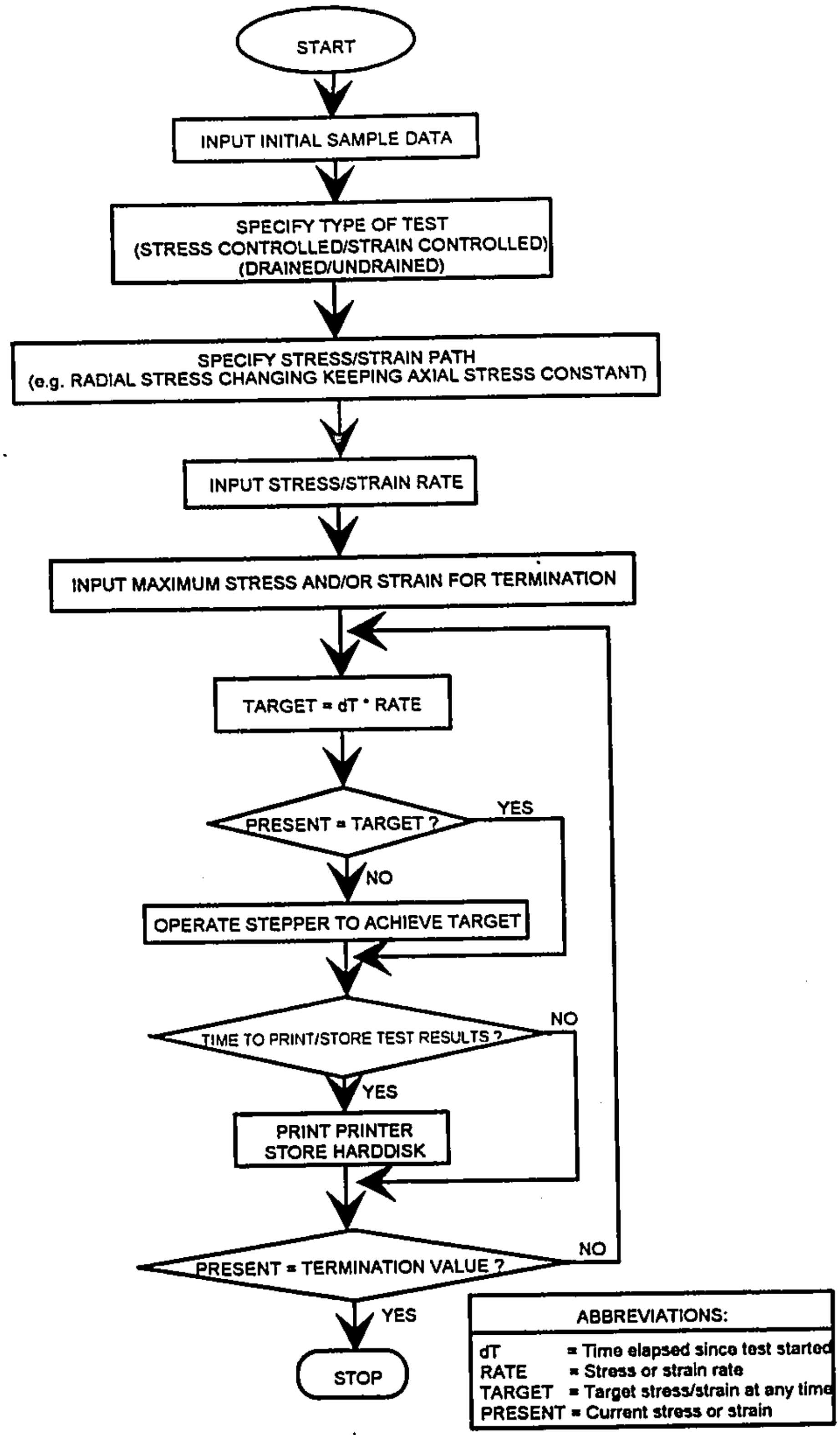

Fig. 5.4. Simplified flow diagram of stress/strain path control program.

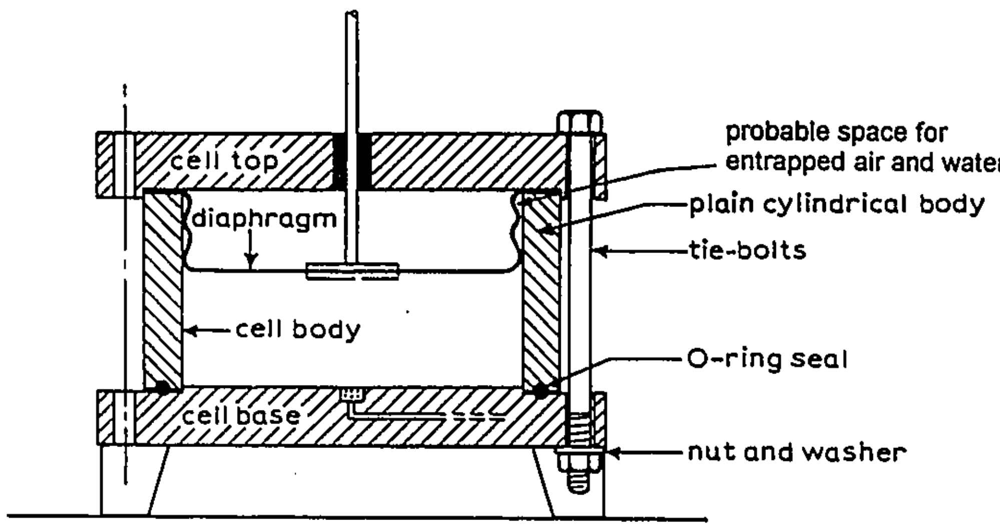

Fig. 5.5. Trapped air and water in a hydraulic consolidometer.

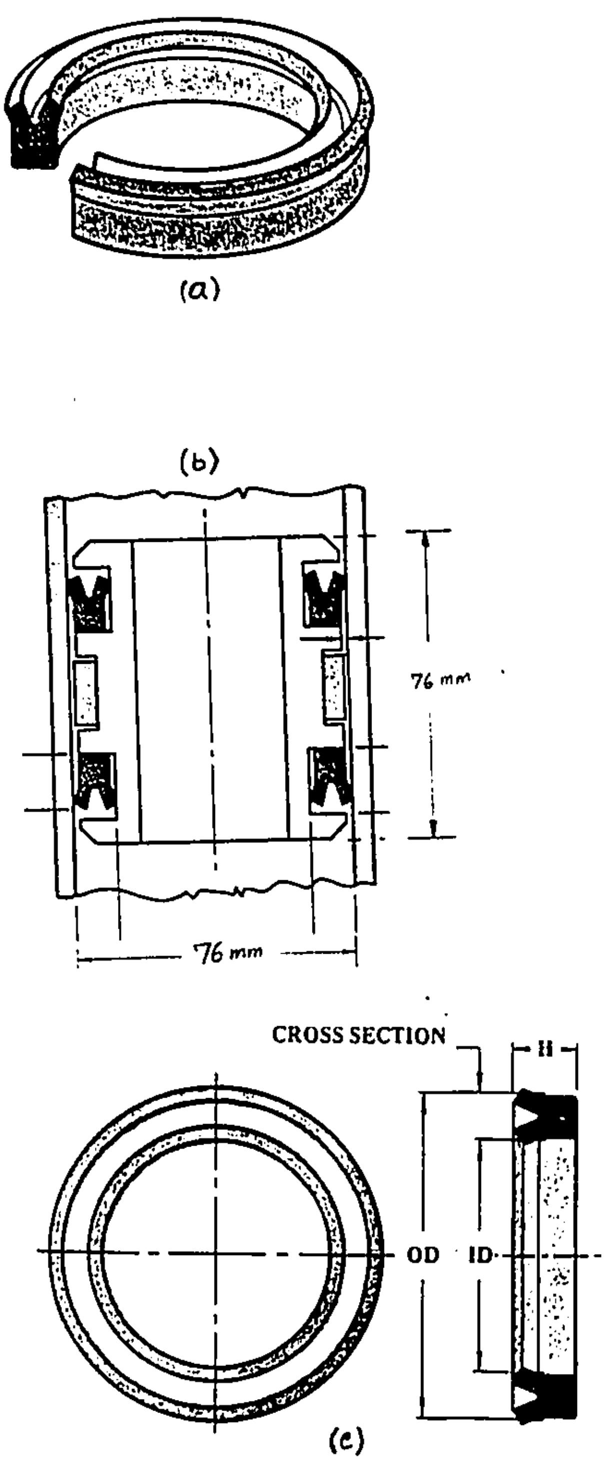

Fig. 5.6. U-cup seal used in a modified hydraulic consolidometer.

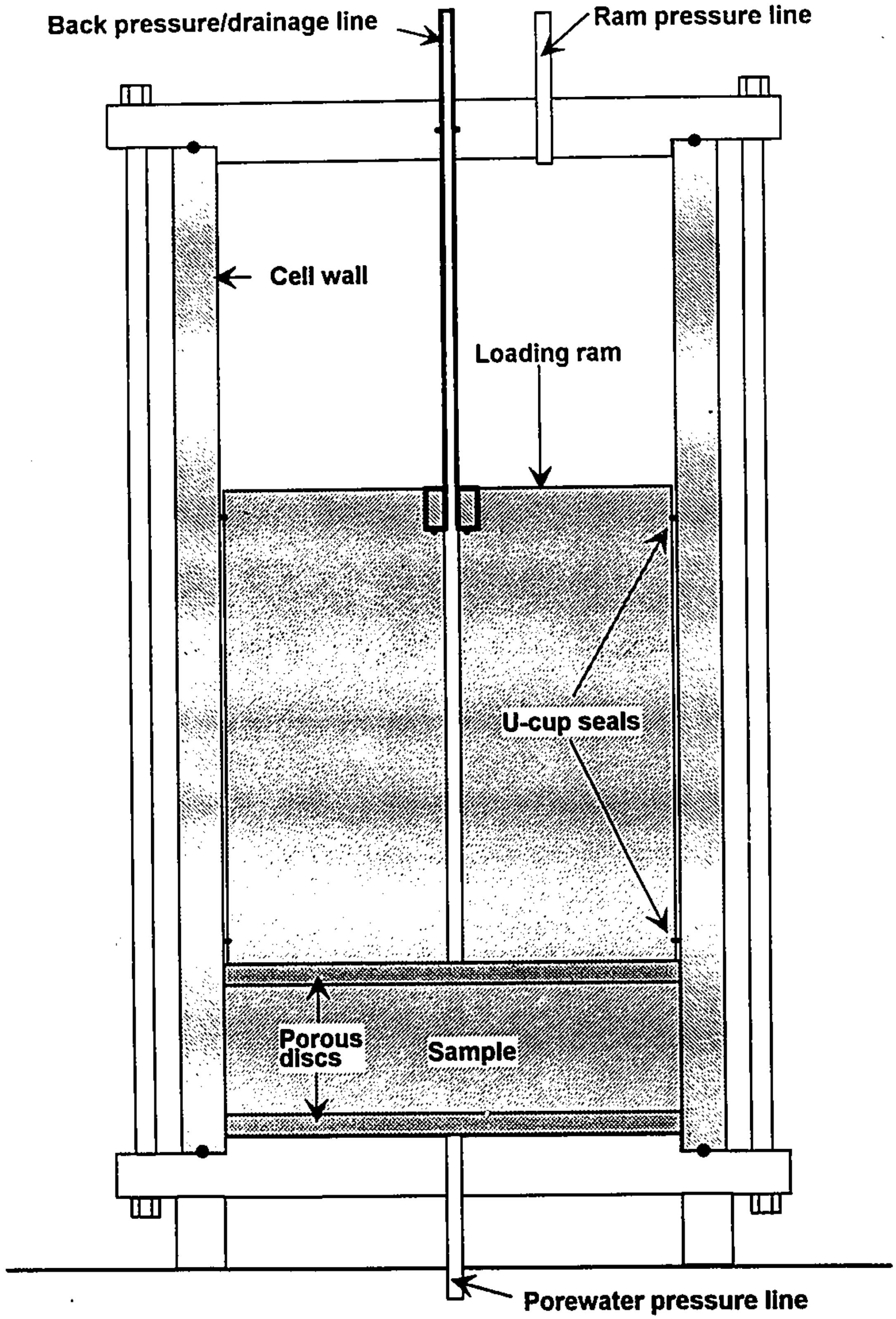

Fig. 5.7. Schematic diagram of modified hydraulic consolidometer.

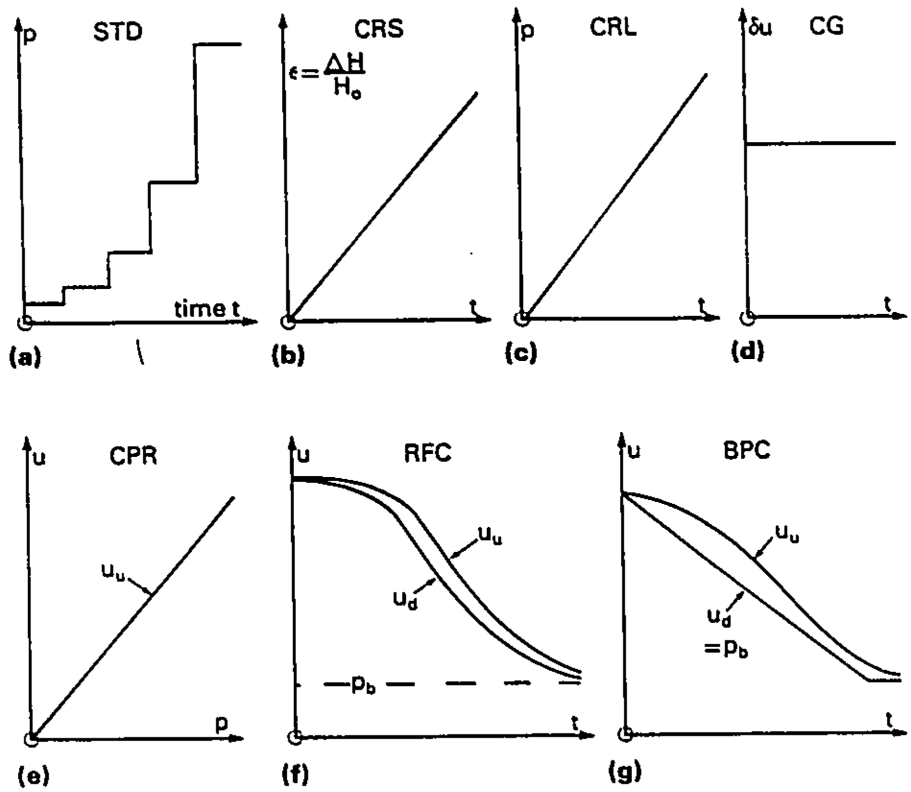

H_0 = initial sample height
ΔH = change in sample height
p = applied consolidation pressure
p_b = back pressure
t = time elapsed from begining of the test
u = pore water pressure
u_u = pore water pressure at the undrained face
u_d = pore water pressure at the undrained face
δu = excess pore water pressure at the undrained face

Fig. 5.8. Loading patterns of various types of consolidation tests.

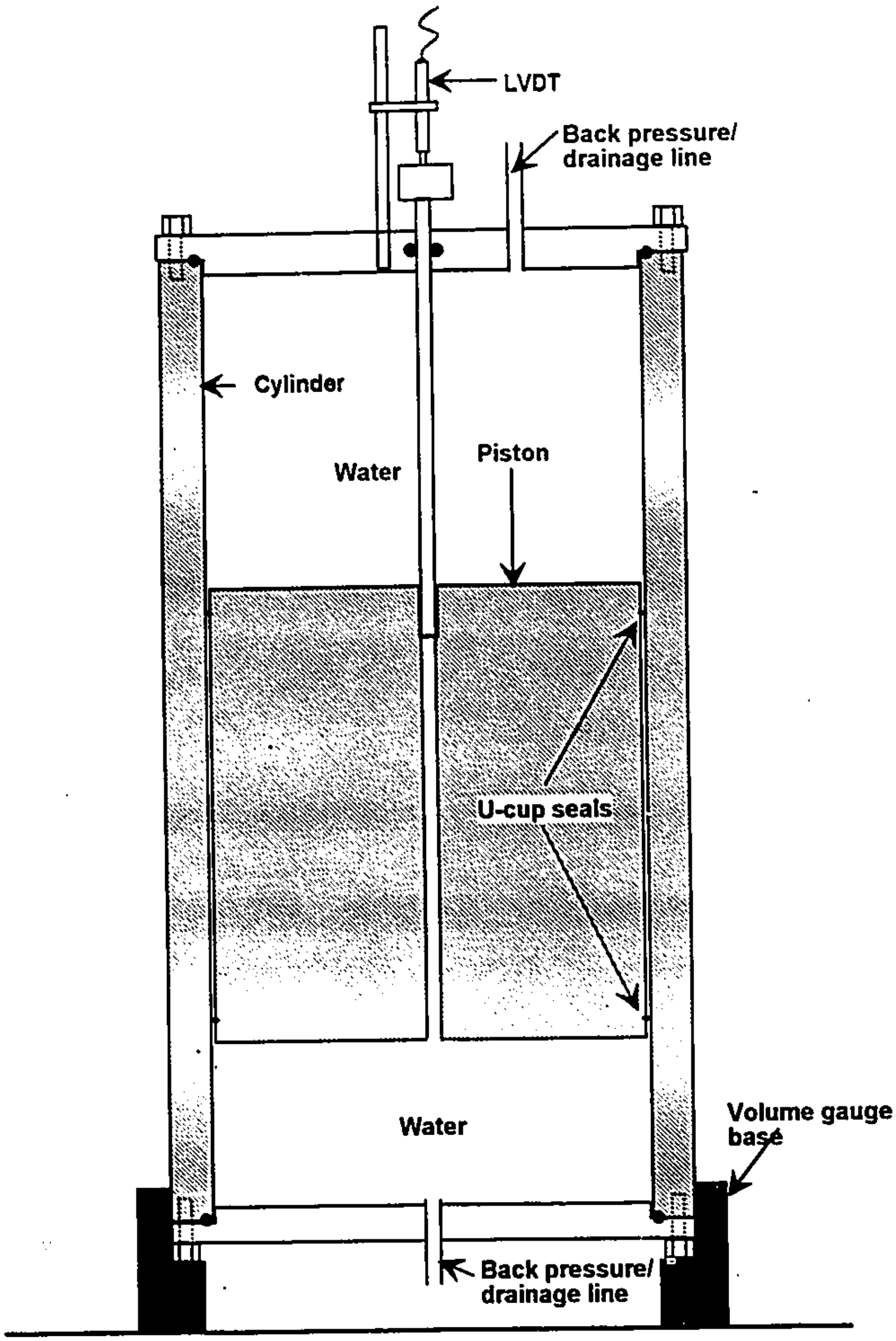

Fig.5.9. Schematic diagram of the new volume gauge.
(See Fig. 5.6 for details of U-cup seals)

CHAPTER 6

DEVELOPMENT OF A METHOD OF K_0 EVALUATION FOR OVERCONSOLIDATED CLAYS

6.1 Introduction

Most of the laboratory testing methods available for the evaluation of *in situ* horizontal stresses are applicable to normally consolidated or lightly overconsolidated clays. This chapter describes a new laboratory method for the determination of *in situ* horizontal stresses of heavily overconsolidated clays using a stress path triaxial apparatus. The proposed method is based on the concept that if the radial stress exceeds the *in situ* horizontal stress, while maintaining the axial stress constant and equal to the *in situ* vertical effective stress, only then will the sample experience significant axial strain. The results obtained for undisturbed samples of an overconsolidated clay crust are found to be in agreement with some available methods. For verification of the applicability of the proposed method, K_0 was determined for artificially prepared samples which had been subjected to known stress paths simulating field stress history.

It is well recognized that the representative strength-deformation behaviour of a soil, specially of an overconsolidated clay, cannot be evaluated unless the *in situ* stresses are known (Henkel 1970). The evaluation of *in situ* stresses in the overconsolidated clay crust is important for problems related to foundations, excavations, and numerical analyses. The *in situ* vertical effective stress at any depth can be easily determined if the unit weight of the soil and location of the water table are known; but the determination of horizontal stress is not easy. Moreover, the determination of horizontal stress for an overconsolidated clay is more problematic than that of a normally consolidated clay. Direct measurements of *in situ* horizontal stresses by field testing methods (e.g., Kenney 1967; Bjerrum and Andersen 1972; Massarsch 1975; Massarsch et al. 1975; Marchetti 1980; Handy et al. 1982; Lutenegger and Timian 1986; Jefferies 1988;) are difficult and introduce uncertainty as a result of changes to initial stress state during installation of the various devices (Tavenas et al. 1975). The hydraulic fracturing method (Bjerrum and Andersen 1972) is applicable only to normally consolidated and lightly overconsolidated clays (Jamiolkowski et al. 1985). Also, there does not appear to be a suitable laboratory method which can be used for the determination of *in situ* horizontal stresses of overconsolidated clays. The only known laboratory test method, for the measurement of *in situ* stresses, was the use of oedometer developed by Skempton (1961). The horizontal stresses determined by this method are normally lower than those of *in situ* values (Skempton and Sowa 1963; Canadian Geotechnical Society 1985). Other methods such as those developed by Becker et al. (1987), and Mesri and Castro (1987) are not applicable to shallow desiccated clay crust found in Eastern Ontario, as discussed later in this chapter.

While there are a number of laboratory methods available for the estimation of K_0 for normally consolidated or slightly overconsolidated clays (Bishop and Henkel 1962; Bishop 1958; Campanella and Vaid 1972; Poulos and Davis 1972; Tavenas et al. 1975; Chang et al. 1977), i.e., for clays with $K_0<1$, the techniques for evaluation of K_0 in overconsolidated clays are non-existent. There are some empirical or indirect methods (e.g., Brooker and Ireland 1965; Mayne and Kulhawy 1982) available for the determination of *in situ* stresses of heavily overconsolidated clays, but all of these methods are dependent on a combination of laboratory tests, such as oedometer consolidation, Atterberg limits determination,or triaxial tests.

Jaky's (1948) well known equation ($K_0 = 1 - \sin\phi'$) is not applicable to overconsolidated clays.

6.2 Stress History of Overconsolidated Clays

A typical stress history of an overconsolidated clay in the field is shown in Fig. 6.1a. The line AB indicates the stress path due to sedimentation process, during which the soil is normally consolidated under K_0 condition. The stress path BC indicates unloading due to some erosional process. The soil is overconsolidated along the stress path BC. Point C is the *in situ* condition with present stresses σ_{h0}' and σ_{v0}'. After subsequent sampling and preparation for laboratory testing, both vertical and horizontal stresses become equal since the total stress as well as the pore water pressure in the sample is isotropic. In the ideal case of perfectly undisturbed sampling, this isotropic stress state lies at point D', located above point D. The state of stress of such a sample may be slightly lower than or equal to point D' on the line AE depending on whether the negative pore water pressure developed in the sample is less than or equal to the mean *in situ* stress. Generally, the state of stress of the prepared specimen has been observed to be less than that at point D' (Skempton and Sowa 1963). Similar observations have also been made in the present investigation.

6.3 The Proposed Method

The proposed method is based on the concept that if an undisturbed overconsolidated soil sample is consolidated isotropically to a stress equivalent to the effective *in situ* vertical stress (σ_{v0}'), and subsequently the radial stress is increased while maintaining the *in situ* vertical stress constant, the sample will experience significant axial strain only when the radial stress exceeds the *in situ* horizontal stress (σ_{h0}'). The concept is illustrated in Fig. 6.1. During the first stage, the sample is consolidated isotropically to the point D where the consolidation pressure is equal to σ_{v0}'. During the second stage, the radial stress (σ_h') is increased while maintaining the axial effective stress constant equal to σ_{v0}'. The sample will experience appreciable axial strain only when σ_h' exceeds σ_{h0}', i.e., when the stress path along DC moves towards right of point C. The corresponding axial strains, which may not necessarily be linear, associated with the stress path are shown in Fig. 6.1(b).

6.4 Testing Procedure

The testing procedure requires a triaxial apparatus with the capability of applying vertical and radial stresses independently to simulate various stress paths. The computer-operated stress path controlled triaxial apparatus discussed in Chapter 5, was used, and is preferable for this purpose.

The sample was initially consolidated to an effective cell pressure equal to the *in situ* effective vertical stress using a back pressure equal to *in situ* pore water pressure. After full consolidation, the test was continued fully drained by increasing radial stress (cell pressure) while keeping the vertical effective stress constant. The rate of application of the radial stress was 1.0 kPa/hour. The rate was slow enough to ensure full dissipation of excess pore water pressure. Values of cell pressure, back pressure, pore water pressure, load, axial deformation, volume change and lateral deformation were recorded by the computer on its hard disk and were simultaneously printed on the printer at a suitable time interval, generally 5 minutes. The test was stopped automatically when the axial strain exceeded 0.20%.

The resolution of the pressure transducers, used for the measuring cell, back and pore water pressures was 0.3 kPa. Two types of linear variable differential transformers (LVDT) with maximum travel of 50 mm and 25 mm were used. In this study, initially a 50 mm travel LVDT with a resolution of 0.03 mm was used. Subsequently, only the 25 mm travel LVDT with a resolution of 0.01 mm was used since the allowable maximum axial displacement was only approximately 0.2 mm for a sample 100 mm in height and 50 mm in diameter.

6.5 Interpretation of Test Data

Among the various data recorded during the test, only the axial strain, cell pressure and back pressure measurements are required for the evaluation of σ_{h0}' using the proposed technique. Test results are plotted on a graph with the σ_h' along the ordinate and the axial extension strain along the abscissa.

An ideal shape of this plot for a truly undisturbed sample is shown in Fig. 6.2, where an abrupt transition must occur when σ_h' exceeds σ_{h0}'. The abruptness of transition is also a function of the resolution of the measuring devices. In practice, this location of σ_{h0}' is not immediately obvious, since experimental data points show a gradual transition as indicated by the curved line in Fig. 6.2. In such cases, the value of σ_{h0}' can be determined by projecting the straight line portion of the inclined arm on the σ_h' axis. The axial extension strain versus σ_h' measurements for undisturbed samples of a weathered crust material are shown in Figs. 6.3(a) - 6.3(f).

6.6 Verification of The Method Using Samples of Known Stress Histories

In order to verify the suitability of the proposed method,some soil samples were artificially prepared to induce a typical stress history of an overconsolidated soil in the field. After simulating a known stress history, the sample was tested to verify whether the proposed method would indicate the same horizontal stress as the one imposed artificially. Preparation of samples and testing method for simulating stress history are described below.

6.6.1 Sample Preparation

The soils used for these artificial samples were obtained from the trimmings of undisturbed samples of weathered crust material overlying the Champlain clay, and for which determination of σ_{h0}' had earlier been made. The original undisturbed samples were overconsolidated and were collected from shallow depths of 1.0-4.0 m. The trimmings were hand-broken into small pieces and then blended into slurry in a large mixing machine. The water content of the slurry was approximately 70% which was well above the liquid limit (45%) of the soil. The slurry was consolidated to a water content (approximately 40%) below the liquid limit in a 50 mm internal diameter cylinder. Dead loads were applied on top of the slurried sample for consolidation. This stage of consolidation was necessary to provide the slurry enough consistency so that it could be easily handled for sample preparation. The vertical consolidation pressures applied in this manner were less than 50 kPa. When the required consolidation was achieved, the sample was extruded from the cylinder and was trimmed at top and bottom to obtain a cylindrical sample, 100 mm high x 50 mm in diameter. The sample was then placed in a computer controlled stress path triaxial cell for further testing as described below.

6.6.2 Simulation of Field Stress History

Two different techniques were used to anisotropically consolidate the samples to the K_0 values greater than unity ($\sigma_h' > \sigma_v'$).

(i) The first method simulated the anisotropic *in situ* stress state in the sample without taking into account the likely field stress history of an overconsolidated soil. In this method, the samples were consolidated arbitrarily to some anisotropic stress state such that $K_c>1$. The consolidation stresses were applied simultaneously in vertical (1.0 kPa/hour) and horizontal directions, where the horizontal stress rate was greater than that of the vertical to provide a value of K_c greater than unity. These rates were, however, slow enough to ensure full consolidation during the test. A condition of zero lateral strain was not maintained during the consolidation stage; hence the final consolidation stress ratio is strictly K_c not K_0. The stress path for this anisotropic consolidation is a straight line from point A to point C in Fig. 6.1, where point C indicates the simulated *in situ* stress.

(ii) The second method attempts to reproduce a more realistic field stress history of an overconsolidated soil. In this method, the sample was brought to its overconsolidated state by consolidating and unloading under K_0 ($\varepsilon_h=0$) condition. The condition of null lateral strain was maintained by using a specially designed K_0 ring equipped with a Hall Effect semiconductor in a manner similar to that described by Clayton et al. (1989). The fine resolution of the device, capable of measuring radial deformation to a precision of 4 μm, made a more realistic simulation of K_0 condition possible than has previously been reported. It is of interest to note that in the classical studies on K_0 determination by Brooker and Ireland (1965), the resolution of lateral deformation indicator was four times coarser than the one used in this research.

The sample was normally consolidated under K_0 condition from point A to point B (Fig. 6.1). During this stage, the vertical stress was increased slowly (1.0 kPa/hour) so that there was no excess pore water pressure developed. The lateral displacement transducer activated an increase in the horizontal stress to maintain the condition of zero lateral strain. In order to simulate the unloading in the field due to some erosional process, the sample was unloaded axially in a drained condition, also under condition of zero lateral strain. Due to continuous unloading in the axial direction, the sample tended to deform laterally (decrease in diameter). The horizontal stress was automatically decreased to counteract this tendency. This process was continued until the desired stress level point C corresponding to the assumed *in situ* stress was achieved.

After achieving the *in situ* stress conditions of an overconsolidated soil by either of the above two methods, sampling was simulated by decreasing both vertical and horizontal stresses simultaneously to zero with the drainage valves being closed. There is a slight uncertainty in the simulation of sampling in this manner, since in reality the sample may tend to expand as the total stress is released. This expansion may induce smaller negative pore water pressure than would otherwise develop in an ideal sample where no volume change under undrained loading occurs. This negative pore water pressure is likely to be small for a fissured soil. Since the drainage valves were closed while unloading to simulate sampling, the residual stress developed in the sample is approximately equal to the mean *in situ* effective stress. In order to verify the effect of drainage conditions during the sampling simulation technique, the drainage valves were left open for 30 minutes during this stage for two samples only (sample Nos. RMD11A and RMD31). It was found that the above procedure did not have any effect on the estimation of *in situ* horizontal stresses.

After the sampling simulation stage, all specimen were left in the triaxial cell for 24 hours with drainage valves closed to simulate storage. The proposed technique was then applied from this stage to determine the *in situ* horizontal stresses.

6.7 Discussion of Test Results

6.7.1 Undisturbed Samples

The undisturbed samples, used in this study, were also obtained from the weathered clay crust overlying Champlain clay in the Fallowfield site. These samples were either obtained by using 250 mm diameter Sherbrooke sampler (Lefebvre and Poulin 1979) or from 225 mm cubical hand-cut blocks from test pits. The crust at this site was typically 3 to 4 m thick. Test results indicated a plasticity index of 22, and an effective angle of internal friction varying between 27° and 30°. An indication of low sample disturbance is provided by the values of recompression strain measured at the *in situ* effective vertical stress in the oedometer tests (Holtz et al. 1986). The average value for the four oedometer tests used in this study is 0.48% which indicates that the ratio of the measured preconsolidation stress to the "best estimate" (Fig. 2 in Holtz et al. 1986) is approximately 0.95, and is a measure of the high quality of these samples.

As a part of a detailed study of this clay crust, other field tests (dilatometer, piezocone, pressuremeter, and field vane) and laboratory tests (stress path triaxial shear, oedometer consolidation, Atterberg limits, and other routine tests) were conducted. A detailed discussion of these test results are given in Chapters 3, 7, and 8. However, the pertinent profiles from dilatometer and self-boring pressuremeter tests used in subsequent analysis are shown in Figs. 6.4 and 6.5, respectively.

The results of axial extension strains versus effective horizontal stresses obtained from the experimental data for six undisturbed samples are plotted in Figs. 6.3(a) - 6.3(f). The values of σ_{h0}' and hence the K_0 values determined by the proposed method are shown in the respective figures.

It is emphasized that the stress-strain relationships shown in Fig. 6.3 correspond to the very early portion of the complete stress-strain curves, at less than 0.20% axial strain. It is therefore important to note that the estimated value of σ_h' at zero axial strain as determined by the proposed technique is *not* related to the conventional estimate of "yielding" indicated in a complete stress-strain curve. This is exemplified in Fig. 6.3(d) where Test No. BS308T2 was continued to a higher strain of approximately 3.3%. The initiation of "yielding", in this test, occurs at axial strain of approximately 0.40%.

The K_0 values evaluated by the proposed method have been compared to those obtained from the other available methods which have been proposed for overconsolidated soils, and are shown in Table 6.1. These include the following techniques:

(a) The dilatometer test (DMT) developed by Marchetti (1980). Fig. 6.4 shows the profile of DMT parameters p_0, p_1, K_D, OCR and K_0 for the site. These profiles were obtained from two test runs conducted at a spacing of 1.5 m. The values of K_0 were obtained from the following empirical equation:

$$K_0 = \left(\frac{K_D}{1.5}\right)^{0.47} - 0.6 \qquad (6.1)$$

where,

$K_D = \frac{p_0 - u_0}{\sigma_{v0}'}$ = Horizontal Stress Index,

p_0 = pressure required to start the expansion of the membrane,

σ_{v0}' = initial effective overburden pressure,

u_0 = *in situ* pore water pressure.

(b) The self-boring pressuremeter (SBP) test where the initial "lift-off" pressure from visual inspection is considered as a measurement of σ_{h0}' (Ghionna et al. 1985). Fig. 6.5 shows the profile of σ_{h0}' and the estimated K_0.

(c) The oedometer consolidation test (Tavenas et al. 1975). In this method, the ratio of horizontal preconsolidation stress σ_{hp}' to vertical preconsolidation stress σ_{vp}' as determined by oedometer tests is suggested as the value of the *in situ* K_0 at "any given site" , i.e.,

$$K_0 = \frac{\sigma_{hp}'}{\sigma_{vp}'} \qquad (6.2)$$

The values of σ_{hp}' is determined by testing a sample oriented along the horizontal direction in a conventional oedometer. Relevant test data from the oedometer tests are shown in Table 6.1 and Fig. 6.6.

(d) The oedometer consolidation test (Mahar and O'Neill 1983) which is similar to method (c). In this method, the ratio of consolidation pressure of a horizontally oriented sample to that of a vertically oriented sample, in the normally consolidated pressure range for the same void ratio, is considered as the *in situ* K_0. Since the ratio was not constant in the normal consolidation range, K_0 was determined as the average from three void ratio levels indicated by points 1,2 and 3 in Fig. 6.6.

(e) The empirical correlation chart developed by Brooker and Ireland (1965). In this method, the determination of K_0 requires a knowledge of the plasticity index as well as of the overconsolidation ratio.

(f) The empirical relationship developed by Mayne and Kulhawy (1982) where the effective friction angle (ϕ') and previous stress history (OCR) from the previously published data have been correlated to the values of K_0. The following empirical formula was suggested:

$$K_0 = (1 - \sin\phi')(OCR)^{\sin\phi'} \tag{6.3}$$

The form of the above equation was first suggested by Schmidt (1966), and subsequently modified by Mayne and Kulhawy (1982).

Table 6.1 and Fig. 6.7 show that the results obtained by the proposed method compare reasonably well with those from methods (a), (e), and (f). It should be noted that the self-boring pressuremeter, method (b) shows significantly higher K_0 values whereas the oedometer test methods (c) and (d) provide appreciably lower estimates. Higher estimates of K_0 by the pressuremeter may be due to the use of the lift-off pressure which is associated with the development of passive pressure (significantly higher than σ_{h0}') during the expansion of the diaphragm. Higher values of K_0 from SBP tests were also obtained by Ghionna et al. (1985, Fig. 1d) for highly overconsolidated Taranto clay. In this study, the average value of K_0 obtained from the Brooker and Ireland (1965) method is approximately 2.5 whereas those obtained from SBP tests range between 3 and 5.6.

The inability of the oedometer test method (c) to predict $K_0 > 1$ is not surprising since a natural soil does not show preconsolidation pressure in a horizontal direction higher than in the vertical direction. The oedometer test method (d) on the other hand, relies on the data for vertically and horizontally trimmed samples in the normally consolidated range only. This method can only estimate maximum values of K_0 close to unity as long as there is no significant difference in soil structures in the two directions.

Two other methods using oedometer tests, Becker et al. (1987), and Mesri and Castro (1987) are cited in the literature for estimation of K_0. The method by Becker et al. (1987), which analyses oedometer tests on horizontally and vertically trimmed samples of clay using work as a criterion for determining *in situ* stresses, is not suitable for clays at low stress levels such as the shallow overconsolidated clay crust overlying Champlain clay in Eastern Ontario. In this method, the consolidation data are plotted in a work/unit volume versus effective stress space. Two transition points are expected from this curve, one at the *in situ* stress and the other at the yield (preconsolidation) stress. In the present investigations, the yield stress was easily obtained, however, the transition at *in situ* stress was not obvious. The *in situ* stresses were too low to obtain adequate number of data points to provide a noticeable transition at the *in situ* stress. The method suggested by Mesri and Castro (1987) is valid only for those cases where the overconsolidation is due to secondary (delayed) compression, and K_0 obtained by this method will never exceed unity. This method cannot be applied to soils where the overconsolidation is due to unloading, desiccation, or cementation.

6.7.2 Artificially Prepared Samples

The axial strains versus σ_h' for artificially prepared samples are plotted in Figs. 6.8 and 6.9. Figures 6.8(a)-6.8(c) show results for samples consolidated anisotropically using the first method, while Figs. 6.9(a) and 6.9(b) show corresponding data for samples with imposed stress history using the second method. The estimated and simulated *in situ* stress parameters are compared in Tables 6.2 and 6.3. In both cases, the proposed method determines simulated σ_{h0}' correctly. It is noticeable from Table 6.3 that the K_0 values estimated from other empirical methods (Brooker and Ireland 1965; Mayne and Kulhawy 1982) consistently indicate smaller values of K_0.

In the first method, the samples were normally consolidated, to an anisotropic stress state with $\sigma_h'>\sigma_v'$. This is unrealistic, since a truly normally consolidated sample in the field cannot be subjected to $\sigma_h'>\sigma_v'$. Even though Method 1 did not simulate overconsolidation on the samples, the purpose of this method was to investigate whether the proposed technique would successfully estimate the previously imposed maximum horizontal stress. The estimated stresses are equal to or very close to the imposed horizontal stresses.

The artificially prepared samples using Method 2 show a significant scatter in observed data points than for the undisturbed samples collected from the field. This scatter may be due to the fact that the laboratory simulations of stress history are done in a short time where the aging effect is absent.

Since the triaxial tests were conducted using computerized servo-controlled apparatus, it is possible to relate the measured values of K_0 to OCR for the two artificially prepared samples by Method 2. This relationship is shown in Fig. 6.10. It should be noted, however, that the verification of the proposed technique was carried out only at overconsolidation ratios of 7.1 and 9.7. These stress states were achieved at the end of unloading of the two samples. The results of K_0 determinations for all undisturbed samples are also shown in Fig. 6.10. The fit is remarkable and indicates that the K_0-OCR relationship for a soil is not significantly affected by its structure. Clearly, equation 6.3 suggested by Mayne and Kulhawy (1982) overestimates K_0 for this clay crust.

Table 6.1 In situ stress parameters for undisturbed clay estimated by proposed and other methods.

Sample No.	Depth (m)	σ_{v0}' (kPa)	Proposed Method σ_{h0}' (kPa)	Proposed Method K_0	Oedometer Tests σ_{vp}' (kPa)	Oedometer Tests σ_{hp}' (kPa)	OCR	K_0 Estimated by Other Methods Brooker & Ireland (1965)	Mayne & Kulhawy (1982)	Mahar & O'Neil (1983)	Oedometer, Tavenas et al. (1975)	Dilatometer, Marchetti (1980)	SBP, Ghionna et al. (1985)
SB421	1.96	26.0	46.0	1.77	240	250	9.2	1.45	1.50	0.93	1.04	1.75	2.85
SB431	2.07	27.0	47.5	1.76	300	260	11.1	1.70	1.66	0.83	0.87	1.75	2.75
SB433	2.07	27.0	47.0	1.74	300	260	11.1	1.70	1.66	0.83	0.87	1.75	2.75
BS308T2	3.08	34.0	46.0	1.35	155	-	4.6	1.10	1.09	-	-	1.51	2.05
BS333T1	3.33	36.4	45.0	1.24	130	-	3.6	0.90	0.97	-	-	1.49	1.95
BS360T3	3.60	38.1	41.5	1.09	120	-	3.2	0.80	0.92	-	-	1.37	1.80

Table 6.2. Artificially prepared samples with simulated *in situ* stress state (method 1)

Sample No.	Simulated Anisotropic Consolidation σ_{vp}' (kPa)	σ_{hp}' (kPa)	K_c	Evaluation by Proposed Method σ_{hp}' (kPa)	K_c	Error (%)
RMD11	100	140	1.40	136	1.36	2.9
RMD11A	160	200	1.25	200	1.25	-
RMD12	94	150	1.60	150	1.60	-

Table 6.3. Artificially prepared samples with reproduced stress history (method 2)

Sample No.	Normally Consolidated K_0 Loading			K_0 Unloading to Simulated *In situ* condition			Proposed Method		OCR	K_0 by Other Methods	
	σ_v' (kPa)	σ_h' (kPa)	K_0	σ_{v0}' (kPa)	σ_{h0}' (kPa)	K_0	σ_{h0}' (kPa)	K_0		Brooker & Ireland (1965)	Mayne & Kulhawy (1982)
RMD21	300	154	0.51	42	68	1.62	65	1.55	7.1	1.27	1.32
RMD31	300	140	0.48	31	60	1.94	54	1.74	9.7	1.50	1.58

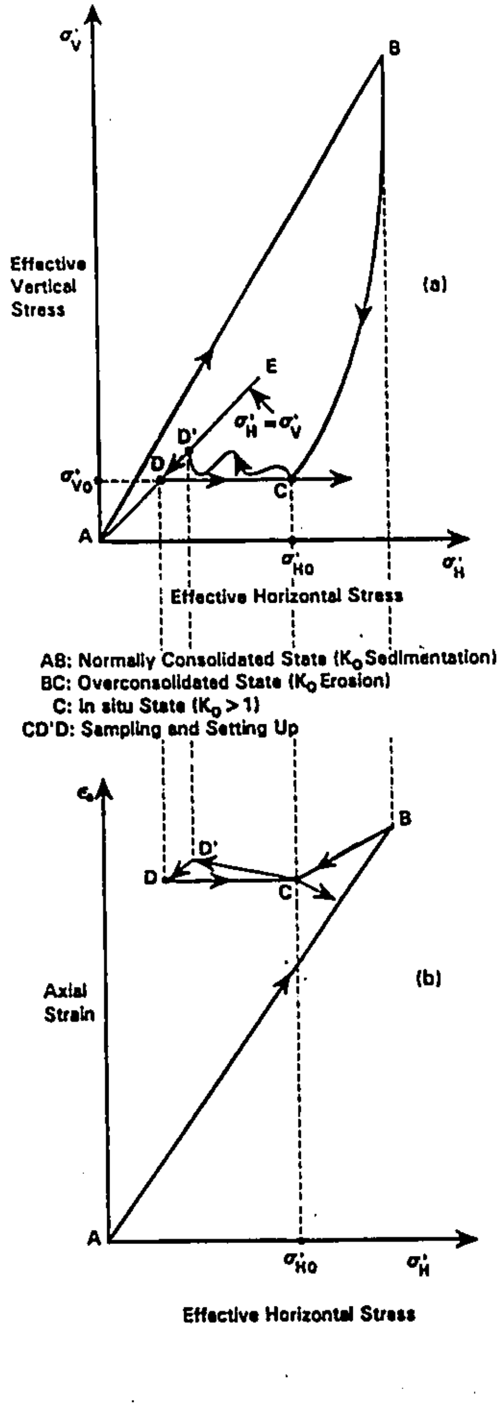

Fig. 6.1. Typical field stress history of overconsolidated clays.

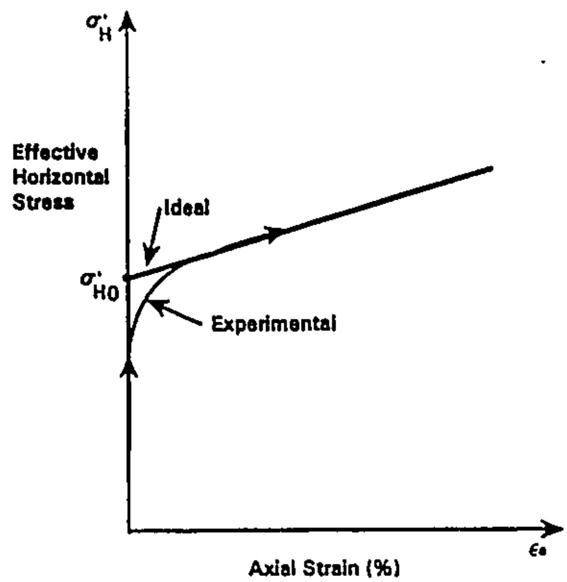

Fig. 6.2. Ideal and experimental ε_a-σ_h' plot.

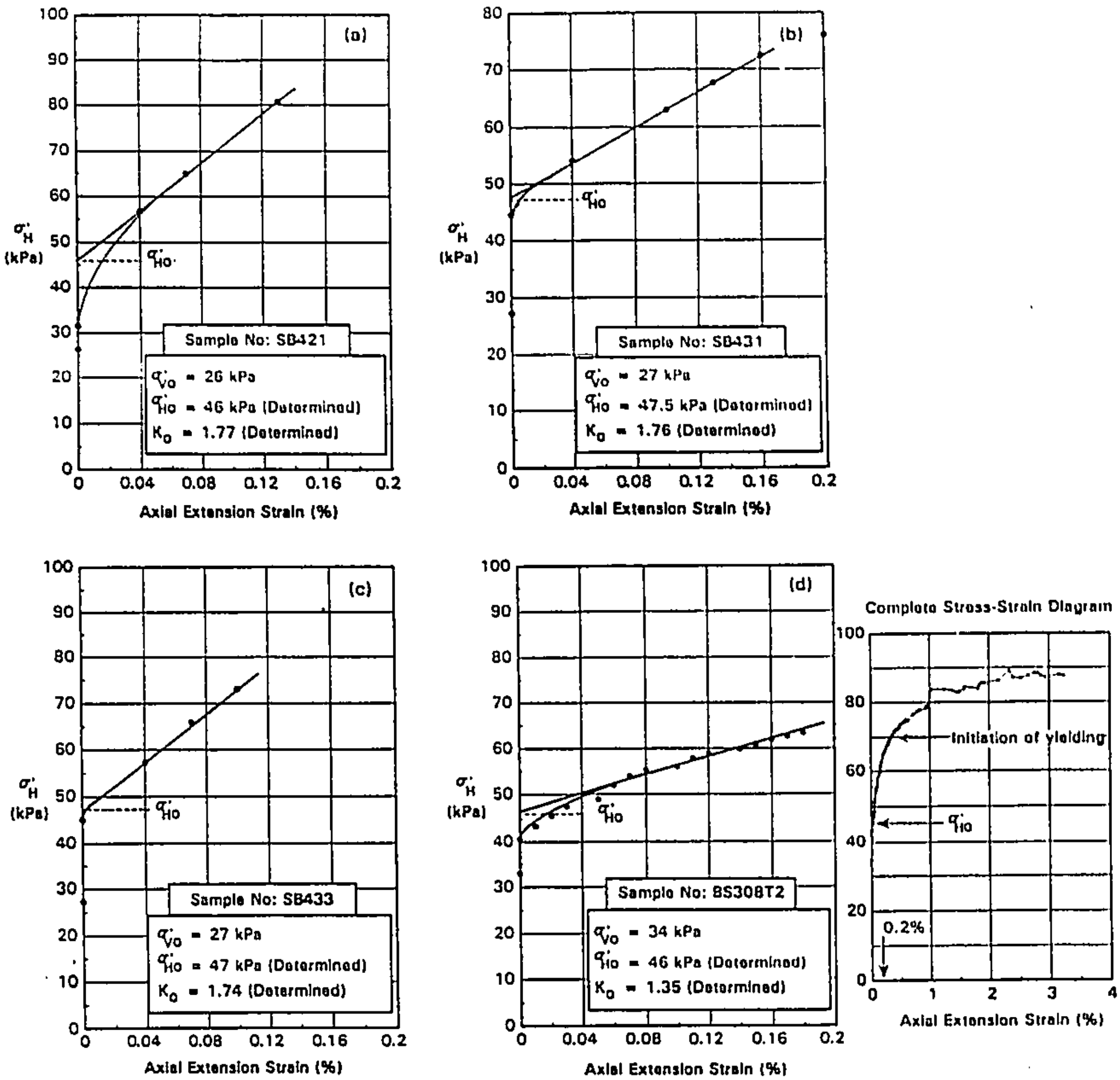

Fig. 6.3. K_0 determination for undisterbed samples of a weathered clay crust.

(Continued to next page)

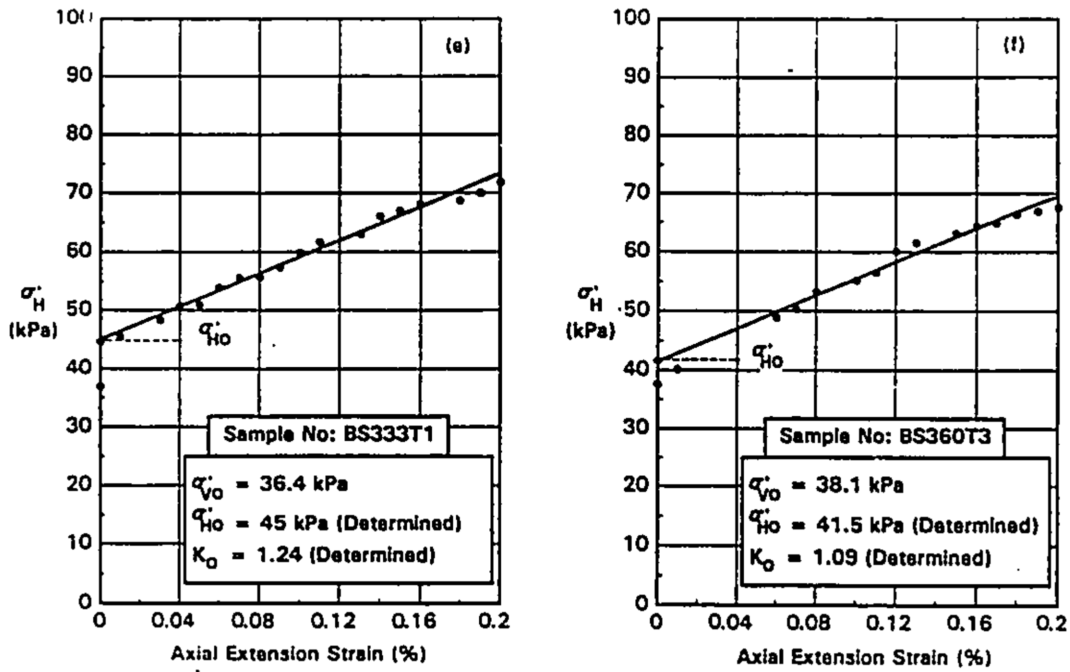

Fig. 6.3. K_0 determination for undisterbed samples of a weathered clay crust.
(Continued from previous page)

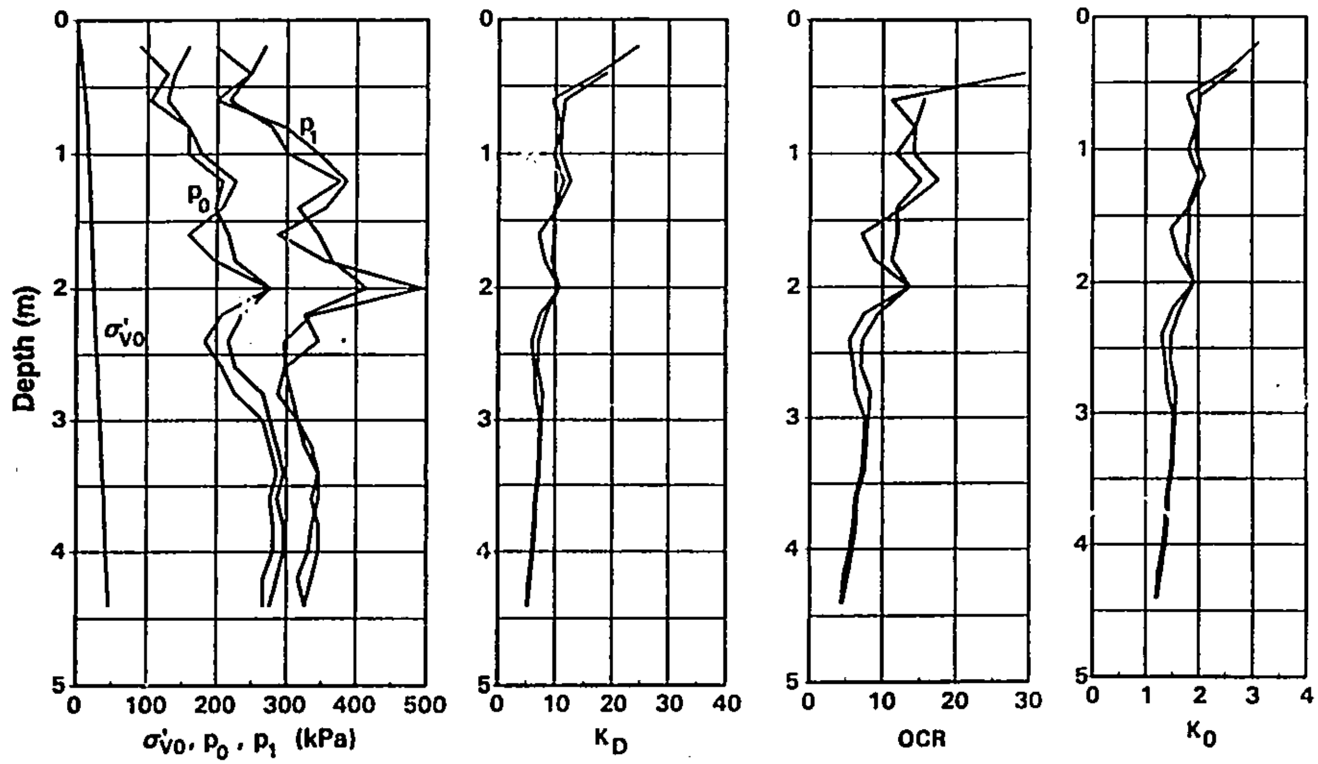

Fig. 6.4. Profiles of dilatometer test results.

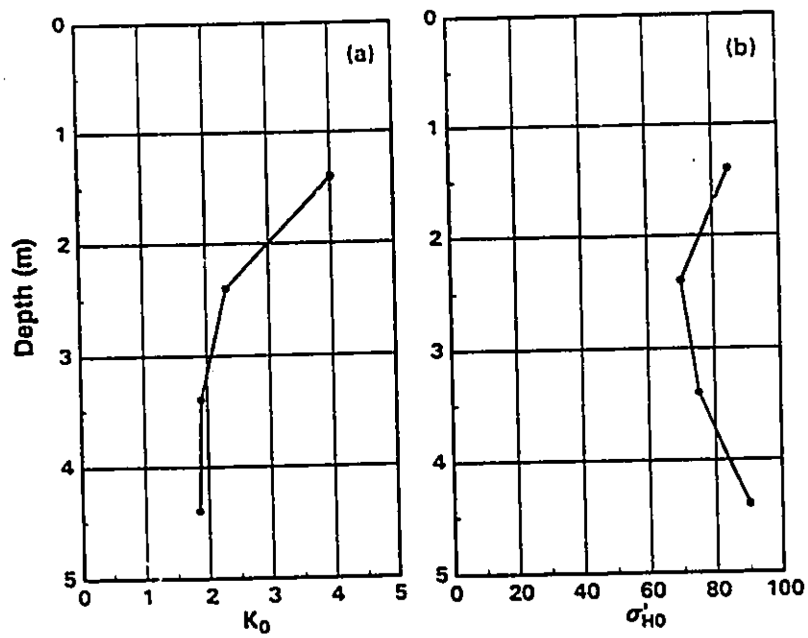

Fig. 6.5. Profiles of self-boring pressuremeter test results.

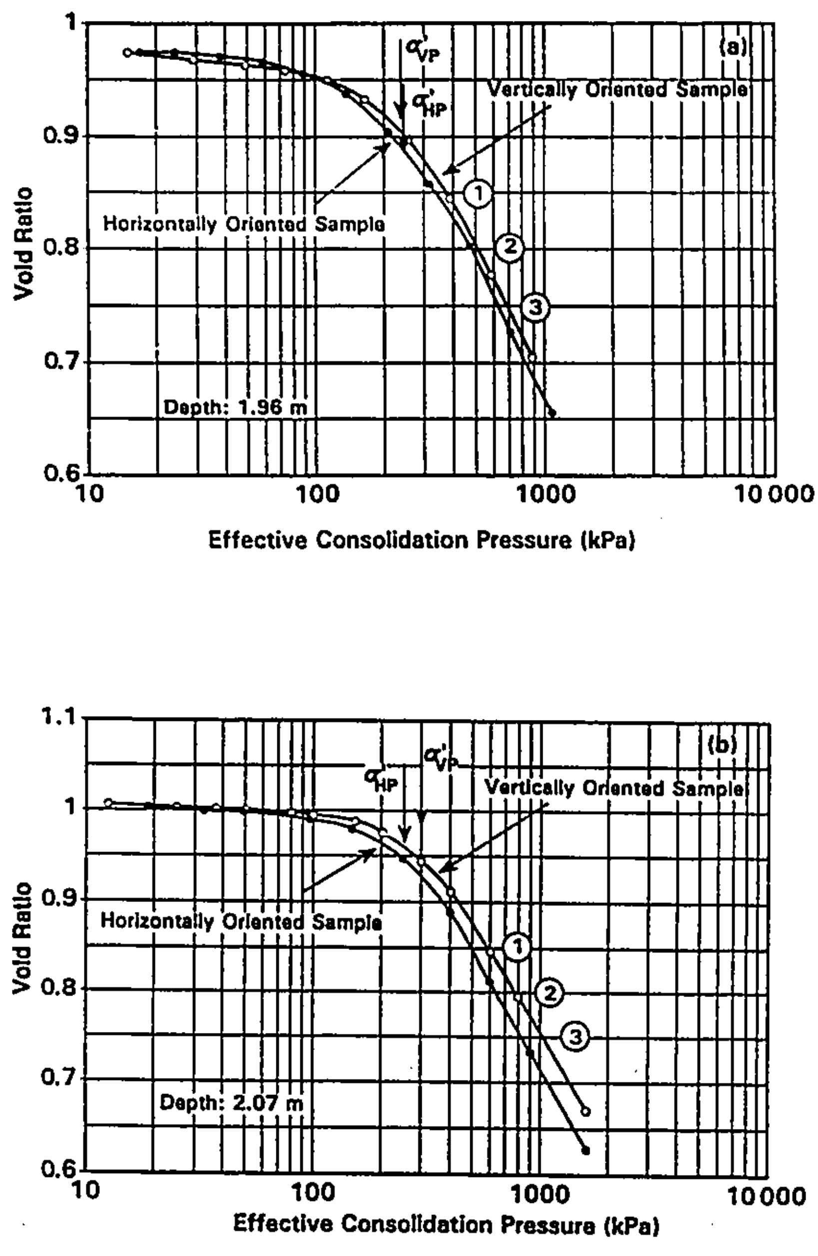

Fig. 6.6. Results from oedometer tests.

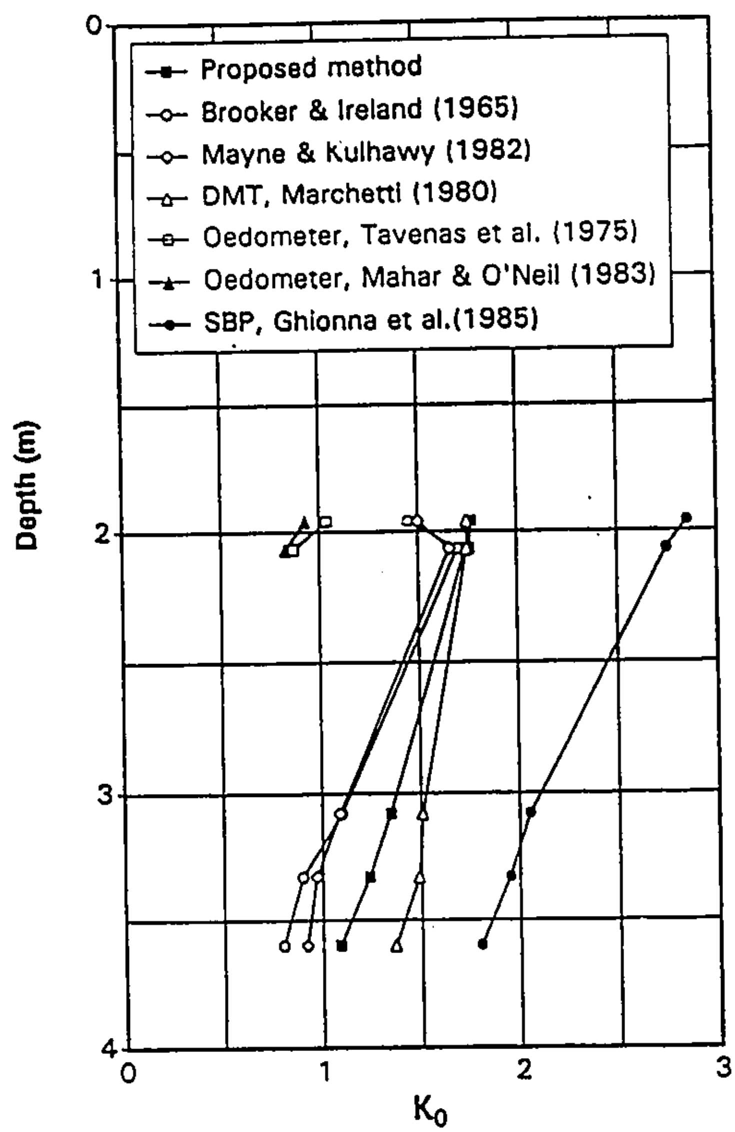

6.7. K_0 for undisturbed clay estimated by proposed and other methods.

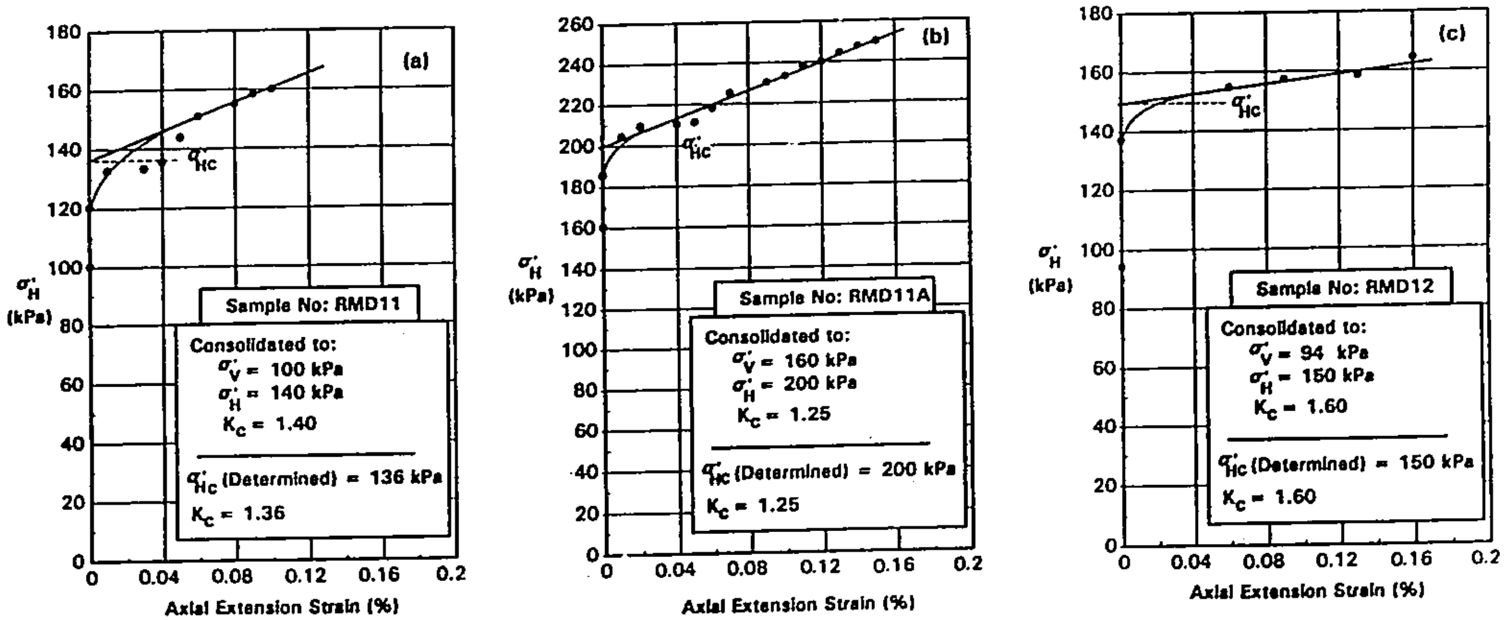

Fig. 6.8. Horizontal stress determination for artificially prepared samples (method 1).

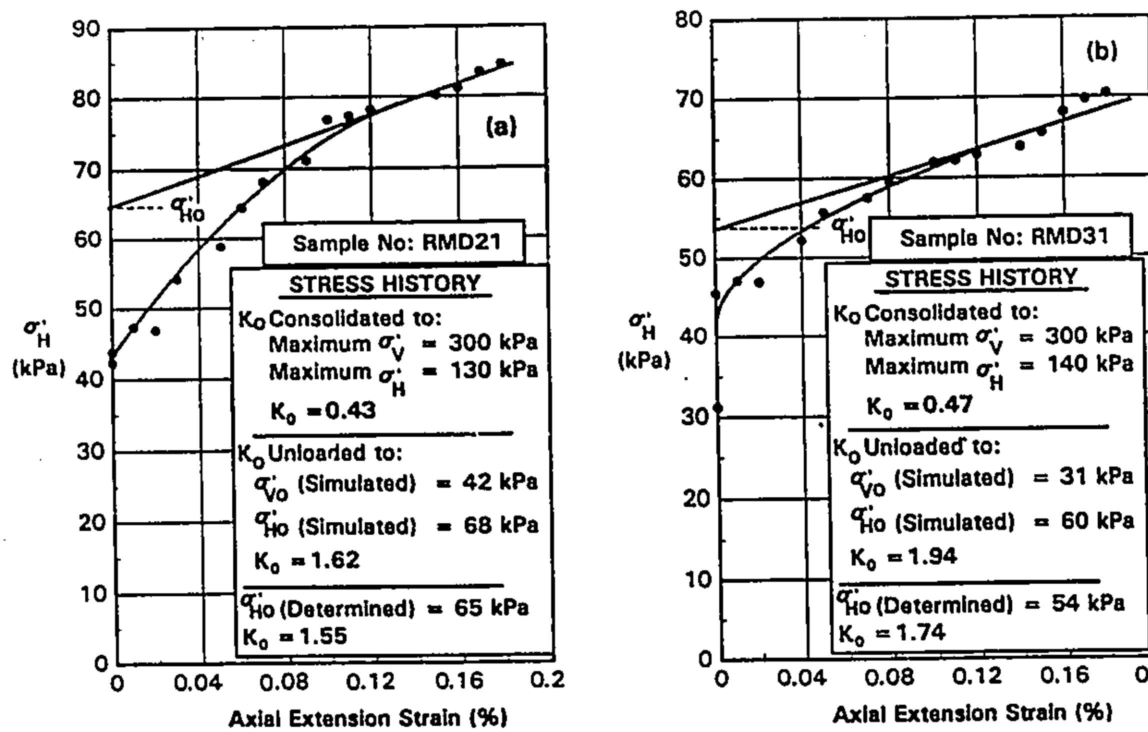

Fig. 6.9. Horizontal stress determination for artificially prepared sampies (method 2).

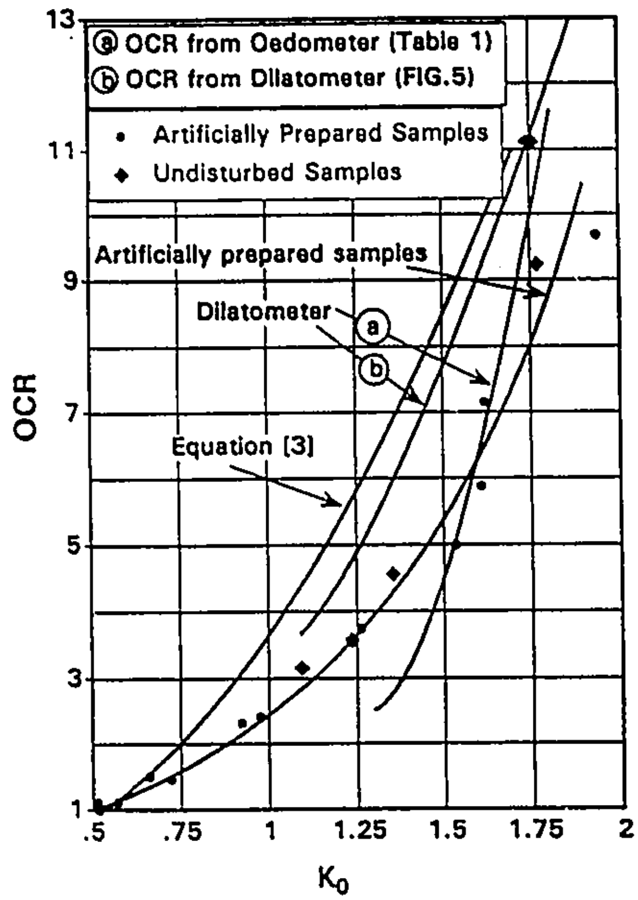

Fig. 6.10. K_0-OCR relationship for artificially prepared and undisturbed samples.

CHAPTER 7

RESULTS AND ANALYSIS OF TRIAXIAL TESTS

This chapter mainly discusses the results of laboratory triaxial tests. However, to provide a preliminary information regarding the soil samples used in the laboratory tests, a brief description of the method of sample collection and the results of routine laboratory tests are given at the beginning of this chapter. The triaxial test results are subsequently presented and discussed.

7.1 Collection of Test Samples

Two types of block samples were collected: hand-cut cubical samples and 250 mm cylindrical samples using the Sherbrooke sampler (Lefebvre and Poulin 1979). Hand-cut block samples were collected in two groups: the first group was collected from 0.40 m to 0.80 m and the second group was collected from 3.0 m to 3.73 m depth. The size of most of these cubes was approximately 225 mm. Some rocks, roots, root-holes and worm-holes were observed in the upper set (0.40 to 0.80 m) of block samples. Limited number of tests were conducted in this group, as shown in Appendix A, because of the uncertainties expected from the presence of these rocks, roots, and holes. Most of the tests were conducted for the depth range of 1.0 m and 3.7 m.

The cylindrical Sherbrooke block samples (Lefebvre and Poulin 1979), approximately 250 mm diameter by 400 mm high, were collected with the help of Geotechnical Section of National Research Council Of Canada (NRCC). These samples were collected from a depth range of 0 - 2.8 m. Uncountable microfissures were observed in both types of samples collected from above 1.75 m depth level.

The locations of these samples with respect to the locations of *in-situ* tests are shown in the site plan (Fig. 3.1). The groundwater table observed, during sample collection and during the *in situ* tests, was at 0.80 m. However, a study of water table fluctuation by O'Shaughnessy (1992) at the same site indicates that the position of water table changes between 0.7 m and 1.1 m in different seasons.

7.2 Routine Laboratory Tests

Routine tests conducted during this research include the determination of bulk unit weight, density of solid particles, natural water content, and grain size. For brevity, only the tabular or graphical form of the test results are provided with short discussions.

In-situ Bulk Unit Weight

The variation of *in-situ* bulk unit weight along the depth is shown in Fig. 7.1a. It is noticeable that the unit weight decreases gradually as the depth increases, showing that the soil pre-consolidation gradually decreased from the shallow depth toward the lower soil. The *in-situ* bulk unit weight varies between 18.7 kN/m^3 at 0.40 m and 17.8 kN/m^3 at 3.70 m.

Density of Solid Particles

Density of soil particles (ρ_s) of the clay crust was determined following the ASTM Standard No. D854-58. Density is approximately constant along the depth of the crust, varying between 2.74 kg/m^3 and 2.77 kg/m^3. From Fig. 7.1b, a constant ρ_s of 2.76 kg/m^3 can be considered as a representative value for the whole crust layer.

Natural Water Content

All specimens for water content determination were oven-dried at 105°C for a minimum of 24 hours and then were kept overnight in the desiccator before the dry weights were taken. Natural water content (w_N) increases with depth (Fig. 7.2a) starting from 23.5% at 0.40 m to 41.5% at 3.70 m (slightly below the crust) indicating that the soil was more preconsolidated toward the surface.

Atterberg Limit

The values of liquid limits (w_L) and the plastic limits (w_P) of the crust are also plotted in Fig. 7.2a. It is noticeable that the value of the plasticity index for the whole crust layer is approximately constant and is equal to 22±2 with a minor deviation at depth 1.50 m where the plasticity index is equal to 25. The liquidity index (Fig.7.2b) increases with depth ranging between 0 and 1 indicating that the sensitivity also increases along the depth. The average Atterberg limit of this soil plots above the A line on a plasticity chart classifying the crust soil as CL (inorganic clay with low to medium plasticity). All these Atterberg Limit tests were performed according to ASTM Standards D-423 and D-424.

Grain Size Analysis

It was found from wet sieving that more than 99% of the soil particles passed sieve No.200. This indicates that the soil contains only silt and clay. Clay and silt fractions obtained from hydrometer analysis, during this research, are shown in Table 7.1. Grain size analysis, by a previous investigator (Bozozuk 1977), showed 37% clay fraction and 63% silt at a depth of 2.0 m, changing almost linearly with depth to 58% clay and 42% silt at a depth of 16.0 m.

7.3 Programme of Triaxial Tests

Various types of triaxial tests, drained or undrained and compression or extension, have been conducted during this research using 51 mm diameter by 102 mm high samples. Test samples were reconsolidated isotropically to *in situ* overburden pressure or anisotropically to *in situ* state of stress before triaxial shearing. Testing procedures described by Bishop and Henkel (1962), and Head (1986) were generally followed.

The complete list of these triaxial tests is given in Table 7.2. Table 7.2 shows, for each of these samples, the depth, the type of test and the stress path followed during the test and the reconsolidation state of stress before the start of triaxial shearing. Abbreviations used in Table 7.2 and in Appendix A for various types of stress paths and various types of tests are listed below:

Abbreviations Used for Stress Paths:

ACRD : Axial stress is kept constant while radial stress decreases (Fig. 5.3, stress path 2).
ACRI : Axial stress is kept constant while radial stress increases (Fig. 5.3, stress path 3).
ADRC : Axial stress decreases while radial stress is kept constant (Fig. 5.3, stress path 4).
ADRI : Axial stress decreases while radial stress increases (Fig. 5.3, stress path 6).
AIRC : Axial stress increases while radial stress is kept constant (Fig. 5.3, stress path 1).
AIRD : Axial stress increases while radial stress decreases (Fig. 5.3, stress path 6).
AIRI : Both axial stress and radial stress increase (Fig. 5.3, stress path 5,7,8).

The stress path abbreviated as AIRI is applicable to three types of tests: (i) K_0 consolidation, i.e, axial and radial stresses are increased such that there is no lateral strain (Fig. 5.3, stress path 5); (ii) isotropic compression/consolidation, i.e, both axial and radial stresses are increased simultaneously at the same rate (Fig. 5.3, stress path 7); and (iii) both stresses are arbitrarily increased but at different rates (Fig. 5.3, stress path 8).

Abbreviations Used for Types of Tests:

CIUC : Isotropically consolidated undrained compression.
CIDC : Isotropically consolidated drained compression.
CIUE : Isotropically consolidated undrained extension.
CIDE : Isotropically consolidated drained extension.
CK_0UC : K_0 consolidated undrained compression.
CK_0DC : K_0 consolidated drained compression.
CK_0UE : K_0 consolidated undrained extension.
CK_0DE : K_0 consolidated drained extension.
CAUC : Anisotropically consolidated undrained compression.
CADC : Anisotropically consolidated drained compression.
CAUE : Anisotropically consolidated undrained extension.
CADE : Anisotropically consolidated drained extension.

The term "K_0 consolidated" (CK_0--), in this section, indicates that the sample was consolidated to K_0 condition, i.e, consolidated to its *in situ* state of stress before triaxial shearing. The term "anisotropically consolidated" (CA--) indicates that the soil sample was anisotropically consolidated to some arbitrary anisotropic stress condition before shearing.

The cell pressures, back pressures, and porewater pressures were measured by pressure transducers with a precision of 0.3 kPa. The LVDTs used for axial strain measurements, the load cells used for vertical load measurements, and the volume gauges used for volume change measurements, were capable of precisions of 0.01 mm, 0.2 N and 0.01 cc, respectively.

For all the undrained tests, samples were saturated by using back pressuring technique, and the back pressure used for final saturation was at least 150 kPa to ensure that the air bubbles are in the diluted form in the porewater of the specimen. At the final stage of saturation, the B value obtained was at least 0.97.

Both stress-controlled and strain-controlled undrained tests were conducted in this investigation. Shearing rates used for strain-controlled and stress-controlled tests were 1.68%/hour and 30 kPa/hour, respectively. Stress-controlled tests were generally performed for drained tests. For most of the drained tests, the test was started initially as a stress-controlled test and then just before failure, stress-control was converted to strain-control to obtain a well-defined stress-strain curve. Detailed discussion on the purpose and technique of converting stress-control to strain-control has been provided in Chapter 5. The shearing rates used in drained tests, for strain-controlled and stress-controlled tests, were 0.09%/hour and 0.75 kPa/hour, respectively.

7.4 Results of Triaxial Tests

Due to the large number of tests (73 tests in total) all conventionally analyzed test curves are presented in Appendix A, only the further analyses of these various triaxial tests and their discussions have been presented in this chapter. Each figure in Appendix A, pertaining to undrained tests, contains the four curves:

(a) axial strain (ε_1) versus deviatoric stress ($q = \sigma_v - \sigma_h$) and ε_1 versus porewater pressure developed (Δu) during the test,
(b) ε_1 versus stress ratio (σ_v'/σ_h'),
(c) mean stress ($p = (\sigma_v' + 2\sigma_h')/3$) versus q, and
(d) t ($= (\sigma_v - \sigma_h)/2$) versus s' ($= (\sigma_v' + \sigma_h')/2$).

The conventional plots for drained tests also show the above set of curves with the exception in Fig. (a) where ε_1 versus Δu has been replaced by ε_1 versus volumetric strain (ε_v).

Since axial strain at failure was small (0.5%-0.7%), it can be considered that the influence of membrane on the measured stress-strain behaviour would not be significant and no membrane correction was applied. Similar approach has been used by Crooks and Graham (1976) for the analysis of Belfast Estuarine deposits where the average ε_1 at failure was approximately 2%.

7.4.1 Undrained Tests

As the geotechnical properties of the weathered crust of Ottawa region had not previously been studied in detail, the present investigation is set out to examine a wide range of soil behaviour. The test conditions and results are summarized in Tables 7.2 and 7.4, respectively.

Evaluation of Shear Strength Parameters: ϕ' and c'

Shear strength parameters, ϕ' and c', have been determined by using two methods. Firstly, the individual undisturbed samples were reconsolidated isotropically by conventional method to various consolidation pressures, and then sheared monotonically. Samples SB210T1 (consolidated to 97 kPa), SB210T2 (consolidated to 194kPa) and SB210T3 (consolidated to 301 kPa) were used for this purpose as shown in Fig. 7.3.

Secondly, the multistage triaxial test as suggested by Kenney and Watson (1961) was also used to determine the values of ϕ' and c'. By this method, the shear strength parameters can be determined from a single sample instead of two or more samples required in the conventional method. In the multistage triaxial test, the same sample is consolidated at stages to various consolidation pressures before each stage of shearing. In each stage, the test is continued until the post-peak stress starts decreasing. The peak stresses, obtained from different consolidation pressures, are used to determine the shear strength parameters. Both undisturbed and reconstituted samples were used for this purpose. A typical example of the calculation of parameters ϕ' and c' is shown in Fig. 7.4. The results of the multistage triaxial tests are shown in Table 7.3 and in Figs. A.66 - A.79.

The values of parameters ϕ' and c' obtained by Method 1 are 28° and 21 kPa, respectively and the average values of these parameters obtained by Method 2, for the crust (within 3 m depth), are 26° and 17 kPa, respectively. The shear strength parameters, for undisturbed samples, obtained by multistage triaxial tests (Method 2) are slightly lower than those values obtained by the conventional method (Method 1). The absence of thixotropic effect in multistage triaxial tests, except the first stage where this effect is present, could be the reason of the lower values of shear strength parameters obtained by this method.

Determination of Failure Stre·

The failure stress, q_f or $(\sigma_v - \sigma_h)_f$ has been determined by three methods:

(1) The peak stress has been taken as the failure stress if an obvious peak stress is developed in the stress-strain diagram (for example, see Fig. A.9).

(2) For some tests, the latter part of the stress-strain diagram becomes approximately horizontal, and the first point where the stress-strain curve becomes horizontal, has been taken as the failure stress (for example, see Fig. A.7).

(3) For the tests where stress-strain diagram becomes hyperbolic, the stress at the peak stress ratio (σ_1'/σ_3') has been considered as the failure stress (for example, see Fig. A.3).

The first method was applicable for most of the samples, whereas, the other methods were mostly applicable for samples above 1.0 m depth.

The samples within 2 m depth, sheared by axial compression, failed by bulging without any visible shear plane. However, the samples below this depth also failed by bulging but with a visible shear plane. The average angle between the failure plane and the horizontal axis was approximately 58°. For all the compression and extension tests, the area correction was made assuming the sample as a right cylindrical sample.

Table 7.4 shows that the samples from shallower depths experienced higher axial strain at failure (ε_{1f}) than those from lower depths. There are two reasons for this behaviour. Firstly, the lower samples are more cemented which require less strain (0.5%-0.7%) for failure than those of less cemented upper soil. Cemented behaviour of the lower samples is easily recognized from the sudden drop of post-peak stress visible in a stress-strain curve of a triaxial compression test (for example, see Fig. A.58), and also from the sudden break immediately after the preconsolidation pressure visible in an e-logσ' curve of a consolidation test (for example, see Fig. B.8a) . Secondly, the upper soil is loose with random microfissures, and produces less pronounced peak stress requiring higher strain for failure.

Where an obvious peak stress has occurred indicating strain-softening behaviour, it has been observed that the q_f and $(\sigma_v'/\sigma_h')_{max}$ developed at the same strain level. For the samples where stress-strain diagram does not indicate strain-softening behaviour (i.e, no obvious peak stress is observed), $(\sigma_v'/\sigma_h')_{max}$ developed at a lower strain level than that for q_f. In all cases, $(\sigma_v'/\sigma_h')_{max}$ was developed at maximum porewater pressure u_{max} and after this point u decreased showing that the dilation has started at this point. From this study, it can be concluded that $(\sigma_v'/\sigma_h')_{max}$ develops when the samples start dilating.

In all consolidated undrained triaxial tests collected from within the crust, i.e, above 3 m depth level, isotropically or anisotropically consolidated, vertically oriented or horizontally oriented, the stress ratio $(\sigma_v'/\sigma_h')_{max}$ was reached before the deviator stress had attained its maximum value. For the lightly overconsolidated Belfast estuarine deposits, as discussed by Crooks and Graham (1976), this sequence of occurrence was opposite where $(\sigma_v'/\sigma_h')_{max}$ occurred after $(\sigma_v - \sigma_h)_{max}$. However, for the intact clay immediately below the crust, both $(\sigma_v - \sigma_h)_{max}$ and $(\sigma_v'/\sigma_h')_{max}$ reached at the same time and at the same strain level. $(\sigma_v'/\sigma_h')_{max}$ is attained where maximum porewater pressure is developed and starts decreasing with the decrease in porewater pressure. The above observation suggests that the maximum deviator stress is a measure of the strength of the soil structure. Whereas the mobilization of the frictional resistance between soil particles is controlled by the ratio σ_v'/σ_h'. This supports the suggestion made by Bjerrum and Kenny (1967), although in their case $(\sigma_v'/\sigma_h')_{max}$ develops after $(\sigma_v - \sigma_h)_{max}$ does, and after significant straining. It is interesting to note that $(\sigma_v'/\sigma_h')_{max}$, in this study also develops after $(\sigma_v - \sigma_h)_{max}$, but for the samples which were reconsolidated to a higher stress than the preconsolidation stress, σ_p'.

The values of q_f shown in Table 7.4 have been calculated as $(\sigma_v - \sigma_h)_f - (\sigma_v - \sigma_h)_c$. For CIU tests, $q_f = (\sigma_v - \sigma_h)_f$ since $(\sigma_v - \sigma_h)_c = 0$ but in CK_0U tests, for $K_0 \neq 1$, $(\sigma_v - \sigma_h)_c$ has a positive value if $K_0 < 1$ and has a negative value when $K_0 > 1$. For the present study, where $K_0 > .1$, for example, for test SB100T3 q_f has been calculated as 118.2 kPa where $(\sigma_v - \sigma_h)_h = 86.1$ kPa and $(\sigma_v - \sigma_h)_c = -32.1$ kPa. The term q_f expressed by $(\sigma_v - \sigma_h)_f - (\sigma_v - \sigma_h)_c$ is the maximum deviatoric stress in the vertical direction and not always the maximum shear stress. The value of maximum shear stress will always be $(\sigma_v - \sigma_h)_f$ and the value of shear strength has always been calculated as $(\sigma_v - \sigma_h)_f/2$. Clearly, there is a difference between deviatoric stress and shear stress for anisotropically consolidated samples but not for isotropically consolidated samples.

Effect of In situ State of Stress and Stress History on the Undrained Behaviour of the Crust

It is understood that the consolidation stress history has considerable effect on the stress-strain behaviour of a soil. To obtain a representative stress-strain behaviour, samples have to be reconsolidated to the *in situ* state of stress (i.e., consolidated to K_0 condition) before starting the triaxial test. It has been observed that the samples reconsolidated to the *in situ* stress state indicated higher undrained strength than the isotropically consolidated samples as shown in Fig. 7.5. However, this comparison will be opposite for a normally consolidated soil where $K_0<1$.

K_0 consolidated samples also showed higher deformation moduli, both $E_{0.1}$ and E_{50}, than the samples consolidated isotropically to σ_{v0}' (Table 7.4 and Fig. 7.7), where $E_{0.1}$ is the secant modulus at 0.1% axial strain and E_{50} is that at 50% of the maximum deviatoric stress. Deformation modulus, E was calculated as q/ε_1 at respective strain or stress levels.

Considerable differences in porewater pressure response were recorded in samples consolidated under different stress systems. K_0 consolidated samples resulted higher A_f values than isotropically consolidated ones even though σ_{vc}' was same for both type of tests.

Fig. 7.6 shows dependence of A_f on the consolidation history, and confirms the general pattern found in other soils (Crooks and Graham 1976; Henkel 1956; Simons 1960). Fig. 7.6a shows that there is a good correlation between OCR and A_f for CIUC tests. Similar observations were also made for overconsolidated Weald clay (Simons 1960). Fig. 7.6 also indicates that A_f values for horizontally oriented samples are higher than the vertically oriented samples although the water content was same for both type of samples. Therefore, it is obvious from this study that the magnitude of A_f is not water content dependent but stress history dependent. This observation also confirms that the samples are less preconsolidated in the horizontal direction giving higher A_f for the horizontal samples than the vertical samples at the same water content. This is expected for a soil with the horizontal preconsolidation pressure, $\sigma_{ph}' = K_{0nc} \cdot \sigma_p'$, where $K_{0nc} = 0.5$ as evaluated by Garga and Khan (1991). It is interesting to note that the values of A_f from CK_0UC tests do not change much with stress history and are approximately same. The reason of this observation is not known; further studies may be undertaken to investigate this aspect.

Previous studies on a variety of soil types have suggested that the ratio E_{50}/S_u lies between 500 and 1000 (Simons 1976, Crooks and Graham 1976). The present study also confirms this general trend. The values of E_{50}/S_u for this study ranges between 600 and 1000 as shown in Table 7.4. It is obvious from Table 7.4 that the stress history or the type of consolidation do not have any effect on the value of E_{50}/S_u.

The relatively elastic porewater pressure response to undrained axial compression of samples anisotropically consolidated to the *in situ* state results is an approximately vertically straight effective stress path up to the yield state (for example, see Fig. A.27). The average value of A for these tests is approximately 0.31. A value of 0.33 is expected if the soil behaves perfectly elastic.

Strength Anisotropy:

Several studies have shown that the undrained strength of overconsolidated post-glacial clays are directional (Aas 1967; Lo and Morin 1972). One method of studying undrained strength anisotropy is by comparing the results of consolidated undrained triaxial compression and extension tests (Bjerrum et al. 1972). Another method is to shear samples in vertical and horizontal directions. Both types of tests have been conducted in this study and the results are summarized in Table 7.4 and Fig. 7.5. The values of S_u obtained from CK_0UC are consistently higher than those obtained from CK_0UE (Fig. 7.5). The ratio of $S_u(CK_0UC)/S_u(CK_0UE)$ varies between 1.25 and 1.65 with an average of 1.50.

The values of S_u for vertical samples were higher than those for the horizontal samples. The ratio of S_u for vertical to horizontal, at various depths, ranges between 1.28 to 1.59 with an average of 1.40. Bishop (1966) and Lo and Milligan (1967) also observed similar behaviour for heavily overconsolidated soils. They mentioned the reason for this behaviour as the reduced resistance to shearing along bedding planes in layered deposits. However, in addition to this reason, the writer believes that the smaller preconsolidation pressure in the horizontal direction as well as the structural anisotropy is also responsible for the lower strengths in the horizontal direction. Samples with lower strengths in horizontal direction had larger strains at maximum deviator stress giving lower deformation moduli.

7.4.2 Drained Tests

In order to examine the importance of variation of stress path, several samples were reconsolidated isotropically to σ_{v0}' or anisotropically to the approximate *in situ* state of stress, and subsequently tested under drained conditions along various stress paths as illustrated in Fig. 7.8. The triaxial samples obtained from various depths, for drained tests, are listed in Table 7.2. The stress paths followed in the triaxial space, the test type (drained/undrained or compression/extension), and the consolidation type (isotropically consolidated or anisotropically consolidated to K_0 condition) including the consolidation stresses are also listed in the Table 7.2.

Effect of Stress-Path on the Soil Behaviour

Conventionally, triaxial compression and oedometer consolidation tests are being performed to evaluate the strength and deformation behaviour of any soil. However, in the field, the stress paths followed by various engineering projects may deviate from the stress paths used in the above laboratory tests. Moreover, the stress-paths followed by different soil elements, under a foundation, are different. It is expected that the strength-deformation behaviour of any foundation soil would depend on the stress path to be followed in the field. In this context, to obtain representative soil parameters from laboratory tests, for any engineering project, the stress path to be maintained in the laboratory test should be similar to that to be followed in the real project.

From the analysis of the data, obtained from various drained stress-path tests as shown in Fig. 7.8, the following two conclusions can be made:

(i) The drained shear strengths decrease (Fig. 7.9a) with the increase in β_c or β_e values, where β_c or β_e are the measurements of angles between the stress-path and the isotropic compression line for compression and extension directions, respectively (Fig. 7.8). On the compression side, the estimation of shear strength was possible for stress-paths 3 (Fig. A.43) and 4 (Fig. A.48) only, with the values of 44 kPa and 36 kPa, respectively. On the other hand, no strength could be calculated for stress-paths 2 and 5. The stress-path 2, which is close to the isotropic compression line, did not show any peak (Fig. A.45), and, the stress-path 5 did not fail when σ_h' was slowly decreased to zero (Fig. A.44) when further decrease of σ_h' was not practical.

On the extension side, the shear strengths calculated for stress paths 7 (Fig. A.39), 8 (Fig. A.49) and 9 (Fig. A.55) are 32 kPa, 24 kPa and 19 kPa, respectively. Although the stress-path 9 did not completely fail, the peak stress of 38 kPa can easily be estimated from the stress-strain curve where the sample approached failure as shown in Fig. A.55 The calculation of shear strength for stress-path 6 (Fig. A.56) was not possible since there was no obvious peak in the stress-strain curve.

(ii) The values of moduli of deformation increase with the increase in β_c or β_e values for both compression and extension directions as illustrated in Fig. 7.9b. The moduli

($E_{0.1}$) were calculated as the ratio of deviatoric stress ($\sigma_1 - \sigma_3$) to axial strain (ε_1) at 0.10% axial strain which can be reasonably approximated as the initial moduli (E_i).

The second observation indicates that farther the stress-path is from the isotropic line, the stiffer the material, as indicated from the trend of $E_{0.1}$ values. However, it is interesting to note that although the crust material shows an initial higher stiffness as the stress-paths move away from the isotropic line, the ultimate stress becomes smaller as discussed in the first observation. This study is limited to depth 3.3 m. Further studies are recommended, for different types of soils, to investigate this aspect.

Triaxial Isotropic Compression Tests:

The stress-strain behaviour of triaxial isotropic compression tests indicated that the compressibility of the soil structure is small before it reaches the preconsolidation pressure, σ_p'. However, after the stress exceeds the σ_p' there is a sudden break in the curve changing from small strain (low compressibility) to large strain (high compressibility) behaviour. Similar observations were made in the one-dimensional oedometer consolidation tests.

7.5 Yield Envelope

The different soil elements, under any structure, experience different stress-paths depending on the location of the element. If the yield envelope of any soil is known, the yield stress for any specific soil element can be obtained for the representative stress-path. The best use of an yield envelope can be made in a numerical analysis, such as boundary element or finite element method, where the equation of the envelope is used. The use of the yield envelope is beyond the scope of this research; however, the determination of the yield envelope has been performed in this study.

The locus of stress states at which the soil structure yields defines a boundary in stress space between small strain and large strain response to loading, and has been termed as the yield envelope (Graham et al. 1983). The yield stress is conventionally defined as that stress below which the material behaves elastically and above which the behaviour is plastic.

In this investigation, the yield stresses have been determined by using the bilinear plotting method suggested by Graham et al. (1983). In this method, two straight lines are expected, in the stress-strain plot, before and after yielding of the sample. The point of intersection of these two straight lines is considered as the yield stress as illustrated in Fig. 7.10. Although well-defined straight lines were not obvious in the stress-strain curves (see curve (a) of all the figures in Appendix A) of the crust, bilinear plotting method can be used with reasonable confidence.

For undrained test, shear strain $\varepsilon = (2/3)(\varepsilon_1-\varepsilon_3)$ versus shear stress $q = \sigma_v-\sigma_h$ and for drained tests, volumetric strain ε_v versus mean effective stress $p' = (\sigma'_v + 2\sigma'_h)/3$ were plotted for determining yield stresses. For an undrained test where the sample is considered incompressible, $\varepsilon = \varepsilon_1$ since $\varepsilon_3 = -0.5\varepsilon_1$. For drained constant p' test, yield stresses were obtained from ε_1 versus σ'_1 curve since ε_v versus p' plotting is not possible. The yield stresses determined by this method are shown in Fig. 7.11a, and the normalized yield stresses are shown in Fig. 7.11b. Normalization has significantly reduced the scatter of data points, from which a well-defined yield envelope can be drawn as shown in Fig. 7.11b.

The yield stresses, obtained from various triaxial tests, have been normalized by the yield stresses obtained from one-dimensional oedometer consolidation test results. The latter is not the conventionally defined preconsolidation pressure obtained from Casagrande method but the yield stresses obtained from bilinear plotting as suggested by Graham et al. (1983). It has been observed from the present study that the yield stress obtained from bilinear plotting is always slightly smaller than the preconsolidation pressure obtained by the Casagrande method. Therefore, in this study, the 'yield stress' by Casagrande method will be termed as the preconsolidation pressure, and only the 'yield stress' by bilinear plotting will be referred to as yield stress.

The samples were tested from six depths where OCR values range between 3 and 16. The yield envelope has been obtained from the test results of 39 triaxial shear tests and 6 one-dimensional oedometer consolidation tests. Various stress paths were followed for these tests. All the possible stress paths as shown in Fig. 5.3 were followed for the depth of 3.3 m where enough number of samples were available to conduct these variety of stress path tests. For other depth levels, number of stress paths followed were limited by the number of available samples. The triaxial tests considered for plotting the yield envelope were either consolidated isotropically to σ'_{v0} or anisotropically to in situ state of stress before starting shearing. Out of 39 triaxial tests, 17 extension and 22 compression (including isotropic compression test) tests were conducted. These triaxial tests were performed for both drained (21 tests) and undrained (18 tests) conditions.

To obtain a well-defined pre-failure and post-failure stress-strain curve, most of the tests were initially started as a stress-controlled test and then just before failure, the test mode was changed from stress-control to strain-controlled test. This combination of stress- and strain-control was used because well-defined pre-failure curve cannot be obtained for a strain-controlled test whereas on the other hand well-defined post-failure curve cannot be obtained for a stress-controlled test. The automatic control system of the triaxial testing apparatus, as discussed in Chapter 5, made this operation possible. The stress rate used for drained tests was 0.75 - 1.0 kPa/hour to allow enough time for the dissipation of excess porewater pressure.

The tests represented by the extreme-left two data points, for 3.3 m depth as shown in Fig. 7.11a, did not fail, and is obvious from their stress strain diagrams (Fig. A.44 and Fig. A.55). However, the locus of the yield envelope plotted from rest of the data points shows that these two tests have reached their yield states. These two tests, one in compression and other one in extension, followed the stress paths 2 and 4, respectively, as illustrated in Fig. 5.3. These tests were continued upto such stages so that σ'_v or σ'_h did not attain negative values in order to always keep the sample in no-tension condition. During the test, when σ'_v or σ'_h approached negative values, the test was stopped automatically at that instant although the sample did not fail. The computer program for stress path control test was also written to take care of this situation.

To obtain p' and q values from one-dimensional (1-D) oedometer consolidation tests, the value of K_0 for normally consolidation K_{0nc} was required. K_{0nc} used in the determination of p' and q values is 0.50 which was evaluated by Garga and Khan (1991) from experimental results. For this purpose, the K_{0nc} was determined from reconstituted soil samples obtained from the slurry prepared from the same soil where the water content of the slurry was higher than the liquid limit of the soil. The procedure of K_{0nc} determination has been described in detail in Chapter 6.

Many researchers (Graham 1972; Tavenas and Leroueil 1977; Parry and Nadarajah 1973) have concluded that the yield envelope is symmetric about the K_{onc} line; on the other hand, Chan (1985) has shown that for the Gennessee clay (OCR = 2, K_0 = 1.2), the yield envelope is symmetric about the q = 0 axis, i.e, the p' line. It should be noted that the envelope obtained by Tavenas and Leroueil 1977 for Champlain Sea clay is not precisely the yield envelope, but the failure envelope or the limit state envelope, and the failure (peak) stresses were used to plot the envelope. Unlike the above-mentioned cases, the yield envelope for the crust material is symmetric about a line which lies between the lines K_{onc} and p' (Fig. 7.11b). The angle between the q = 0 axis and the axis of yield envelope symmetry is approximately 15°, and the ratio p'/q along the line of symmetry is approximately 3.6. Therefore, in this context, it can be concluded that the axis of symmetry of yield envelope is not always same, and is soil dependent. The parameters on which the position of this axis of symmetry depends are not yet understood. More research is required to acquire better understanding of this subject.

7.5.1 Strain Contours

The stress-path tests provide various types of strains, e.g. vertical/axial strain, horizontal/lateral strain, volumetric strain, shear strain, etc. The only strain which may be evaluated from all the path tests, is the axial strain. The lateral strain cannot be measured in a K_0 triaxial test, the volumetric strain is not measurable in an undrained triaxial test and the shear strain does not develop in an isotropic triaxial compression test. Therefore, axial strain which is measurable in any stress path test is used in this section for strain contour plotting.

It is understood that the strain is stress path dependent (Henkel 1960). Contours of five strain levels (0.1%, 0.2%, 0.4%, 0.6%, 0.8% and 1.0%) are plotted in Fig.7.12. Although a strain contour has been drawn for 0.1%, it shows more scatter (Fig.7.12a) than the other contours (Fig.7.12b-f). However, for other strain levels (0.2%, 0.4%, 0.6%, 0.8% and 1.0%) the scatter is less prominent and well-defined contours can be plotted (Fig.7.12b-f). The increased scatter of stress states for 0.1% strain level is believed to be due to the disturbance effects during sample preparation or due to loose seating of loading ram on the specimen top. These problems are unavoidable at such a low strain level.

It is obvious from Fig. 7.13 that the yield state on the extension side reaches at a lower strain level (0.4%) than those on the compression side (0.6%). It is also noticeable that the strain close to the yield state on the isotropic line is even smaller than that of compression or extension yield states.

The strain contour for any strain level, within the yield envelope, has a regular shape. However, when the contour line goes beyond the yield envelope, i.e, from elastic to plastic range, some irregularities are observed. This is expected for a strain softening soil where the shear stress reduces after the peak shear stress. For an isotropic compression test, the stress state for any strain level is much higher than that of any other stress path test. This explains why the strain contours for higher strain levels go beyond the yield envelope when these contour lines approach the isotropic line i.e, p' line, and the yield envelope makes an apex on this line. To obtain a smooth yield envelope, the data points for isotropic compression tests have been avoided.

Strain contours have been plotted as long as the contour lines are within the yield envelope (Figs.7.12a-c). On the compression side, yield envelope and contour lines for 0.6%, 0.8% and 1.0% are approximately the same. Although the average strain contour passes through the yield envelope, some stress levels decrease at higher strains after failure since these specimens show strain-softening behaviour. Strain-softening behaviour is more prominent for undrained compression tests and for stress paths making higher angles with the isotropic compression line. However, on the extension side, the stress levels corresponding to these strain levels go beyond the yield envelope. This is expected since the soil shows less prominent strain-softening behaviour for extension tests.

7.6 Some Further Comments on Triaxial Test Results

The results described in the preceding sections demonstrate the importance of soil structure in controlling the behaviour of the weathered crust of Champlain clay. The structure of the soil is different in horizontal and vertical directions giving different strength-deformation behaviour in these directions (Table 7.4, and Figs. 7.5, 7.6 and 7.7).

One of the more significant consequences of the brittle nature of the soil structure is the yield envelope. Straining of the soil at stress states lying inside this locus is essentially small and elastic. Further straining moves the stress state outside the yield envelope, for continuous straining the stress state comes back within the yield envelope. This is due to the strain-softening behaviour of the soil. The ability of the soil structure to sustain stresses greater than the *in situ* stresses is directly related to the degree of overconsolidation. It was suggested in a previous section that the small strain undrained strength of a soil is essentially a measure of the strength of the soil structure.

The yield envelope provides a qualitative criterion for estimating the response of the soil to applied loading. Where field loading produces increased shear stresses with little corresponding change in mean normal stress, the yielding will be abrupt. In sensitive soils, yielding produces increased strain rates and a tendency towards quickly occurring failures. The results of this study emphasize the problem of how to define the strength of the Champlain Sea clay crusts. The criterion to be used in a given problem clearly depends on the importance of, strains preceding failure and the direction of the stress path.

Field loading under the edges of foundations increases both normal and shear stresses in the soil. In this case, settlements and porewater pressures at stresses below yielding will be small and largely elastic. At higher stresses, much larger non-elastic settlements can be expected. Drained and undrained behaviour are largely identical up to yielding; thereafter, however, they differ considerably.

Table 7.1 Clay and silt fractions from hydrometer analysis.

Depth (m)	Clay Fraction (%)	Silt Fraction (%)
1.0	41	58
1.8	40	59
2.6	38	61
3.3	44	55
3.6	45	54

Table 7.2 Record of triaxial tests: stress path, test type, and consolidation state at the start of test (continued to next page).

Sample No.	Depth (m)	Stress path	Test type	σ_{hc}' (kPa)	σ_{vc}' (kPa)	$\sigma_{hc}'/\sigma_{vc}'$	Remarks
BS065T1	0.65	AIRC	CIUC	23.5	23.5	1.0	
SB075T1	0.75	AIRC	CIUC	106	106	1.0	
SB075T2	0.75	AIRC	CIUC	105	105	1.0	
SB075T3	0.75	AIRC	CIDC	107	107	1.0	
SB090T1	0.90	ADRC	CIUE	105	105	1.0	
SB090T2	0.90	ACRD	CIUC	107	107	1.0	
SB100T1	1.00	AIRC	CIUC	16.2	16.2	1.0	
SB100T2	1.00	ACRI	CIDE	16.7	16.7	1.0	
SB100T3	1.00	AIRC	CK_0UC	47.1	15	3.14	
SB100T4	1.00	ACRI	CK_0UE	46.5	16.2	2.87	
SB120T1	1.20	ADRC	CIDE	109	109	1.0	
SB120T2	1.20	ACRI	CIUE	110	110	1.0	
SB150T1	1.50	AIRC	CIUC	20.9	20.9	1.0	Horizontal sample
SB180T1	1.80	AIRC	CIUC	23.6	23.6	1.0	
SB180T2	1.80	ACRI	CIDE	22.8	22.8	1.0	
SB180T3	1.80	AIRC	CK_0UC	48.4	23.8	2.03	
SB180T4	1.80	ACRI	CK_0UE	47.9	23.4	2.05	
SB210T1	2.10	AIRC	CIUC	97.1	97.1	1.0	
SB210T2	2.10	AIRC	CIUC	194	194	1.0	
SB210T3	2.10	AIRC	CIUC	301	301	1.0	
SB220T1	2.20	AIRC	CIUC	26.2	26.2	1.0	Horizontal sample
SB250T1	2.50	ACRI	CIDE	29	29	1.0	
SB250T2	2.50	AIRC	CIDC	28	28	1.0	
SB250T3	2.50	ADRC	CK_0DE	50.9	32.9	1.55	
SB260T1	2.60	ACRI	CIDE	30.8	30.8	1.0	
SB260T2	2.60	AIRC	CIUC	30.1	30.1	1.0	
SB260T3	2.60	AIRC	CK_0UC	47.1	30.1	1.56	
SB260T4	2.60	ACRI	CK_0UE	46.7	29.5	1.58	
SB260T5	2.60	AIRC	CK_0UC	47.1	30.1	1.56	
SB273T1	2.73	AIRC	CIUC	31.4	31.4	1.0	Horizontal sample
BS308T1	3.08	AIRD	CK_0DC	47.4	35.4	1.34	Constant p'
BS308T2	3.08	ACRI	CIDE	33.6	33.6	1.0	
BS308T3	3.08	AIRC	CK_0DC	46.9	32.6	1.44	
BS308T5	3.08	AIRC	CK_0DC	46.7	32.9	1.42	
BS308T6	3.08	ADRI	CK_0DE	46.6	33.2	1.40	Constant p'

Table 7.2 Record of triaxial tests: stress path, test type, and consolidation state at the start of test (continued from previous page).

Sample No.	Depth (m)	Stress path	Test type	σ_{hc}' (kPa)	σ_{vc}' (kPa)	$\sigma_{hc}'/\sigma_{vc}'$	Remarks
BS333C1	3.33	AIRC	CIUC	36.5	36.5	1.0	Cyclic test
BS333C2	3.33	AIRC	CIUC	35.9	35.9	1.0	Cyclic test
BS333C3	3.33	AIRC	CIUC	36.1	36.1	1.0	Cyclic test
BS333T1	3.33	ACRI	CIDE	36.5	36.5	1.0	
BS333T2	3.33	AIRC	CK_0UC	45	36	1.25	
BS333TC3	3.33	AIRI	CIDC	13.1	13.1	1.0	Isotropic consolidation
BS333T3	3.33	AIRC	CIUC	100.4	100.4	1.0	Cont. from BS333TC3
BS333T4	3.33	AIRC	CIUC	36.6	36.6	1.0	
BS333T5	3.33	AIRC	CIDC	38.1	38.1	1.0	
BS333T6	3.33	ACRD	CIDC	36.5	36.5	1.0	did not fail
BS333T7	3.33	AIRI	CIDC	37.4	37.4	1.0	2(v):1(h) consolidation
BS333T8	3.33	AIRC	CAUC	124.8	223.1	0.56	
BS333T9	3.33	ACRI	CK_0UE	44.2	35.7	1.24	
BS333T10	3.33	AIRD	CIDC	38.9	38.9	1.0	Constant p'
BS333T11	3.33	ADRI	CIDE	39.1	39.1	1.0	Constant p'
BS333T12	3.33	AIRC	CIUC	73.3	73.3	1.0	
BS333T13	3.33	ADRC	CIDE	36.3	36.3	1.0	
BS333T14	3.33	AIRI	CIDE	35.5	35.5	1.0	1(v):2(h) consolidation
BS333T15	3.33	AIRC	CAUC	211.6	116.2	1.82	
BS333T16	3.33	AIRC	CIUC	35.3	35.3	1.0	Horizontal sample
BS333T17	3.33	ADRC	CIDE	36.7	36.7	1.0	
BS333T18	3.33	AIRI	CIDE	36.9	36.9	1.0	1(v):2(h) consolidation
BS333T19	3.33	ADRC	CAUC	249.1	126.8	1.96	
BS360T1	3.60	AIRC	CIUC	37.9	37.9	1.0	
BS360T3	3.60	ACRI	CIDE	37	37	1.0	
BS360T4	3.60	AIRC	CK_0UC	41.9	38.3	1.09	
BS360T5	3.60	AIRC	CK_0UC	41.9	38.5	1.09	Unsaturated
BS360T6	3.60	ACRI	CK_0UE	42.1	38.6	1.09	
BS370T1	3.70	AIRC	CIUC	39.3	39.3	1.0	Horizontal sample
RMDT1		AIRC	CIUC	300	300	1.0	
RMDT2		AIRC	CIUC	20	20	1.0	

Table 7.3 Results of multistage triaxial tests
(Isotropically consolidated undrained, strain-controlled)

Sample No.	Depth (m)	Stage	σ_c' (kPa)	w.c. (%)	ε_{1f} (%)	s_f' (kPa)	t_f (kPa)	c' (kPa)	ϕ'
RMDMT1	2.0 (remoulded)	1	99		0.6	129	74	18.3	26.1
		2	200		0.9	218	109		
		3	300	27.16	1.15	281	141		
RMDMT2	2.0 (remoulded)	1	102		2	127	73	18.9	26.1
		2	199		1.5	193	101		
		3	398	27.36	1.6	303	150		
SB200MT1	2.0	1	98		1.1	83	49	13.8	25.5
		2	200		1.25	150	77		
		3	400		1.98	286	137		
		4	602	28.6	1.99	413	192		
SB360MT1	3.6	1	17.3		0.5	31.1	26.9	17.1	21.1
		2	37.9		0.46	53.7	35.4		
		3	58.9		0.61	69.9	41.1		
		4	89	39.06	0.94	83.6	45.7		

Table 7.4 Results of undrained triaxial compression tests for samples isotropically consolidated to σ_{v0}' and anisotropically consolidated to *in situ* state.

Sample No.	q_f (kPa)	ε_{1f} (%)	A_f	$(\sigma_v'/\sigma_h')_{max}$	ε_1 at $(\sigma_v'/\sigma_h')_{max}$	A at $(\sigma_v'/\sigma_h')_{max}$	$E_{0.1}$ (MPa)	E_{50} (MPa)	S_u (kPa)	E_{50}/S_u
CIUC tests for vertical samples										
SB100T1	68.1	3.89	0.10	8.96	1.04	0.16	21.1	14.3	34.1	419
SB180T1	72.8	1.29	0.16	8.84	0.72	0.20	25.4	23.9	36.4	657
SB260T2	70.8	0.64	0.22	6.53	0.33	0.28	30.5	29.6	35.4	836
BS333T4	89.1	0.58	0.28	8.56	0.58	0.28	30.3	27.9	44.6	626
BS360T1	82.9	0.67	0.29	6.76	0.67	0.29	32.0	25.8	41.5	622
CK_0UC tests for vertical samples										
SB100T3	118.2	1.59	0.28	7.50	1.18	0.40	37.1	26.5	43.1	615
SB180T3	104.1	2.45	0.34	9.27	0.63	0.52	37.7	33.7	39.8	847
SB260T5	92.1	0.72	0.31	5.10	0.72	0.31	37.9	33.3	37.6	886
BS333T2	101.7	0.65	0.30	7.22	0.65	0.30	35.5	30.4	46.4	655
BS360T4	89.1	0.64	0.31	6.94	0.64	0.31	31.4	28.1	42.8	657
CIUC tests for horizontal samples										
SB150T1	54.8	5.91	0.19	6.75	2.82	0.29	25.3	22.1	27.4	807
SB220T1	59.6	4.10	0.29	8.40	2.16	0.32	27.4	26.4	29.8	886
SB273T1	53.7	1.36	0.34	5.86	0.66	0.41	27.0	27.0	26.9	1004
BS333T16	49.8	0.79	0.55	7.34	0.79	0.55	23.3	21.3	24.9	855
BS370T1	53.2	0.76	0.57	6.81	0.76	0.57	25.8	25.0	26.6	934

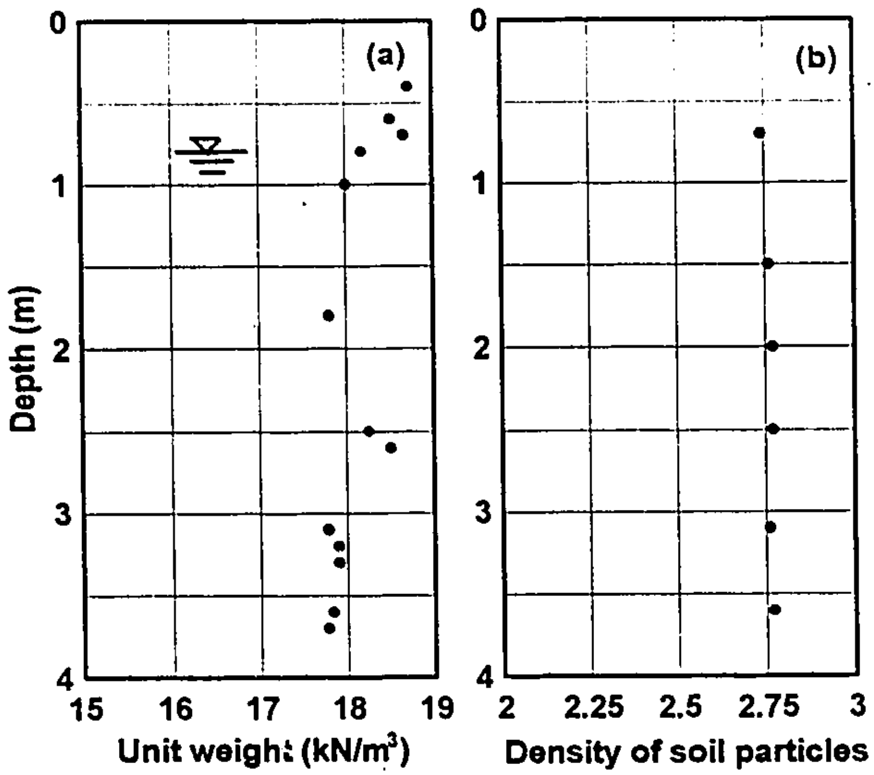

Fig. 7.1. Variation of (a) bulk unit weight, and (b) Density of soil particles.

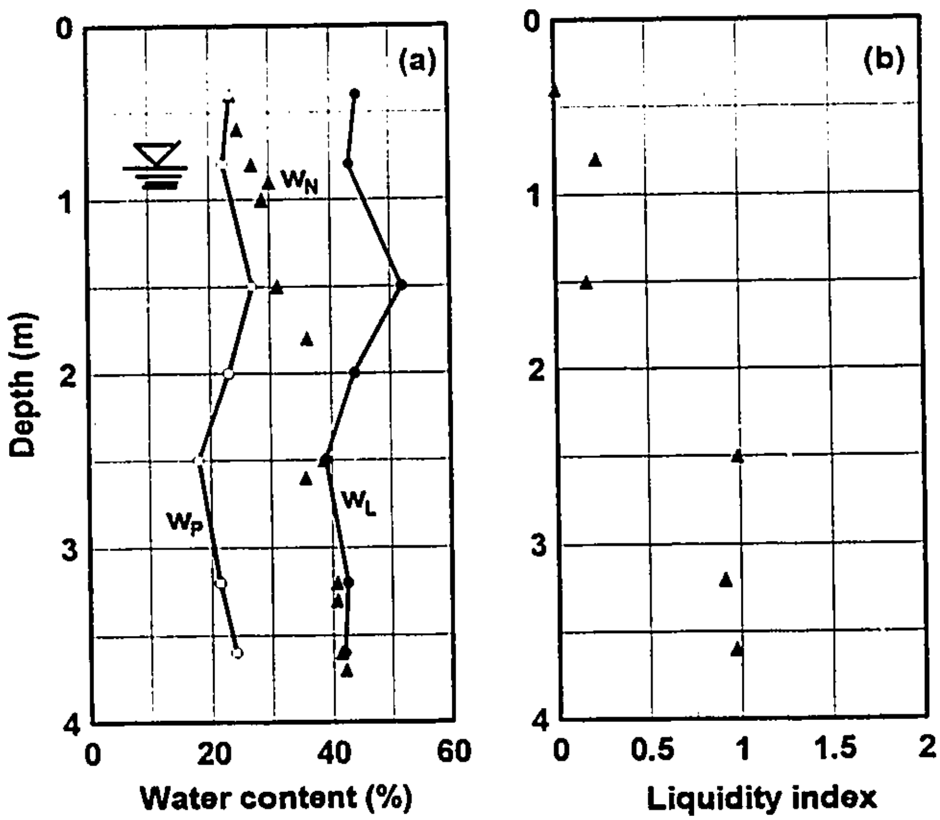

Fig. 7.2. Variation of Atterberg limits with depth.

Sample #	Conf.Pr.	s' (kPa)	t' (kPa)
SB210T1	98	101	68
SB210T2	196	156	87
SB210T3	302	215	121

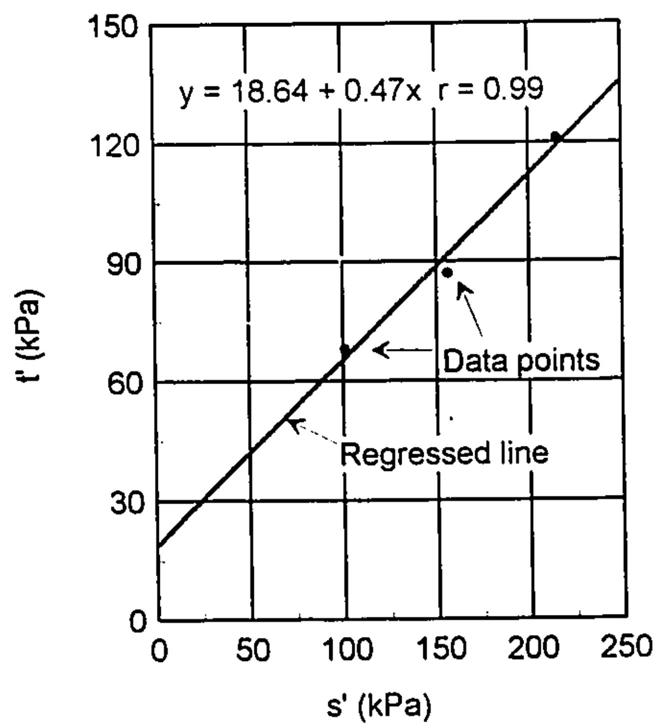

$s' = (\sigma_1' + \sigma_3')/2$

$t' = (\sigma_1' - \sigma_3')/2$

$\tan\alpha' = 0.47$ $\alpha' = 25.2^{\circ}$

$\sin\phi' = \tan\alpha'$ $\phi' = 28.0^{\circ}$

$a' = 18.64$ $c' = 18.64/\cos\phi' = 21.1$ kPa

Fig. 7.3 Determination of shear strength parameters ϕ' and c' using three different tests with different consolidation pressures.

Stage	Conf.Pr.	s' (kPa)	t' (kPa)
1	98	83	49
2	200	150	77
3	400	286	137
4	602	413	192

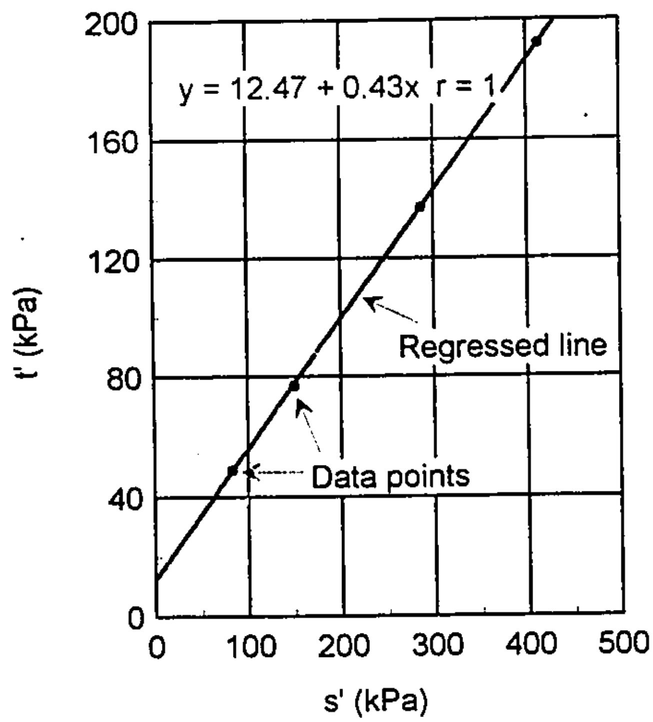

$s' = (\sigma_1' + \sigma_3')/2$

$t' = (\sigma_1' - \sigma_3')/2$

$\tan\alpha' = 0.43$	$\alpha' = 23.3^o$
$\sin\phi' = \tan\alpha'$	$\phi' = 25.5^o$
$a' = 12.47$	$c' = 12.47/\cos\phi' = 13.8$ kPa

Fig. 7.4 Determination of shear strength parameters ϕ' and c' using single multistage triaxial test (Sample No: SB200MT).

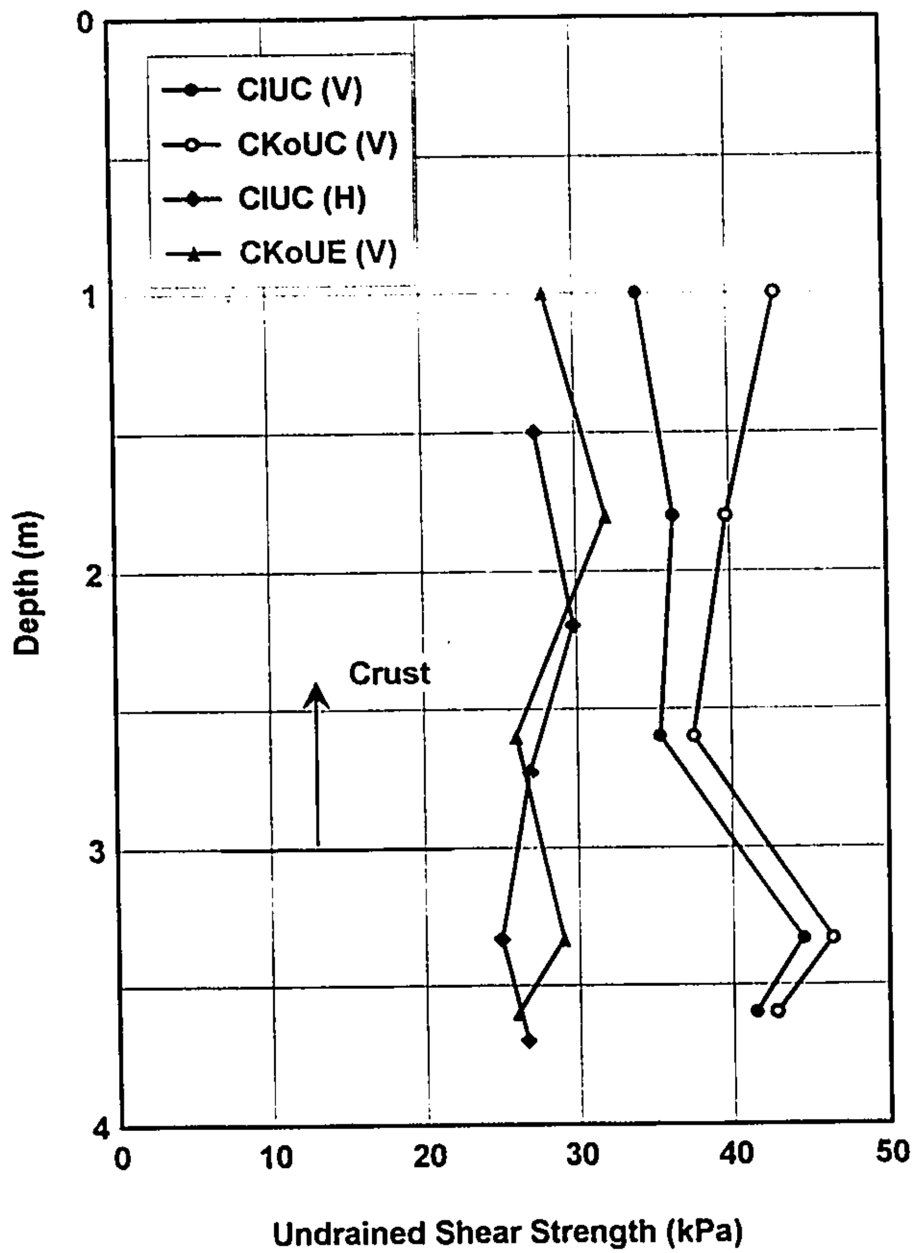

Fig. 7.5 Undrained shear strengths from triaxial tests for vertically and horizontally oriented samples.

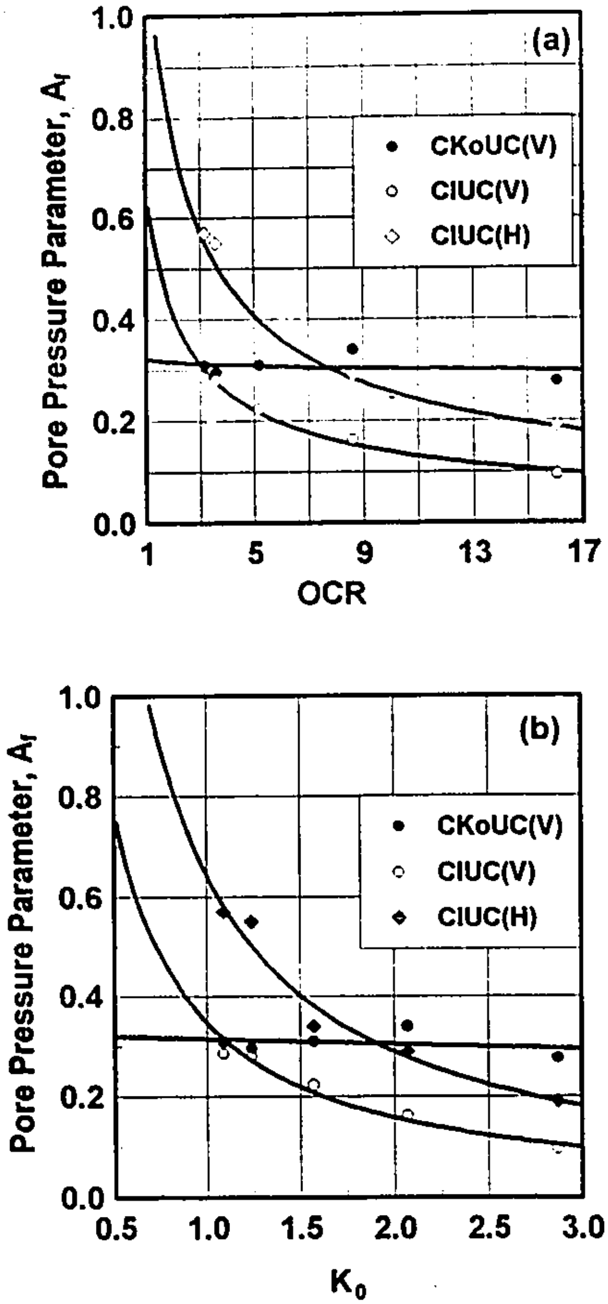

Fig. 7.6. Correlation between porewater pressure parameter, A_f and *in situ* stress histories, OCR and K_0: (a) OCR versus A_f, (b) K_0 versus A_f.

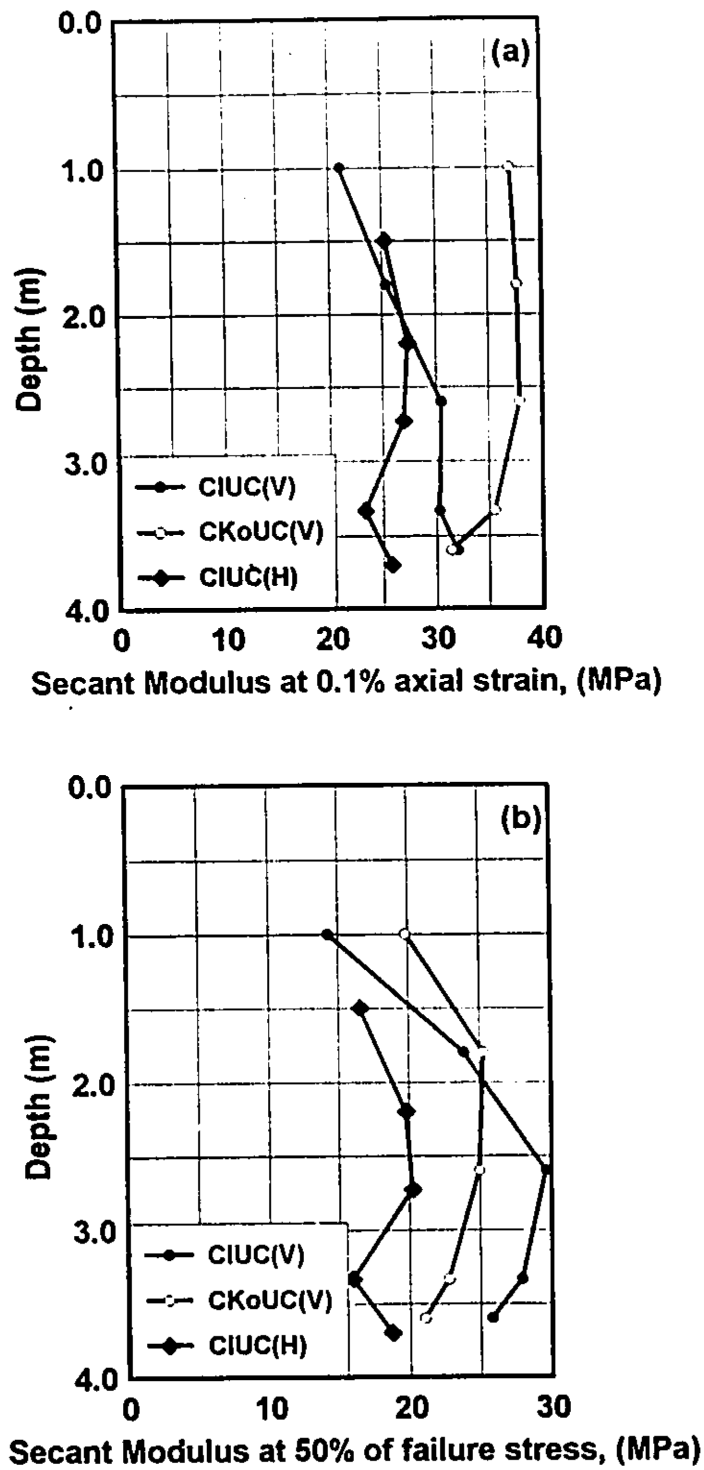

Fig. 7.7. Secant modulus of deformation: (a) at 0.1% of axial strain $E_{0.1}$, and (b) at 50% of failure stress, E_{50}.

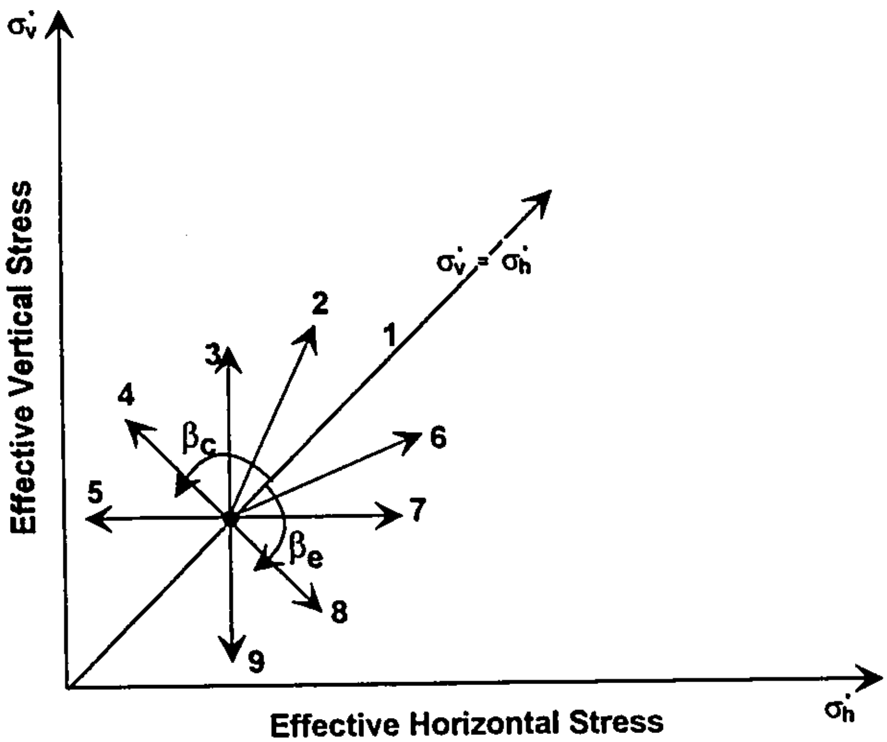

Stress-path 1:	Isotropic compression.
Stress-path 2:	Represents Test No. BS333T7 (Fig. A.45).
Stress-path 3:	Represents Test No. BS333T5 (Fig. A.43).
Stress-path 4:	Represents Test No. BS333T10 (Fig. A.48).
Stress-path 5:	Represents Test No. BS333T6 (Fig. A.44).
Stress-path 6:	Represents Test No. BS333T18 (Fig. A.56).
Stress-path 7:	Represents Test No. BS333T1 (Fig. A.39).
Stress-path 8:	Represents Test No. BS333T11 (Fig. A.49).
Stress-path 9:	Represents Test No. BS333T17 (Fig. A.55).

Fig. 7.8 Stress paths followed to study the stress-path dependent behaviour.

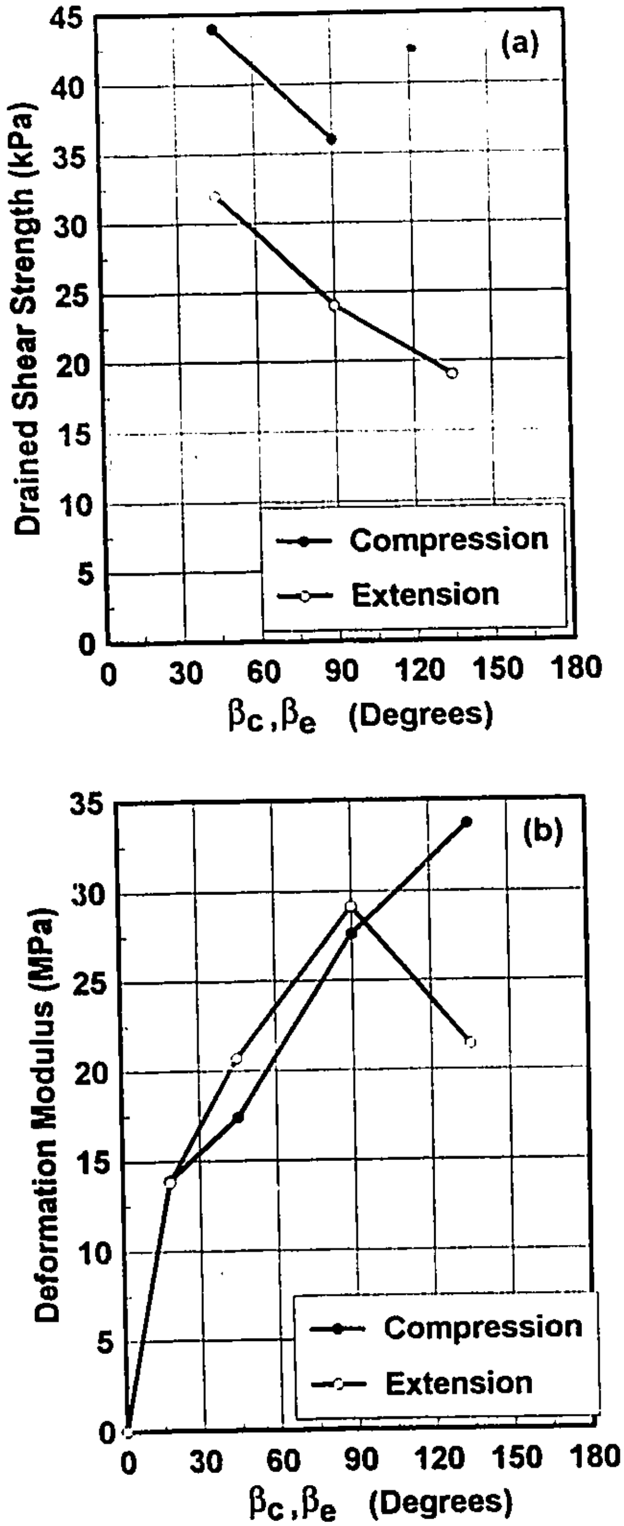

Fig. 7.9 Effect of stress path on shear strength (a) and deformation modulus (b).

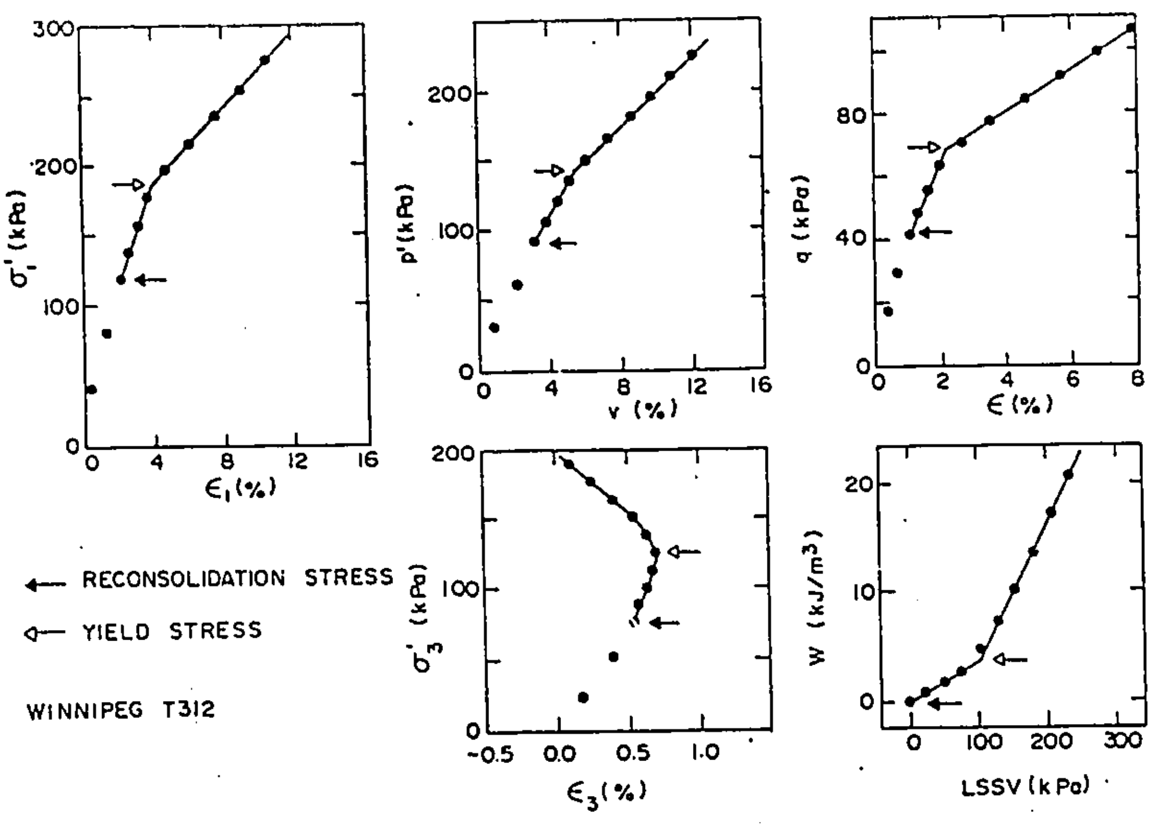

Fig. 7.10 Yielding identification from bilinear plot of various stress-strain criteria (Graham et al. 1983).

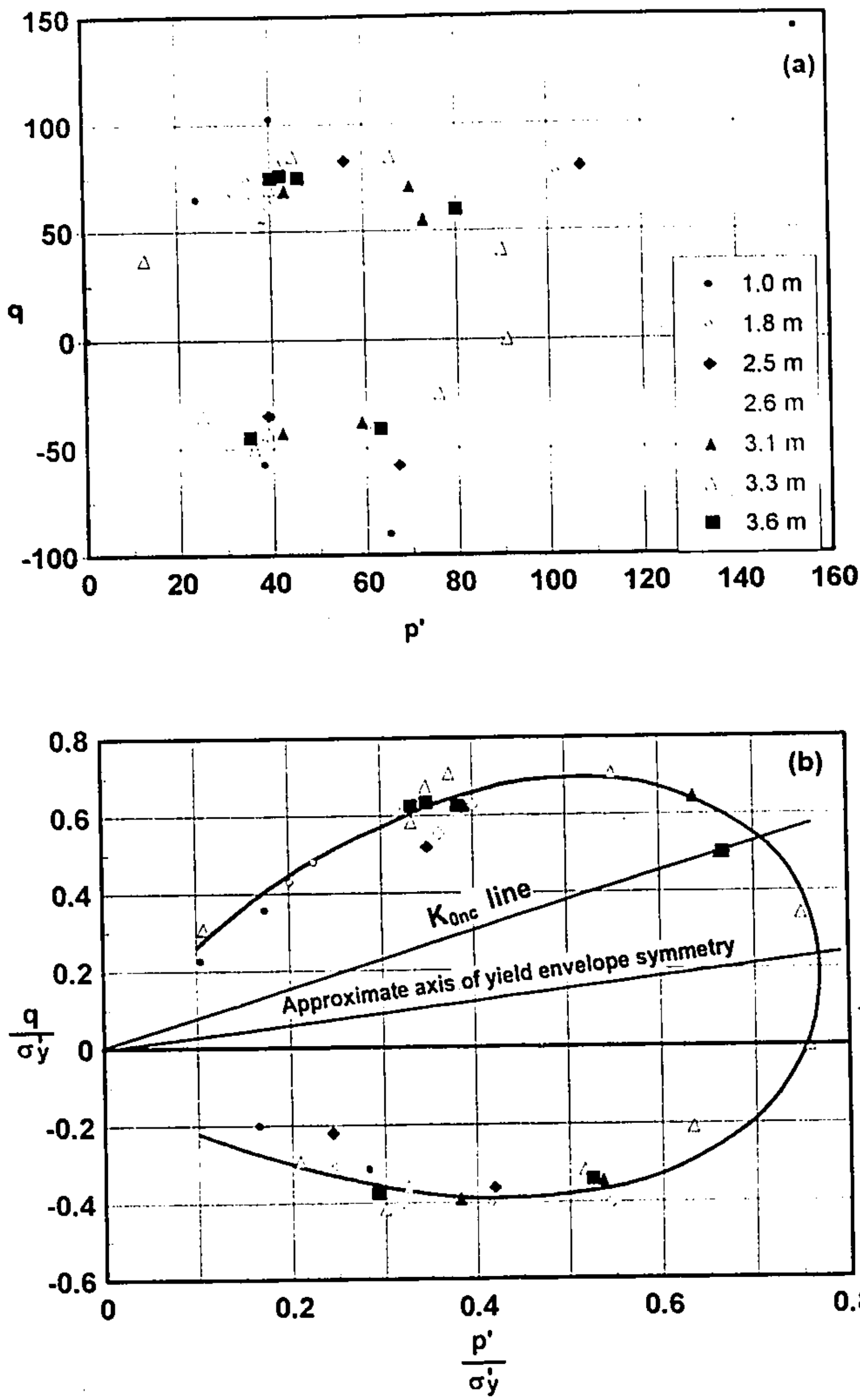

Fig. 7.11. (a) Yield stresses for various stress paths, (b) Yield envelope from normalized yield stresses.

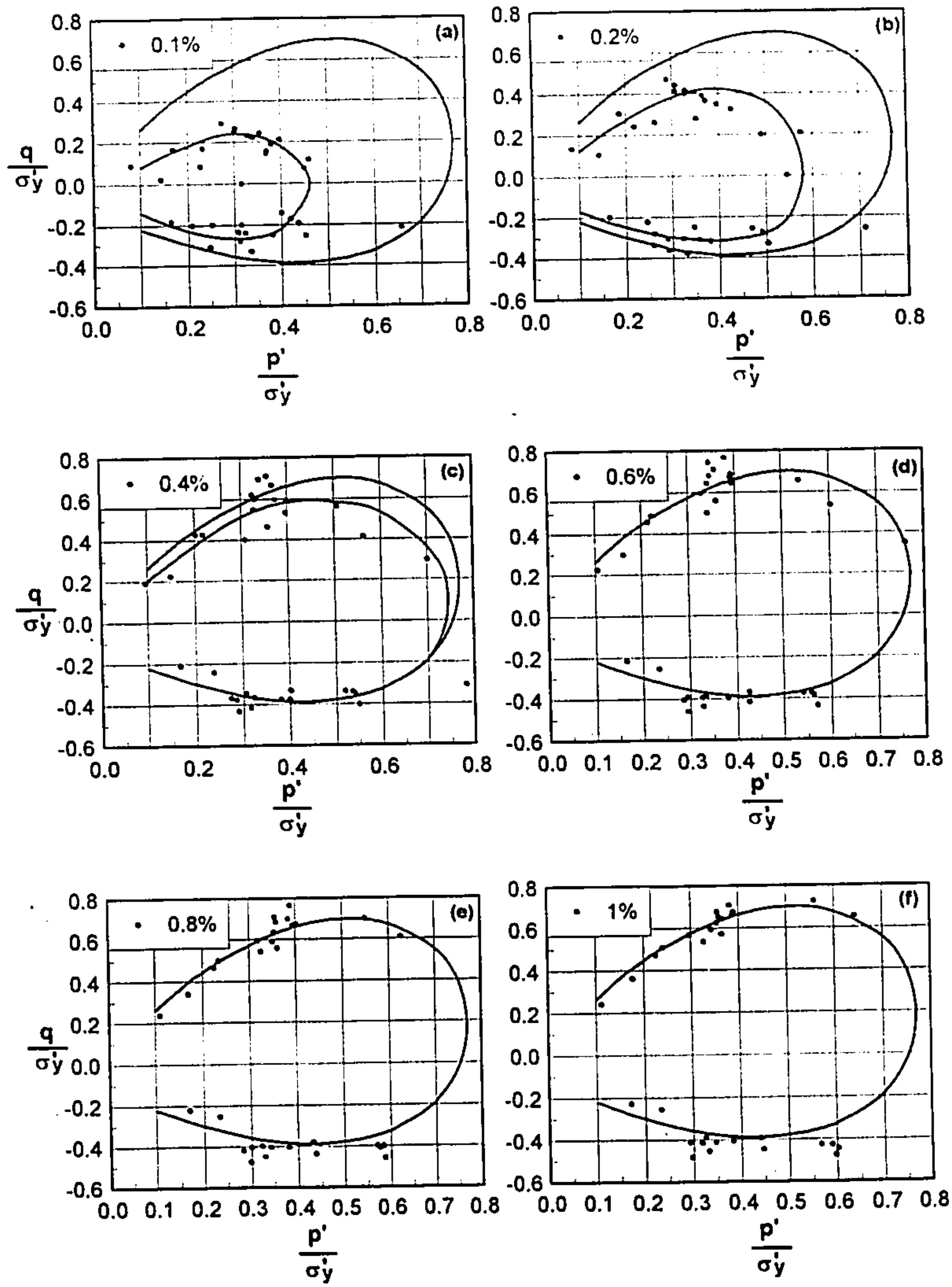

Fig. 7.12. Strain contours for various strain levels
(the outermost curve in each plot is the yield envelope).

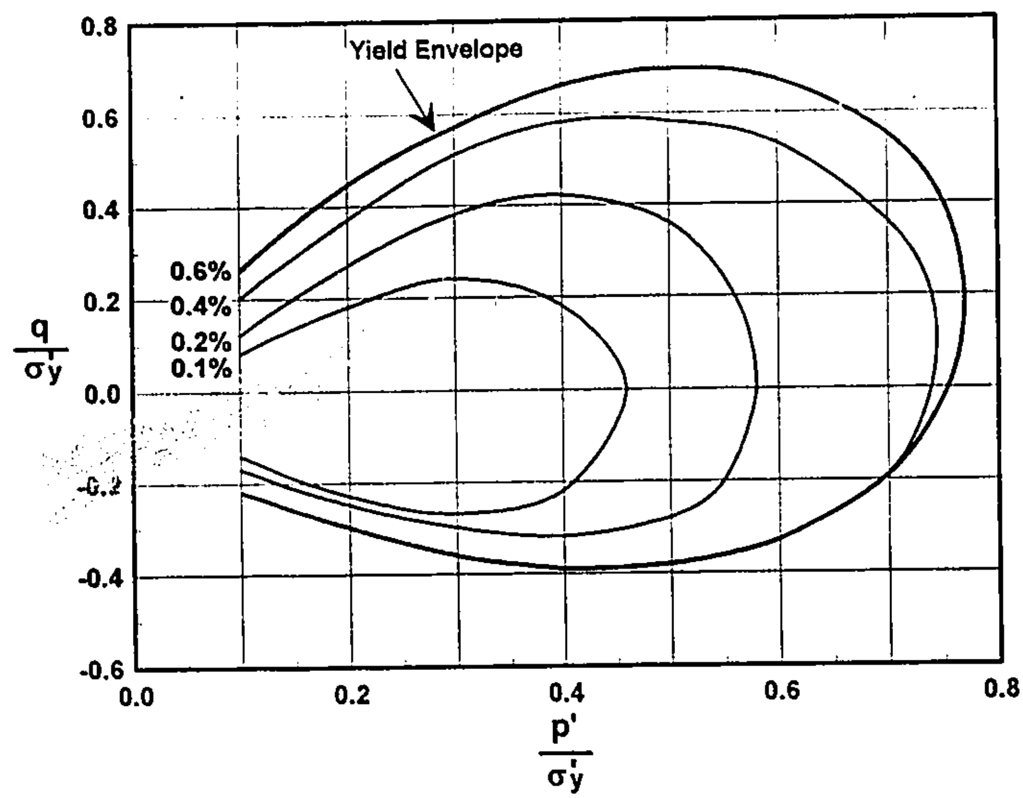

Fig. 7.13. Strain contours within the yield envelope.

CHAPTER 8

RESULTS AND ANALYSIS OF CONSOLIDATION TESTS

8.1 Introduction

The consolidation of a saturated soil is a process of volume reduction due to the expulsion of water from the void space of the soil. If the process is slow, it can occur without the generation of significant pressures in the porewater; if it is rapid, the compression induced by stress change is inhibited by the inability of the water to drain away quickly enough, and this results in a temporary increase in the porewater pressure. The build-up and the dissipation of porewater pressures is related to the magnitude and rate of loading, the length of the drainage path, the permeability of the soil, and the compressibility of the soil structure.

The conventional oedometer test, based on Terzaghi's one-dimensional consolidation theory, has been commonly used in practice for settlement analyses. A standard procedure (ASTM D2435-65T) is mostly used to perform the test and to interpret the data. Commonly load-increment ratio of unity is applied, and each stress increment is applied for 24 hours to obtain the characteristic time-settlement curves from which coefficient of consolidation (c_v) is computed. The use of this procedure may take several weeks to complete a consolidation test in a clayey soil. The resulting void ratio (e) versus logarithm of vertical effective stress (σ_v'), from the limited number of data points, can be ill-defined giving a poor estimation of preconsolidation (maximum past) pressure.

Comparison with field rates of loading shows that the conventional laboratory test rates are fast and unrealistic (Crawford 1964). It has been suggested that the rate of loading is a much more influential factor than many of the other known factors of testing. Therefore, this incremental step-loading test for the evaluation of consolidation properties is being replaced by controlled rate of strain tests (Crawford 1988).

To speed up the testing procedure and to avoid the sudden impact of step-loading tests, three continuous type of loading tests have been reported: (1) the constant rate of strain (CRS) test (Smith and Wahls 1969), (2) the controlled gradient (CG) test (Lowe et al. 1969), and (3) the constant rate of loading (CRL) test (Aboshi et al. 1970). To study the influence of testing method on the consolidation characteristics of the weathered crust, these three types of continuous loading and the conventional 24-hour step-loading tests have been conducted during this research. The versatile consolidation apparatus developed during this research as described in Chapter 5 is capable of performing all these four types of tests, and was used for this study. For all the tests performed with this new apparatus, samples were saturated using the back-pressuring technique, before the start of consolidation tests.

8.2 Testing Programme

Four different types of consolidation tests were carried out during this study. Specimens used for conventional oedometer tests were 49.92 mm in diameter and 19.15 mm in height, and the specimens for the three types of continuous loading consolidation tests were 76.10 mm in diameter and 30.63 mm in height. The room temperature maintained for all these testing was approximately 21°C. Test methods used are briefly described as follows:

(a) ***Oedometer consolidation test:*** Specimens were loaded in steps using a load increment ratio $\Delta p/p = 0.5$ at an interval of 24 hours; drainage was allowed at both ends of the specimen and no porewater pressure measurements were made for these tests. Few tests were also conducted with load increment ratio LIR = 1 to study the effect of different LIRs on consolidation behaviour.

(b) ***Constant rate of strain (CRS) test:*** Strain rate used varied between 1.26×10^{-4} - 1.90×10^{-4} %/sec. The CRS tests performed in this study were slightly different than the commonly known CRS tests where gear-operated strain-control is used. The strain-control used in this research was computer-controlled from the feed-back of the LVDT with time. At a convenient time interval, the computer increases the vertical stress to achieve the required strain level.

(c) ***Controlled gradient (CG) test:*** The porewater pressure difference Δu_b between the top and bottom of the specimen maintained was approximately 15 kPa. As shown by Wissa et al. (1971), the pore pressure difference Δu_b is related, among other parameters, to the strain rate of the specimen. Therefore, varying the magnitude of Δu_b in the CG tests will have an effect on the stress-strain behaviour of the clay similar to that observed when varying strain rate in the CRS tests. The rate of stress increase was comparatively fast at the beginning of the test as the computer-control system attempted to achieve the value of Δu_b from zero to the desired level.

(d) ***Constant rate of loading (CRL) test:*** Rate of loading or rate of stress used was 0.005 kPa/sec. Maximum Δu_b generated for this rate of stress was approximately 11 kPa. The increase in the value of Δu_b continued up to the consolidation stress equal to the preconsolidation stress; thereafter Δu_b decreased.

In test type (a), where 24-hr incremental loading was used, the samples were double-drained. Single drainage was used in all the samples in tests (b), (c) and (d) where continuous loading was applied. For these continuous loading tests, the back pressure, which was equal to the *in situ* effective overburden pressure σ_{v0}', was applied from the top of the specimen, and the porewater pressure was measured at the bottom of the sample. The duration of continuous loading tests was 1-2 days, and that for oedometer tests was 10-14 days for the loading stress up to 1000 kPa.

8.3 Results of Consolidation Tests

A complete list of all the consolidation tests, conducted during this research, is tabulated in Table 8.1. Table 8.1 shows the various conditions and the values of natural water contents and preconsolidation pressures determined from these tests. Respective overconsolidation ratios for vertically oriented samples are also shown in Table 8.1. These tests have been conducted for the depth range of 0.75 m to 3.70 m. The plots for void ratio, coefficient of consolidation, coefficient of volume compressibility and permeability are provided in Appendix B. All these consolidation characteristics have been plotted against logσ_v'. Among the total of 22 consolidation tests, 16 conventional 24-hour step-loading tests and 6 non-conventional continuous loading (constant rate of strain, constant rate of loading, controlled gradient) consolidation tests have been conducted. Both horizontally and vertically oriented samples were used in the conventional testing program to determine the anisotropy in consolidation behaviour.

8.3.1 Evaluation of Preconsolidation Pressure

It is important to determine the preconsolidation pressure (σ_p') by a reliable method since this is the single most value which controls the behaviour of a clay (Leroueil et al. 1983). Preconsolidation pressures (σ_p') were determined by the Casagrande (1936) method. There is some uncertainty in the determination of σ_p' from the Casagrande (1936) method since different individuals will get different values of σ_p' by this method. This uncertainty occurs because of the freedom the individuals have while selecting the point of maximum curvature and drawing the tangent at this point of the e-logσ_v' curve using eye estimation. However, it has been observed that more consistent results can be obtained by different individuals when the intersection point of the projected straight lines of reloading and virgin compression parts is considered as the preconsolidation pressure. In this study, this point of intersection has been considered as the yield stress (σ_y') while the preconsolidation pressure has been estimated from the Casagrande (1936) method. It has also been observed that the σ_y' is always slightly smaller than σ_p'. This value of σ_y' is also known as the minimum preconsolidation pressure.

Continuous loading tests yielded higher values (10%-15%) of preconsolidation pressures (Figs. 8.6a and 8.7a) than the conventional oedometer tests. This may be for either of the following two reasons: (i) due to the higher rates of strain used in the continuous loading tests, or (ii) due to the sample size effect. Larger samples (76 mm diameter) were used in all the continuous loading tests whereas 50 mm samples were used for all the oedometer consolidation tests.

The difference in LIRs does not have significant influence on the value of preconsolidation pressure (Fig. 8.7a). However, it has been observed that the e-logσ_v' curve for LIR = 0.5 was smoother and more consistent than that for LIR = 1 (Fig. 8.7a).

8.3.2 Anisotropy in Consolidation Behaviour

To study the anisotropic consolidation behaviour, both vertically and horizontally oriented samples were tested in the oedometer for five depth levels (1.96 m, 2.03 m, 2.60 m, 3.30 m and 3.70 m).

The preconsolidation pressures obtained for horizontal samples are slightly smaller than those of vertical samples with the exception of 2.60 m. At 2.60 m, the preconsolidation pressure in the horizontal direction is higher than that of the vertical direction which may be due to some experimental error. In the vicinity of preconsolidation pressure, the portion of the e-logσ_v' curve for horizontal direction is always below that of the vertical direction. This indicates that the sample is more rigid in the vertical direction than in the horizontal direction which could be for two reasons; (i) the variation in stress history, and (ii) the variation in orientation of soil structure, in these two orthogonal planes.

The values of coefficient of consolidation (c_v) and permeability (k) are always higher in the horizontal direction than those values in the vertical direction for respective depth levels (Figs 8.1b,d - 8.5b,d). This indicates that the *in situ* soil particles are oriented along the horizontal direction providing more surface area in the vertical direction.

In addition to the permeability values obtained from the consolidation tests, these values were also measured *in situ* as well as in the laboratory using the constant-head method. The *in situ* permeability of the crust at this site lies in the range of 2×10^{-7} to 3×10^{-5} m/s (O'Shaughnessy 1993). Permeability values measured from laboratory constant-head tests, conducted on samples that were consolidated to *in situ* vertical stresses in a 76 mm hydraulic oedometer, lie in the range of 1.9×10^{-9} to 2.5×10^{-8} m/s. The field c_v values may be estimated by a combination of *in situ* k and laboratory m_v values.

Although there are some differences in horizontal and vertical directions for σ_p', c_v and k, virtually no significant difference is observed in the volume compressibility values (Figs.

8.1c-8.5c). The volume compressibility, which is defined as the volume change per unit volume per unit increase in effective stress, was determined directly by dividing the unit volume change by the stress increase at the various stress levels. The coefficient m_v appears to relatively independent of the direction of the application of consolidation stress, for the stress range covered in the experimental programme.

8.4 Effect of Rate of Loading

The laboratory rates of compression are considerably faster than known field rates. The maximum known rate for Champlain Clay, for a foundation of earth-fill consisting of both crust and lower clay, is approximately 1%/year (Crawford 1964). Obviously, if rate of compression affects the compressibility of the soil, the risk of extrapolating laboratory test results to actual problems is great. The estimation of permeability from consolidation testing is particularly suspect, because of the rapid loading required to produce porewater pressure in a small element of soil. Crawford (1964) suggested that the laboratory consolidation test be conducted at a steady rate of compression sufficiently slow to prevent the development of significant porewater pressures. Such a test should provide a more realistic evaluation of soil compressibility by avoiding the impact and extremely rapid rates of strain caused by incremental loading.

Estimation of soil settlement is likely to be seriously in error when load increments in the field and in the test are not similar (Crawford 1964). Field loading is seldom applied in increments. The following two consequences are evident for incremental loading tests: (1) Sudden large increments cause a shock to the soil structure; and (2) the induced porewater pressure gradients cause internal rupture of the soil structure. The continuous loading tests, in which the stress is increased gradually, simulates the field situation better than the conventional incremental loading tests, and should be used to estimate the field consolidation behaviour.

Preconsolidation pressure, coefficient of consolidation and permeability values seem to be dependent on the testing procedure as well as the direction of consolidation. The controlled gradient test yielded the highest value of c_v whereas the oedometer test provided the lowest (Fig. 8.7b). However, it is interesting to note that the value of m_v is neither sensitive to the testing procedure nor to the direction of consolidation, and is almost same for any specific depth irrespective of testing method and sample orientation (Figs. 8.1-8.7).

For conventional oedometer tests, the range of infered permeability values for the same test at different stress levels is different by several order of magnitude, and that range obtained from continuous type of consolidation tests is within one order of magnitude (Figs. 8.1b-8.5b).

The load increment ratio (LIR), $\Delta p/p$ of 0.5, which is mostly used (Leroueil et al. 1983) for similar type of clays in Eastern Canada, has been used for most of the tests. However, few tests have also been conducted with LIR = 1 to investigate the effect of different LIRs. It has been observed that the LIR = 0.5 gives better and consistent e-logσ_v' curve.

It is interesting to note that the values of permeability and the coefficient of volume compressibility m_v become minimum before approaching the vicinity of the preconsolidation pressure σ_p' and become maximum when the stress level exceeds the preconsolidation pressure (Figs. 8.1c-d through 8.7c-d). The reason for this observation may be that the soil particles get closer due to the expulsion of water from the pore spaces, resulting in less value of permeability and volume compressibility, just before reaching preconsolidation pressure, and beyond the σ_p' the soil specimen tends to dilate resulting in higher permeability.

Table 8.1 Results of Consolidation Tests.

Sample No.	Depth (m)	Initial H x D (mm)	Loading Type	Orienta-tion	Drainage type	Natural w.c.	σ_p' (kPa)	OCR
SB100DV	1.00	19.2 x 49.9	LIR=0.5	V	Double	0.30	260	16.05
SB180DV	1.80	19.2 x 49.9	LIR=0.5	V	Double	0.36	200	8.64
SB196DV	1.96	19.2 x 49.9	LIR=0.5	V	Double	0.35	220	8.71
SB203DV	2.03	19.2 x 49.9	LIR=0.5	V	Double	0.35	280	11.07
SB245DV	2.45	19.2 x 49.9	LIR=0.5	V	Double	0.36	200	6.8
SB260DV	2.60	19.2 x 49.9	LIR=0.5	V	Double	0.36	155	5.20
BS315DV	3.15	19.2 x 49.9	LIR=1.0	V	Double	0.41	110	3.14
BS316DV	3.16	19.2 x 49.9	LIR=0.5	V	Double	0.42	130	3.71
BS330DV	3.30	19.2 x 49.9	LIR=0.5	V	Double	0.41	130	3.64
BS370DV	3.70	19.2 x 49.9	LIR=0.5	V	Double	0.43	120	3.08
BS075DH	0.75	19.2 x 49.9	LIR=1.0	H	Double	0.26	190	-
SB196DH	1.96	19.2 x 49.9	LIR=0.5	H	Double	0.34	220	-
SB203DH	2.03	19.2 x 49.9	LIR=0.5	H	Double	0.35	250	-
SB260DH	2.60	19.2 x 49.9	LIR=0.5	H	Double	0.33	160	-
BS335DH	3.35	19.2 x 49.9	LIR=0.5	H	Double	0.41	110	-
BS370DH	3.70	19.2 x 49.9	LIR=0.5	H	Double	0.41	100	-
BS369HV	3.69	76.1 x 30.6	LIR=0.5	V	Single	0.41	145	-
BS315G	3.15	76.1 x 30.6	Gradient	V	Single	0.41	145	-
BS315N	3.15	76.1 x 30.6	Strain	V	Single	0.41	140	-
SB246S	2.46	76.1 x 30.6	Stress	V	Single	0.38	220	-
BS308S	3.08	76.1 x 30.6	Stress	V	Single	0.41	155	-
BS333TC3	3.33	101 x 50.6	Isotropic	V	Single	0.41	-	-

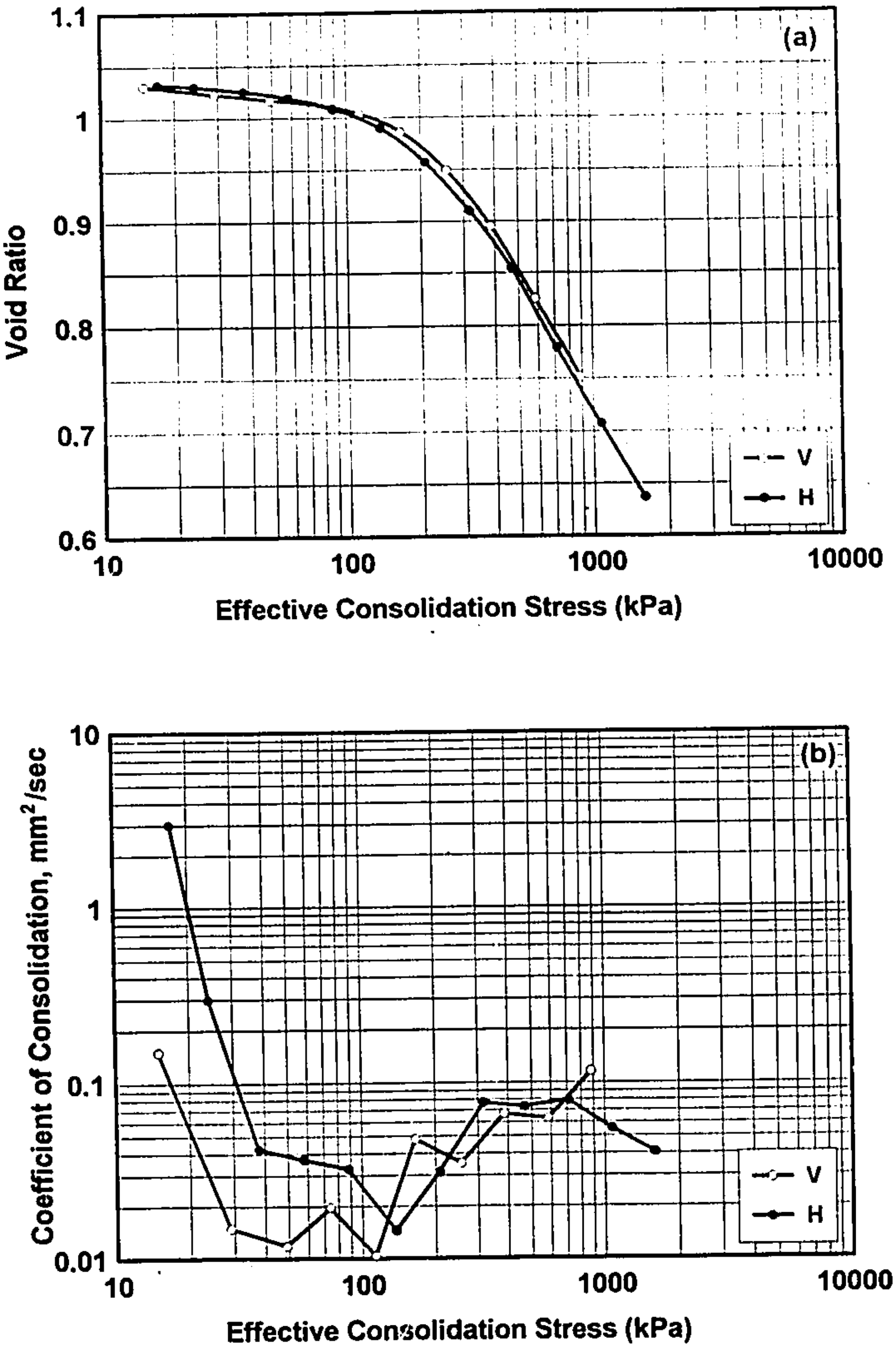

Fig. 8.1. Comparison of consolidation tests for vertical and horizontal samples (Depth = 1.96 m).

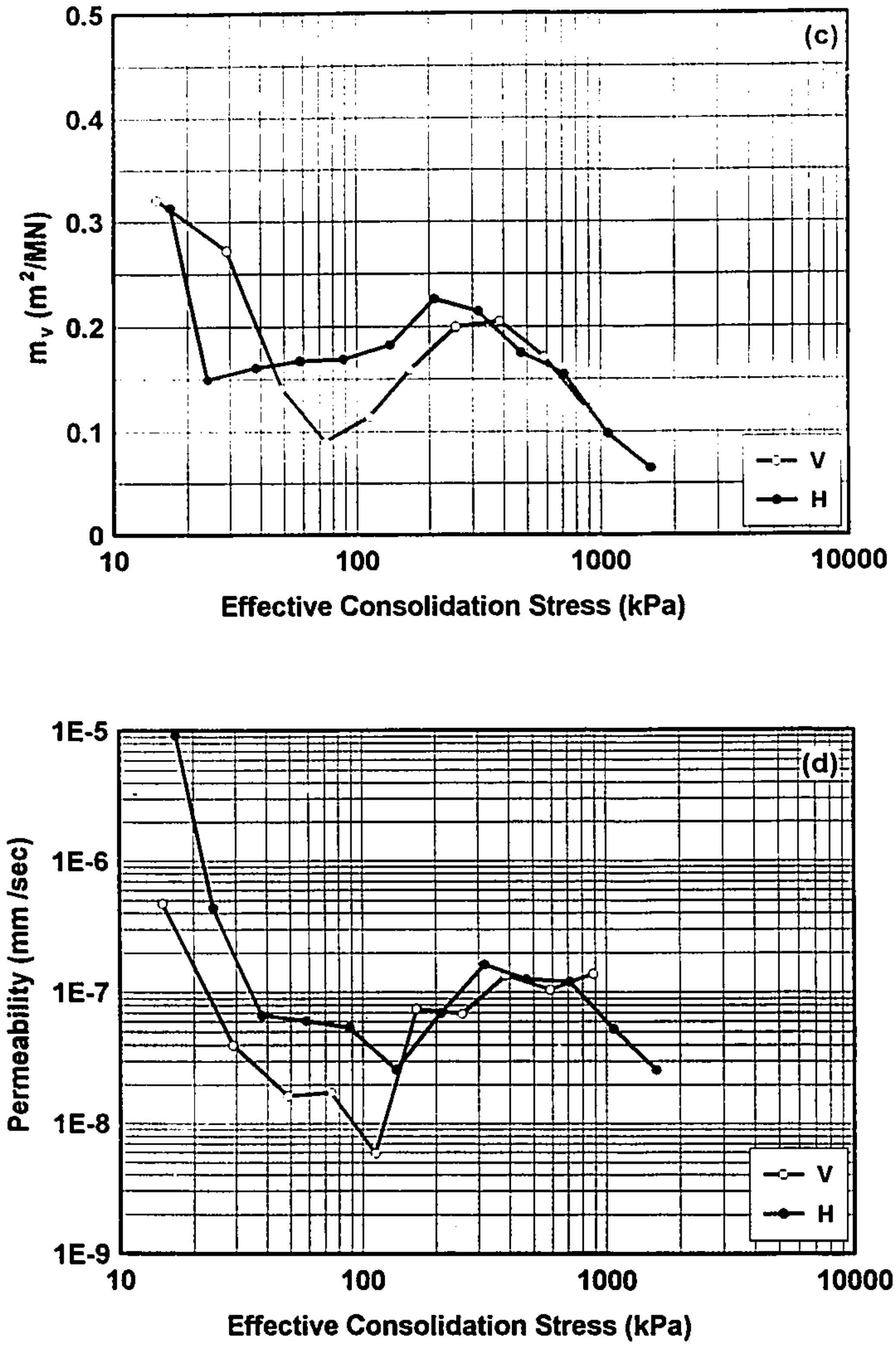

Fig. 8.1. Comparison of consolidation tests for vertical and horizontal samples (Depth = 1.96 m).

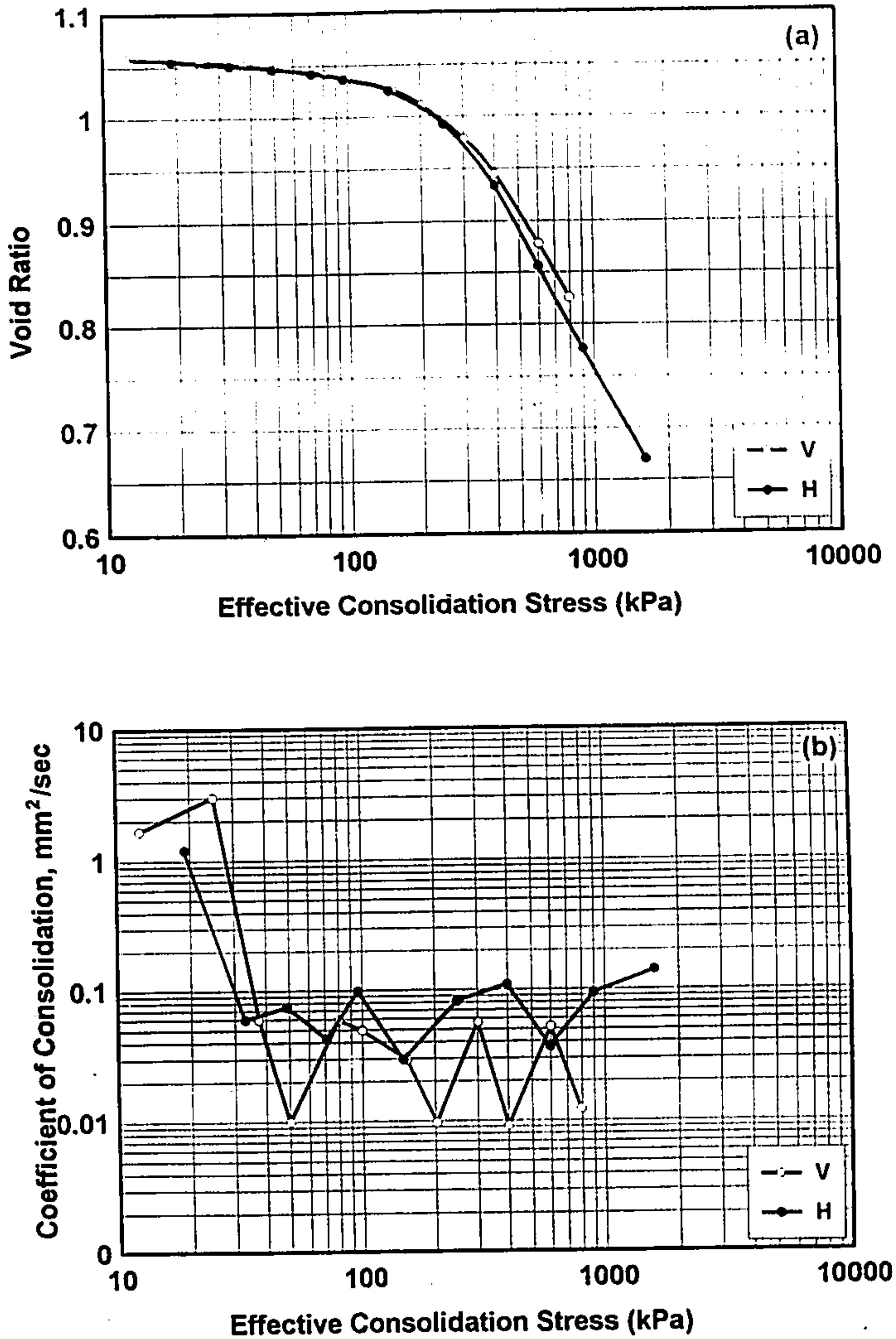

Fig. 8.2. Comparison of consolidation tests for vertical and horizontal samples (Depth = 2.03 m).

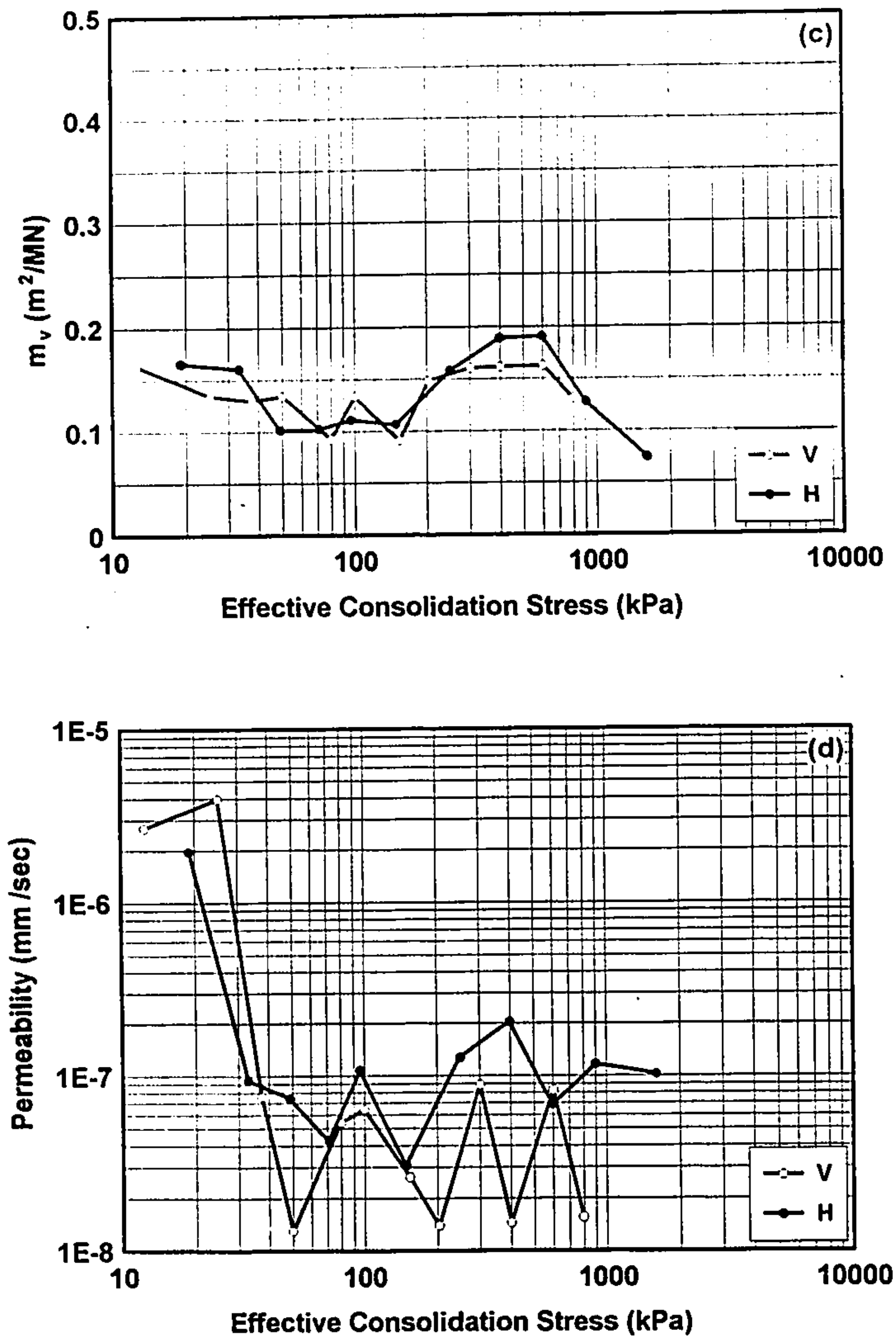

Fig. 8.2. Comparison of consolidation tests for vertical and horizontal samples (Depth = 2.03 m).

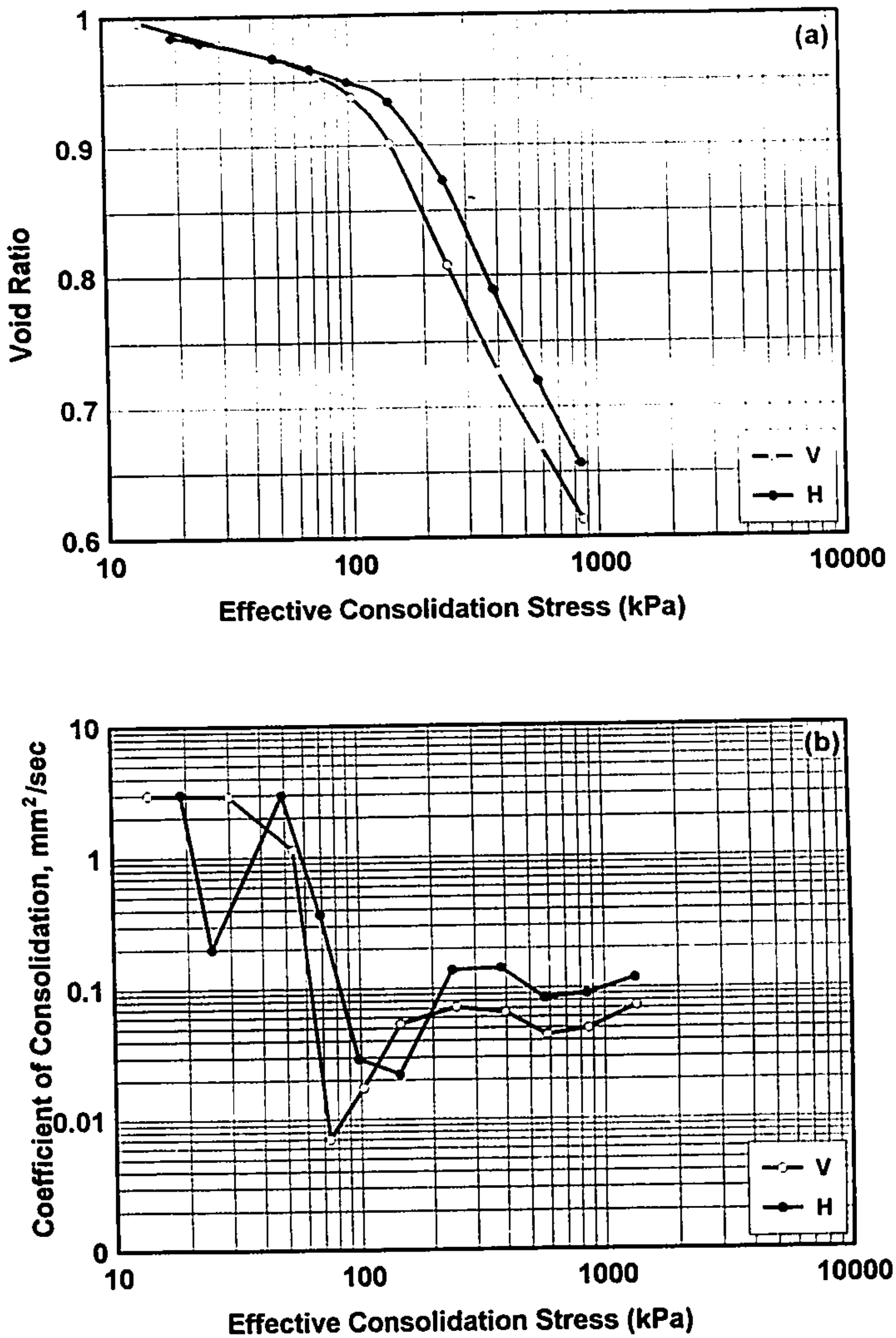

Fig. 8.3. Comparison of consolidation tests for vertical and horizontal samples (Depth = 2.60 m).

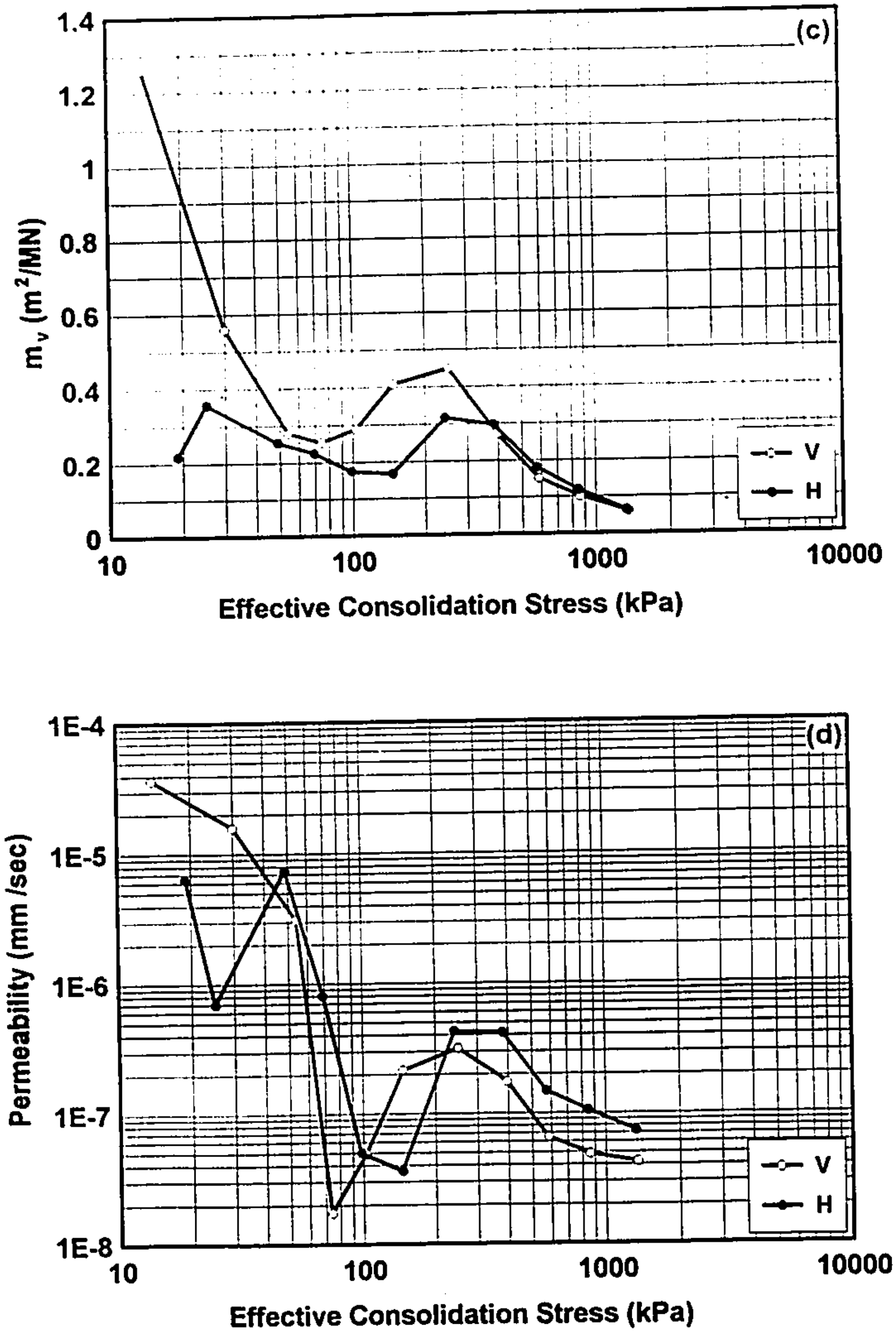

Fig. 8.3. Comparison of consolidation tests for vertical and horizontal samples (Depth = 2.60 m).

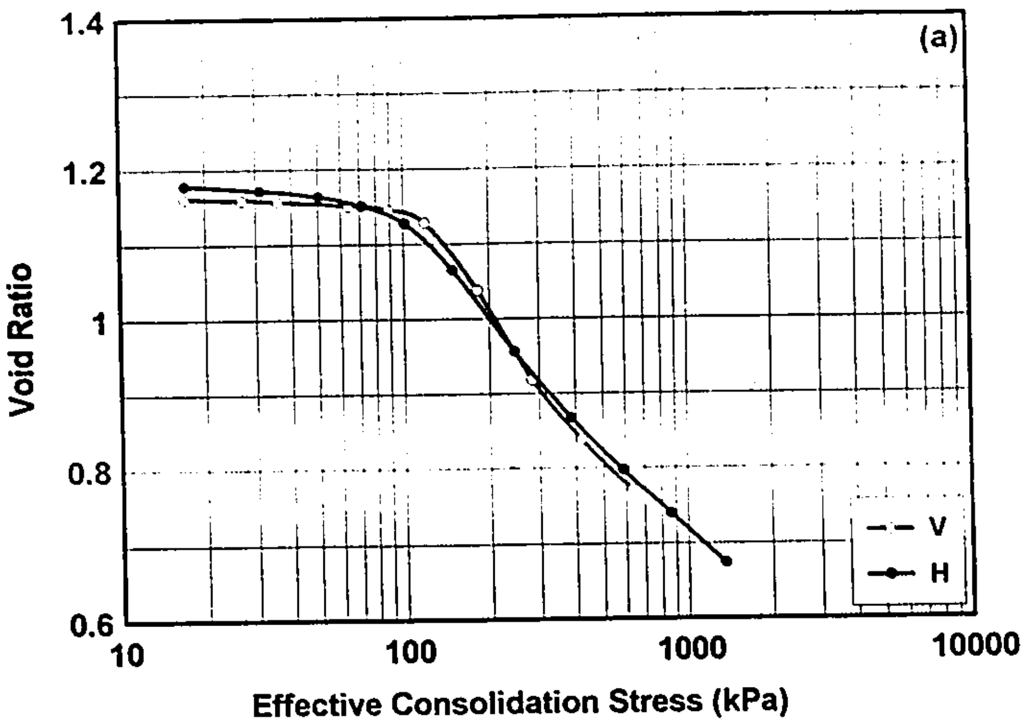

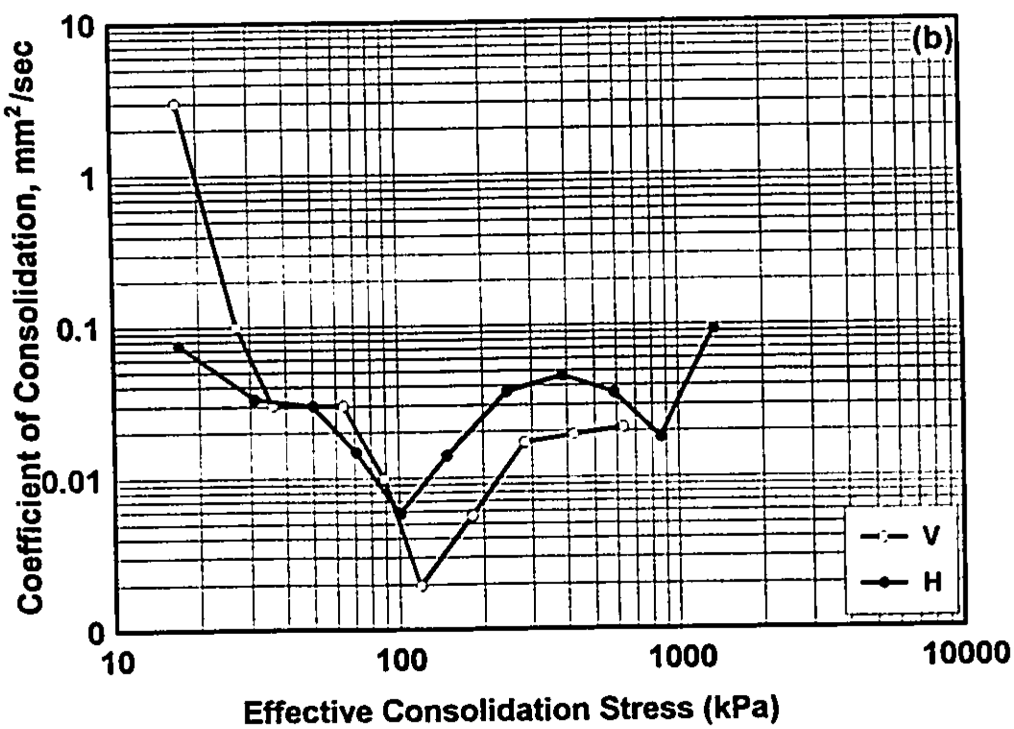

Fig. 8.4. Comparison of consolidation tests for vertical and horizontal samples (Depth = 3.30 m).

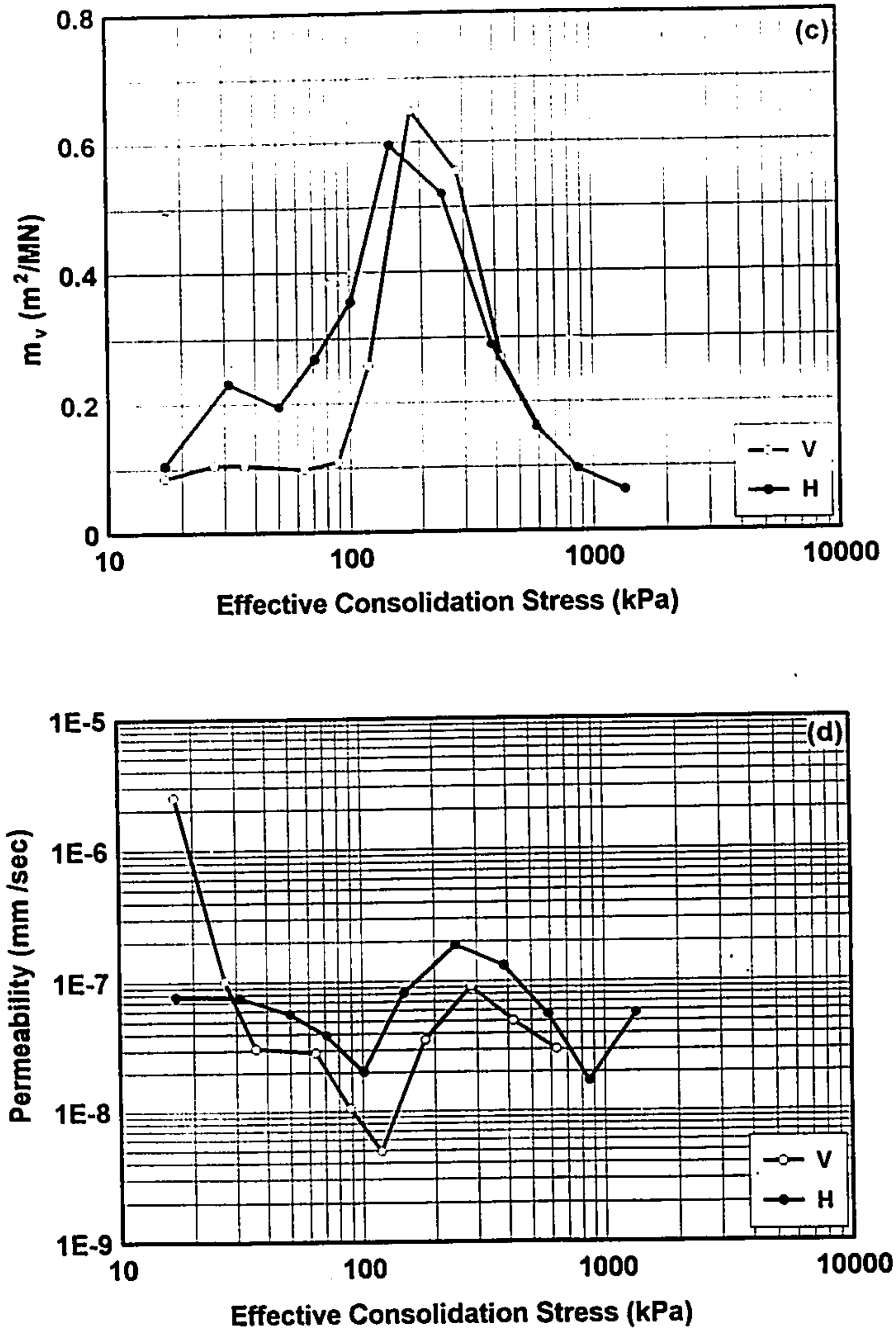

Fig. 8.4. Comparison of consolidation tests for vertical and horizontal samples (Depth = 3.30 m).

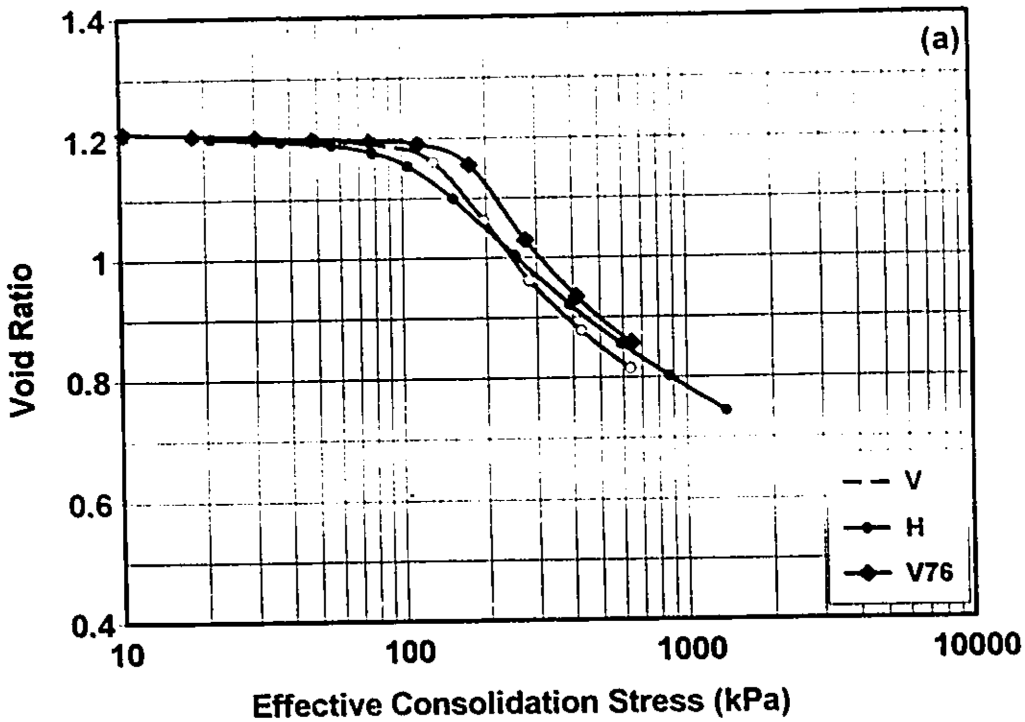

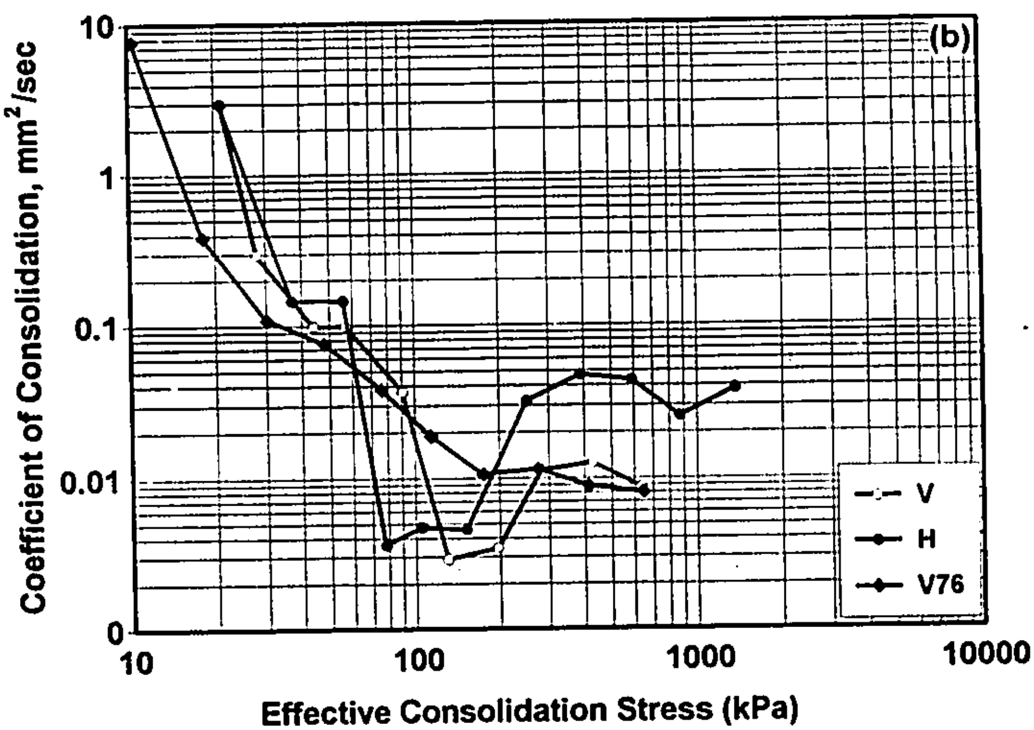

Fig. 8.5. Comparison of consolidation tests for vertical and horizontal samples (Depth = 3.70 m).

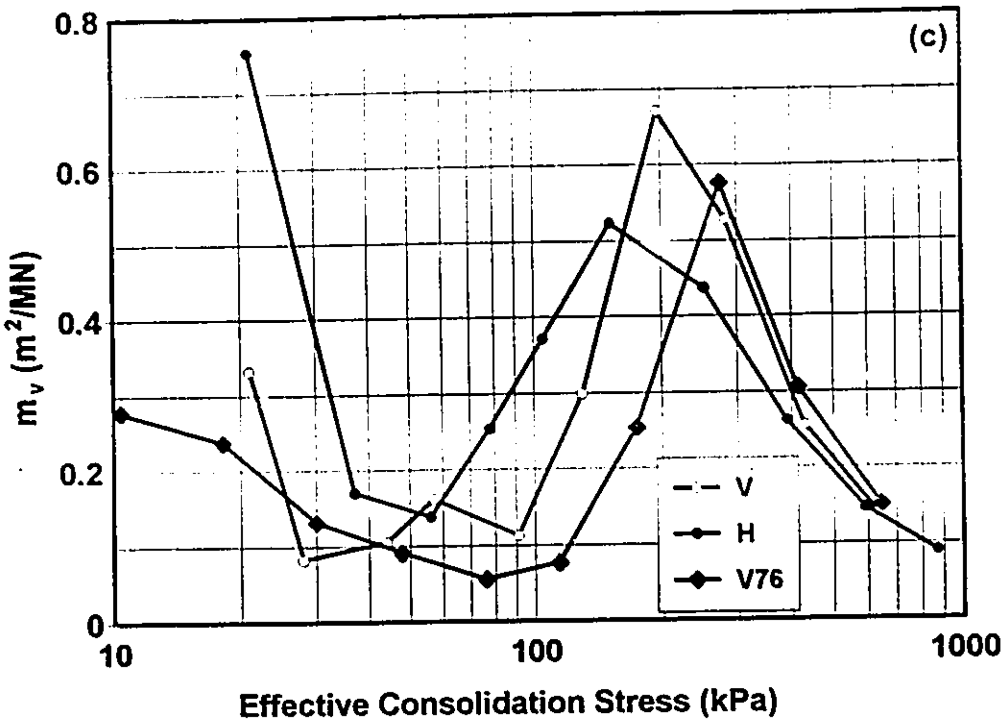

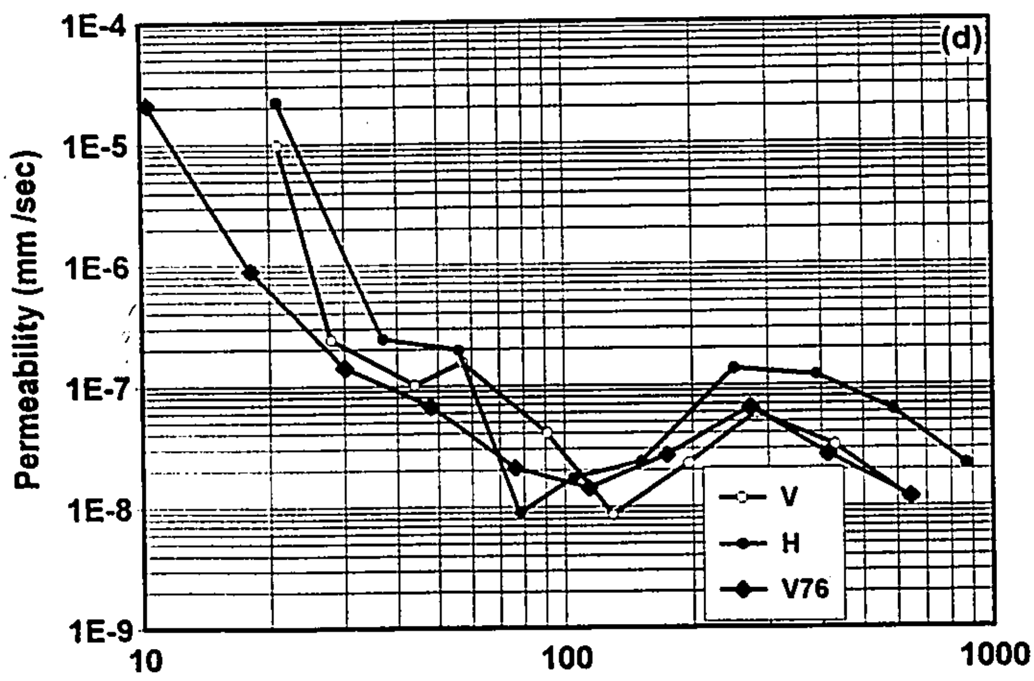

Fig. 8.5. Comparison of consolidation tests for vertical and horizontal samples (Depth = 3.70 m).

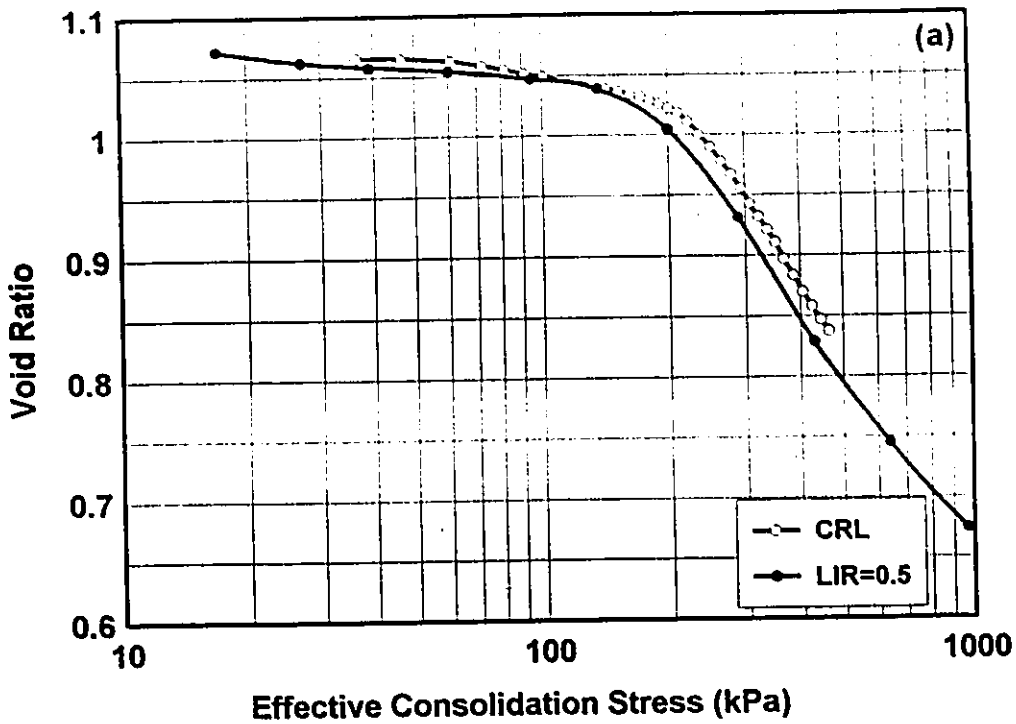

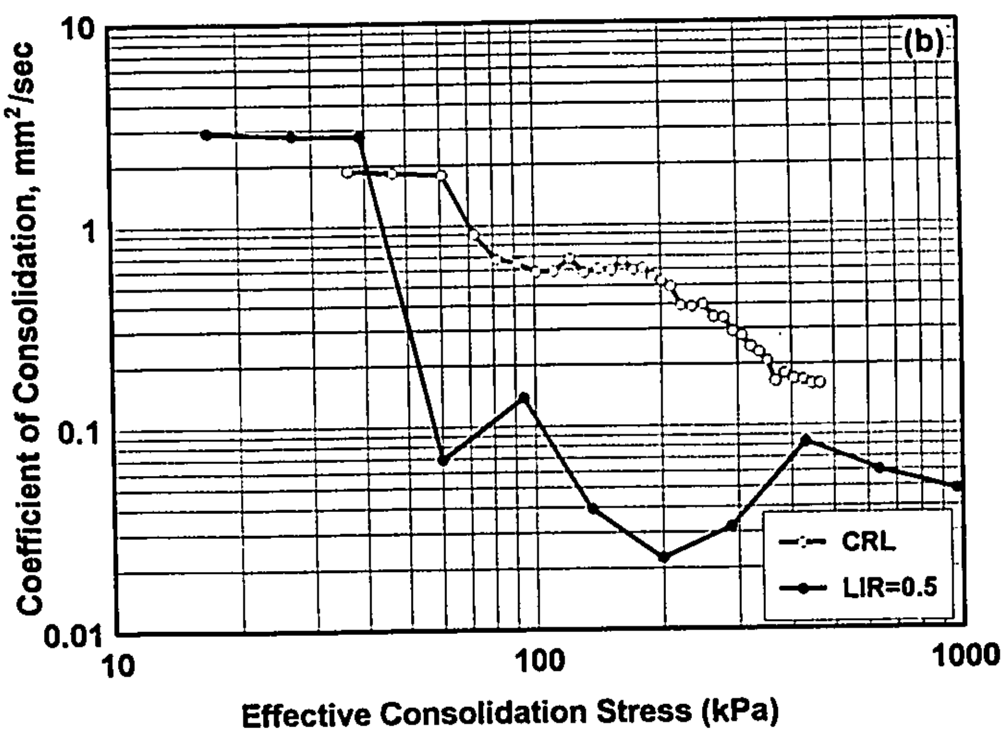

Fig. 8.6. Comparison of various types of consolidation tests (Depth = 2.45 m).

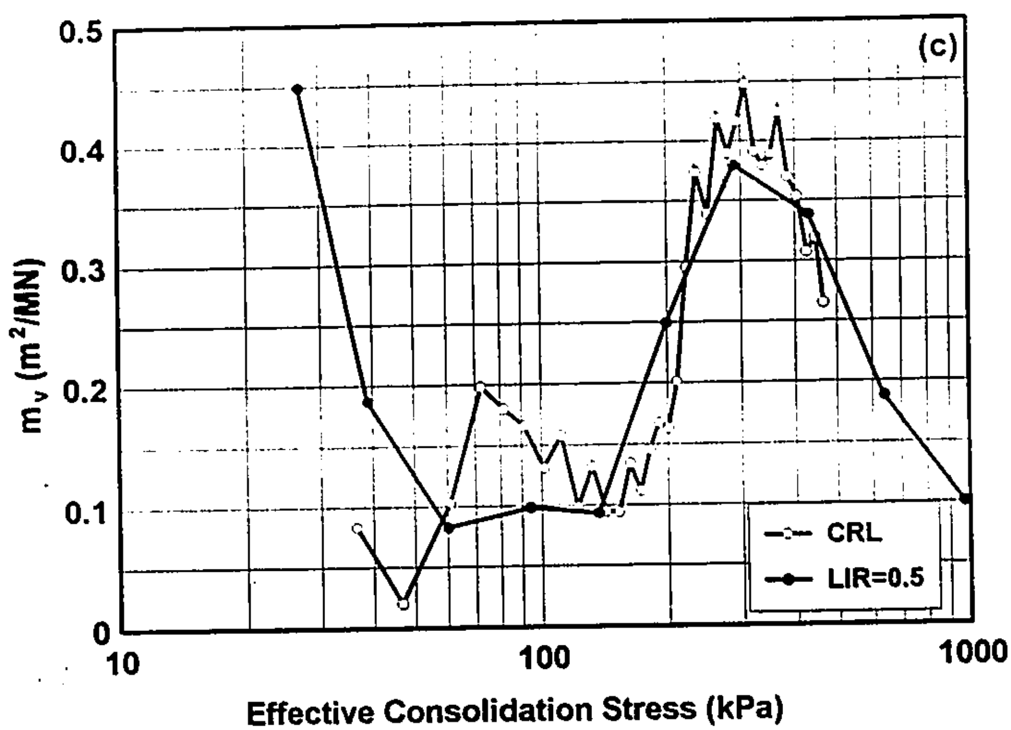

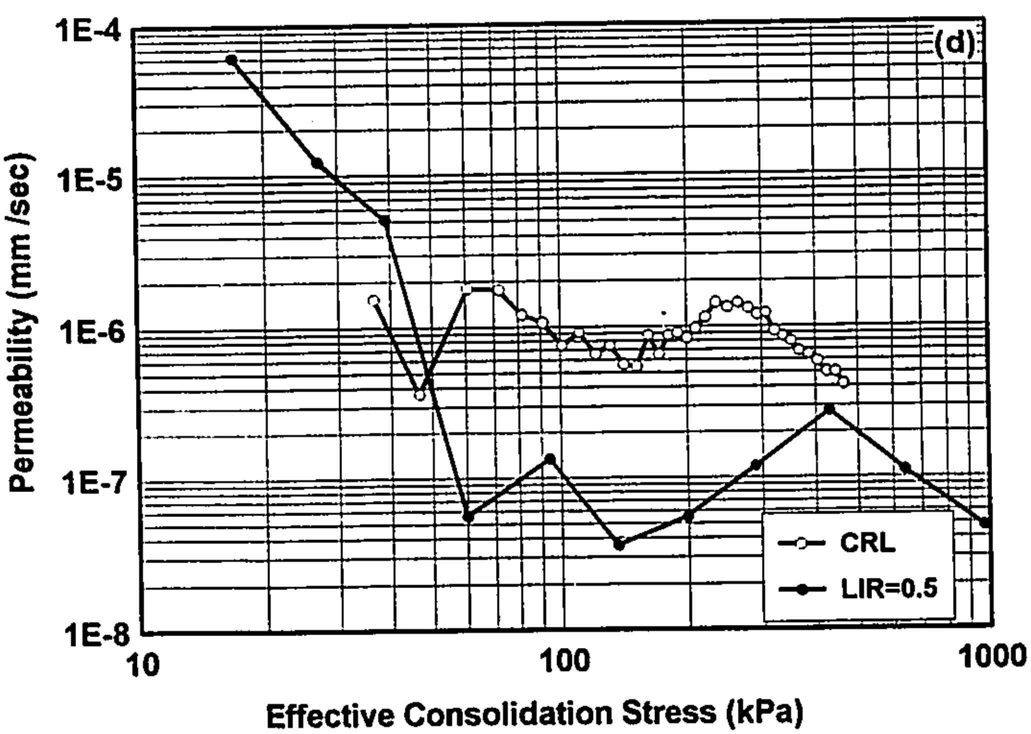

Fig. 8.6. Comparison of various types of consolidation tests (Depth = 2.45 m).

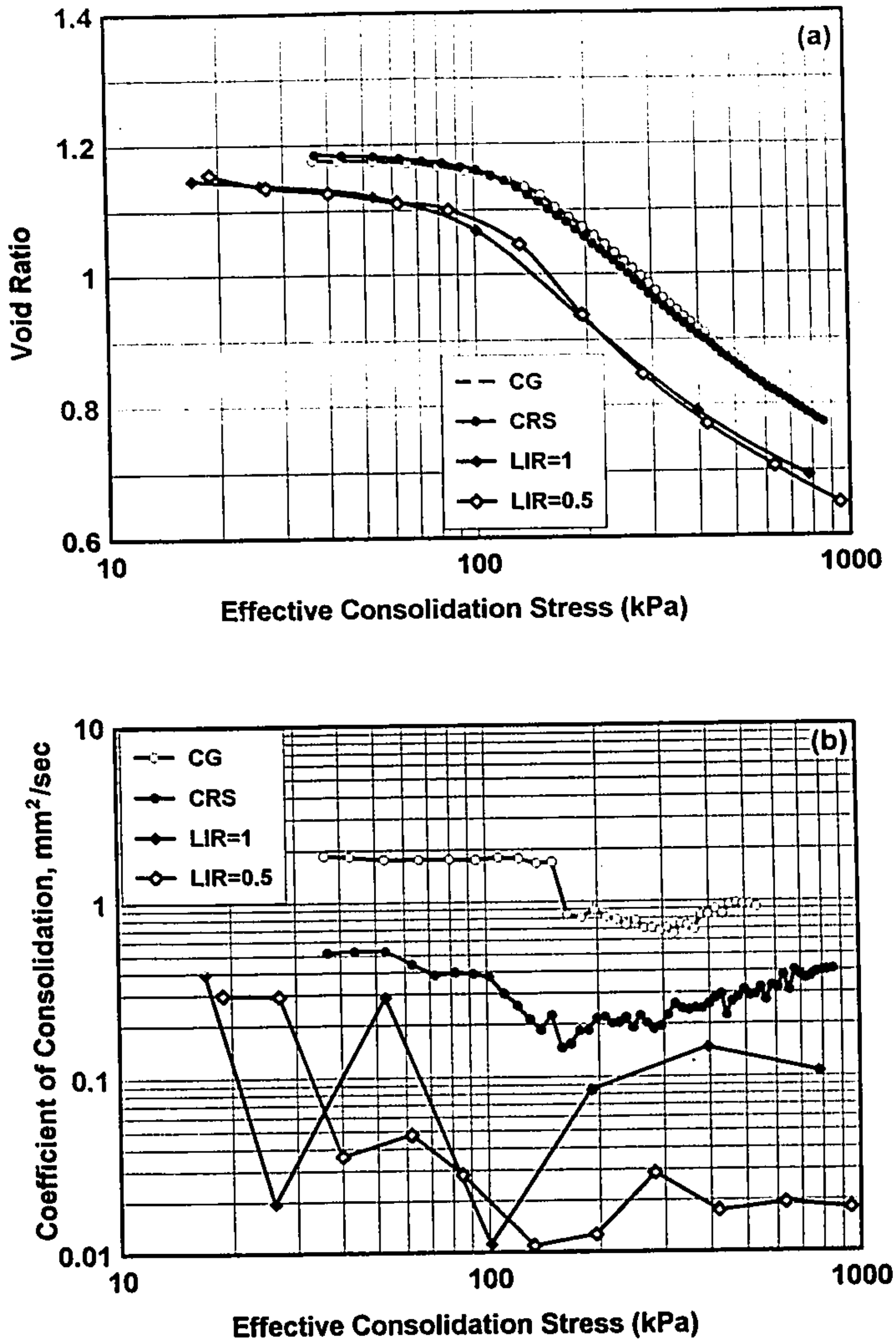

Fig. 8.7. Comparison of various types of consolidation tests (Depth = 3.15 m).

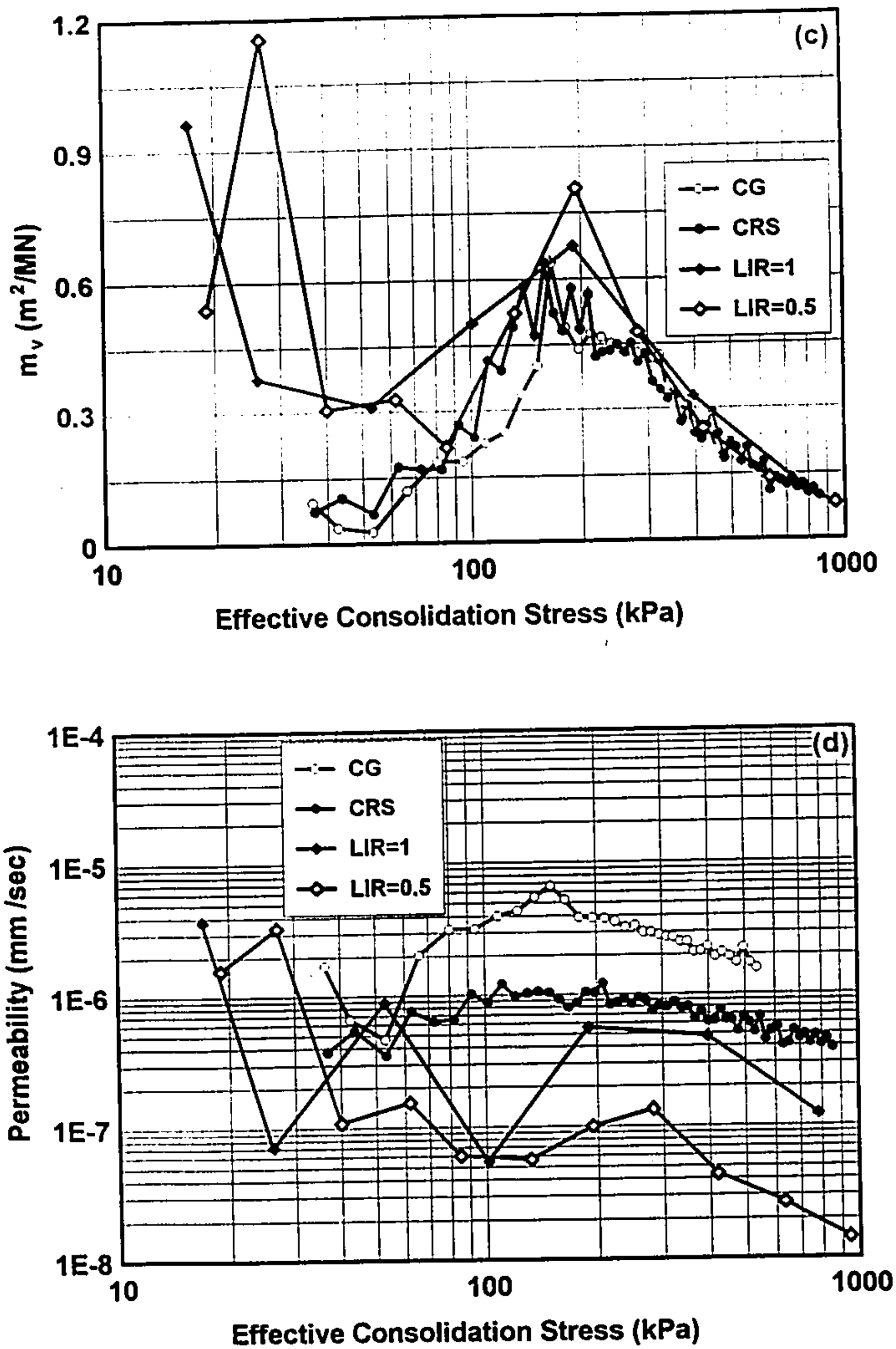

Fig. 8.7. Comparison of various types of consolidation tests (Depth = 3.15 m).

CHAPTER 9

COMPARISON OF SOIL PARAMETERS OBTAINED FROM TESTS AND CASE STUDIES

The comparison of soil parameters has been presented in two groups:

(i) the comparison between the test results obtained from various field and laboratory tests, and,

(ii) the comparison between the soil parameters obtained from the test results (both laboratory and field) and those obtained from the case studies (Bozozuk 1977; Haile 1977) of silo foundations at the same site.

The soil parameters included in this comparison are the undrained shear strength and the deformation modulus.

9.1 Comparison Between Field and Laboratory Tests

9.1.1 Comparison of Undrained Shear Strength

The comparison of the values of undrained shear strength S_u obtained from various field and laboratory tests, carried out during the course of this research, are presented in

Fig. 9.1. Results from eight different types of tests are shown in this figure. Within the crust, all the field testing methods, except the dilatometer (DMT) test, indicate higher values of S_u than the laboratory testing methods. The DMT provides comparable values of S_u with those from laboratory tests. The DMT values scatter within a narrow range staying between triaxial compression and extension tests for the whole soil profile, covering both the weathered crust and the underlying intact clay.

Although the values of S_u obtained from conventional analysis of the field vane test are significantly higher than those obtained from the laboratory tests, the S_u values for the horizontal surface of the field vane, S_{uh}(FV), are comparable to the K_0 consolidated triaxial tests as shown in Fig. 4.6. The detailed discussion of this aspect has been provided in Chapter 4.

It is interesting to note that although the S_u values in the crust obtained from field tests (except DMT) are higher than the laboratory tests, all the S_u values below the crust obtained from field tests (including DMT) lie between the S_u values obtained from triaxial compression and extension tests. The *in situ* stress anisotropy within the overconsolidated crust and the normally consolidated nature of the soil below the crust may be the reason of this behaviour.

9.1.2 Comparison of Undrained Modulus

The comparison of the values of undrained deformation modulus E_u, obtained from various field and laboratory tests, are presented in Fig. 9.2a. The calculation of E_u for field tests was possible only for self-boring pressuremeter (SBP) test. The procedure of interpretation of E_u(SBP) has been presented in Chapter 3.

The values of E_u, within the crust, obtained from SBP tests are slightly higher (3-18%) than those obtained from K_0 consolidated (CK_0UC) triaxial tests. However, the values of E_u(SBP) are significantly higher than those for the isotropically consolidated (CIUC) triaxial tests. The E_u(SBP) values, for below the crust, are lower than those obtained from both type of triaxial tests. The correspondence between the SBP and CK_0UC triaxial tests is good.

9.1.3 Comparison of Drained Modulus

The comparison of the values of drained modulus E_d obtained from field and laboratory tests are presented in Fig. 9.2b. The only field test and the two laboratory tests, from which the calculation of E_d was possible, are the dilatometer (DMT), oedometer, and the drained triaxial compression (CIDC) tests, respectively. The empirically derived constrained modulus M obtained from DMT test has been considered as the drained modulus since the M defined by Schmertmann (1986) is "M=the constrained modulus of soil compressibility. Tangent value from vertical, drained loading, applicable at the in situ effective stress. Also = $1/m_v$, where m_v = the coefficient of volume change in one-dimensional compression."

The comparison between the values of E_d obtained from DMT and oedometer tests is very good. However, the E_d values obtained from triaxial (CIDC) tests are significantly higher (by more than 100%) than those obtained from oedometer and DMT tests as shown in Fig. 9.2b. However, the good comparison between oedometer and DMT may be because of the empirical derivation of DMT constrained modulus.

9.2 Comparison Between Test Results and Case Studies

Full-scale behaviour of two tower silos, founded within the crust, was studied at the same site of this research. These studies were made by Bozozuk (1977) on the foundation failure of a tower silo, and by Haile (1977) on the load-deformation behaviour of a tower silo which was instrumented with load cell, strain gauges, and piezometers. In the first case, failure occurred during the filling of the silo, and in the second case, foundation performance of the instrumented silo was studied during construction and post-construction loading.

These case studies have provided an opportunity to evaluate the probable field strength mobilized at failure and the bulk deformation characteristics of the crust. Soil parameters obtained from these analyses have been used to provide comparisons with the results obtained in the present study. Similar comparative study was also conducted by Tanaka

(1986) which has also been discussed in this chapter, along with the discussions of the present study. These two case histories are discussed separately in the following section, thereafter the comparative study has been presented.

9.2.1 Review of The Case Histories

Foundation Failure of a Tower Silo

The failure of this silo, 32.3 m high and 9.14 m diameter, has been documented by Bozozuk (1977). The silo foundation consisted of a circular concrete ring, 610 mm thick with outside and inside diameters of 11.9 and 7.6 m, respectively. The total weight of the structure, at the time of failure, was estimated as 22150 kN. Bozozuk (1977) estimated the contact area, at the time of failure, as 91 m^2 in order to have a factor of safety of unity. This data was used by Tanaka (1986), in order to assess the mobilized undrained shear strength in the crust. The strength mobilized in the crust corresponds to 23% of the total slip surface which indicates a high contribution of the crust. The schematic diagram of the failed concrete silo is given in Fig. 9.3 and the section of the silo and the soil profile is given in Fig. 9.4. From the parametric slope stability analysis, Tanaka obtained the values of S_u for the crust of 60, 43 and 27 kPa for corresponding S_u values of 30, 35 and 40 kPa in the underlying clay, respectively. However, the value of 35 kPa was selected as a representative value for the underlying soil which provided the S_u of 43 kPa for the crust. These values were used in the comparative study by Tanaka (1986) as well as in the present study.

Performance of an Instrumented Tower Silo

The monitoring and the analyses of this instrumented tower silo has been documented by Haile (1977). The silo was founded on a heavily reinforced raft. A section through the silo raft and the underlying soil including the location of instrumentation is shown in Fig. 9.5.

The silo has an inside diameter of 7.6 m and a height of 26.1 m. The concrete raft foundation of the silo is 13.7 m in diameter and 1.0 m in thickness, and it was founded at

0.7 m below the ground surface. The deep settlement gauges were installed at a radial distance of approximately 4.6 m away from the centre of the raft foundation.

The loading steps of the silo can be summarized as follows: after the raft was completed, the silo structure was assembled in three days. Within 25 days after completion, the silo was loaded with corn silage to a stress intensity of 55 kPa. Filling of the silo was interrupted for about 30 days until more silage became available. Thereafter, it was completely filled to an estimated bearing pressure of 72.5 kPa. This pressure was maintained for a relatively short period of time, since gradual unloading by feeding began. The design pressure was 88 kPa, which was considerably lower than the preconsolidation pressure (average value of approximately 200 kPa) of the crust.

The measured vertical displacements versus the net applied pressure (total pressure minus the stress relief due to the excavation of the raft foundation) is shown in Fig. 9.6. The load-settlement curve due to the applied pressure of 55 kPa which was kept constant for 30 days as shown in Fig. 9.6.

53% of the total observed settlement of 7.0 mm took place within a depth of approximately 3.4 m below the raft which corresponds to a Z/D (depth to diameter) ratio of 0.25. 90% of the total settlement took place within a depth of 13.3 m, i.e., at a Z/D ratio of 0.97. This observation indicates that the portion of settlement within the crust is significant. Therefore, deformation behaviour of the crust should be included for the structures to be founded within the crust.

Haile (1977) computed undrained modulus from settlement measurements obtained from various stresses at different depth levels below the raft. Modulus values were computed using Giroud's (1972) solution for stresses and deformations below a rigid loaded area in an ideal semi-infinite elastic half-space. The variation of soil modulus with depth was found to be as 5.7 MPa at a depth of 1.5 m below the raft foundation, 32 MPa at 3.0 m, and 41 MPa at 7.3 m. These values are plotted in Fig. 9.10.

9.2.2 Comparison of Undrained Shear Strength

The comparison of the undrained shear strengths, obtained from the back-analysis of the silo failure and the field tests, and the same comparison between the silo failure and the laboratory tests, are presented in Figs. 9.7 and 9.8, respectively. Fig. 9.7 shows that none of the field testing methods show good comparison with the back-analyzed result for the crust. The DMT shows the closest comparison. The study by Tanaka (1986) also shows a good agreement between the S_u(DMT) and the S_u(Silo) as shown in Fig. 9.9. From the observations from this study and those from Tanaka's study, it can be concluded that, among the field tests used by Tanaka and in this study, the DMT has the best potential for the estimation of undrained shear strength for the weathered crust.

The undrained shear strength obtained for the horizontal face of the field vane S_{uh}(FV), evaluated by the new interpretation method as discussed in Chapter 4, compares well with that of the silo failure. The match between S_{uh}(FV) and S_u(Silo), for the crust, will be even better if the gradual decrease in S_u(Silo) is considered. The comparison of strengths below the crust is good for all the field testing methods. This good match for all the field testing methods may be due to the fact that the interpretation methods were developed on the assumption of isotropic soil behaviour.

The comparison between the values of S_u(Silo) and those from various laboratory tests indicates that only the K_0 consolidated triaxial compression test (CK_0UC) compares well with the back-analysis (Fig. 9.8). Again, the match will be better if the gradual decrease in S_u(Silo) is considered in the back-analysis. The value of S_u(Silo), below the crust, is approximately the average of triaxial compression and extension tests.

The good match between S_u(Silo) and S_{uh}(FV), and S_u(Silo) and S_u(CK_0UC) indicates the importance of *in situ* state of stress in the experimental and interpretation methods. Therefore, it can be concluded that the in situ state of stress of any soil must be known, and be applied in the experimental studies as well as in the interpretation methods, to obtain the representative parameters of that soil.

9.2.3 Comparison of Deformation Modulus

The comparison of deformation moduli, obtained from various field and laboratory tests and those obtained from back-analysis of silo failure, is shown in Fig. 9.10. For clarity, the undrained and drained moduli are plotted separately in Figs. 9.10a and 9.10b, respectively. The comparison of deformation moduli, obtained from various field tests including the screw plate test (SCT) and those from the monitored silo, studied by Tanaka (1986) is presented in Fig. 9.11.

The comparison of E_u(Silo) with E_u from other field and laboratory tests is poor for the soil above 2.5 m depth (Figs. 9.10a). However, the E_u(Silo) compares very well with triaxial tests below the depth of 2.5 m. The undrained modulus obtained by Tanaka for screw plate tests is approximately 2 to 6 times (Fig. 9.11) those obtained from other *in situ* methods.

The comparison of the values of drained modulus (Figs. 9.10b) obtained from the silo E_d(Silo) and those obtained from the DMT and the oedometer tests is good above 2.5 m depth, and is poor below this depth which is in contrast to the above comparison of E_u above and below 2.5 m depth.

The above contradictory observation may be for the reason that the soil above 2.5 m depth was more fissured, and the drainage within this depth was fast during the silo construction and loading. In contrast, the soil below 2.5 m was intact, significantly less fissured and with slow drainage. Therefore, the deformation within the crust is instantaneous and drained, while below the crust, the undrained modulus of deformation is measured in the field tests. Hence, the undrained modulus below the crust from the silo field loading test compare well with the values obtained from the undrained triaxial tests.

Effect of Fissures

The weathered crust is highly fissured with random microfissures and pores. Very limited data are available for the crust in terms of density of fissures and the sample-size effect. The number of fissures and the number of pores studied by O'Shaughnessy (1993) for the crust of the same field are 20 to 70 and 10 to 100, respectively, per 10,000 mm^2. On the basis of this study, a triaxial sample of 51 mm diameter by 102 mm high will contain 41 to 143 fissures and 20 to 204 pores. This high number of fissures in a test sample may be considered representative of the *in situ* condition.

Lefebvre et al. (1987) performed large *in situ* shear box (600 x 600 mm square by 400 mm high) tests and laboratory triaxial (35.5 mm diameter x 71 mm high) tests to study the sample-size effect due to fissuring in the crust. The shear strengths obtained from these two different types of tests compared very well. The shear strengths obtained from *in situ* shear box tests ranged between 14 and 20 kPa and that obtained from triaxial tests ranged between 15 and 20 kPa. The *in situ* shear box tests were conducted with the normal stresses close to the *in situ* vertical stresses and the triaxial tests were conducted anisotropically reconsolidating the samples to *in situ* stresses. From the above-mentioned two studies it can be concluded that the small laboratory samples contained enough number of fissures to represent the field condition and consequently there is little sample-size effect on the shear strength behaviour of the crust.

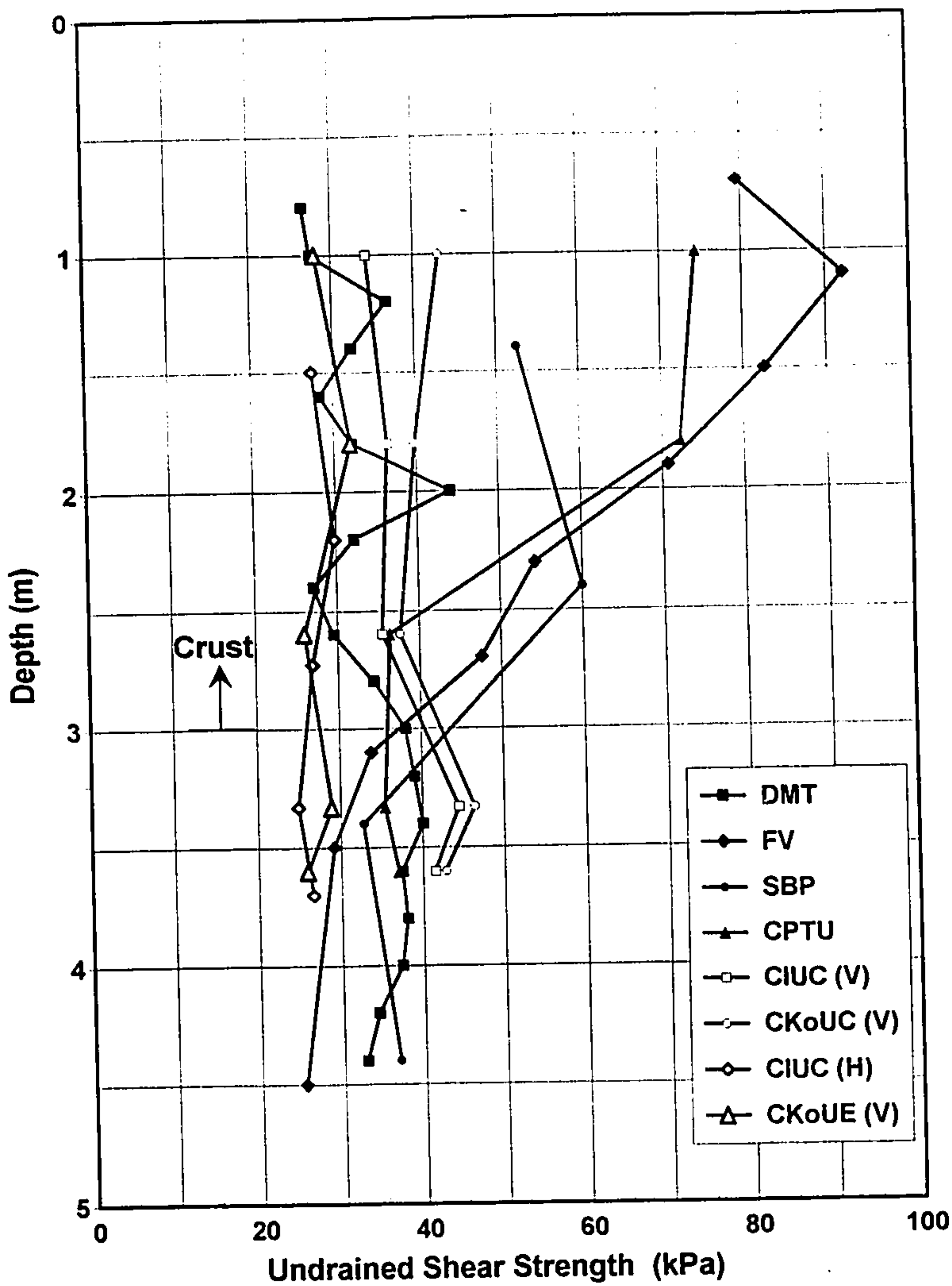

Fig. 9.1 Comparison of undrained shear strength obtained from various field and laboratory tests.

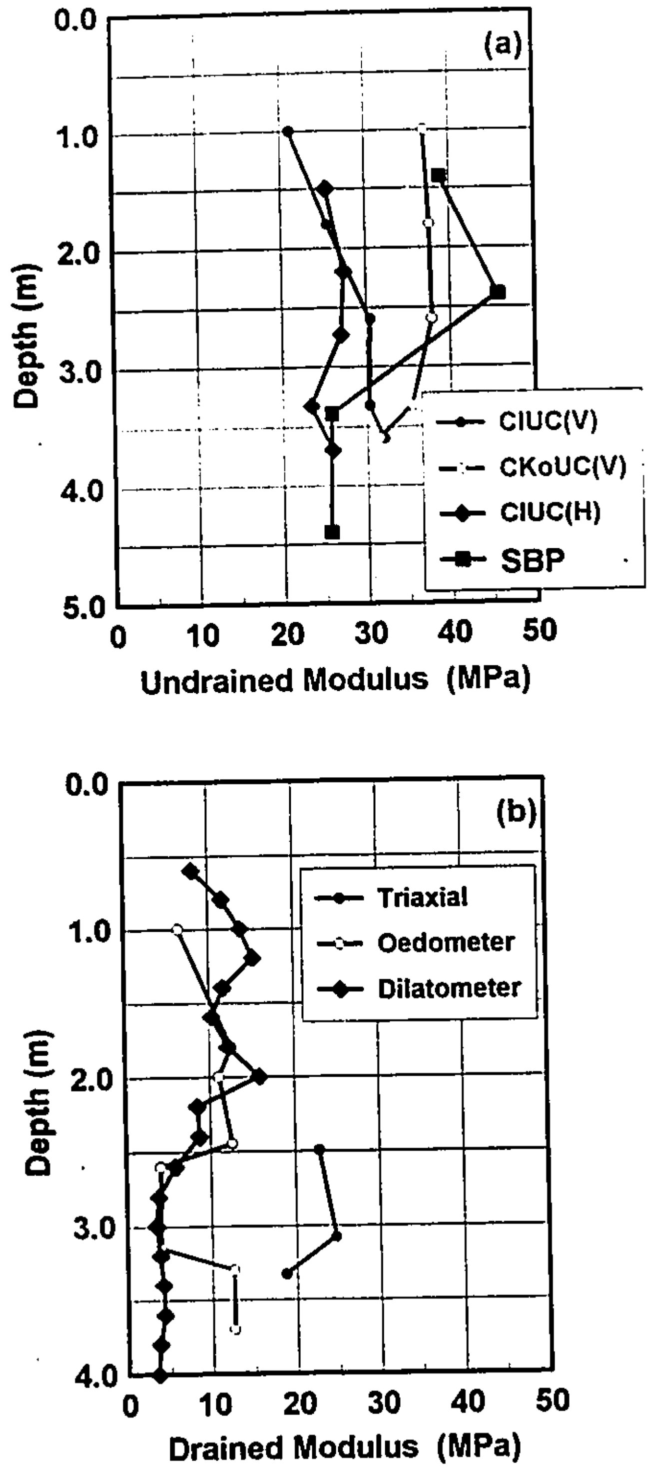

Fig. 9.2 Comparison of deformation moduli obtained from various field and laboratory tests.

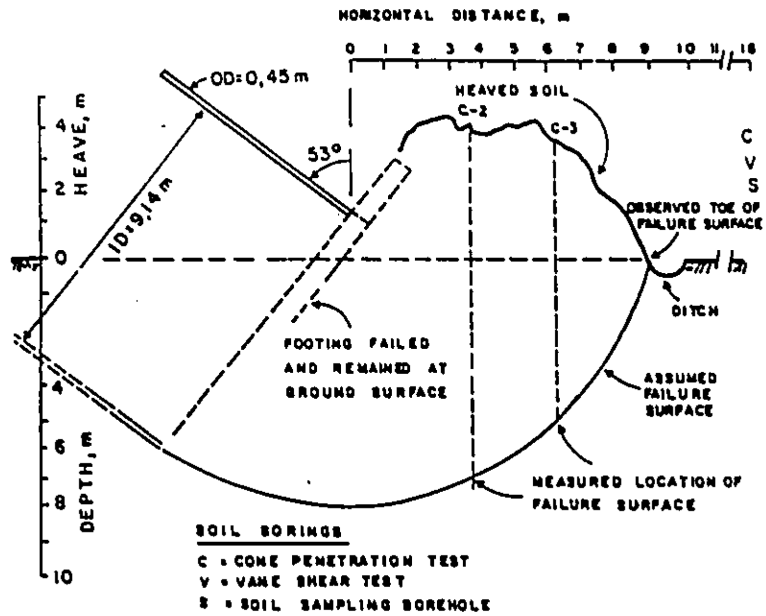

Fig. 9.3 Failed concrete silo (after Tanaka 1986).

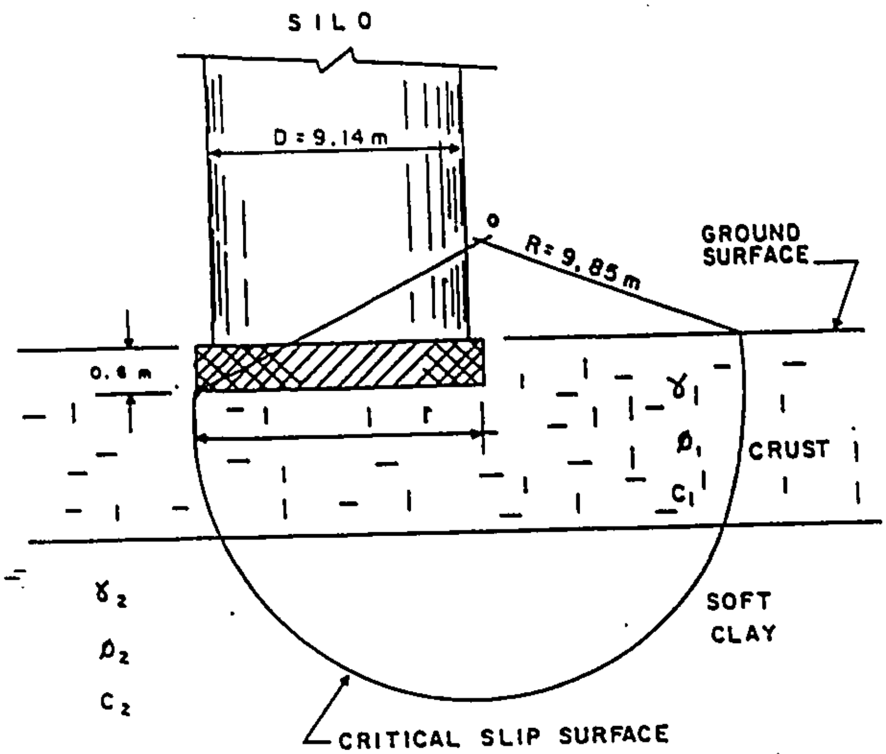

Fig. 9.4 Section of the silo and the soil profile (after Tanaka 1986).

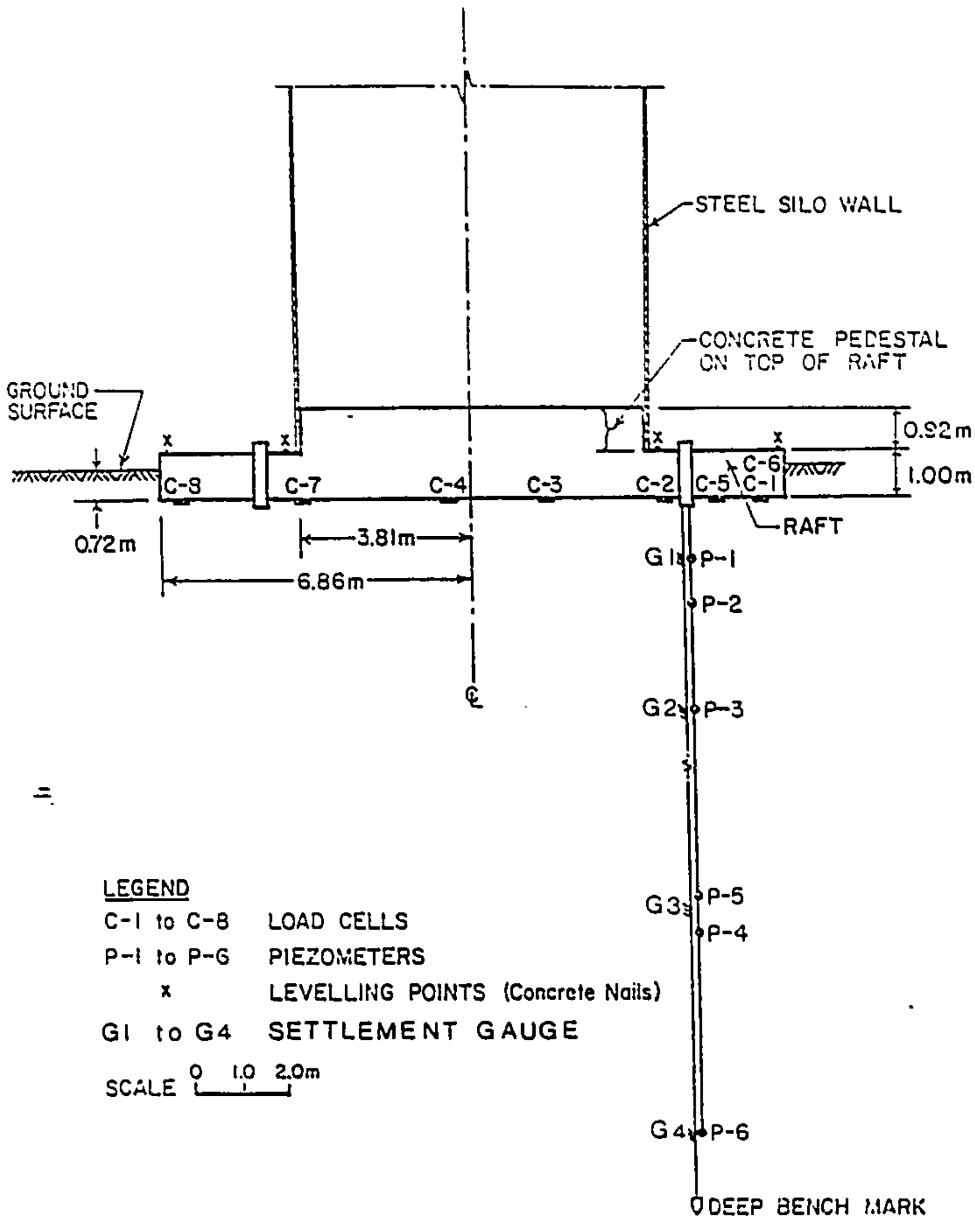

Fig. 9.5 Section of the silo raft and instrumentation locations (after Haile 1977).

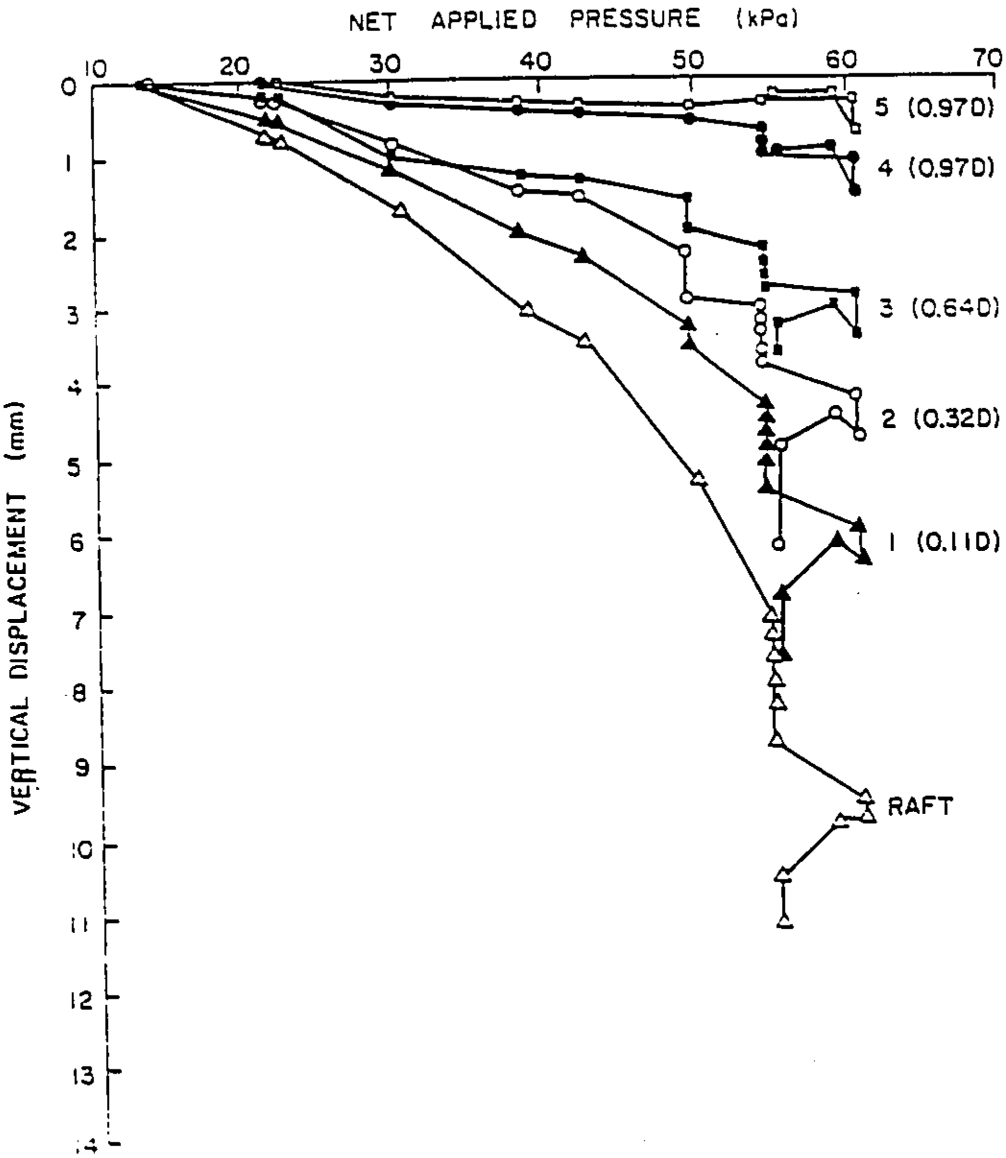

Fig. 9.6 Load-displacement curve of the instrumented silo (after Haile 1977).

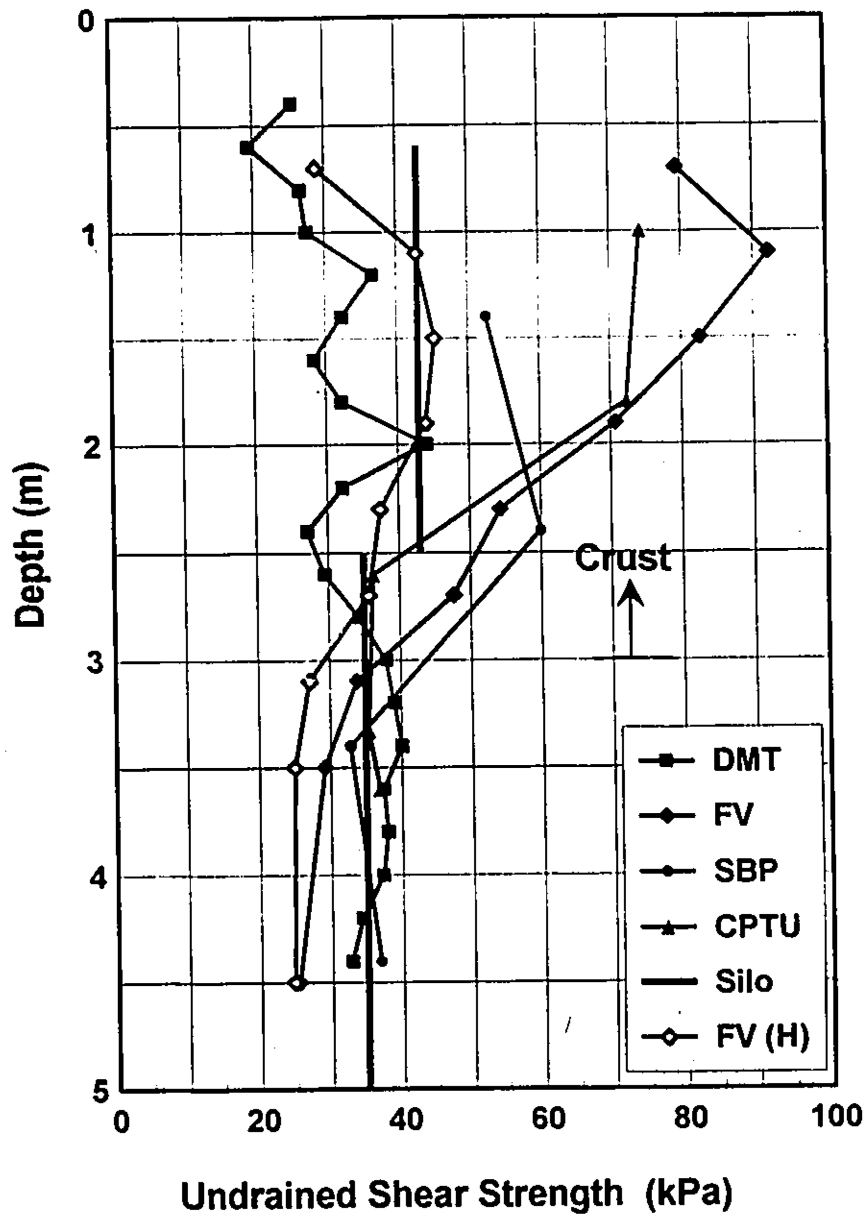

Fig. 9.7 Comparison of undrained shear strengths obtained from various field tests and silo failure.

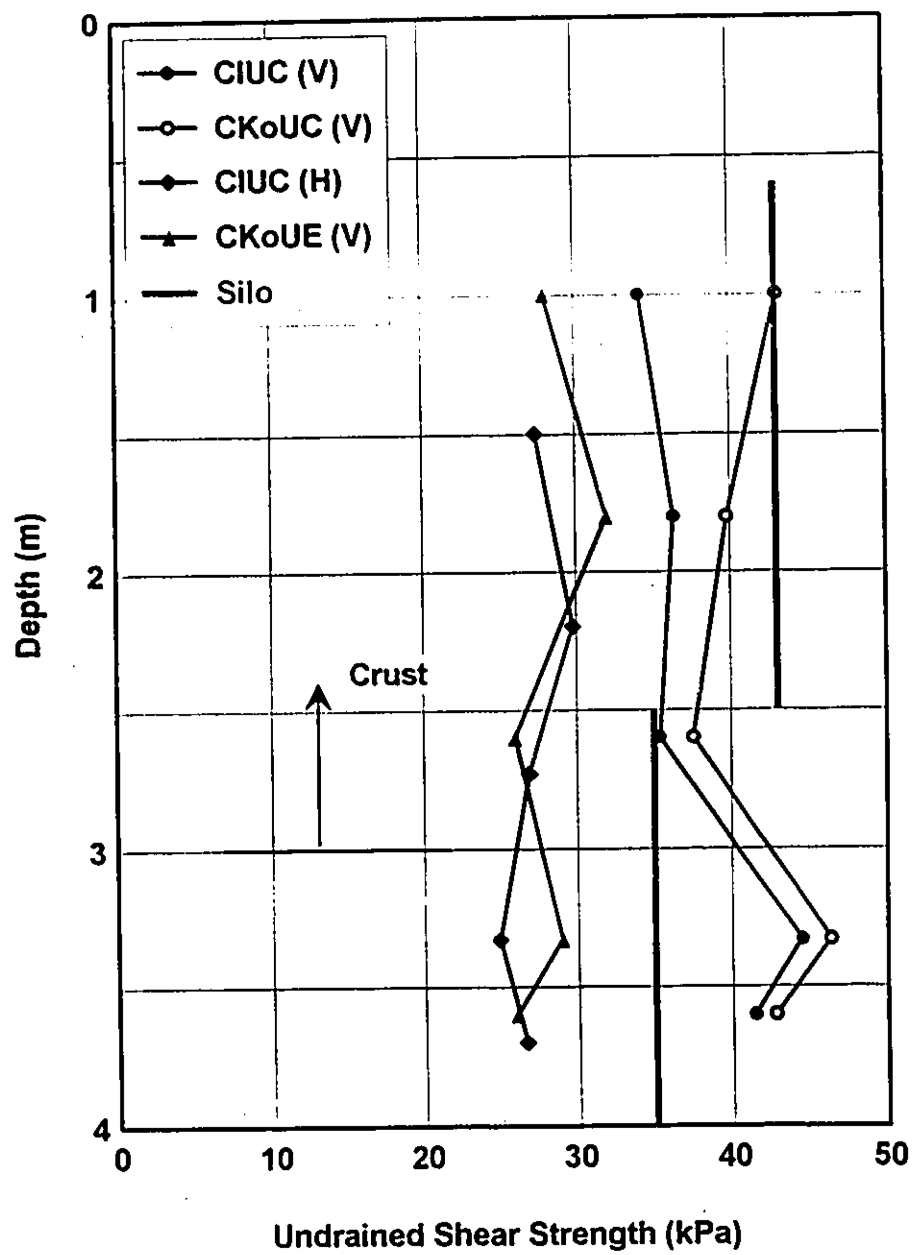

Fig. 9.8 Comparison of undrained shear strengths obtained from various laboratory tests and silo failure.

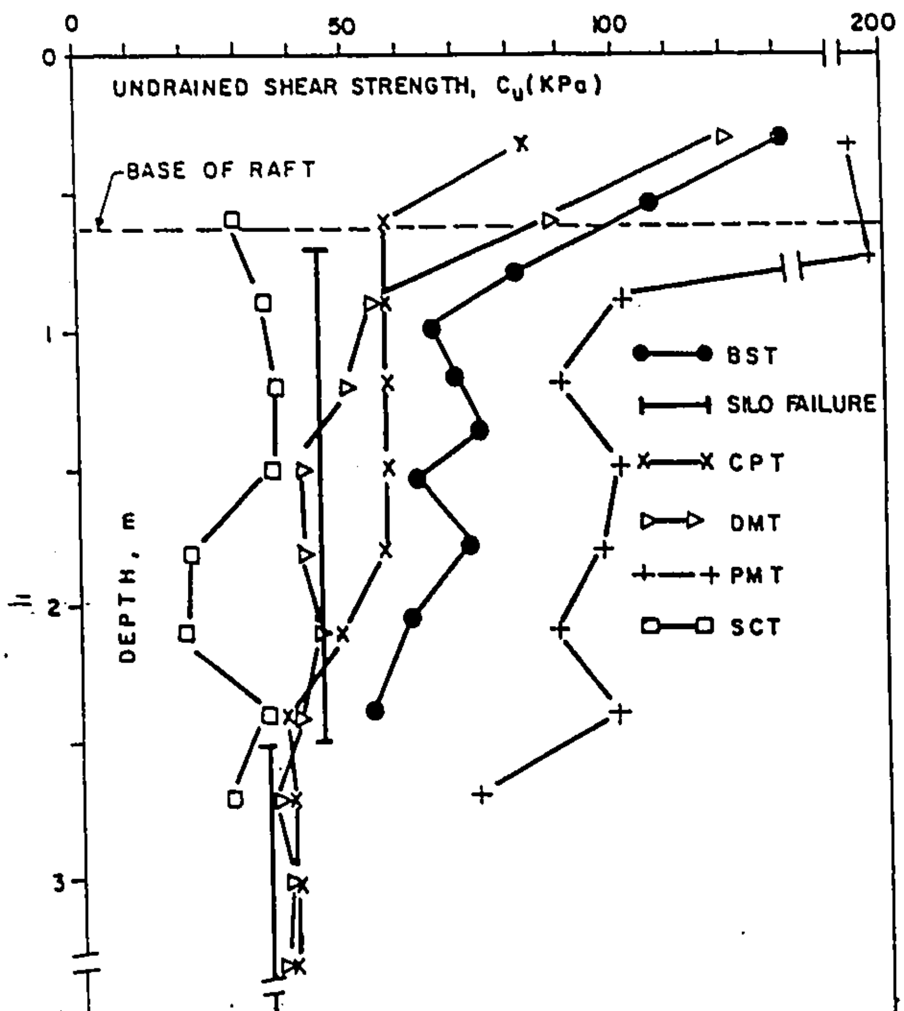

Fig. 9.9 *In situ* shear strength versus depth (after Tanaka 1986).

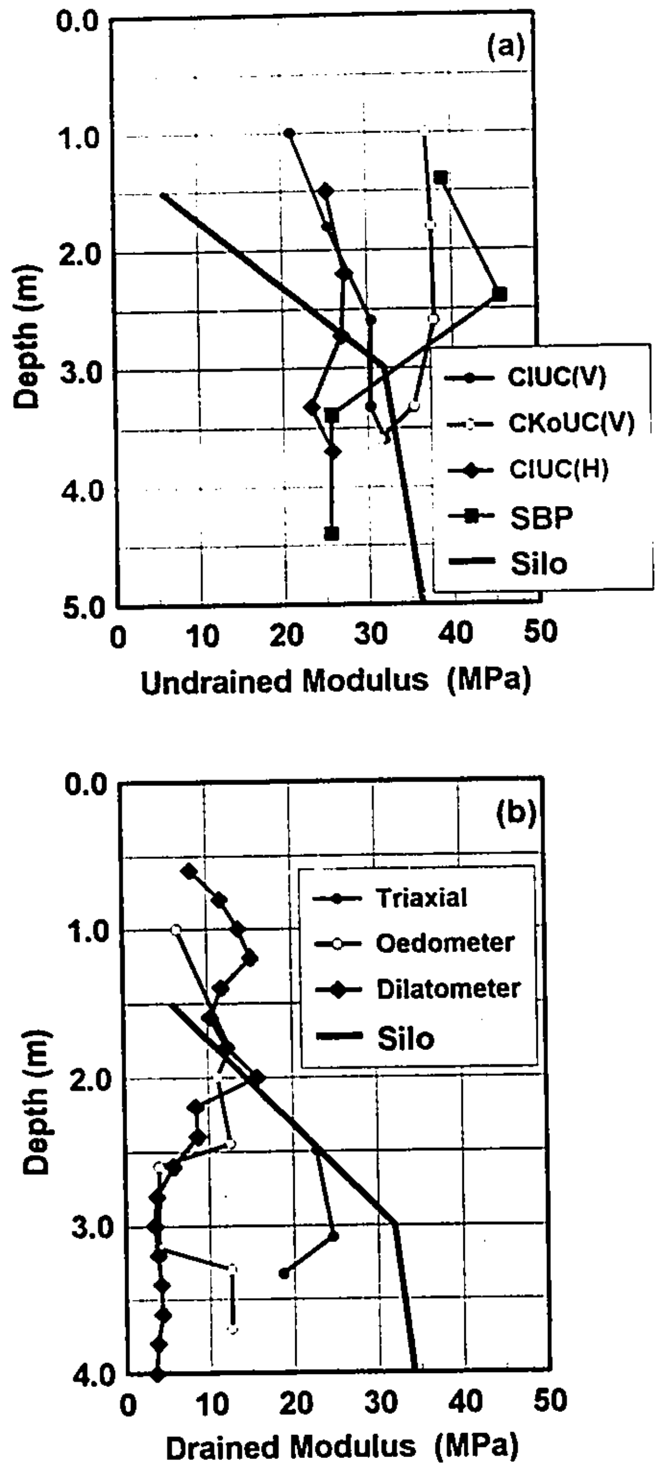

Fig. 9.10 Comparison of deformation moduli obtained from various field tests, laboratory tests and silo failure.

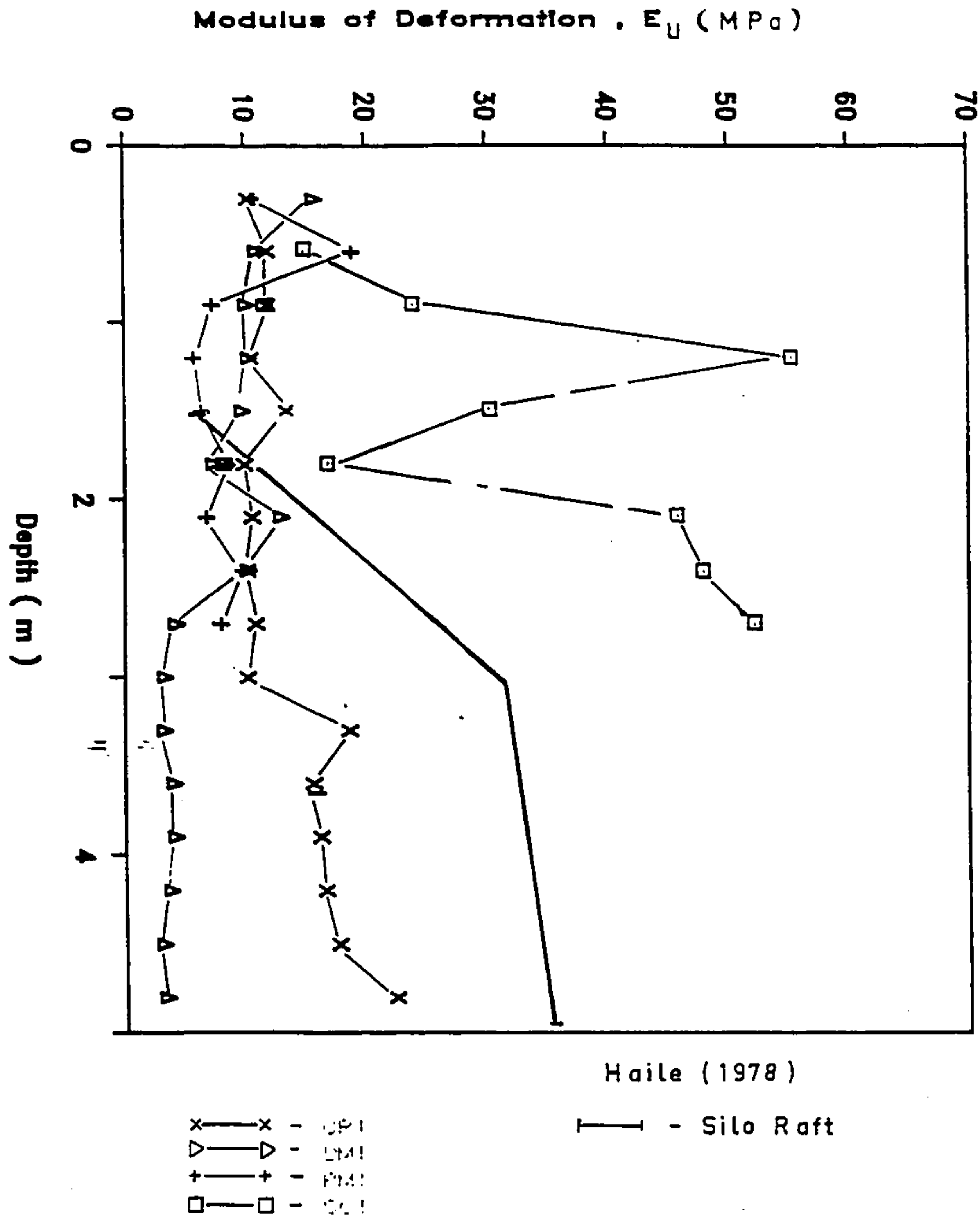

Fig. 9.11 Comparison of deformation moduli (after Tanaka 1986).

CHAPTER 10

CONCLUSIONS AND RECOMMENDATIONS

10.1 Conclusions

The conclusions drawn from this experimental research are:

1. The sensitivity obtained from the field vane test is low, within the crust, when compared with the soil immediately below the crust. Sensitivity increases suddenly immediately below the crust. The values of sensitivity obtained from the piezocone test are consistently lower, by approximately 50%, than those from the field vane test.

2. The comparison of the values of undrained shear strengths within the crust, calculated from various field testing methods, indicates that the field vane (FV) provides the highest value and the dilatometer (DMT) provides the lowest. The piezocone also provides high values of S_u which are comparable to FV results. The scatter in the values of S_u within the crust, obtained from different field tests, is appreciably larger in contrast to that below the crust material.

3. The values of K_0 obtained from the self-boring pressuremeter (SBP) test are significantly higher than those obtained from the DMT test. The K_0 values obtained

from the DMT test, however, compare well with the new laboratory method developed during this research as well as with some other empirical methods (Brooker and Ireland 1965; and Mayne and Kulhawy 1982).

4. A laboratory method has been developed for the evaluation of K_0 for highly overconsolidated clays. The results from the reconstituted samples which have been simulated to the field *in situ* conditions and field stress histories, and subsequently tested for the determination of K_0 using the proposed method, support the validity of the new method. Comparison of K_0 values, obtained from the proposed method and the other empirical and field testing methods, indicate that the dilatometer test provides the closest estimate of K_0.

5. There is a unique correlation between K_0 and OCR, independent of whether the soil is undisturbed or remoulded.

6. Conventional interpretation of field vane strength considers the soil as an isotropic material, i.e., uniform stress distribution around the vane blade and same shear strength on vertical and horizontal directions. In reality, most of the soils existing in the field are anisotropic. Because of this anisotropic behaviour of the soils, unrealistic values of undrained shear strengths are obtained from conventional interpretation of field vane test results. A new interpretation method has been developed, during the course of this research, in which non-uniform stress distribution around the vane blade, strength anisotropy, effect of shearing rate and disturbance due to vane insertion have been included.

7. Stress conditions during laboratory reconsolidation strongly influence the stress-strain behaviour and porewater pressure generation during subsequent shearing. To obtain a representative stress-strain behaviour, samples have to be reconsolidated to the *in situ* state of stress (i.e., consolidated to K_0 condition) before starting the triaxial test. The samples reconsolidated to the *in situ* stress state indicated higher undrained strength than the isotropically consolidated samples. K_0 consolidated samples also showed higher (20-60%) deformation moduli than the samples consolidated isotropically to σ_{v0}'. Considerable differences in porewater pressure response were recorded in samples consolidated under different stress systems. K_0 consolidated samples resulted in higher A_f values than isotropically consolidated ones even though σ_{vc}' was same for both type of tests.

8. The stress-path has a significant effect on the strength-deformation behaviour of the weathered crust. To obtain representative soil parameters from laboratory tests, the stress-path to be followed in the laboratory must be similar to that in the field. The study shows that the value of drained shear strength decreases and the value of the deformation modulus increases with the increase in angle between the stress-path and the isotropic compression line for both compression and extension directions.

9. The behaviour of the Champlain Sea clay crust examined in the laboratory shows anisotropic strength-deformation characteristics (such as shear strength, deformation modulus, porewater pressure, etc.) indicating different values in vertical and horizontal directions.

10. A well-defined yield envelope has been obtained for the weathered crust which is symmetric about a line located in between the lines K_{onc} and p'. Within the yield envelope the strain response of the soil structure to applied loading is small, while outside the strain response is large. The angle between the q = 0 axis and the axis of yield envelope symmetry is approximately 15°, and the ratio p'/q along the line of symmetry is approximately 3.6. The shape of the yield envelope appears to depend on soil type and on the geological history of the deposit. Samples tested for compression require more axial strain (0.6%) than the extension tests (0.4%) to reach the yield stress.

11. Continuous loading consolidation tests (constant rate of strain, constant rate of stress, and controlled gradient) yielded higher values (10%-15%) of preconsolidation pressure than the oedometer consolidation tests (conventional 24-hour step-loading).

12. The value of preconsolidation pressure in the horizontal direction is lower than in the vertical direction whereas the values of coefficient of consolidation (c_v) and permeability (k) are always higher in the horizontal direction than the corresponding values in the vertical direction.

13. The values of preconsolidation pressure, coefficient of consolidation and permeability obtained from various tests have been found to be dependent on the testing procedure whereas the value of volume compressibility is independent of testing method and sample orientation.

14. The controlled gradient test yielded the highest value of c_v whereas the oedometer test provided the lowest.

15. Among the field tests used by Tanaka (1986) and in this study, the DMT has the best potential for the estimation of undrained shear strength for the weathered crust.

16. The *in situ* state of stress of any soil must be known, and be applied in the experimental studies as well as in the interpretation methods, to obtain the representative parameters of that soil.

Finally, three laboratory apparatuses were also developed during the course of this research: (i) a versatile computer-operated stress path control system including the software to operate the system. (ii) an automated consolidation apparatus, capable of performing stress-, strain-, or gradient-controlled test as well as conventional step-loading test including porewater pressure measurement; and (iii) an improved volume gauge with larger volume measurement capacity.

10.2 Recommendations for Further Research

For the continuation of the present research, further studies may be undertaken on the following aspects:

1. Crust materials are not generally fully saturated. Tests on unsaturated crust may provide better estimation of soil parameters. Therefore, further research is recommended to investigate this aspect.

2. The laboratory method to determine K_0 for overconsolidated soils developed during this research was tested only for the clay crust. This research may be extended to check the validity of this method for other overconsolidated soils including sand.

3. The piezocone test provides high values of S_u within the crust which are comparable to the values of S_u obtained from conventional interpretation of FV test results. The high values of $S_u(CPTU)$ within the crust could be due to the high anisotropic *in situ* state

of stress where σ_{h0}' is greater than σ_{v0}'. Further research may be undertaken to study this aspect to develop a new interpretation technique of piezocone data for a soil with anisotropic *in situ* state of stress, especially, where $K_0>1$.

4. For clayey soils, the most critical condition occurs during or at the end of construction. However, certain type of structures such as grain silos, storage tanks where the foundation soil is subjected to cyclic/seasonal loading, may fail during service period after a certain number of cyclic/repeated loadings. Some slow cyclic undrained tests may be conducted to simulate this situation to check whether the repeated loading has any effect on the strength-deformation behaviour. Only three repeated loading (slow cyclic) tests have been conducted during this research in order to demonstrate the capability of the triaxial control system developed in this study.

5. This research may be extended toward numerical analysis. If the equation of the yield envelope, obtained from the stress-path tests, is developed and incorporated in a boundary element or finite element program, numerical analysis of a full-scale structure is possible.

REFERENCES

AAS, G. 1965. A study of the effect of vane shape and rate of strain on the measured values of *in situ* shear strength of clays. Proceedings, Sixth International Conference on Soil Mechanics and Foundation Engineering, Montreal, Canada, Vol.1, pp. 141-145.

AAS, G. 1967. Vane tests for investigation of anisotropy of undrained shear strength of clays. Proceedings of the Geotechnical Conference, Oslo, Vol.1: 3-8.

AL-DAHIR, Z.A. and TAN, S.B. 1968. A note on one dimensional constant head permeability tests. Geotechnique, **18**: 499-505.

ALLAM, M. M. and SRIDHARAN, A. 1980. Influence of the back pressure technique on the shear strength of soils. Geotechnical Testing Journal. **3**: 35-40.

AMPADU, S. and TATSUOKA, F. 1989. An automated stress-path control triaxial system. ASTM Geotechnical Testing Journal, **12:** 238-243.

ARMOUR, D.W.Jr. and DRNEVICH, V.P., 1986. Improved techniques for the constant rate of strain consolidation test. In Consolidation of Soils, ASTM STP 892, pp. 170-183.

ARNOLD, N. 1981. An empirical evaluation of pressuremeter test data. Canadian Geotechnical Journal, **18**: 455 - 459.

ATKINSON, J.H., 1973. Elasticity and plasticity in soils. Geotechnique, Vol.23, No.4, pp. 565-571.

ATKINSON, J.H. 1975. Anisotropic elastic deformations in laboratory tests on undisturbed London Clay. Geotechnique, **25**: 357-374.

ATKINSON, J.H., 1978. The mechanics of soils, an introduction to critical state soil mechanics. McGraw-Hill Book Company (UK)Limited, England.

ATKINSON, J.H. 1985. Simple and inexpensive pressure control equipment for conventional and stress path triaxial testing of soils. Geotechnique, **35**: 61-63.

ATKINSON, J.H., 1988. Undrained triaxial strength and stress-strain characteristics of a glacial till soil. Canadian Geotechnical Journal, Vol. 25, No.3, pp. 428-439.

ATKINSON, J.H., EVANS, J.S. and HO, E.W.L., 1985. Non-uniformity of triaxial samples due to consolidation with radial drainage. Geotechnique 35, No.3, pp. 353-355.

ATKINSON, J.H. and FARRAR, D.M. 1985. Stress path tests to measure soil strength parameters for shallow landslips. 11th International Conference on Soil Mechanics and Foundation Engineering, San Francisco, **2**: 983-986.

ATKINSON, J.H. and RICHARDSON, D., 1985. Elasticity and normality in soil - experimental examinations. Geotechnique 35, No.4, pp. 443-449.

ATKINSON, J.H. and RICHARDSON, D., 1987. The effect of local drainage in shear zones on the undrained strength of overconsolidated clay. Geotechnique. Vol.37. No.3, pp. 393-403.

AZZOUZ, A.S., BALIGH, M.M. and LADD, C.C. 1983. Corrected field vane strength for embankment design. ASCE Journal of Geotechnical Engineering, **109**: 730-734.

BAUER, G.E.A., SCOTT, J.D. and SHIELDS, D.H., 1973. The deformation properties of a clay crust. 8th International Conference on Soil Mechanics and Foundation Engineering, Moscow, **1**: 31-38.

BECKER, D.E., CROOKS, J.H.A. and BEEN, K., 1988. Interpretation of the field vane test in terms of *in situ* and yield stresses. *In* Vane shear strength testing in soils: field and laboratory studies, ASTM STP 1014. *Edited by* A.F. Richards, pp. 71-87.

BECKER, D.E., CROOKS, J.H.A., BEEN, K., and JEFFERIES, M.G., 1987. Works as a criterion for determining *in situ* and yield stresses in clays. Canadian Geotechnical Journal, **24:** 549-564.

BISHOP, A.W., 1958. Test requirements for measuring the coefficient of earth pressure at rest. Proc. Conf. on Earth Pressure Problems, Brussels, Vol. 1, pp. 2-14.

BISHOP, A.W., 1966. The strength of soils as engineering materials. 6th Rankine Lecture. Geotechnique, Vol.16, pp. 131-171.

BISHOP, A. W. 1967. Progressive failure - with special reference to the mechanism causing it. Proceedings of the Geotechnical Conference, Oslo, Session 2 - Panel Discussion, Vol. 2, pp. 142-150.

BISHOP, A. W. 1971. Shear strength parameters for undisturbed and remoulded soil specimens. In: Stress-Strain Behaviour of Soils, Roscoe Memorial Symposium, editor: R.H.G. Parry, Oxfordshire, Foulis, pp. 3-58.

BISHOP, A.W., ALPAN, I., BLIGHT, G.E. and DONALD, I.B., 1960. Factors controlling the strength of partly saturated cohesive soils. ASCE Research Conf. on Shear Strength of Cohesive soils, Boulder, Colorado, pp. 503-532.

BISHOP, A.W. and BLIGHT, G.E., 1963. Some aspects of effective stress in saturated and partly saturated soils. Geotechnique **13**, pp. 177-197.

BISHOP, A.W. and HENKEL, D.J. 1962. The measurement of soil properties in the triaxial test. 2nd ed., Edward Arnold, London, U.K.

BISHOP, A.W., WEBB, D.L. and LEWIN, P.I. 1965. Undisturbed samples of London clay from the Ashford Common shaft: strength-effective stress relationships. Geotechnique, **15**: 1-31.

BISHOP, A.W. and WESLEY, L.D. 1975. A hydraulic triaxial apparatus for controlled stress path testing. Geotechnique, **25**: 657-670.

BERRE, T. and BJERRUM, L. 1973. Shear strength of normally consolidated clays. Proc. 8th International Conference on Soil Mechanics and Foundation Engineering, Moscow,**1**: 39-49.

BJERRUM, L. 1972. Embankments on soft ground. Proceedings, Specialty Conference on Performance of Earth and Earth-Supported Structures, Purdue University, pp. 1-54.

BJERRUM, L. 1973. Problems of soil mechanics and construction on soft soils. Proc. 8th International Conference on Soil Mechanics and Foundation Engineering, Moscow, **3**: 109-159.

BJERRUM, L. and ANDERSEN, K.H., 1972. *In situ* measurement of lateral pressures in clay. Publication No.91, Norwegian Geotechnical Institute, Oslo, pp. 29-38.

BJERRUM, L. and KENNEY, T. C. 1967. Effect of structure on the shear behaviour of normally consolidated quick clays. Proceedings of the Geotechnical Conference, Oslo, Vol. 2, pp. 19-27.

BLACK, D.K. and LEE, K.L. 1973. Saturating laboratory samples by back pressure. ASCE Journal of the Geotechnical Engineering Division, **99**: 93.

BLIGHT, G.E. 1963. The effect of non-uniform pore pressures on laboratory measurements of the shear strength of soils. ASTM Symposium on Laboratory Shear Testing of Soils, ASTM STP 361, pp. 173-184.

BLIGHT, G.E., 1966. Strength characteristics of desiccated clays. ASCE, Journal of Geotechnical Engineering, Vol. 92, SM6, pp.19-37.

BOZOZUK, M. 1963. The modulus of elasticity of Leda clay from field measurements. Canadian Geotechnical Journal, **1:** 43-51.

BOZOZUK, M. 1977. Evaluating strength tests from foundation failures. Proceedings, Ninth International Conference on Soil Mechanics and Foundation Engineering, Tokyo, Vol.1, pp. 55-59.

BOZOZUK, M., 1983. Foundation Design for Silos on Clay Soils. Proc. of the 31st Annual Soil Mechanics and Foundation Engineering Conference, University of Minnesota, pp. 112-178.

BRANDON, T.L., DUNCAN, J.M. and CADDEN, A.W. 1990. Automated back-pressure saturation device for triaxial testing. ASTM Geotechnical Testing Journal, **13**: 77-82.

BRIAUD,J-L., LYTTON, R.L., and HUNG, J-T., 1983. Obtaining moduli from cyclic pressuremeter tests. ASCE Journal of Geotechnical Engineering, pp. 657-665.

BROOKER, E.W. and IRELAND, H.O., 1965. Earth pressures at rest related to stress history. Canadian Geotechnical Journal, **2:** 1-15.

BURLAND, J.B. 1969. Deformation of soft clay beneath loaded areas. Seventh International Conference on Soil Mechanics and Foundation Engineering, Mexico, **1**: 55-63.

BURLAND, J.B. 1971. A method of estimating the pore pressures and displacements beneath embankments on soft, natural clay deposits. Roscoe Memorial Symposium, editor: R.H.G. Parry, Oxfordshire, Foulis, pp. 505-536.

BURLAND, J.B. 1990. On the compressibility and shear strength of natural clays. Thirtieth Rankine Lecture, Geotechnique, **40**: 329-378.

BYRNE, P.M. AND AOKI, Y., 1969. The strained controlled consolidation test. Soil Mechanics Series No.9, Department of Civil Engineering, University of British Columbia, Vancouver, Canada.

CALABRESI, G. and RAMPELLO, S. 1987. Swelling of overconsolidated clays in excavations. Proceedings, Ninth European Conference on Soil Mechanics and Foundation Engineering. Vol. 1, pp. 11-15.

CAMPANELLA, R.G. and VAID, Y.P. 1972. A simple K_0 triaxial cell. Canadian Geotechnical Journal, **9**: 249-260.

CANADIAN GEOTECHNICAL SOCIETY, 1985. Canadian Foundation Engineering Manual. Second Edition. The Canadian Geotechnical Society, c/o BiTech Publishers Ltd., Vancouver.

CASAGRANDE, A. 1936. The determination of preconsolidation load and its practical significance. Proceedings, First International Conference on Soil Mechanics, Cambridge, Mass., Vol. 3, pp. 60-64.

CHANDLER, R.J. 1988. The *in situ* measurement of the undrained shear strength of clays using the field vane. *In* Vane shear strength testing in soils: field and laboratory studies, ASTM STP 1014. *Edited by* A.F. Richards, pp. 13-44.

CHANG, M.F., MOH, Z.C., LIU, H.H. and VIRANUVUT, S., 1977. A method for determining the *in situ* K_0 coefficient. Proc. 9th Intl. Conf. SMFE, Tokyo, Vol.1, pp. 61-64.

CLAYTON, C.R.I., KHATRUSH, S.A., BICA, A.V.D. and SIDDIQUE, A. 1989. The use of Hall Effect semiconductors in geotechnical instrumentation. ASTM Geotechnical Testing Journal, **12:** 69-76.

CLOUGH, G.W. and DENBY, G.M. 1980. Self-boring pressuremeter study of San Francisco Bay Mud. ASCE Journal of the Geotechnical Engineering Division, **106**: 45-63.

COSTA FIEHO, L. DE M. 1985. Measurement of axial strains in triaxial tests on London clay. Geotechnical Testing Journal, **8:** 3-13.

CRAWFORD, C.B. 1964. Interpretation of the consolidation test. ASCE Journal of the Geotechnical Engineering Division, **90**: 87-102.

CRAWFORD, C.B. 1988. On the importance of rate of strain in the consolidation test. Geotechnical Testing Journal, **11**: 60-62.

CROOKS, J.H.A. and GRAHAM, J. 1976. Geotechnical properties of the Belfast estuarine deposits, Geotechnique, **26**: 293-315.

DASCAL, O., TOURNIER, J.P., TAVENAS, F. and LAROCHELLE, P. 1972. Failure of a test embankment on sensitive clay. Proceedings, ASCE Specialty Conference on Performance of Earth and Eart-Supported Structures, Purdue University, Lafayette, Indiana, Vol.1, pp. 129-158.

DENBY, G. M. and CLOUGH, G. W. 1980. Self-boring pressuremeter tests in clay. ASCE Journal of the Geotechnical Engineering Division, **106**: 1369-1387.

DENBY, G. M. and HUGHES, J. M. O. 1982. Horizontal stress interpretation of pressuremeter tests. Proc. conf. on Updating Subsurface Sampling of Soils and Rocks and their *In situ* Testing. Santa Barbara California, pp. 227-244.

DONALD, I.B., JORDAN, D.O. and PARKER, R.J. 1975. Interpretation of vane testing in clays. Fifth Symposium on *In situ* Testing for Design Parameters, Melbourne, Australia, pp. 1-25.

DONALD, I.B., JORDAN, D.O., PARKER, R.J. and TOH, C.T. 1977. The vane test - a critical appraisal. Ninth International Conference on Soil Mechanics and Foundation Engineering, Tokyo, Vol.1, pp. 81-88.

DUNCAN, J.M., JAVETE, D.F. and STARK, T.D. 1991. The importance of a desiccated crust on clay settlements. Soils and Foundations, **31**: 77-90.

EDEN, W.J. and BOZOZUK, M. 1969. Earth pressures on Ottawa outfall sewer tunnel. Canadian Geotechnical Journal, **6**: 17-32.

EDEN, W.J. and CRAWFORD, C.B. 1957. Geotechnical properties of Leda clay in the Ottawa area. 4th International Conference on Soil Mechanics and Foundation Engineering, London, Vol.1, pp. 22-27.

EDEN, W.J. and JARRET, P.M., 1971. Landslide at Orleans, Ontario. National Research Council of Canada, DBR, Technical Papaer No. 321.

EDEN, W.J. and LAW, K.T. 1980. Comparison of undrained shear strength results obtained by different test methods in soft clays. Canadian Geotechnical Journal, **17**:369-381.

EDEN, W.J., and MITCHELL, R.J., 1970. The mechanics of landslides in Leda clay. Canadian Geotechnical Journal, Vol. 7, pp. 285-296.

EDEN, W.J., and MITCHELL, R.J., 1973. Landslides in sensitive marine clay in Eastern Canada. Highway Research Record No. 463, pp. 18-27.

EIGENBROD, K.D., BURAK, J.-P. and GRAHAM, J. 1987. Drained deformation and failure due to cyclic pore pressures in soft natural clay at low stresses. Canadian Geotechnical Journal **24**: 208-215.

FAHEY, M. and FOLEY, P. A., 198.. *In situ* measurement of the coefficient of consolidation. Proceedings, Ninth European Conference on Soil Mechanics and Foundation Engineering. Vol. 1, pp. 29-33.

FLAATE, K. 1966. Factors influencing the results of vane tests. Canadian Geotechnical Journal, **3**: 18-31.

GARGA, V.K., 1988. Experience with field vane testing at Sepetiba test fills. *In:* Vane Shear Strength Testing in Soils: Field and Laboratory Studies, ASTM STP 1014, A.F. Richards, ed., pp. 267-276.

GARGA, V.K. and KHAN, M.A. 1991. Laboratory evaluation of K_o for overconsolidated clays. Canadian Geotechnical Journal, **28**: 650-659.

GARGA, V.K. and KHAN, M.A. 1992. Interpretation of field vane strength of an anisotropic soil. Canadian Geotechnical Journal, **29:** 627-637.

GARGA, V.K. and KHAN, M.A. 1994. Evaluation of K_0 and its influence on the field vane strength of a weathered crust. International Conference for Soil Mechanics and Foundation Engineering, New Delhi, India (accepted for publication).

GHIONNA, V., JAMIOLKOWSKI, M., LACASSE, S., LADD, C. C., LANCELLOTTA, R., and LUNNE, T. 1985. Evaluation of self-boring pressuremeter. Norwegian Geotechnical Institute, Oslo, Report 159, pp. 1-9.

GIBSON, R.E. 1966. A note on the constant head test to measure soil permeability *in situ*. Geotechnique , **16**: 256-259.

GIBSON, R.E. 1970. An extension to the theory of the constant head insitu permeability test. Geotechnique, **20**: 193-197.

GORMAN, C. T., HOPKINS, T. C., DEEN, R. C., and DRNEVICH, V. P. 1978. Constant-rate-of-strain and controlled-gradient consolidation testing. Geotechnical Testing Journal. **1:** 3-15.

GRAHAM, J. 1979. Embankment stability on anisotropic soft clays. Canadian Geotechnical Journal, **16**: 295-308.

GRAHAM, J. and HOULSBY, G.T. 1983. Anisotropic elasticity of a natural clay. Geotechnique, **33**: 165-180.

GRAHAM, J. and LI, C.C., 1985. Comparison of natural and remoulded plastic clay. ASCE, Journal of Geotechnical Engineering, Vol. 111, No.7, pp. 865-881.

GRAHAM, J., CROOKS, J.H.A. and LAU, S.L.K. 1983. Yield envelopes: identification and geometric properties. Geotechnique, **38**: 125-134.

GRAHAM, J., NOONAN, M.L. and LEW, K.V. 1983. Yield states and stress-strain relationships in a natural plastic clay. Canadian Geotechnical Journal, **20**: 502-516.

GRAHAM, J., PINKNEY, R.B., LEW, K.V. and TRAINOR, P.G.S. 1982. Curve-fitting and laboratory data. Canadian Geotechnical Journal, **19**: 201-205.

GRIFFITHS. D.V. and LANE, P.A. 1990. Finite element analysis of the shear vane test. Computers and Structures, **37(6)**: 1105-1116.

HAILE, G. 1977. Foundation performance of a tower silo. M.A.Sc. Thesis, Department of Civil Engineering, University of Ottawa, Canada.

HANDY, P L., REMMES, B., MOLDT, S., LUTENEGGER, A.J. and TROTT, G. 1982. *In situ* stress determination by Iowa Stepped Blade. ASCE Journal of Geotechnical Engineering Division, **108**: 1405-1422.

HANNA, A. and GHALY, A. 1992. Effects of K_o and overconsolidation on uplift capacity. ASCE Journal of Geotechnical Engineering, **118**: 1449-1469.

HEAD, K.H. 1986. Manual of soil laboratory testing, Vol.3, John Wiley & Sons, Toronta, Canada.

HENKEL, D.J. 1960. The shear strength of saturated remoulded clays. ASCE Research Conference on Shear Strength of Cohesive soils, Boulder, Colorado, pp. 533-554.

HENKEL, D.J., 1970. Geotechnical considerations of lateral stresses. ASCE Spec. Conf. Earth Retaining Structures, Cornell University, pp. 1-49.

HENKEL, D.J. 1971. The relevance of laboratory-measured parameters in field studies. In: Stress-Strain Behaviour of Soils, Roscoe Memorial Symposium, editor: R.H.G. Parry, Oxfordshire, Foulis, pp. 669-675.

HOLTZ, R.D., JAMIOLKOWSKI, M.B. and LANCELLOTTA, R. 1986. Lessons from oedometer tests on high quality samples. ASCE Journal of the Geotechnical Engineering Division, **112**: 768-776.

HOULSBY, G.T. and WROTH, C.P. 1991. The variation of shear modulus of a clay with pressure and overconsolidation ratio. Soils and Foundations, **31**: 138-143.

HRYCIW, R.D. 1990. Small-atrain-shear modulus of soil by dilatometer. ASCE Journal of the Geotechnical Engineering Division, **116**: 1700-1716.

HVORSLEV, M.J. 1960. Physical components of the shear strength of saturated clays. ASCE Research Conf. on Shear Strength of Cohesive Sils, Boulder, Colorado, pp. 169-273.

JAKY, J., 1944. The coefficient of earth pressure at rest. Journal of the Society of Hungarian Architects and Engineers, pp. 355-358.

JAKY, J. 1948. Pressure in soils. Proceedings, 2nd International Conference on Soil Mechanics and Foundation Engineering, Rotterdam, Vol. 1, pp. 103.

JAMIOLKOWSKI, M., LADD, C.C, GERMAINE, J.J. and LANCELLOTTA, R. 1985. New developments in field and laboratory testing of soils, Proceedings, 11th International Conference on Soil Mechanics and Foundation Engineering, San Francisco, **1**: 57-154.

JANBU, N., TOKHEIM,O. and SENNESET, K. 1981. Consolidation tests with continuous loading. Proc. 10th International Conference on Soil Mechanics and Foundation Engineering, Stockholm, Vol.1, pp. 645-654.

JARDINE, R.J., SYMES, M.J. and BURLAND, J.B. 1984. The measurement of soil stiffness in the triaxial apparatus. Geotechnique **34**: 323-340.

JARRET, P.M., 1970. The mechanics of landslides in Leda clay: Discussion. Canadian Geotechnical Journal, Vol. 7, pp. 504-505.

JEFFERIES, M.G., 1988. Determination of horizontal geostatic stress in clay with self-bored pressuremeter. Canadian Geotechnical Journal **25**: 559-573.

JEFFERIES, M. G., CROOKS, J. H. A., BECKER, D. E., and HILL, P. R. 1987. Independence of geostatic stress from overconsolidation in some Beaufort Sea clays. Canadian Geotechnical Journal, **24**: 342-356.

KABBAJ, M., OKA, F., LEROUEIL, S. and TAVENAS, F., 1986. Consolidation of natural clays and laboratory testing, in Consolidation of Soils, ASTM STP 892, pp. 378-404.

KAMEI, T. and NAKASE, A. 1989. Undrained shear strength anisotropy of K_0-consolidated cohesive soils. Soils and Foundations, **29**: 145-151.

KENNEY, T.C., 1967. Field measurement of *in situ* stresses in quick clays. Proc. of the Geotechnical Conf. Oslo, Vol.1, pp. 49-55.

KENNEY, T.C. and LANDVA, A. 1965. Vane-triaxial apparatus. Sixth International Conference on Soil Mechanics and Foundation Engineering, Montreal, Vol.1, pp. 269-272.

KENNEY, T.C. and WATSON, G.H., 1961. Multiple-stage triaxial test for determining c' and i' of saturated soils. Proc. 5th International Conference on Soil Mechanics and Foundation Engineering, Paris, pp. 191-195.

KHAN, M.A. and GARGA, V.K. 1991. Evaluation of undrained shear strength of a clay crust. 44th Canadian Geotechnical Conference, Calgary, Paper No. 3, pp. 3.1-3.10.

KHAN, M.A. and GARGA, V.K. 1990. Evaluation of *in-situ* horizontal stresses of overconsolidated clays. Proceedings, 43rd Canadian Geotechnical Conference, pp. 689-696.

KIETKAJORNKUL, C. and VASINVARTHANA, V. 1989. Influence of different vane types on undrained strength of soft Bangkok Clay. Soils and Foundations. **29**: 146-152.

KOLISOJA, P., SAHI, K. and HARTIKAINEN, J. 1989. An automatic triaxial-oedimeter device. 12th International Conference on Soil Mechanics and Foundation Engineering, Rio de Jeneiro, Vol.1, pp. 61-64.

KONRAD, J-M. and LAW, K.T. 1987a. Undrained shear strength from piezocone tests. Canadian Geotechnical Journal, **24**: 392-405.

KONRAD, J-M. and LAW, K.T. 1987b. Preconsolidation pressure from piezocone tests in marine clays. Geotechnique, **37**: 177-190.

KOUTSOFTAS, D.C. and LADD, C.C. 1985. Design strengths for an offshore clay. ASCE Journal of the Geotechnical Engineering Division, **111**: 337-355.

KONRAD, J-M. and LAW, K.T. 1987b. Preconsolidation pressure from piezocone tests in marine clays. Geotechnique, **37**: 177-190.

LACASSE, S., JAMIOLKOWSKI, M., LANCELLOTTA, R., and LUNNE, T. 1981. *IN SITU* characteristics of two Norwegian clays. 10th International Conference on Soil Mechanics and Foundation Engineering, Stockholm. Vol. 2, pp. 507-511.

LACASSE, S. and LUNNE, T. 1982. *In situ* horizontal stress from pressuremeter tests. Proc. Symp. on the Pressuremeter and its Marine Applications, Editions Techniq, Paris, pp. 187-208.

LADANYI, B. 1970. The mechanics of landslides in Leda clay: Discussion. Canadian Geotechnical Journal, Vol. 7, pp. 506-507.

LADANYI, B. 1972. *In situ* determination of undrained stress-strain behaviour of sensitive clays with the pressuremeter. Canadian Geotechnical Journal, **9**: 313-319.

LADD, C. C. 1964. Stress-strain modulus of clay in undisturbed shear. ASCE Journal of the Geotechnical Engineering Division, **90**: 103-132.

LADD, C. C. 1991. Stability evaluation during staged construction. ASCE Journal of the Geotechnical Engineering Division, **117**: 537-615.

LADD, C. C. and FOOTT, R. 1974. New design procedure for stability of soft clays. ASCE Journal of the Geotechnical Engineering Division. **100**: 763-786.

LADD, C. C., FOOTT, R., ISHIHARA, SCHLOSSER and POULOS, H.G. 1977. Stress-deformation and strength characteristics. International Conference on Soil Mechanics and Foundation Engineering, Tokyo, **2**: 421-494.

LADE, P.V. and DUNCAN, J.M. 1976. Stress-path dependent behaviour of cohesionless soil. ASCE Journal of the Geotechnical Engineering Division, **102**: 51-68.

LAFLEUR, J., GIROUX, F., and HUOT, M. 1987. Field permeability of the weathered Champlain clay crust. Canadian Geotechnical Journal **24**: 581-589.

LAFLEUR, J., LEFEBVRE, G., MARCOTTE, M. and SILVESTRI, V., 1982. Shear strength of the weathered Champlain clay measured in a large diameter triaxial test. Canadian Geotechnical Journal, **19**: 413-420.

LAMB, J.H. and ANDERSON, J.A. 1973. A versatile control system for triaxial testing of soils. Journal of Testing and Evaluation, **1**: 144-148.

LAMBE, T.W., 1964. Methods of estimating settlement. ASCE Journal of Geotechnical Engineering Division, **90**: 43-67.

LAMBE, T.W., 1967. Stress path method. ASCE, Journal of Geotechnical Engineering, **93**: 309-331.

LAMBE, T.W., 1979. Stress path method: second edition. ASCE, Journal of Geotechnical Engineering, Vol. 105, GT6, pp. 309-331.

LA ROCHELLE, P., ROY, M. and TAVENAS, S. 1973. Field measurements of cohesion in Champlain clays. International Conference on Soil Mechanics and Foundation Engineering, Moscow, Vol.1, pp. 229-236.

LA ROCHELLE, P., TRAK, B., TAVENAS, F., and ROY, M. 1974. Failure of a test embankment on a sensitive Champlain clay deposit. Canadian Geotechnical Journal, **11**: 142-164.

LARSSON, R. and SALLFORS, G., 1986. Automatic continuous consolidation testing in Sweden. In Consolidation of Soils, ASTM STP 892, pp. 299-328.

LAW, K.T. 1979. Triaxial vane tests on a soft marine clay. Canadian Geotechnical Journal, **16**: 11-18.

LAW, K.T., 1981. A servo system for controlled stress path test. In: Laboratory Shear Strength of Soil. ASTM STP 740, Eds: R.N. Yong and F.C. Townsend. pp. 164-179.

LAW, K.T. and LO, K.Y. 1976. Analysis of shear-induced anisotropy in Leda clay. Proceedings, Engineering Conference on Numerical Methods in Geomechanics, BlacksBurg, VA, Vol.1, pp. 329-344.

LEFEBVRE, G., LADD, C.C. and PARE, J.J. 1988. Comparison of field vane and laboratory undrained shear strength in soft sensitive clays. Vane Shear Strength Testing in Soils: Field and Laboratory Studies. ASTM STP 1014, A.F. Richards, Ed., pp. 233-246.

LEFEBVRE, G., PARE, J.J., and DASCAL, O. 1987. Undrained shear strength in the surficial weathered crust. Canadian Geotechnical Journal, **24**: 23-34.

LEFEBVRE, G., and POULIN, C. 1979. A new method of sampling in sensitive clay. Canadian Geotechnical Journal, **16**: 226-233.

LEROUEIL, S., KABBAJ, M., TAVENAS, F., and BOUCHARD, R., 1985. Stress-strain-strain rate relation for the compressibility of sensitive natural clays. Geotechnique, **35**: 159-180.

LEROUEIL, S., LEBIHAN, J.P. and TAVENAS, F. 1980. An approach for the determination of the preconsolidation pressure in sensitive clays. Canadian Geotechnical Journal, **17**: 446-453.

LEROUEIL, S., SAMSON, F. and BOZOZUK, M., 1983. Laboratory and field determination of preconsolidation pressures at Gloucester. Canadian Geotechnical Journal, **20**: 477-490.

LEROUEIL, S., TAVENAS, F., SAMSON, F. and MORIN, P., 1983. Preconsolidation pressure of Champlain clays. Part II, Laboratory determination, Canadian Geotechnical Journal, Vol. 20, No.4, pp. 803-816.

LEWIN, P.I. 1971. Use of Servo mechanisms for volume change measurement and K_0 consolidation. Geotechnique, **21**: 259-262.

LO, K.Y. 1972. An approach to the problem of progressive failure. Canadian Geotechnical Journal, **9**: 407-429.

LO, K.Y. and MORIN, J.P. 1972. Strength anisotropy and time effects of two sensitive clays. Canadian Geotechnical Journal, 9: 261-277.

LOWE, J. and JOHNSON, T.C. 1960. Use of back pressure to increase degree of saturation of triaxial test specimens. Proc. Conf. on Shear Strength of Cohesive soils, Boulder, Colorado, pp. 819-826.

LUTENEGGER, A.J. and TIMIAN, D.A., 1986. *In situ* tests with K_0 stepped blade. Proc. Use of *In situ* Tests in Geotechnical Engineering, ASCE, Geotechnical Special Publication No. 6, pp. 730-751.

MAHAR, L.J. and O'NEILL, M.W. (1983). Geotechnical characterization of desiccated clay. ASCE Journal of the Geotechnical Engineering Division **109**: 56-71.

MAIR, R.J. and WOOD, D.M., 1987. Pressuremeter testing: methods and interpretation. CIRIA Ground Engineering Report: *In situ* Testing, Butterworths, London.

MARCHETTI, S. 1975. A new *in situ* test for measurement of horizontal soil deformability. Proc. ASCE Speciality Conf. on *In situ* Measurement of Soil Properties, Raleigh, NC, Vol.II, pp. 255-259.

MARCHETTI, S. 1980. *In situ* tests by flat dilatometer. ASCE Journal of Geotechnical Engineering, **106**: 299-321.

MARSLAND, A. 1971. The shear strength of stiff fissured clays. In: Stress-Strain Behaviour of Soils, Roscoe Memorial Symposium, editor: R.H.G. Parry, Oxfordshire, Foulis, pp. 59-68.

MASSARSCH, K.R., 1975. New method for measurement of lateral earth pressure in cohesive soils. Canadian Geotechnical Journal, **12:** 142-146.

MASSARSCH, K.R., HOLTZ, R.D., HOLM, B.G. and FREDRIKSSON, A., 1975. Measurement of horizontal *in situ* stresses. Proc. Conf. on *In Situ* Measurement of Soil Properties. Specialty Conf. ASCE Geotechnical Engineering Divn., Raleigh, NC, Vol. 1, pp. 266-286.

MAYNE, P. W. 1980. Cam-clay predictions of undrained strength. ASCE Journal of the Geotechnical Engineering Division, **106** : 1219-1242.

MAYNE, P.W., 1984. K_0-C_u/σ_{vo}' trends for overconsolidated clays. ASCE Journal of Geotechnical Engineering Divn., Vol.110, No.10, pp. 1511-1516.

MAYNE, P. W. 1985. Stress anisotropy effects on clay strength. ASCE Journal of the Geotechnical Engineering Division, **111**: 356-366.

MAYNE, P.W. and KULHAWY, F.H., 1982. K_0-OCR relationships in soil. ASCE, Journal of Geotechnical Engineering, **106:** 851-872.

MAYNE, P.W. and MITCHELL, J.K., 1988. Profiling of over-consolidation ratio in clays by field vane, Canadian Geotechnical Journal, **25**: 150-157.

McMANIS, K. and ARMAN, A., 1986. Sampling and testing in stiff crustal clays. In: Geotechnical Aspects of Stiff and Hard Clays, Editors: Raj P. Khera and C.W. Lovell, ASCE, Geotechnical Special Publication No. 2, pp. 1-13.

MENARD, L.F. 1956. An apparatus for measuring the strength of soils in place. M.Sc. Thesis, University of Illinois, at Urbana, Illinois, USA.

MENZIES, B.K. 1976. An approximate correction for the influence of strength anisotropy on conventional shear vane measurements used to predict field bearing capacity. Geotechnique, **26**: 631-634.

MENZIES, B.K. 1988. A computer controlled hydraulic triaxial testing system. Advanced Triaxial Testing of Soil and Rock, ASTM STP 977, Robert T. Donaghe, Ronald C. Chaney, and Marshall L. Silver, Eds., pp. 82-94.

MENZIES, B.K. and HOOKER, P. 1991. Discussion of "Automated triaxial testing of soft clays: an upgraded commercial system" by T.C. Sheahan, J.T. Germaine and C.C. Ladd. ASTM Geotechnical Testing Journal, **14**: 110-112.

MENZIES, B.K. and MAILEY, L.K. 1976. Some measurements of strength anisotropy in soft clays using diamond-shaped shear vanes. Geotechnique, **26**: 535-538.

MENZIES, B.K. and MERRIFIELD, C.M. 1980. Measurements of shear stress distribution on the edges of a shear vane blade. Geotechnique, **30**: 314-318.

MESRI, G. 1989. A reevaluation of $S_{u(mob)}=0.22\sigma_p'$ using laboratory shear tests. Canadian Geotechnical Journal, **26**: 162-164.

MESRI, G. and CASTRO, A. 1987. C_α/C_c concept and K_0 during secondary compression. ASCE Journal of the Geotechnical Engineering Division, **113**: 230-247.

MITCHELL, R.J., 1970. On the yielding and mechanical strength of Leda clays. Canadian Geotechnical Journal, Vol. 7, pp. 297-312.

MITCHELL, R.J., 1975. Strength parameters for permanent slopes in Champlain Sea clays. Canadian Geotechnical Journal, Vol. 12, No. 4, pp. 447-455.

MITCHELL, R.J., SANGREY, D.A. and WEBB, G.S. 1972. Foundations in the crust of sensitive clay deposits. Proc. Specialty Conf. Performance of Earth and Earth upported Structures, Purdue University, pp. 1051-1072.

NAGARAJ, T.S., MURTHY, M.K. and SRIDHARAN, A., 1981. Incremental loading device for stress path and strength testing of soils. ASTM Geotechnical Testing Journal, **4**: 74-78.

NASR, A.N. and GANGOPADHYAY, C.R., 1988. Study of S_u predicted by pressuremeter test. ASCE, Journal of Geotechnical Engineering, **114**: 1209-1226.

O'SHAUGHNESSY, V. 1993. The hydrological and contamination transport properties of fractured weathered Leda clay in Eastern Ontario. M.A.Sc. Thesis, Department of Civil Engineering, University of Ottawa, Ottawa, Canada.

PANDE, G. N. and PIETRUSZCZAK , S. 1986. A critical look at constructive models for soils. In: Geotechnical Modelling in Engineering Practice. Editors: R. Dungar and J.A. Studer. pp. 369-395.

PARRY, R.H.G. 1970. Overconsolidation in soft clay deposits. Geotechnique, **20**: 442-446.

PARRY, R.H.G. 1971. Undrained shear strength of clays. Proc. 1st ANZ Geomechanics conf., Melbourne, pp. 11-15.

PARRY, R.H.G. and NADARAJAH, V. 1973. A volumetric yield locus for lightly overconsolidated clay. Geotechnique, **23**: 451-453.

POTTS, D.M., DOUNIAS, G.T. and VOUGHAN, P.R. 1987. Finite element analysis of the direct shear box test. Geotechnique, **37**: 11-23.

POULOS, H.G. and DAVIS, E.H., 1972. Laboratory determination of *in situ* horizintal stress in soil masses. Geotechnique, **22:** 177-182.

PRADHAN, T:B.S., TATSUOKA, F., MOHRI, Y. and SATO,Y., 1989. An automated triaxial testing system using a simple triaxial cell for soils. Soils and Foundations, **29**: 151-160.

RICHARDSON, A.M., BRAND, E.W. and MEMON, A. 1975. *In situ* determination of anisotropy of a soft clay. Proceedings, ASCE Specialty Conference on *In situ* Measurement of Soil Properties, Raleigh, North Carolina, Vol.1, pp. 336-349.

ROBERTSON, P.K. and CAMPANELLA, R.G. 1983. Interpretation of cone penetration tests. Part I: Sand and Part II: Clay. Canadian Geotechnical Journal, **20**: 718-745.

ROBERTSON, P.K., CAMPANELLA, R.G. and WIGHTMAN, A. 1983. SPT-CPT correlations. ASCE Journal of Geotechnical Engineering, **109**: 1449-1459.

ROWE, P.W. and BARDEN, L. 1966. A new consolidation cell. Geotechnique, **16**: 162-170.

ROY, M. and LEBLANC, A. 1988. Factors affecting the measurements and interpretation of the vane strength in soft sensitive clays. *In* Vane shear strength testing in soils: field and laboratory studies, ASTM STP 1014. *Edited by* A.F. Richards, pp. 117-128.

SANGREY, D.A. 1972. On the causes of natural cementation in sesitive soils. Canadian Geotechnical Journal, **9**: 117-119.

SANDBAEKKEN, G., BERRE, T. and LACASSE, S., 1986. Oedometer testing at the Norwegian Geotechnical Institute. In Consolidation of Soils, ASTM STP 892, pp. 329-353.

SCHMERTMANN, J.H. 1975. Measurement of *in situ* shear strength. Proceedings, ASCE Specialty Conference on *In situ* Measurement of Soil Properties. Vol.II, Raleigh, NC, pp. 57-138.

SCHMERTMANN, J.H. 1981. Discussion (Marchetti, 1980) and closure by S. Marchetti. ASCE Journal of Geotechnical Engineering, **107**: 831-837.

SCHMERTMANN, J.H., 1985. Measure and use: the *in situ* lateral stress. The Practice of Foundation Engineering- a volume honoring J.O. Osterberg, Published by: The Department of Civil Engineering, Northwestern University.

SCHMERTMANN, J.H., 1986. Suggested method for performing the flat dilatometer test. ASTM Geotechnical Testing Journal, **9**: 93-101.

SCHMIDT, B. 1966. Discussion: Earth pressure at rest related to stress history. Canadian Geotechnical Journal **3**: 239-242.

SEED, H.B. and CHAN, C.K. 1959. Structure and strength characteristics of compacted clays, ASCE Journal of Geotechnical Engineering Division, **85**: 87-128.

SHEAHAN, T.C., GERMAINE, J.T. and LADD C.C. 1990. Automated triaxial testing of soft clays: an updated commercial system. ASTM Geotechnical Testing Journal, **13**: 153-163.

SHARIFOUNNASAB, M. and ULLRICH, C.R. 1985. Rate of shear effects on vane shear strength. ASCE Journal of the Geotechnical Engineering Division, **111**: 135-139.

SHEN, C.K., LI, X.S., CHAN, C.K. and WANG, Z. 1989. Microcomputer-based laboratory apparatus for soil testing. 12th International Conference on Soil Mechanics and Foundation Engineering, Vol.1, pp. 119-122.

SHIELDS, D.H. 1976. Consolidation tests. Geotechnique, **26**: 209-212.

SHIELDS, D.H. and BAUER, G.E., 1975. Determination of modulus of deformation of a sensitive clay using laboratory and *in situ* tests. Proc. Conf. Insitu Measurement of Soil Properties, Raleigh, North Carolina, pp. 395-421.

SILVESTRI, V. and AUBERTIN, M. 1988. Anisotropy and *in situ* vane tests. *In* Vane shear strength testing in soils: field and laboratory studies, ASTM STP 1014. *Edited by* A.F. Richards, pp. 88-103.

SILVESTRI, V., YONG, R.N., SOULIE, M. and GABRIEL,F., 1986. Controlled-strain, controlled-gradient and standard consolidation testing of sensitive clays. In Consolidation of Soils: Testing and Evaluation, ASTM STP 892, R.N. Yong and F.C. Townsend, Eds., pp. 433-450.

SIMONS, N., 1958. Discussion on Test requirements for measuring the coefficient of earth pressure at rest. Proc. Conf. on Earth Pressure Problems, Brussels, Vol. 3, pp. 2-14.

SIMONS, N. E. 1971. The stress path method of settlement analysis applied to London clay. In: Stress-Strain Behaviour of Soils, Roscoe Memorial Symposium, editor: R.H.G. Parry, Oxfordshire, Foulis, pp. 241-252.

SIMONS, N. E. and SOM, N.N. 1969. The influence of lateral stresses on the stress deformation characteristics of London clay. Seventh International Conference on Soil Mechanics and Foundation Engineering, **1**: 369-377.

SIVAKUGAN, N., CHAMEAU, J.L., HOLTZ, R.D. and HUANG, A.B. 1991. Inexpensive automatic control system for soil testing. Transportation Research Record 1309, pp. 1-4.

SKEMPTON, A.W. 1960. Effective stress in soils, concrete and rocks. Proc. Conf. on Pore Pressure and Suction in Soils, Butterworths, London, pp. 4-16.

SKEMPTON, A.W. 1961. Horizontal stresses in an overconsolidated Eocene clay. Proc. 5th International Conference on Soil Mechanics and Foundation Engineering, Paris, Vol. 1, pp. 351-357.

SKEMPTON, A.W. 1964. Long-Term Stability of Clay Slopes, 4th Rankine Lecture, Geotechnique, Vol. 14, No. 2, pp. 77-102.

SKEMPTON, A.W. and HUTCHINSON, J. 1969. Stability of natural slopes and embankment foundations. Proc. Seventh International Conference on Soil Mechanics and Foundation Engineering, Mexico, 291-340.

SKEMPTON, A.W. and SOWA, V.A., 1963. The behaviour of saturated clays during sampling and testing. Geotechnique, **13:** 269-290.

SMITH, R.E. and WAHLS, H.E., 1969. Consolidation under constant rates of strain. ASCE Journal of Geotechnical Engineering Divn., Vol.95, No. SM2, pp. 519-539.

SOM, N.N. 1968. The effect of stress path on the deformation and consolidation of London Clay. PhD thesis, Imperial College, University of London, U.K.

STRACHAN, P. 1985. Alternative test method for ensuring full saturation in triaxial samples. Geotechnical Testing Journal, **8**: 43-44.

TANAKA, A. 1986. *In situ* measurements for shear strength and deformation characteristics of a fissured clay soil. Ph.D. Thesis, Department of Civil Engineering, Carleton University, Ottawa.

TANAKA, A., BAUER, G. and QUEIROZ DE CARVALHO, J.B. 1989. Failure and analysis of a concrete silo. 12th International Conference on Soil Mechanichs and Foundation Engineering, Rio de Janeiro, **1**: 345-348.

TAVENAS, F., DES ROSIERS, J.-P., LEROEIL, S., LA ROCHELLE, P. and ROY, M., 1979. The Use of Strain Energy as a Yield and Creep Criterion for Lightly Overconsolidated Clays. Geotechnique 29, No.3, pp. 285-303.

TAVENAS, F., and LEROEIL, S., 1977. Effects of stresses and time on yielding of clays. Proc. 9th ICSMFE, Tokyo, **1**, pp. 319-326.

TAVENAS, F.A., BLANCHETTE, G., LEROUEIL, L., ROY, M. and LA ROCHELLE, P., 1975. Difficulties in the *in situ* determination of K_0 in soft sensitive clays. Proc., Conf. on *In Situ* Measurement of Soil Properties. Specialty Conf. ASCE Geotechnical Engineering Divn., Raleigh, NC, Vol. 1, pp. 266-286.

TOWNSEND, D.L., SANGREY, D.A. and WALKER, L.K. 1969. The brittle behaviour of naturally cemented soils. Seventh International Conference on Soil Mechanics and Foundation Engineering, Mexico, **1**: 411-417.

TSUCHIDA, T. and KIKUCHI, Y. 1991. K_0 consolidation of undisturbed clays by means of triaxial cell. Soils and Foundations, **31**: 127-137.

VAID, Y.P., CAMPANELLA, R.G. and KELLY, W.E., 1972. Discussion: Consolidation at constant rate of strain. ASCE Journal of Geotechnical Engineering, Vol. 98, pp. 508-512.

VAID, Y.P., ROBERTSON, P.K. and CAMPANELLA, R.G. 1979. Strain rate behaviour of Saint-Jean-Vianney clay. Canadian Geotechnical Journal, **16**: 34-42.

WARD, W.H., MARSLAND, A. and SAMUELS, S.G., 1965. Properties of the London Clay at the Ashford Common Shaft: *in situ* and undrained strength tests. Geotechnique, Vol.15, No.4, pp. 321-344.

WEBB, G.S. 1971. Geotechnical properties of the weathered crust of Leda Clay. M.Sc. Thesis, Queen's University, Kingston, Canada.

WINDLE, D. and WROTH, C.P. 1977. The use of a self-boring pressuremeter to determine the undrained properties of clays, Ground Engineering, **10**: 37-46.

WISSA, A.E.Z., CHRISTIAN, J.T., DAVIS, E.H. and HEIBERG, S., 1971. Consolidation at constant rate of strain. ASCE Journal of Geotechnical Engineering Divn., Vol.97, No. SM10, pp. 1393-1413.

WROTH, C.P. 1971. Some aspects of the elastic behaviour of overconsolidated clay. In: Stress-Strain Behaviour of Soils, Roscoe Memorial Symposium, editor: R.H.G. Parry, Oxfordshire, Foulis, pp. 347-361.

WROTH, C.P. 1984. The interpretation of *in situ* soil tests, 24th Rankine Lecture, Geotechnique **34**: 449-480.

WROTH, C.P. AND HOULSBY, G.T. 1985. Soil Mechanics - Property characterization and analysis procedures. 11th International Conference on Soil Mechanics and Foundation Engineering, San Francisco, **1**, 1-55.

WROTH, C.P., and HUGHES, J.M.O. 1973. An instrument for the *in situ* measurement of the properties of soft clays. Proceedings of the Eighth International Conference on Soil Mechanics and Foundation Engineering, Moscow, USSR, Vol. 1.2, pp. 487-494.

APPENDIX A

PLOTS OF TRIAXIAL TEST RESULTS

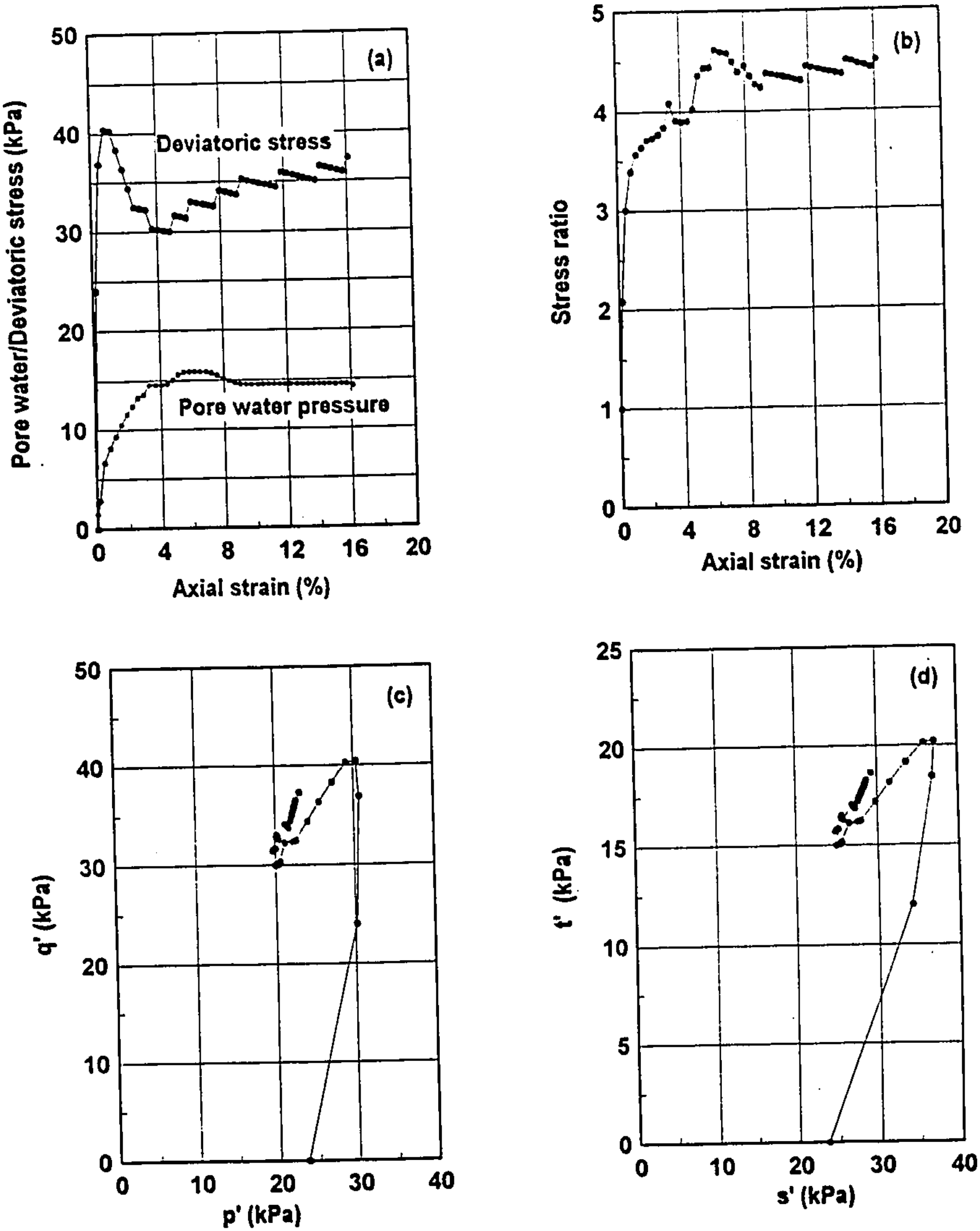

Fig. A.1. CIU triaxial compression test: Sample No. BS065T1.

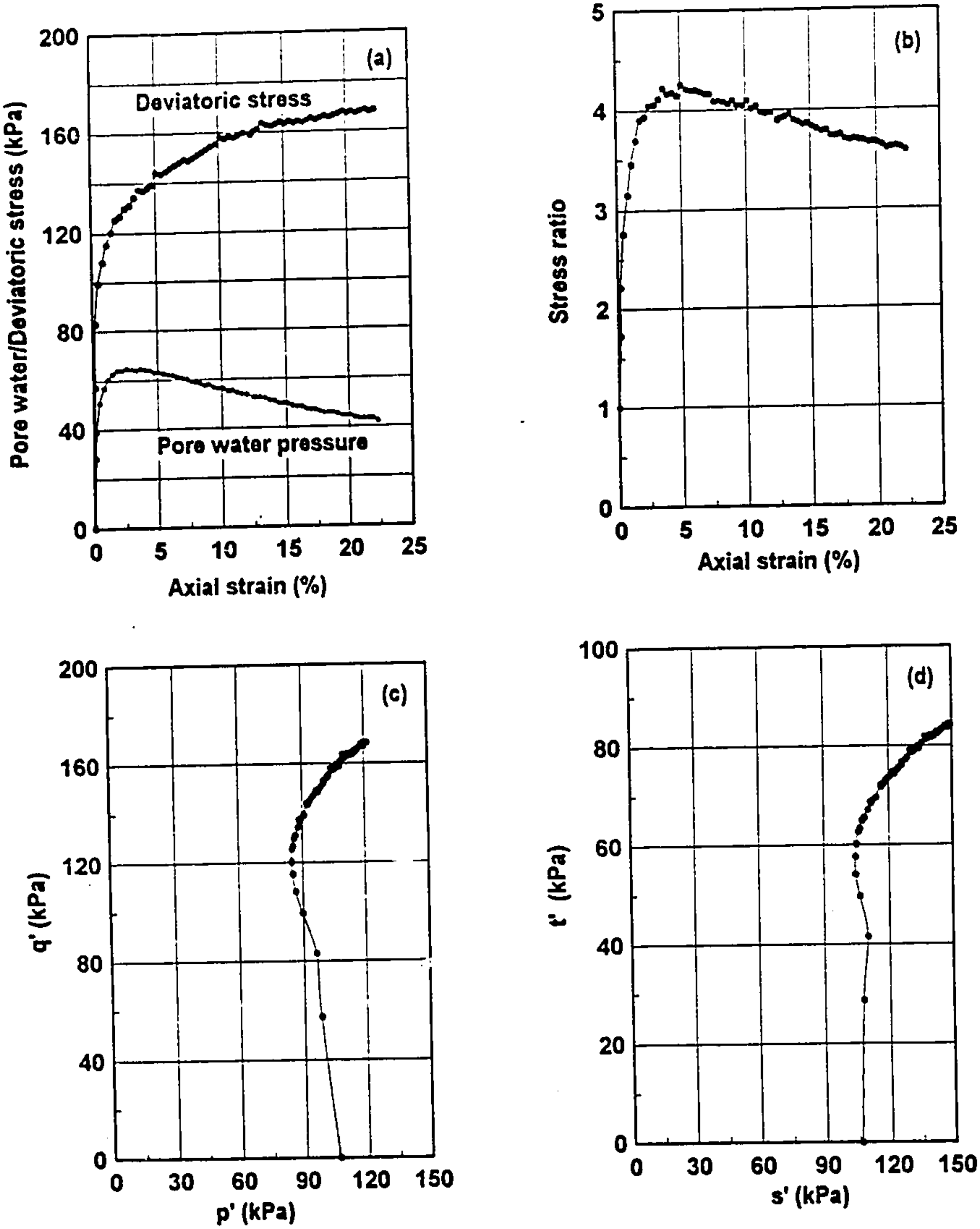

Fig. A.2. CIU triaxial compression test: Sample No. SB075T1.

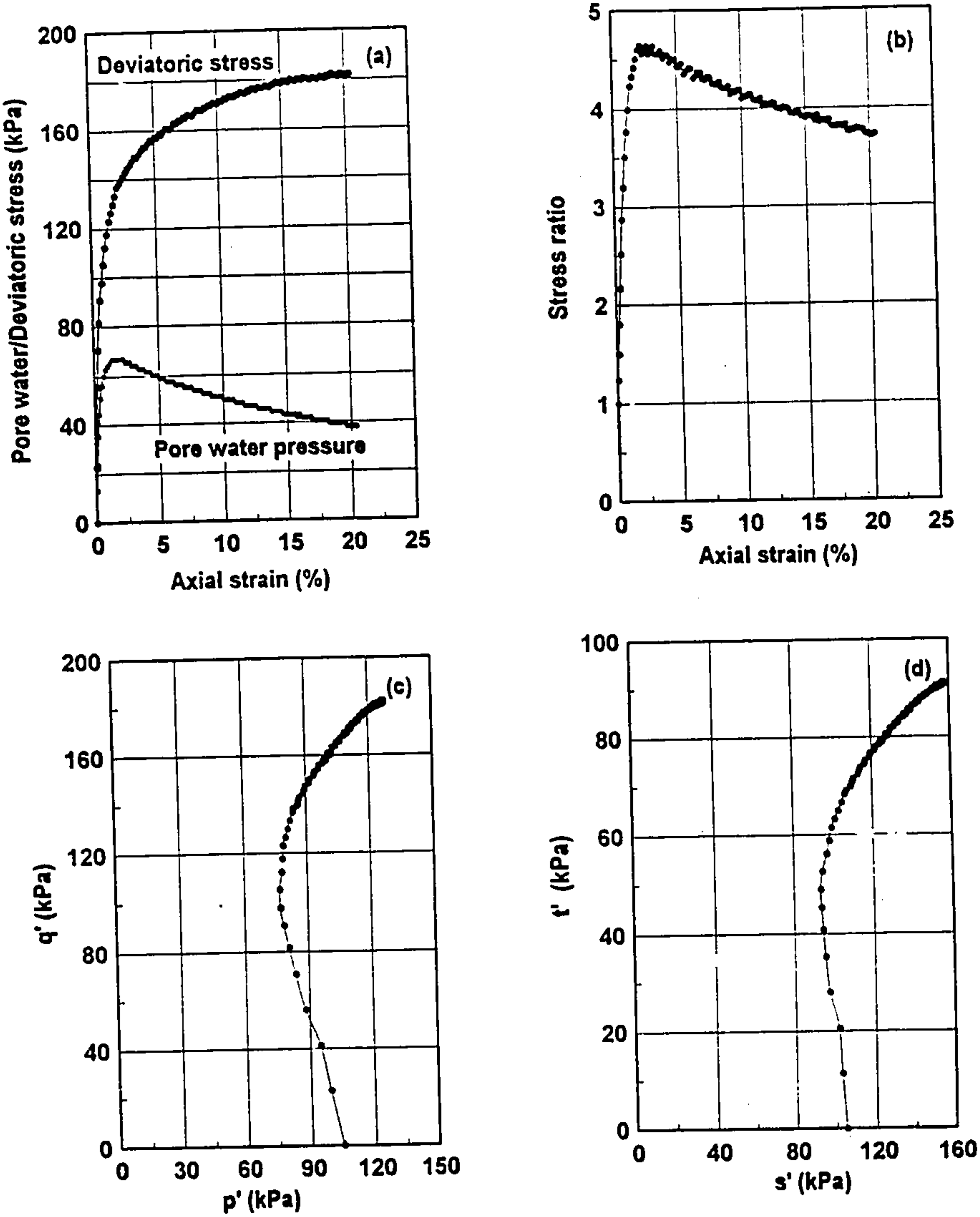

Fig. A.3. CIU triaxial compression test: Sample No. SB075T2.

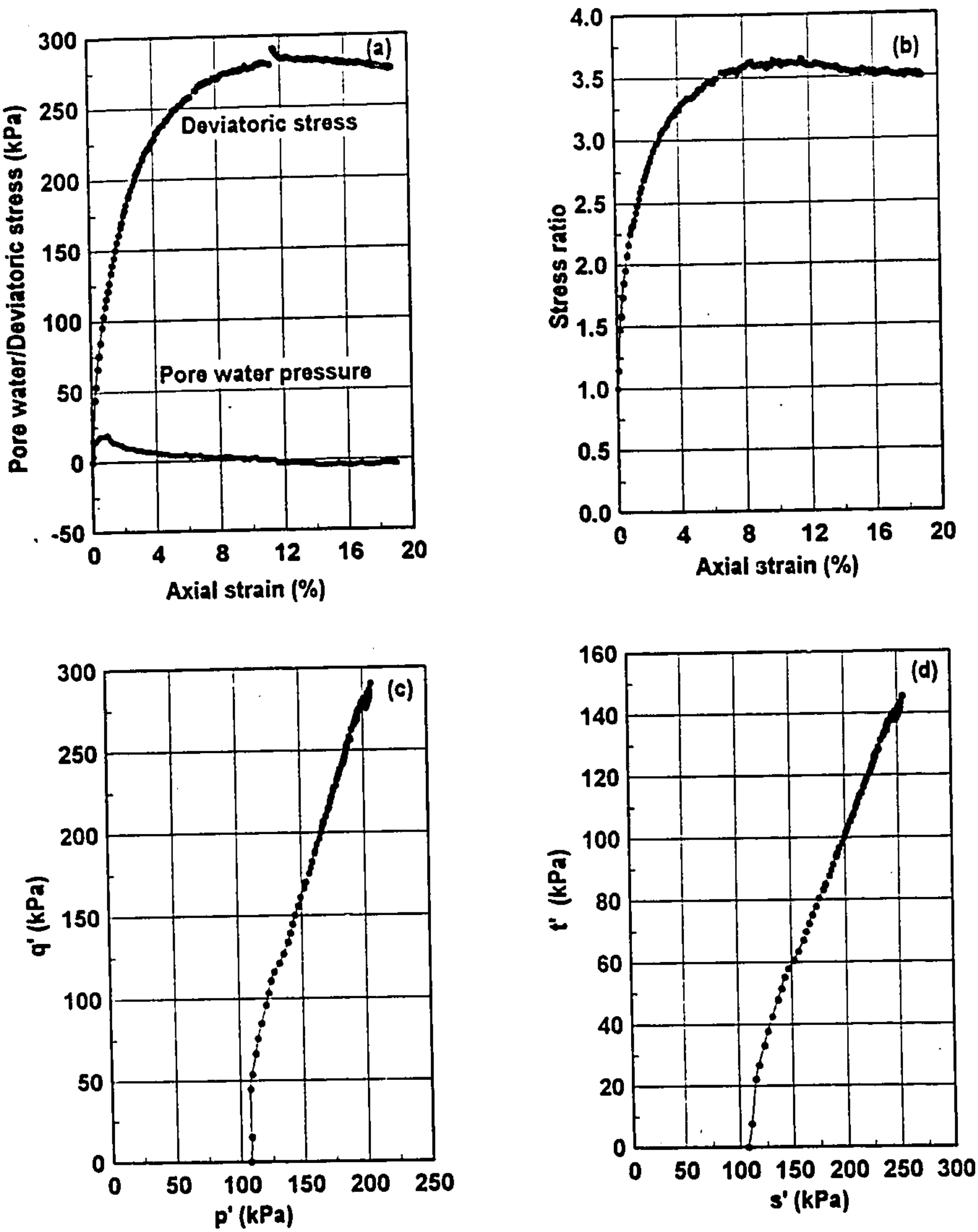

Fig. A.4. CID (partially drained) triaxial compression test: Sample No. SB075T3.

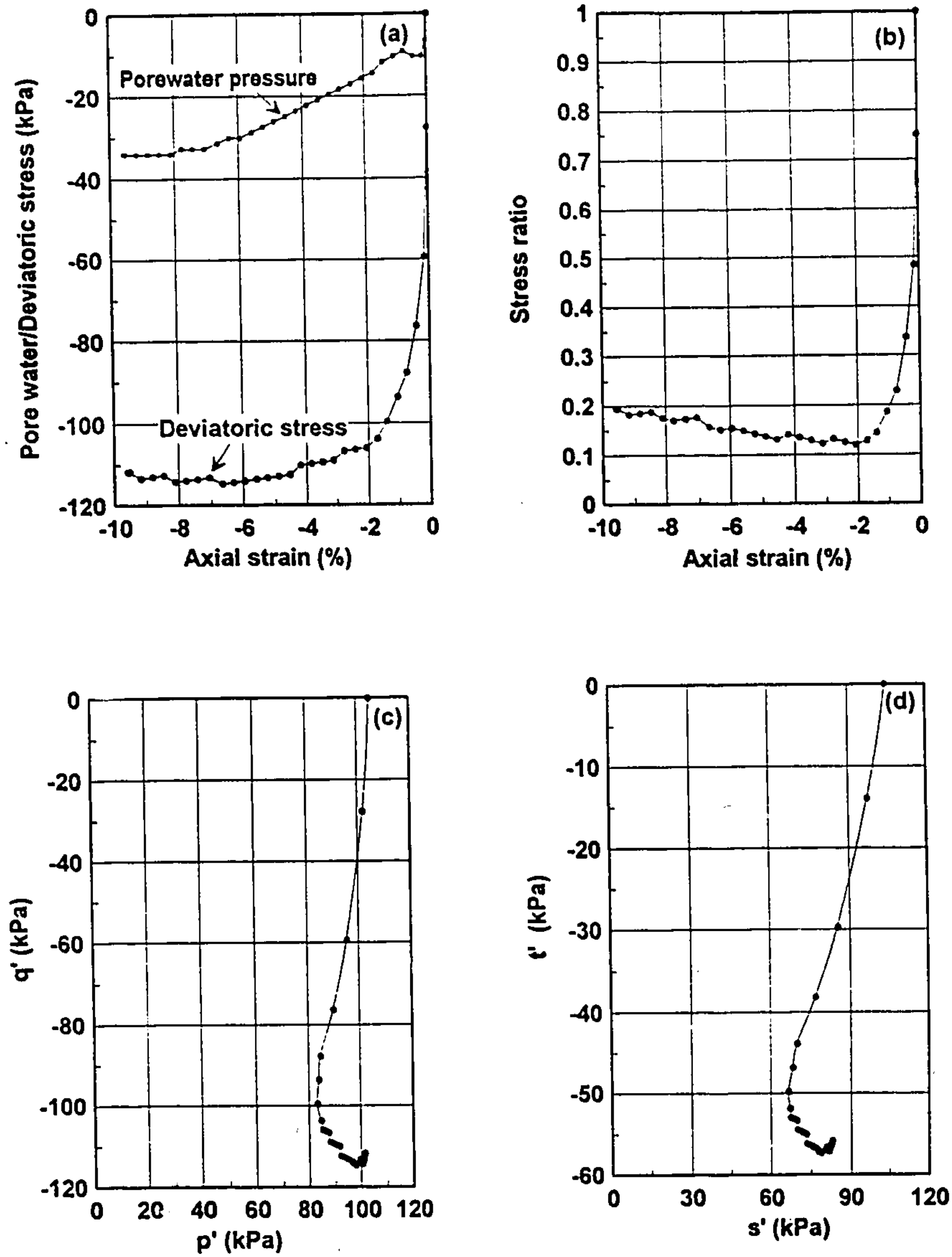

Fig. A.5. CIU triaxial extension test: Sample No. SB090T1.

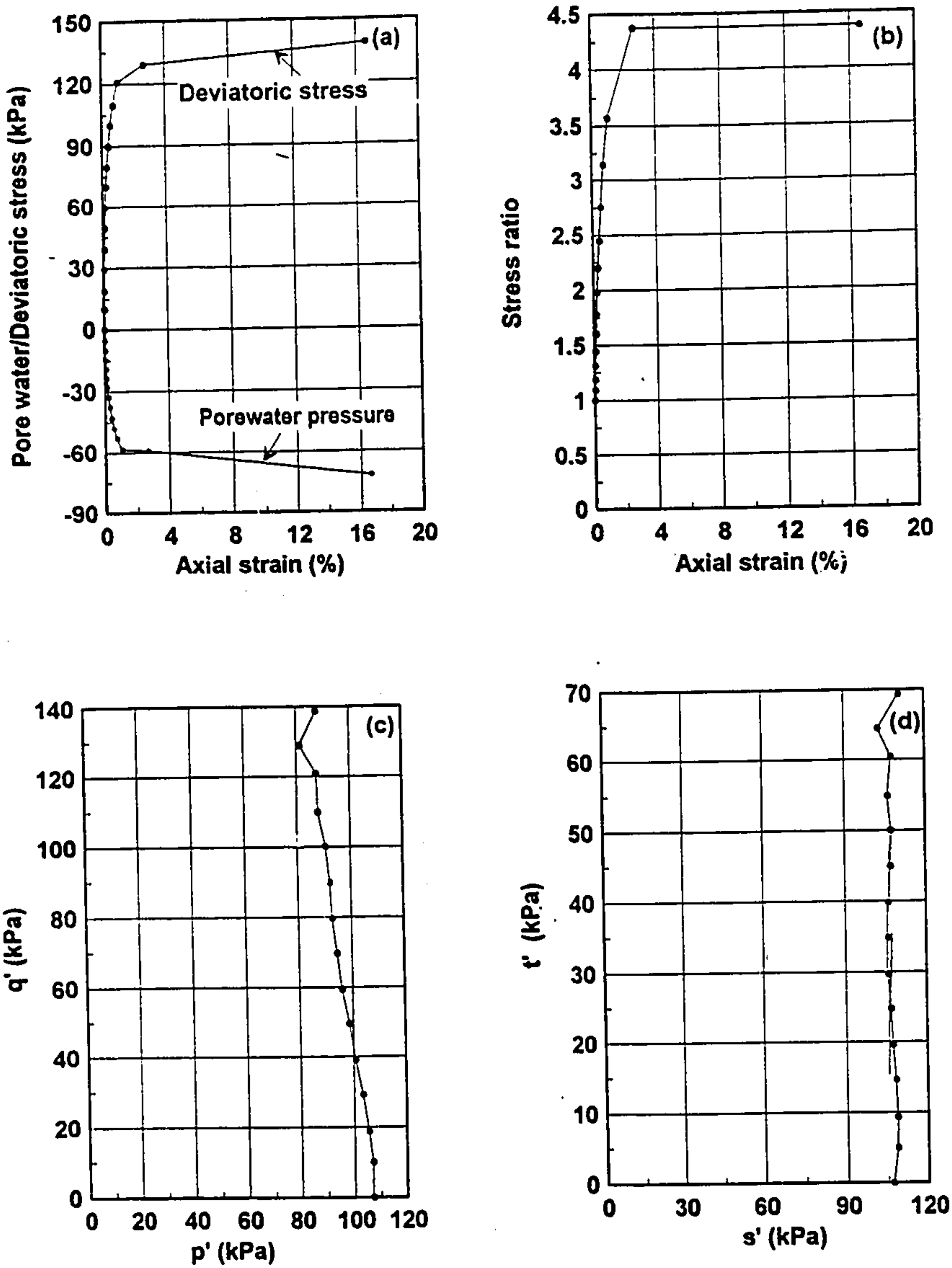

Fig. A.6. CIU triaxial compression test: Sample No. SB09T2.

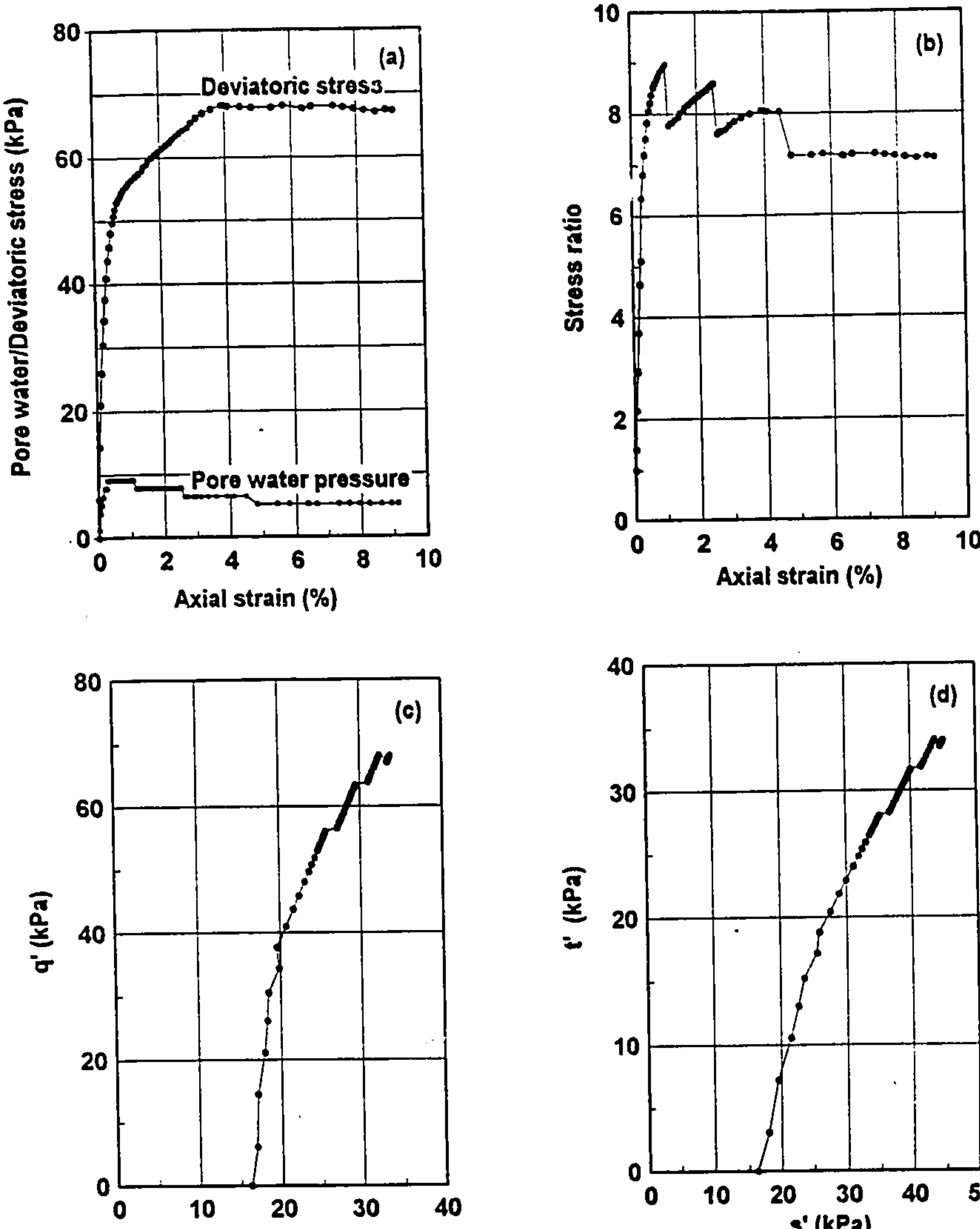

Fig. A.7. CIU triaxial compression test: Sample No. SB100T1.

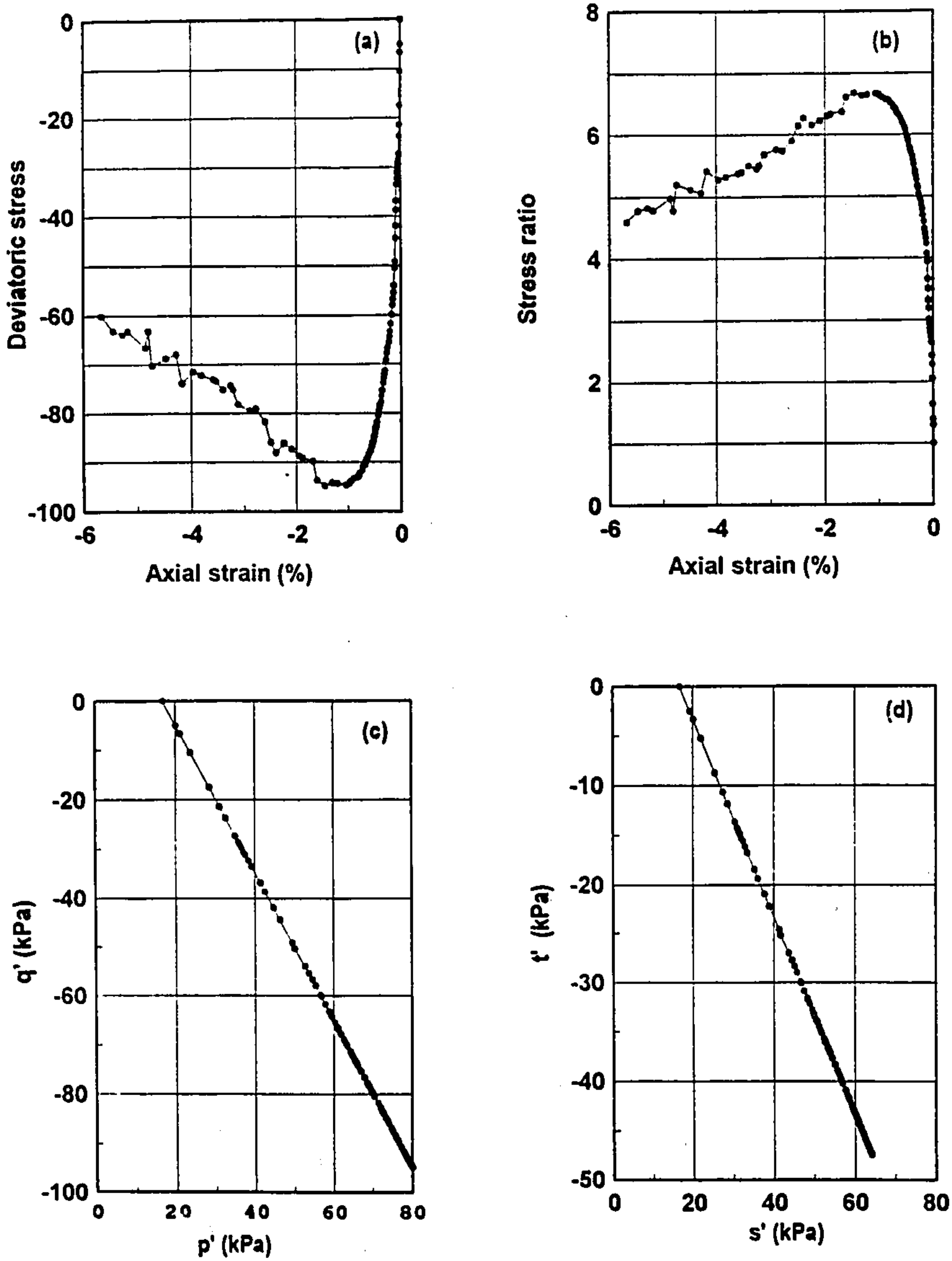

Fig. A.8. CID triaxial extension test: Sample No. SB100T2.

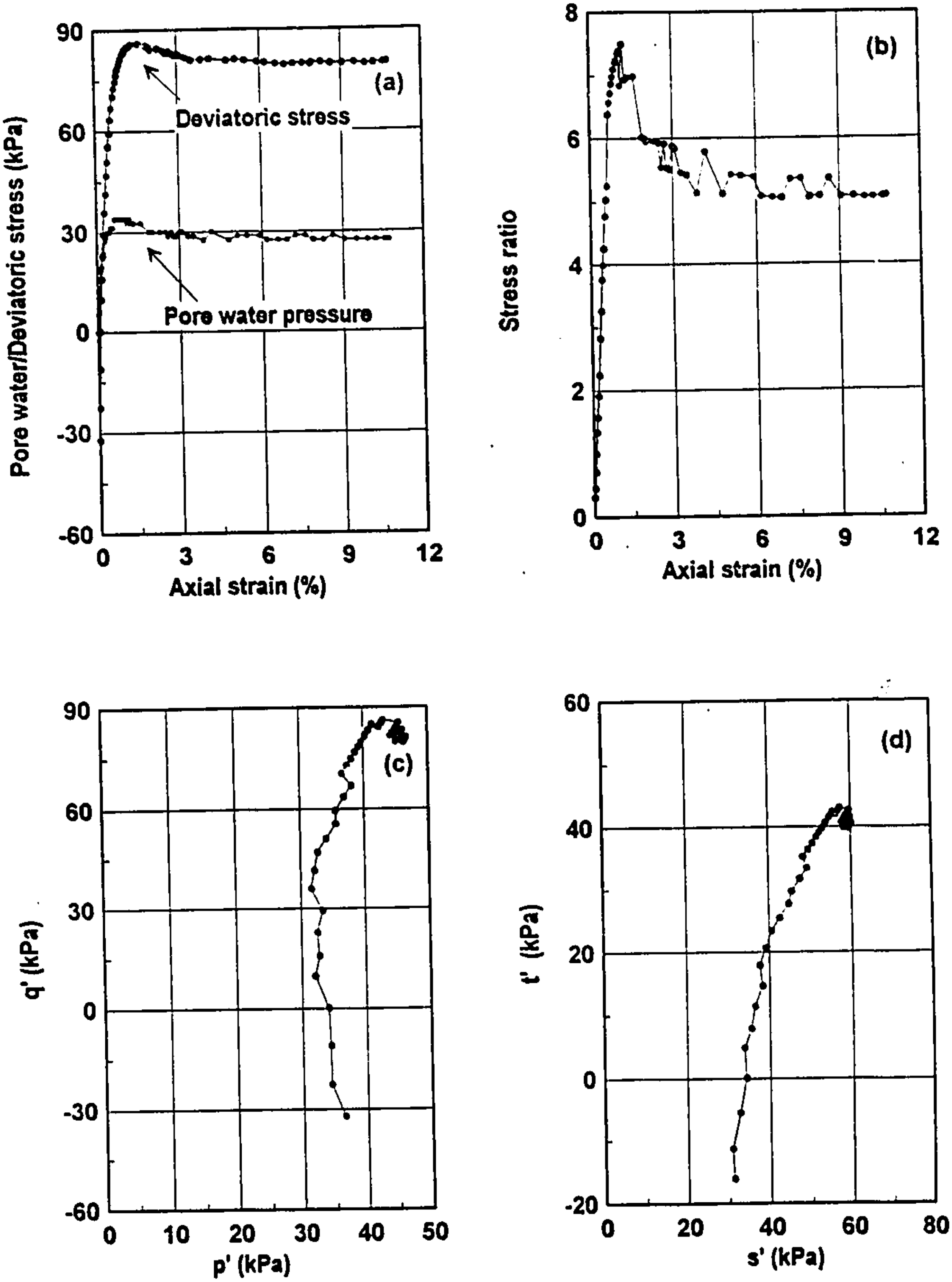

Fig. A.9. CK_0U triaxial compression test: Sample No. SB100T3.

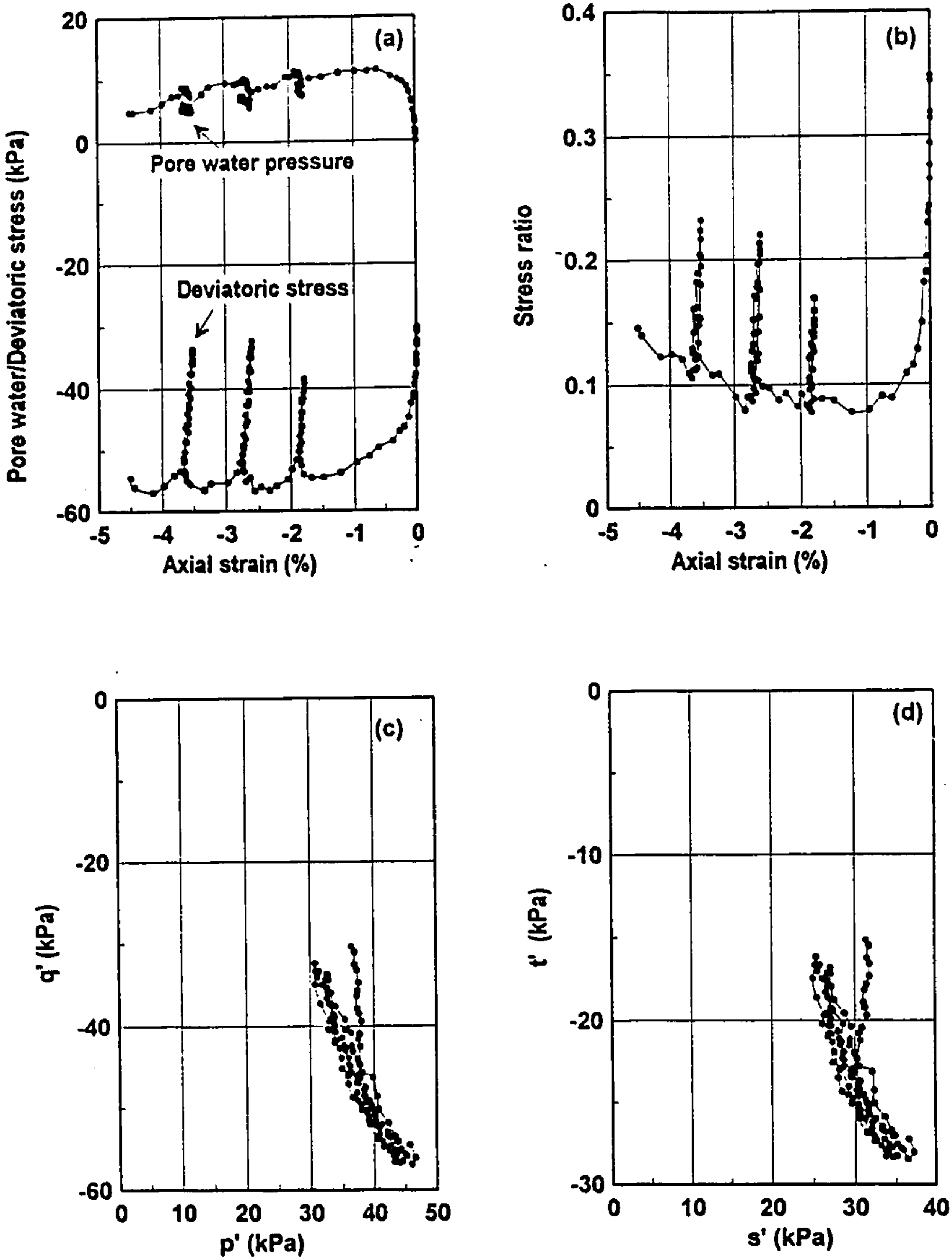

Fig. A.10. CK_0U triaxial extension test: Sample No. SB100T4.

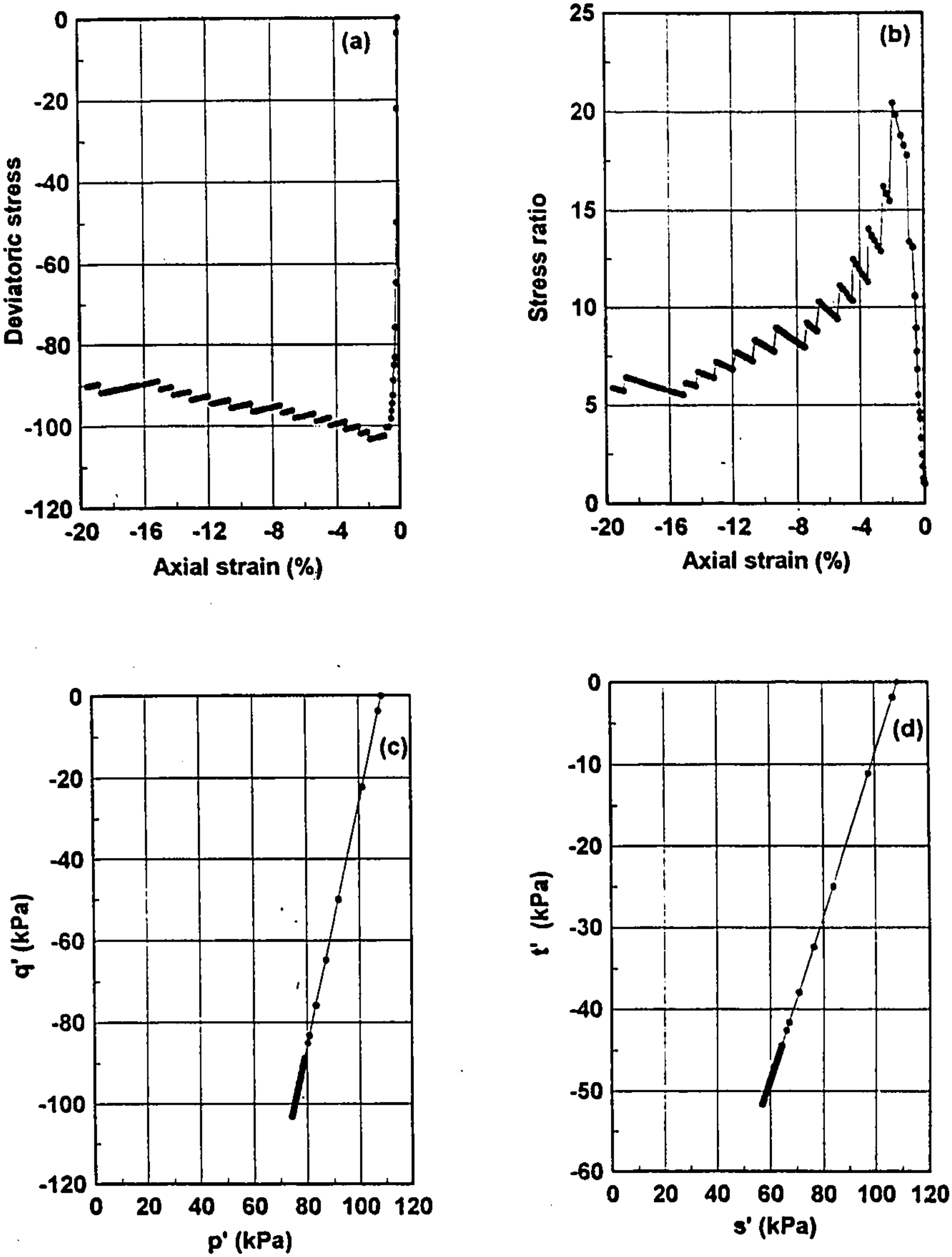

Fig. A.11. CID triaxial extension test: Sample No. SB120T1.

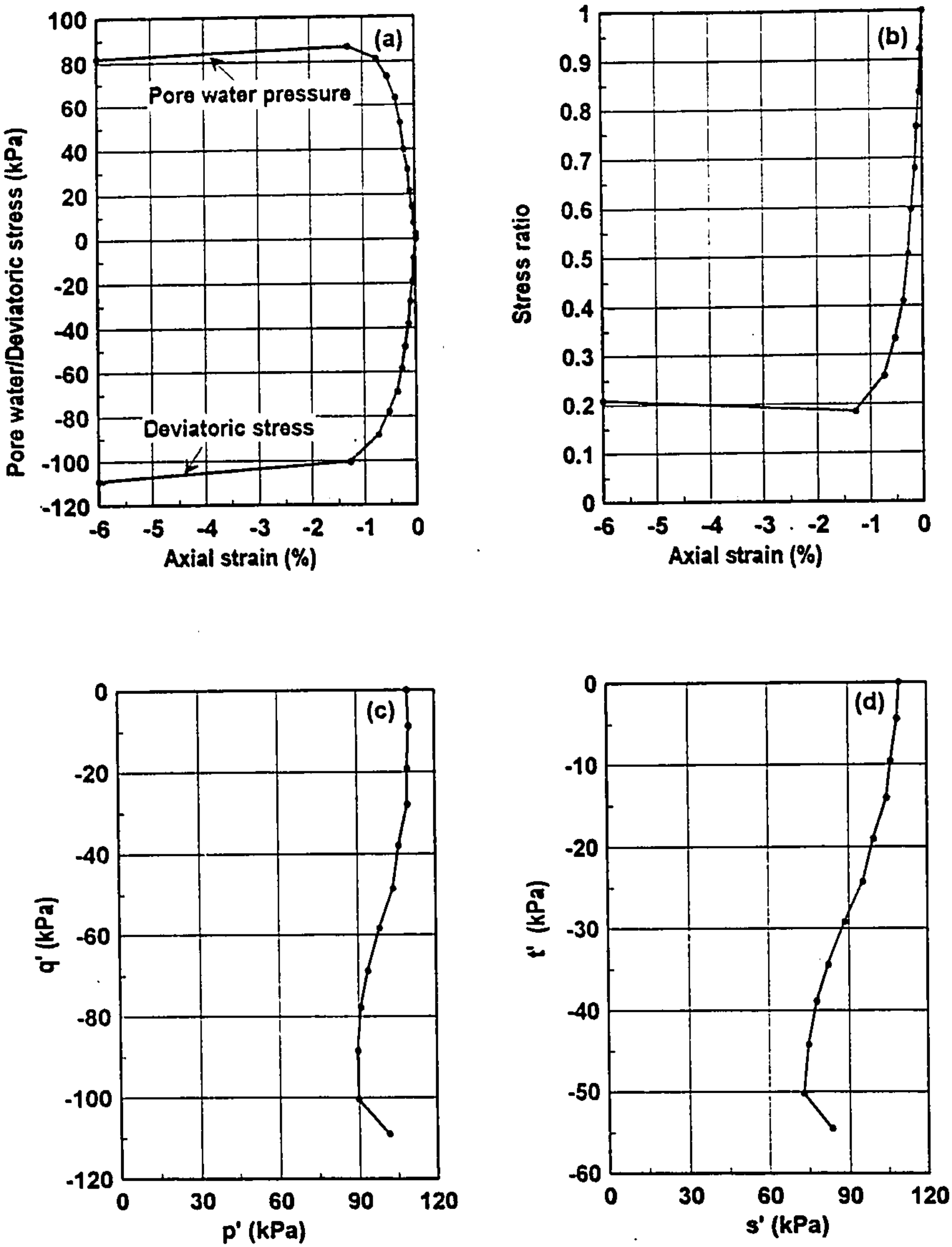

Fig. A.12. CIU triaxial extension test: Sample No. SB120T2.

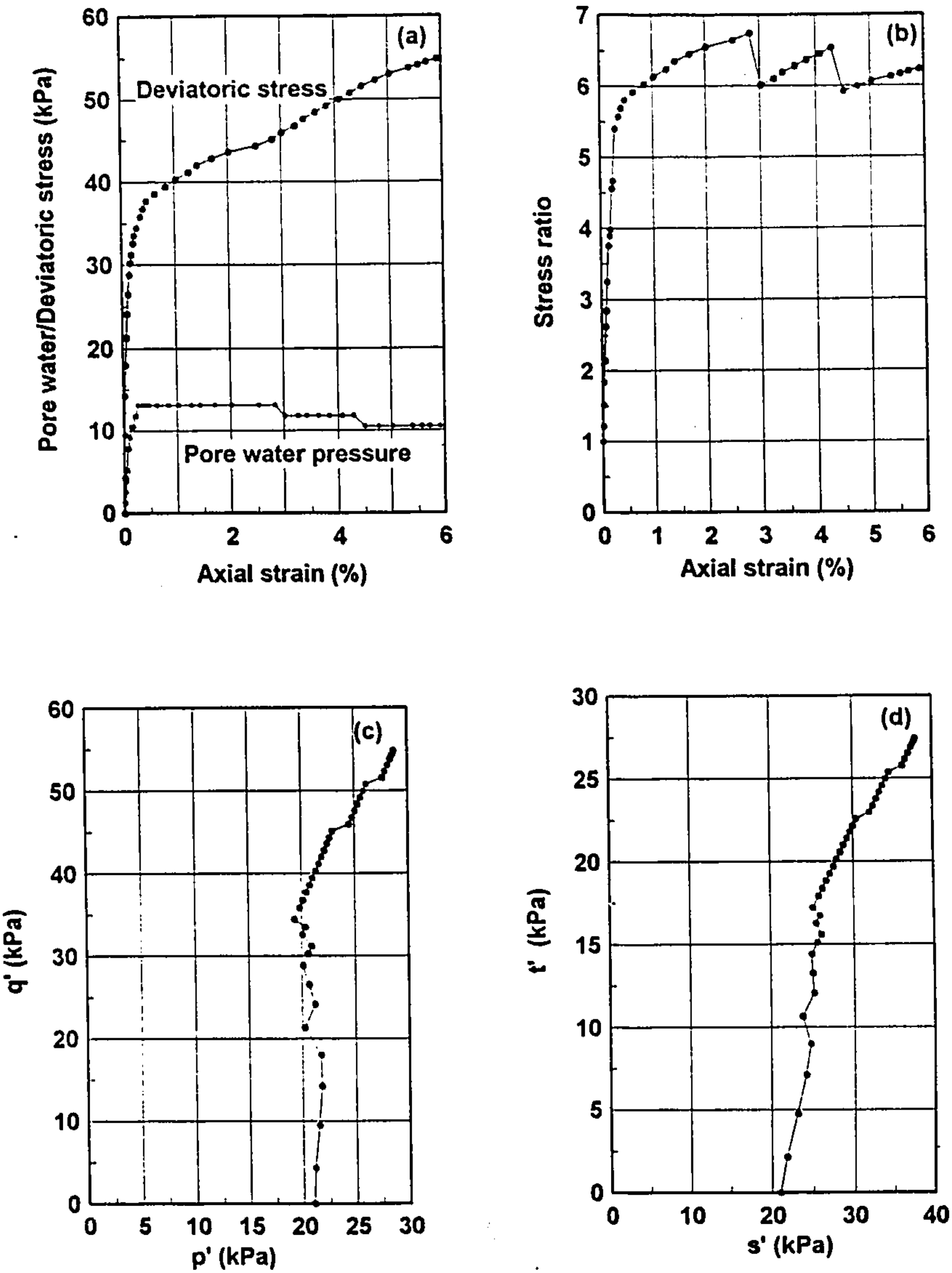

Fig. A.13. CIU triaxial compression test: Sample No. SB150T1 (horizontal sample).

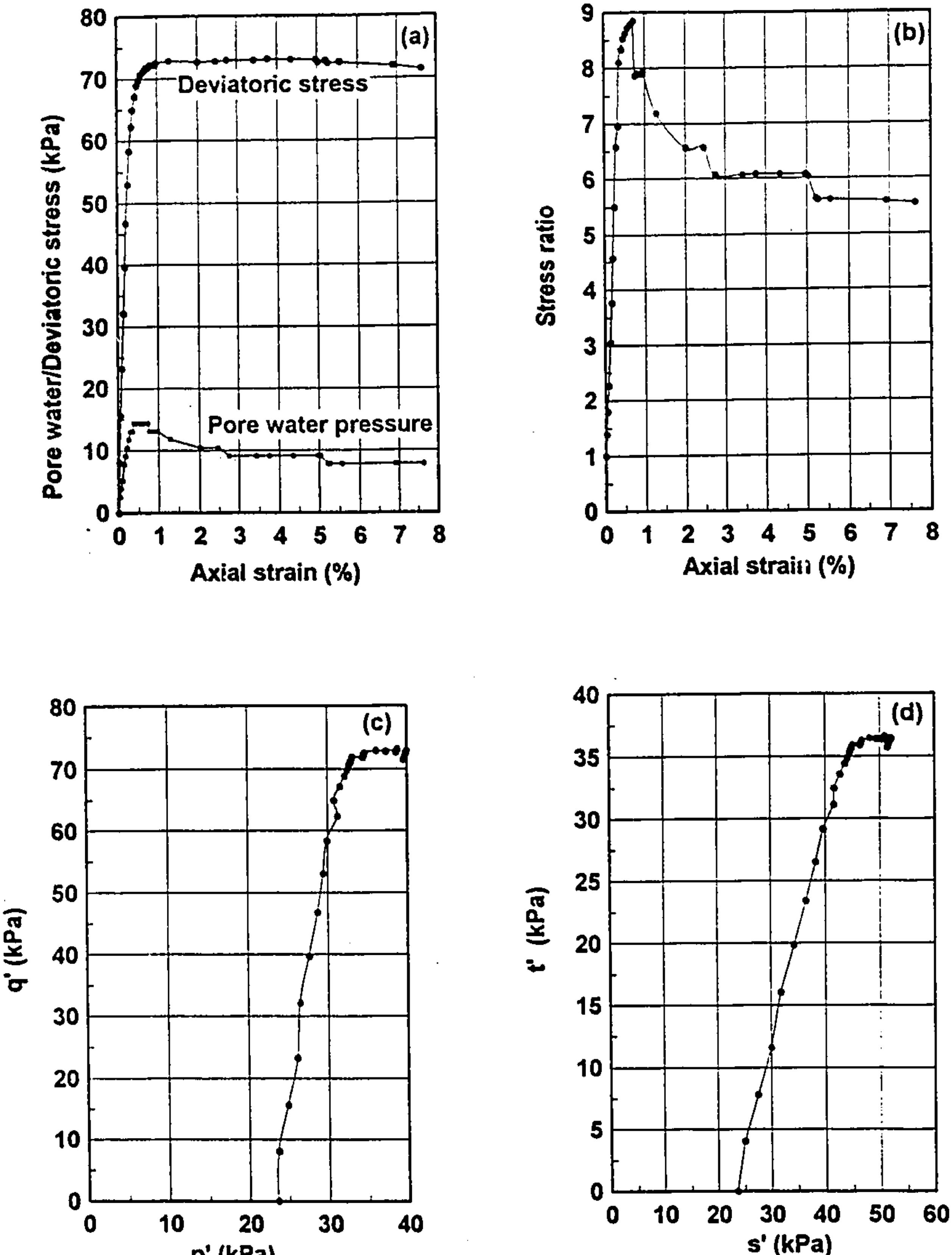

Fig. A.14. CIU triaxial compression test: Sample No. SB180T1.

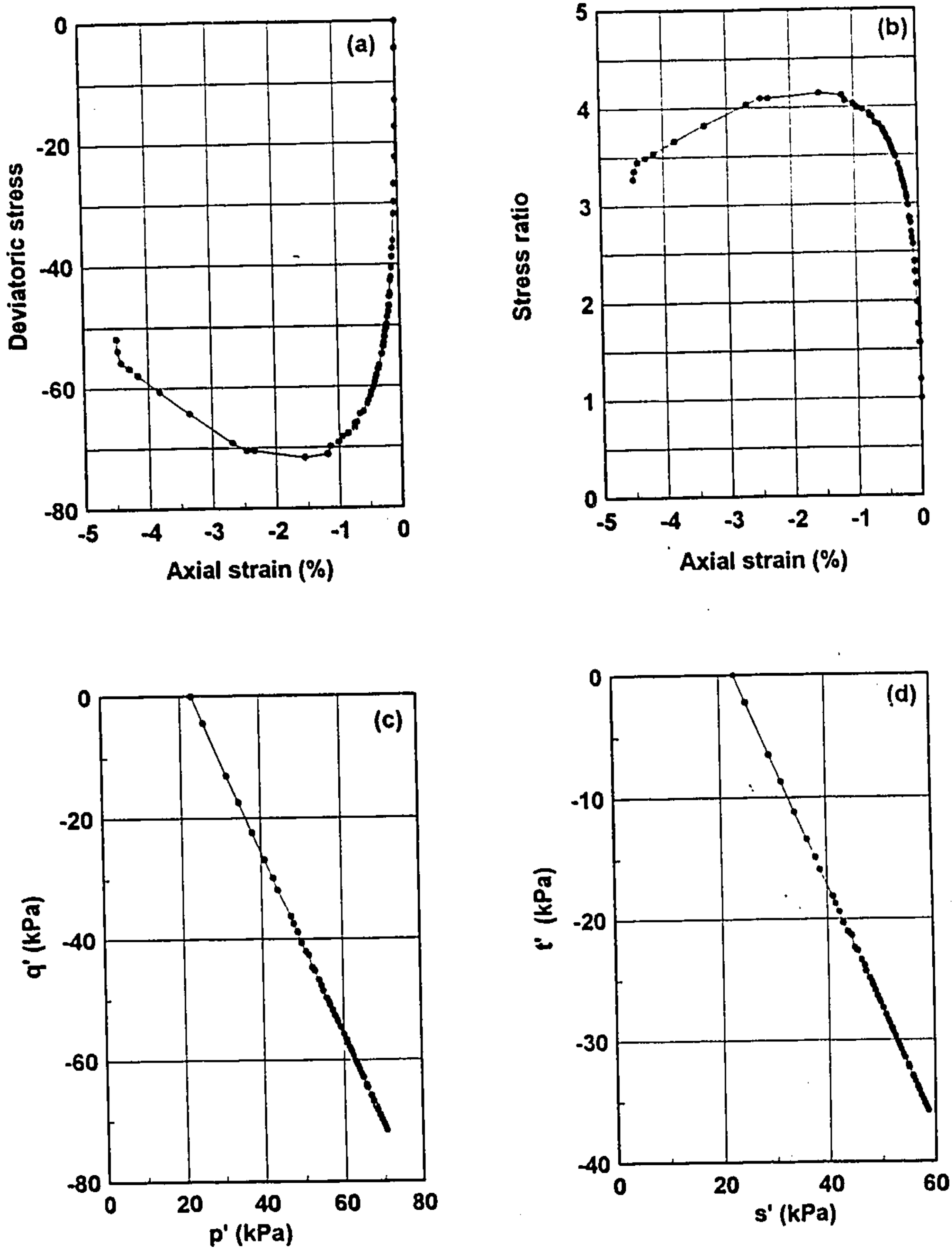

Fig. A.15. CID triaxial extension test: Sample No. SB180T2.

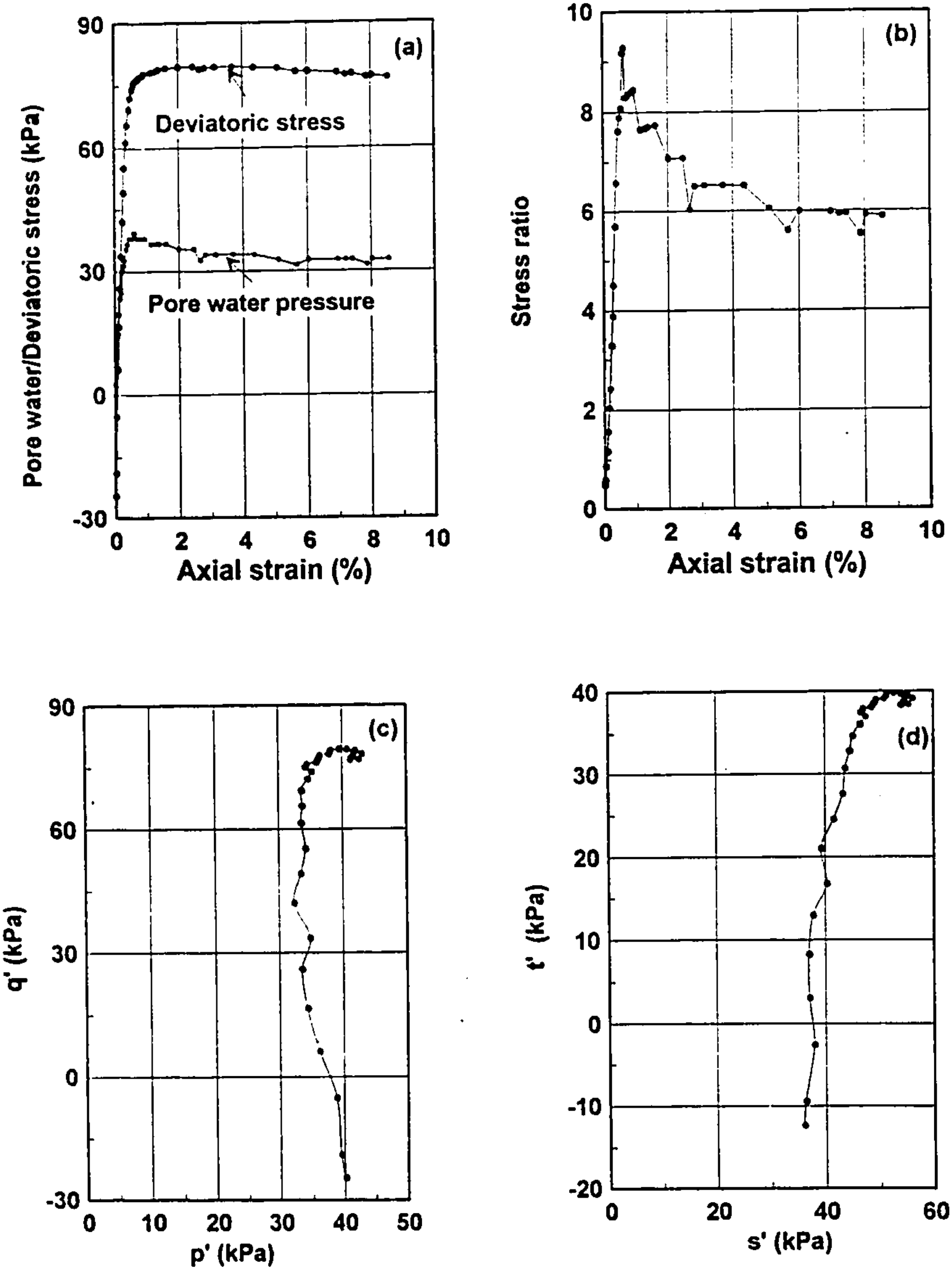

Fig. A.16. CK_0U triaxial compression test: Sample No. SB180T3.

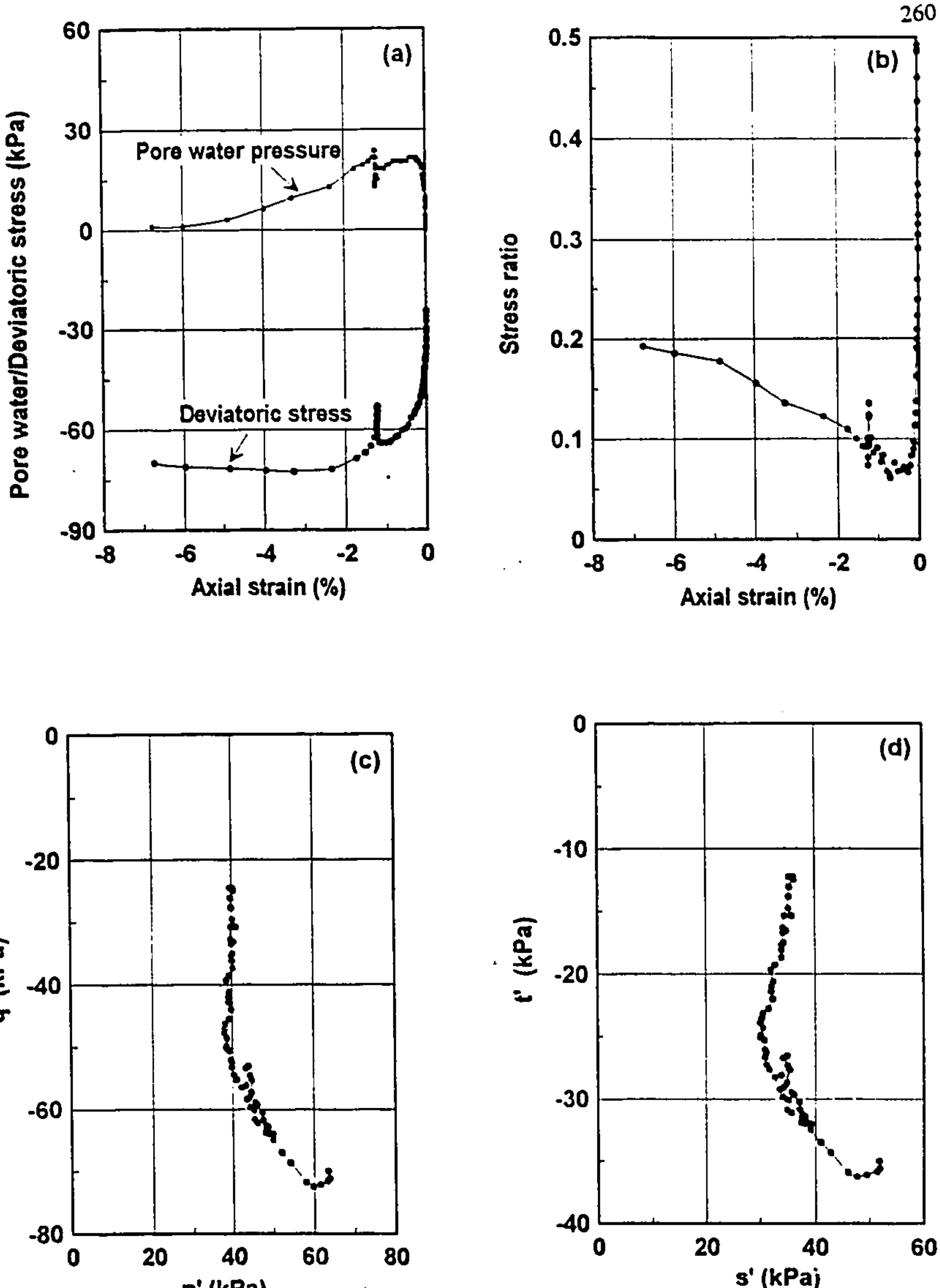

Fig. A.17. CK_0U triaxial extension test: Sample No. SB180T4.

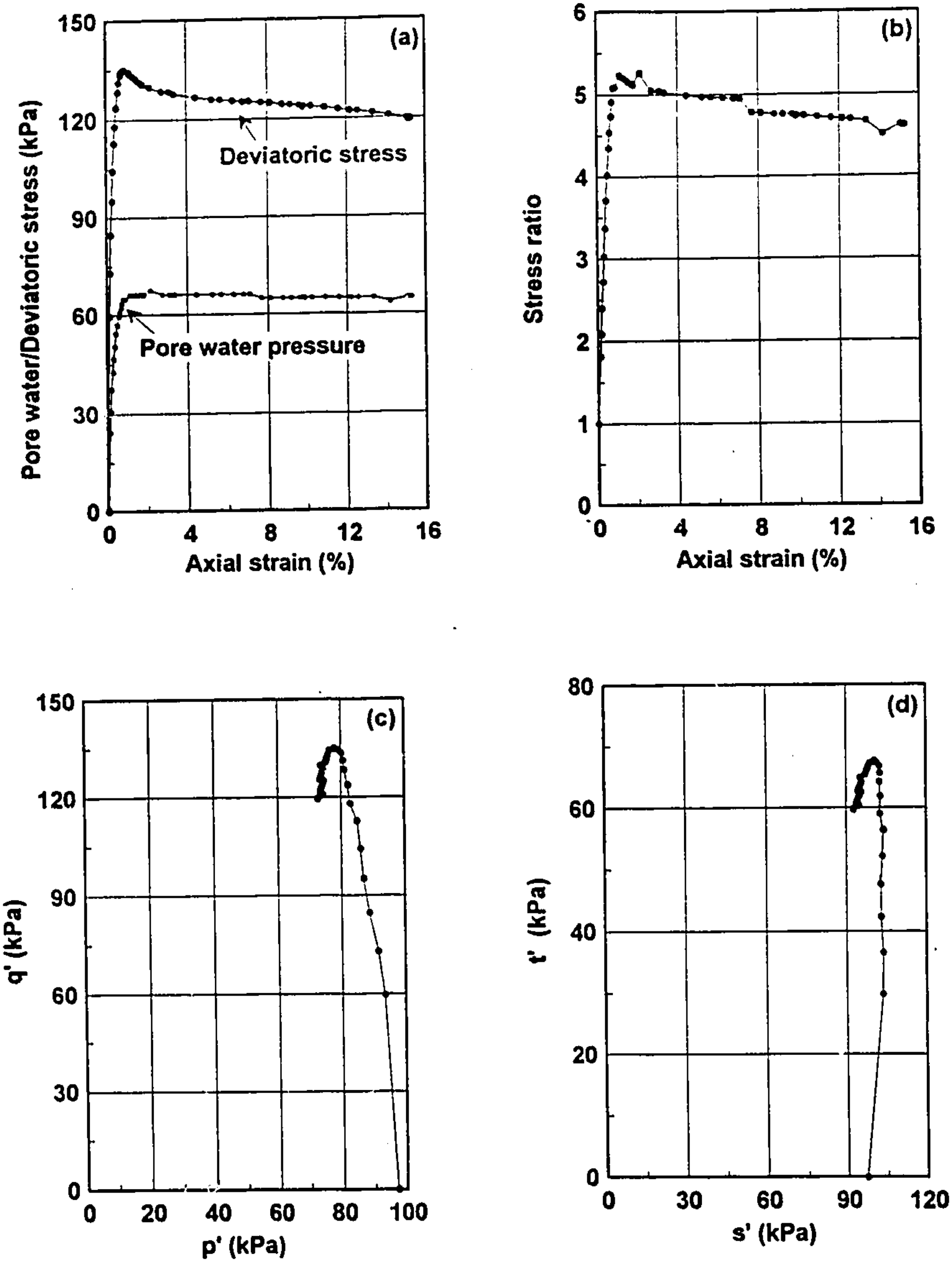

Fig. A.18. CIU triaxial compression test: Sample No. SB210T1.

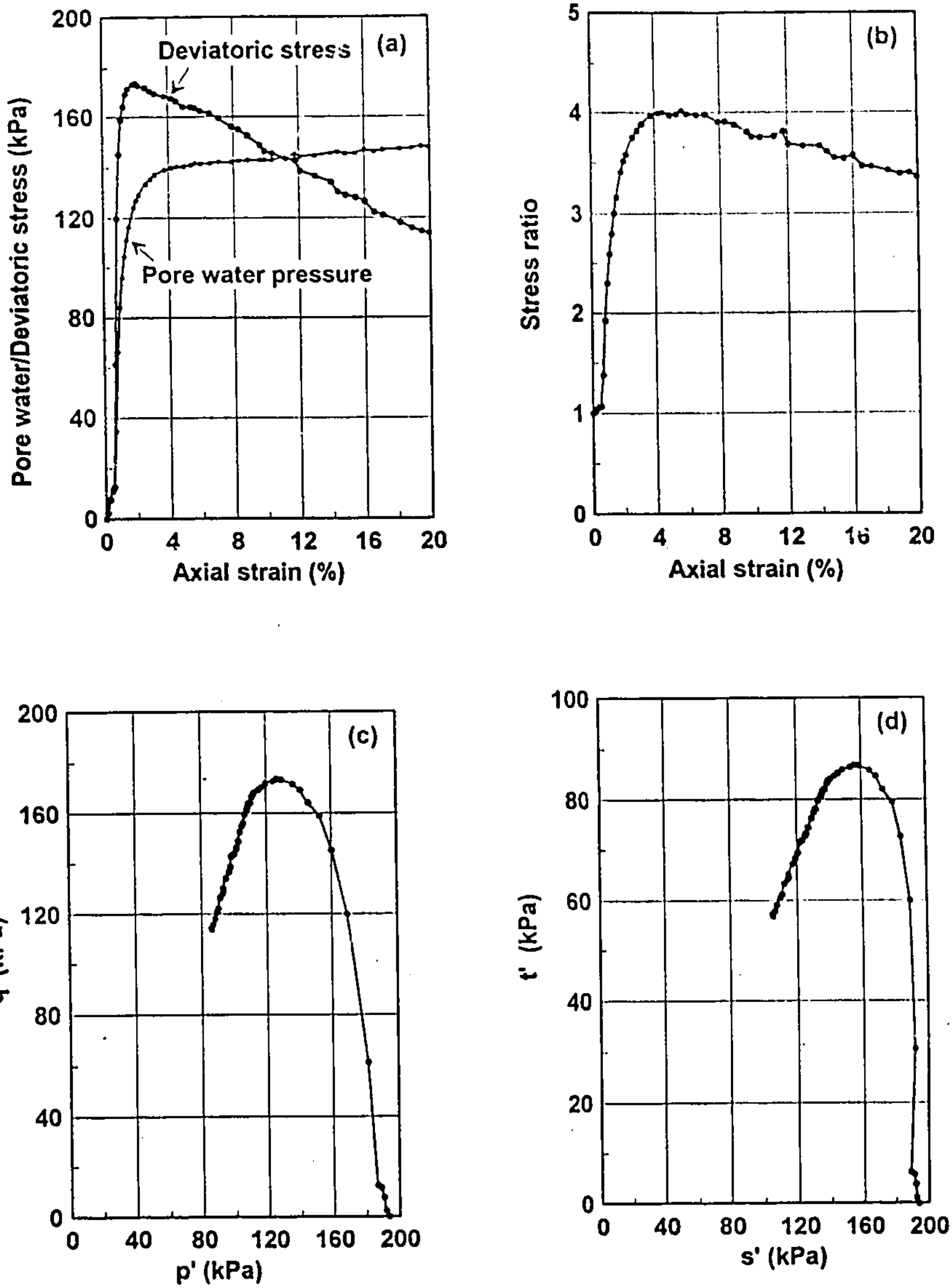

Fig. A.19. CIU triaxial compression test: Sample No. SB210T2.

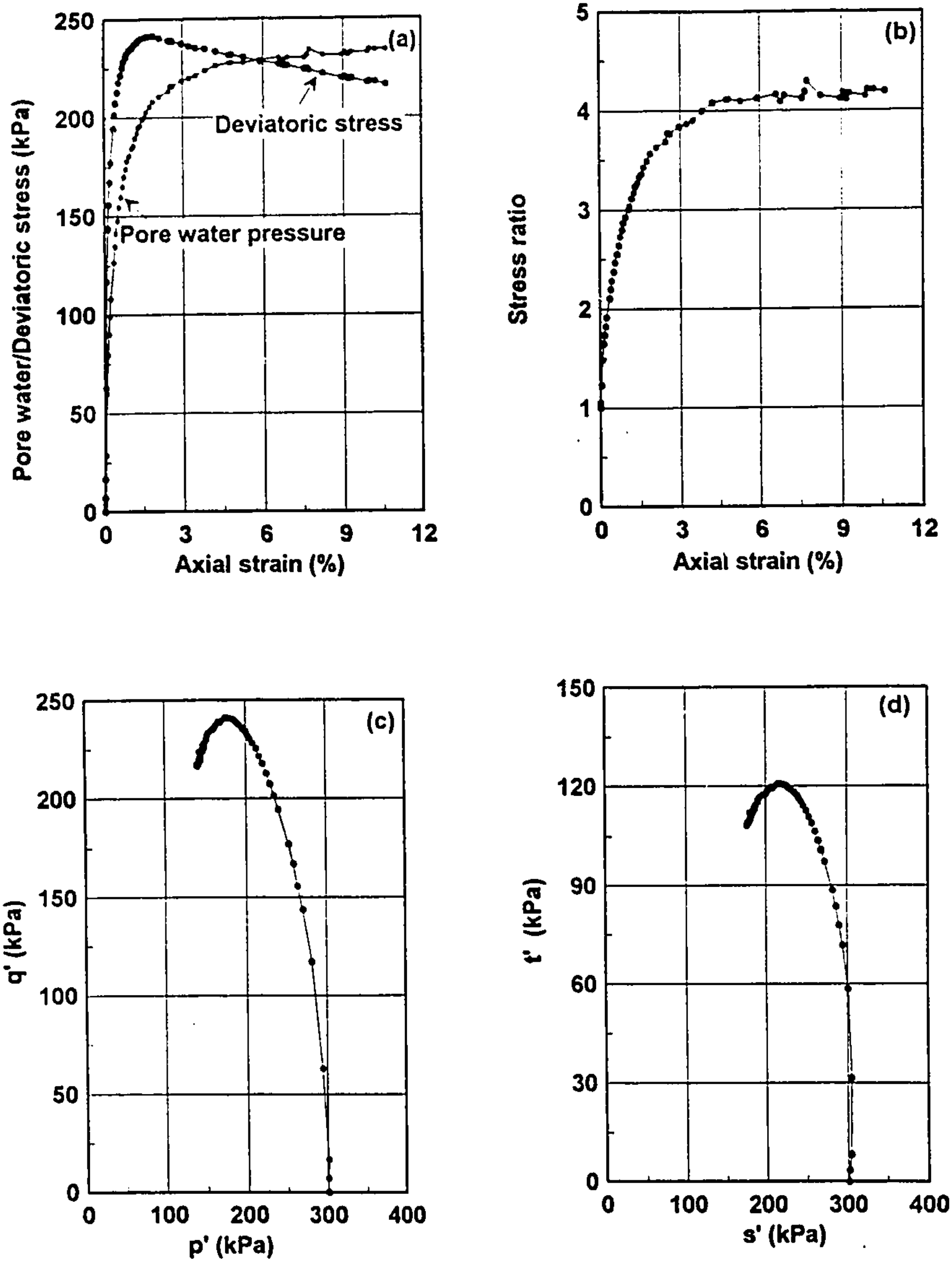

Fig. A.20. CIU triaxial compression test: Sample No. SB210T3.

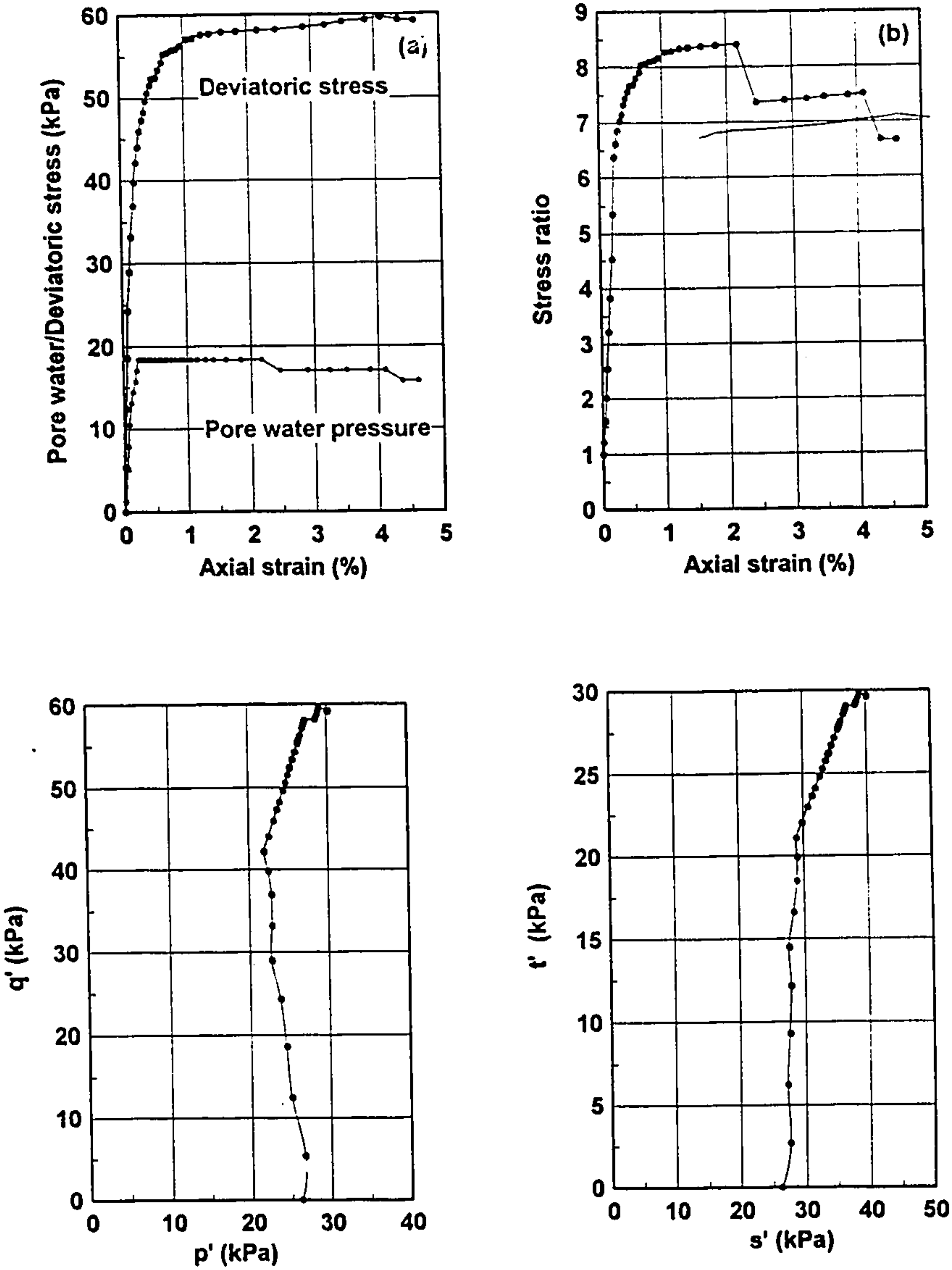

Fig. A.21. CIU triaxial compression test: Sample No. SB220T1.

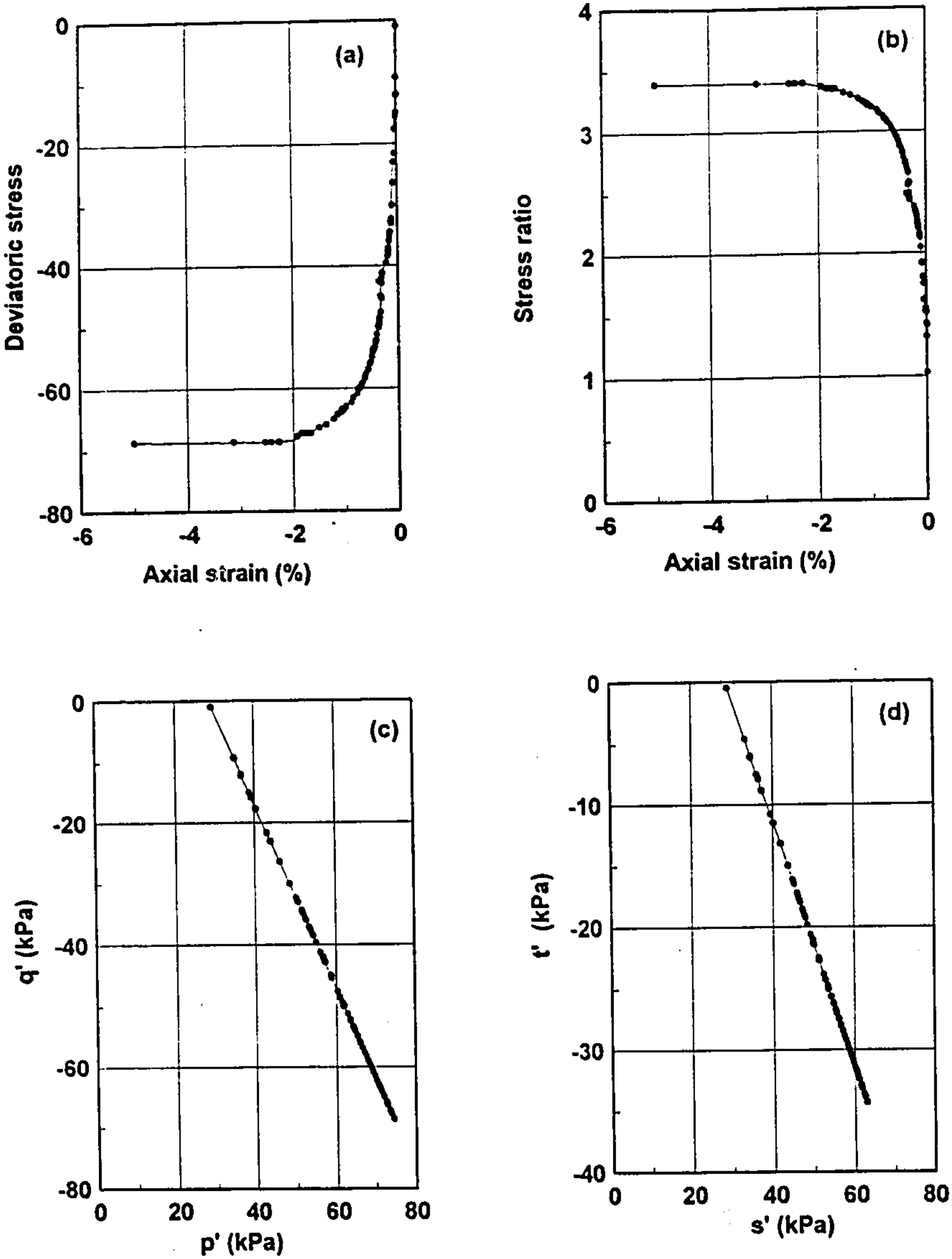

Fig. A.22. CID triaxial extension test: Sample No. SB250T1.

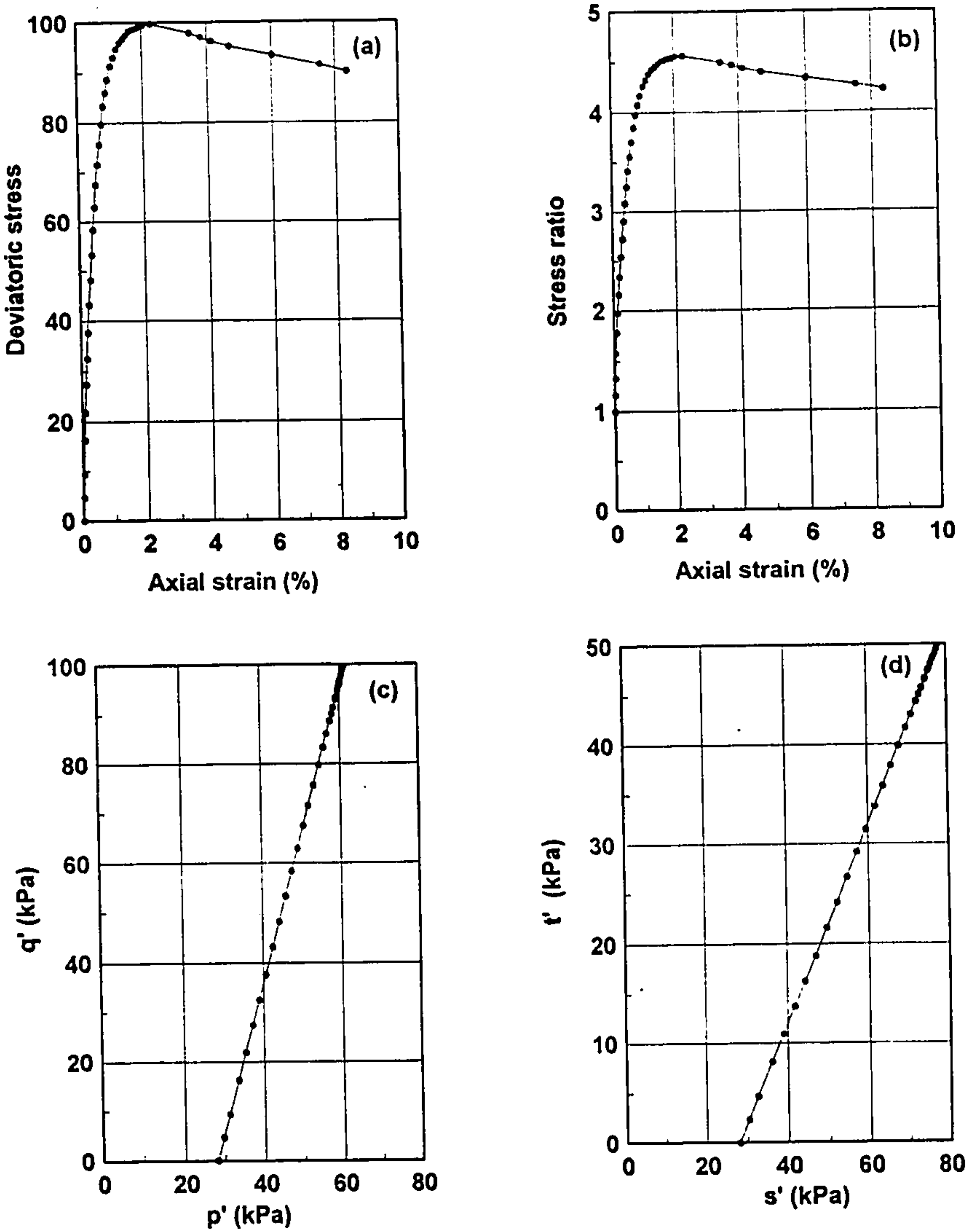

Fig. A.23. CID triaxial compression test: Sample No. SB250T2.

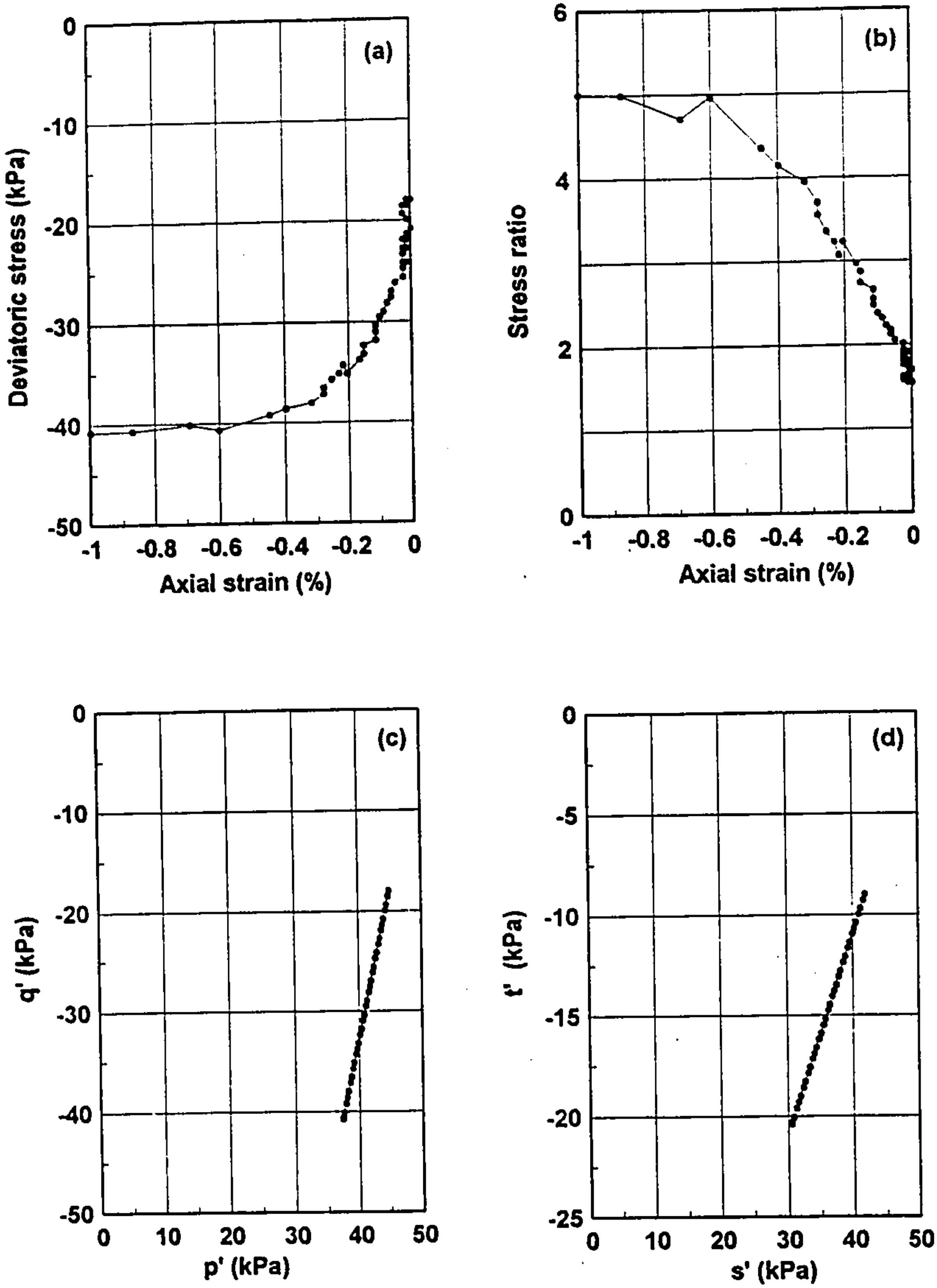

Fig. A.24. CK_0D triaxial extension test: Sample No. SB250T3.

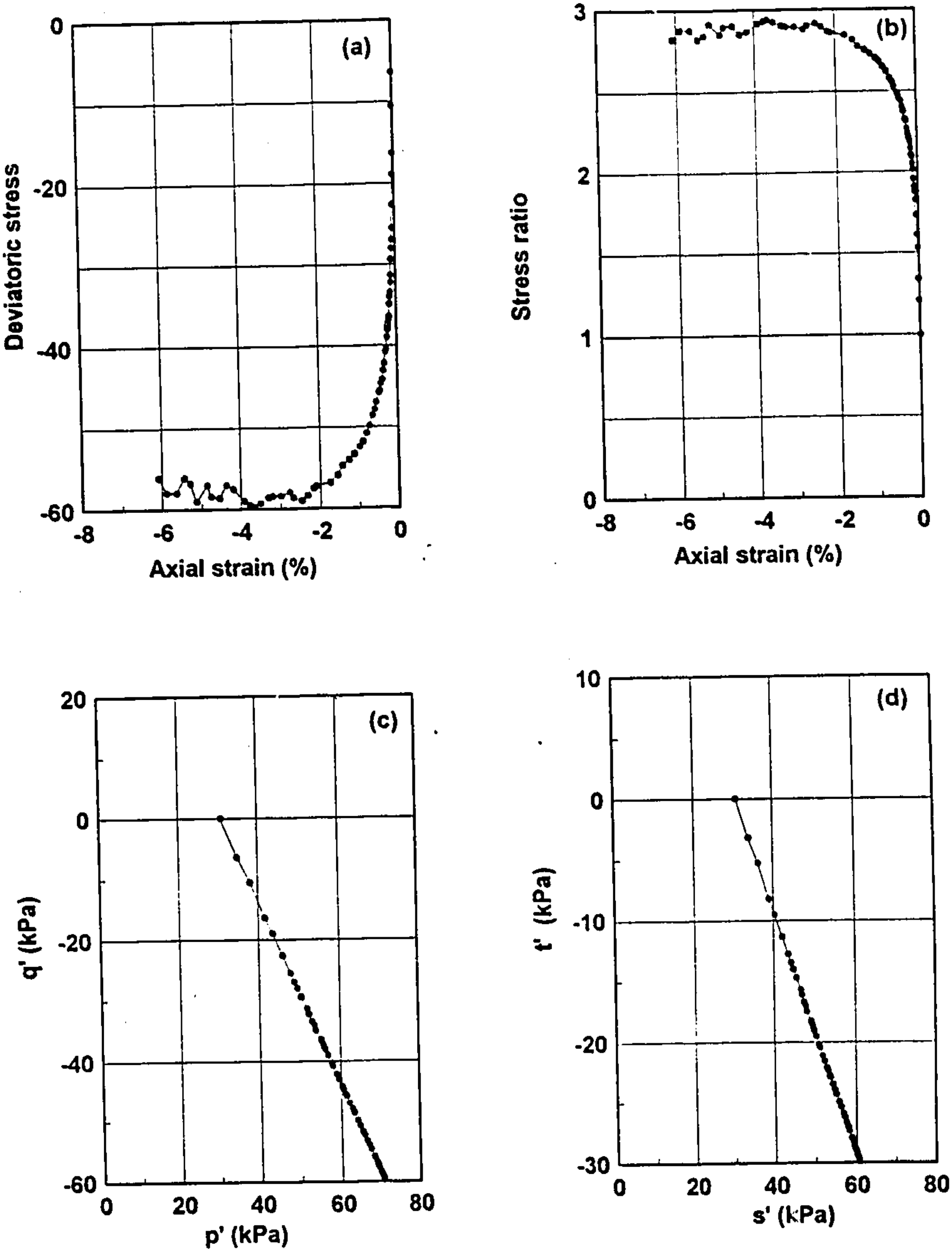

Fig. A.25. CID triaxial extension test: Sample No. SB260T1.

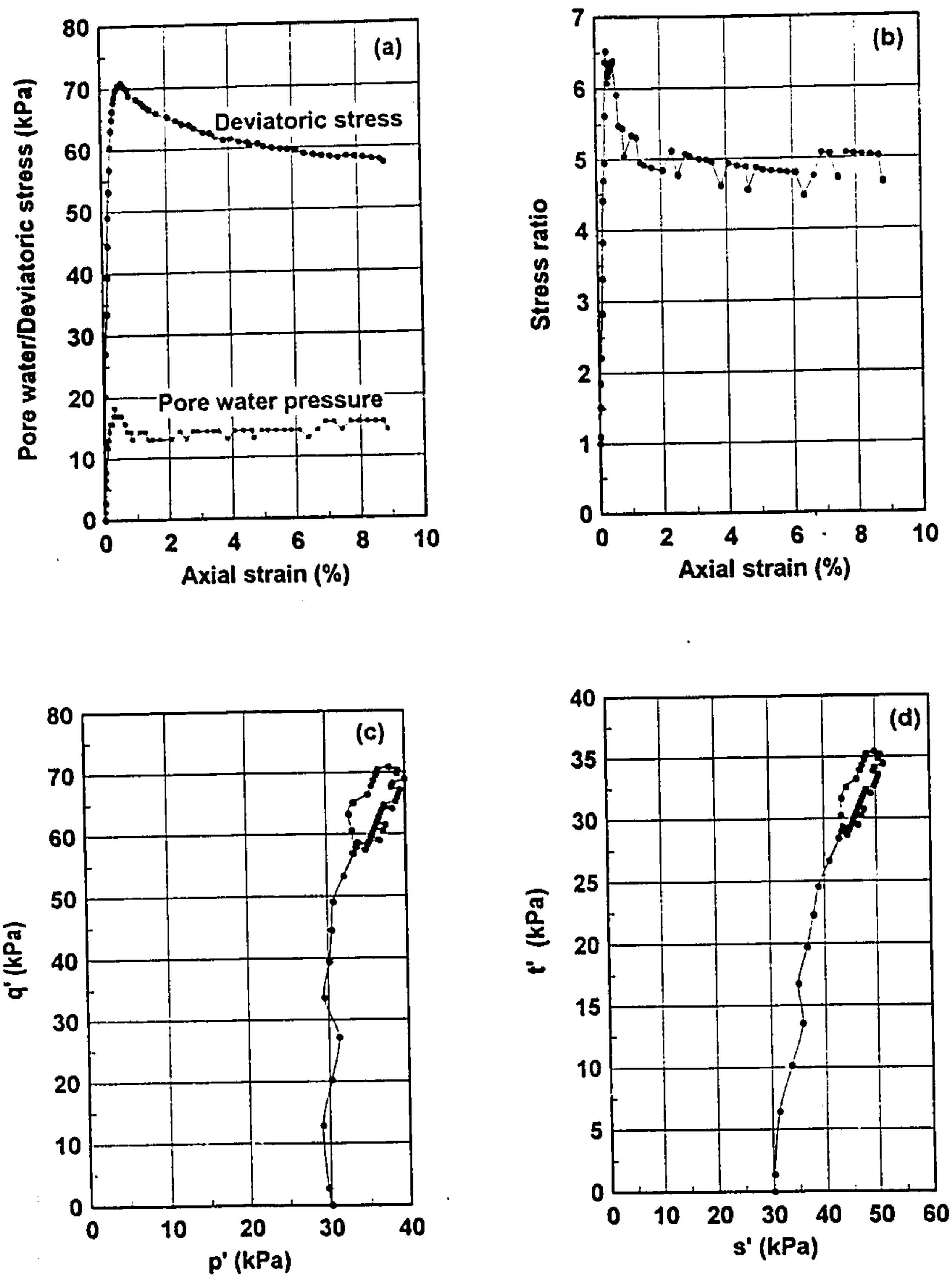

Fig. A.26. CIU triaxial compression test: Sample No. SB260T2.

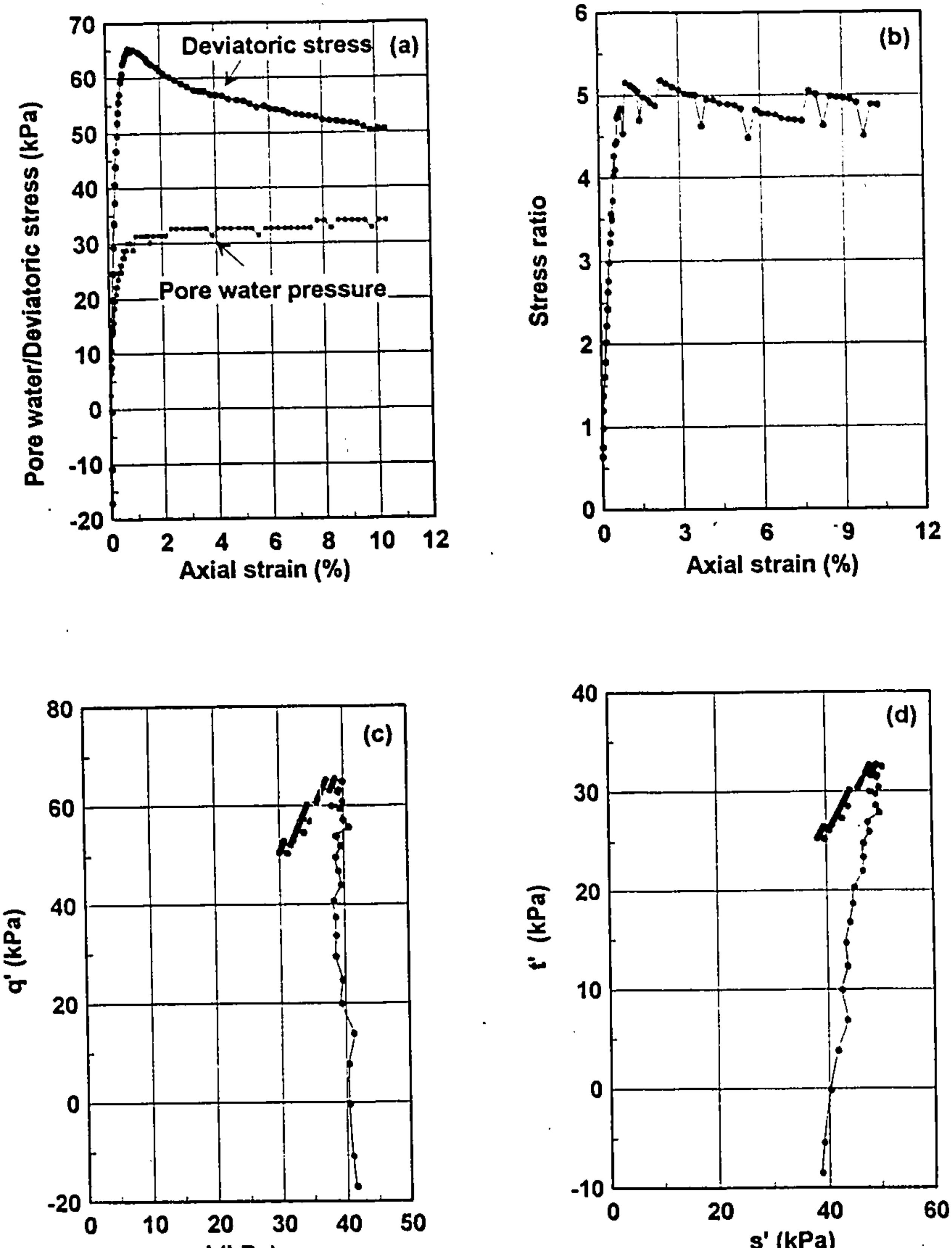

Fig. A.27. CK_0U triaxial compression test: Sample No. SB260T3.

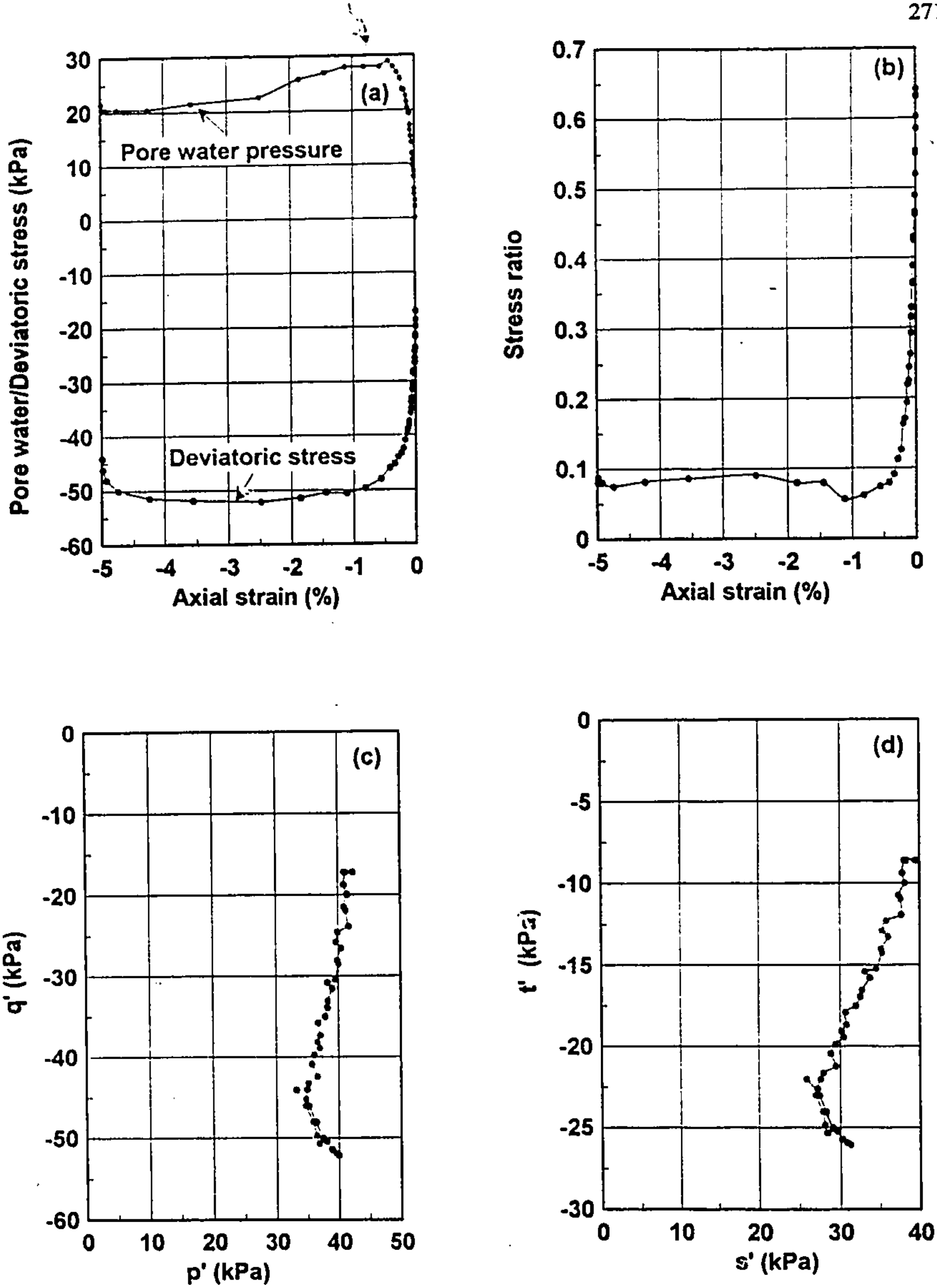

Fig. A.28. CK_0U triaxial extension test: Sample No. SB260T4.

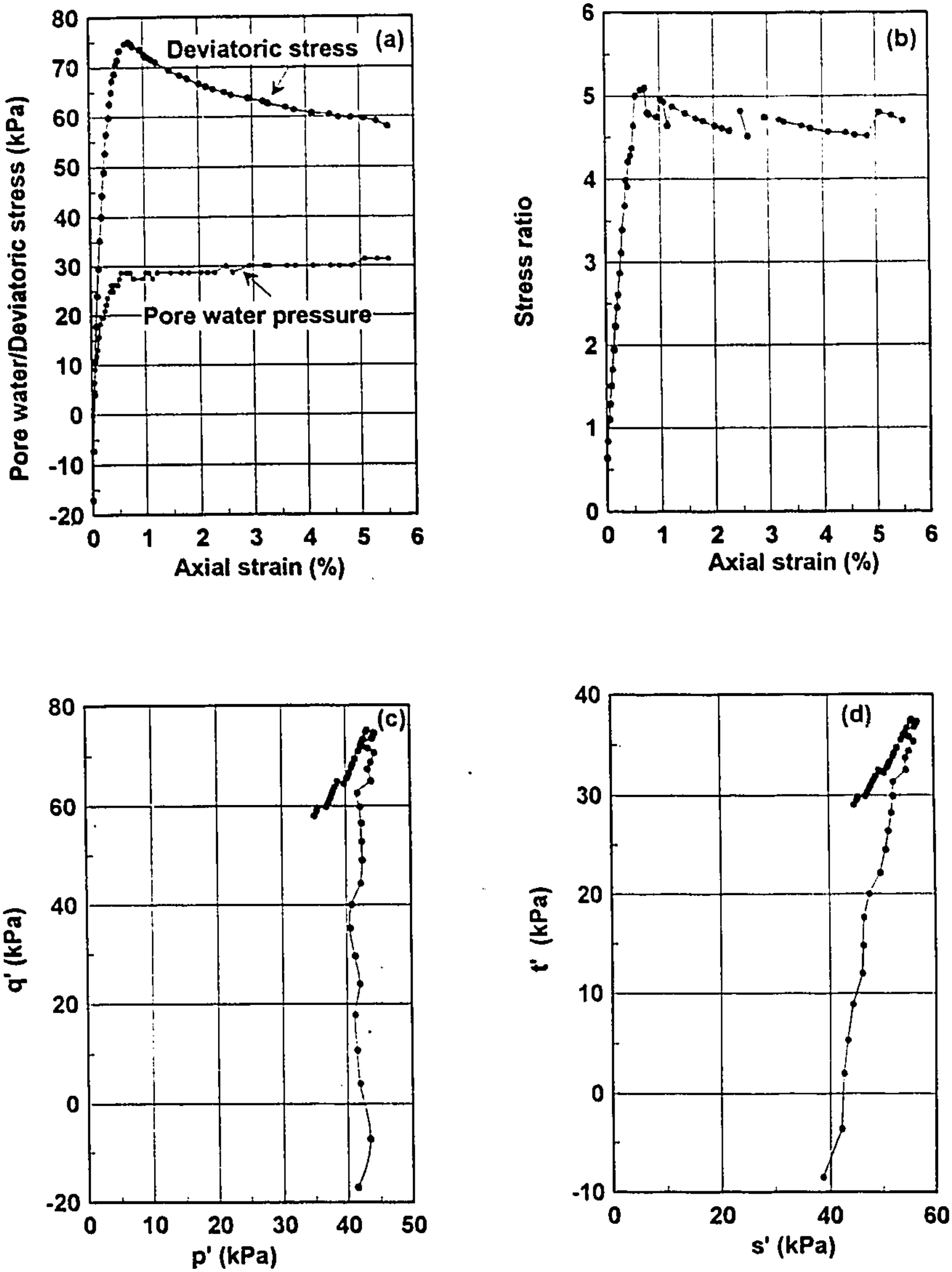

Fig. A.29. CK_0U triaxial compression test: Sample No. SB260T5.

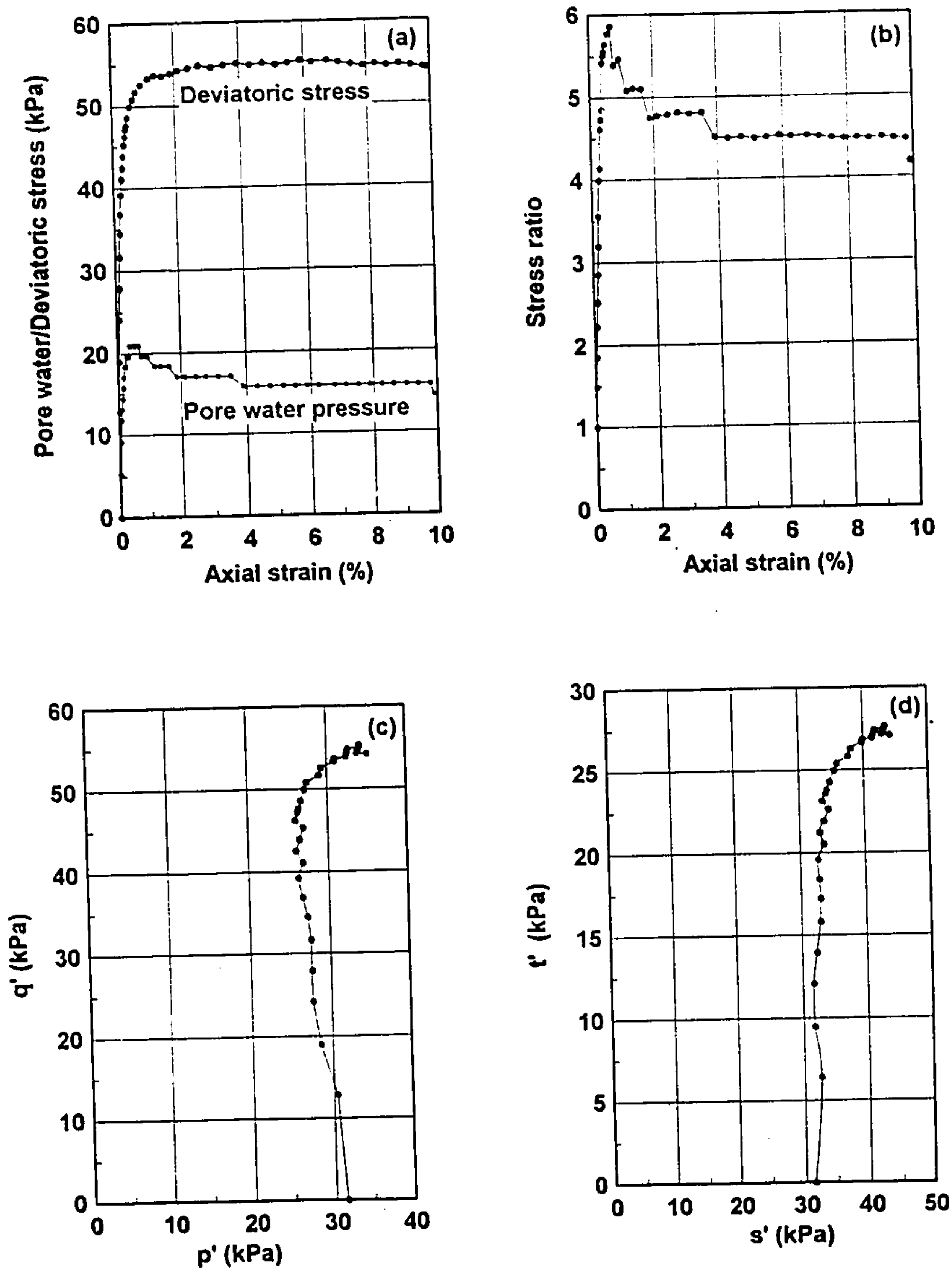

Fig. A.30. CIU triaxial compression test: Sample No. SB273T1 (horizontal sample).

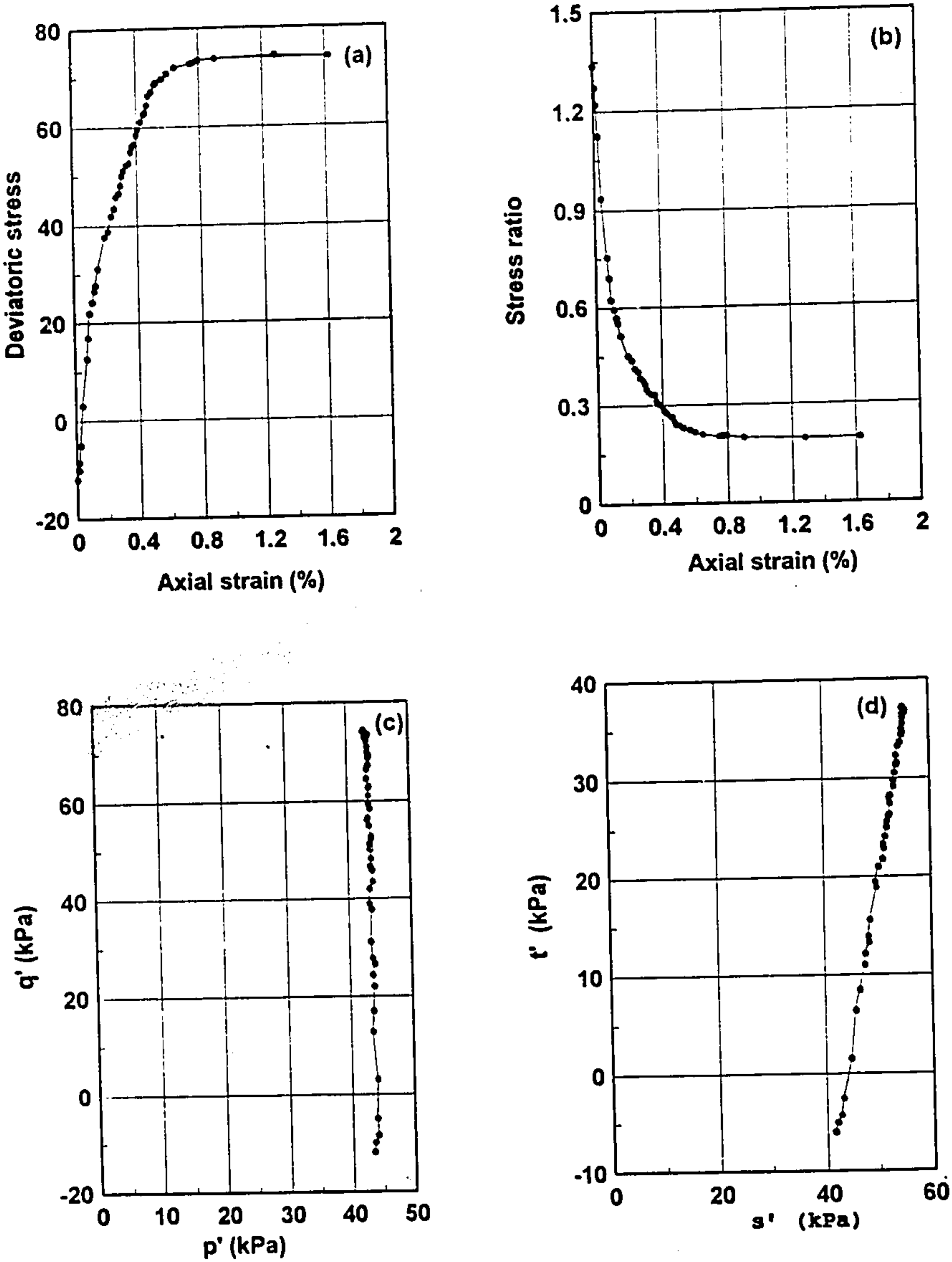

Fig. A.31. CK_0D triaxial compression test: Sample No. SB308T1.

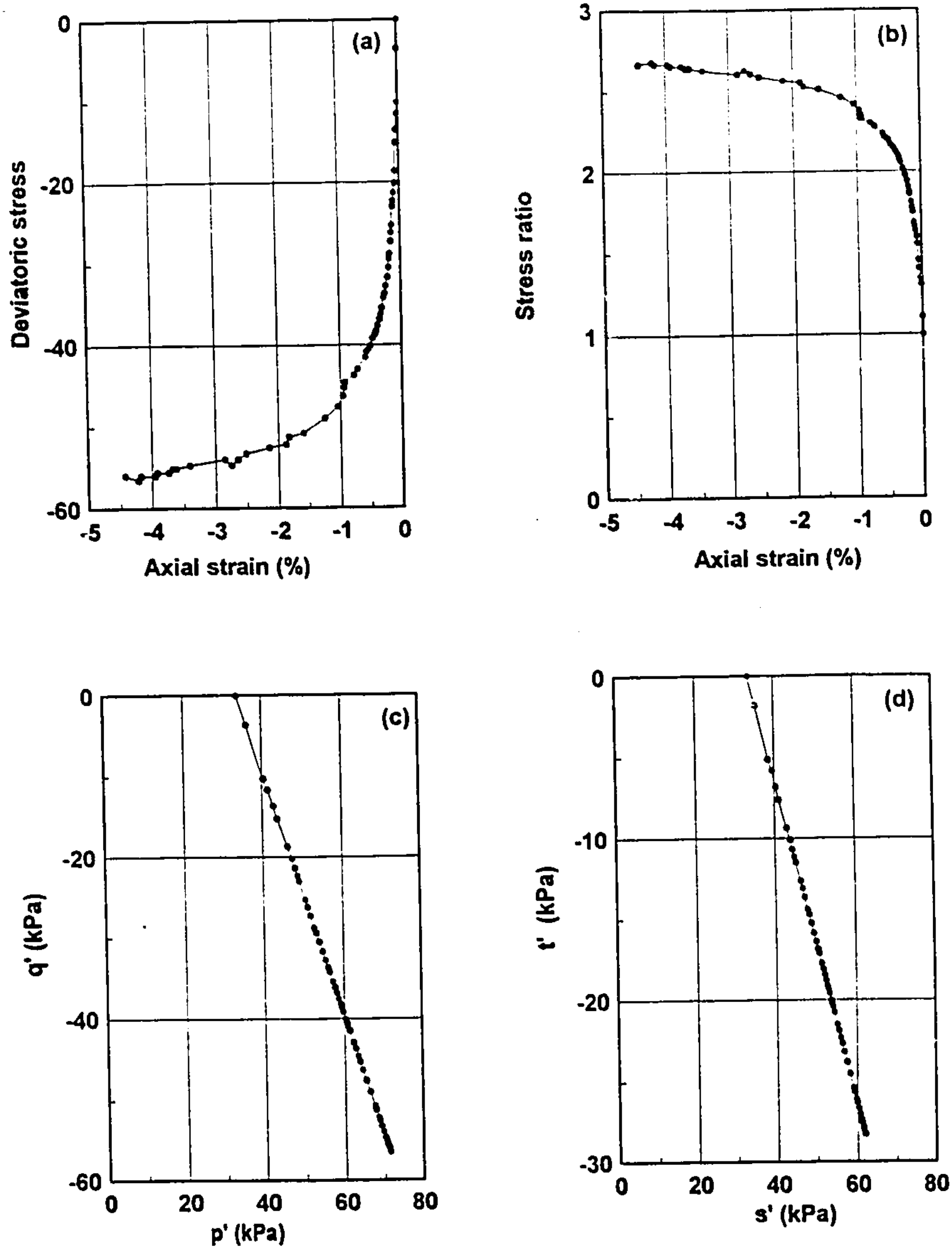

Fig. A.32. CID triaxial extension test: Sample No. SB308T2.

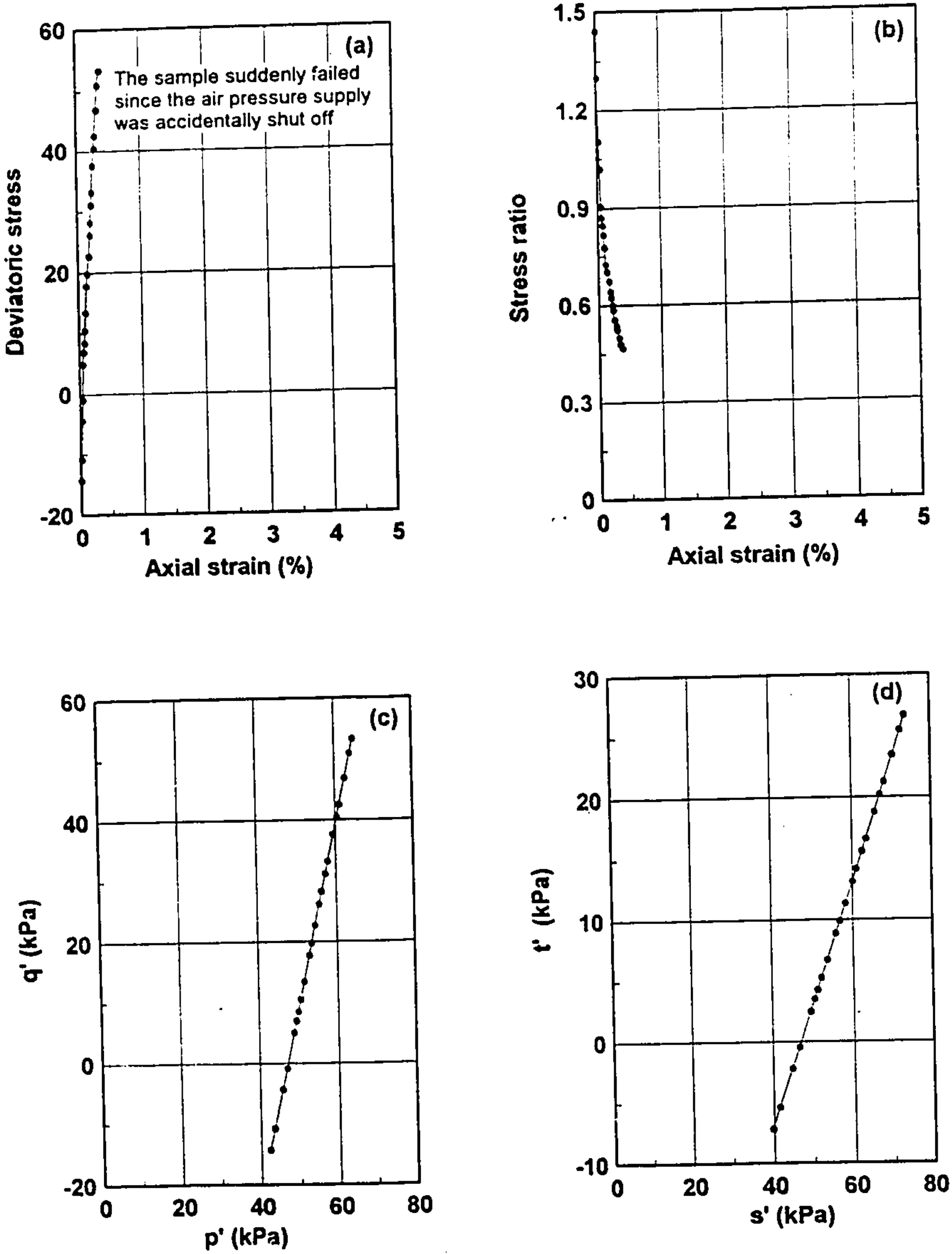

Fig. A.33. CK_0D triaxial compression test: Sample No. SB308T3.

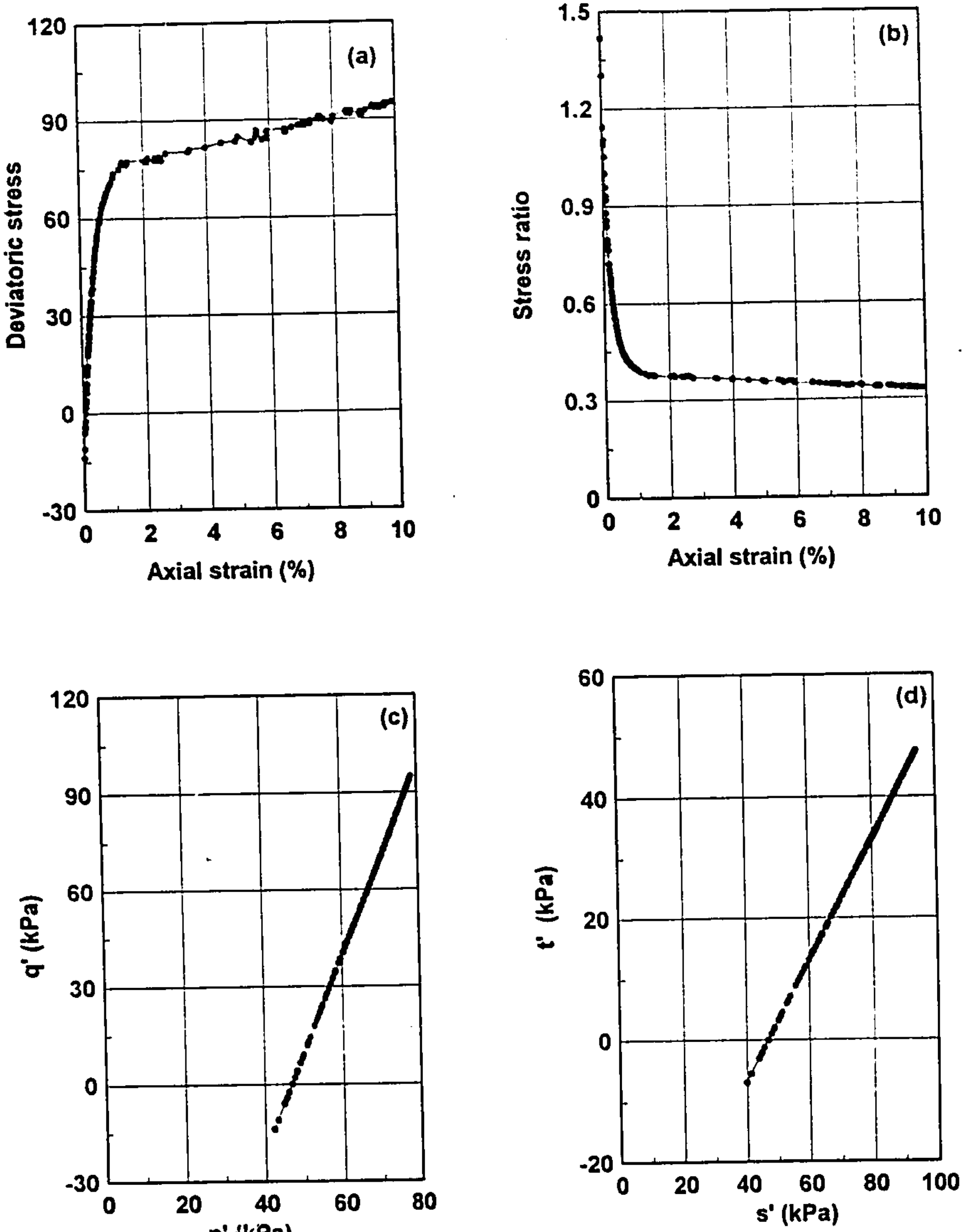

Fig. A.34. CK_0D triaxial compression test: Sample No. SB308T5.

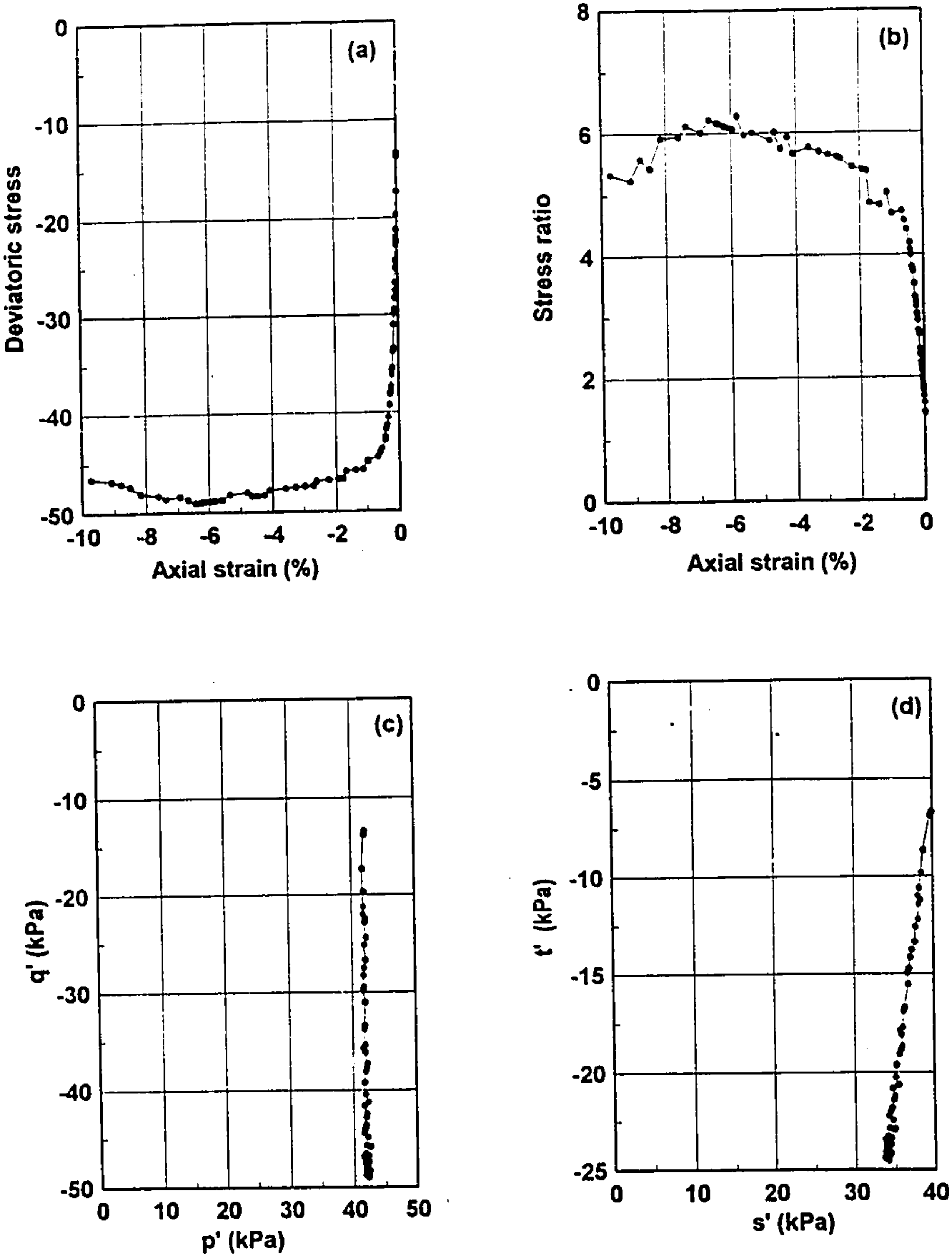

Fig. A.35. CK_0D triaxial extension test (constant p'): Sample No. SB308T6.

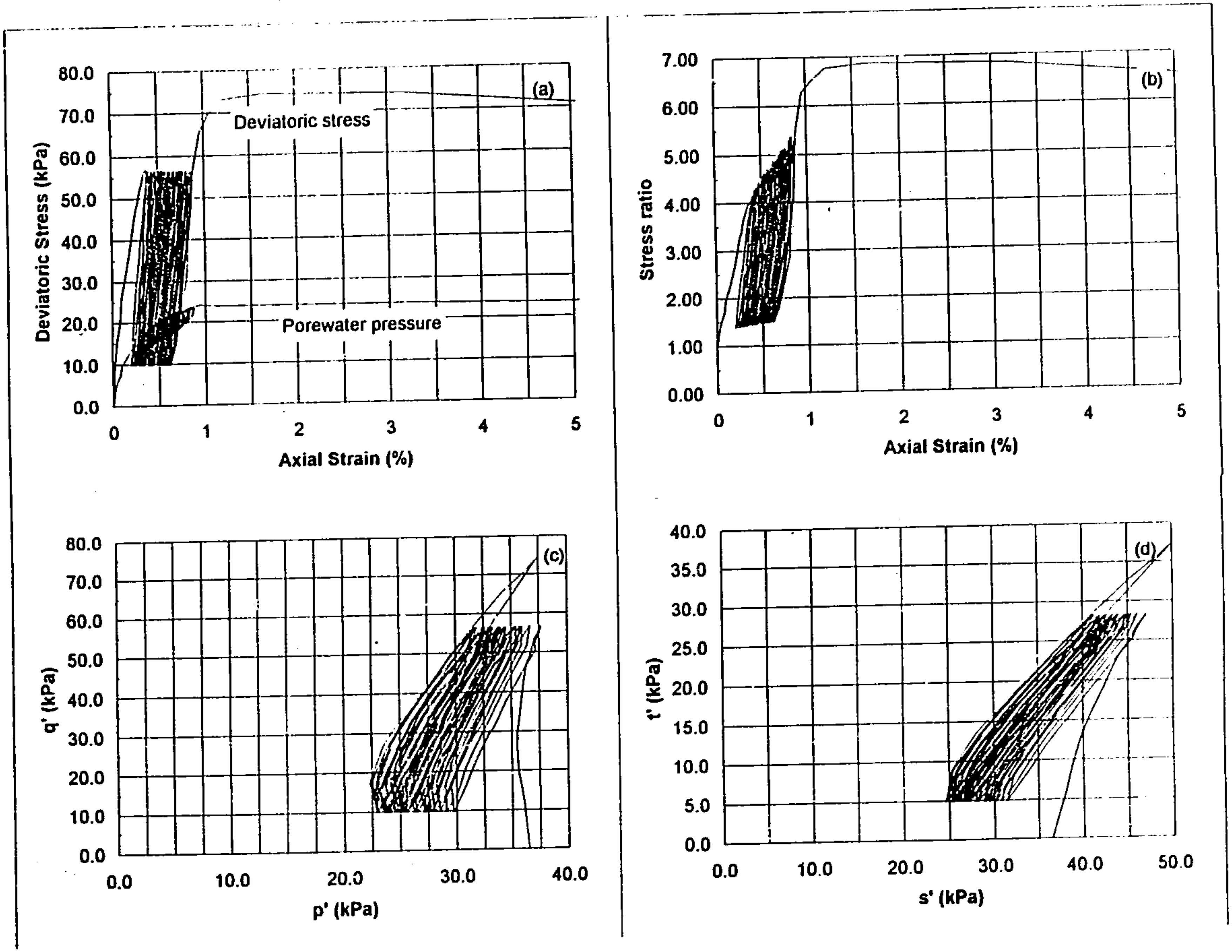

Fig. A 36. CIU cyclic triaxial compression test: Sample No. BS333TC1.

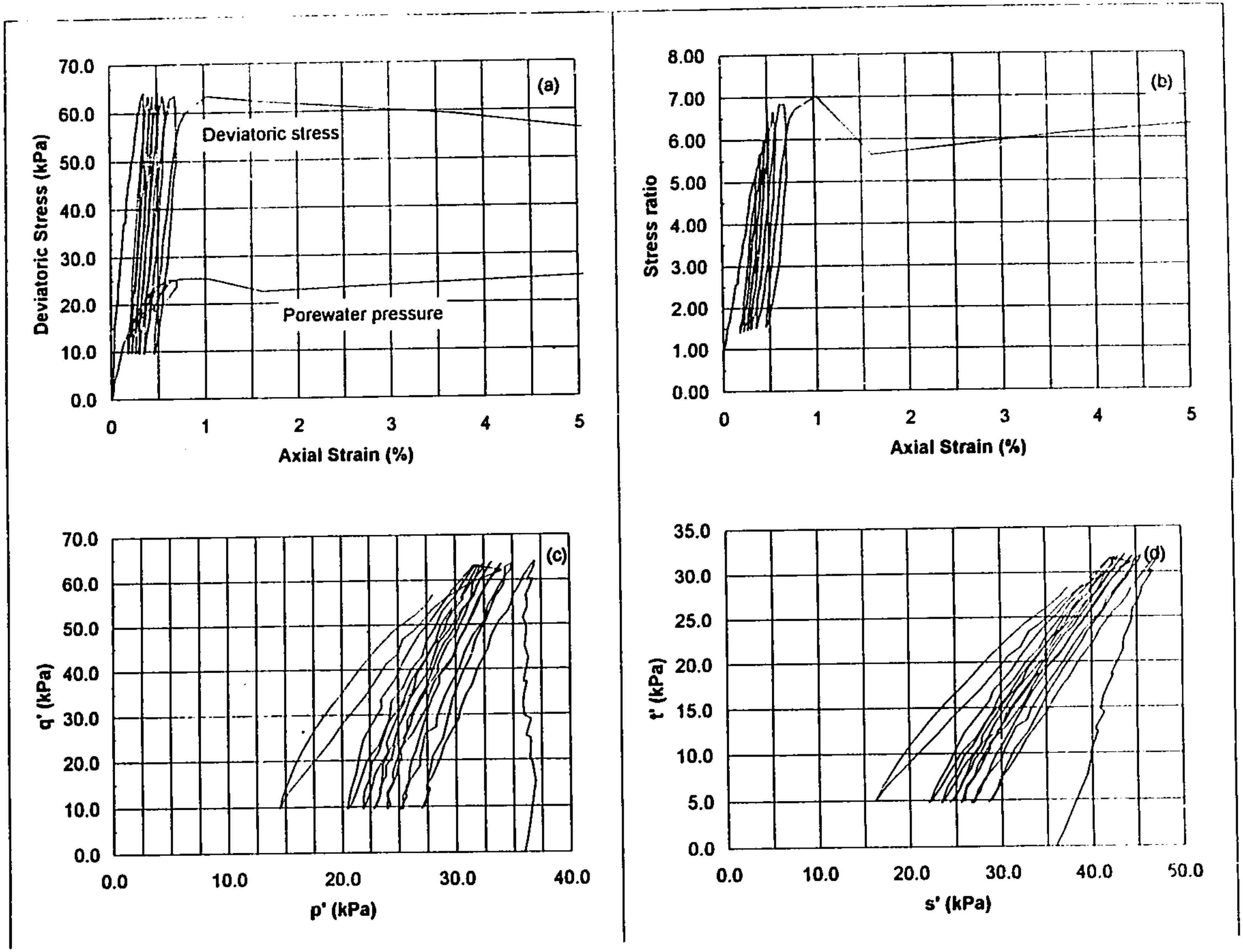

Fig. A.37. CIU cyclic triaxial compression test: Sample No. BS333TC2.

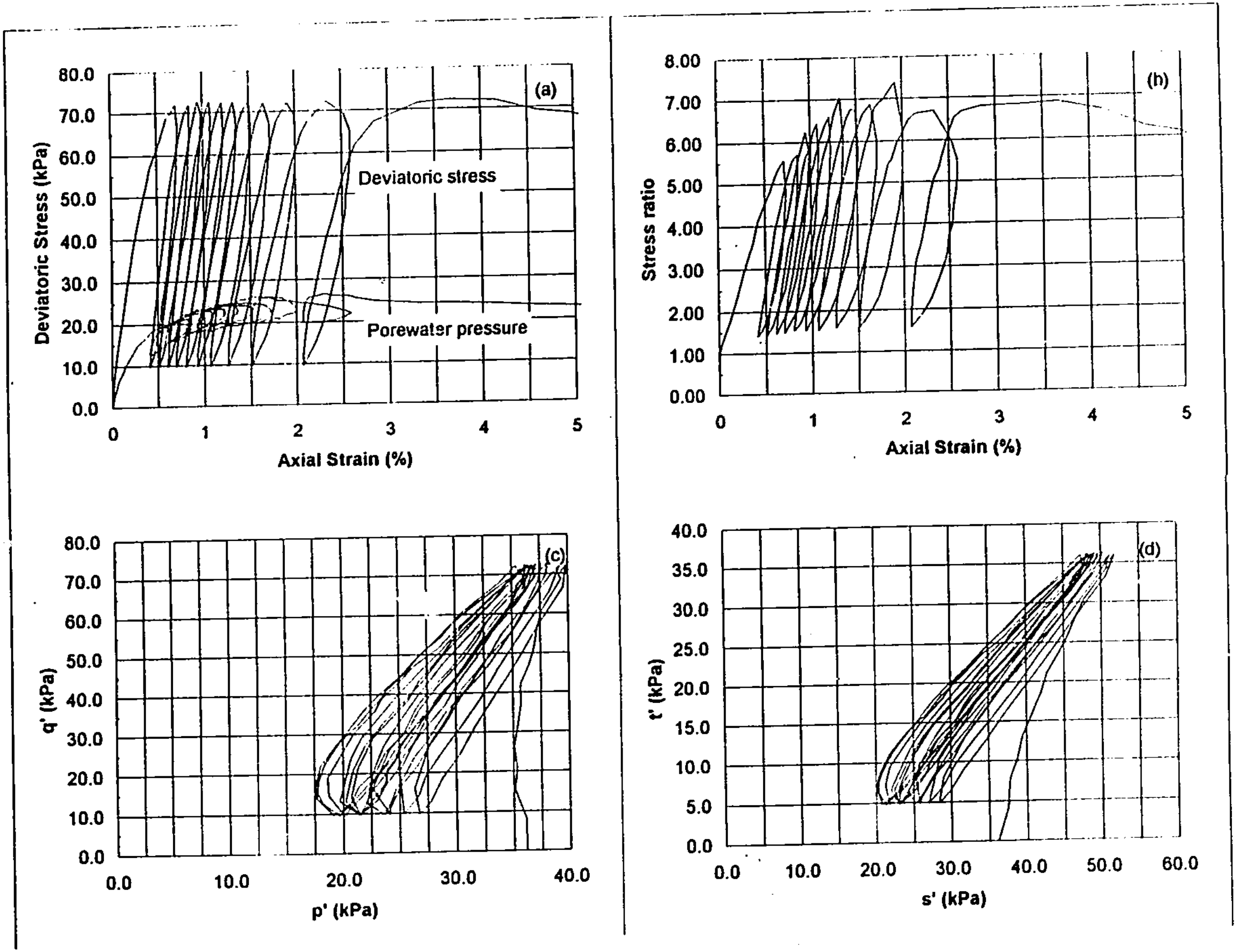

Fig. A.38. CIU cyclic triaxial compression test: Sample No. BS333TC3.

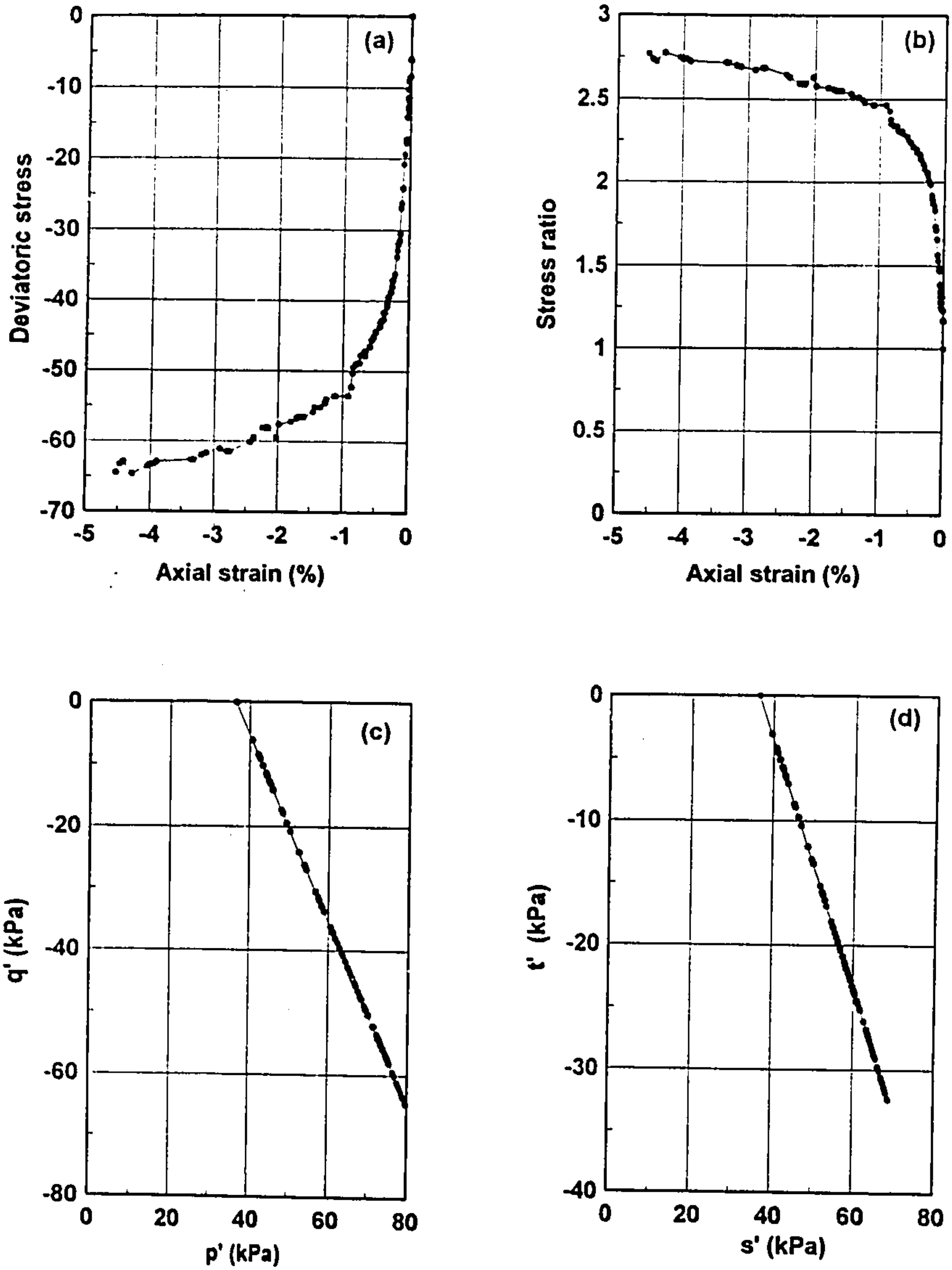

Fig. A.39. CID triaxial extension test: Sample No. BS333T1.

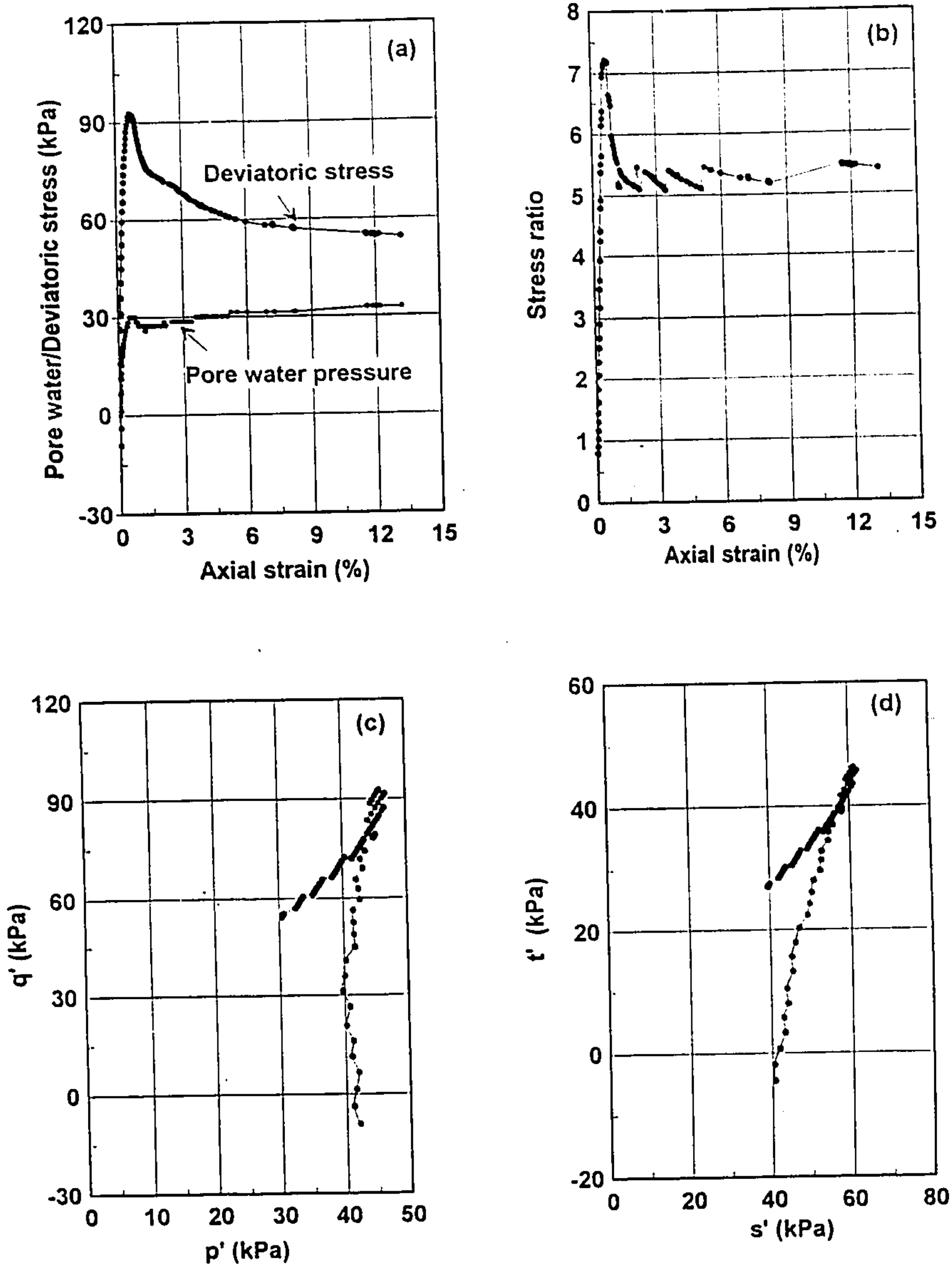

Fig. A.40. CK_0U triaxial compression test: Sample No. BS333T2.

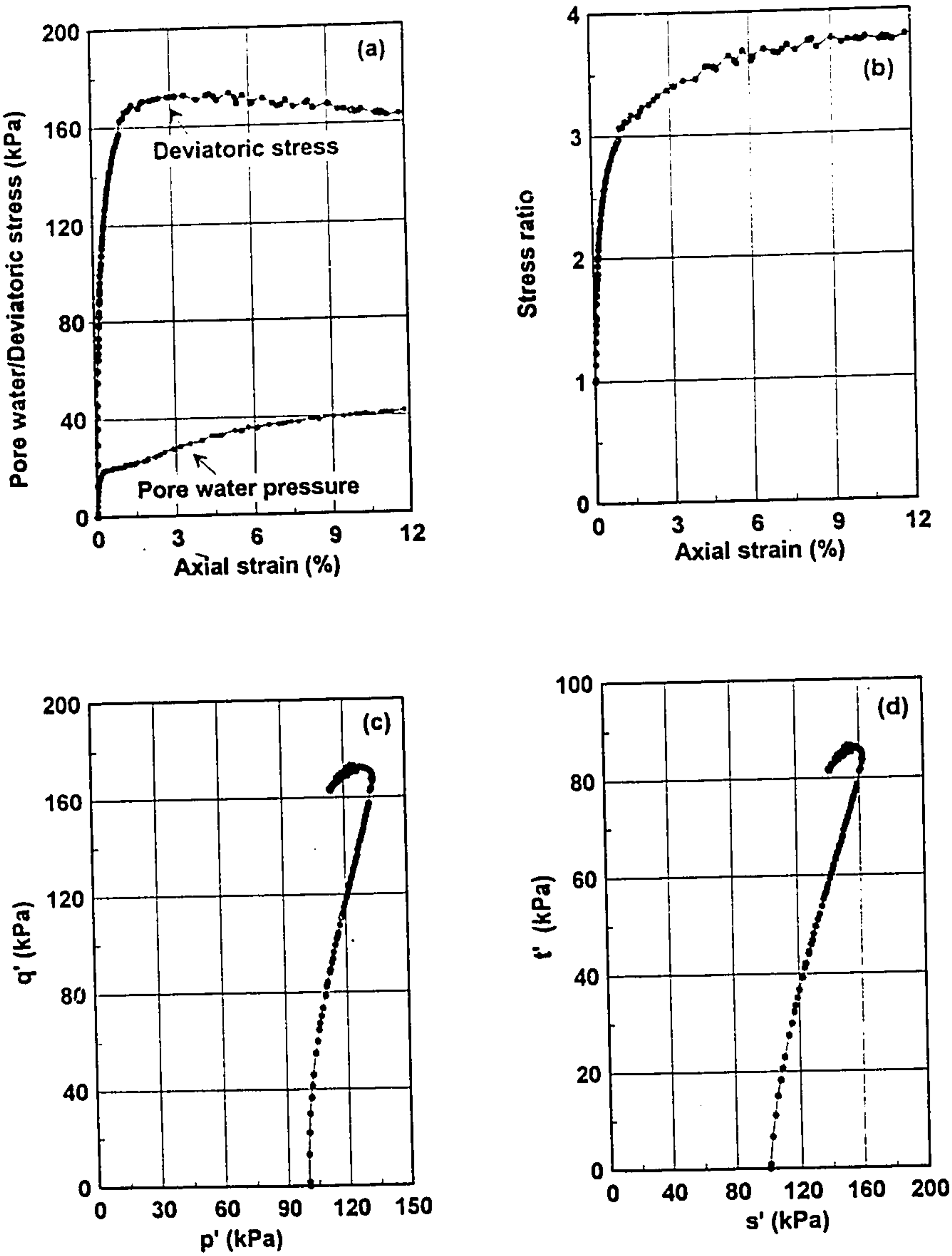

Fig. A.41. CIU triaxial compression test: Sample No. BS333T3.

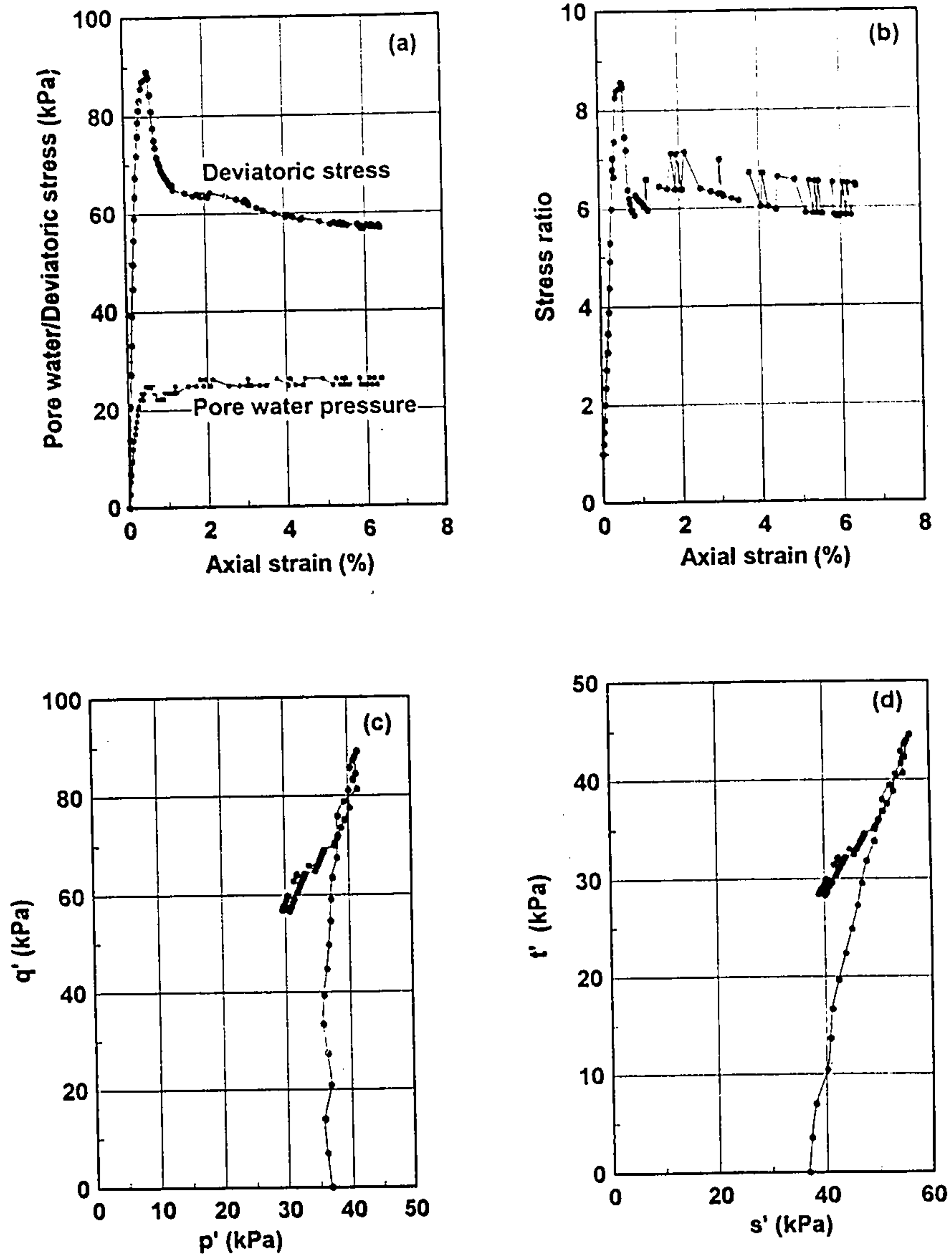

Fig. A.42. CIU triaxial compression test: Sample No. BS333T4.

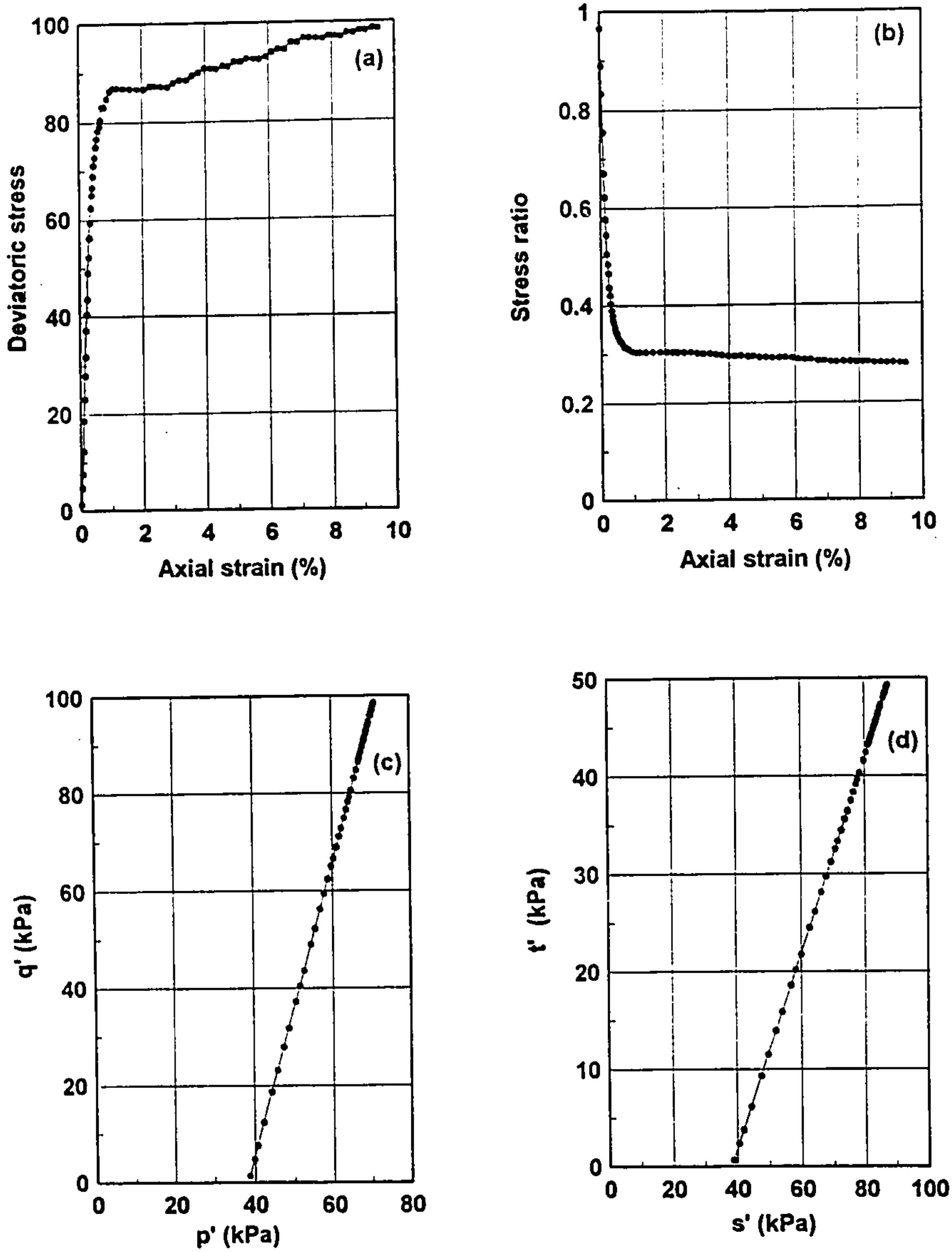

Fig. A.43. CID triaxial compression test: Sample No. BS333T5.

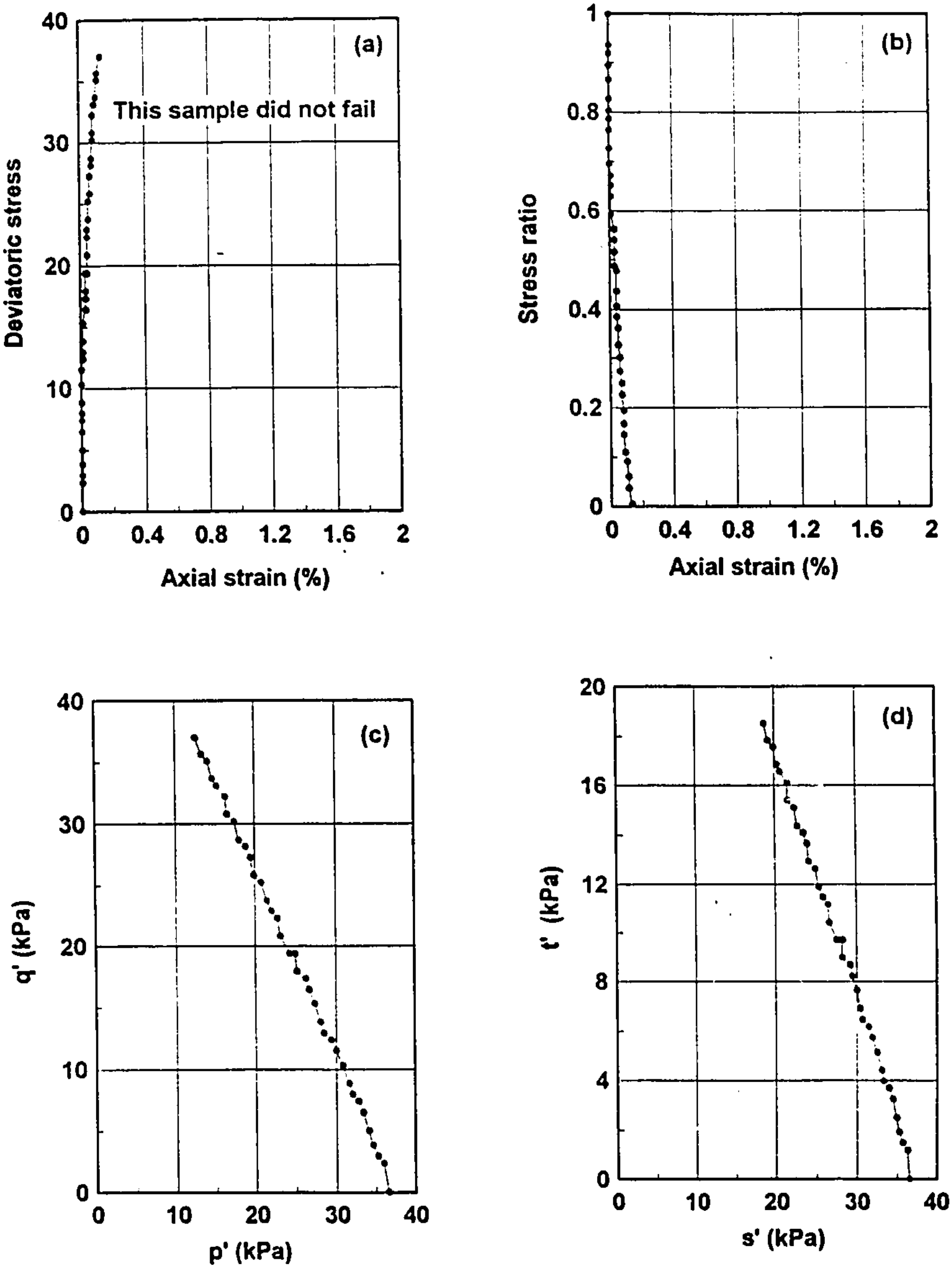

Fig. A.44. CID triaxial compression test: Sample No. BS333T6.

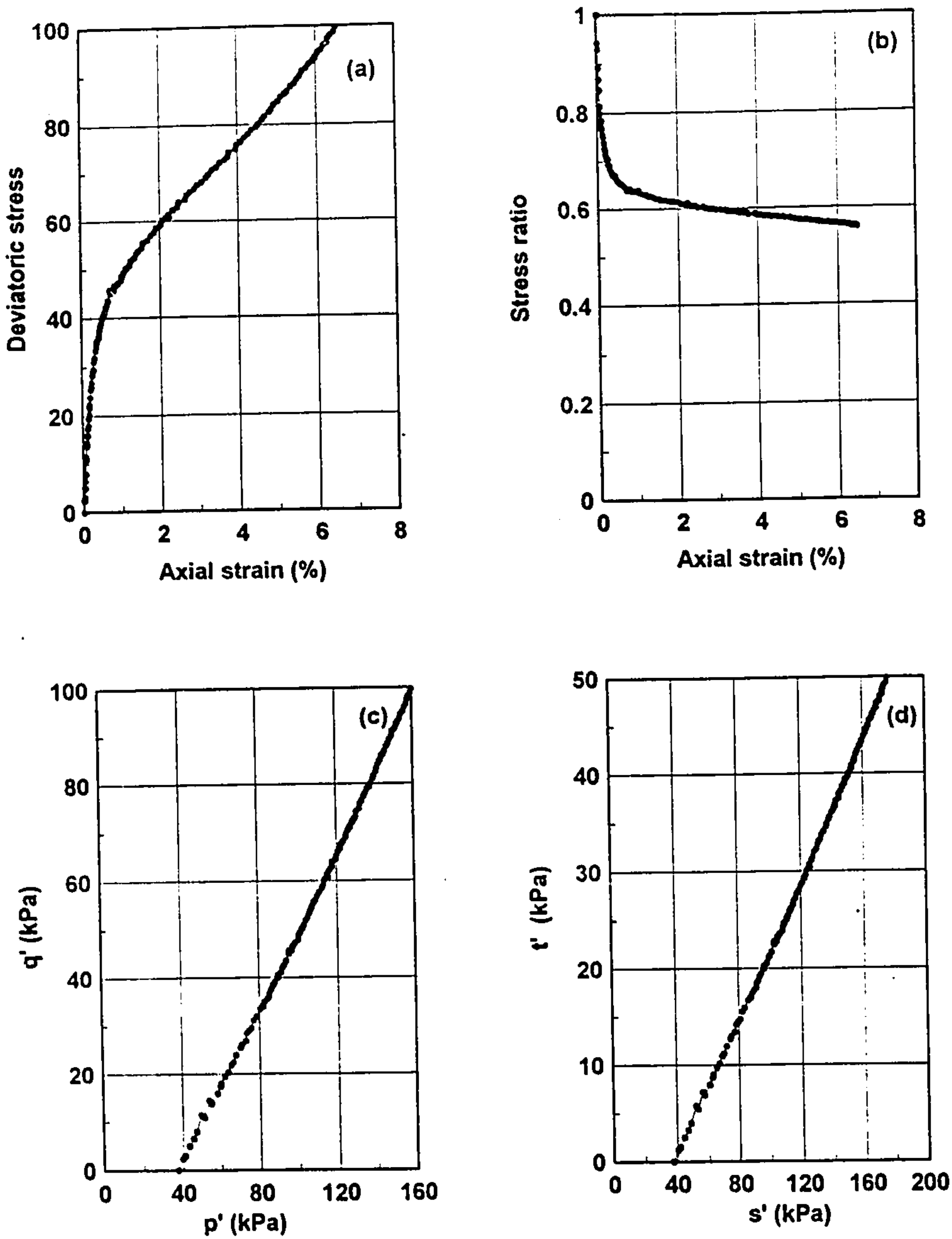

Fig. A.45. CID triaxial compression test: Sample No. BS333T7.

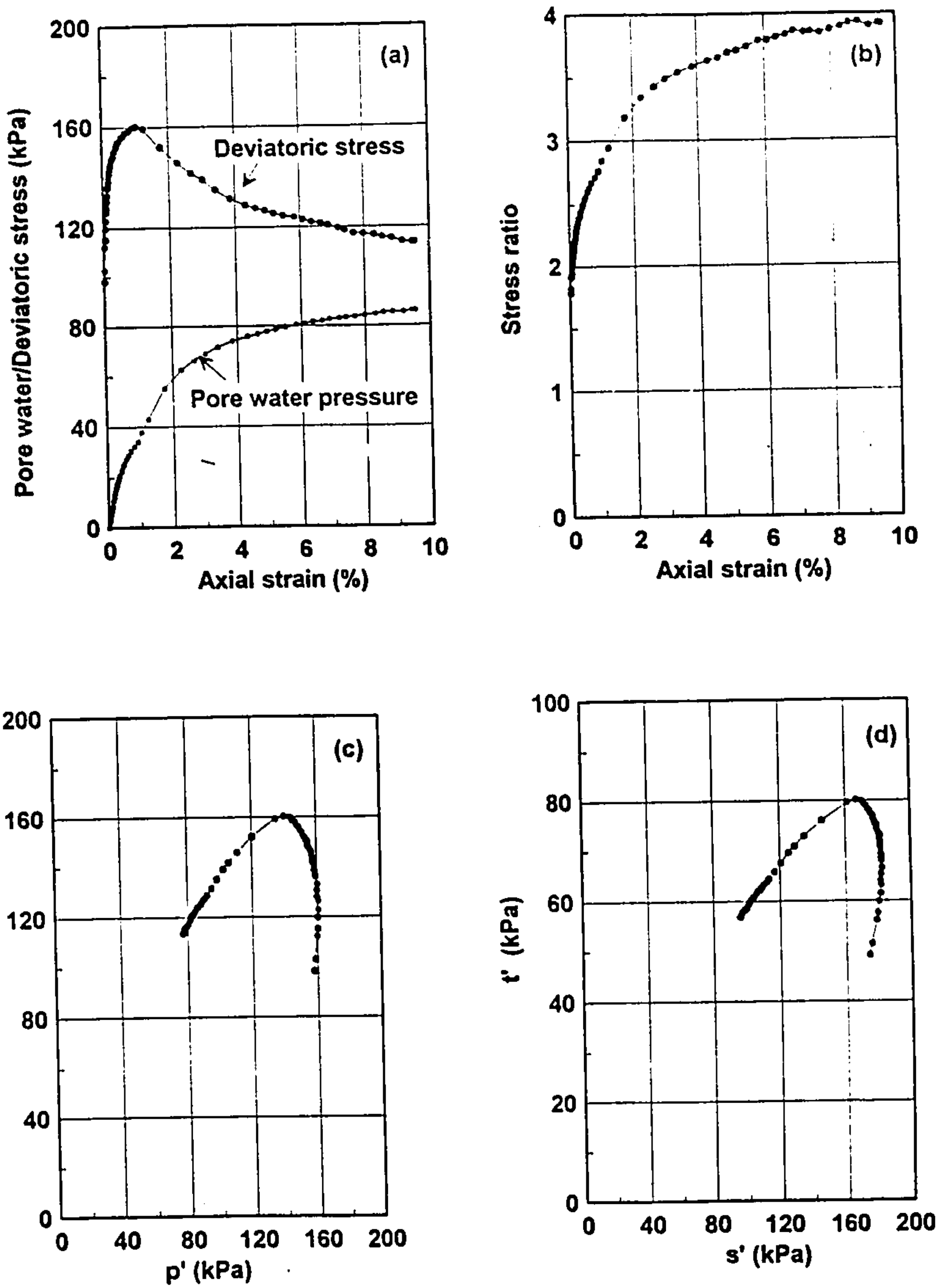

Fig. A.46. CAU triaxial compression test: Sample No. BS333T8.

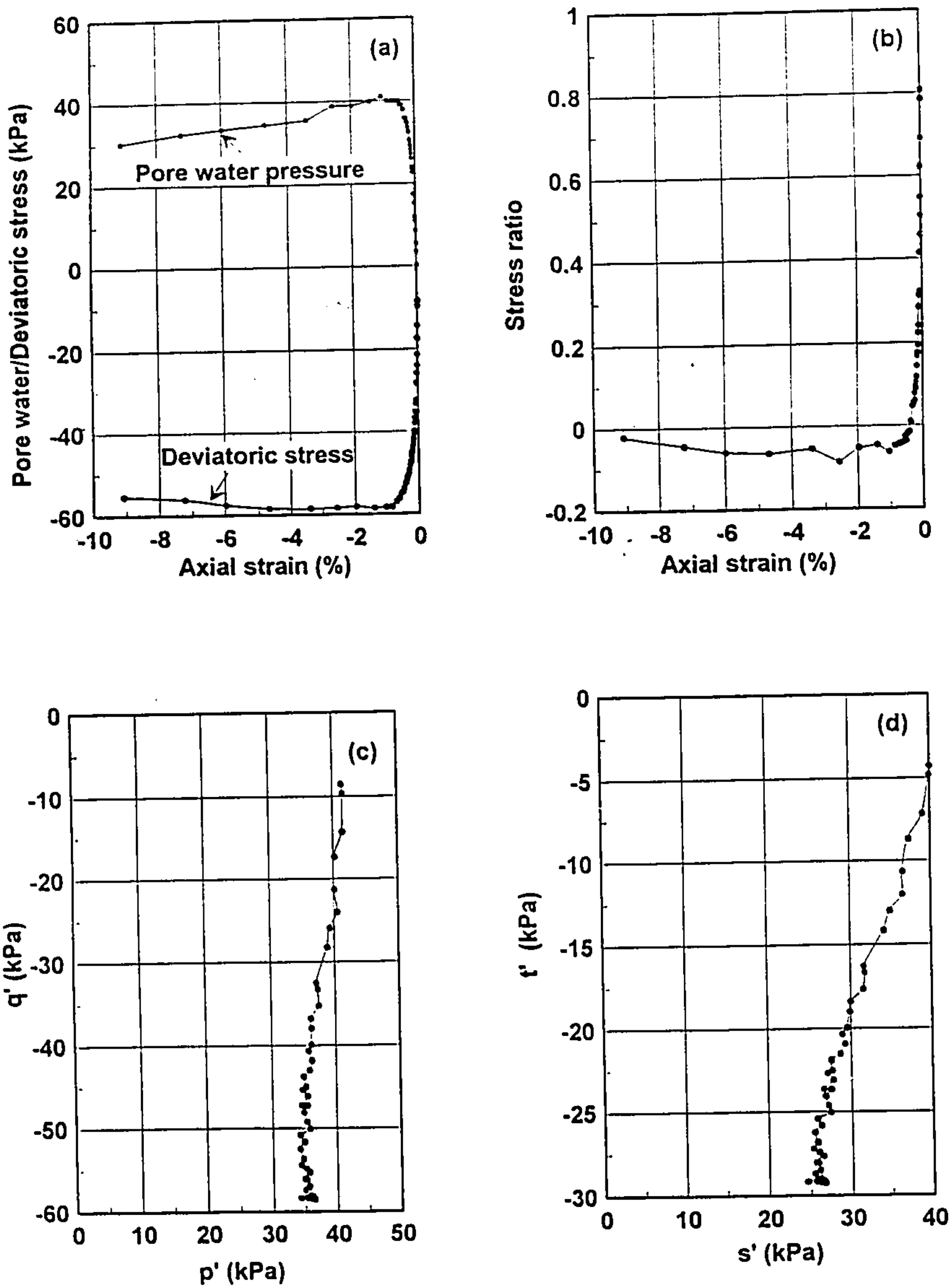

Fig. A.47. CK_0U triaxial extension test: Sample No. BS333T9.

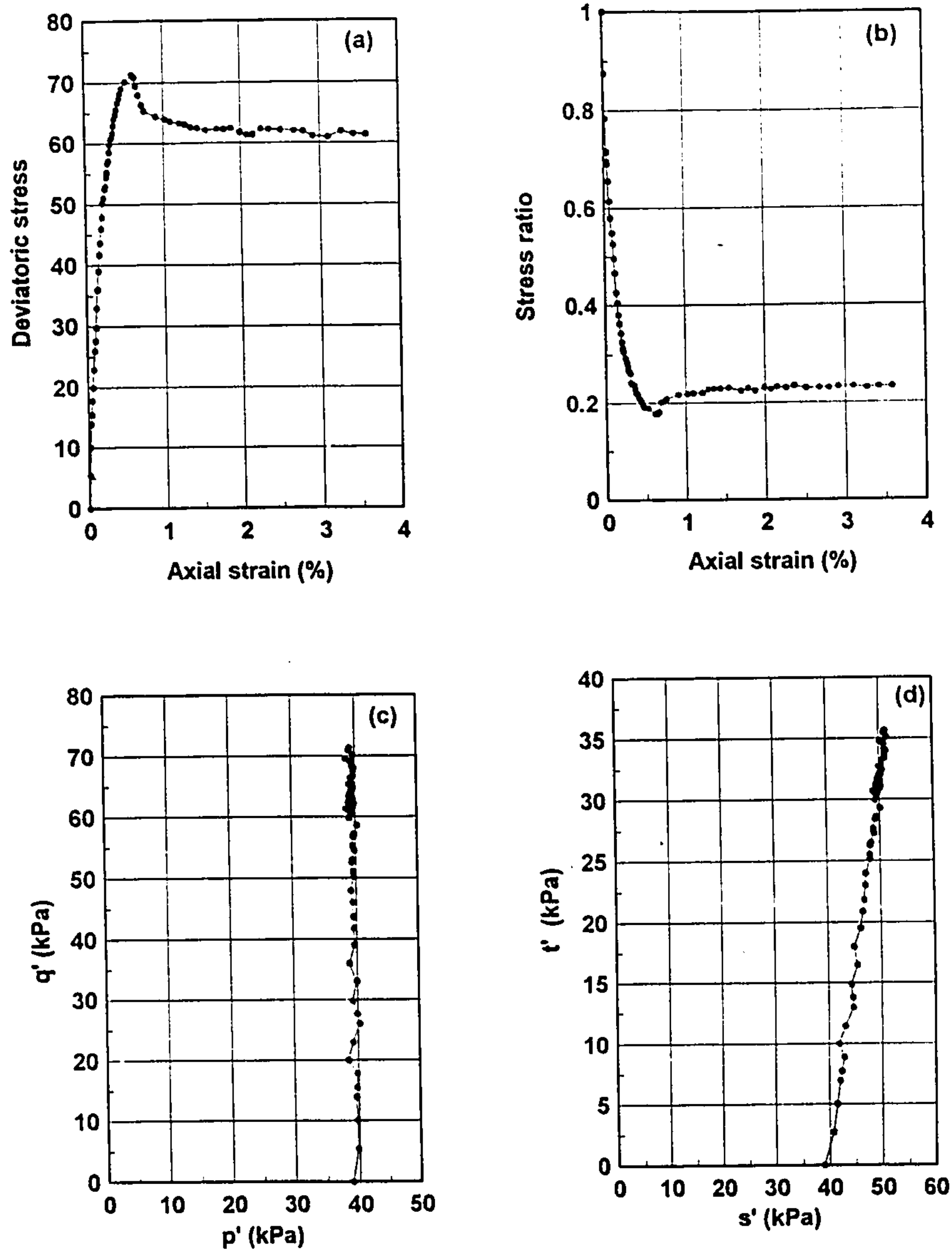

Fig. A.48. CID triaxial compression test (constant p'): Sample No. BS333T10.

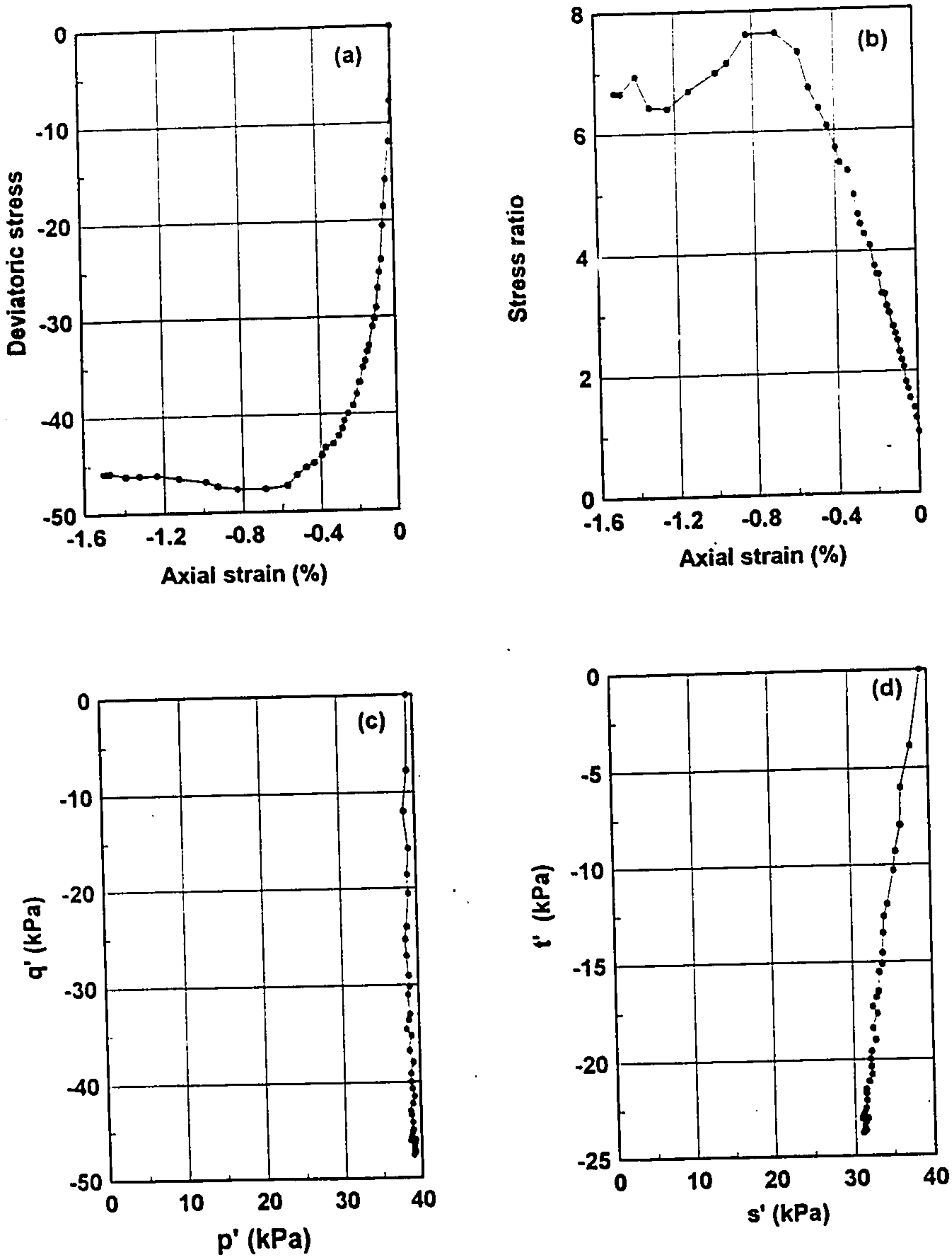

Fig. A.49. CID triaxial extension test (constant p'): Sample No. BS333T11.

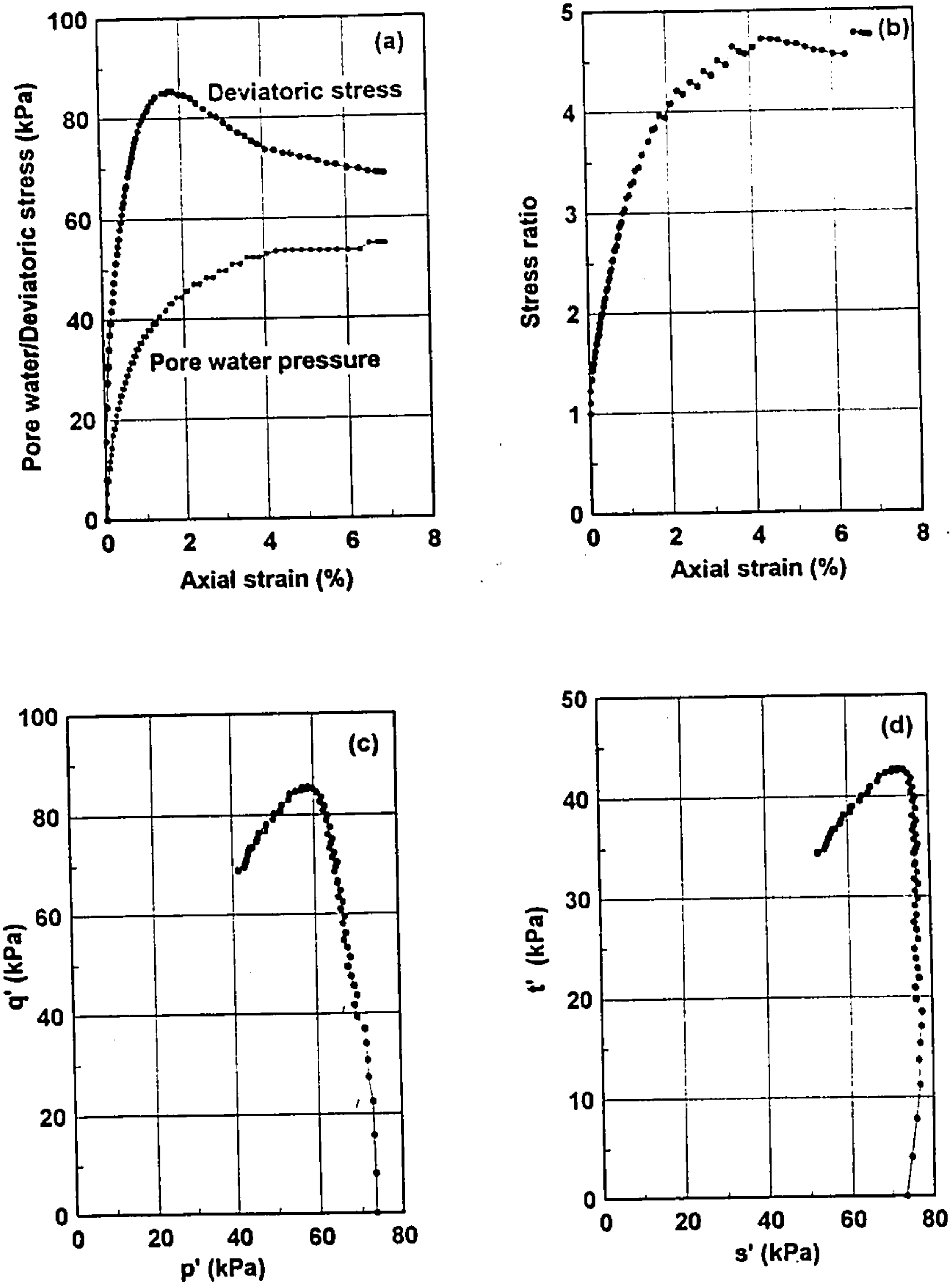

Fig. A.50. CIU triaxial compression test: Sample No. BS333T12.

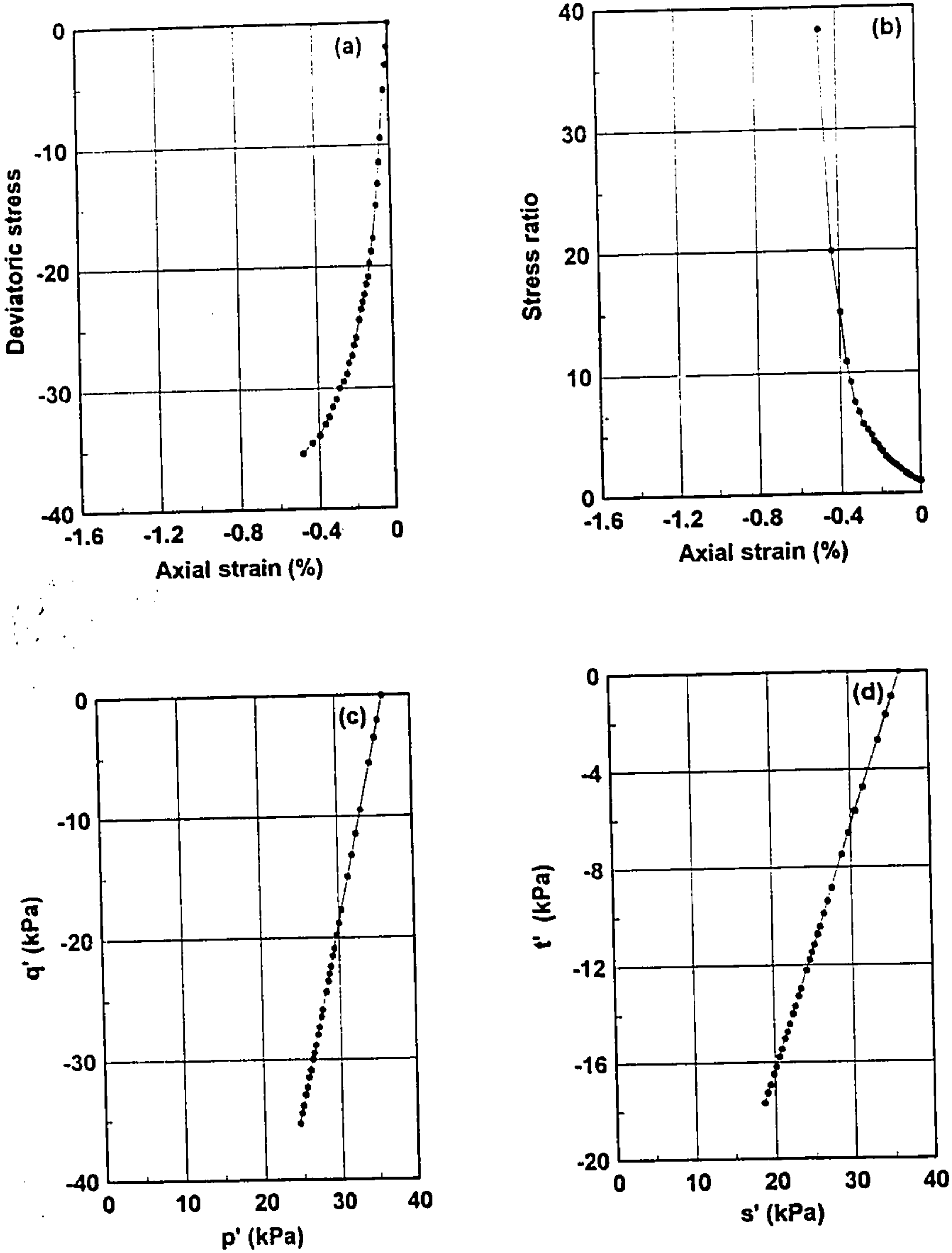

Fig. A.51. CID triaxial extension test: Sample No. BS333T13.

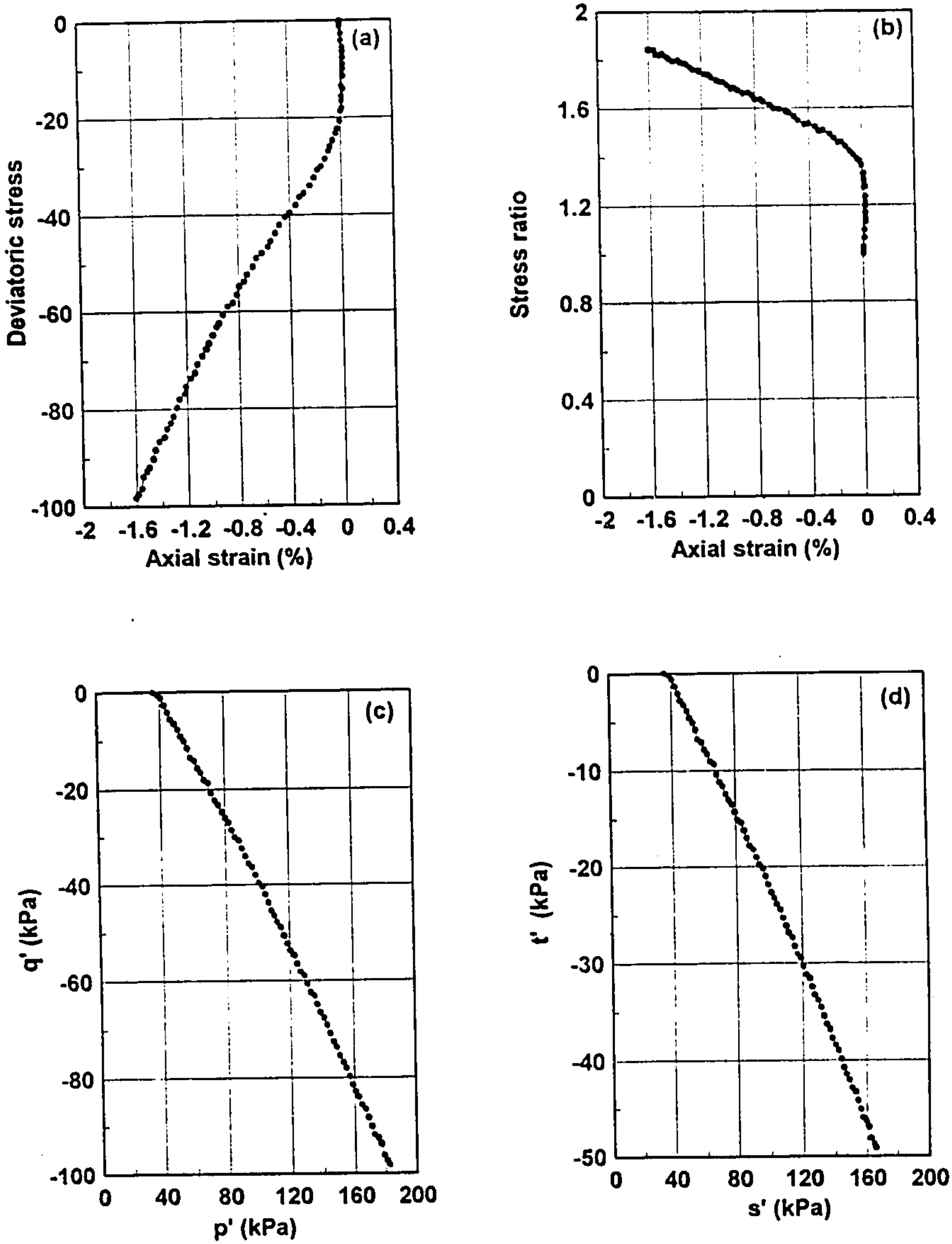

Fig. A.52. CID triaxial consolidation (vertical : horizontal = 1:2) test:
Sample No. BS333T14.

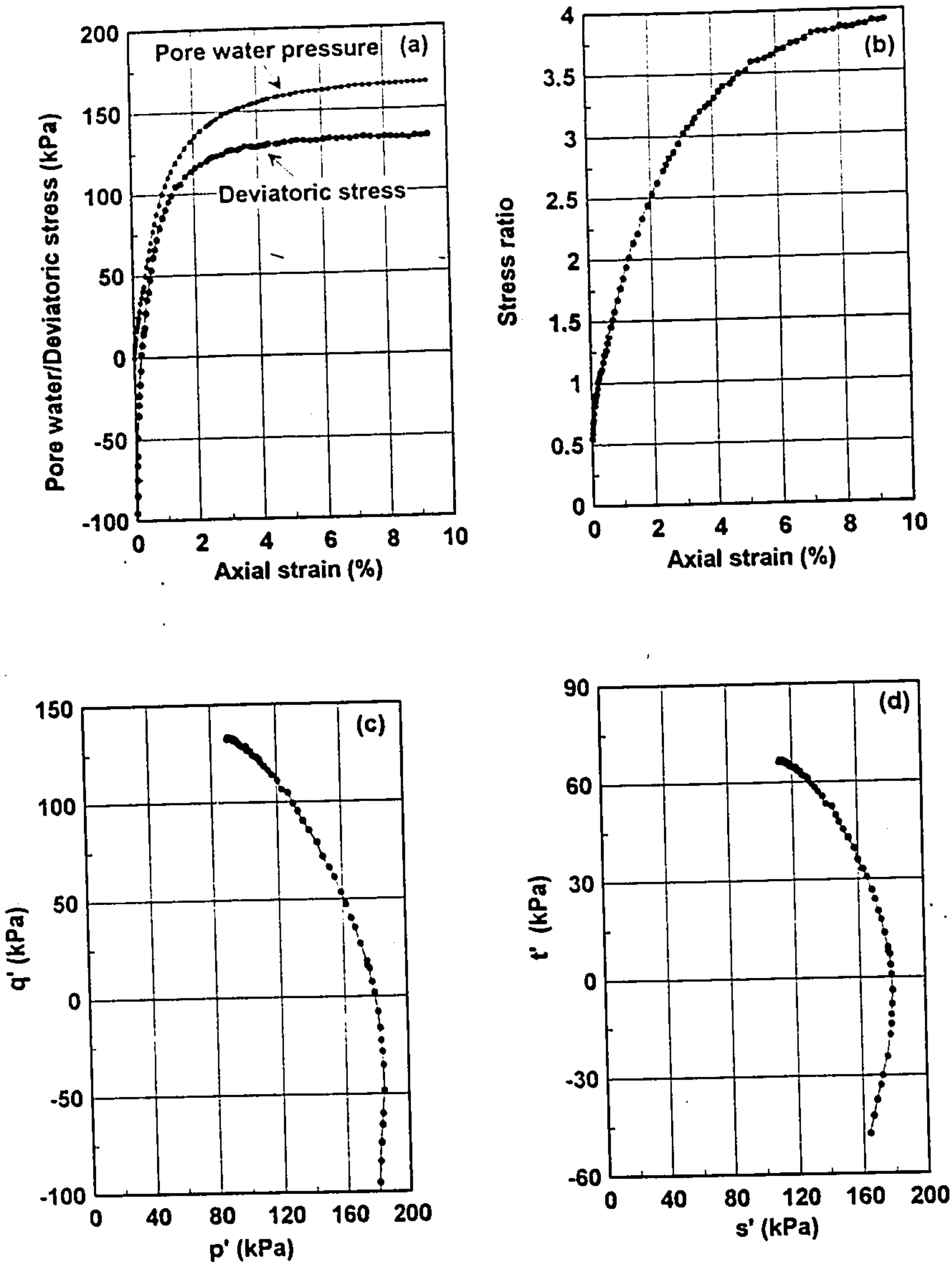

Fig. A.53. CAU triaxial compression test: Sample No. BS333T15.

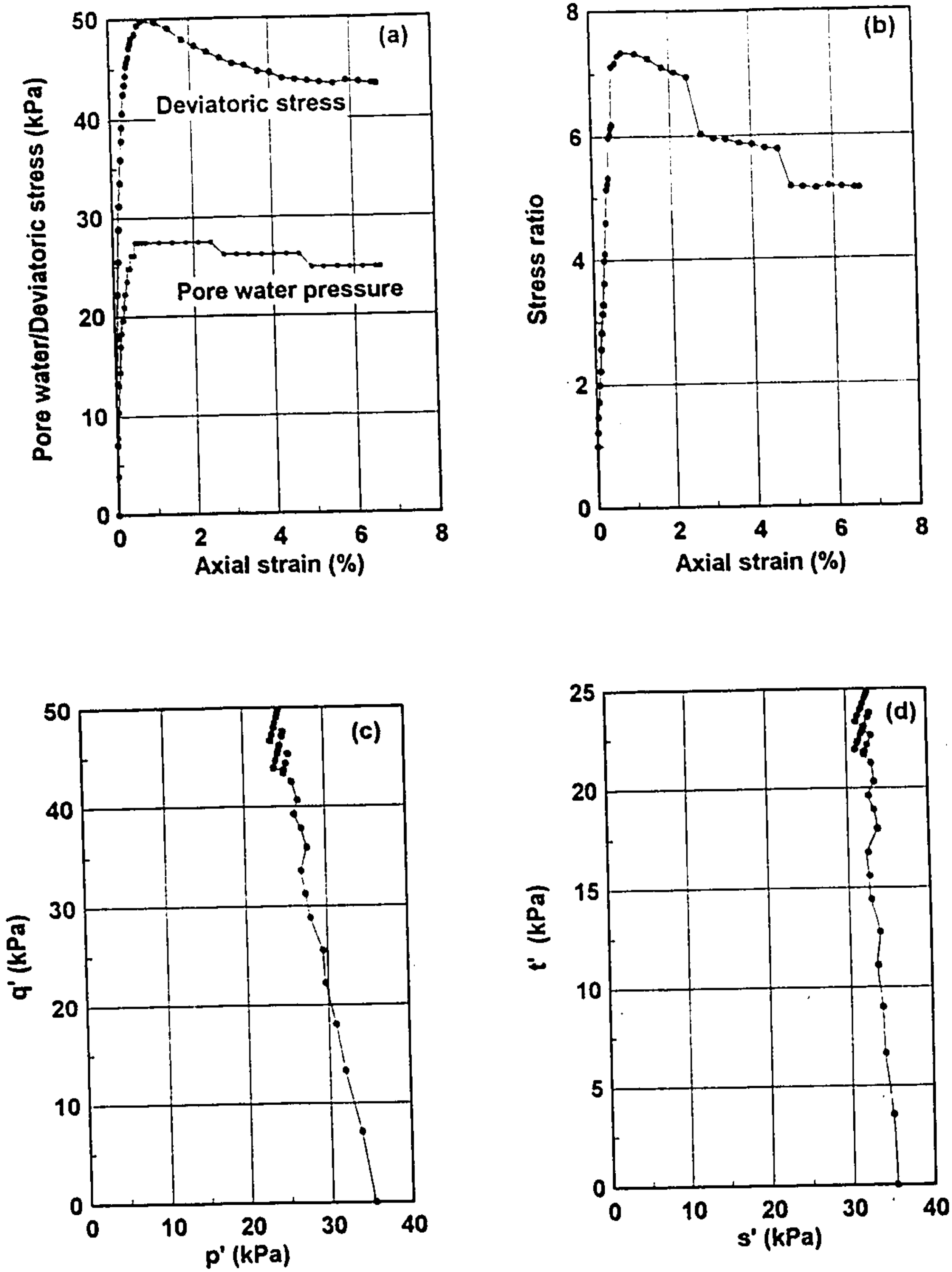

Fig. A.54. CIU triaxial compression test: Sample No. BS333T16 (horizontal sample).

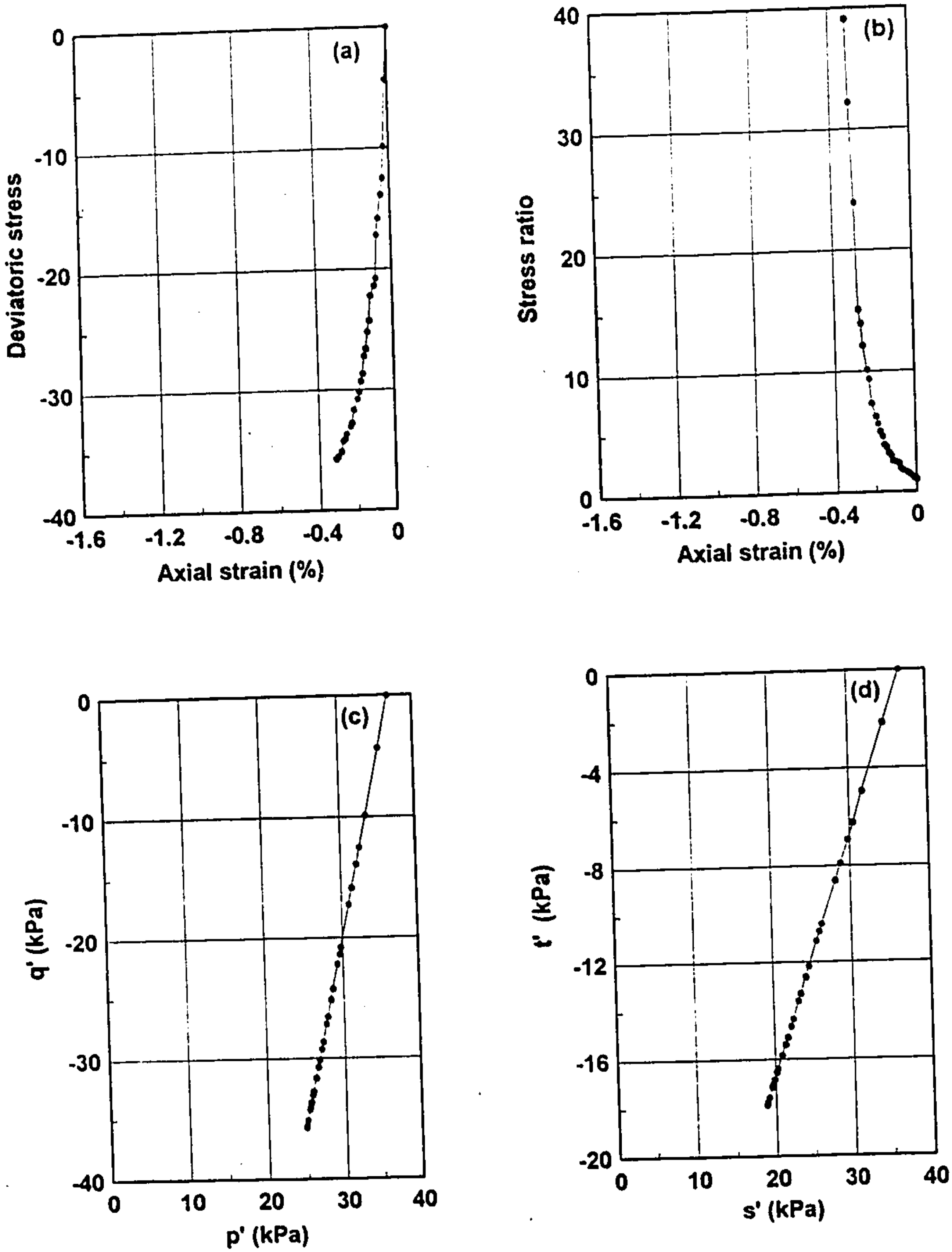

Fig. A.55. CID triaxial extension test: Sample No. BS333T17.

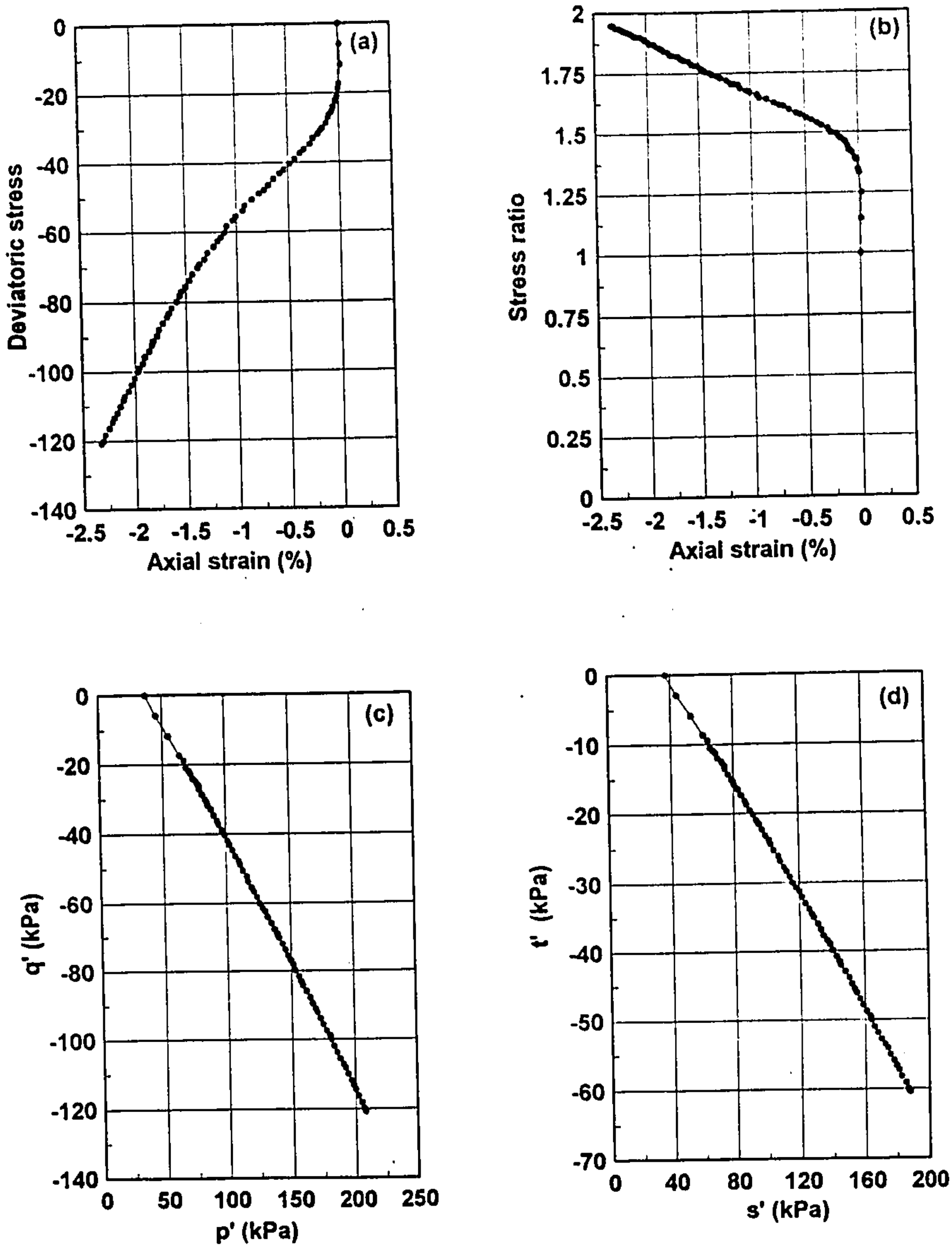

Fig. A.56. CID triaxial consolidation (vertical : horizontal = 1:2) test:
Sample No. BS333T18.

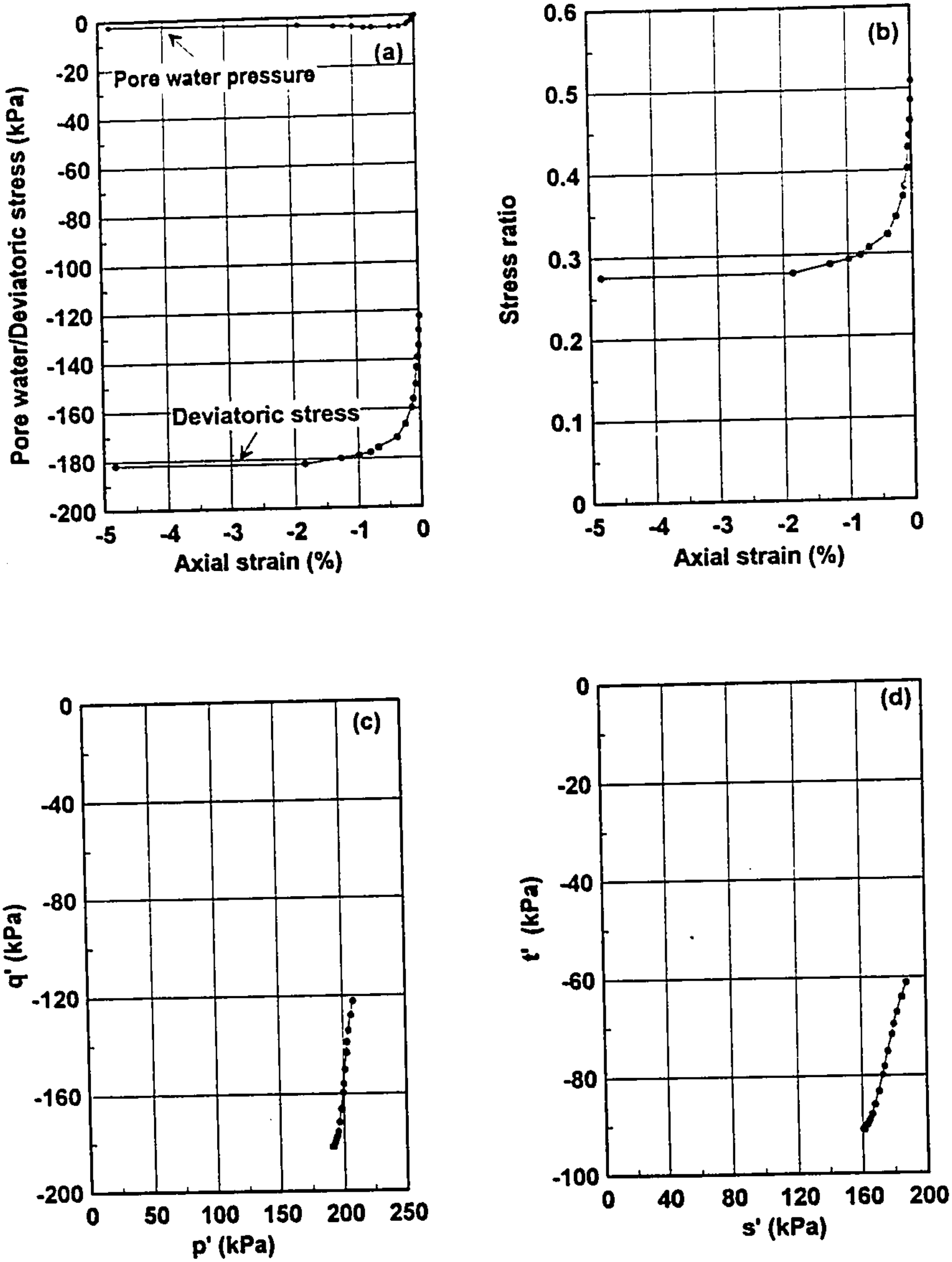

Fig. A.57. CAU triaxial compression test: Sample No. BS333T19.

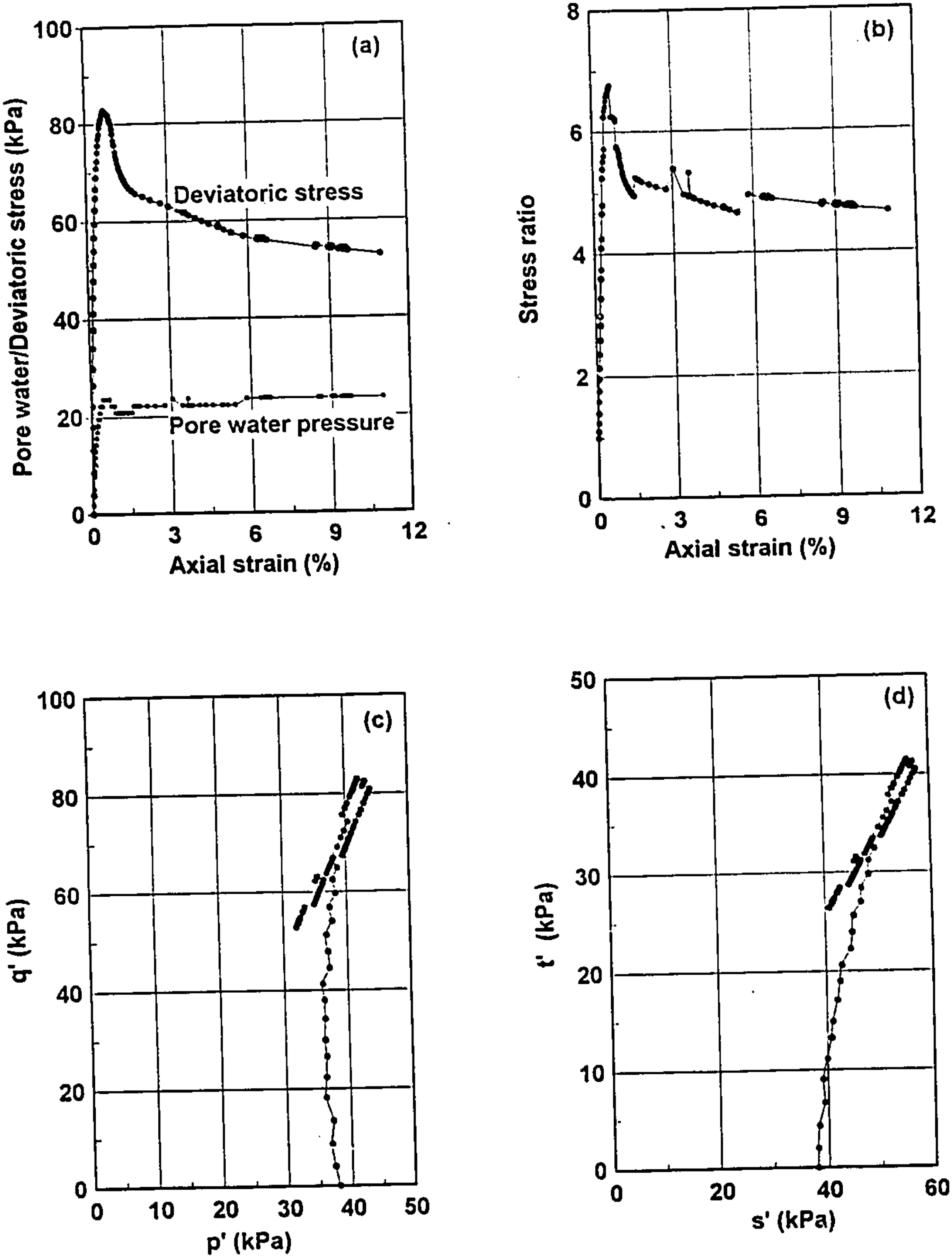

Fig. A.58. CIU triaxial compression test: Sample No. BS360T1.

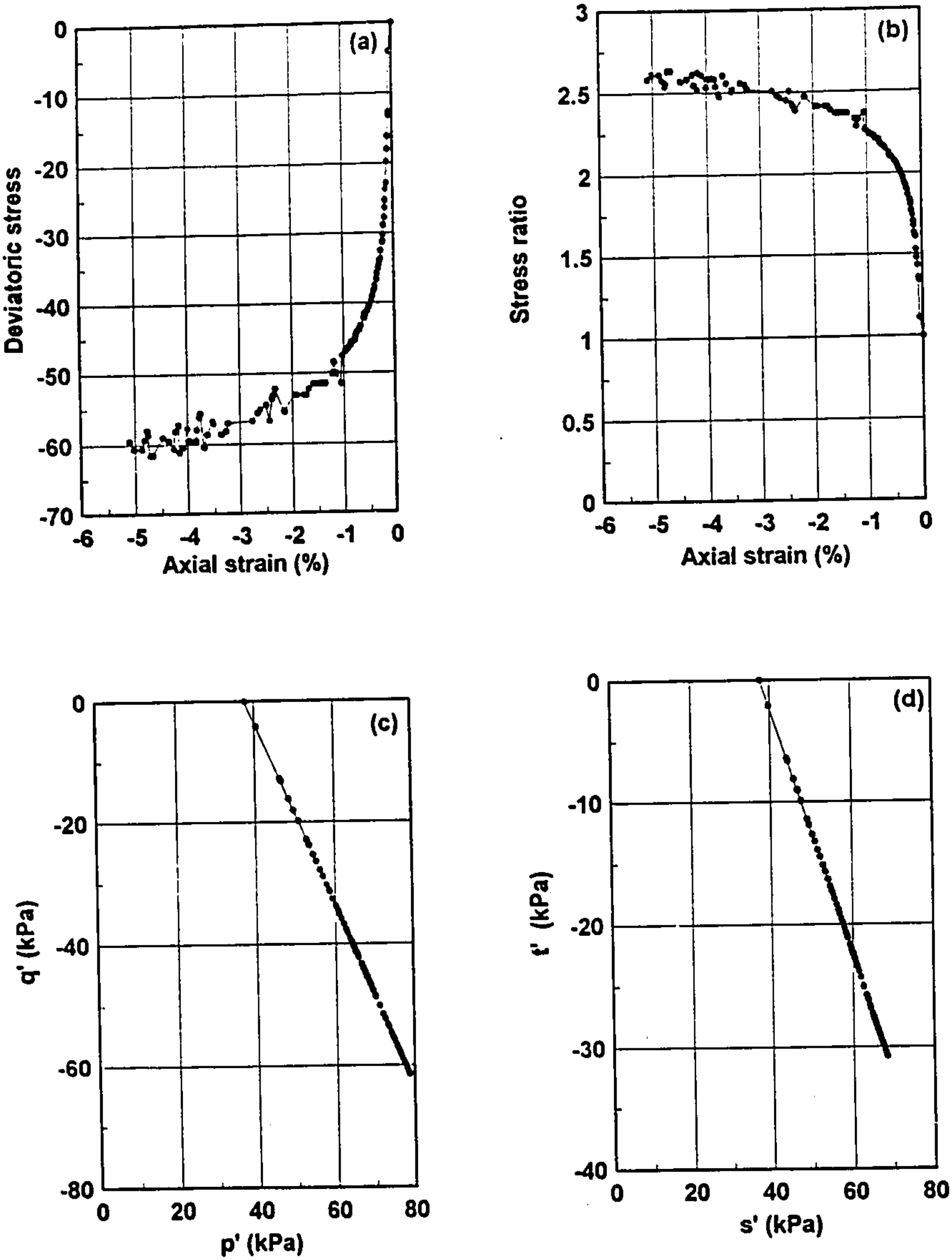

Fig. A.59. CID triaxial extension test: Sample No. BS360T3.

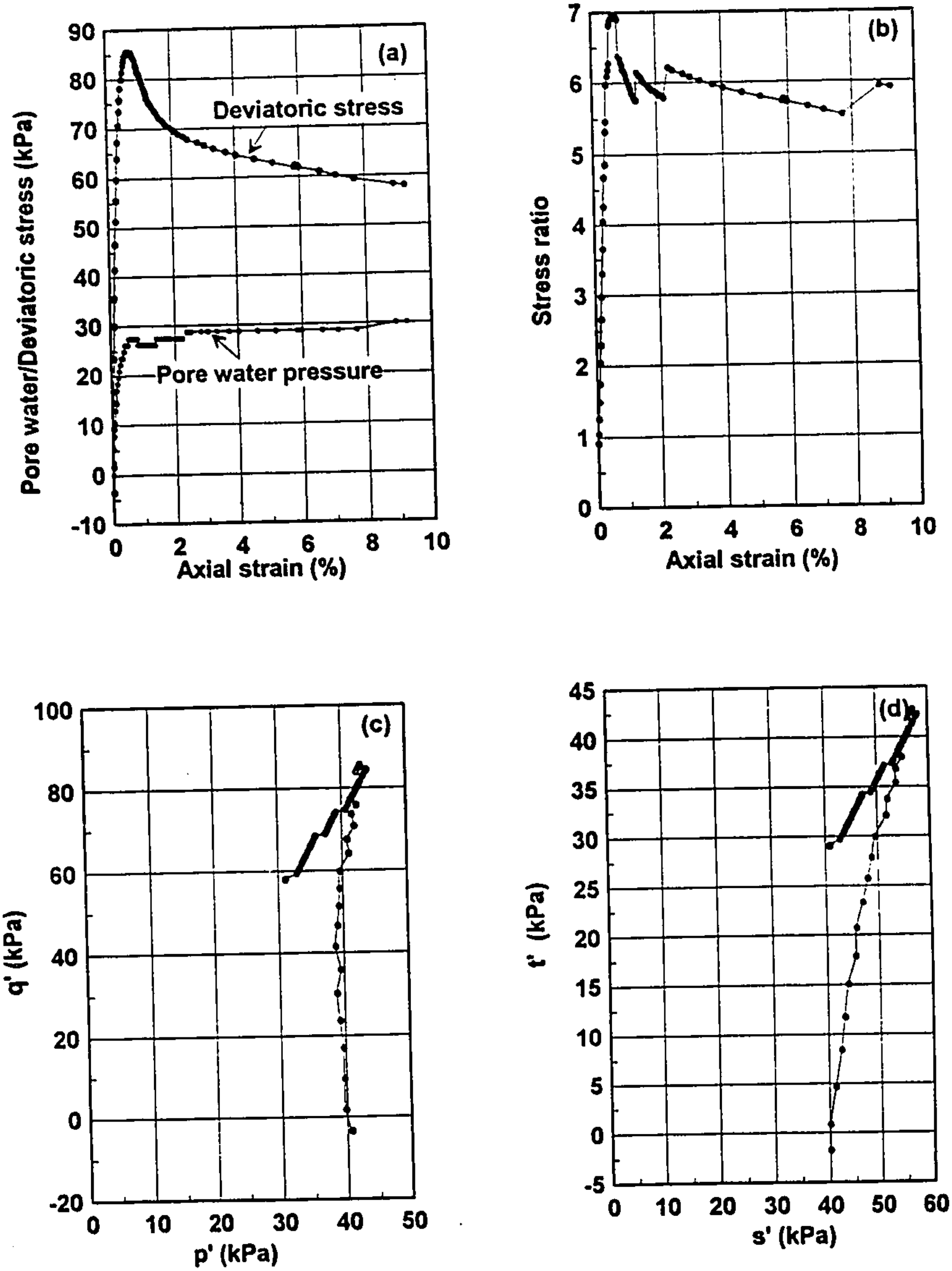

Fig. A.60. CK_0U triaxial compression test: Sample No. BS360T4.

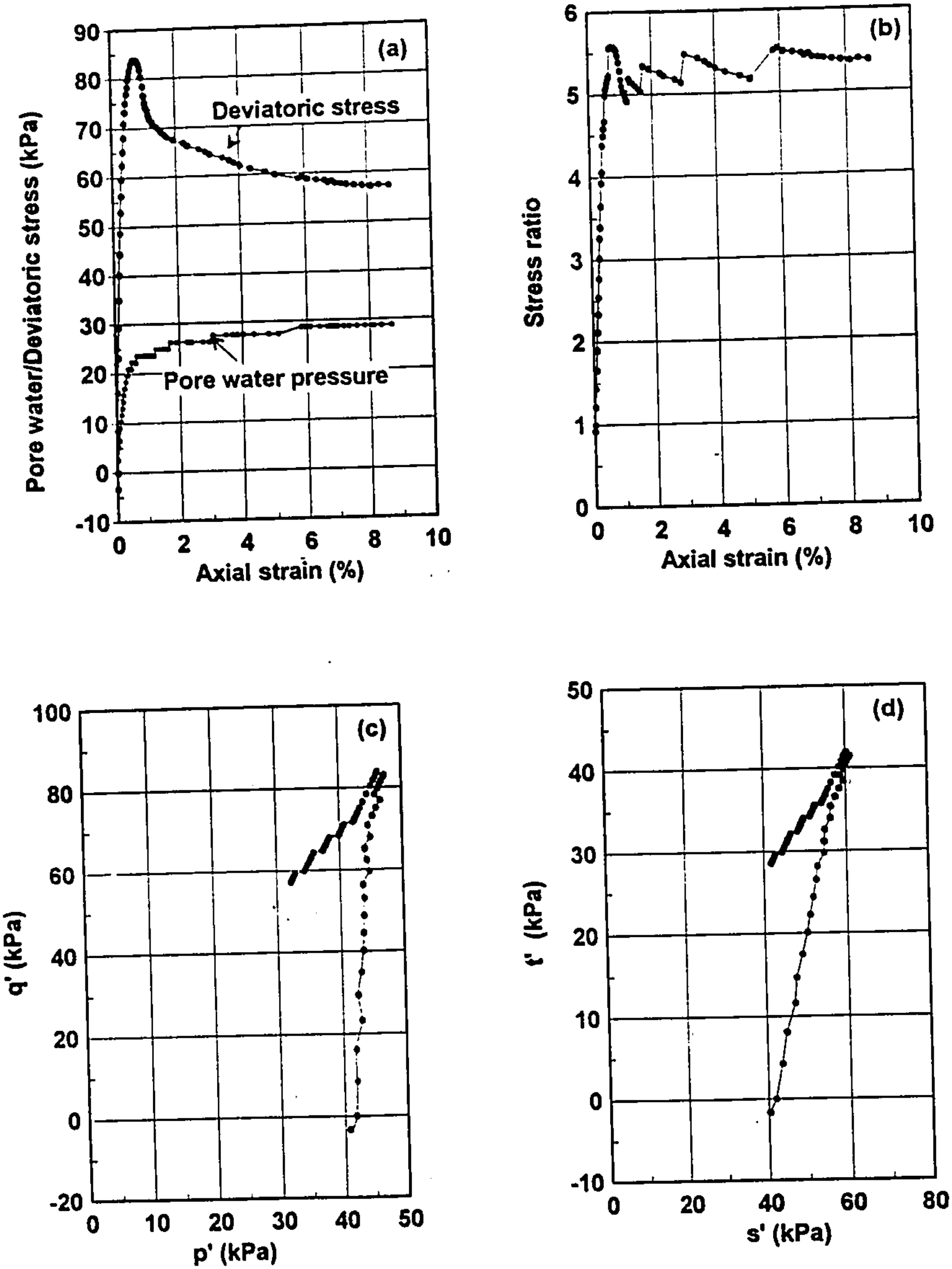

Fig. A.61. CK_0U triaxial compression test (unsaturated): Sample No. BS360T5.

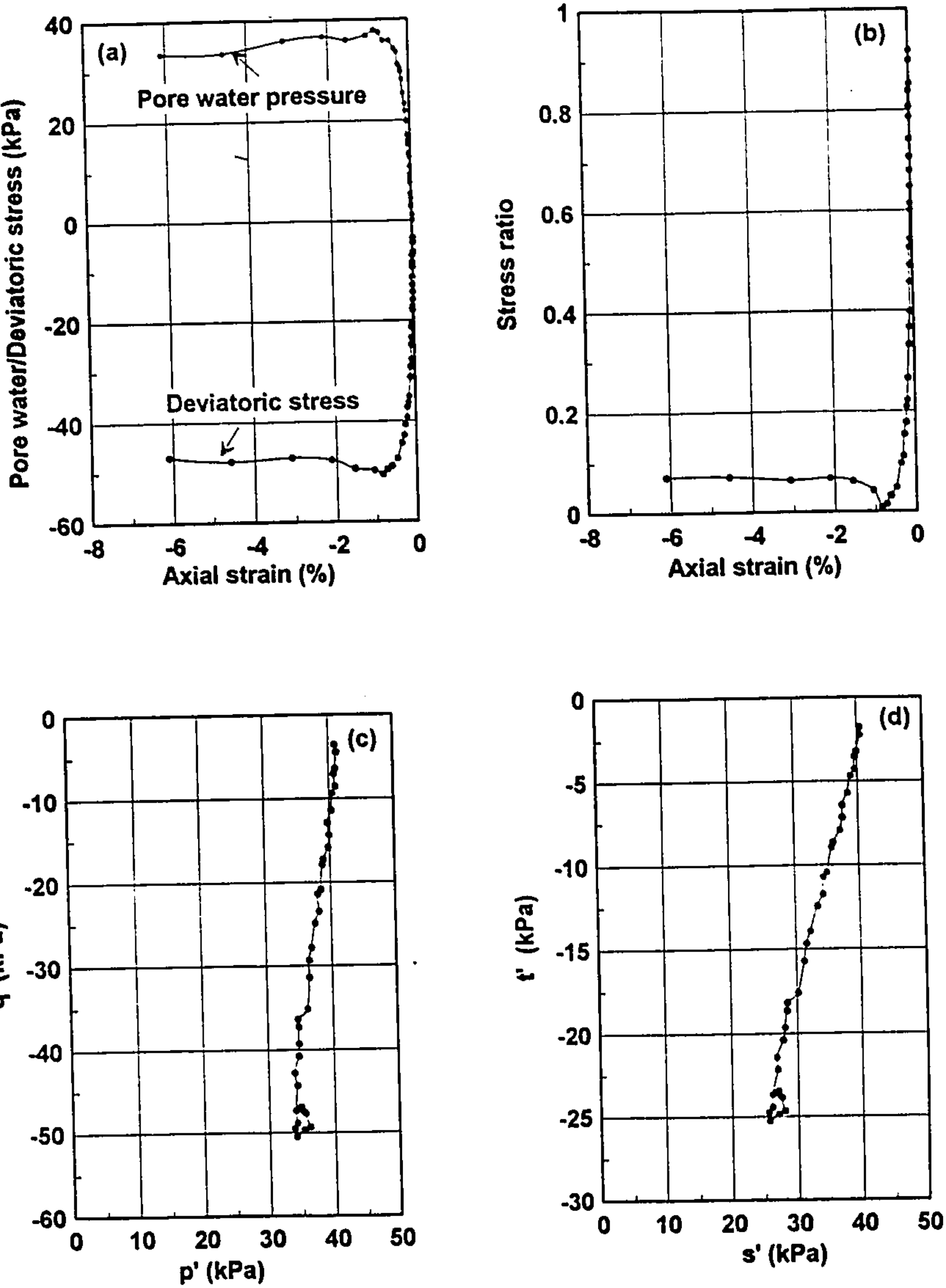

Fig. A.62. CK_0U triaxial extension test: Sample No. BS360T6.

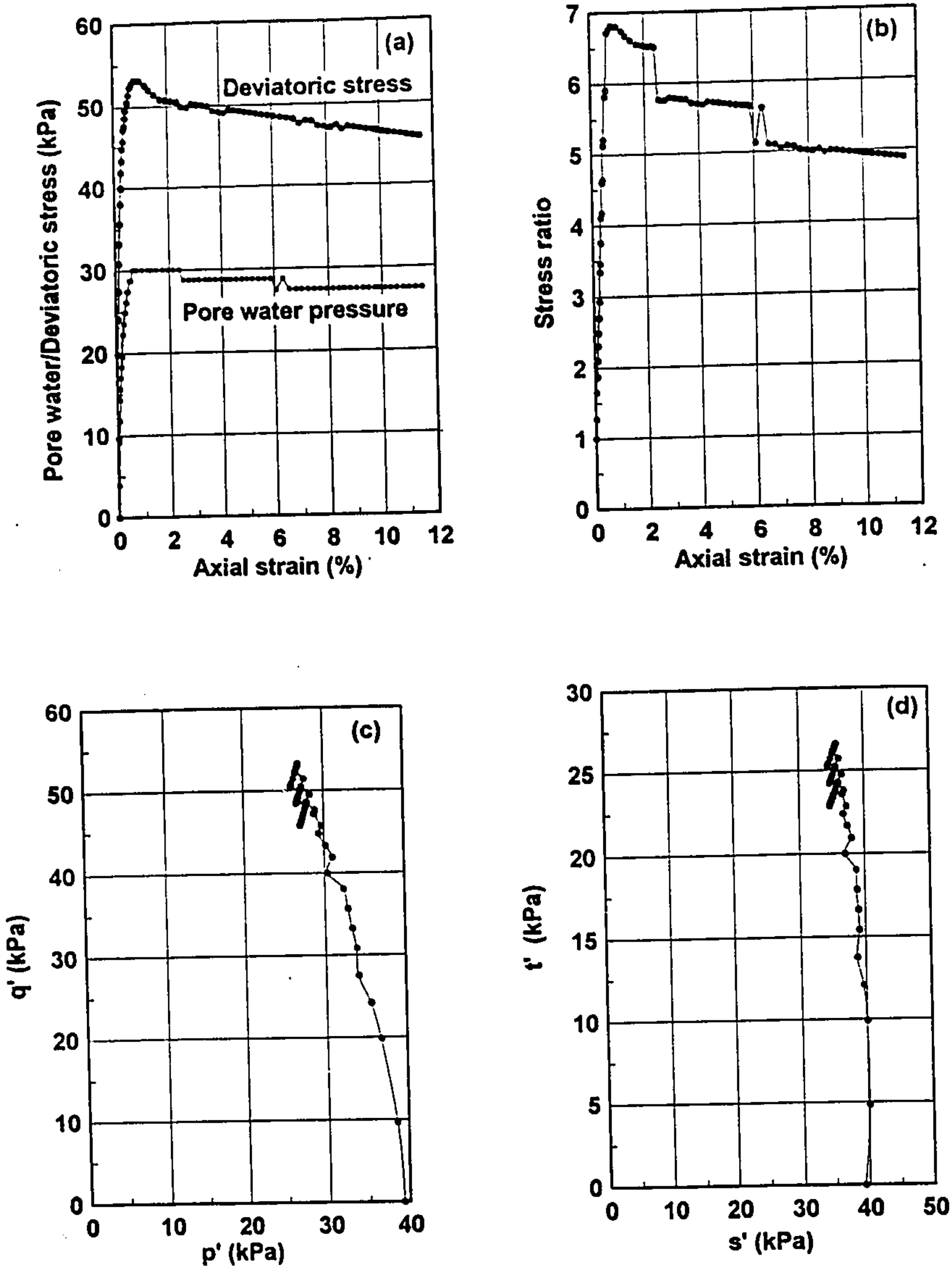

Fig. A.63. CIU triaxial compression test: Sample No. BS370T1 (Horizontal sample).

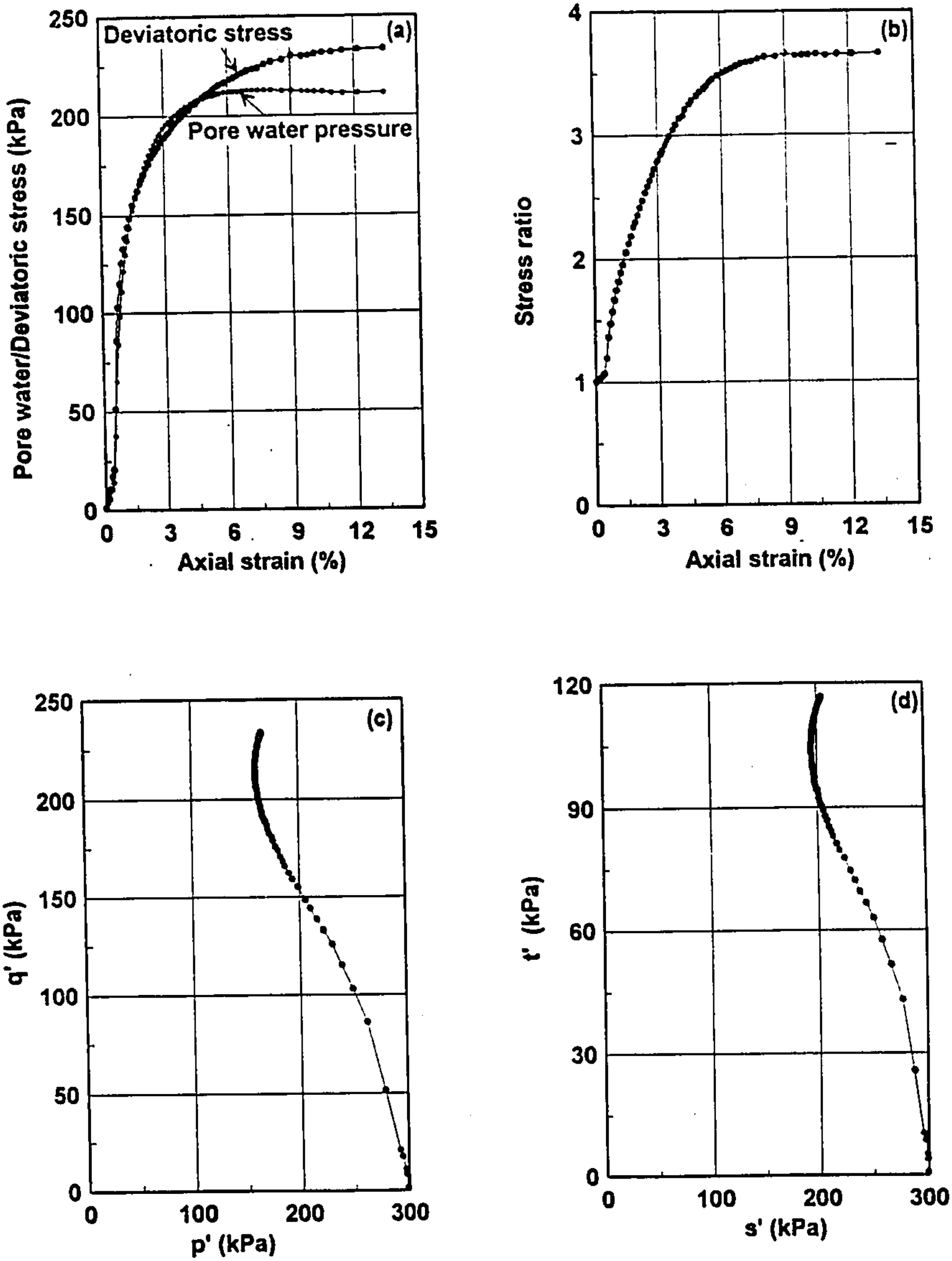

Fig. A.64. CIU triaxial compression test: Sample No. RMDT1 (Reconstituted sample).

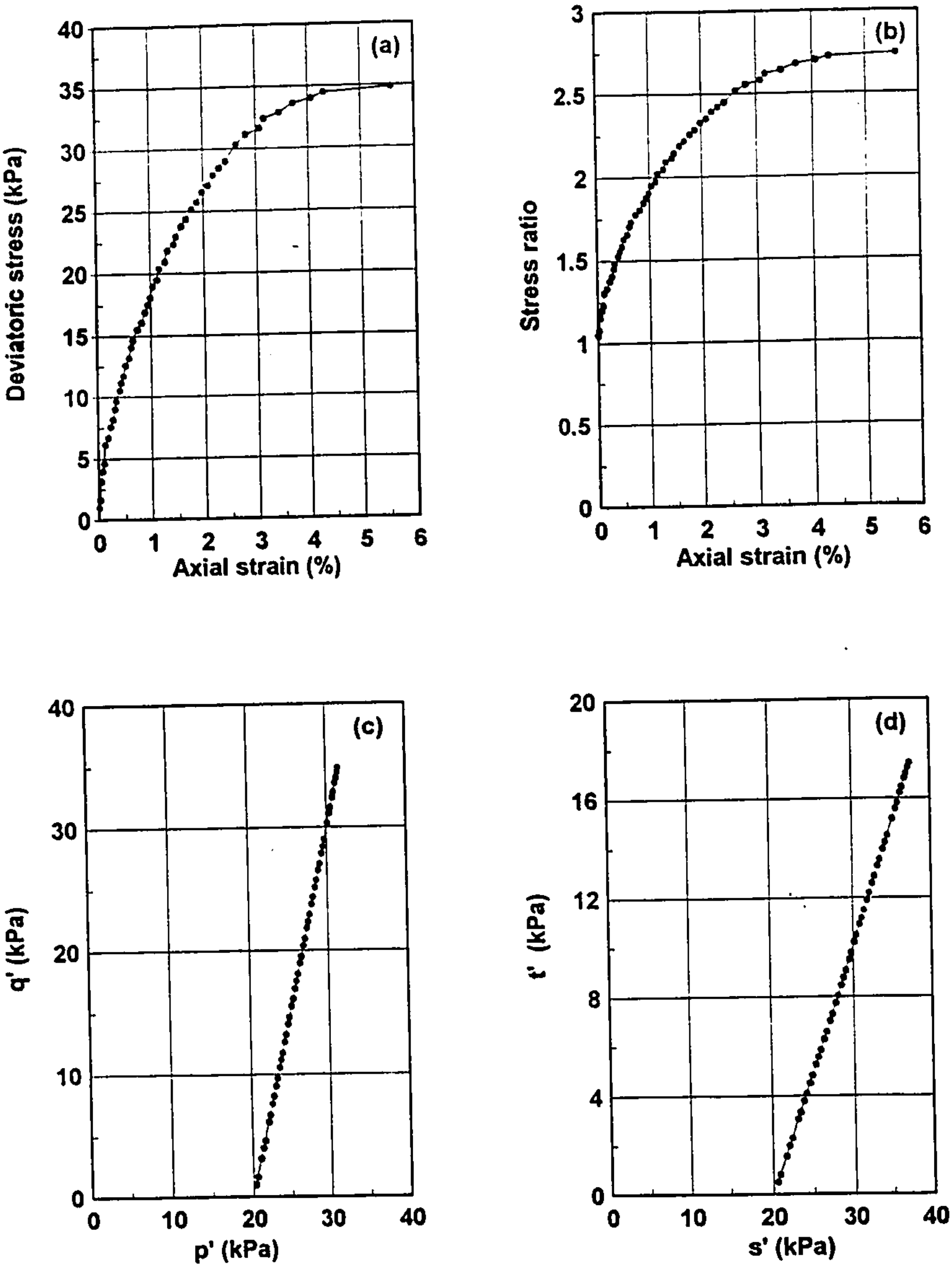

Fig. A.65. CIU triaxial compression test: Sample No. RMDT2 (Reconstituted sample).

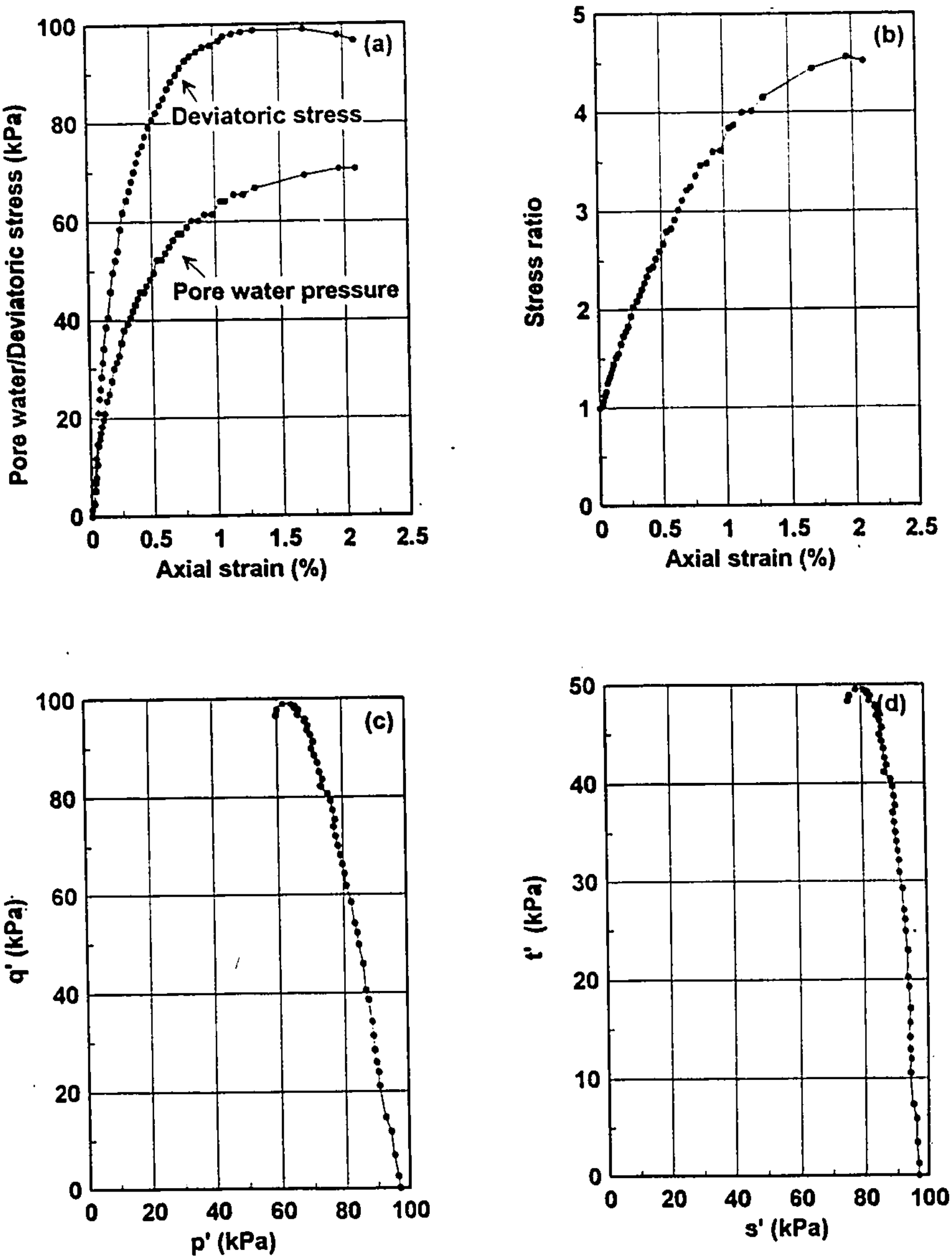

Fig. A.66. CIU multistage triaxial compression test: Sample No. SB200MT (Stage 1).

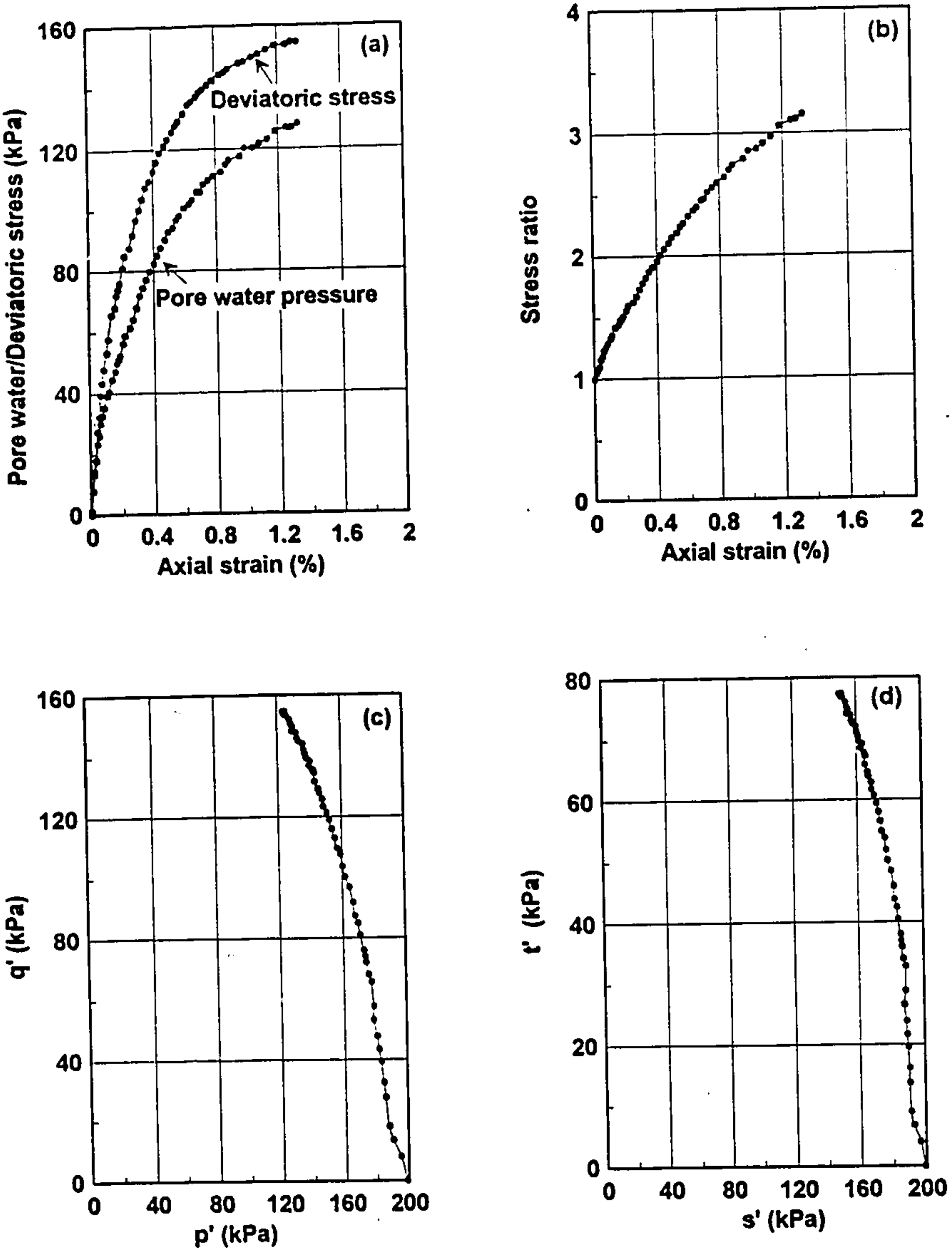

Fig. A.67. CIU multistage triaxial compression test: Sample No. SB200MT (Stage 2).

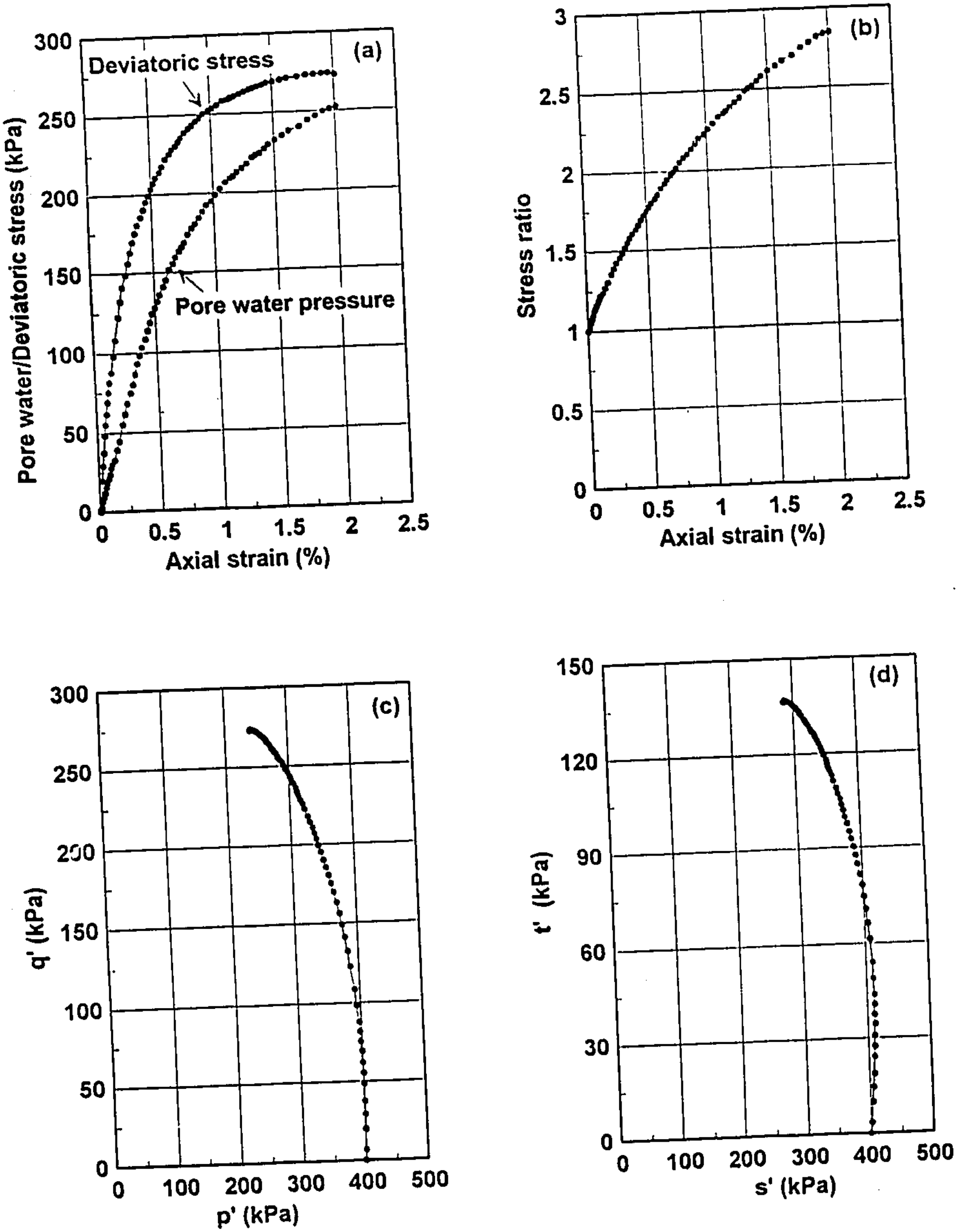

Fig. A.68. CIU multistage triaxial compression test: Sample No. SB200MT (Stage 3).

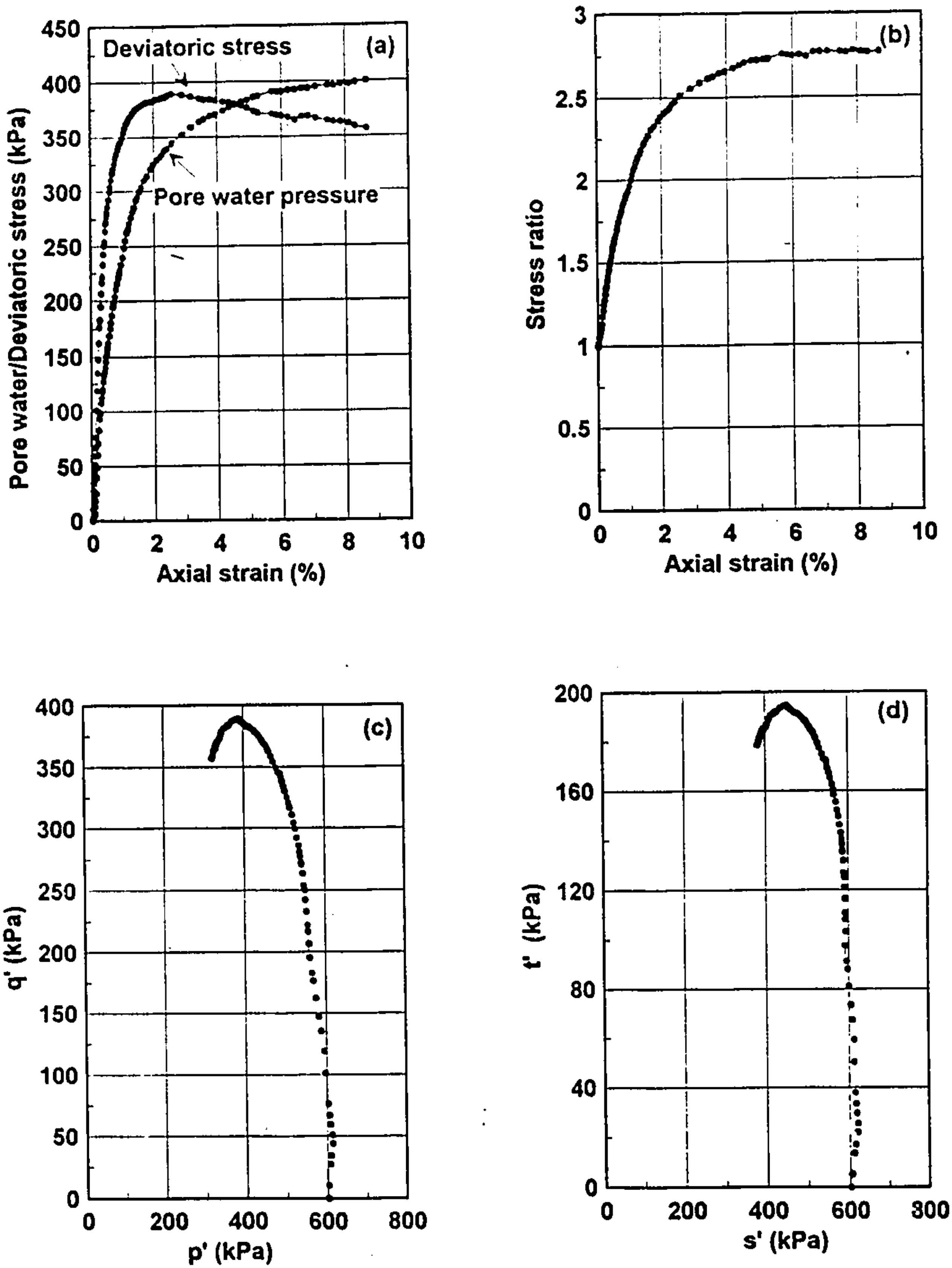

Fig. A.69. CIU multistage triaxial compression test: Sample No. SB200MT (Stage 4).

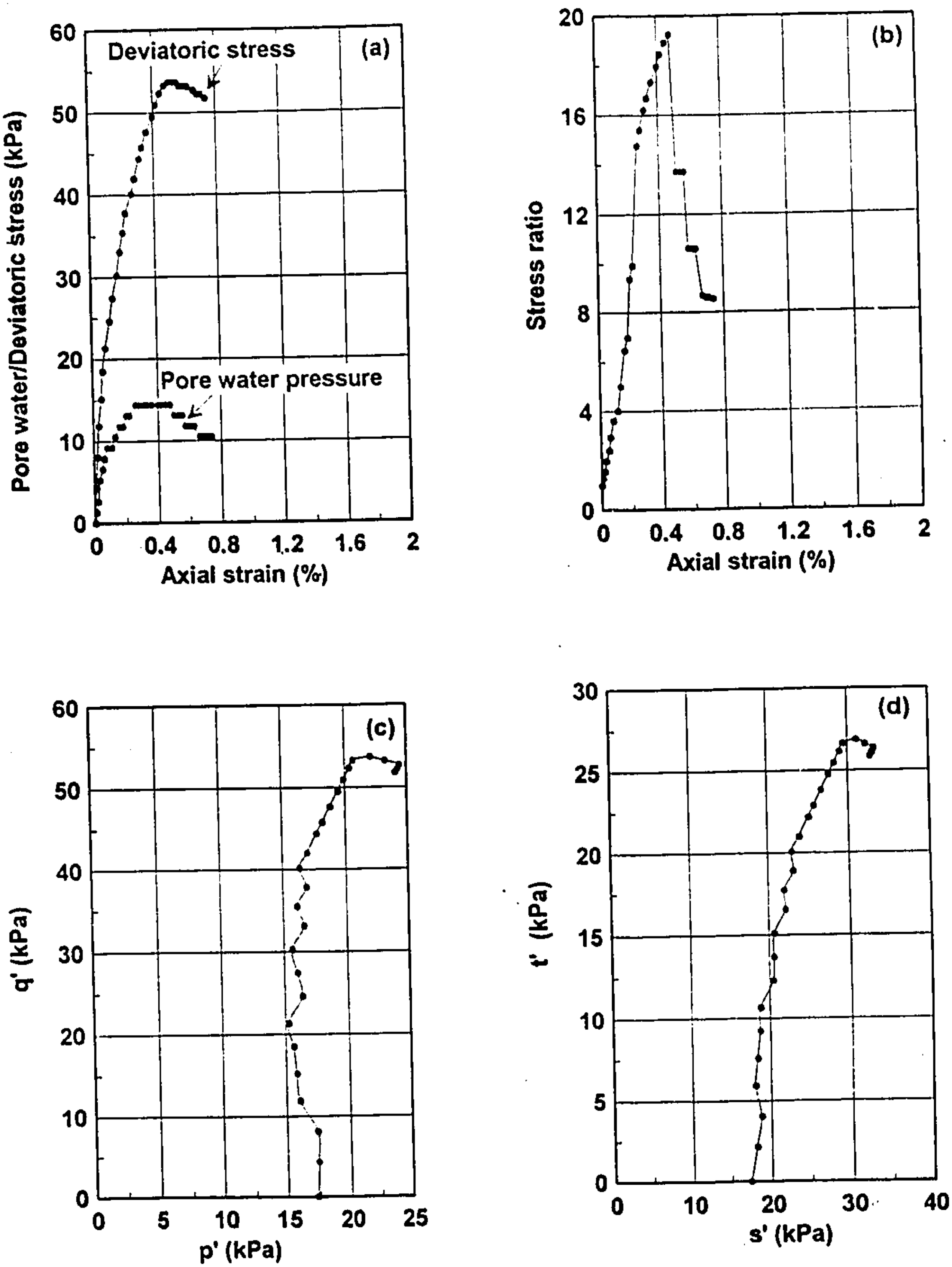

Fig. A.70. CIU multistage triaxial compression test: Sample No. SB360MT (Stage 1).

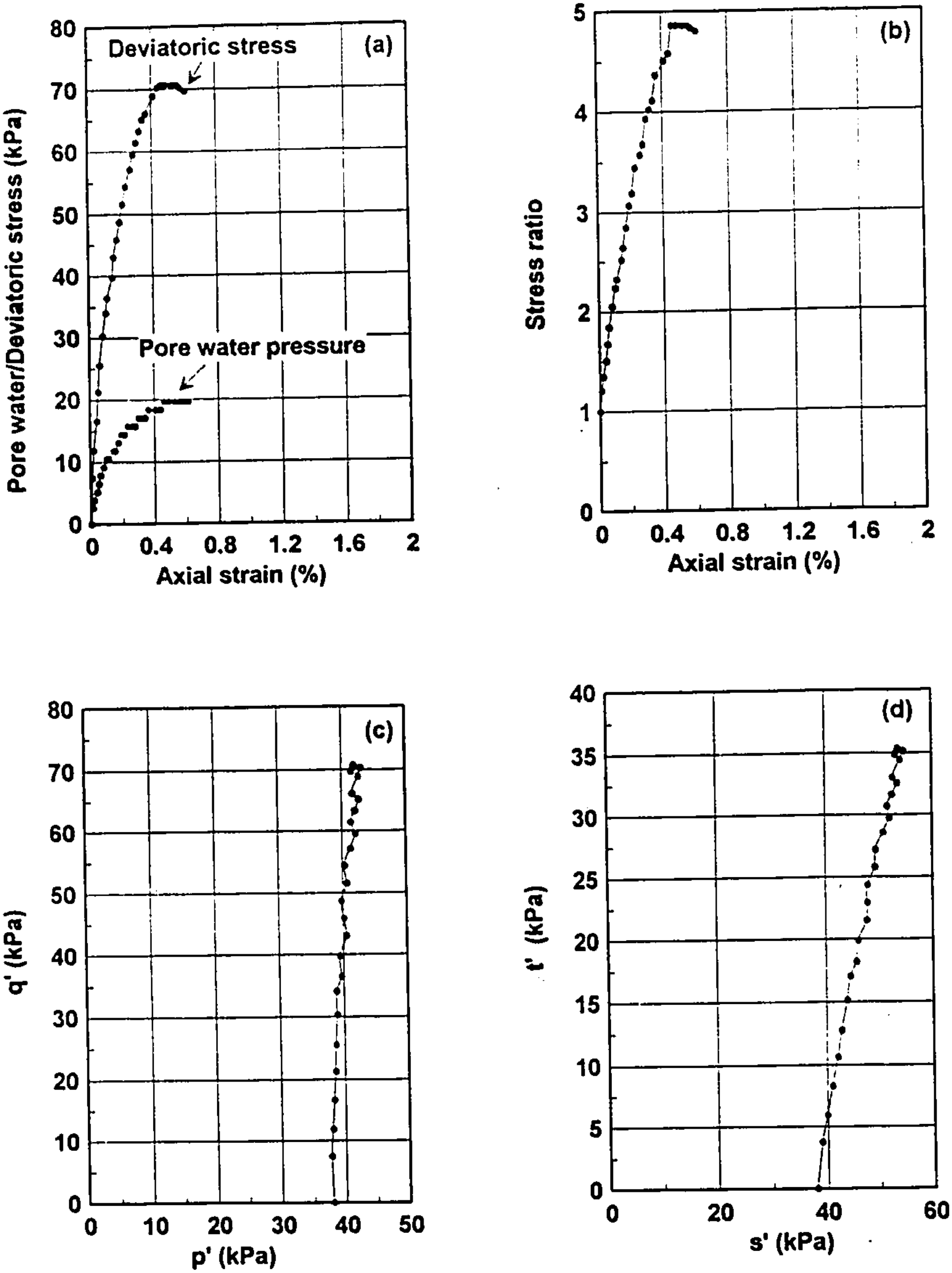

Fig. A.71. CIU multistage triaxial compression test: Sample No. SB360MT (Stage 2).

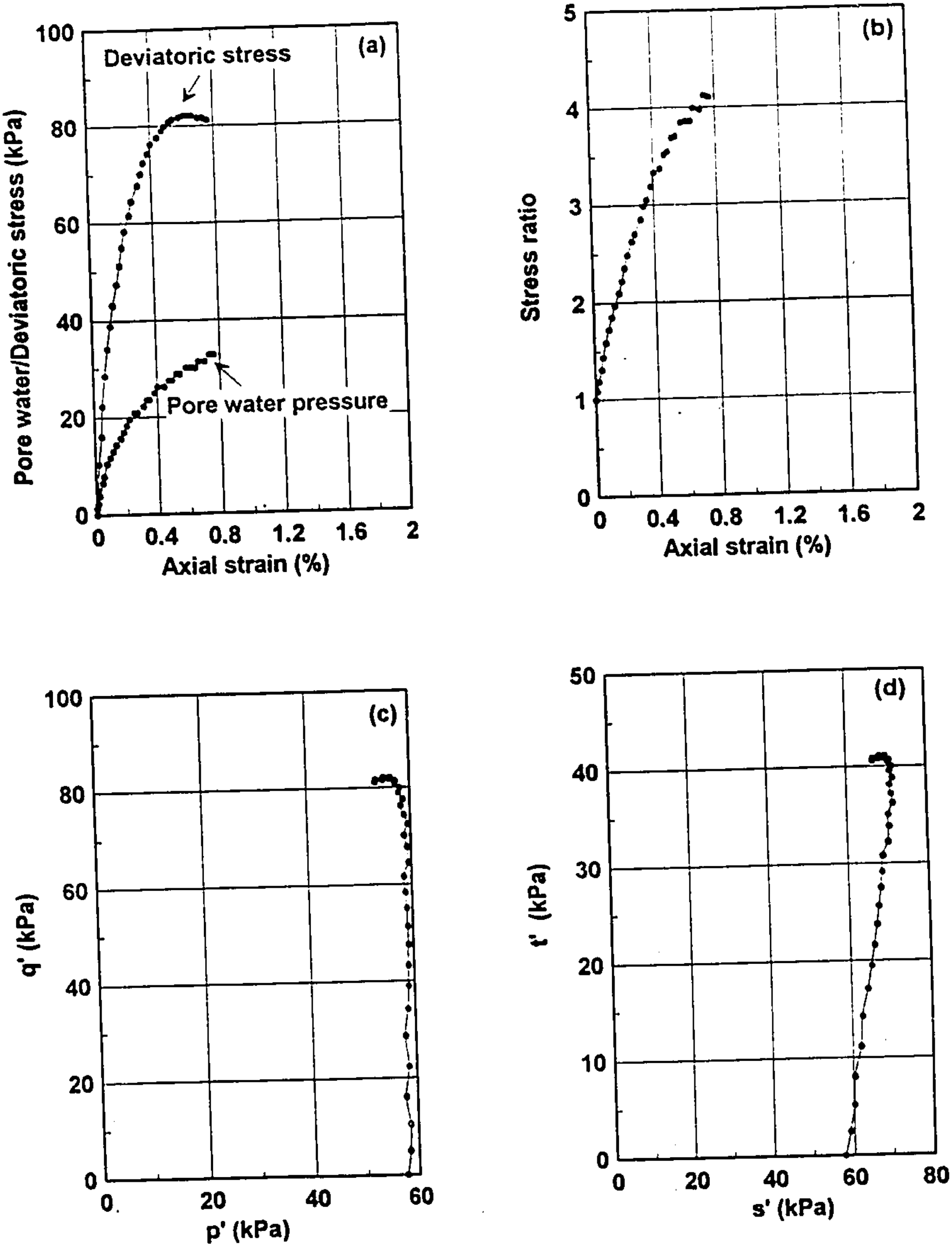

Fig. A.72. CIU multistage triaxial compression test: Sample No. SB360MT (Stage 3).

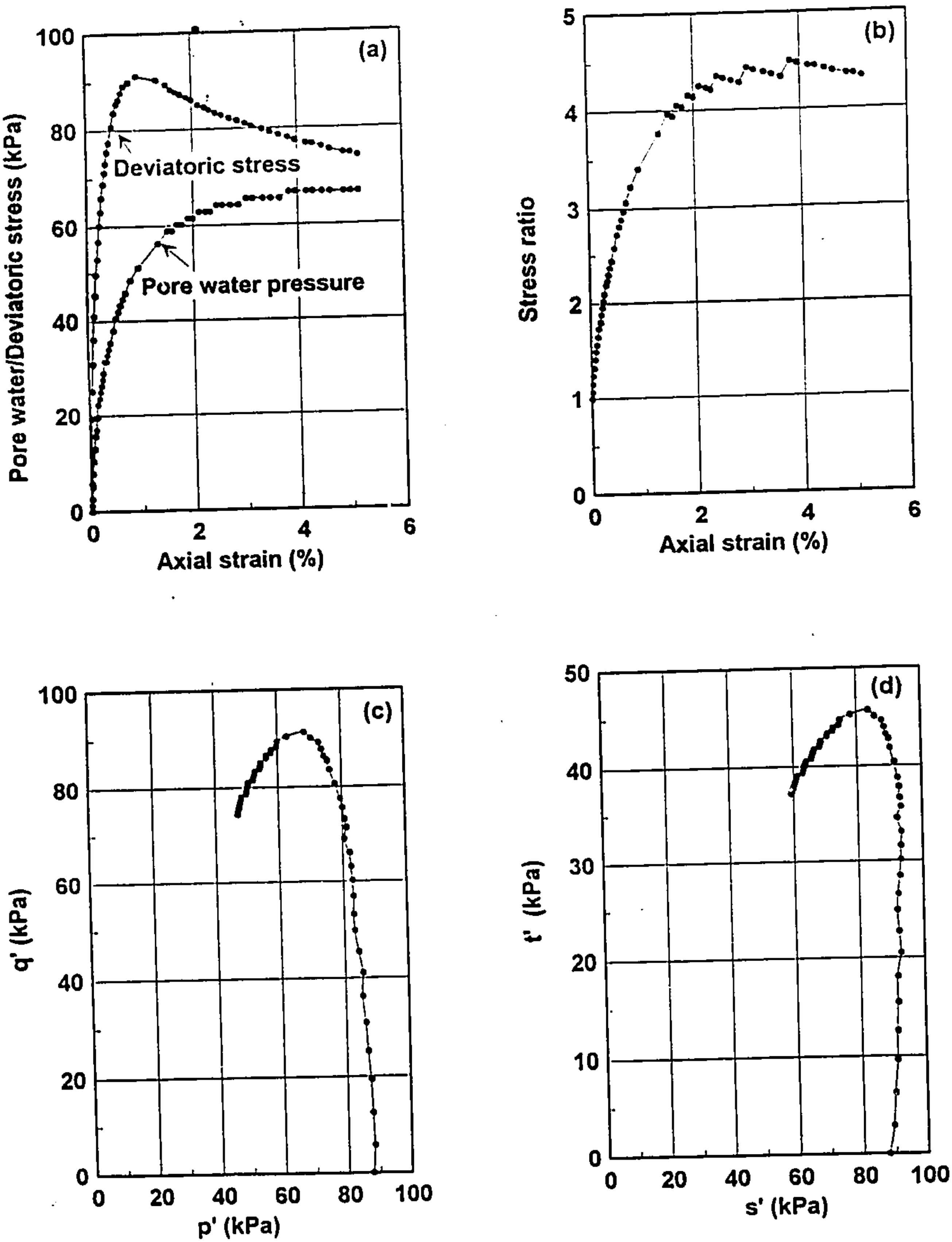

Fig. A.73. CIU multistage triaxial compression test: Sample No. SB360MT (Stage 4).

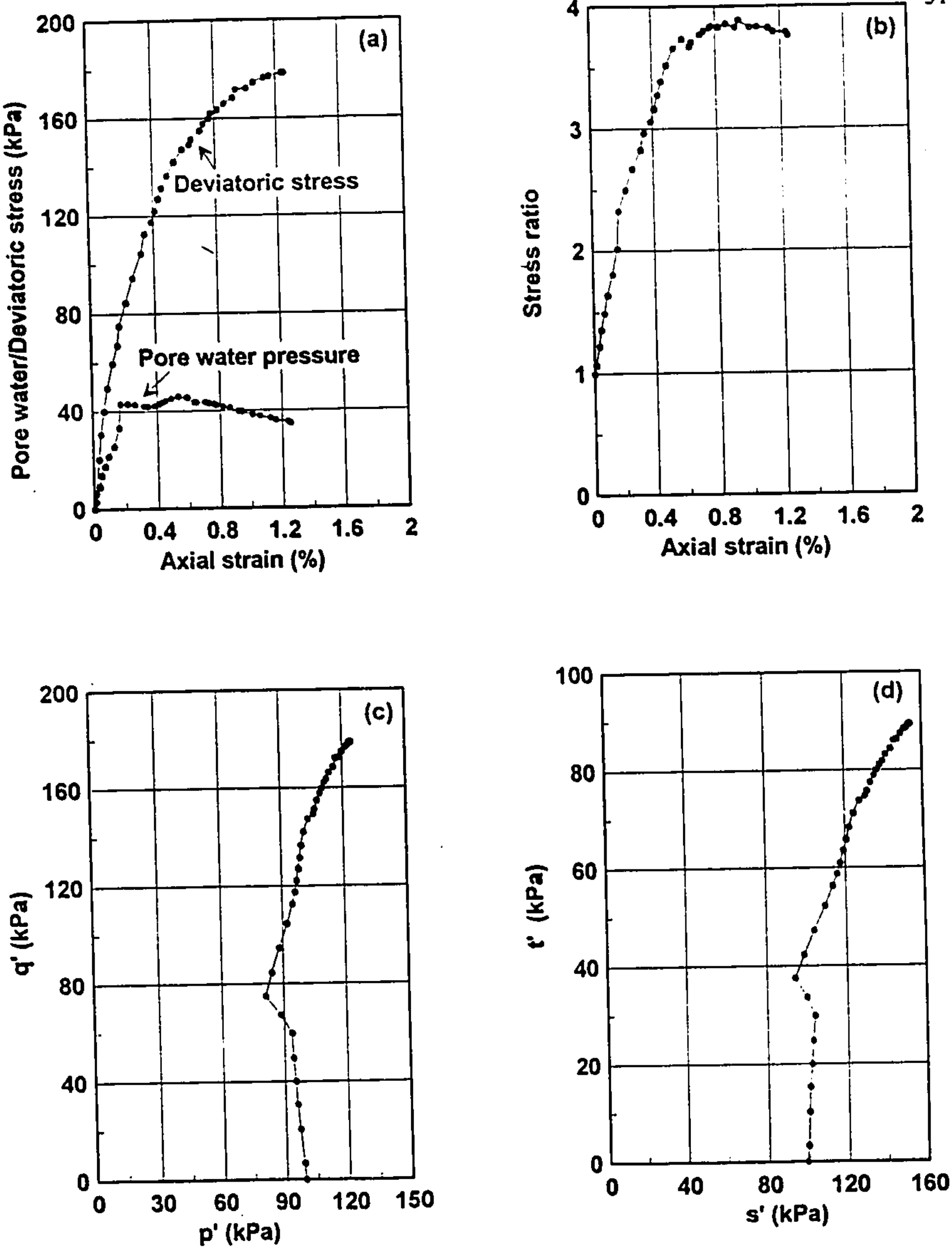

Fig. A.74. CIU multistage triaxial compression test: Sample No. RMDMT1 (Stage 1).

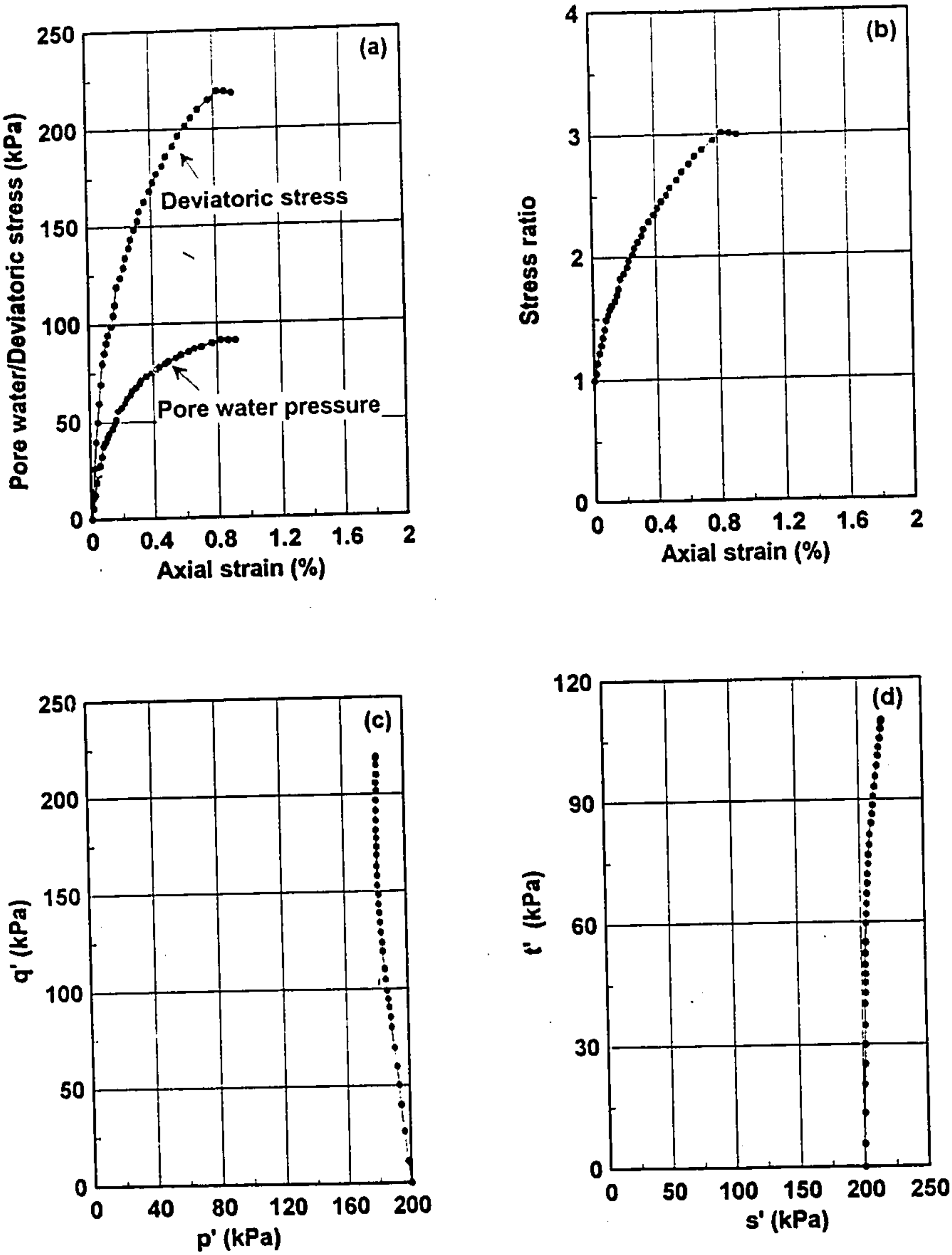

Fig. A.75. CIU multistage triaxial compression test: Sample No. RMDMT1 (Stage 2).

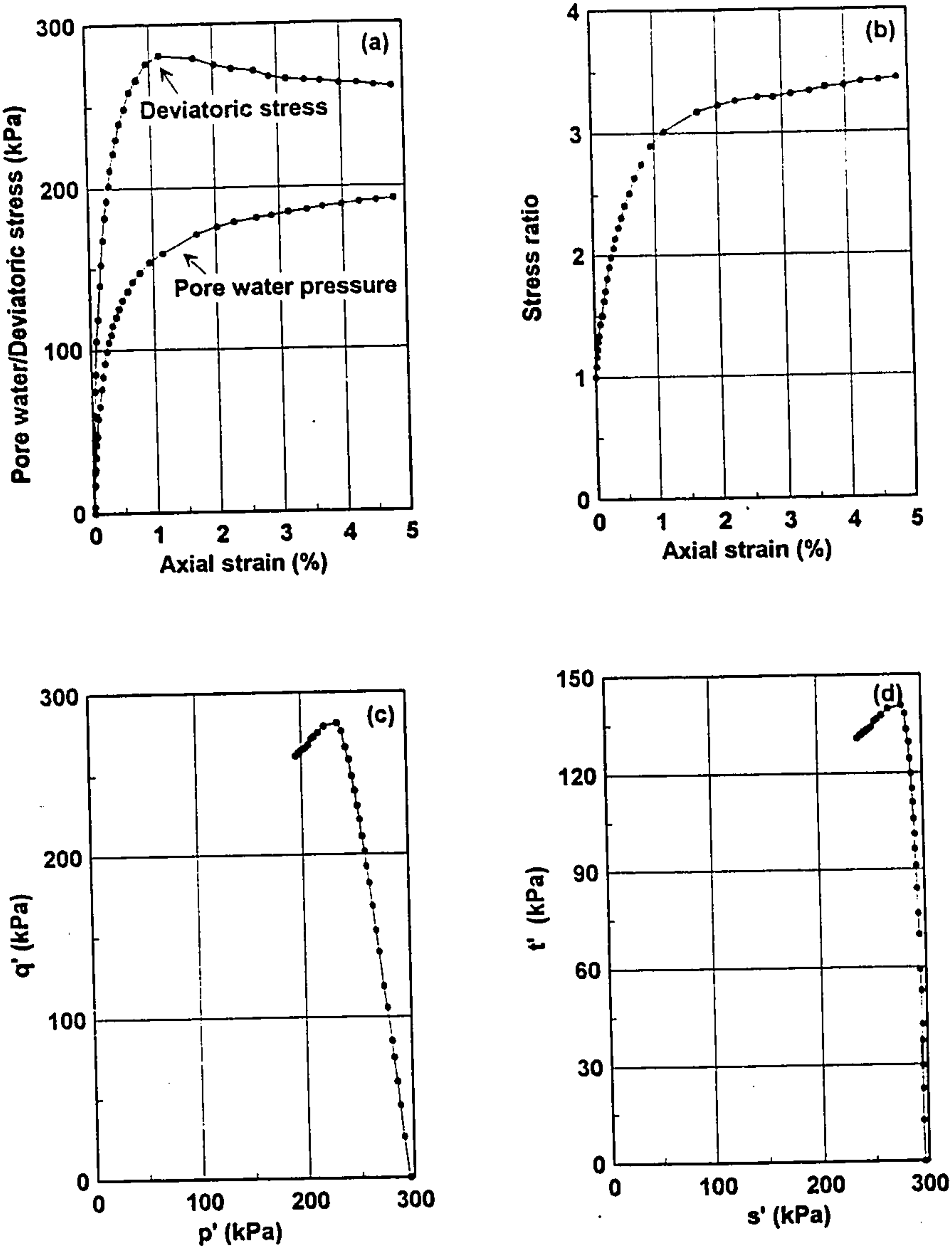

Fig. A.76. CIU multistage triaxial compression test: Sample No. RMDMT1 (Stage 3).

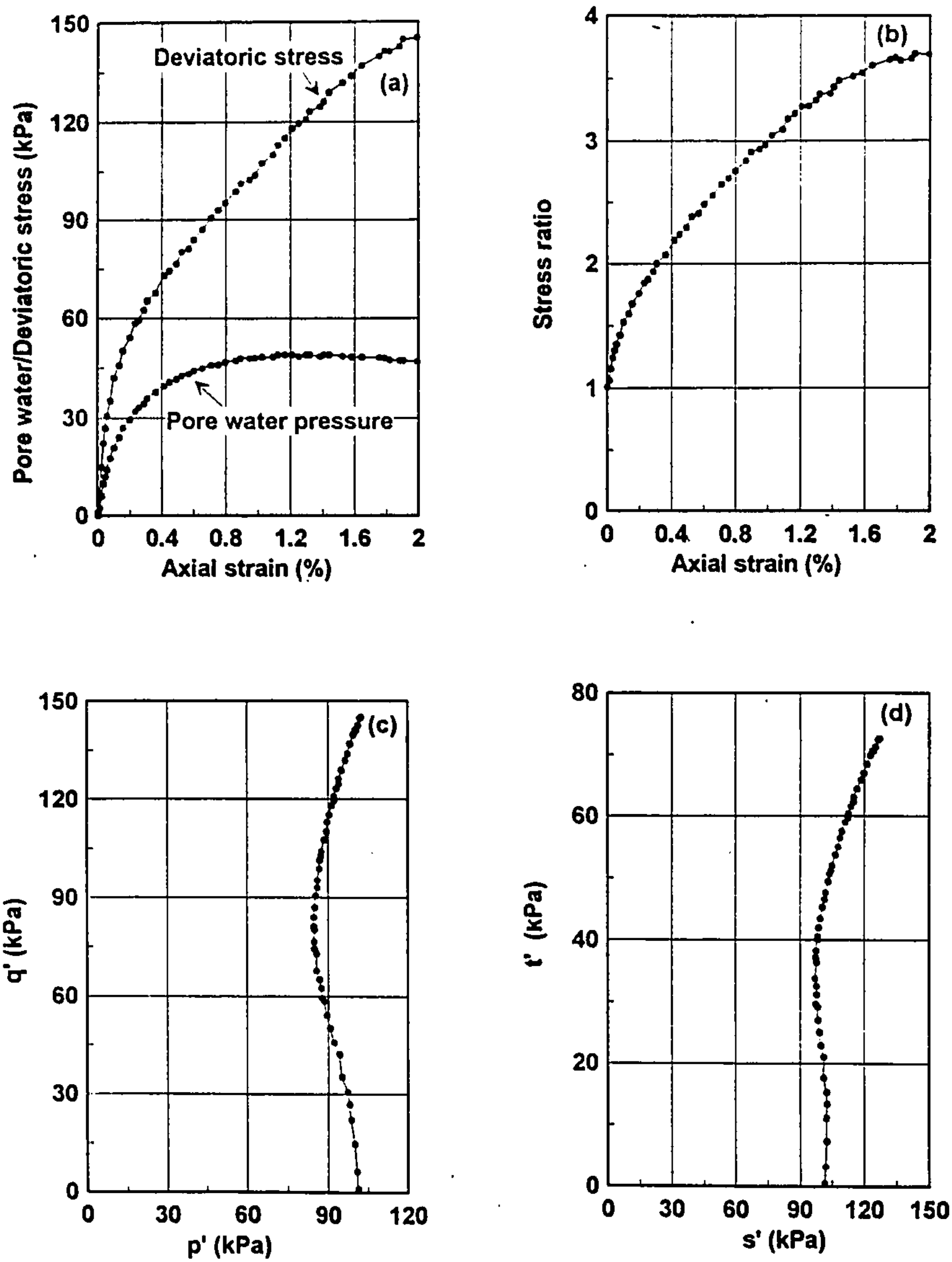

Fig. A.77. CIU multistage triaxial compression test: Sample No. RMDMT2 (Stage 1).

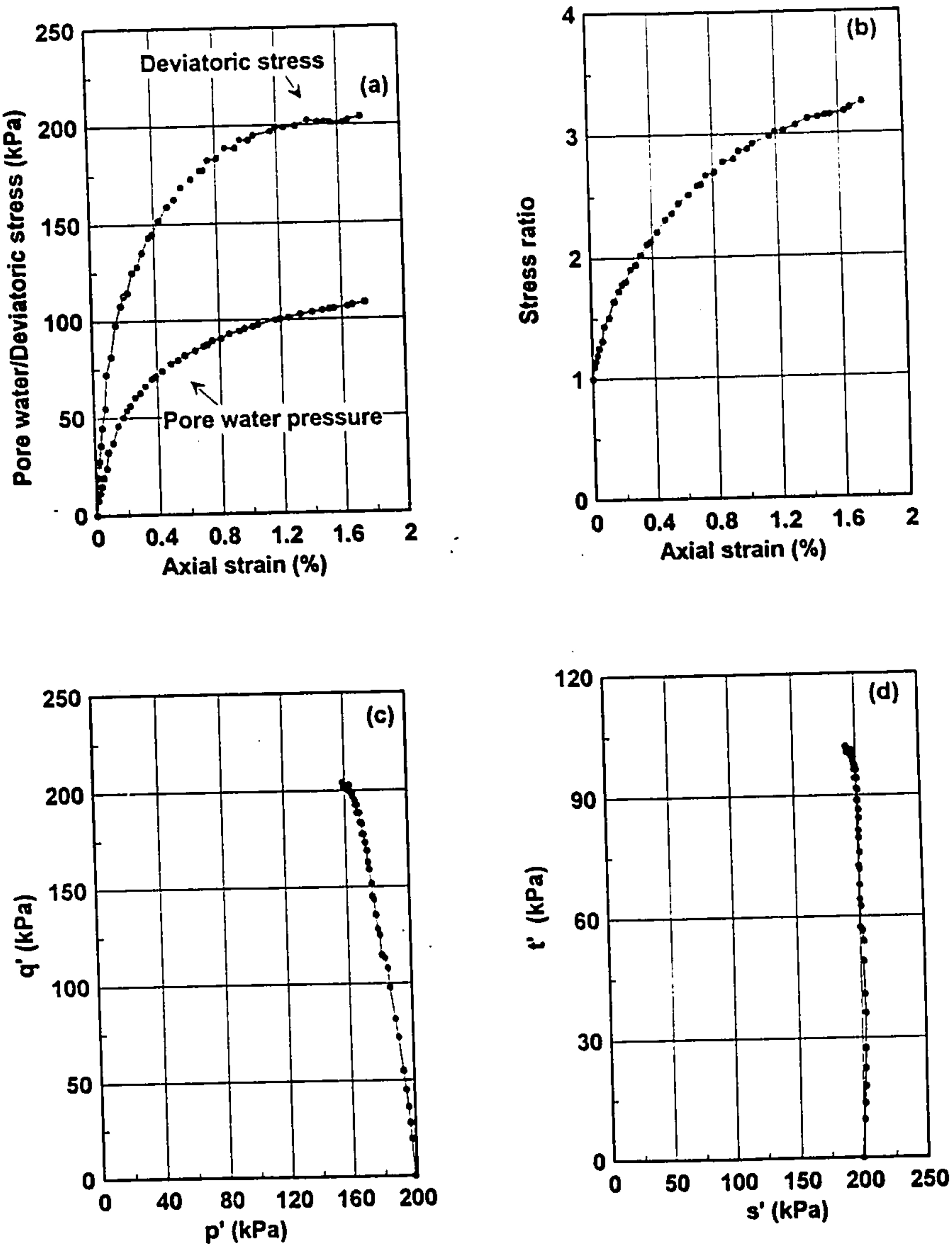

Fig. A.78. CIU multistage triaxial compression test: Sample No. RMDMT2 (Stage 2).

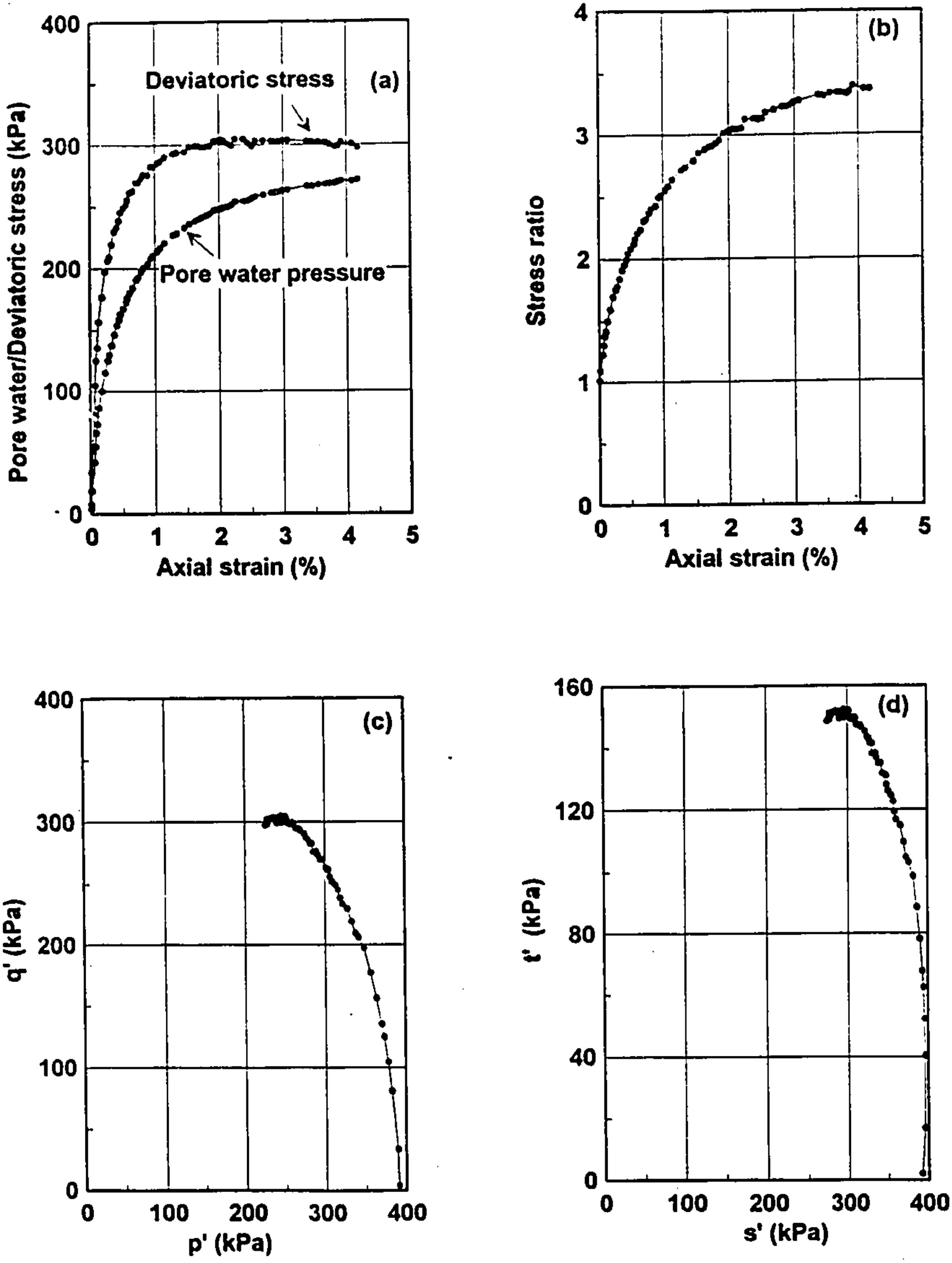

Fig. A.79. CIU multistage triaxial compression test: Sample No. RMDMT2 (Stage 3).

APPENDIX B

PLOTS OF CONSOLIDATION TEST RESULTS

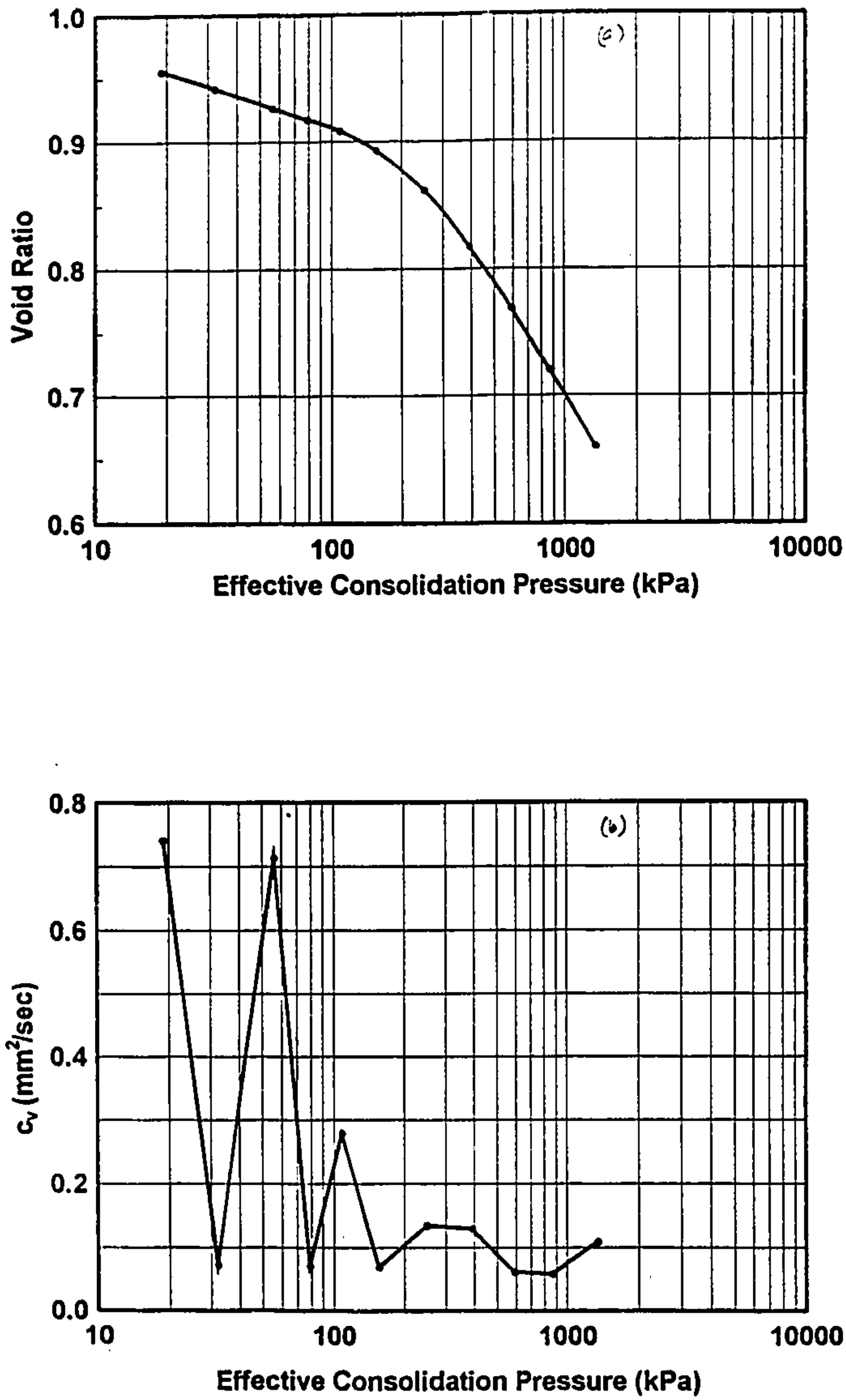

Fig. B.1. Results of oedometer consolidation test for vertical samples (Depth = 1.00 m).

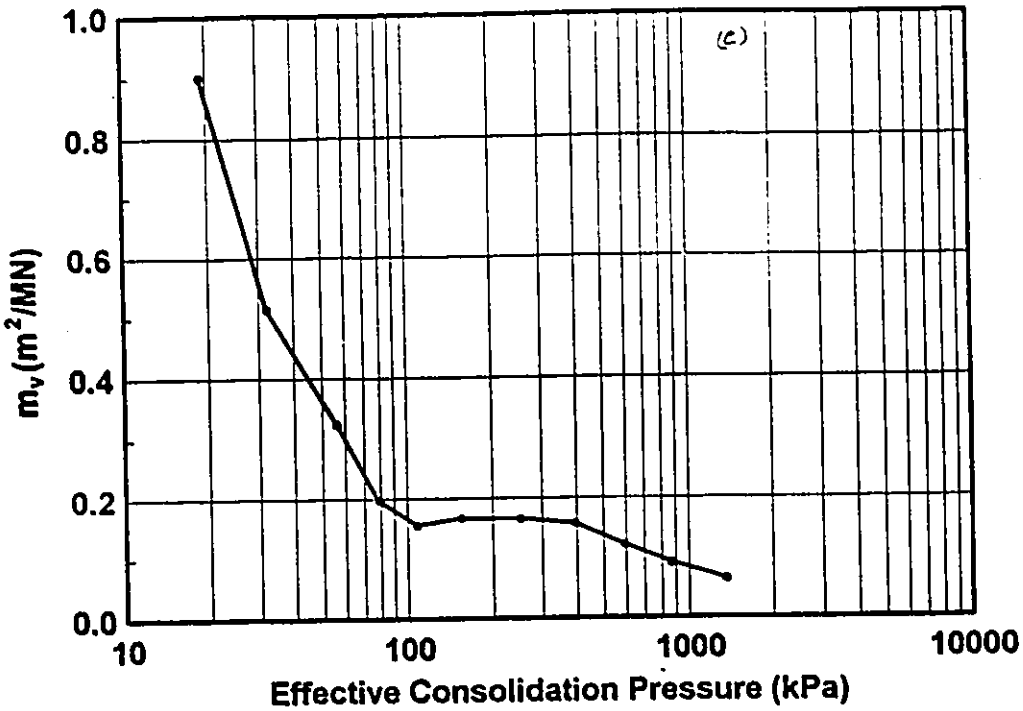

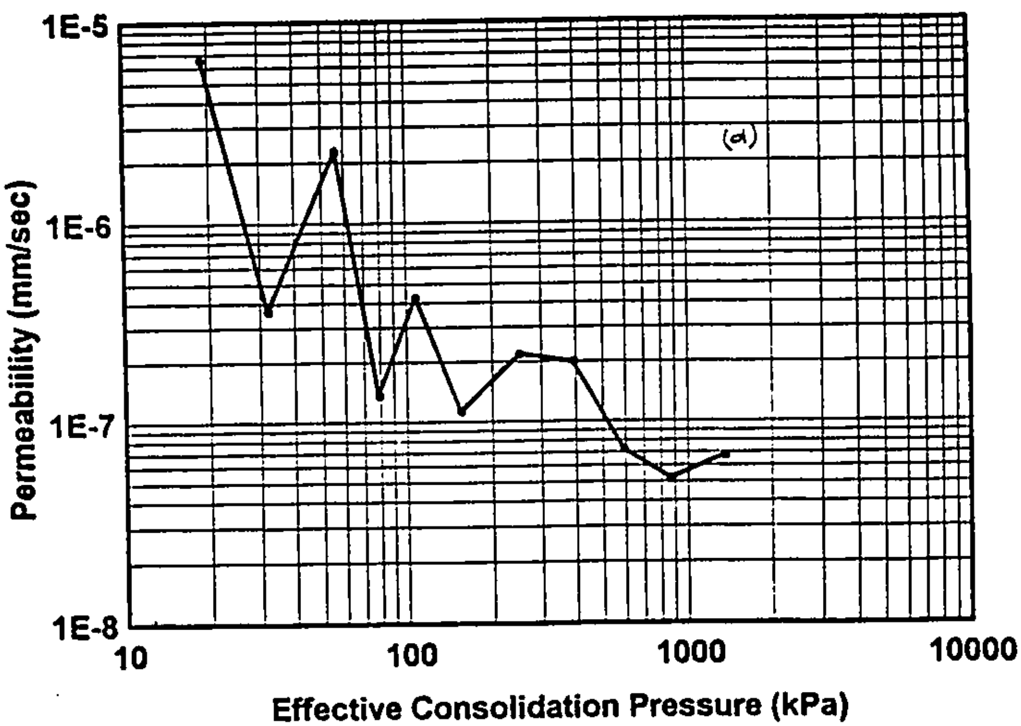

Fig. B.1. Results of oedometer consolidation test for vertical samples (Depth = 1.00 m).

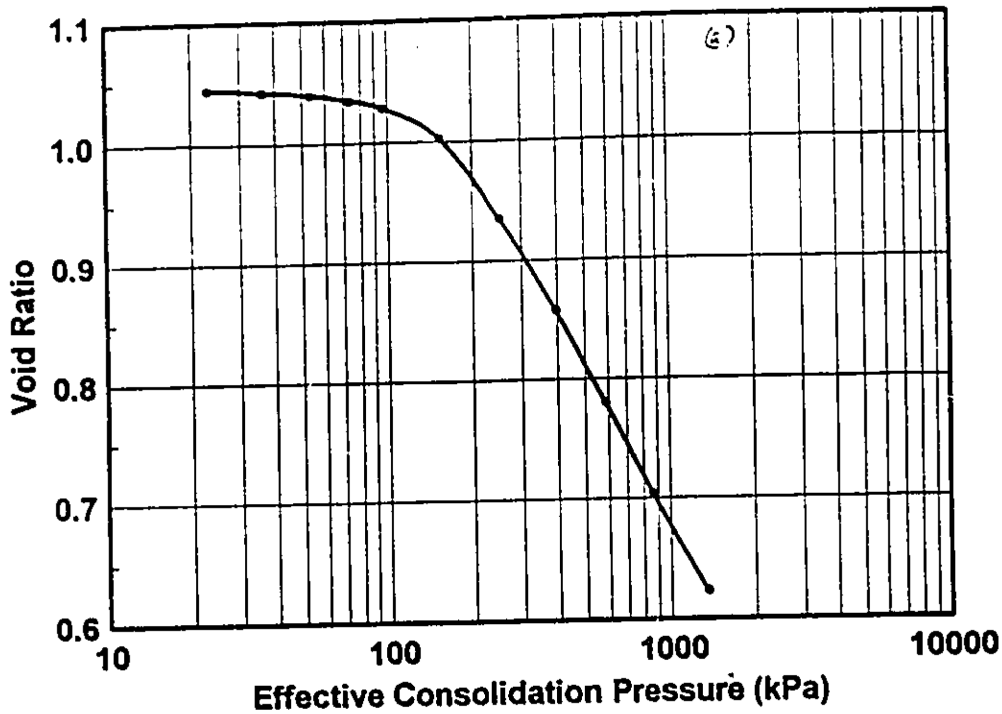

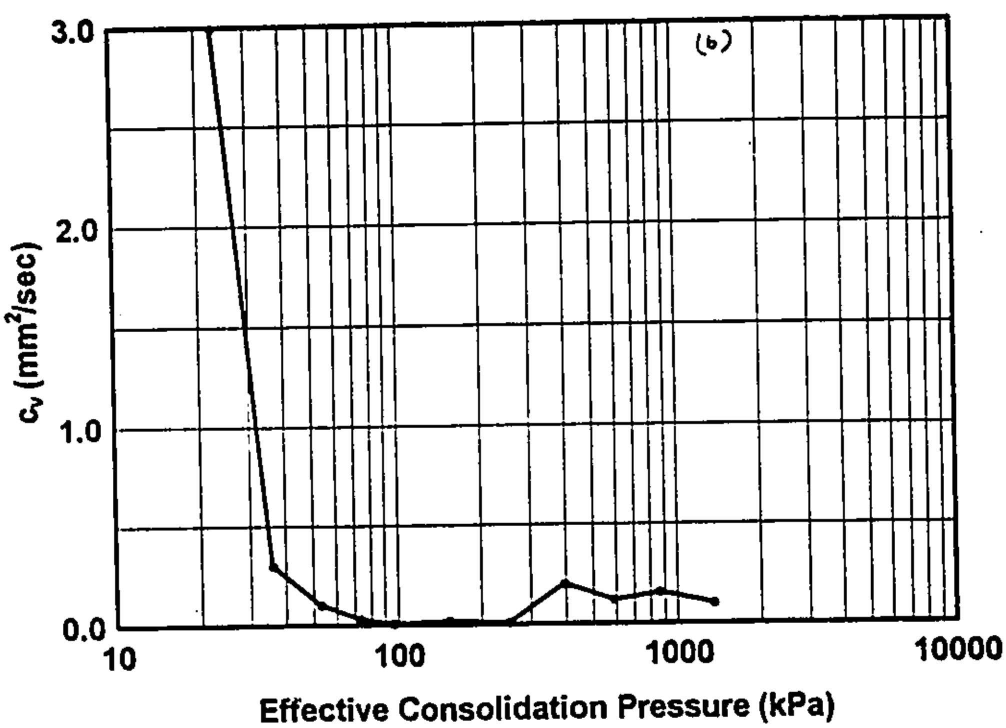

Fig. B.2. Results of oedometer consolidation test for vertical samples (Depth = 1.80 m).

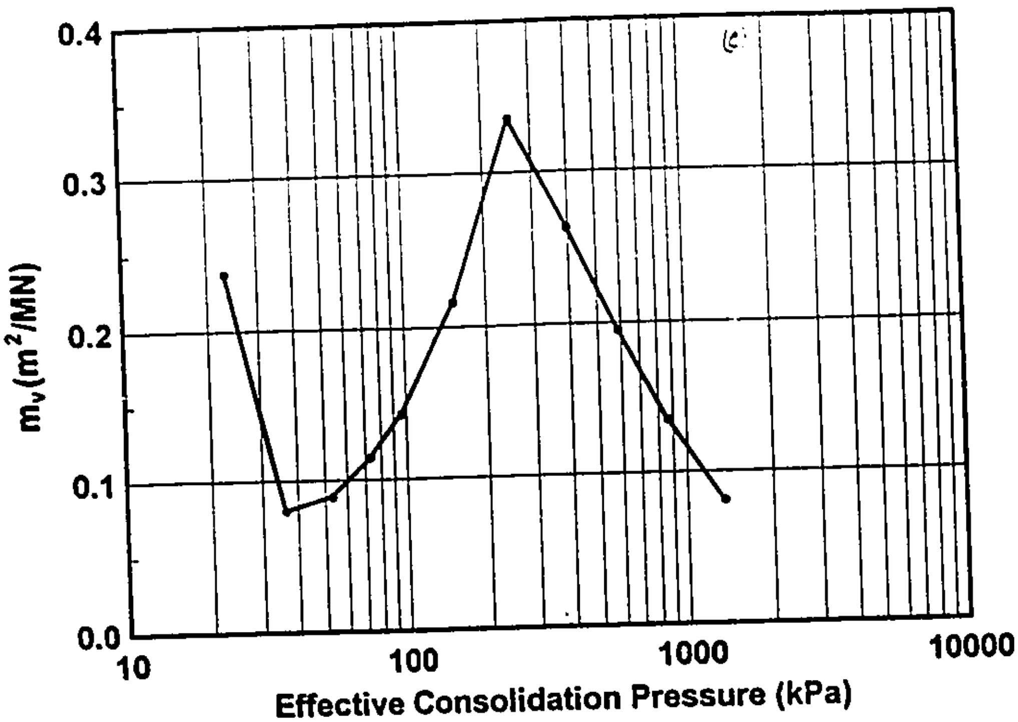

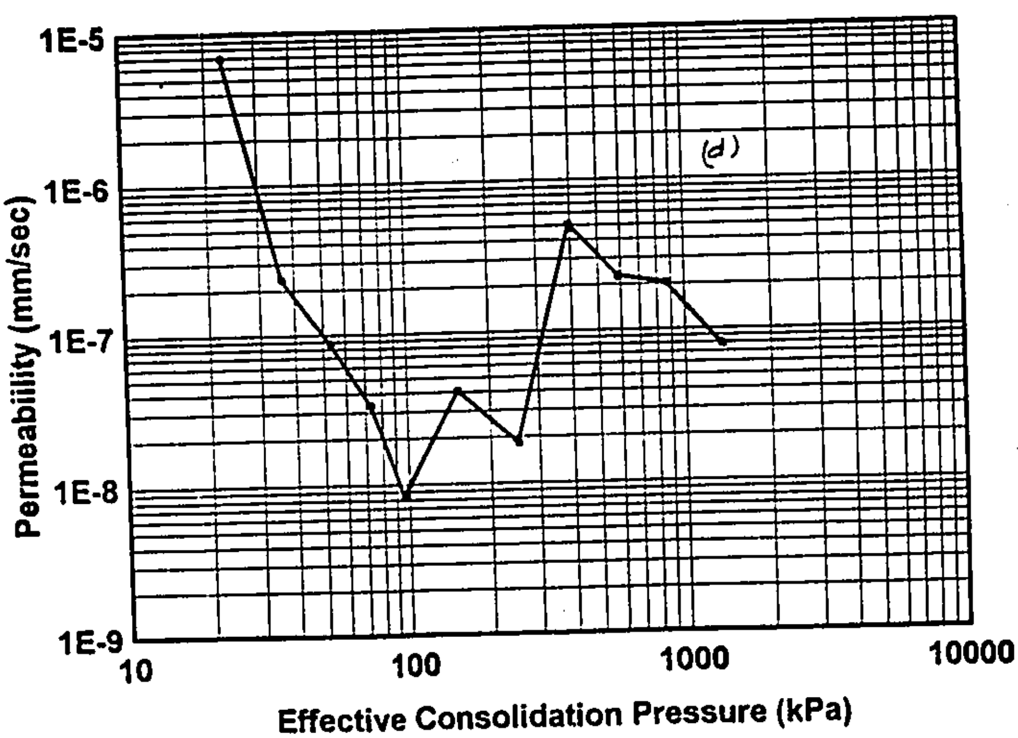

Fig. B.2. Results of oedometer consolidation test for vertical samples (Depth = 1.80 m).

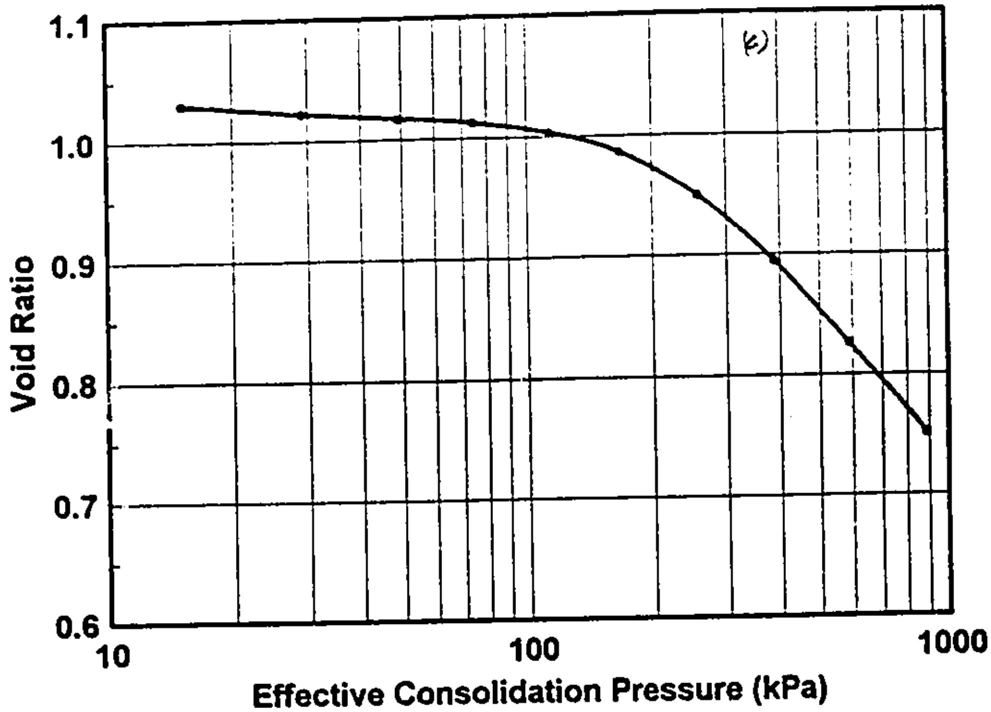

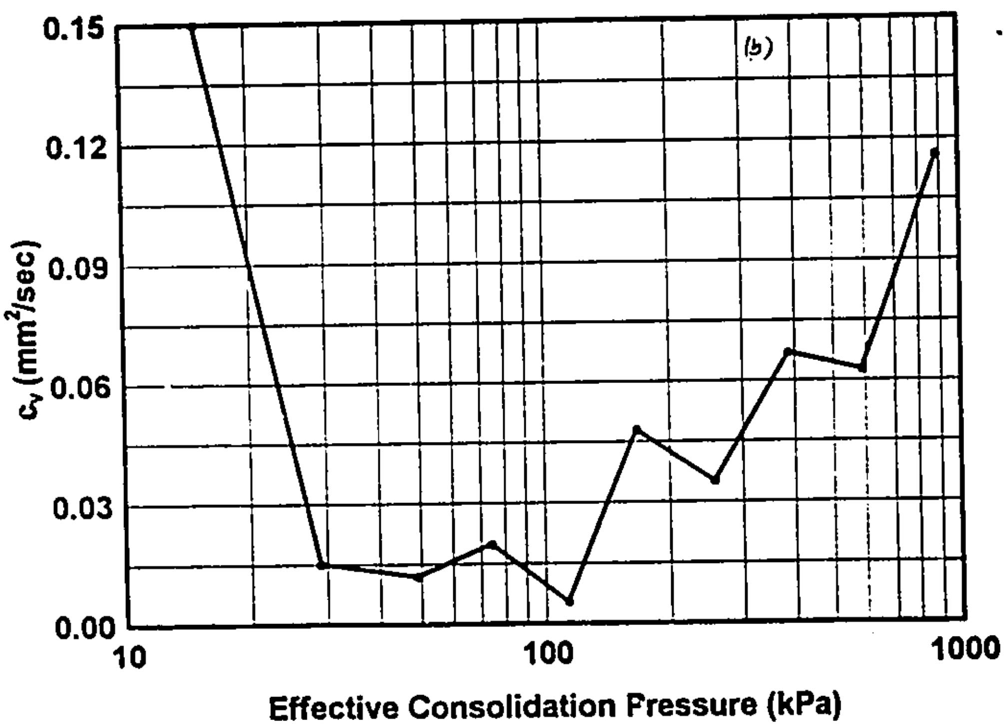

Fig. B.3. Results of oedometer consolidation test for vertical samples (Depth = 1.96 m).

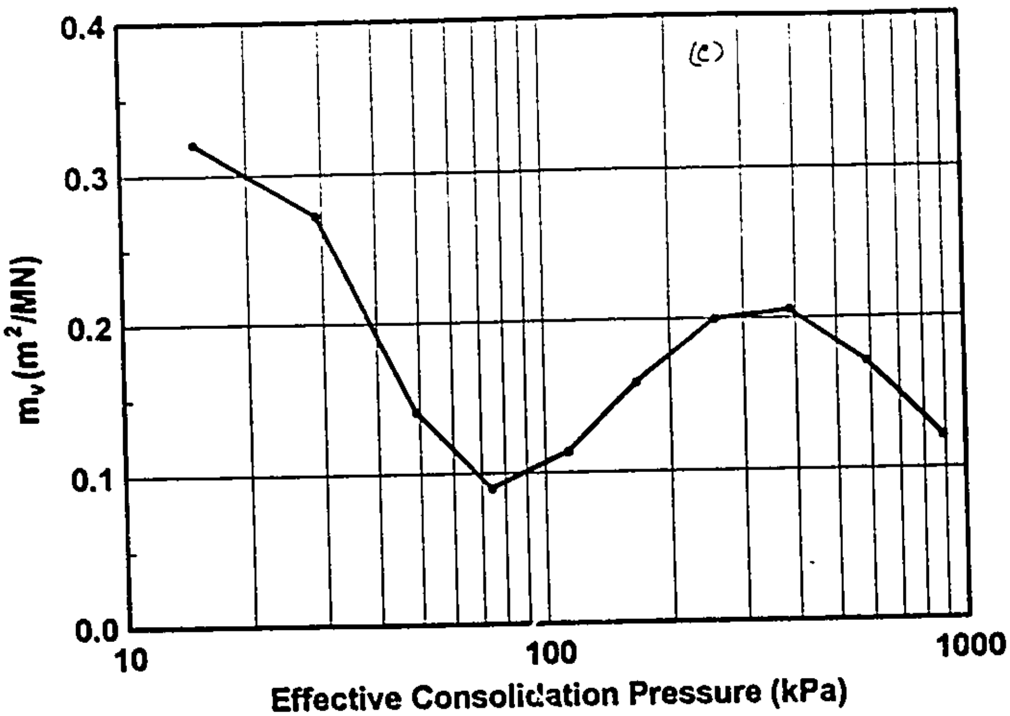

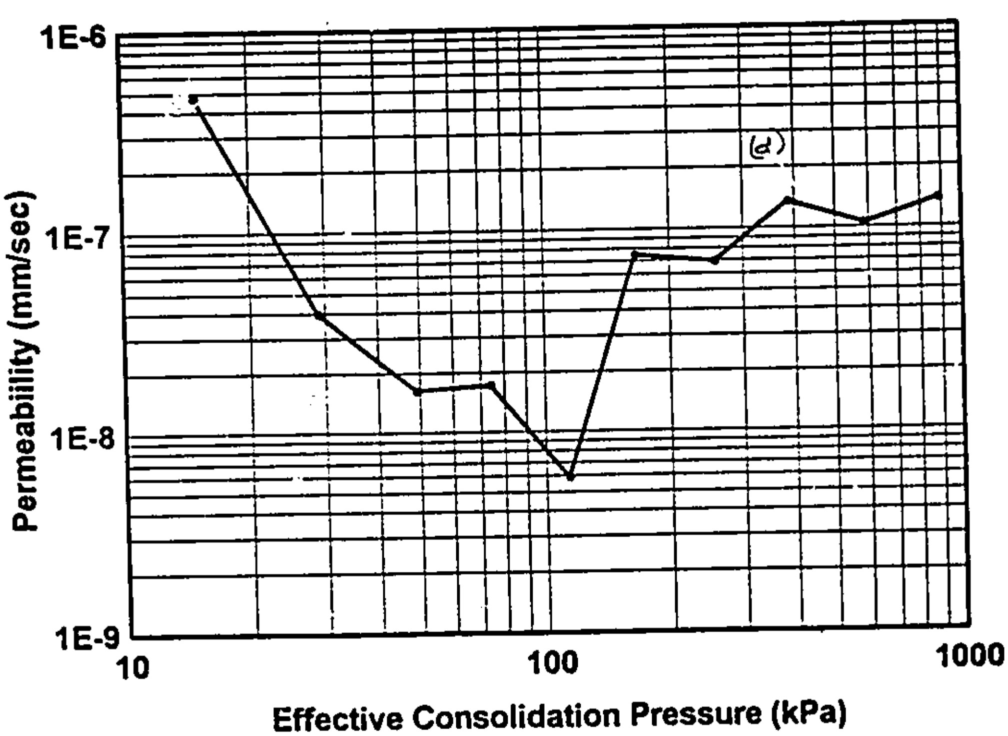

Fig. B.3. Results of oedometer consolidation test for vertical samples (Depth = 1.96 m).

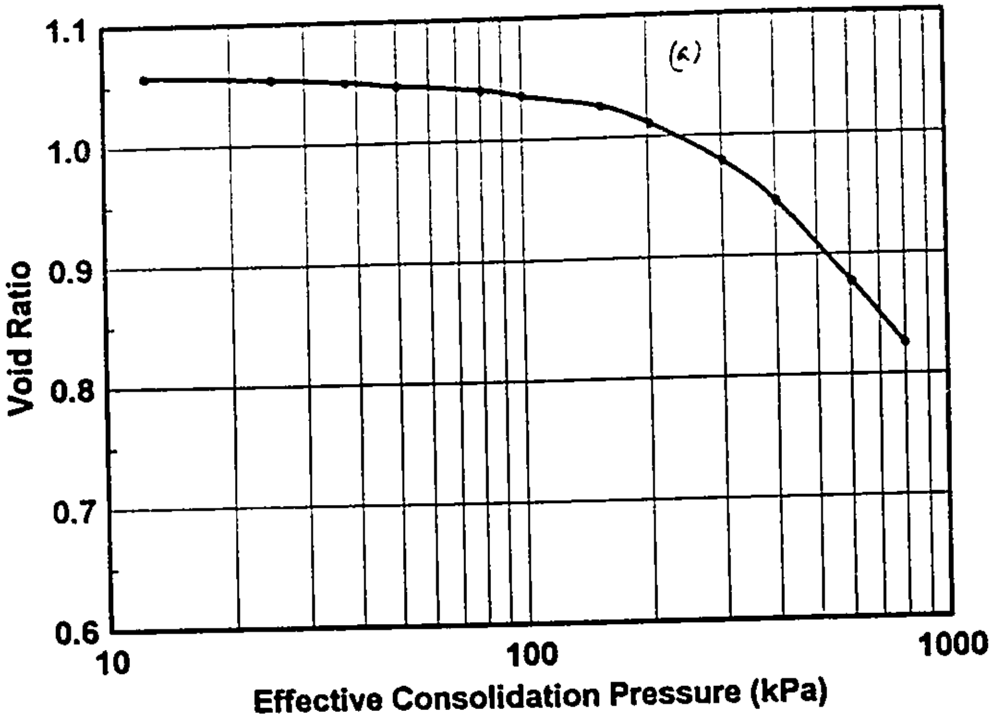

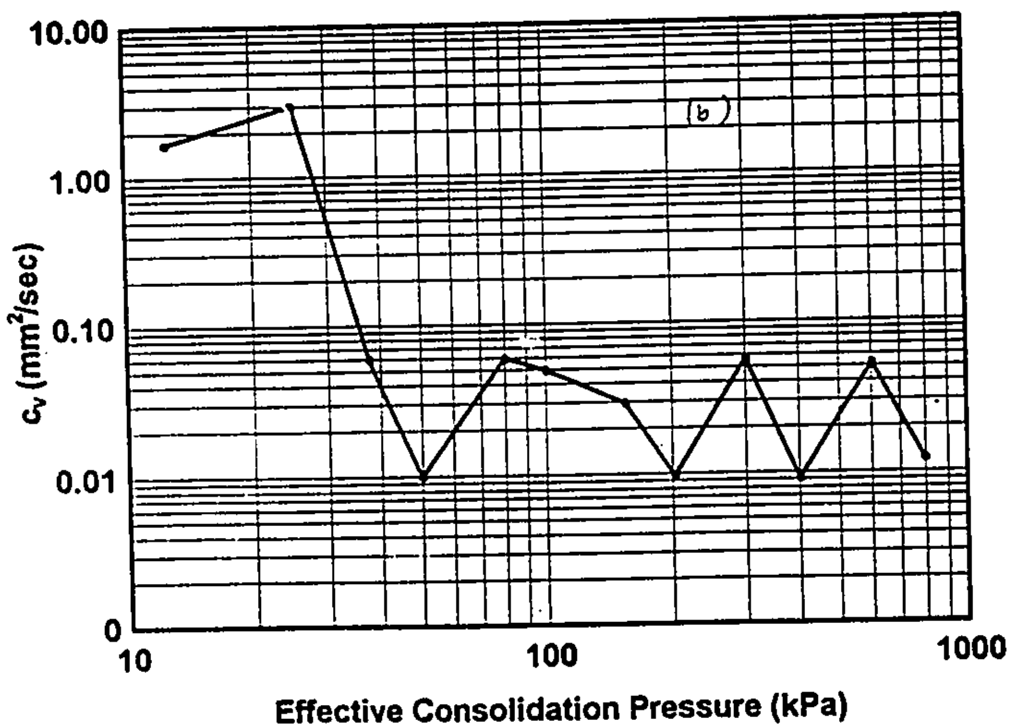

Fig. B.4. Results of oedometer consolidation test for vertical samples (Depth = 2.03 m).

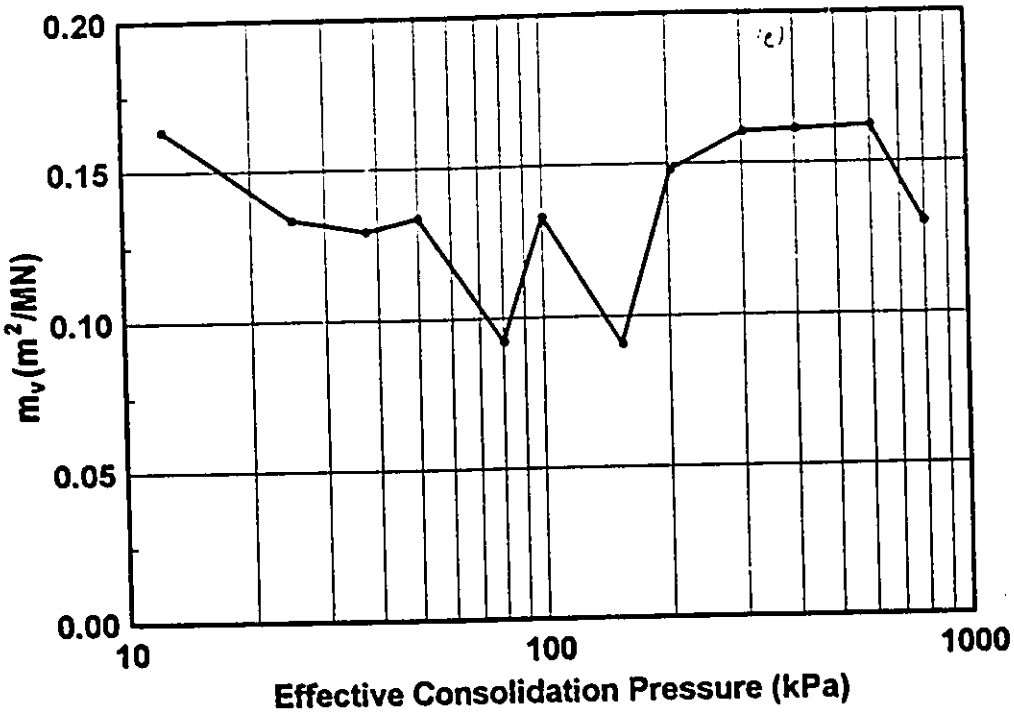

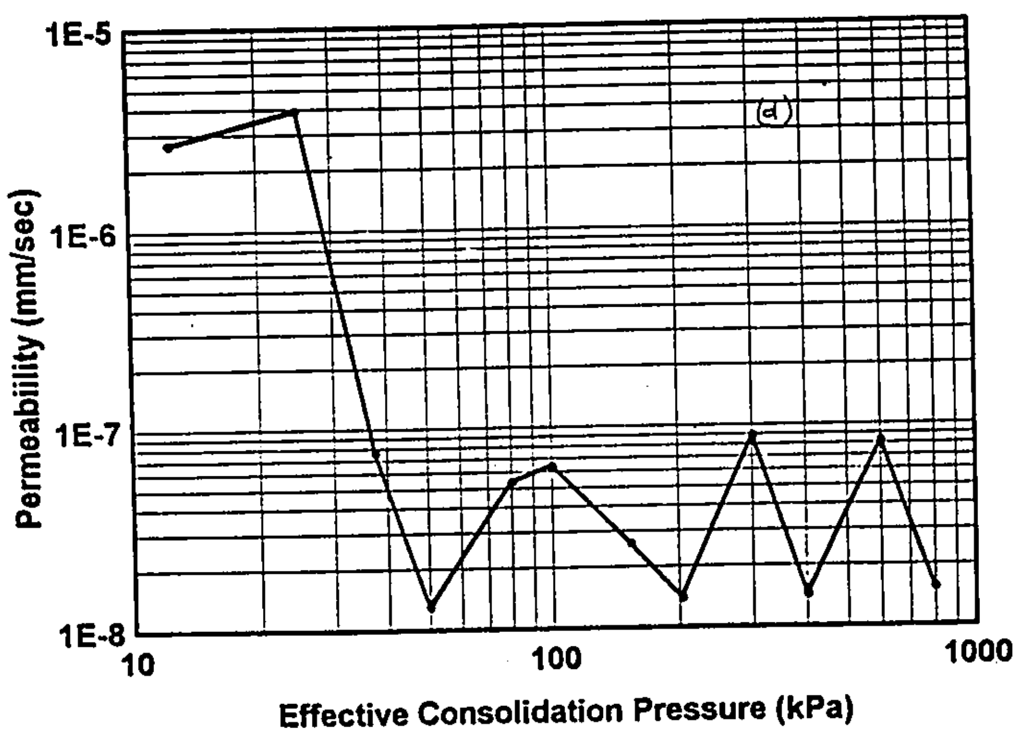

Fig. B.4. Results of oedometer consolidation test for vertical samples (Depth = 2.03 m).

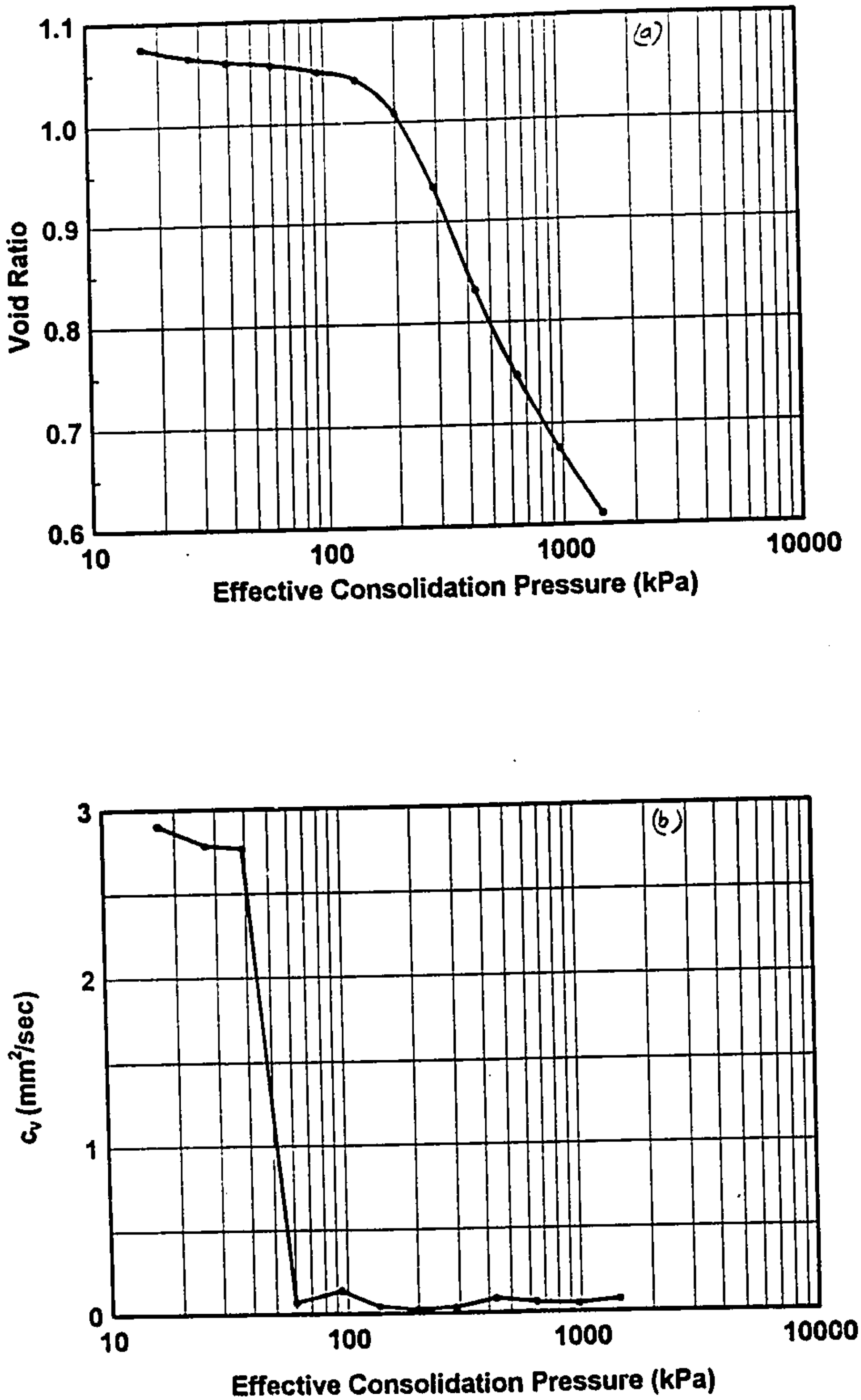

Fig. B.5. Results of oedometer consolidation test for vertical samples (Depth = 2.45 m).

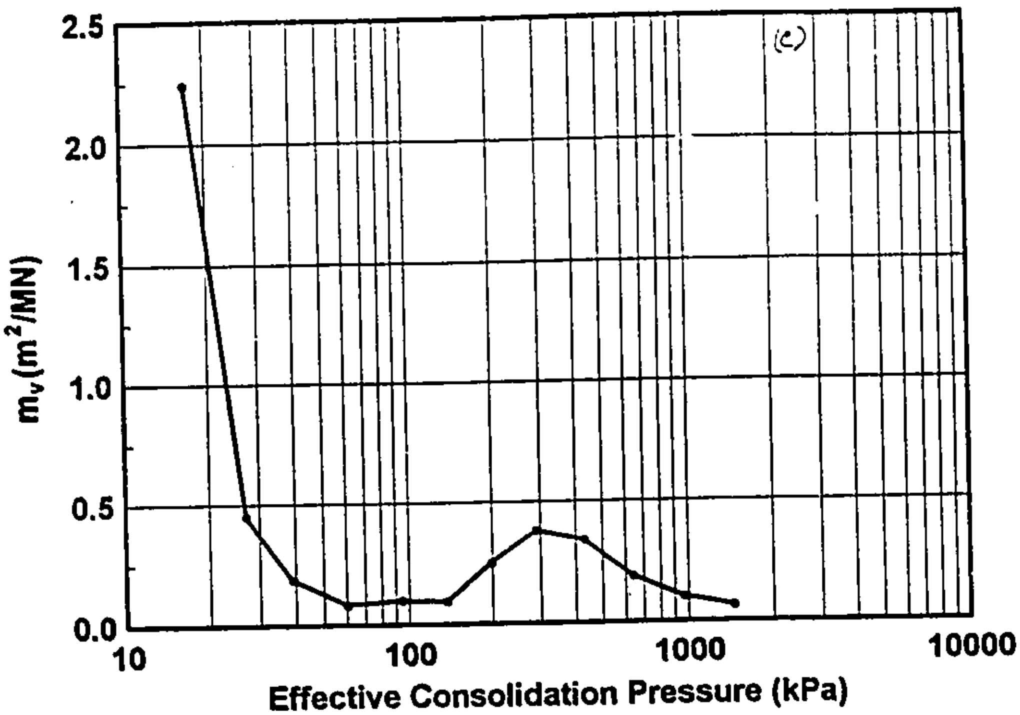

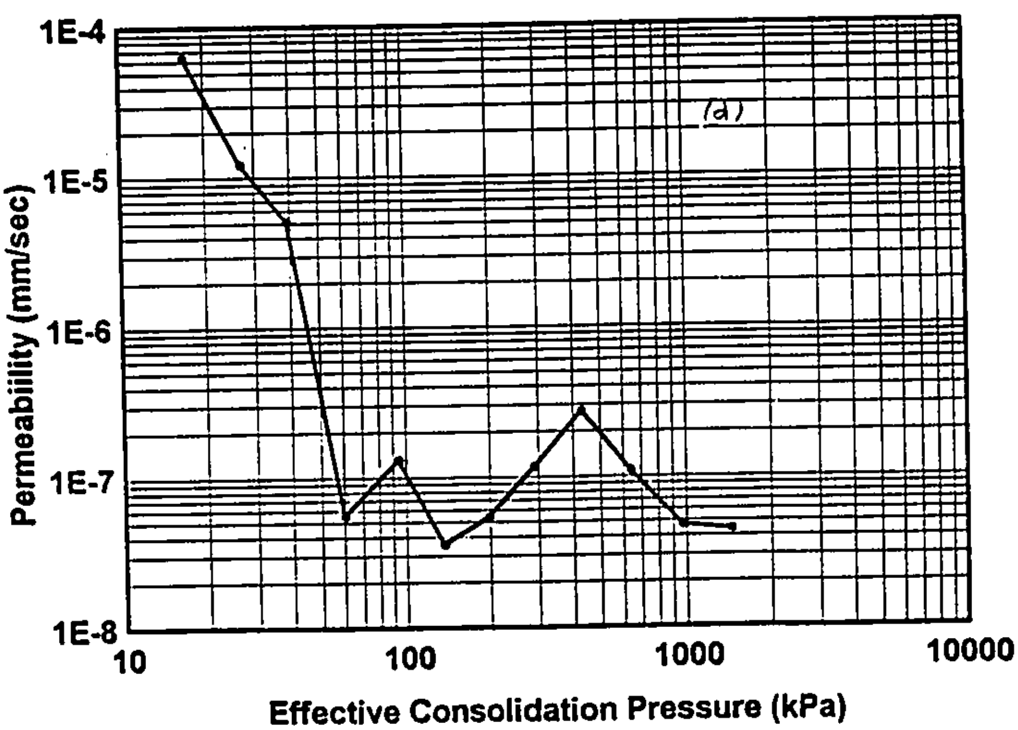

Fig. B.5. Results of oedometer consolidation test for vertical samples (Depth = 2.45 m).

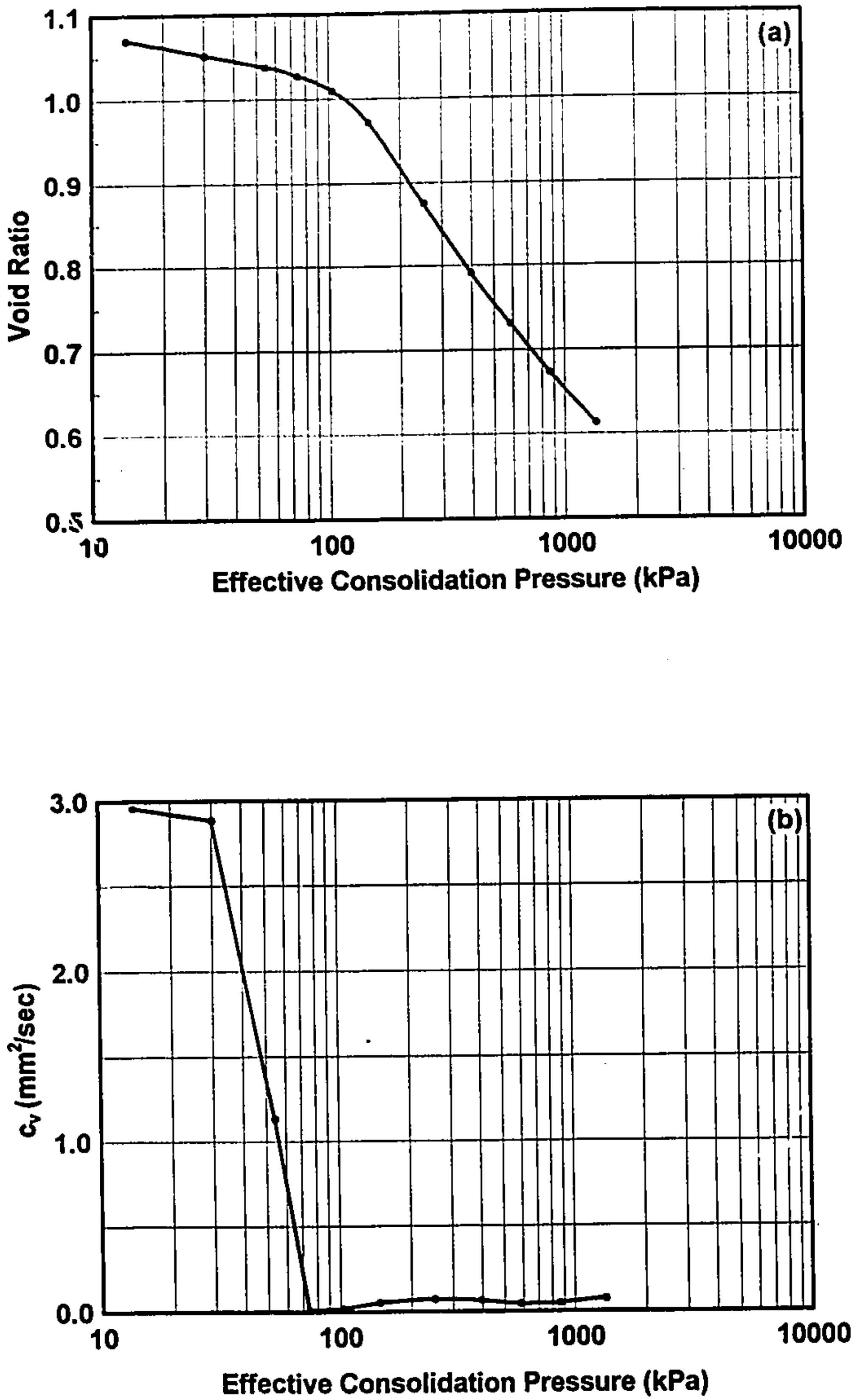

Fig. B.6. Results of oedometer consolidation test for vertical samples (Depth=2.60 m).

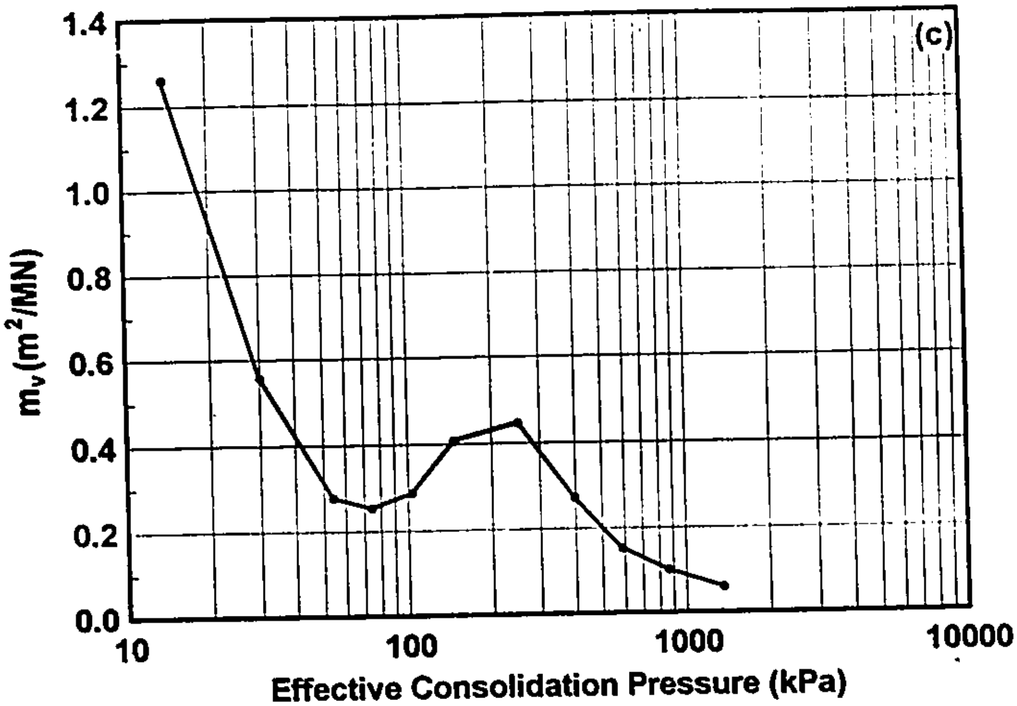

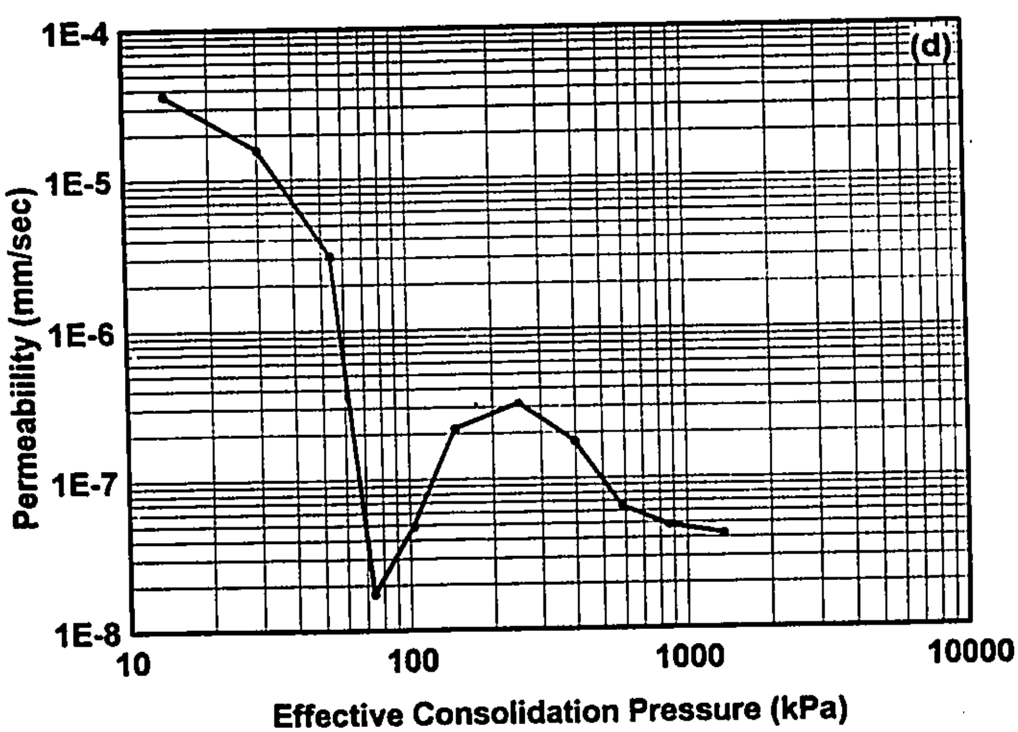

Fig. B.6. Results of oedometer consolidation test for vertical samples (Depth=2.60 m).

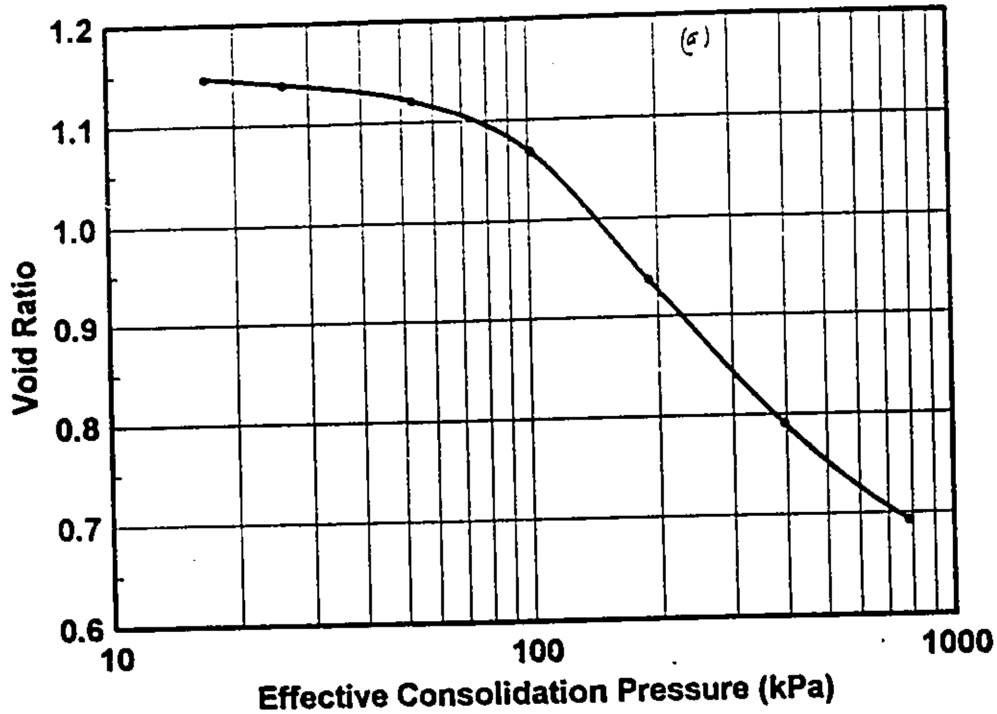

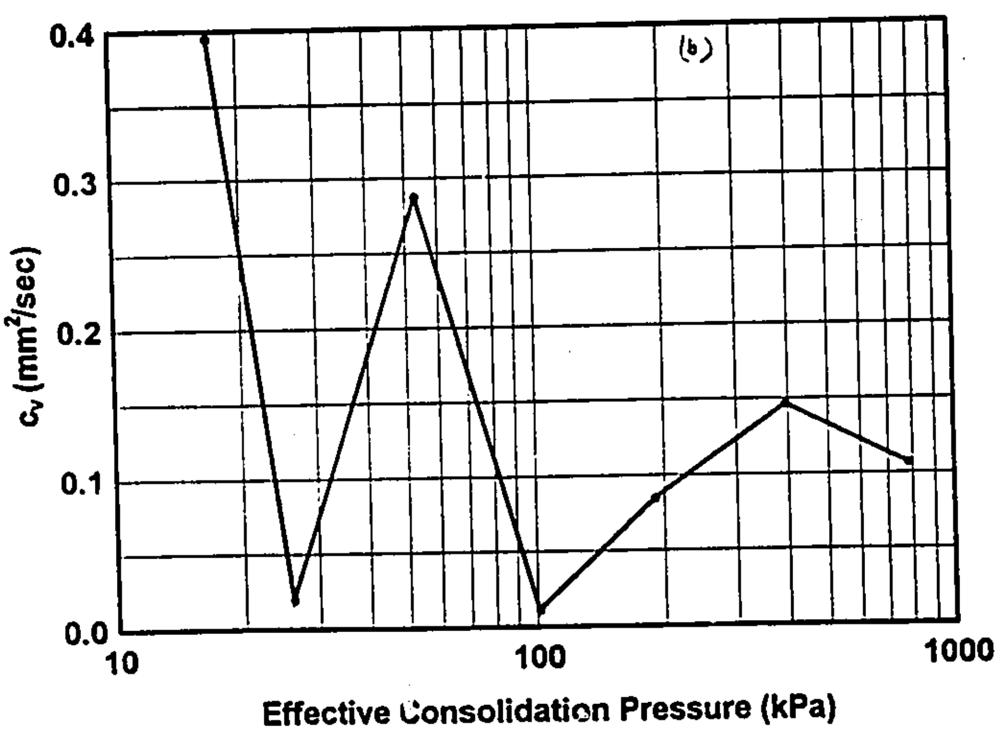

Fig. B.7. Results of oedometer consolidation test for vertical samples (Depth = 3.15 m).

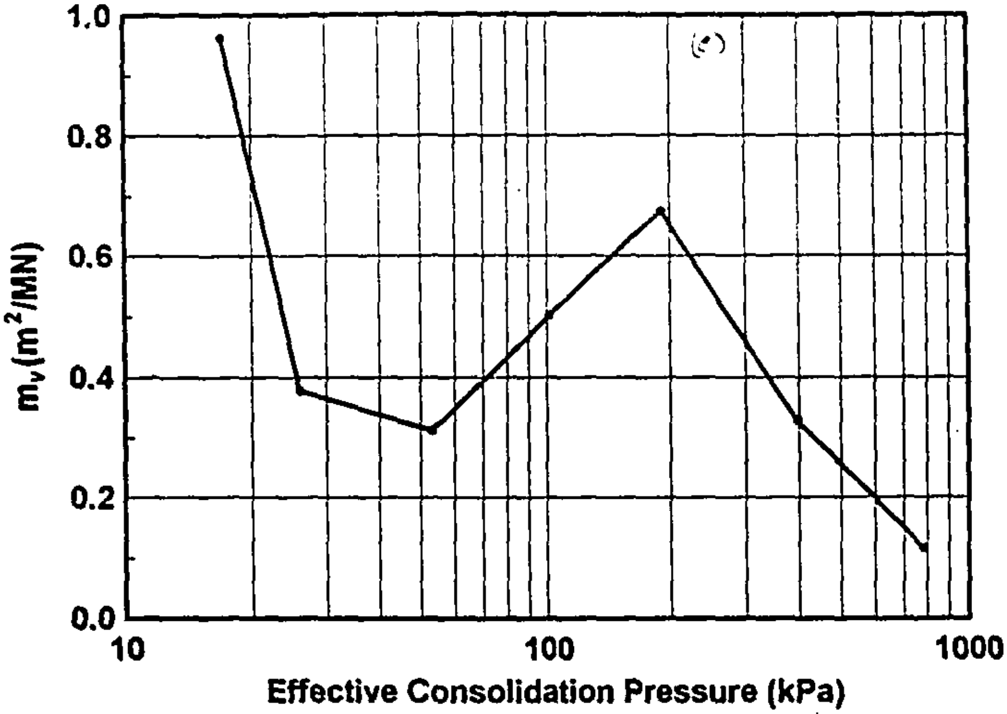

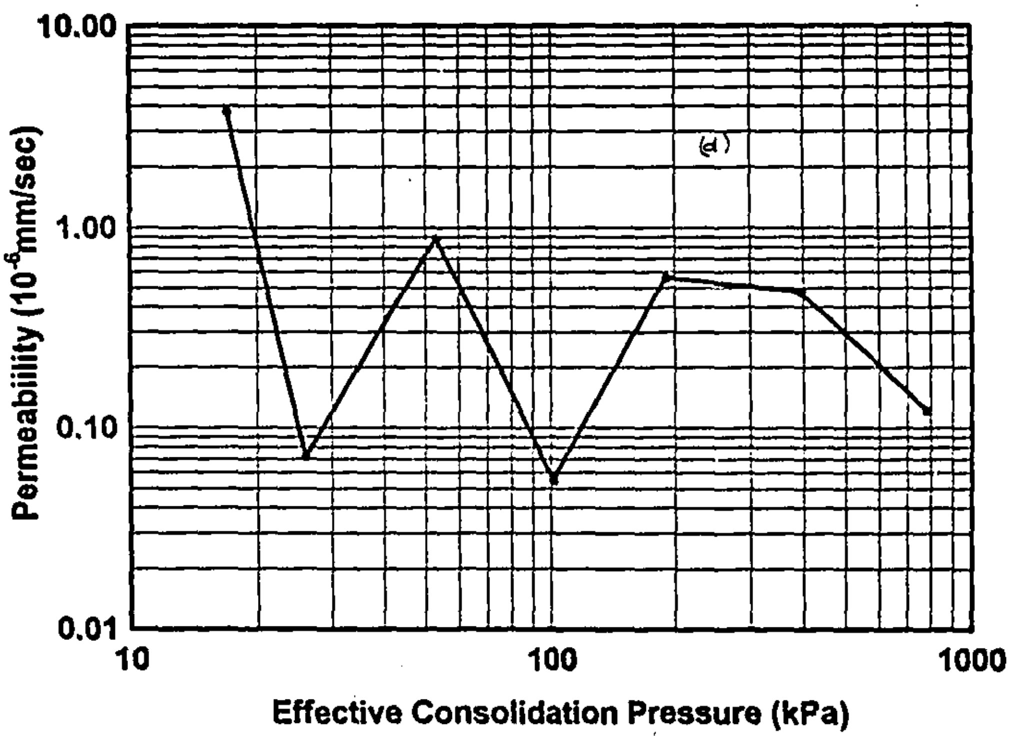

Fig. B.7. Results of oedometer consolidation test for vertical samples (Depth = 3.15 m).

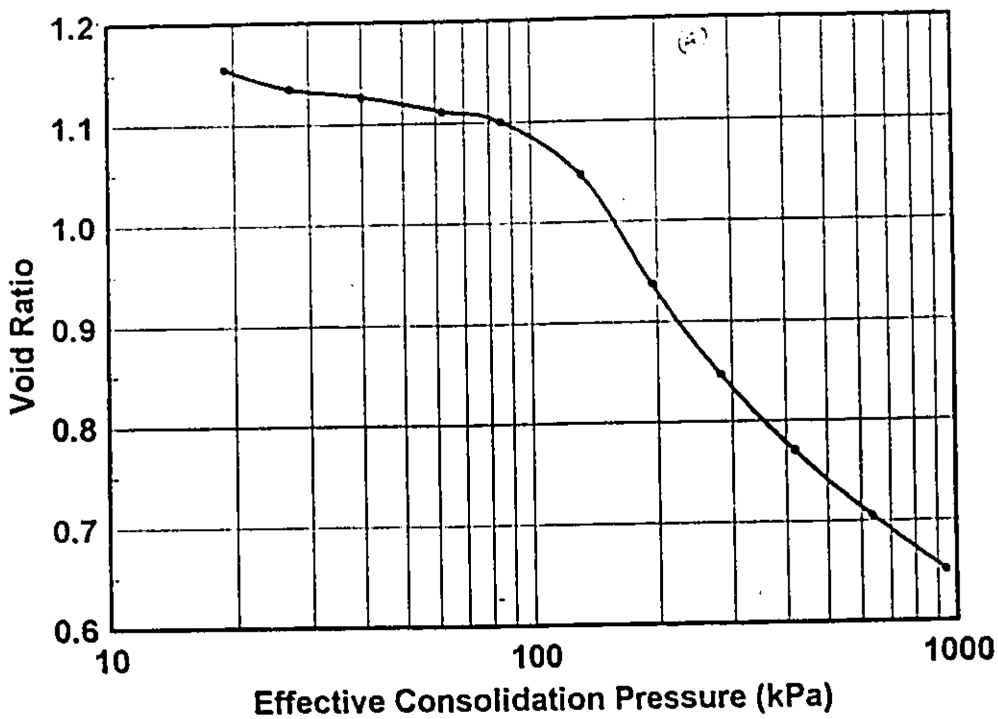

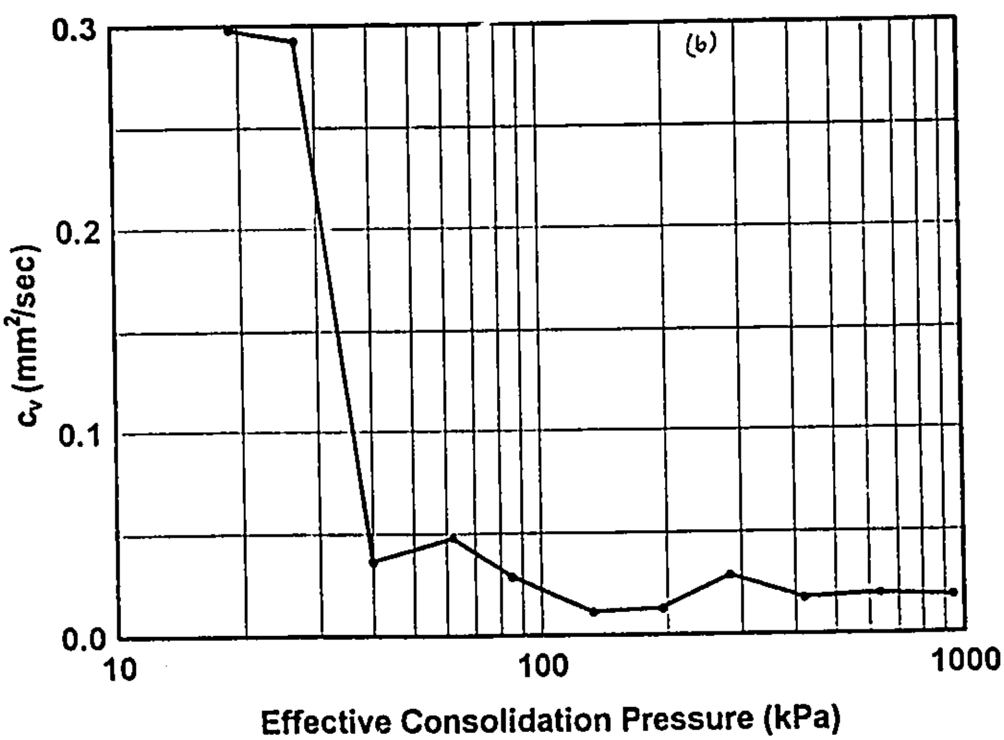

Fig. B.8. Results of oedometer consolidation test for vertical samples (Depth = 3.16 m).

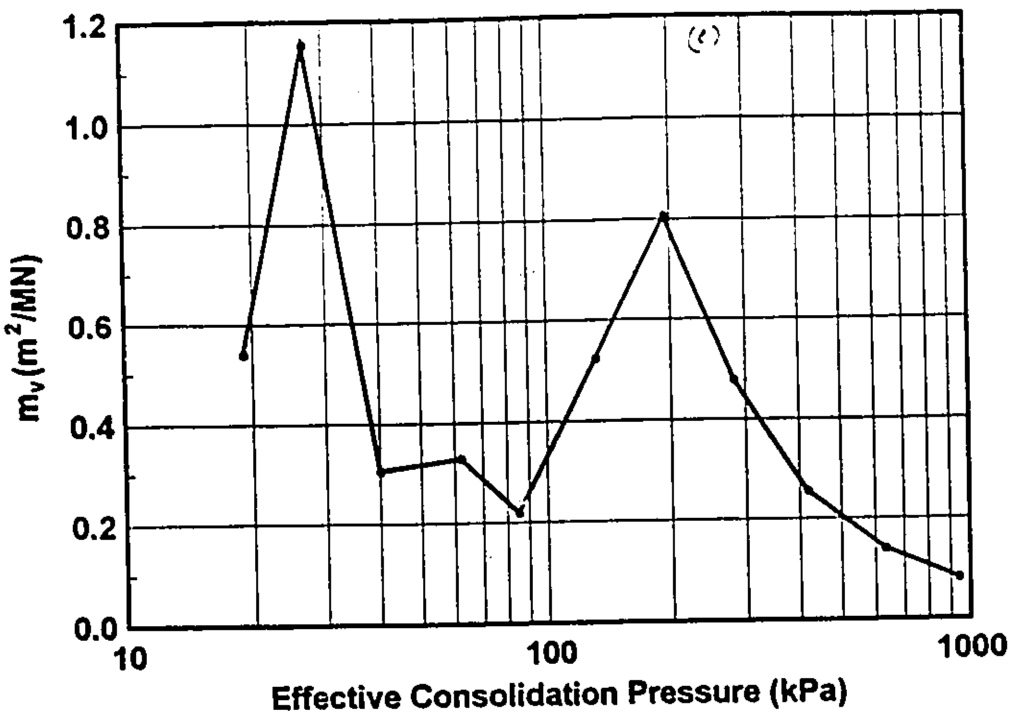

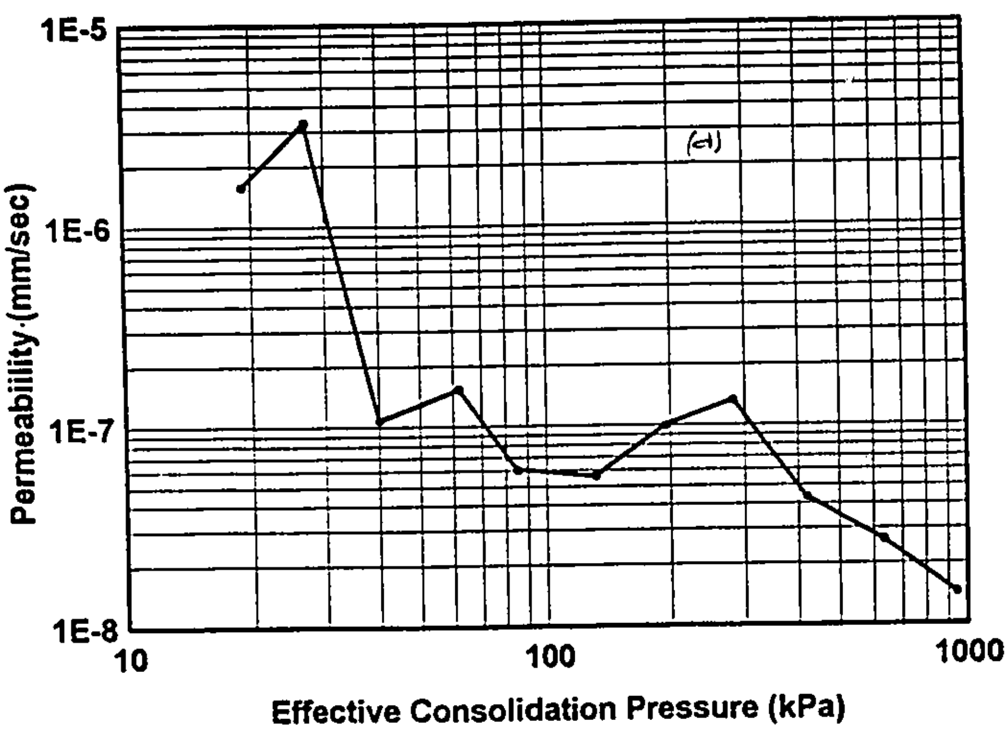

Fig. B.8. Results of oedometer consolidation test for vertical samples (Depth = 3.16 m).

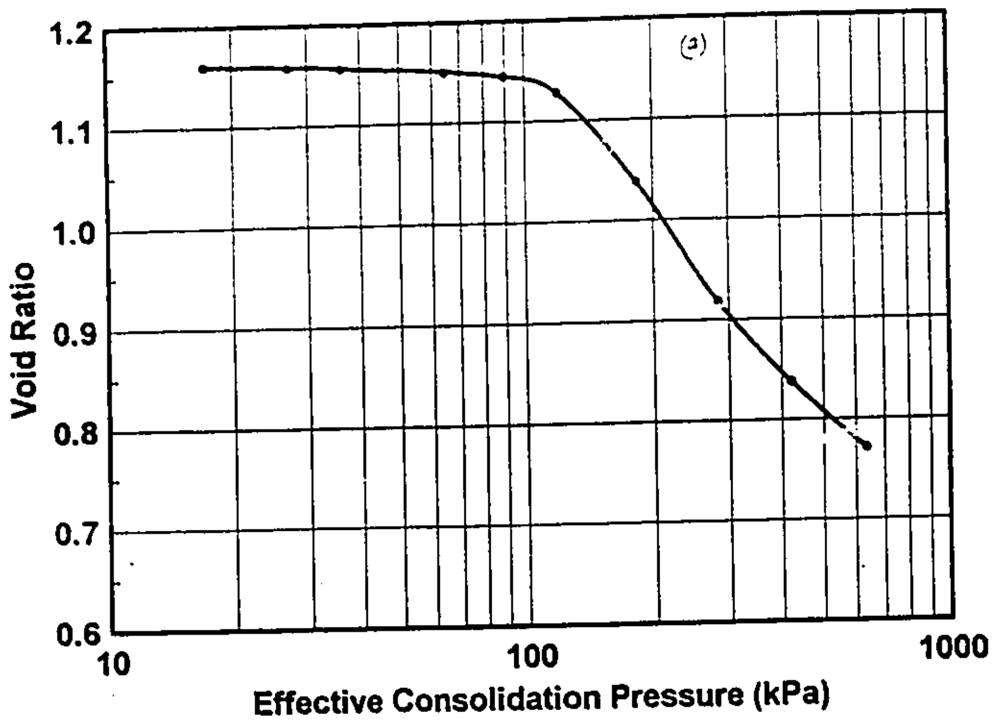

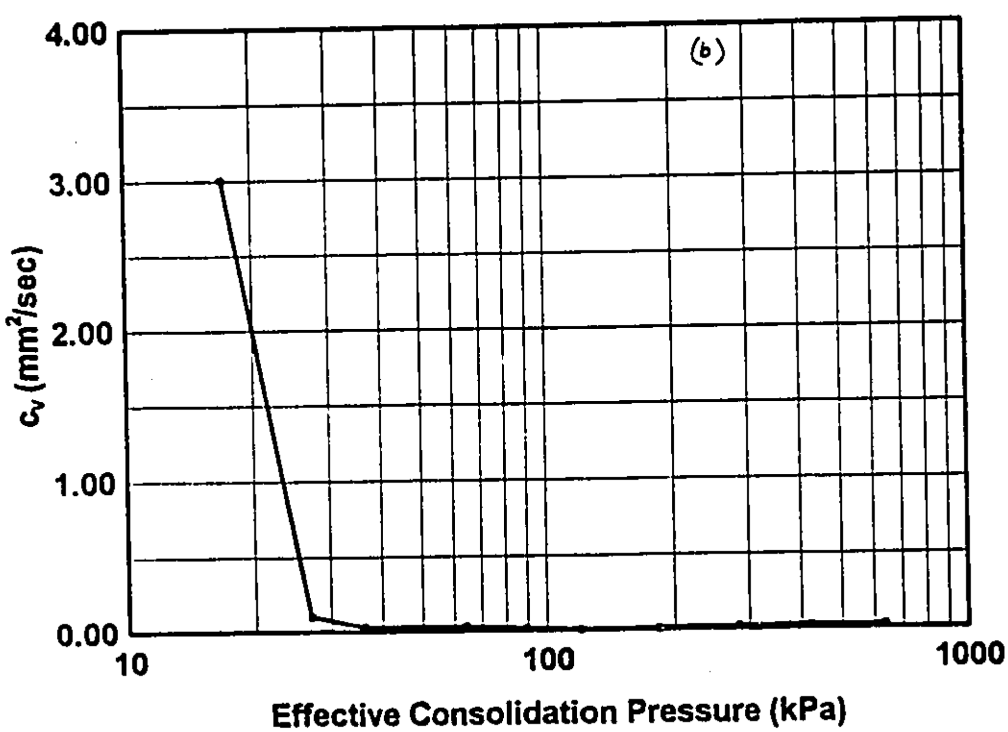

Fig. B.9. Results of oedometer consolidation test for vertical samples (Depth = 3.30 m).

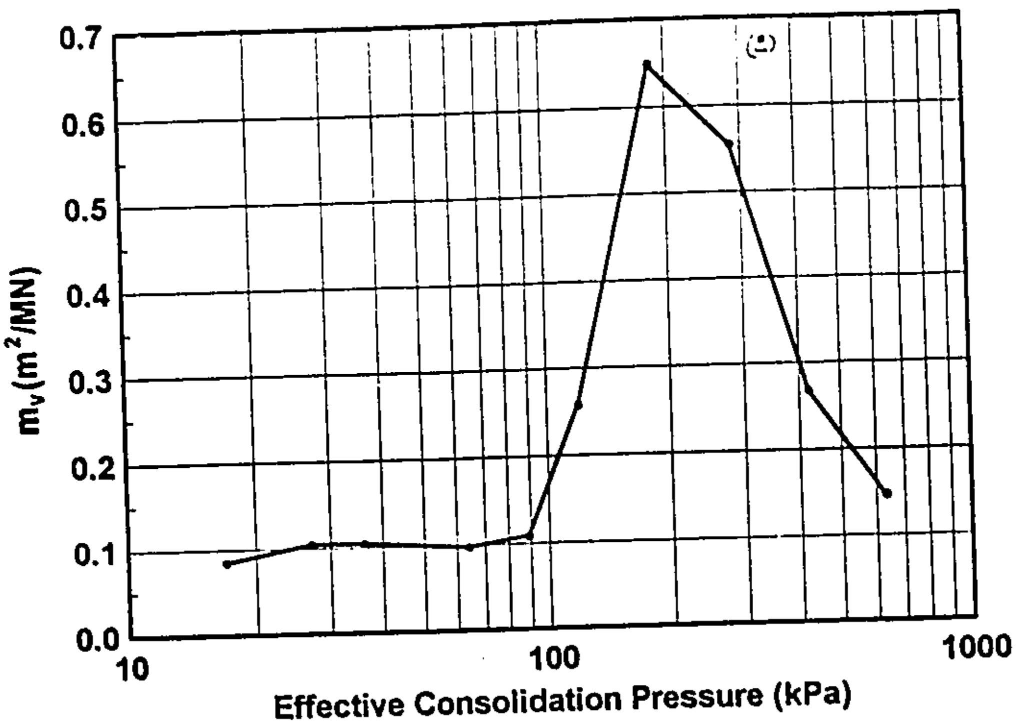

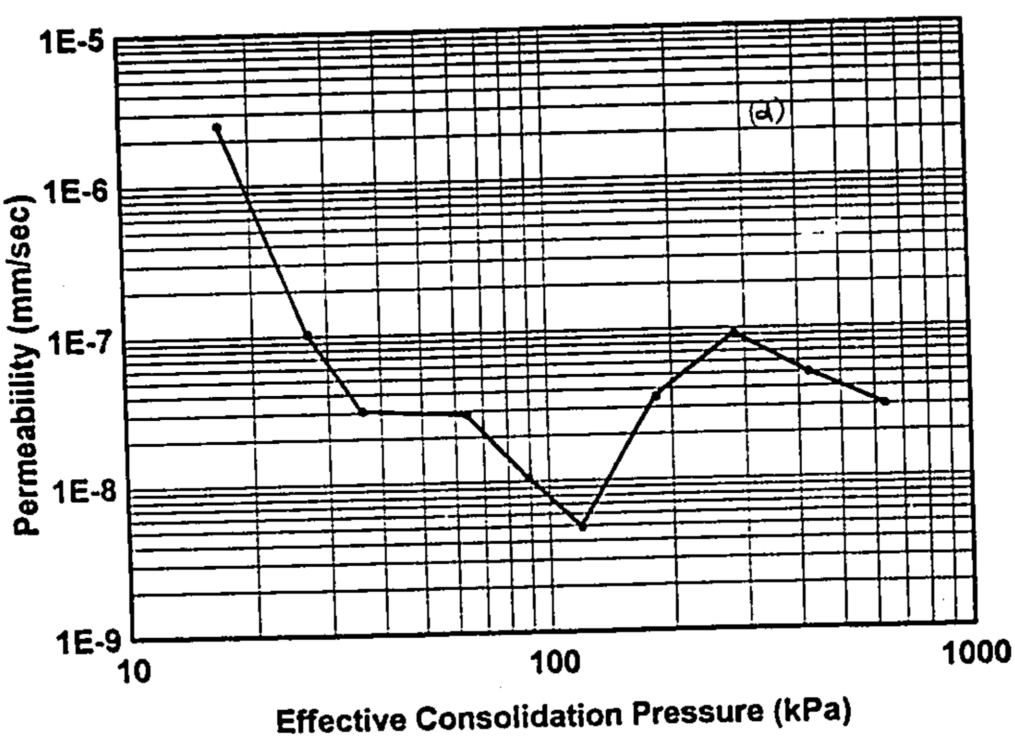

Fig. B.9. Results of oedometer consolidation test for vertical samples (Depth = 3.30 m).

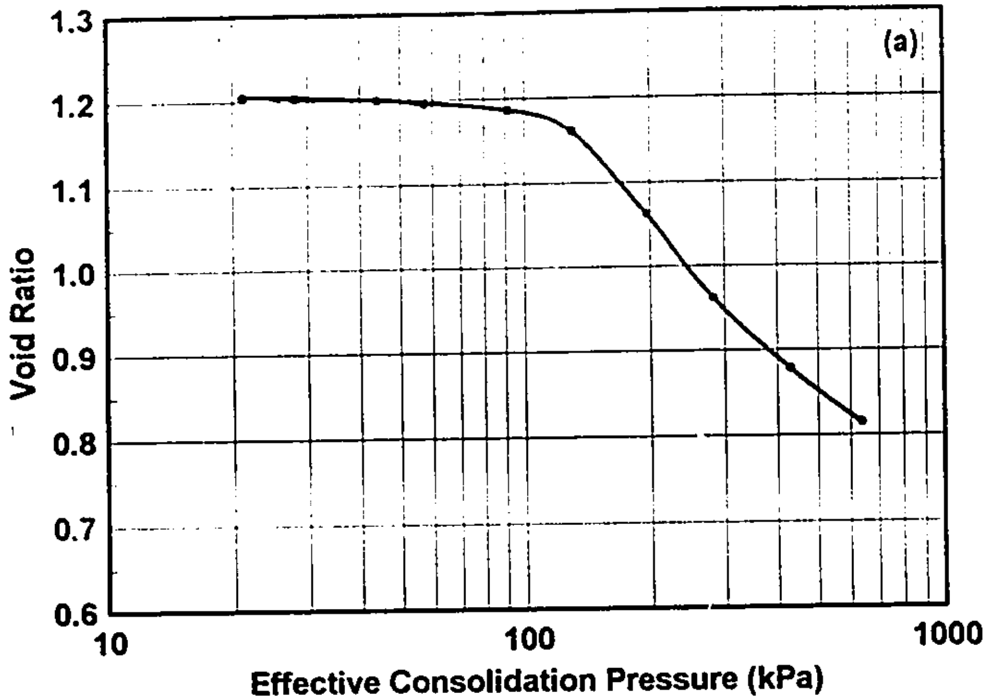

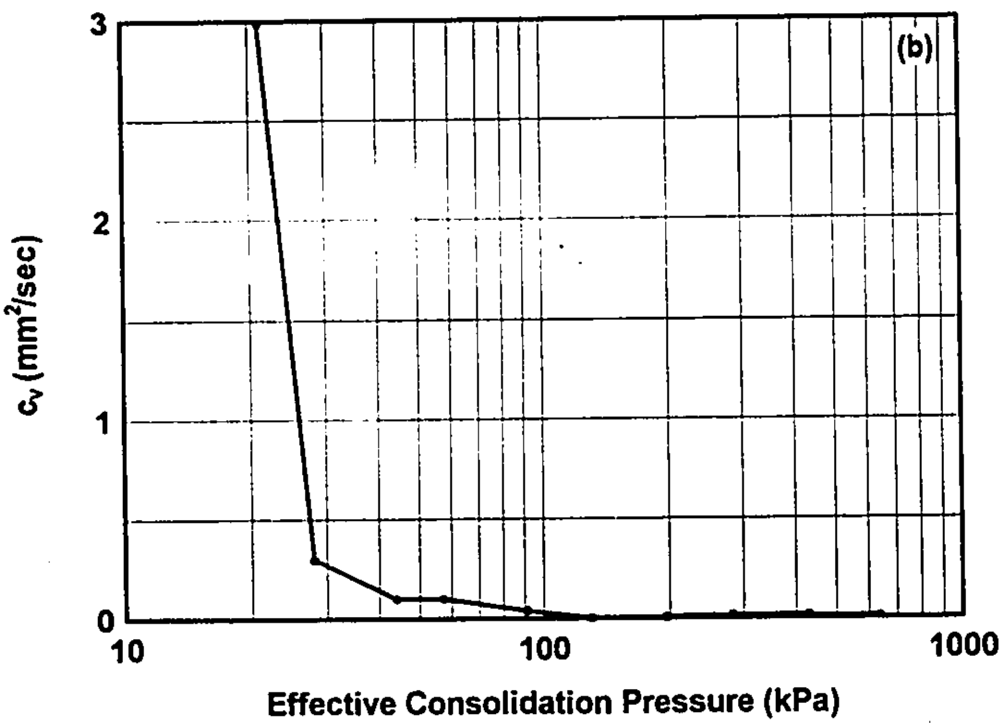

Fig. B.10. Results of oedometer consolidation test for vertical samples (Depth=3.70 m).

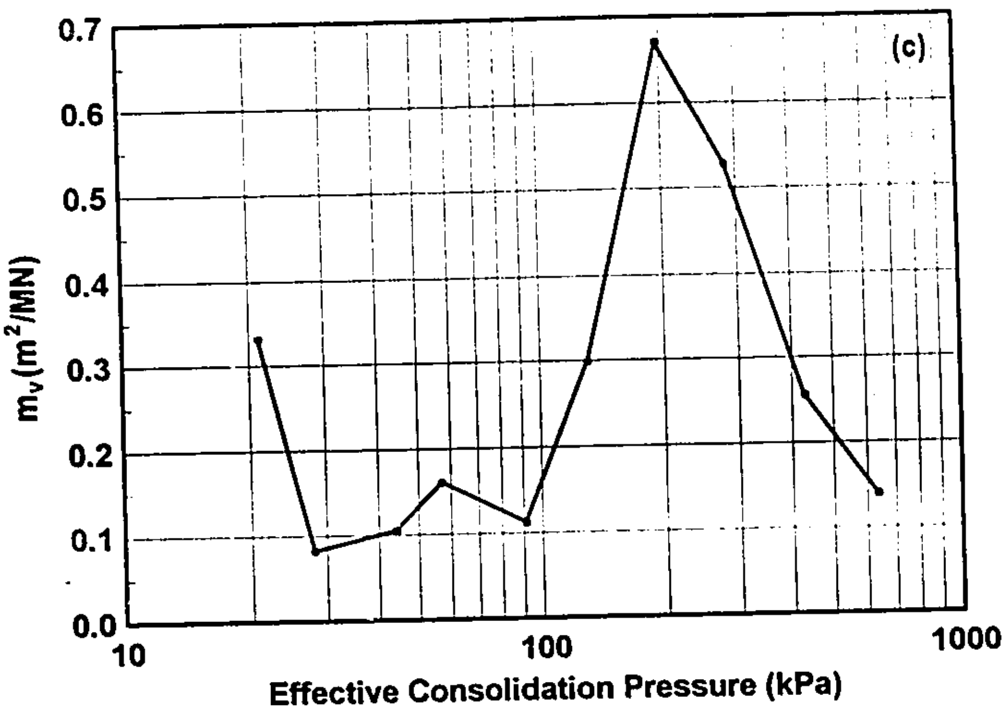

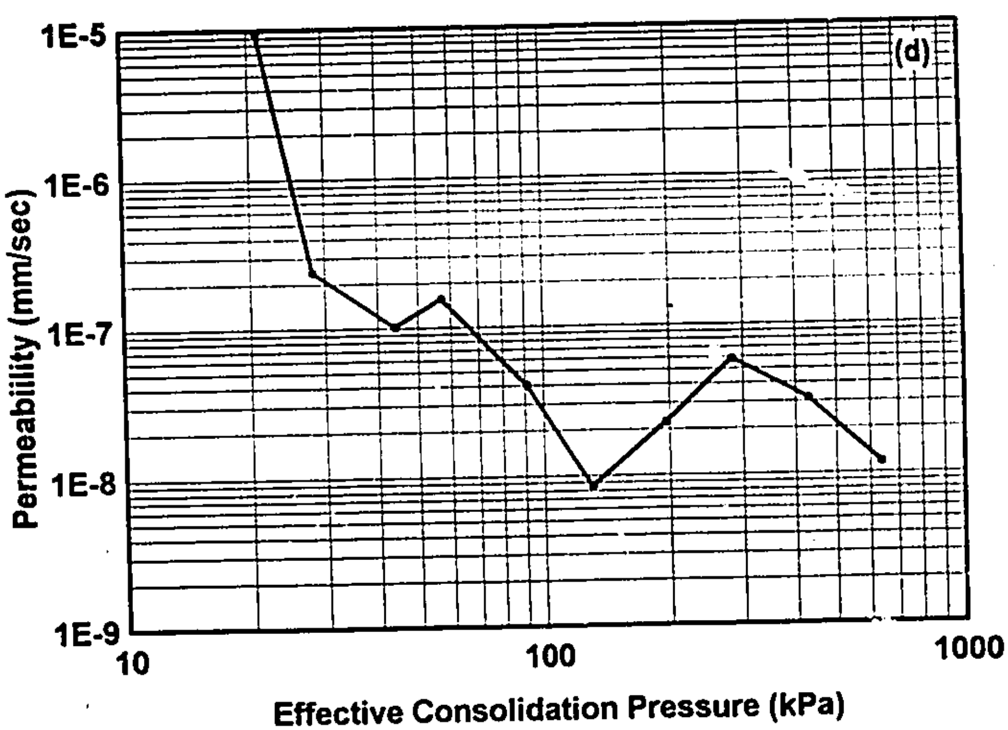

Fig. B.10. Results of oedometer consolidation test for vertical samples (Depth=3.70 m).

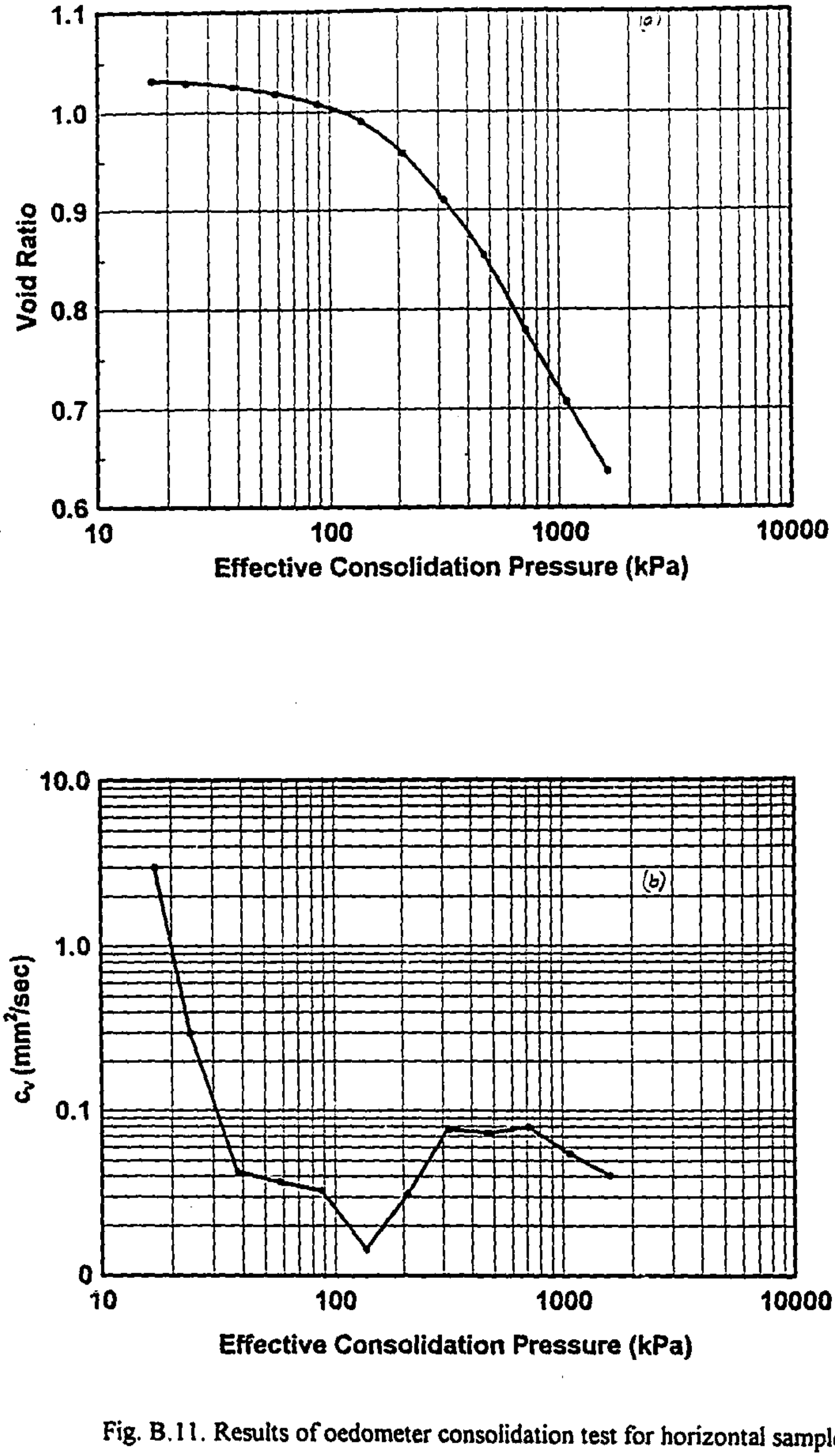

Fig. B.11. Results of oedometer consolidation test for horizontal samples (Depth = 1.96 m).

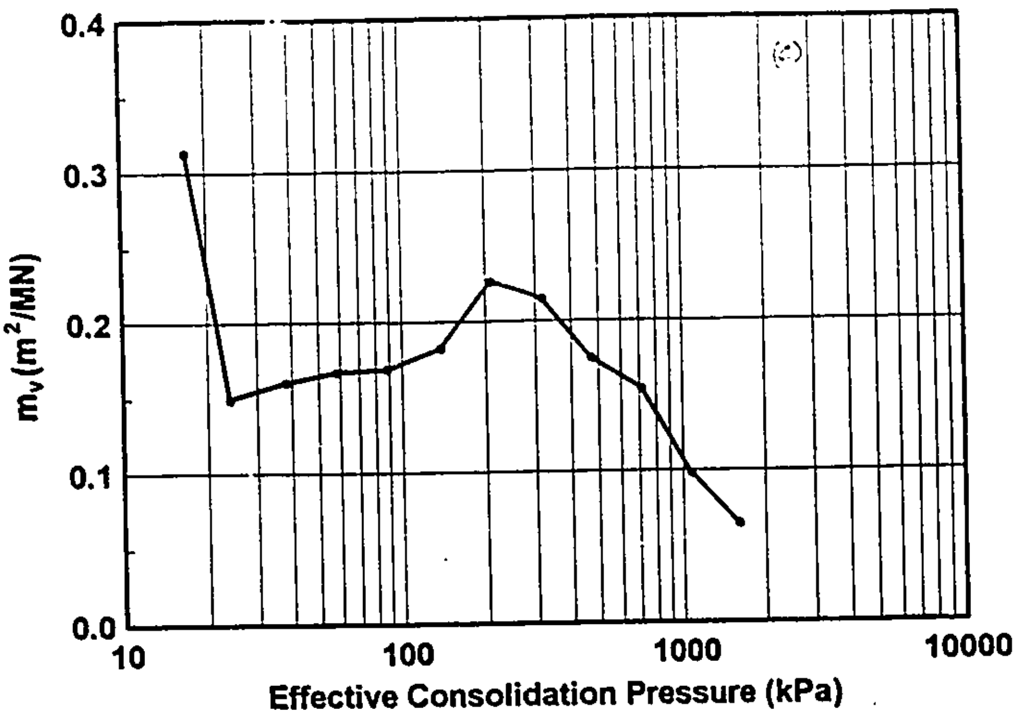

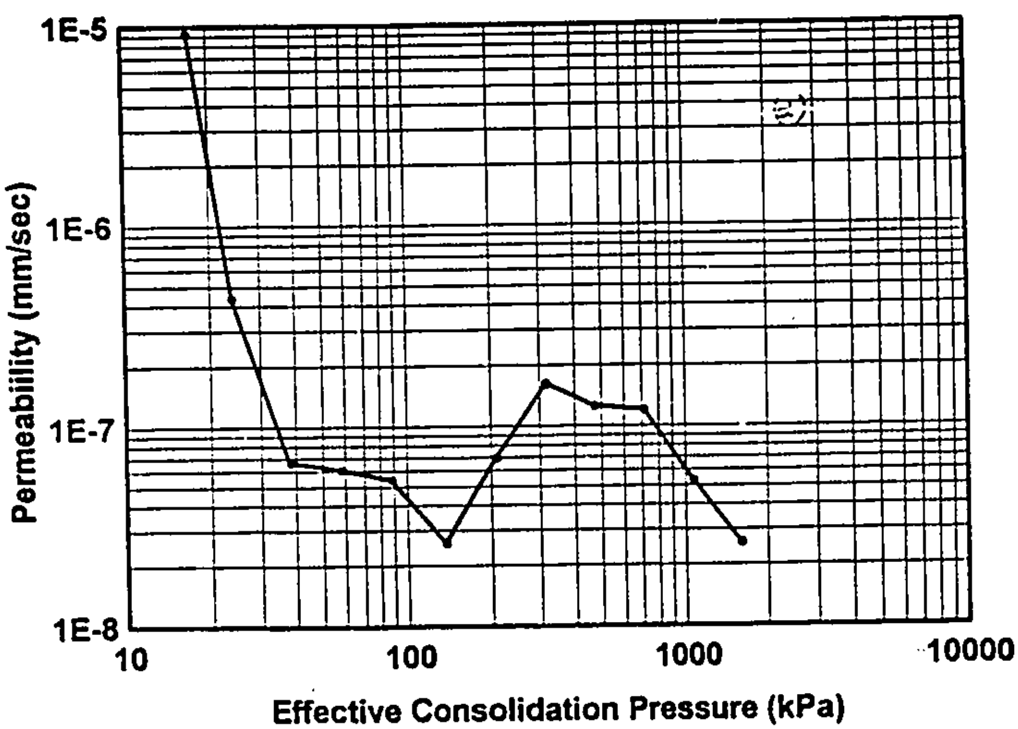

Fig. B.11. Results of oedometer consolidation test for horizontal samples (Depth = 1.96 m).

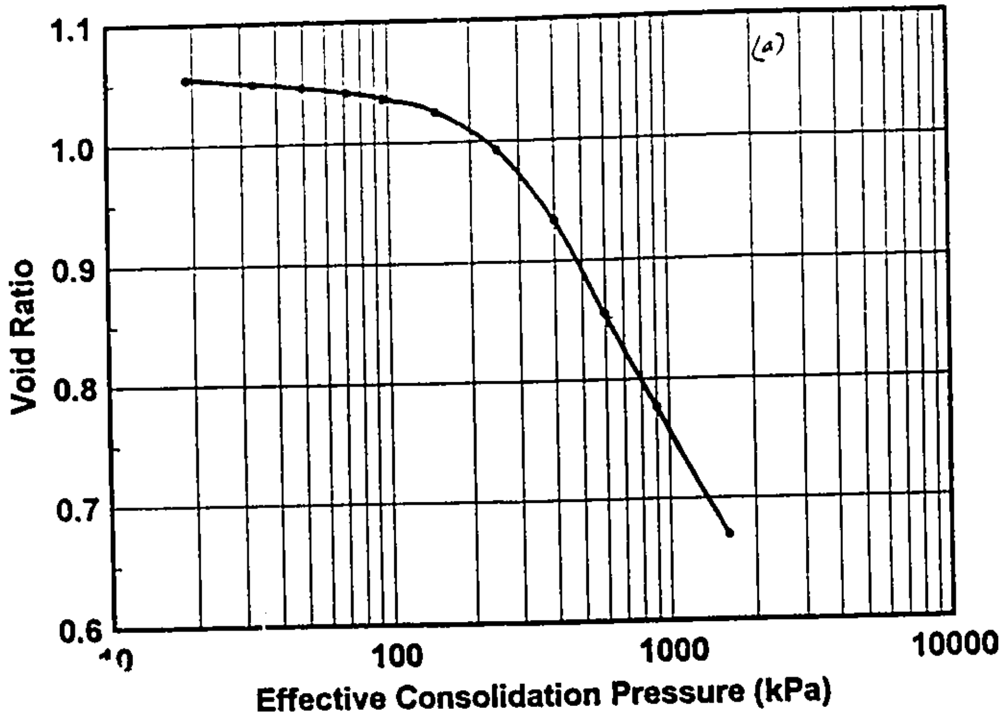

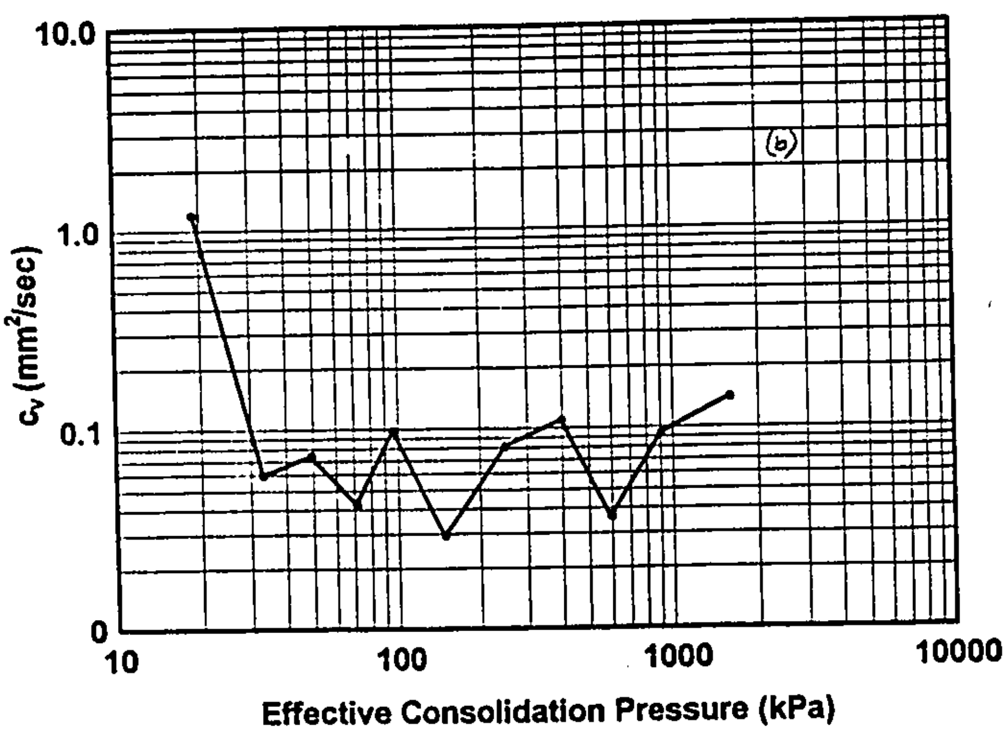

Fig. B.12. Results of oedometer consolidation test for horizontal samples (Depth = 2.03 m).

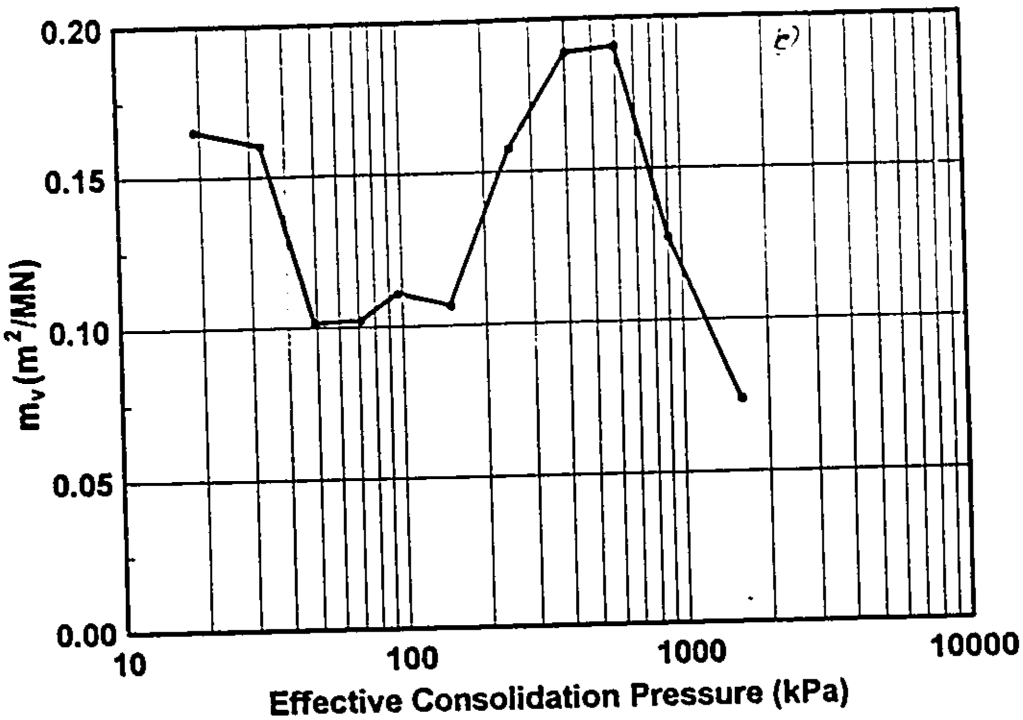

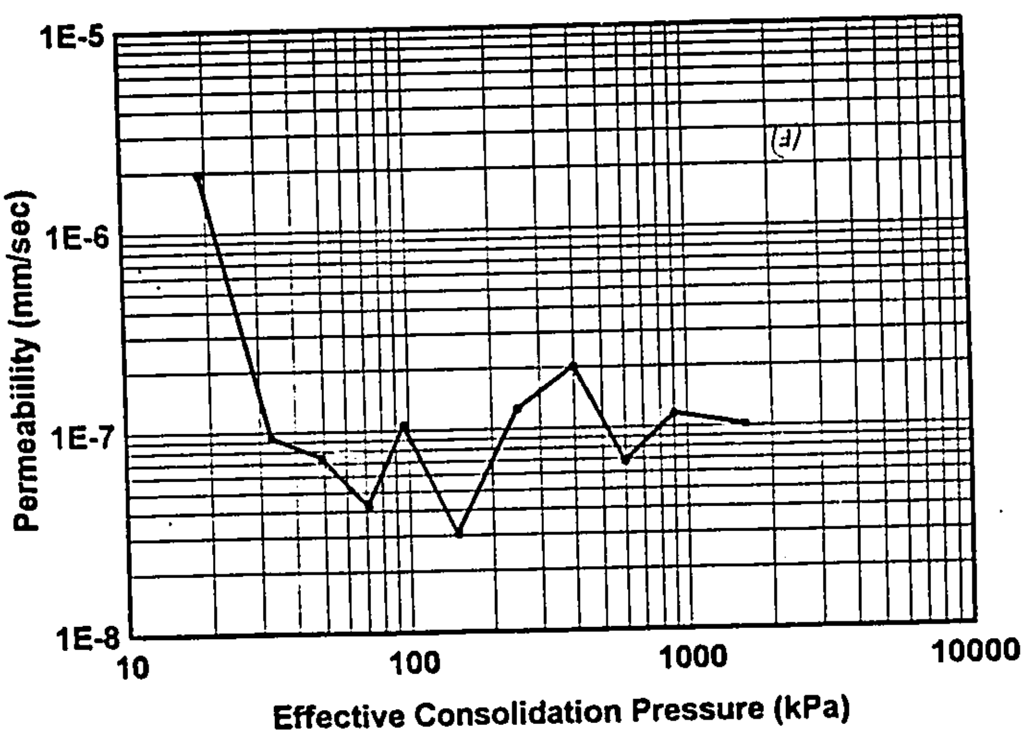

Fig. B.12. Results of oedometer consolidation test for horizontal samples (Depth = 2.03 m).

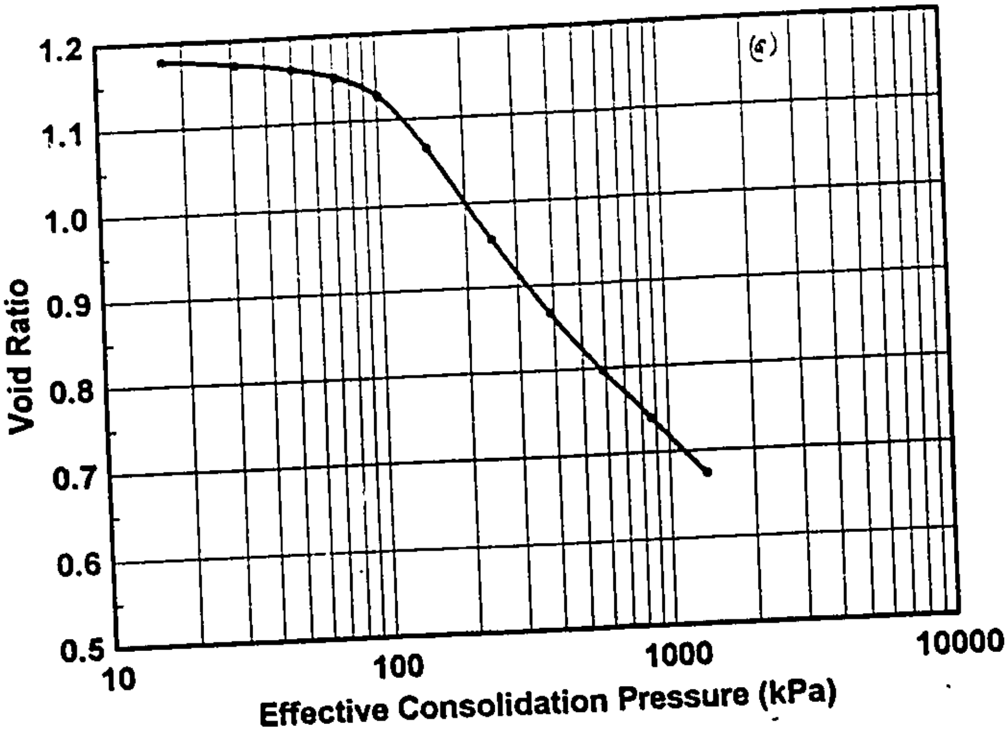

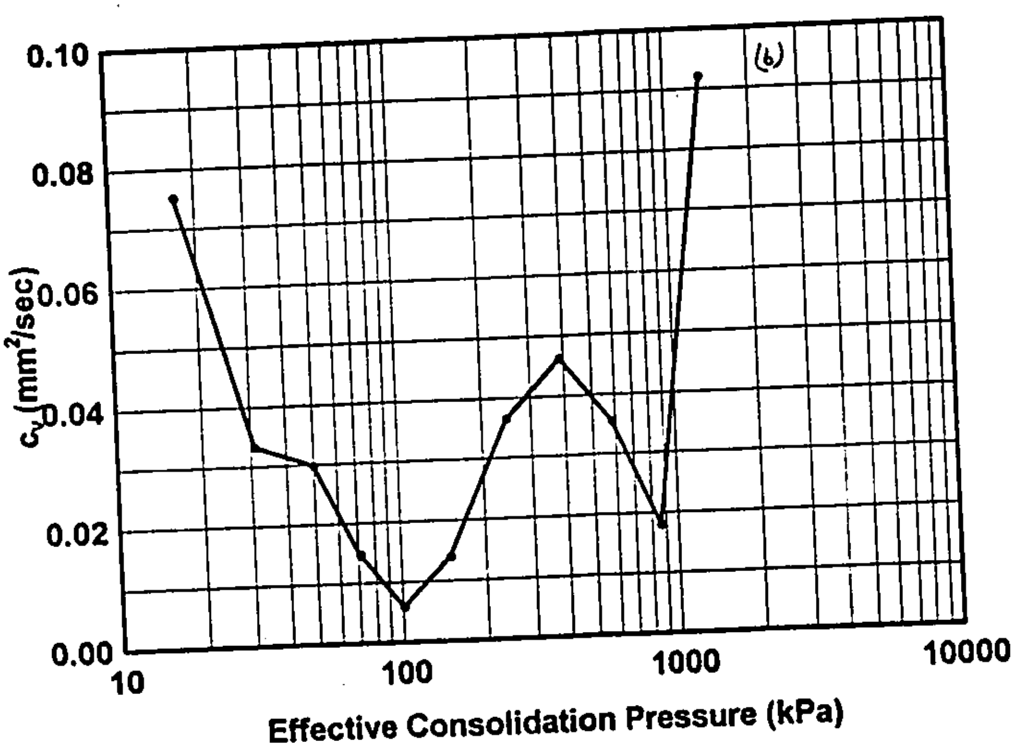

Fig. B.13. Results of oedometer consolidation test for horizontal samples (Depth = 3.35 m).

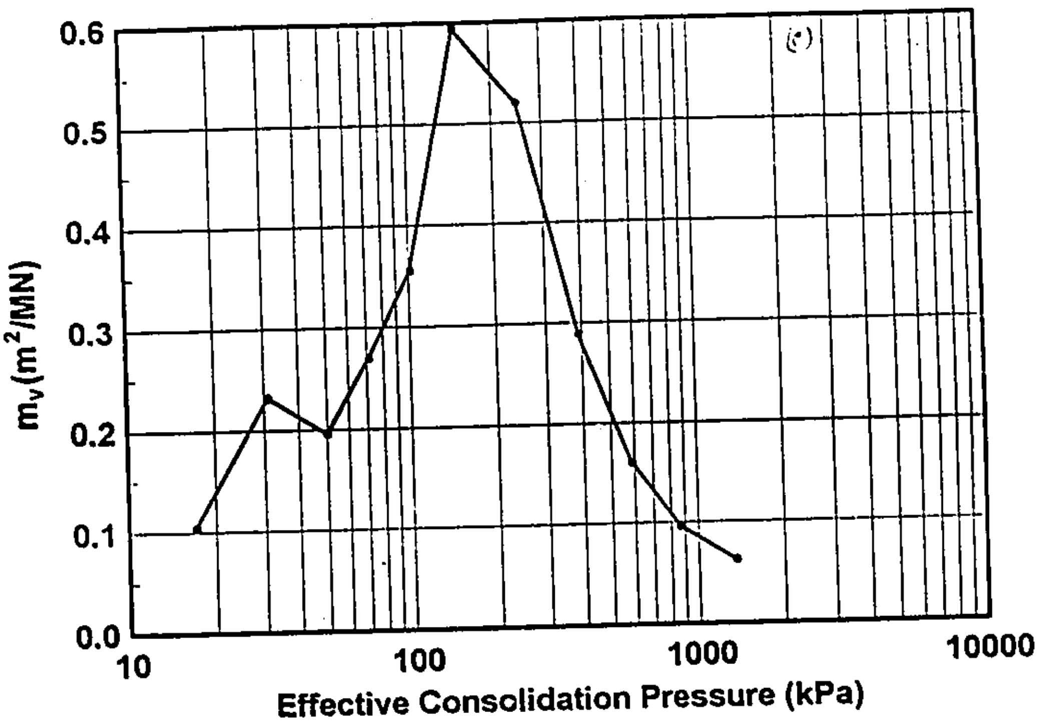

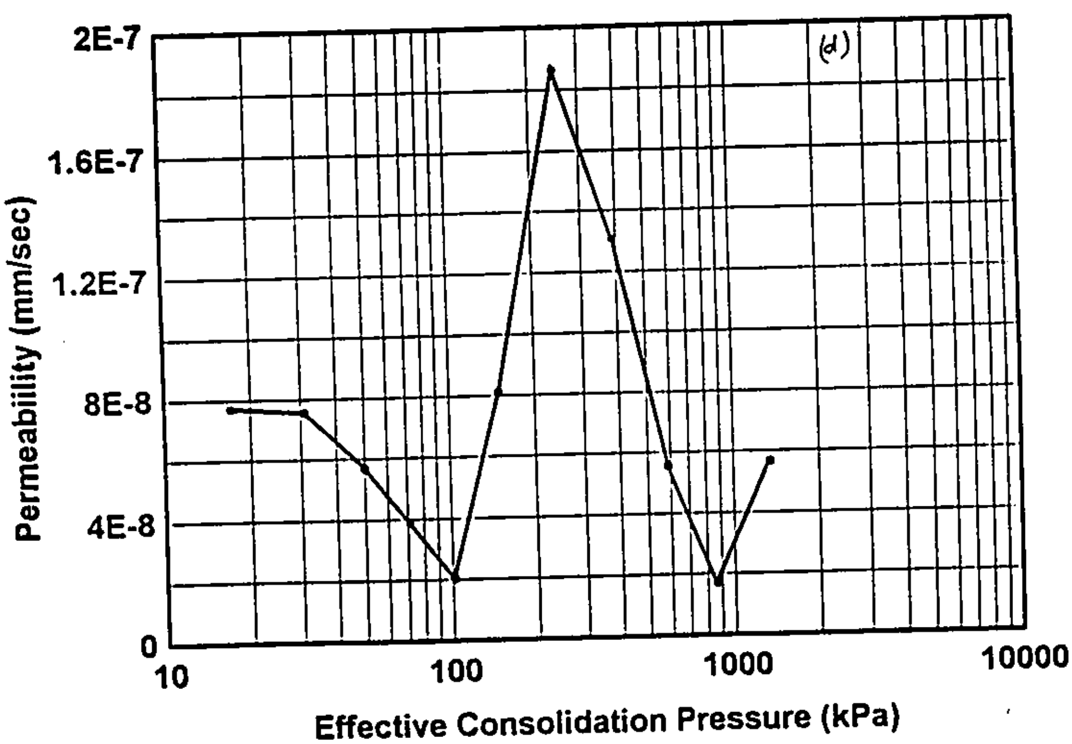

Fig. B.13. Results of oedometer consolidation test for horizontal samples.
(Depth = 3.35 m).

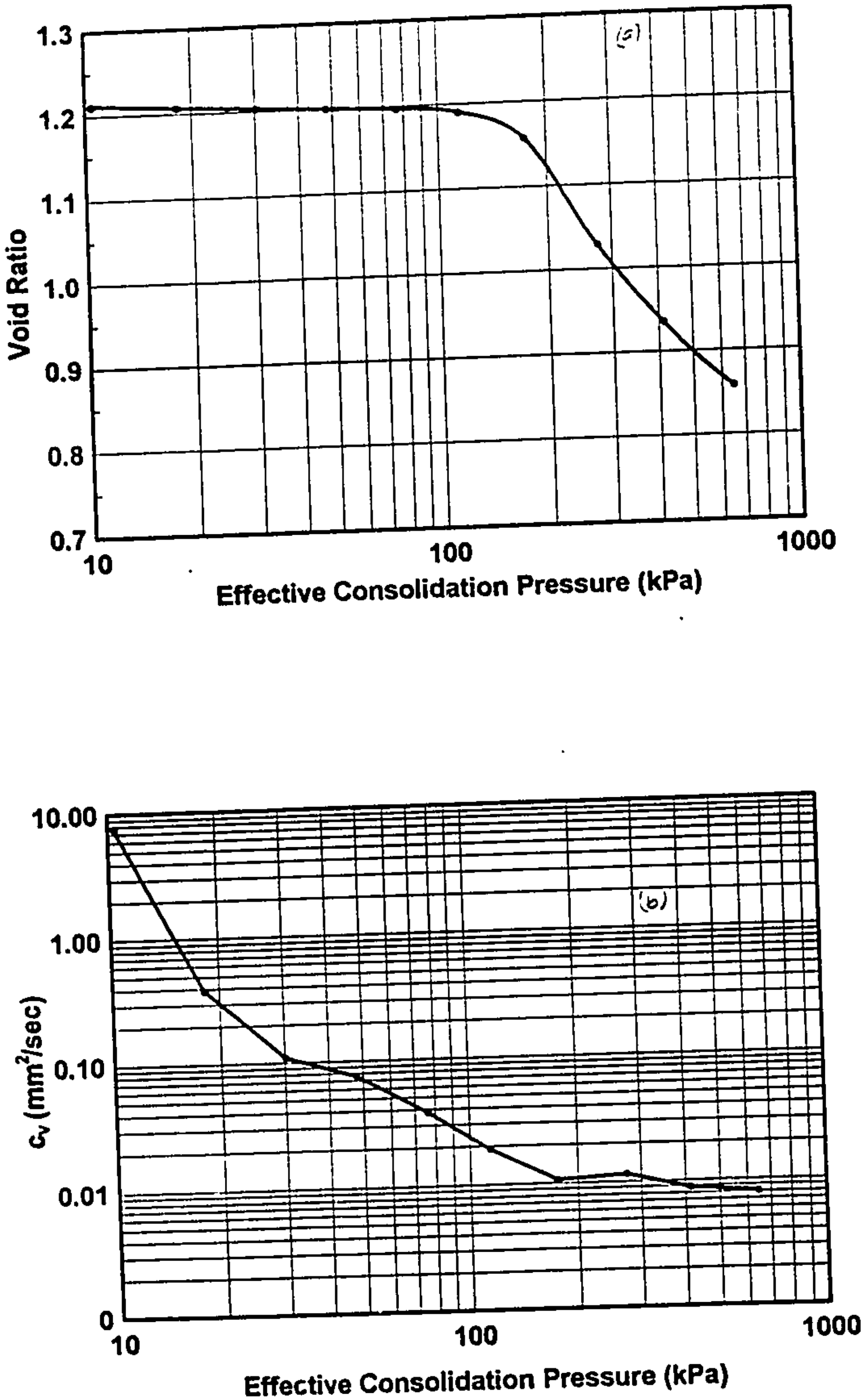

Fig. B.14. Results of hydraulic oedometer (76 mm) consolidation test for vertical samples (Depth = 3.69 m).

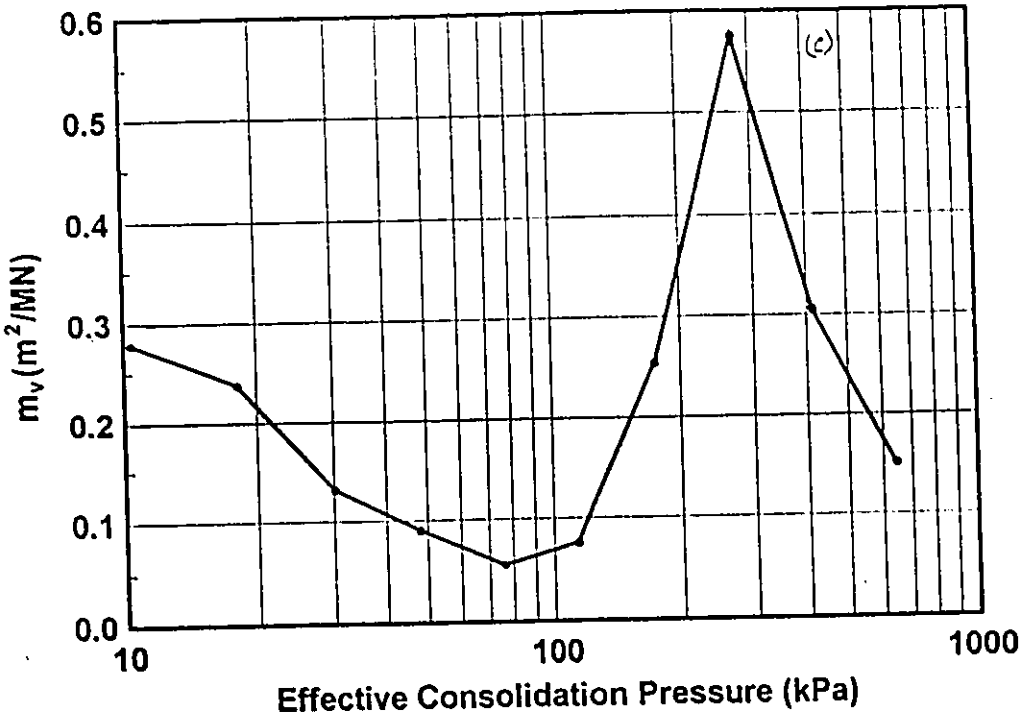

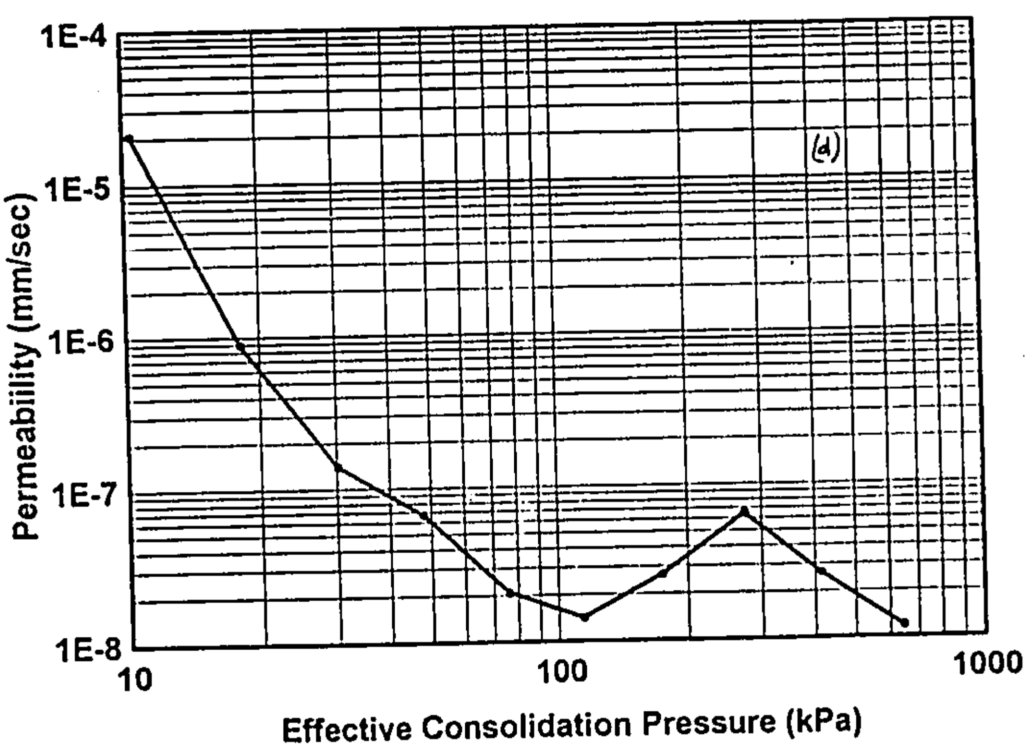

Fig. B.14. Results of hydraulic oedometer (76 mm) consolidation test for vertical samples (Depth = 3.69 m).

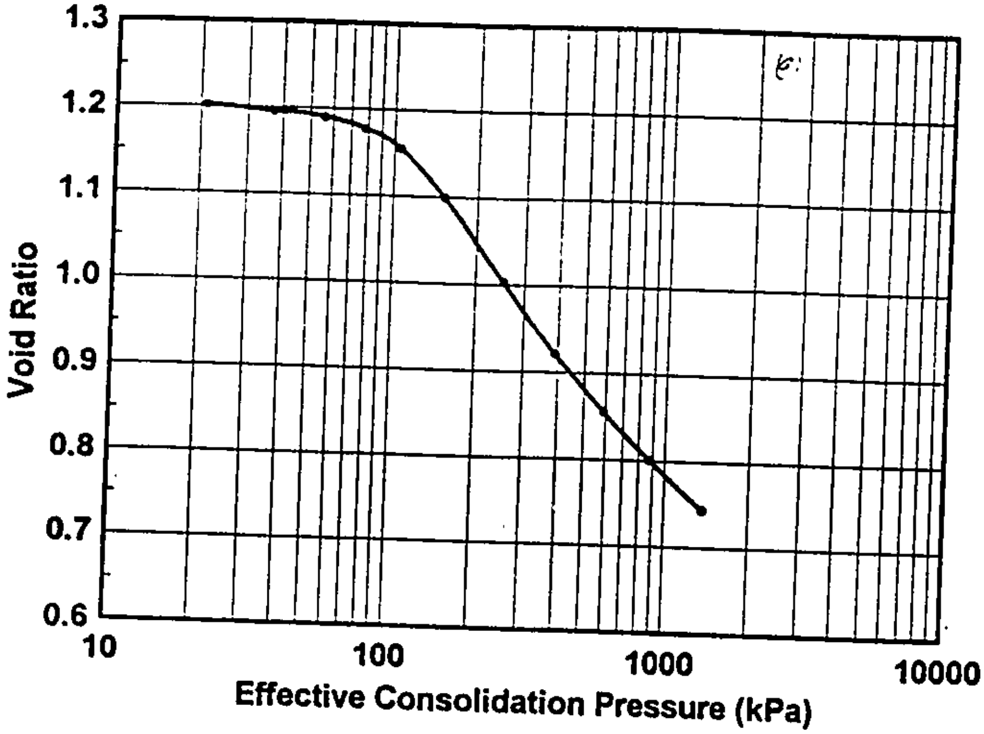

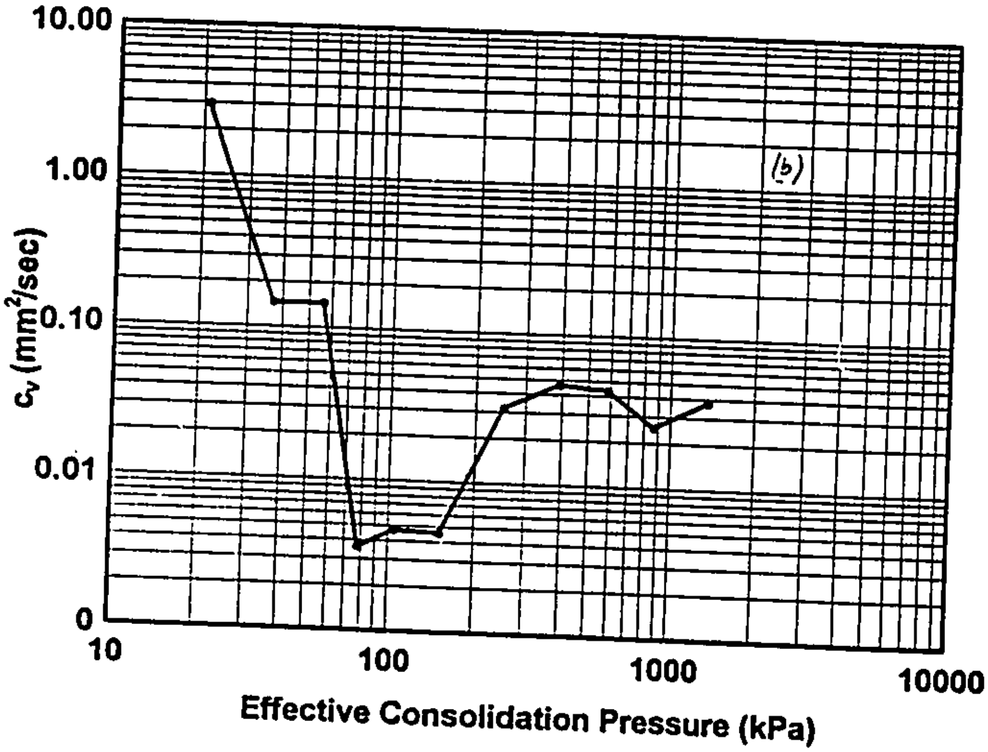

Fig. B.15. Results of oedometer consolidation test for horizontal samples (Depth = 3.70 m).

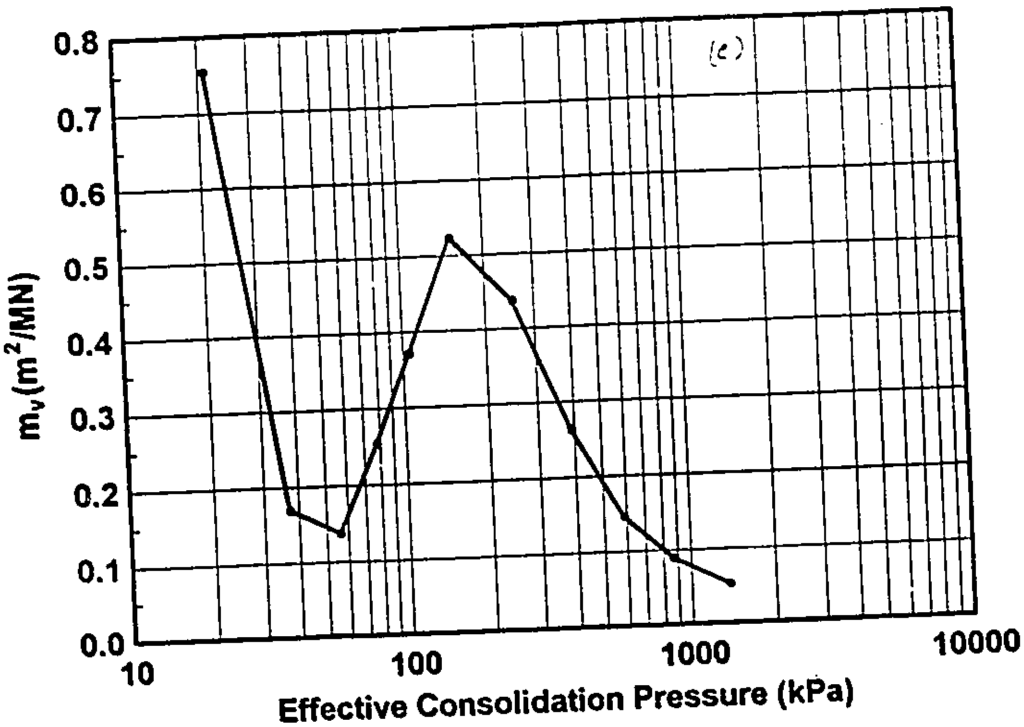

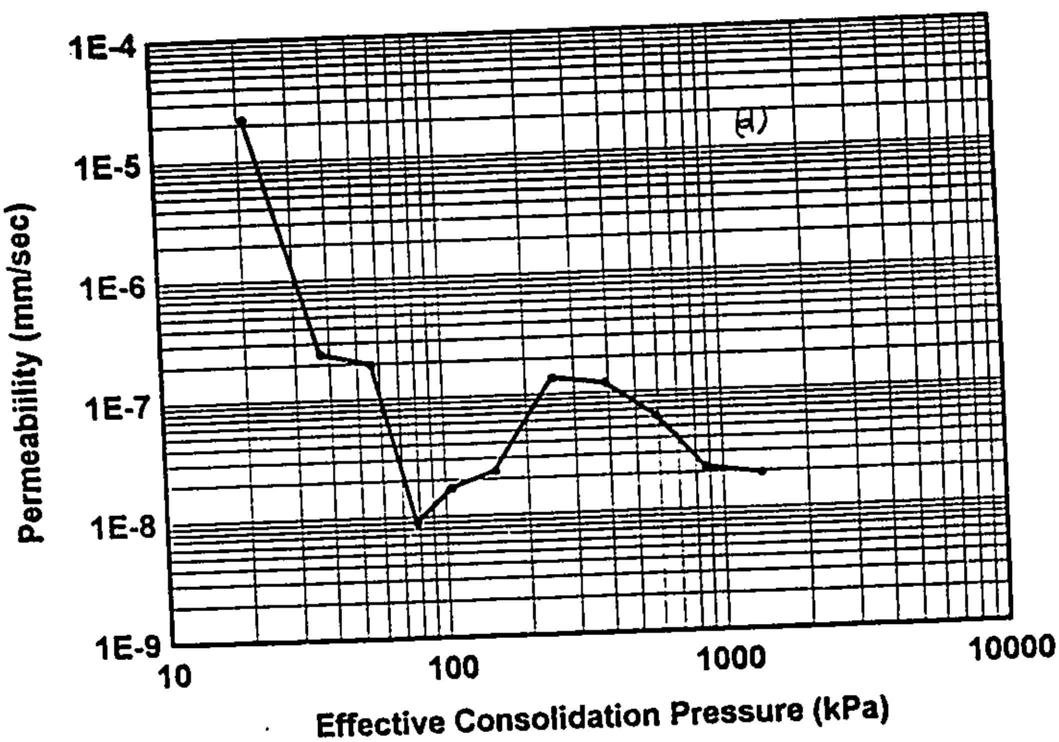

Fig. B.15. Results of oedometer consolidation test for horizontal samples (Depth = 3.70 m).

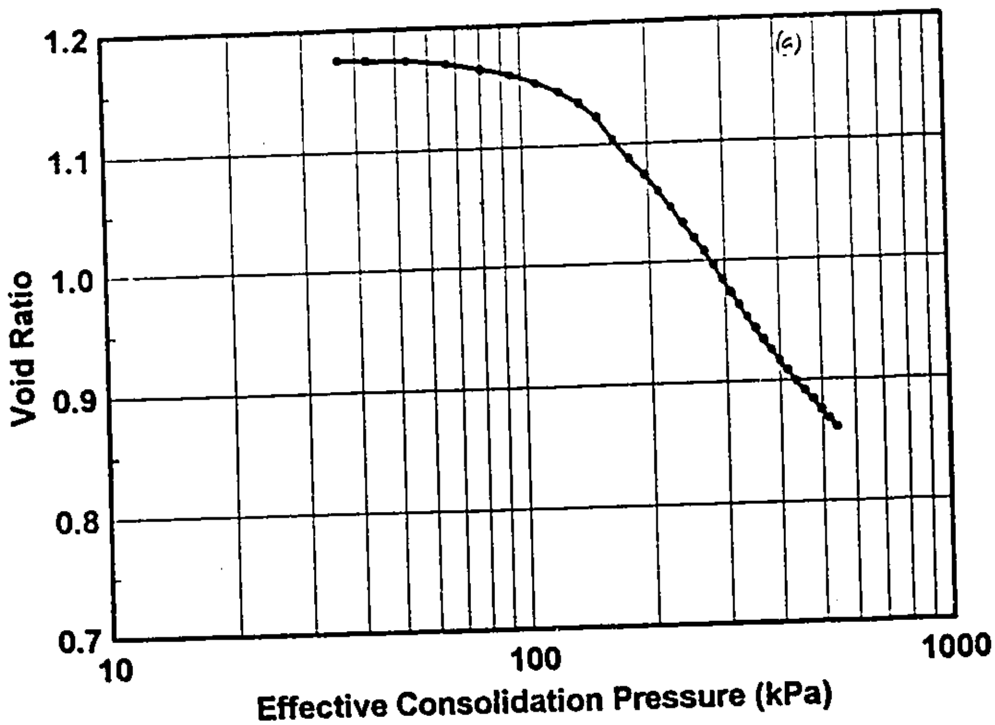

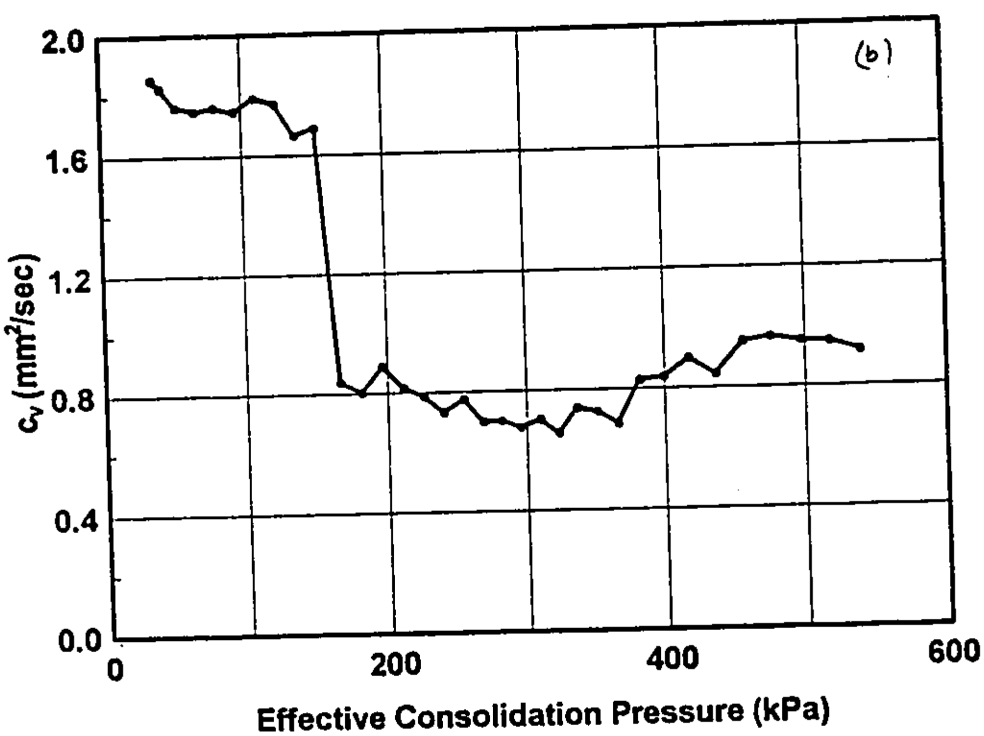

Fig. B.16. Results of controlled gradient (CG) consolidation test for vertical samples (Depth = 3.15 m).

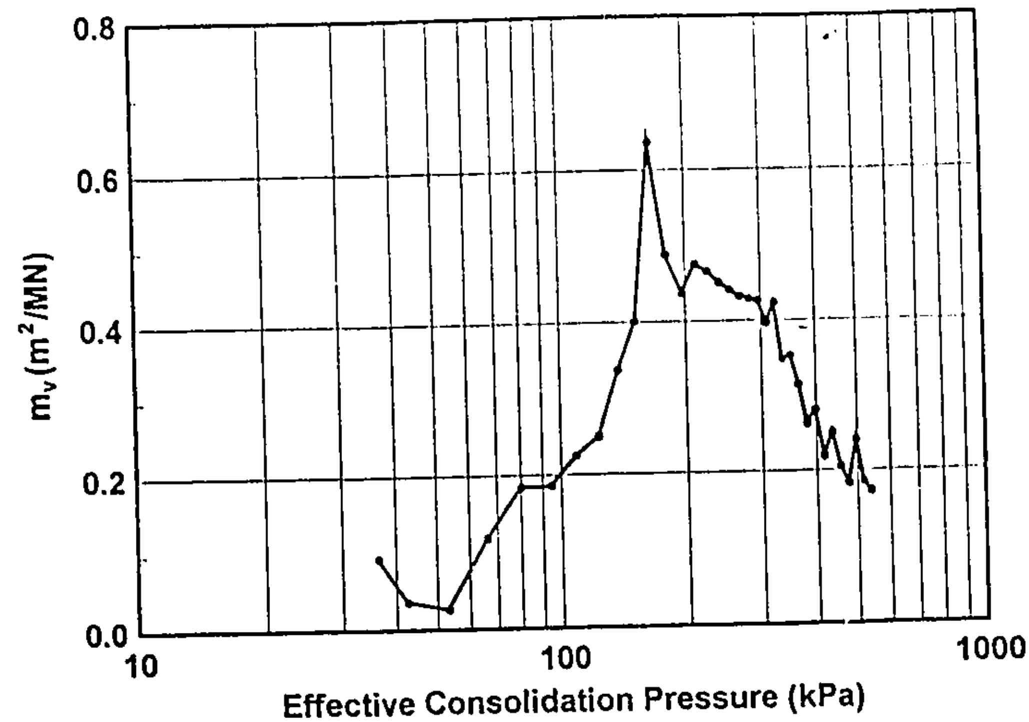

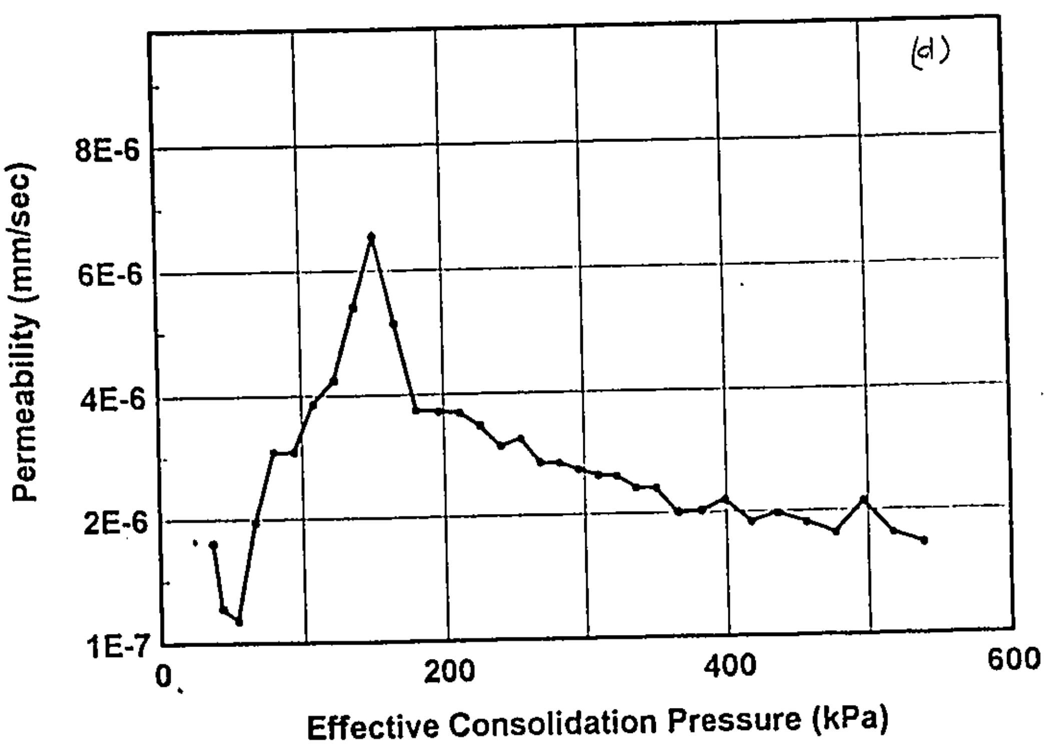

Fig. B.16. Results of controlled gradient (CG) consolidation test for vertical samples (Depth = 3.15 m).

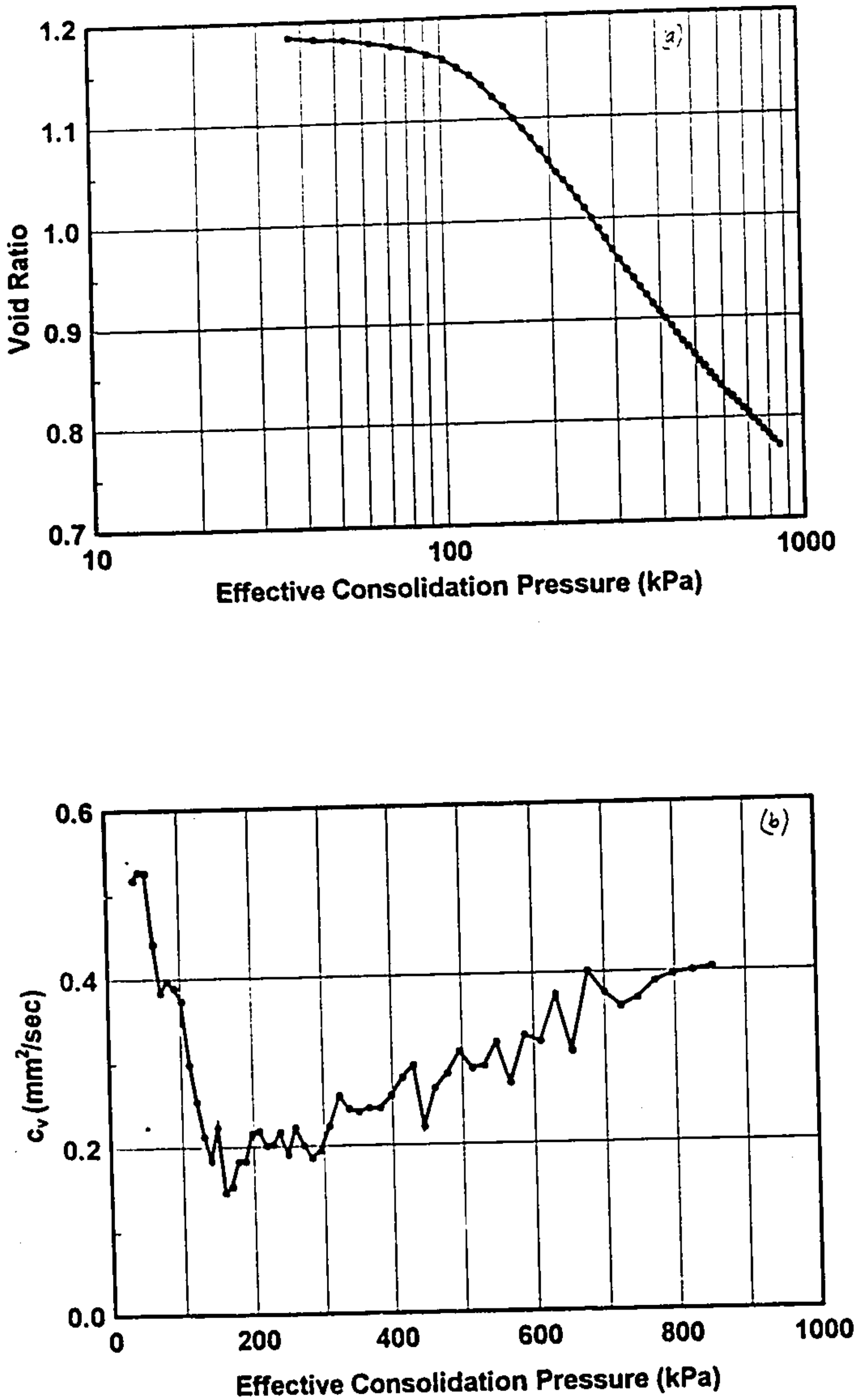

Fig. B.17. Results of constant rate of strain (CRS) consolidation test for vertical samples (Depth = 3.15 m).

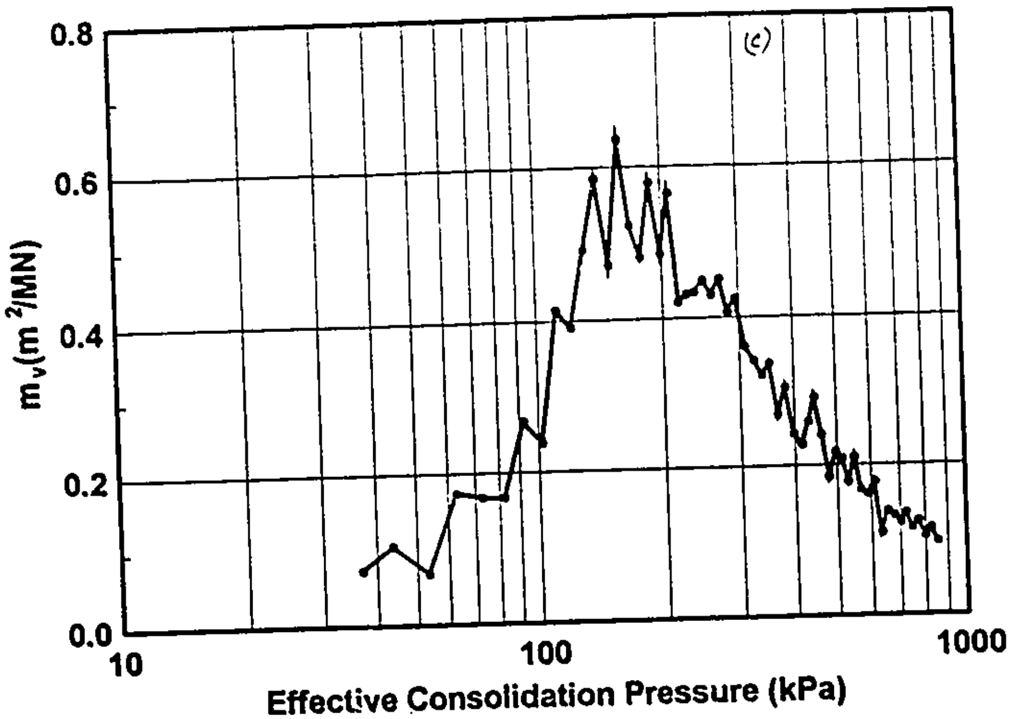

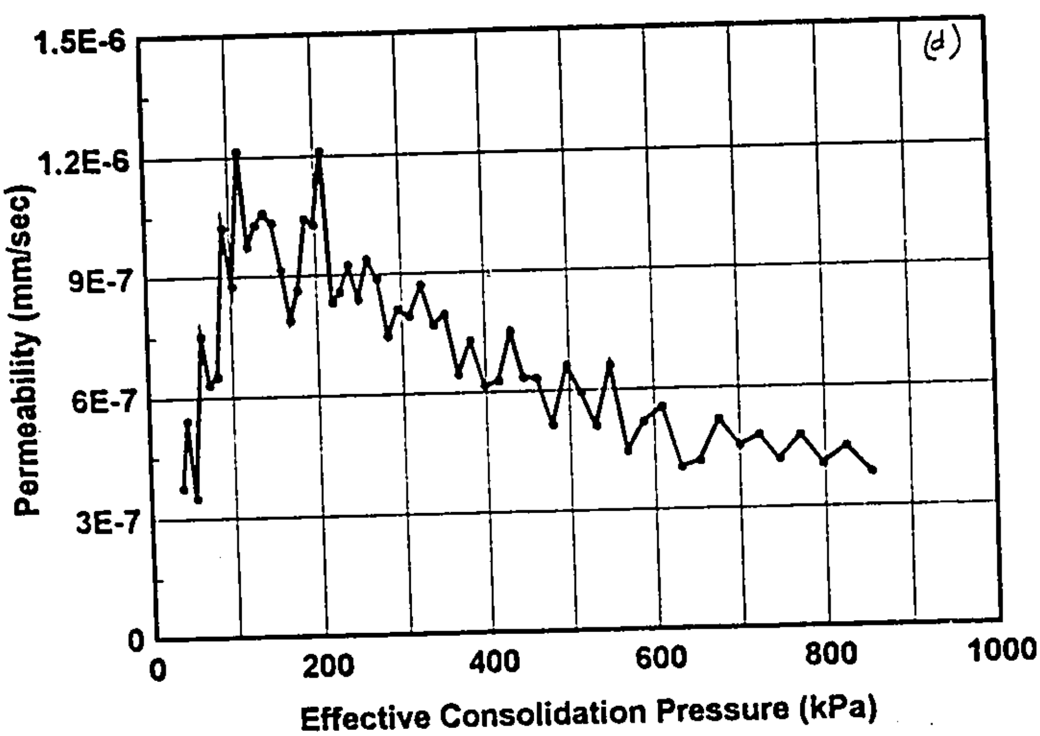

Fig. B.17. Results of constant rate of strain (CRS) consolidation test for vertical samples (Depth = 3.15 m).

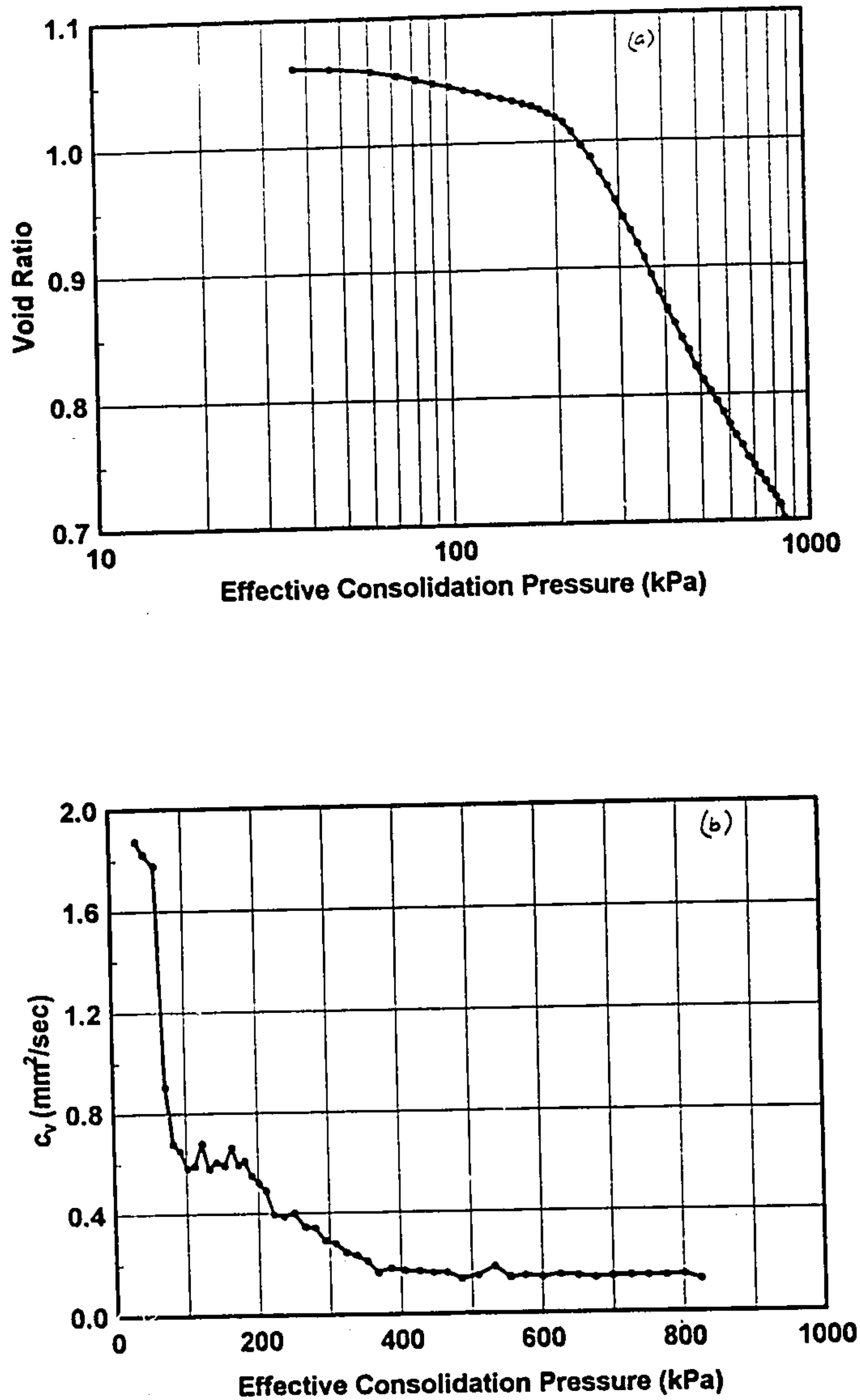

Fig. B.18. Results of constant rate of loading (CRL) consolidation test for vertical samples (Depth = 2.46 m).

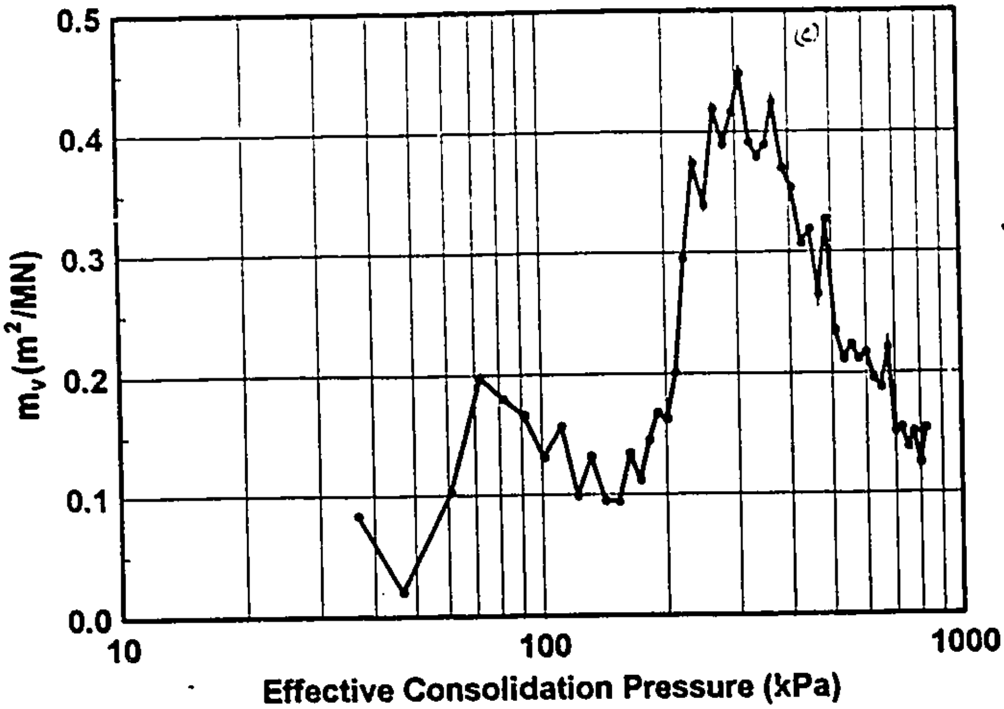

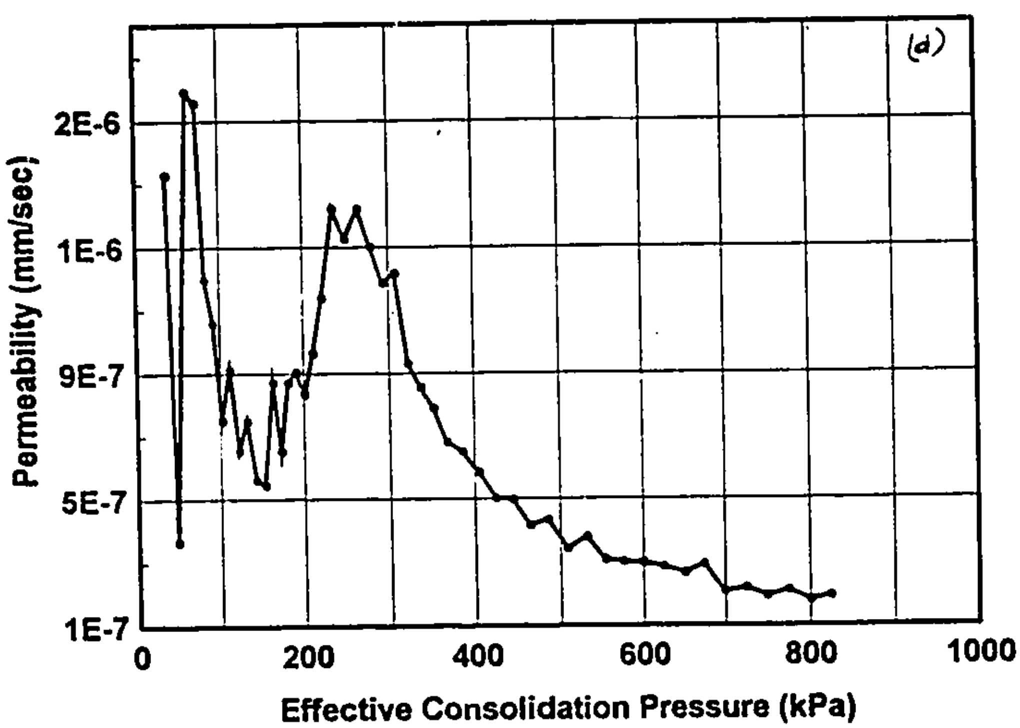

Fig. B.18. Results of constant rate of loading (CRL) consolidation test for vertical samples (Depth = 2.46 m).

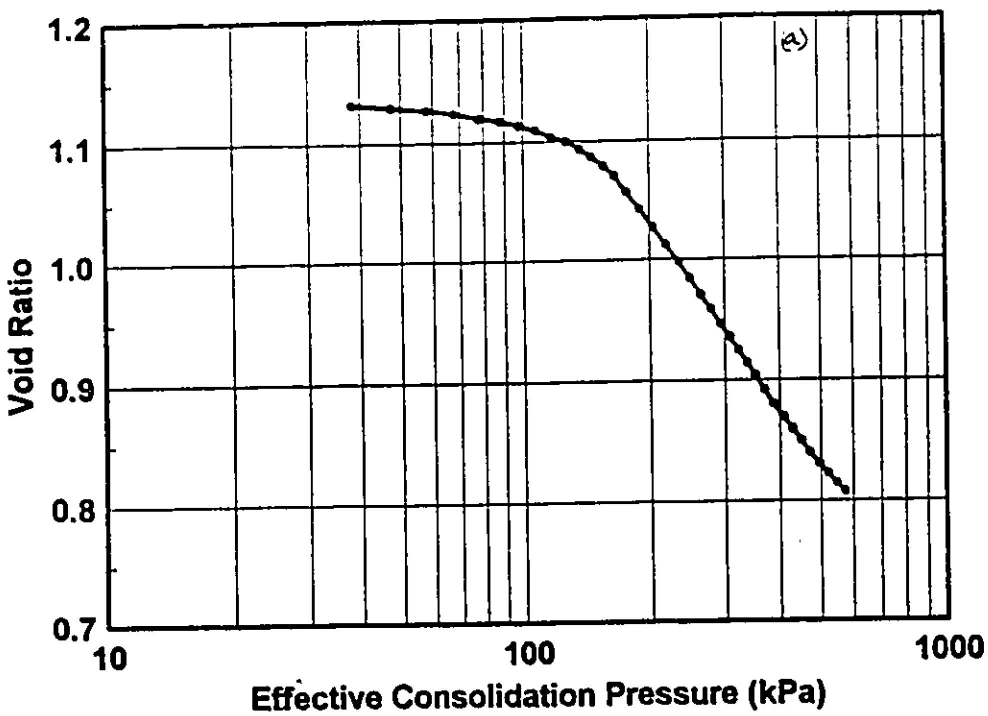

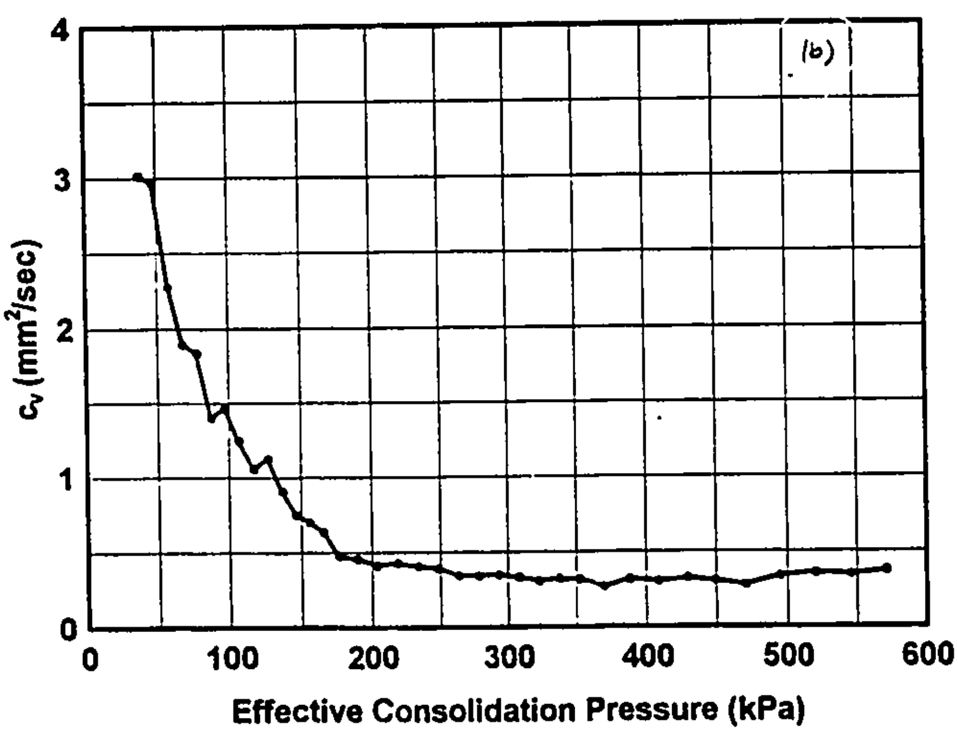

Fig. B.19. Results of constant rate of loading (CRL) consolidation test for vertical samples (Depth = 3.08 m).

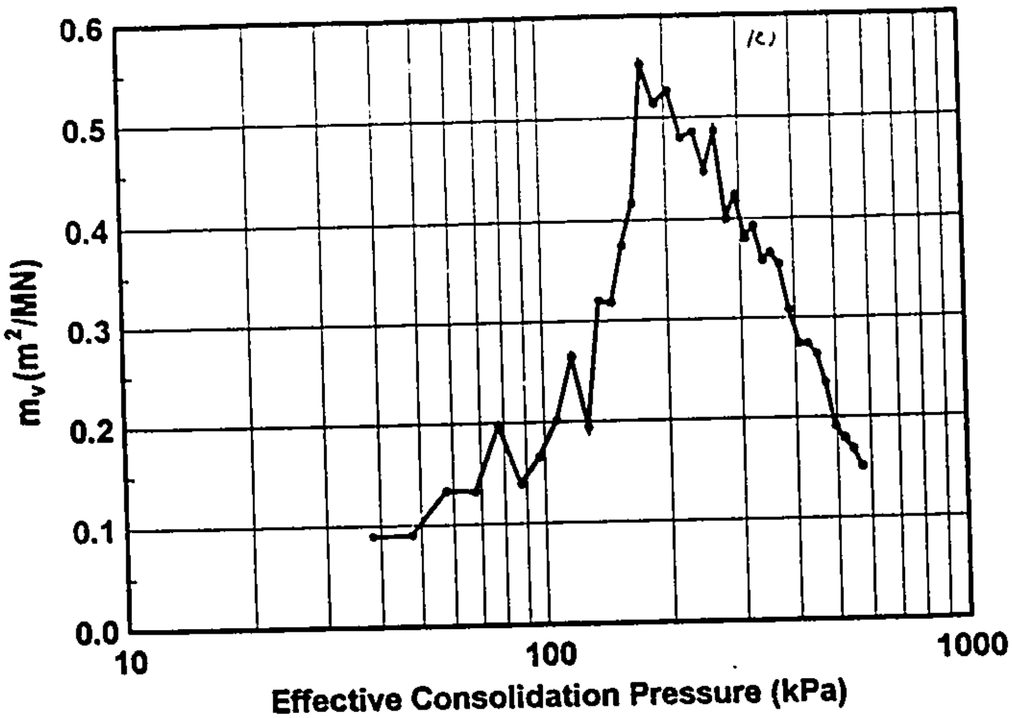

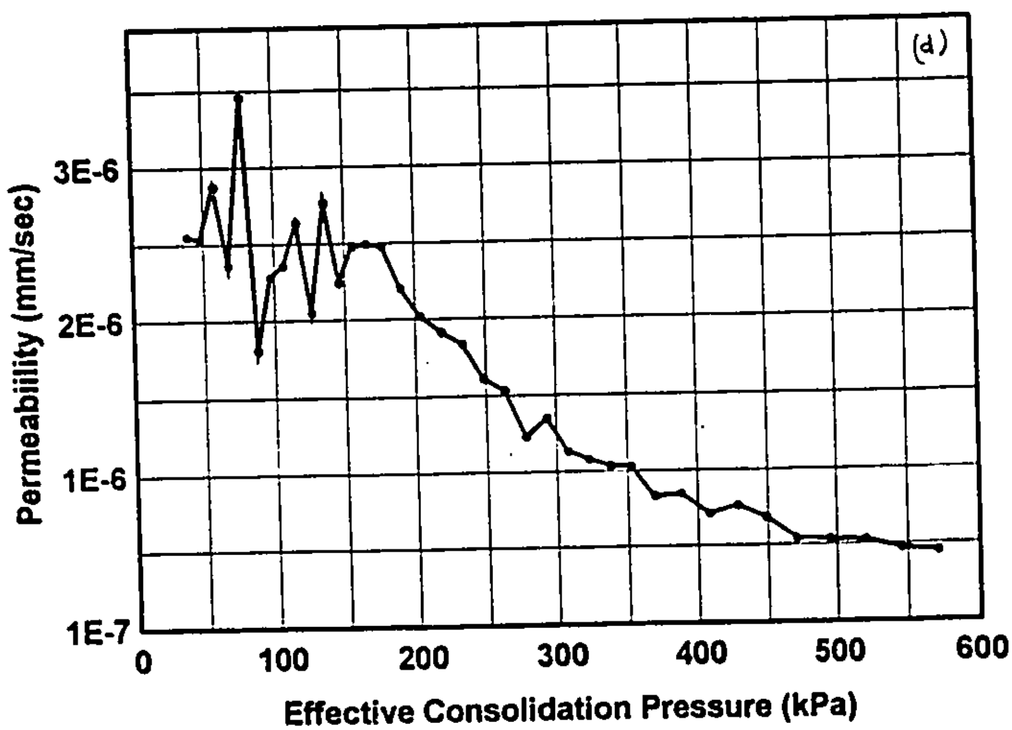

Fig. B.19. Results of constant rate of loading (CRL) consolidation test for vertical samples (Depth = 3.08 m).